Proceedings of the I·R·E

A Journal of Communications and Electronic Engineering

(Including the WAVES AND ELECTRONS Section)

Schleimann
Jensen addre

November, 1947

Volume 35 Number 11

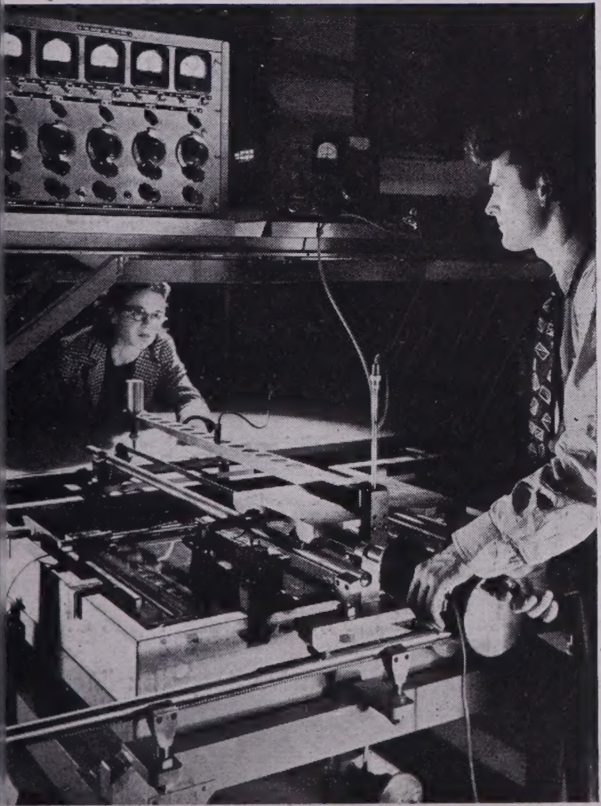

Sylvania Electric Products, Inc.

CTROLYTIC SIMULATION OF CATHODE-RAY-TUBE CONDITIONS

trolytic tank shown above is used for plotting the electrostatic field of
ray-tube focusing and deflecting systems. A pair of deflecting plates,
nes normal size, is immersed in the electrolyte. The field is explored with
Potential picked up by the probe is measured on a vacuum-tube volt-
he bank of five vacuum-tube voltmeters permits measurements at five
multaneously for use in gun design and similar problems. A push button
carriage permits working dots on the plotting board behind the tank.

PROCEEDINGS OF THE I.R.E.

Microwave Converters
Fluctuation Noise in Pulse-Height Multiplex Links
Wave Propagation in the Lower Troposphere
Ionospheric Electron Distribution
Design of Radar I.F. Amplifiers
Target Detectability and Discriminability on Remote Projection P.P.I.
Testing Repeaters with Circulated Pulses
Distortion in Pulse-Duration Modulation
A Method of Virtual Displacements Applied to Pulse Transformers
Transadmittance and Input Conductance of Lighthouse Triodes
The Cyclophon
Video Storage by Secondary Emission from Simple Mosaics
Signal and Noise in Microwave Tetrodes
Motion of Electrons Subject to Transverse Forces
Oscillographic Presentation of Impedances
Parabolic-Antenna Design for Microwaves
Hybrid Circuits for Microwaves
Mathematical Theory of Directional Couplers
Corner-Bend Equivalent Circuits in Wave Guide
Microwave Filters Using Quarter-Wave Couplings
Broad-Band Noncontacting Short Circuits—Part III

Waves and Electrons Section

Postwar Educational Emphasis
Dynamic Performance of Peak-Limiting Amplifiers
Radio Doppler for Aircraft Speed Measurements
Force at the Stylus Tip in Lacquer Disk Recording
Coaxial-Cable Networks
Mutual Impedance Between Unequal-Height Antennas
Wide-Band 550-Mc. Amplifier
Special Magnetic Amplifiers for Computers
Dimensional Analysis of Electromagnetic Equations
Abstracts and References

TABLE OF CONTENTS FOLLOWS PAGE 32A

The Institute of Radio Engineers

the **LITTLE** differences make the **BIG** difference

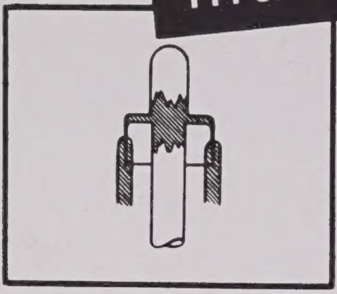

Pigs ain't pigs, we say. There are differences even within the litter. Sometimes they're visible, but often you can only tell the result of good breeding by checking the result.

It's the same with our Amperex 892. There is one of those little differences in the grid arm. It's much easier to assemble this by brazing a few parts together, but we know that a braze often offers resistance to the passage of current, sometimes enough resistance to make a big difference.

So we start this grid arm as a solid rod of oxygen-free copper and make it out of one piece, and it takes some mighty fine skill, Amperex skill, to turn that feather-edged seal from the solid. But that Amperex skill in manufacture, plus Amperex skill in design, produces a grid arm that offers the best operating conditions for both DC and RF . . . just another of the many little differences that make a big difference in the design and construction of the many, many types of tubes that comprise the extensive Amperex line.

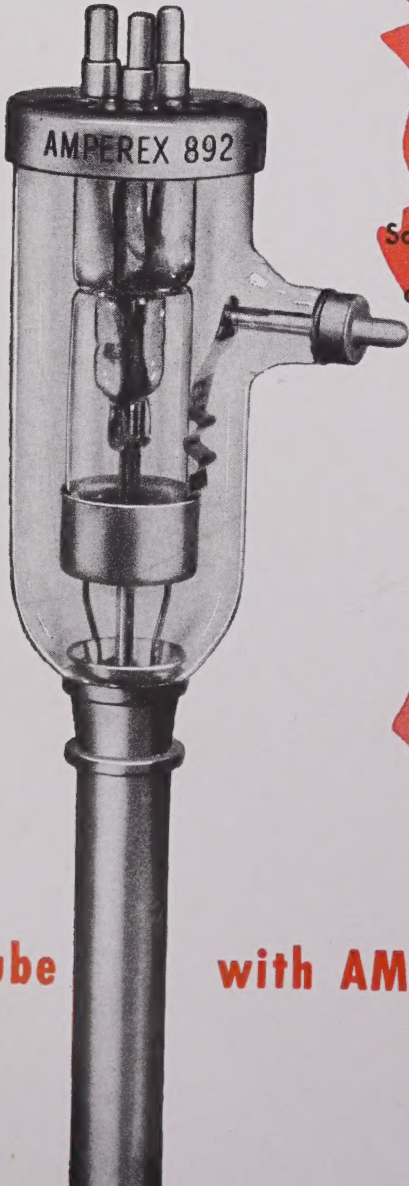

re-tube with AMPEREX

AMPEREX ELECTRONIC CORPORATION

25 WASHINGTON STREET, BROOKLYN 1, N. Y.
In Canada and Newfoundland: Rogers Majestic Limited
11-19 Brentcliffe Road, Leaside, Toronto, Ontario, Canada

BOARD OF DIRECTORS, 1947
Walter R. G. Baker
President
Noel Ashbridge
Vice-President
Raymond F. Guy
Treasurer
Haraden Pratt
Secretary
Alfred N. Goldsmith
Editor
William L. Everitt
Senior Past President
Frederick B. Llewellyn
Junior Past President
1945–1947
Stuart L. Bailey
Keith Henney
B. E. Shackelford
1946–1948
Virgil M. Graham
Donald B. Sinclair
1947–1949
Murray G. Crosby
Raymond A. Heising
1947
J. E. Brown
Frederick R. Lack
Jack R. Poppele
David Smith
William C. White
●
Harold R. Zeamans
General Counsel
●
George W. Bailey
Executive Secretary
Laurence G. Cumming
Technical Secretary
●
BOARD OF EDITORS
Alfred N. Goldsmith
Chairman
●
PAPERS REVIEW COMMITTEE
Murray G. Crosby
Chairman
●
PAPERS PROCUREMENT COMMITTEE
Dorman D. Israel
General Chairman
●

PROCEEDINGS OF THE I.R.E.

(Including the WAVES AND ELECTRONS Section)

Published Monthly by
The Institute of Radio Engineers, Inc.

VOLUME 35 *November, 1947* NUMBER 11

PROCEEDINGS OF THE I.R.E.

Raymond A. Heising, Board of Directors—1947 1179
What's in a Technical Name? .... Duane Roller 1180
2902. Microwave Converters .... C. F. Edwards 1181
2903. Fluctuation Noise in Pulse-Height Multiplex Radio Links .... L. L. Rauch 1192
2904. Propagation of Radio Waves in the Lower Troposphere .... J. B. Smyth and L. G. Trolese 1198
2905. The Determination of Ionospheric Electron Distribution .... Laurence A. Manning 1203
2906. Considerations in the Design of a Radar Intermediate-Frequency Amplifier .... Andrew L. Hopper and Stewart E. Miller 1208
2907. Detectability and Discriminability of Targets on a Remote Projection Plan-Position Indicator .... W. R. Garner and Ferdinand Hamburger 1220
2908. Testing Repeaters with Circulated Pulses ...... A C. Beck and D. H. Ring 1226
2909. Distortion in Pulse-Duration Modulation .... Ernest R. Kretzmer 1230
2910. A Method of Virtual Displacements for Electrical Systems with Applications to Pulse Transformers .. Prescott D. Crout 1236
2911. Transadmittance and Input Conductance of a Lighthouse Triode at 3000 Megacycles .. Norman T. Lavoo 1248
2912. The Cyclophon: A Multipurpose Electronic Commutator Tube ..... D. D. Grieg, J. J. Glauber, and S. Moskowitz 1251
2913. Video Storage by Secondary Emission From Simple Mosaics .... Robert A. McConnell 1258
2914. Space-Charge and Transit-Time Effects on Signal and Noise in Microwave Tetrodes ... L. C. Peterson 1264
2915. The Motion of Electrons Subject to Forces Transverse to a Uniform Magnetic Field .... Paul K. Weimer and Albert Rose 1273
2916. An Oscillographic Method of Presenting Impedances on the Reflection-Coefficient Plane .... A. L. Samuel 1279
2917. Parabolic-Antenna Design for Microwaves .... C. C. Cutler 1284
2918. Hybrid Circuits for Microwaves .... W. A. Tyrrell 1294
2919. A Mathematical Theory of Directional Couplers .... Henry J. Riblet 1307
2920. The Equivalent Circuit of a Corner Bend in a Rectangular Wave Guide .... John W. Miles 1313
2921. Microwave Filters Using Quarter-Wave Couplings .... R. M. Fano and A. W. Lawson 1318
2922. Broad-Band Noncontacting Short Circuits for Coaxial Lines. Part III.—Control of Parasitic Resonances in the S-Type Plunger ...... W. H. Huggins 1324

(Table of Contents continued on page 1178)

Copyright, 1947, by The Institute of Radio Engineers, Inc.

EDITORIAL DEPARTMENT
Alfred N. Goldsmith
Editor

Clinton B. DeSoto
Technical Editor

Mary L. Potter
Assistant Editor

William C. Copp
Advertising Manager

Lillian Petranek
Assistant Advertising Manager

Responsibility for the contents of papers published in the PROCEEDINGS OF THE I.R.E. rests upon the authors. Statements made in papers are not binding on the Institute or its members.

Changes of address (with advance notice of fifteen days) and communications regarding subscriptions and payments should be mailed to the Secretary of the Institute, at 450 Ahnaip St., Menasha, Wisconsin, or 1 East 79 Street, New York 21, N. Y. All rights of republication, including translation into foreign languages, are reserved by the Institute. Abstracts of papers, with mention of their source, may be printed. Requests for republication privileges should be addressed to The Institute of Radio Engineers.

MEMBER AUDIT BUREAU OF CIRCULATIONS

Board of Editors

Alfred N. Goldsmith,
Chairman

F. W. Albertson
J. S. Allen
G. M. K. Baker
W. L. Barrow
R. R. Batcher
A. E. Bowen
R. M. Bowie
Ralph Bown
R. S. Burnap
O. H. Caldwell
C. W. Carnahan
L. W. Chubb
L. M. Clement
J. D. Cobine
M. G. Crosby
R. B. Dome
W. G. Dow
E. W. Engstrom
W. L. Everitt
W. G. H. Finch
D. G. Fink
H. C. Forbes
I. A. Getting
G. W. Gilman
P. C. Goldmark
A. W. Graf
F. W. Grover
L. B. Headrick
E. W. Herold
J. A. Hutcheson
C. M. Jansky, Jr.
J. K. Johnson
L. F. Jones
H. S. Knowles
J. D. Kraus
J. B. H. Kuper
J. T. Lawson
D. G. Little
F. B. Llewellyn
S. S. Mackeown
Nathan Marchand
E. D. McArthur
Knox McIlwain
J. W. McRae
L. A. Meacham
G. F. Metcalf
E. L. Nelson
D. O. North
H. F. Olson
R. M. Page
H. O. Peterson
G. W. Pickard
Haraden Pratt
C. A. Priest
J. R. Ragazzini
Simon Ramo
H. J. Reich
J. D. Reid
F. X. Rettenmeyer
P. C. Sandretto
S. W. Seeley
V. W. Sherman
L. C. Smeby
C. E. Smith
J. A. Stratton
W. C. Tinus
K. S. Van Dyke
E. K. Van Tassel
E. C. Wente
H. A. Wheeler
J. R. Whinnery
W. C. White
L. E. Whittemore
G. W. Willard
William Wilson
I. G. Wolff
V. K. Zworykin

TABLE OF CONTENTS (Continued)

Contributors to the Proceedings of the I.R.E. . . 1328
Correspondence:
2923. "Quantitative Radar Measurements" . . . . Martin Katzin 1333
2807. "Ultra-Short-Wave Propagation Studies Beyond the Horizon" . . . . . . A. H. Waynick 1334
2804. "Scalar and Vector Potential Treatment" . . . . Paul I. Richards 1334
2796. "Selective Demodulation" . . . B. Starnecki 1335
2763. "Resonant Frequencies of *n*-Meshed Tuned Circuits" . . . . Lotfi A. Zadeh 1335
2662. "Nodal Method of Circuit Analysis" . . . . Albert Preisman 1335
2924. "Federal, Elwell, and Stone" . . . . Ellery W. Stone 1335

INSTITUTE NEWS AND RADIO NOTES
SECTION

Industrial Engineering Notes 1337
Books:
2925. "Klystron Tubes," by A. E. Harrison . . . . Reviewed by J. R. Whinnery 1339
2926. "Antennae: An Introduction to Their Theory," by J. Aharoni . . . . Reviewed by S. A. Schelkunoff 1339
2927. "Vector and Tensor Analysis," by Louis Brand . . . . Reviewed by Nathan Marcuvitz 1339
2928. "The Strange Story of the Quantum," by Banesh Hoffmann . . . . Reviewed by William H. Crew 1340
2929. "Electronic Engineering Patent Index, 1946," edited by Frank A. Petraglia . . . . Reviewed by Alois W. Graf 1340
Sections 1341
I.R.E. People 1342

WAVES AND ELECTRONS
SECTION

Murray Hill Labs., Bell Telephone Laboratories 1344
John E. Keto, Chairman, Dayton Section—May 1946–May 1947 1345
2930. Postwar Curriculum Emphasis . . . . Otto J. M. Smith 1346
2931. Dynamic Performance of Peak-Limiting Amplifiers . . . . Donald E. Maxwell 1349
2932. Radio Doppler Effect for Aircraft Speed Measurements . . . . Leonard R. Malling 1357
2933. Force at the Stylus Tip While Cutting Lacquer Disk-Recording Blanks . . . . H. E. Roys 1360
2934. Coaxial-Cable Networks . . Frank A. Cowan 1364
2935. Mutual Impedance Between Vertical Antennas of Unequal Heights . . C. Russell Cox 1367
2936. A Wide-Band 550-Megacycle Amplifier . . . . Raymond O. Petrich 1371
2937. Special Magnetic Amplifiers and Their Use in Computing Circuits . . . . H. S. Sack, R. T. Beyer, G. H. Miller, and J. W. Trischka 1375
2938. Dimensional Analysis of Electromagnetic Equations . . . . A. M. Winzemer 1383
Contributors to the Waves and Electrons Section 1384
2939. Abstracts and References 1387
News—New Products 30A
Section Meetings . . 35A
Membership 36A
Positions Open 50A
Positions Wanted . . 62A
Advertising Index . . 78A

Papers Procurement
Committee

Dorman D. Israel,
Chairman

E. D. Alcock
Andrew Alford
B. B. Bauer
R. M. Bowie
A. B. Bronwell
J. W. Butterworth
I. F. Byrnes
T. J. Carroll
Madison Cawein
K. A. Chittick
B. J. Chromy
J. T. Cimorelli
Harry Diamond
E. Dietze
G. V. Eltgroth
M. K. Goldstein
H. Grossman
R. C. Guthrie
D. E. Harnett
J. R. Harrison
J. V. L. Hogan
F. V. Hunt
T. A. Hunter
Hans Jaffe
J. J. Jakosky
Martin Katzin
C. E. Kilgour
A. V. Loughren
I. G. Maloff
H. B. Marvin
W. P. Mason
Pierre Mertz
B. J. Miller
I. E. Mouromtseff
A. F. Murray
J. R. Nelson
L. L. Nettleton
G. M. Nixon
D. E. Noble
T. M. Odarenko
H. F. Olson
W. E. Reichle
J. D. Reid
F. X. Rettenmeye
H. W. G. Salinger
Robert E. Shelby
W. P. Short
Daniel Silverman
P. L. Smith
J. Q. Stansfield
G. R. Town
L. G. Trolese
H. J. Tyzzer
K. S. Van Dyke
W. L. Webb
J. R. Whinnery
W. C. White
G. S. Wickizer
R. H. Williamson
R. J. Wise
C. J. Young

Papers Review
Committee

Murray G. Crosby,
Chairman

H. A. Affel
E. W. Allen
C. F. Baldwin
B. de F. Bayly
F. J. Bingley
H. S. Black
F. T. Bowditch
H. A. Chinn
J. K. Clapp
I. S. Coggeshall
S. B. Cohn
J. M. Constable
F. W. Cunningham
H. D. Doolittle
O. S. Duffendack
R. D. Duncan, Jr.
I. E. Fair
E. H. Felix
V. H. Fraenckel
R. L. Freeman
Stanford Goldman
W. M. Goodall
W. C. Hahn
G. L. Haller
O. B. Hanson
A. E. Harrison
J. R. Harrison
T. J. Henry
C. N. Hoyler
F. V. Hunt
Harley Iams
D. L. Jaffe
Hans Jaffe
W. R. Jones
D. C. Kalbfell
A. G. Kandoian
J. G. Kreer, Jr.
Emil Labin
V. D. Landon
H. C. Leuteritz
C. V. Litton
H. R. Lubcke
Louis Malter
W. P. Mason
R. E. Mathes
H. F. Mayer
H. R. Mimno
R. E. Moe
R. M. Morris
F. L. Mosely
I. E. Mouromtseff
G. G. Muller
A. F. Murray
J. R. Nelson
K. A. Norton
H. W. Parker
L. J. Peters
A. P. G. Peterson
W. H. Pickering
A. F. Pomeroy
S. O. Rice
T. H. Rogers
H. E. Roys
M. W. Scheldorf
Samuel Seely
Harner Selvidge
C. M. Slack
J. E. Smith
P. L. Smith
E. E. Spitzer
E. K. Stodola
H. P. Thomas
Bertram Trevor
Dayton Ulrey
A. P. Upton
G. L. Usselman
L. Vieth
S. N. Van Voorhies
R. M. Wilmotte
J. W. Wright
H. R. Zeamans

Raymond A. Heising

Board of Directors—1947

Raymond A. Heising was born in Albert Lea, Minn. on August 10, 1888. He received the degrees of E.E. from the University of North Dakota in 1912 and M.S. (in physics) from the University of Wisconsin in 1914. The University of North Dakota awarded him the D.Sc. degree in 1947 in recognition of his contributions to science and engineering.

Dr. Heising has been associated with the Western Electric Company and Bell Telephone Laboratories since 1914. For over thirty years he was a radio research engineer, and since 1945 has been patent engineer. His work in 1914 through 1917 on power amplifiers and modulation played a major part in the early development of radiotelephony in the Bell System and resulted in many firsts in this field.

After World War I, he participated in the research, development, and engineering for the pioneer transoceanic radiotelephone circuits, both long and short wave; and the services to liners and other ships. Under his supervision there has been carried out much research on ultra-short waves, electronics, and piezoelectric devices. His department made the major basic researches on low-temperature-coefficient quartz-crystal cuts, culminating in the production of millions of crystal plates for the Government in World War II.

Dr. Heising has made many important inventions, covered by more than 100 United States patents, the constant-current or Heising modulation system being one of his most noted. He has published numerous papers in the Proceedings of the I.R.E. and in other technical journals.

Joining The Institute of Radio Engineers in 1920, Dr. Heising was made a Fellow in 1923. He was President of the Institute in 1939; Treasurer, 1943 through 1945; and has been a member of the Board of Directors for seven years prior to serving as an officer. He has served on many committees of the Institute, and as chairman of those on Admissions, Sections, Constitution and Laws, and Office Quarters. He was awarded the Morris-Liebmann Memorial Prize in 1921.

People in general take for granted language and its use. Most persons are perilously unaware of the dangers lurking in vague terminology and ambiguous verbal usage. Occasionally these dangers are made sadly evident by international quarrels centering on differing interpretations of treaty language.

It is therefore particularly necessary that science and technology shall adopt and maintain a common and unequivocal vocabulary. This need, and related matters, are searchingly analyzed in the following guest editorial from one who is especially qualified to discuss such questions as the result of many years of experience as Editor of the *American Journal of Physics*, as Chairman of the Committee on Terminology of the American Association of Physics Teachers, and as Professor of Physics at Wabash College.—*The Editor.*

What's in a Technical Name?

DUANE ROLLER

With a few scientists it is still the fashion to affect disdain for language. As they would say, it is only *things* that are important, not *words*. In an earlier day this attitude could have meant a healthy reaction to prescientific aversions for *facts*. Yet, even the first scientists were not mere fact-collectors. They sought relations between facts and tried to explain these relations, usually in terms of abstractions having no direct referents in Nature; and relations cannot be found or explained, let alone communicated, without using language of some kind.

The symbology and framework of the language which we use for communication are in truth the very tools with which we *think*. Moreover, the peculiar way in which scientists have managed to fashion and use these tools has come to be one of two main ways in which scientific behavior is distinguished from the nonscientific. The other distinguishing characteristic is, of course, systematic observation.

The experienced engineer or other scientist is most likely to be conscious of the role of language in his thinking when he faces new problems that are very fundamental or complicated, or when he is engaged in technical work, old or new, of an industrial or commercial character. As many readers of the PROCEEDINGS are in a position to know, intelligible and unambiguous language is essential in framing commercial specifications, contracts, and descriptions of patents. Doubtless this is one reason why scientists in industries usually are sympathetic toward proposals for improving technical language and often are active in promoting language reforms.

Also especially sensitive to language difficulties are those relatively few scientists who work on the very frontiers of physical knowledge—for instance, physicists working on theory in the submicroscopic domain. Here ordinary technical language may prove to be inadequate or even to hamper thought. Such language is after all an ethnic language that has been so modified and subjected to restrictions as to make it more useful for scientific purposes. Since it originated in prescientific thinking carried out solely on the macroscopic level, there should be no surprise if it turns out to be inadequate for a domain completely outside previous human experience. Fortunately, such a breakdown of language would affect only a few scientists, at least for a long time to come.

For practically all purposes, our current technical language is so effective as to make us confident that in no field of knowledge other than physical science is it *possible* to record and transmit ideas and meanings with so much exactness and clarity. So efficient a mode of communication must not be allowed to deteriorate and is worth improving in any way possible.

Clearly it is the workers in each specialized branch of a science who can best assess their own language needs and who should assume first responsibility for reforms. Yet no one is likely to contend that such reforms should be carried out independently of similar studies in all other branches. Any tendency toward the development of independent nomenclatures in physics, on the one hand, and, say, communications and electronics engineering, on the other, is sure to retard the integration and consequent simplification of knowledge that are essential if each of these fields is in the long run to progress most rapidly.

Various committees on terminology probably can co-operate most successfully when all employ a similar approach to the problem. Certainly they will all agree that each concept must be carefully defined before any attempt is made to select the best name for it. Also essential is a list of all existing synonyms for each concept. Finally, before selecting the single best term, there must be agreement as to what principles of selection are to be used.

An ideal technical term is one that meets five requirements: *nonambiguity*, *meaningfulness*, *internationality*, *simplicity*, and *euphony*. By examining many existing terms in the light of these general requirements, any committee can formulate a number of specific rules that will simplify materially its task of selecting terms and constructing a technical glossary. When such a glossary has been made, it is not enough that it be accepted by those directly concerned. The terms in it should be compared with those in overlapping fields and reconciled with them until a single list of definitions and terms results. Then all scientists will in a measure be able to speak one another's language.

Microwave Converters*

C. F. EDWARDS†, ASSOCIATE, I.R.E.

Summary—**Microwave converters using point-contact silicon rectifiers as the nonlinear element are discussed, with particular emphasis on the design of the networks connecting the rectifier to the input and output terminals. Several converters which have been developed during recent years for use at wavelengths between 1 and 30 centimeters are described, and some of the effects of the impedance-versus-frequency characteristics of the networks on the converter performance are discussed.**

INTRODUCTION

THE TECHNIQUE by which a high-frequency signal may be converted to a lower intermediate frequency to obtain greater ease of amplification and frequency selection is an old and extremely important part of the radio-receiving-system design art, and the methods used to accomplish this at signal frequencies from the lowest up to a few hundred megacycles are well known. In the development during recent years of radar and radio systems operating in the microwave range, where frequencies are measured in thousands of megacycles, this technique has been used to great advantage. Although the fundamental principles employed have not changed, converters operating in the microwave range bear little physical resemblance to those used in the past. The purpose of this paper is to discuss some of the fundamental problems associated with the design and testing of microwave converters and to describe in some detail several converters for use in radar and communication systems which have been developed during the past few years.

The process by which frequency conversion is accomplished rests fundamentally on the use of some device whose impedance varies in a nonlinear way with the applied voltage, and may be regarded somewhat crudely as one in which the wave shape of the applied voltage is distorted in a useful way by the nonlinear element. When two sinusoidal voltages of frequencies f_1 and f_2 are applied to such a device, this distortion gives rise to new frequencies given by $nf_1 \pm mf_2$ where n and m are integers, zero included. In a receiving converter the applied frequencies are those of the signal and beating oscillator, and the difference frequency $f_1 - f_2$ generated in the nonlinear impedance is then selected as the output or intermediate frequency. If the beating-oscillator voltage is large compared to that of the signal, the conversion may be made linear and the output voltage will be linearly proportional to the input voltage.

It is interesting to note that, in selecting a nonlinear element suitable for use in the microwave range, it has been found expedient to resort to a device which was in use in the very early days of radio; namely, the crystal detector. The extremely high frequencies encountered preclude the use of ordinary vacuum tubes due to the losses arising from electron-transit-time effects. In crystal detectors the electrode spacing is of the order of atomic dimensions and the electron-transit time is thus reduced to a negligible value, and by the use of a very small contact point the electrode capacity may be kept sufficiently small to prevent serious loss.

The crystal detectors in use thirty years ago were somewhat erratic in their operation. However, as a result of an intensive development program, growing out of a need for such devices in microwave converters, detectors using silicon as the nonlinear material have been developed to the point where they rank with vacuum tubes in uniformity and reliability. In view of the fact that the crystalline state of the silicon is more nearly like that of iron and copper, which are not ordinarily regarded as crystals, than it is like such crystals as quartz, it seems desirable to eliminate the terms "crystal" and "crystal detector" and designate these devices by the term "point-contact rectifier."

DESIGN CONSIDERATIONS

It is beyond the scope of this paper to give a detailed mathematical analysis of the general converter problem, since this has been extensively covered by other investigators.[1,2] For the same reason any consideration of the problems associated with the design of point-contact rectifiers will be omitted.[3] Within these limits, then, the problem of converter design becomes one of devising suitable networks to connect the nonlinear device to the beating oscillator and the input and output terminals of the converter. A converter is defined as a device having two input and two output terminals and containing within its structure a nonlinear impedance, a beating oscillator, and appropriate connecting networks, which is capable of delivering an output that is linearly proportional to the input in amplitude but differs from it in frequency. The term "mixer" has been frequently applied to such a device, but when the beating oscillator is included as an indispensable component the device may properly be termed a converter.

A basic converter circuit with the nonlinear impedance and the three networks connected in series is shown in Fig. 1. We are concerned here with the design of the three networks and the influence of design variations on the converter performance. What may be termed the

---

* Decimal classification: R361.124×R310. Original manuscript received by the Institute, August 30, 1946; revised manuscript received, November 15, 1946. Presented, 1946 I.R.E. Winter Technical Meeting, New York, N. Y., January 25, 1946.

† Bell Telephone Laboratories, Inc., Holmdel, N. J.

[1] L. C. Peterson and F. B. Llewellyn, "The performance and measurement of mixers in terms of linear network theory," PROC. I.R.E., vol. 33, pp. 458–476; July, 1945.

[2] E. W. Herold, R. R. Bush, and W. R. Ferris, "Conversion loss of diode mixers having image-frequency impedance," PROC. I.R.E., vol. 33, pp. 603–609; September, 1945.

[3] J. H. Scaff and R. S. Ohl, "Development of silicon crystal rectifiers for microwave radar receivers," *Bell Sys. Tech. Jour.*, vol. 26, pp. 1–30; January, 1947.

basic requirements for these networks are readily arrived at by assuming that there are currents in the nonlinear impedance at the input, output, and beating-oscillator frequencies only. In order to obtain the maximum efficiency, each of these currents obviously must be absorbed in the appropriate network only, and not dissipated uselessly in the other networks. The resistance required at the interior terminals of each network at its associated frequency is determined by the rectifier characteristic and the magnitude of the current due to the beating oscillator. There is, however, an interaction between the input and output network impedances, which becomes greater the lower the conversion loss, and this complicates the design procedure in that it requires that the two impedances be optimized simultaneously. Thus, with the components connected in series as shown, the input network must transform the input impedance to the required value and introduce no resistance into the circuit at the output frequency. Similarly, the output network must provide the desired impedance transformation at the output frequency and introduce no resistance at the input frequency. The third network need not match the beating oscillator to the rectifier since in most cases a considerable excess of beating-oscillator power is available; for the same reason the impedance of the input and output networks at the beating-oscillator frequency is not especially important. However, it is important that the beating-oscillator network introduce no resistance into the circuit at the input and output frequencies. The components may, of course, be connected in parallel, in which case the network conductances would be required to be zero.

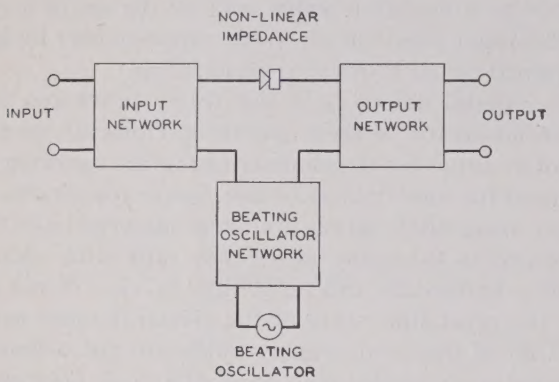

Fig. 1—Converter consisting of a nonlinear impedance, a beating oscillator, and connecting networks.

Such a simple consideration of the problem is obviously inadequate since there are currents in the nonlinear impedance at other frequencies given by $nf_1 \pm mf_2$, some of which derive an appreciable part of their power from the input and output frequencies, and these also cannot be dissipated without adding to the conversion loss. In addition, it has been found that the reactances at some of these frequencies influence the impedances required at the input and output frequencies, so that rather complex interaction effects are introduced. Here, again, the extent of the interaction is dependent on the conversion loss.

From the foregoing it is seen that the converter design problem could become rather formidable should it become necessary to insure that the networks are nondissipative and have the correct reactance at a large number of frequencies. This is especially true in the microwave range where distributed circuit constants are the rule rather than the exception, and it is difficult to construct a simple network having the desired impedance at one frequency and zero impedance, for example, at all higher frequencies. However, the present state of the art is such that a minimum conversion loss of the order of 6 decibels is generally obtained, which is associated with the point-contact rectifier and is, of course, undesirable from a system-performance standpoint. But from the standpoint of network design this loss is helpful, in that it reduces the interaction effects mentioned above to the point where the number of frequencies at which impedance adjustments need to be made are relatively few.

When the ratio of f_1 to f_2 is near unity, as is generally the case in microwave converters, the frequencies given by $nf_1 \pm mf_2$ tend to group themselves about the signal and beating-oscillator frequencies and their harmonics and differ from them by only a few per cent. Thus, selective networks are required if the impedance at one frequency is to be different from that at another frequency in the same group. If selective networks are not employed the impedance will be nearly the same at all frequencies in a group, but, since the groups are substantially in harmonic relation, the impedance for one group will in general be different from that of another.

The experience gained to date indicates that, in addition to the input and output frequencies, it is necessary to consider the impedances at the interior terminals of the networks at the image frequency $(2f_{osc} - f_{sig})$ and at the group of frequencies in the vicinity of the signal and beating-oscillator second harmonic. The frequency of importance in this group has not been identified, but for design purpose a precise knowledge of which frequency one needs to consider is not necessary since they all lie within a narrow band. Only very small effects have been found due to impedance variations at frequencies near the beating-oscillator third harmonic, and no attempts to optimize the impedance in this frequency range have been made.

The performance characteristics of a converter which are of major importance are, generally speaking, the same as those of any four-terminal network and are measured in the same way, taking into account the fact that the input and output frequencies are different. These include the impedance match between the signal source and the input terminals, the match between the output terminals and the load, the conversion loss, the usable frequency bandwidth, and the noise figure.

The input impedance of converters operating in the microwave range is readily measured in terms of the impedance of the input transmission line by means of a standing-wave detector. This is a convenient starting point in the design procedure since the input impedance is almost entirely a function of the rectifier used and the beating-oscillator drive. By turning off the beating oscillator and applying power at the input frequency through the input network, sufficient to give the same value of rectified current as that given by the beating oscillator, the input network may be adjusted so that the rectifier impedance is matched to that of the input line. For commercial rectifiers the rectified beating-oscillator current is usually between 0.7 and 1.5 milliamperes. When the beating oscillator is applied in the normal way it is found that the impedance match to a low-level signal is quite good, and furthermore, because of the conversion loss, this match is not greatly affected by variations in the output network impedance at the output frequency.

The output impedance of the converter may be determined in either of two ways. One method makes use of an output network whose impedance transformation is variable and which may be adjusted to give the maximum output power into the load, under which condition the output network is matched to the converter output impedance. Such a transformer may be made up of a one-eighth wavelength low-impedance transmission line shorted at one end and tuned to antiresonance by means of a variable capacitor at the other. The high-impedance end then forms the internal terminals of the output network and a low-impedance load may then be connected to a sliding tap on the line and the tap position varied to give a wide range of impedance transformations. In the second method the direction of transmission through the converter is reversed and the same technique employed as in the case of the input network. The standing-wave detector in this case may be a quarter-wavelength transmission line with three taps at which the voltage across the line may be measured, and from these measurements the converter output impedance in terms of the line impedance may be determined.

Since the input and output frequencies of a converter are different, conversion-loss measurements based on the ratio of the output to the input power involve power measurements at two frequencies. Methods for measuring power in the microwave range using thermistors have been developed to the point where they present no particular difficulty, and these methods may also be used to measure the output power. The frequency bandwidth may, of course, be measured on a relative basis, and merely involves determining the variation in output as the input frequency is varied and the amplitude kept constant.

The effect of the converter on the over-all noise of the receiving system in which it is used is a matter of especial concern, since, in the absence of suitable amplifiers for use at microwave frequencies, the converter must be located at the point in the system where the signal level is lowest and where the signal-to-noise ratio is most susceptible to deterioration. The manner in which the converter influences the over-all noise figure F of the receiving system is given in the relation

$$F = F_a + L(F_b - 1) \tag{1}$$

where F_a is the converter noise figure, L is the conversion loss, and F_b is the noise figure of the intermediate-frequency amplifier. The noise figure of a network may be defined as the ratio of the apparent noise power at the signal-generator terminals to the available thermal noise power at that point.[4] Each of the terms in (1) is the ratio of two powers, and, while it is generally more convenient to measure these terms in decibels, such measurements must be converted to pure-number ratios for use in the above and subsequent equations.

The noise figure F of the receiving system may be measured directly without regard to its components, L, F_a, and F_b. However, a direct determination of F is somewhat difficult in that it involves a precise evaluation of the large attenuation which must be used between the signal generator and the converter when this measurement is made. An easier method of determining F rests on a measurement of the ratio of the noise-power outputs of the receiver when the converter is active and passive; this ratio is called the Y factor. This measurement is comparatively easy to make, since the passive condition is readily attained by substituting an impedance across the intermediate-frequency-amplifier input terminals equal to the converter output impedance. L and F_b may be measured separately, and the over-all noise figure is then given by

$$F = LYF_b. \tag{2}$$

All the terms in (1) represent fundamental properties of the converter and amplifier. It should be noted, however, that the Y factor is a property of the combination only, and is used to facilitate the measurement of F. The term which specifies the noise in the converter alone is the noise ratio N_r, given by the relation

$$N_r = \frac{F_a}{L}. \tag{3}$$

This term, sometimes referred to as the equivalent noise temperature, is the ratio of the available noise power at the converter output terminals to the available noise power in a resistor at room temperature.

EARLY CONVERTERS

With the foregoing design considerations in mind, we may now turn to the converter problem itself and consider the actual means by which the design objectives are attained. This is perhaps most readily done by describing various converters and showing the changes made as ideas about their design developed. In the early stages only the basic requirements mentioned above were incorporated in the design, and it was not until after a considerable background of experience had been obtained that steps could be taken to optimize the network impedances at frequencies different from the input and output frequencies.

---

[4] H. T. Friis, "Noise figures of radio receivers," PROC. I.R.E., vol. 32, pp. 419–422; July, 1944. By this definition the apparent noise power would be N/G as shown in his equation 5, p. 420. In (1) above $L=1/G$.

The first requirement in the construction of a converter is, of course, a nonlinear device of some kind. It was in 1937 that work was begun on the development of point-contact rectifiers of improved stability and reliability for use in converters operating in the centimeter wavelength range. Fig. 2 shows one of these rectifiers. It employs a sharply pointed contact spring bearing on a highly polished silicon surface. This unit was very rugged and could withstand severe mechanical shock without changing its electrical characteristic. Provision was made for adjusting the contact when necessary, but this feature was found to be of limited value since repeated adjustment tended to flatten the contact point and impair the efficiency. This unit is of interest mainly in that it represents a stage in the development of the cartridge-type rectifiers in widespread use today.

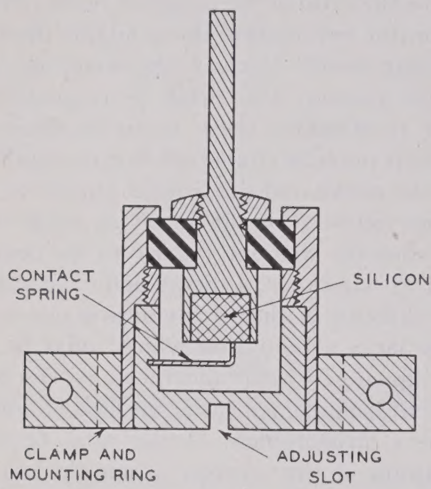

Fig. 2—Early type of semipermanent silicon point-contact rectifier.

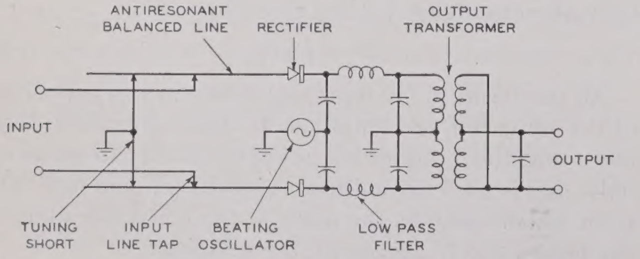

Fig. 3—Balanced converter using silicon rectifiers, operating at a wavelength of 30 centimeters.

Early in 1938 two of these rectifiers were used in a 30-centimeter balanced converter, the circuit of which is shown in Fig. 3. The input network consists of a balanced transmission line tuned to 1000 megacycles by means of an adjustable short circuit, with provision for matching this to the balanced line from the antenna. The beating oscillator is connected between the two rectifiers and ground, and the output is connected to a 65-megacycle amplifier by means of a balanced-to-unbalanced transformer. The low-pass filters are of the simplest form and serve to present the required low impedance to the input frequency, while the input network, by virtue of its design, presents a low impedance to the output frequency. One of the advantages of balanced converters is that the beating oscillator is isolated from the input network by the balance which accomplishes the function of the beating-oscillator network (shown in Fig. 1) in an efficient manner. This converter was made primarily for use in transmission studies, and few measurements were made of its performance. The only data available indicate that the conversion loss was about the same as that of a converter using a similar circuit and special small diodes instead of point-contact rectifiers.

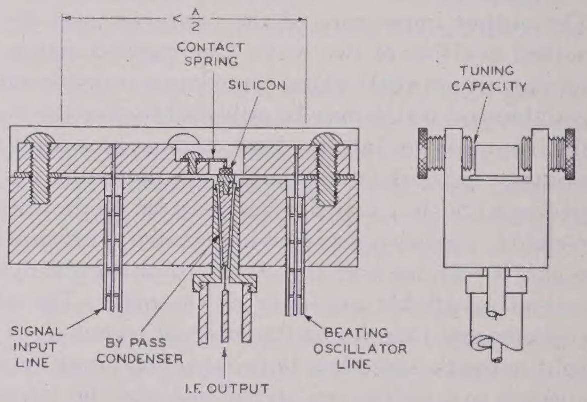

Fig. 4—Converter with integral silicon rectifier tunable over the 9-to-11-centimeter wavelength range.

A converter operating in the 10-centimeter range which was in use in 1940 is shown in Fig. 4. The input network here consists of a "tape" transmission line formed by the rectangular bar located in a channel in the main block. This line is a little less than a half-wavelength long, and is shorted at both ends. By means of the tuning screws capacitance may be added across the central portion of the line which brings it into resonance at the desired frequency. The tuning range is from about 9 to 11 centimeters. The input line is a small coaxial connected to the resonant line at such a distance from the end as to provide the required impedance transformation. The beating-oscillator line is also a small coaxial, and this is connected as near to the shorted end of the resonant line as is consistent with the available beating-oscillator power. In this way a large mismatch loss is interposed between the beating oscillator and the remainder of the circuit which minimizes the loss of signal power into the beating oscillator. The resonant line is of very heavy construction and is used to support the point contact of the silicon rectifier, and the silicon wafer is soldered to a small stud which is screwed into the coaxial capacitor. This capacitor acts as a by-pass for the input frequencies and as a tuning capacitance for the output transformer, which is not shown. The sleeve carrying the by-pass capacitor and the silicon wafer is held in place by set screws which are locked after the proper contact between the silicon and the spring has been made. This converter, using a rectifier selected for the best performance, had a conversion loss of 8 decibels.

CONVERTERS USING STANDARD POINT-CONTACT RECTIFIERS

With the development of the cartridge-type point-contact rectifier, it was necessary to approach the problem of converter design with the viewpoint of accommodating a pre-established set of mechanical and electrical characteristics. With regard to the latter, the problem of converter design was simplified to the extent that by means of factory adjustment and selection a degree of uniformity in the electrical characteristics could be obtained which assured that any unit could be used in a converter designed about a rectifier of average characteristics. A cross section of a Western Electric Company cartridge-type rectifier of the 1N series is shown in Fig. 5. This unit is quite rugged, mechanically, but is easily damaged by minute static discharges, and considerable care must be exercised to protect it from such discharges as might occur between an operator's body and ground during handling, or as might arise when a soldering-iron tip is applied, to any electrical circuit connected to it. If properly protected, however, it will maintain its electrical characteristics unchanged over a period of many months.

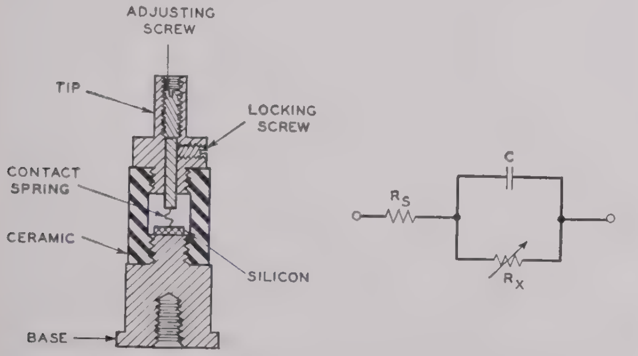

Fig. 5—Cross section of the 1N-series silicon rectifier and an equivalent circuit for the rectifying contact.

The equivalent circuit of this rectifier, of course, contains reactive elements connecting the base and tip to the point of rectification. These, however, are unimportant from a loss standpoint, since they may be tuned out by other external reactances. The equivalent circuit shown in Fig. 5 applies only to the rectifying point contact. R_s represents the resistance of the body of the silicon wafer, C the capacitance between the point contact and the silicon surface, and R_x the nonlinear resistance at this point contact. This equivalent circuit is of present interest only to the extent that it enables us to recognize that the terminals of the nonlinear resistance R_x are not available, that the resistance R_s and the capacitance C are present in such a way as to add to the circuit loss, and that this loss increases with frequency. R_s and C thus tend to increase the loss for the components in the harmonic-frequency range, and the necessity for designing the networks to present the proper impedances at these frequencies is dependent to some extent upon how near the signal frequency is to the maximum operating frequency of the rectifier.

The first rectifier, of the type shown in Fig. 5, to be standardized and manufactured in large quantities was the 1N21, which was designed to operate in the 10-centimeter wavelength range. A coaxial-type converter designed to accommodate this unit is shown in Fig. 6. This converter is tunable over the 9- to 11-centimeter wavelength range. The main tuning element consists of a coaxial line, approximately three-quarters of a wavelength long, which may be adjusted to resonance at the input frequency. The rectifier is located at the high-impedance end, and the other end is shorted at the input frequency by a by-pass capacitor. The input line is coupled to this resonant line by an adjustable capacitance, and by means of these two adjustments the correct impedance transformation may be obtained. The by-pass capacitor, in conjunction with an intermediate-frequency transformer (not shown), constitute the output network. The beating oscillator is weakly loss-coupled to the input line to provide a large reflection, as in the converter shown in Fig. 4.

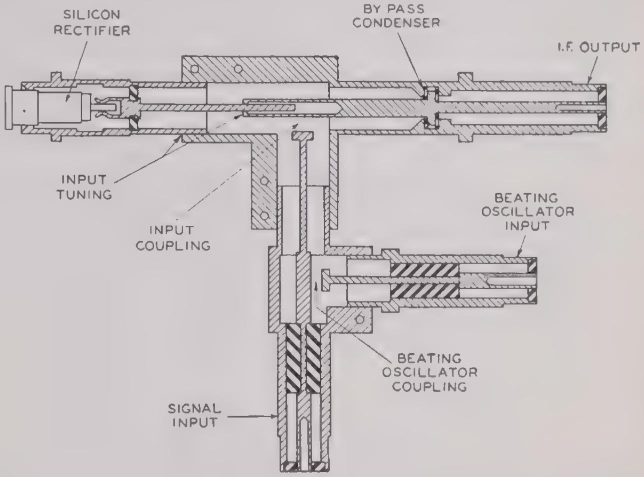

Fig. 6—Converter using a 1N21 silicon rectifier mounted in a coaxial line and tunable over the 9-to-11-centimeter wavelength range.

The first observations of the effect of variations in the impedance of the input network at the higher-order frequencies were made using a converter of this type. The resonant line connected to the rectifier has an impedance irregularity near its center which is necessary for mechanical reasons in order to have the line length adjustable. It was found that this irregularity was affecting the conversion loss, and that, by varying the length of the larger-diameter portion of the inner conductor, variations in conversion loss of over 1 decibel could be caused. The effect of these changes on the input-network impedance transformation was nullified by always adjusting the input and coupling for minimum loss. This effect of the input-network impedance on the conversion loss was also investigated by means of a coaxial tuner coupled to the resonant line after the manner of the input line at a point 1.25 centimeters from the shorted end of the resonant line. At resonance, this tuner absorbed power and caused the conversion loss to increase about 1.5 decibels, and from its behavior it was determined that the frequency at which the power was absorbed was near the second harmonic of the signal and beating oscillator. Effects were also observed near the third harmonic, but these were quite small.

The converter shown in Fig. 7 is one designed for operation at wavelengths in the 3-centimeter range, and employs a 1N23 point-contact rectifier connected across $\frac{1}{2}$-×1-inch wave guide. It is largely fortuitous that the physical design of the 1N23 makes it adaptable to this type of connection to the wave guide. The 1N23 rectifier is similar to the 1N21 but has had improvements made in the silicon and the point contact which reduce its conversion loss at 3 centimeters. The proper impedance transformation between the wave guide and the rectifier is obtained by displacing the rectifier from the center of the wave guide an amount sufficient to cause the conductance component of the rectifier admittance to match the guide, and by adjusting the location of the piston until the susceptance component is reduced to zero. This matching procedure was carried out using a rectifier of average characteristics. When other rectifiers of nonaverage characteristics are used the admittance is found to vary to the extent that input standing-wave ratios up to 8 decibels are obtained. The normalized conductance presented to the guide varies between 0.7 and 1.5, while the normalized susceptance lies between −0.9 and 1.1. The susceptance may be reduced to zero by adjusting the piston so that the mismatch may be reduced to a standing-wave ratio of less than 3.5 decibels, corresponding to a reflected power loss of less than 0.2 decibel.

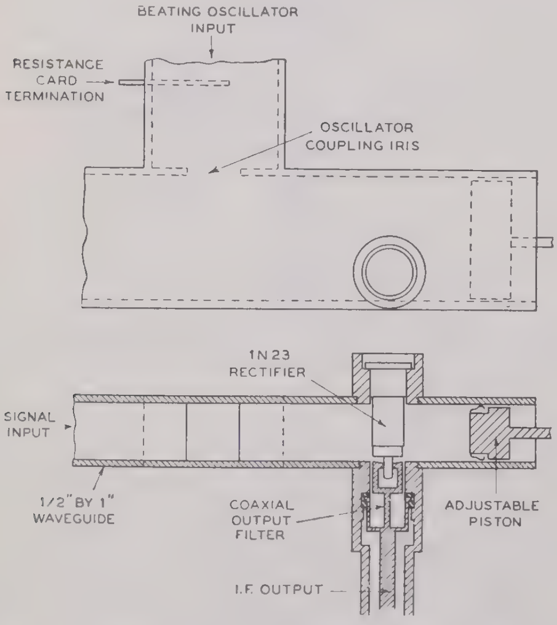

Fig. 7—Converter using a 1N23 silicon rectifier mounted in $\frac{1}{2}$×1-inch wave guide.

This converter was designed to operate over a wide range of input frequencies without adjusting the input tuning. The variation in input standing-wave ratio is such that a rectifier which has been adjusted to match the wave guide at a wavelength of 3.33 centimeters will have a standing-wave ratio of about 6 decibels at wavelengths of 3.13 and 3.53 centimeters, corresponding to a reflected power loss of 0.5 decibel. A frequency-selective network if required may be employed at the input, and the converter will provide a satisfactory load impedance over the 3.13- to 3.53-centimeter range.

The beating oscillator may be coupled to the rectifier in a number of ways. In the method shown in Fig. 7 it is coupled to the wave guide by means of an iris in the side wall. A termination for the beating oscillator is provided by the resistance card located about one-quarter wavelength in front of the coupling iris, and in this way the condition wherein the beating oscillator works into a highly reactive load is avoided. In some applications the iris has been made adjustable so that the beating-oscillator level may be readily controlled. When this method of beating-oscillator coupling is used in the absence of a frequency-selective network at the input, it is possible to lose some of the signal power in the beating-oscillator wave-guide branch, particularly if the available beating-oscillator power is low. When an input frequency-selective network is used, however, it may be so located with respect to the iris as to effectively double the beating-oscillator voltage at the rectifier. The size of the coupling iris may then be decreased to restore the beating-oscillator drive to its original value and the loss of signal power in this branch considerably reduced.

Special precautions have been taken in this converter to provide a low impedance across the output network at the input frequency. This low impedance is obtained by means of a coaxial line one-half wavelength long which is shorted at one end, and the impedance is kept low over a range of frequencies by making the characteristic impedance of the open quarter wavelength of line much lower than that of the shorted quarter wavelength. This structure is supported at its high-impedance point, as shown in Fig. 7, by insulating rings which form a by-pass capacitor and prevent the loss of signal power in the output network more effectively than a capacitor alone.

The effect of variations in the impedance of the input network at frequencies near the signal and beating-oscillator second harmonic was investigated in this converter by means of the arrangement shown in Fig. 8. Here the piston has been replaced by an adjustable metal septum extending across the guide and dividing it into two smaller guides. These smaller guides are beyond cutoff at wavelengths near 3.33 centimeters, so that this septum acts as a piston at these wavelengths. At wavelengths near 1.67 centimeters, however, they are not beyond cutoff, so that by means of two other septa located as shown an independent piston effective only at frequencies near the second harmonic is obtained. By varying the position of this harmonic piston the conversion-loss-variation curve shown in Fig. 9 was obtained. The variation shown amounts to 0.6 decibel, which is about half that obtained with the converter shown in Fig. 6. This variation, however, differed greatly with the particular rectifier used. Several 1N23 rectifiers showed no variation, while nearly all of a special group designed for operation at 1.25 centimeters showed some variation, the greatest being 1 decibel.

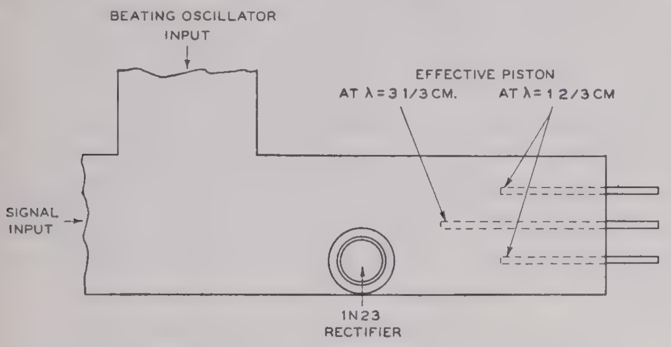

Fig. 8—Wave-guide piston arrangement for measuring the effect of harmonics.

The average spacing between the maxima and minima of the curve in Fig. 9 is 1.25 centimeters. The beating-oscillator wavelength was 3.33 centimeters, and the calculated wavelength of the beating-oscillator second harmonic in the two guides formed by the central septum is 2.54 centimeters. A half wavelength is thus 1.27 centimeters, which is quite close to the value obtained from the curve, and shows that the frequency involved in the conversion-loss variation lies near the beating-oscillator second harmonic. This method of measurement is not sufficiently precise to permit any closer identification of the frequency involved. As an additional test the secondary septa were removed and resistance cards used which absorbed the harmonic frequencies. When this was done the conversion loss assumed a value indicated by the dotted line in Fig. 9. The tuning arrangement shown in Fig. 8 was not used in the final converter design since the decrease in conversion loss was so small as to be hardly worth the added complication.

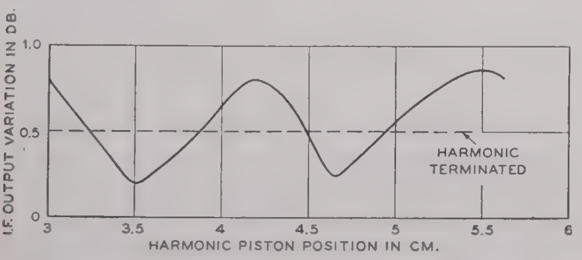

Fig. 9—Variation in conversion loss with harmonic piston position.

The converter shown in Fig. 7 is readily adaptable for use with a wave-guide hybrid junction to form a balanced converter. This is shown in Fig. 10. The hybrid junction (also widely known as a "magic tee"), shown at the right of the figure, performs as a network having four pairs of terminals and an internal structure such that power fed into any one pair will appear equally at two other pairs but not at the third pair. Referring to the figure, it will be seen that power fed into the input branch will appear equally in the output branches but will be balanced out of the beating-oscillator branch. Similarly, power fed into the beating-oscillator branch appears equally in the load branches but is balanced out of the input branch. The purpose of the input matching rod is to provide an impedance match between the input and the load branches, and the beating-oscillator matching rod is an inductance so located as to match that branch to the load branches. When the load branches are terminated in their characteristic impedance, the standing-wave ratio at the input branch is less than 1 decibel, and that at the beating-oscillator branch is less than 3 decibels at all wavelengths between 3.13 and 3.53 centimeters. Since a mismatch at the beating-oscillator input is less important than a mismatch at the signal input, the choice of functions for the various branches has been selected as shown in the figure.

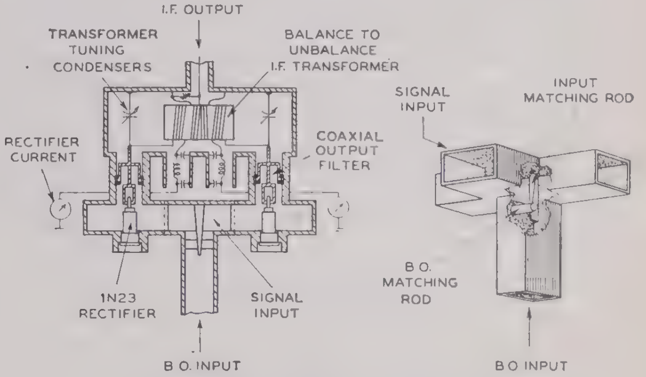

Fig. 10—Balanced 3-centimeter converter using a wave-guide hybrid junction.

The converter in Fig. 7, having been designed to match the wave-guide impedance, may thus be connected to the load branches of the hybrid junction and, with the addition of a balanced-to-unbalanced output transformer, a balanced converter obtained. Since the hybrid junction itself introduces only a small mismatch, the balanced converter will terminate the input line nearly as well as the converter in Fig. 7. A balanced converter has several advantages over an unbalanced converter which arise from the conjugate relationship which can be obtained between the signal and beating-oscillator terminals. The circuit of a converter using a hybrid junction is essentially the same as the converter shown in Fig. 3. The degree of balance that can be obtained depends on the similarity of the two rectifiers, and by selecting pairs it is not difficult to obtain a balance such that the loss between the input and beating-oscillator terminals is in excess of 25 decibels. The loss of signal power into the beating oscillator is thus effectively prevented, and similarly the beating-oscillator power level at the input terminals is considerably reduced. Since no mismatch loss between the signal and beating-oscillator terminals is required, the rectifiers will absorb the full applied beating-oscillator power, so that considerably less available power is required.

Another advantage obtained by the use of a balanced converter is the protection against beating-oscillator noise. In applications where the signal frequency is extremely high and the intermediate frequency low enough to be a very small fraction of this frequency, the beating oscillator may have noise sidebands in the signal-frequency range. An analysis of the phase relations shows that, when the signal and beating oscillator are applied to the same terminals, as would be the case for an oscillator with noise sidebands, the output from the two rectifiers will be balanced out by the output transformer.

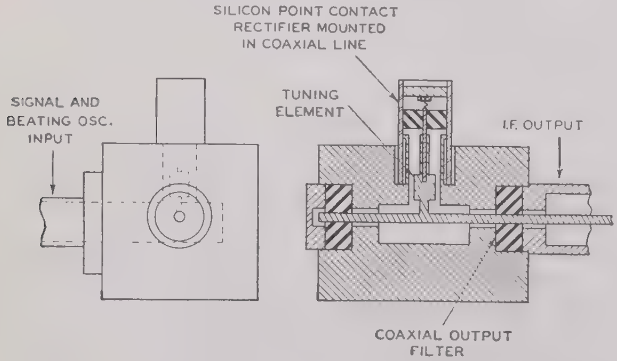
SILICON POINT CONTACT RECTIFIER MOUNTED IN COAXIAL LINE
SIGNAL AND BEATING OSC. INPUT
TUNING ELEMENT
I.F. OUTPUT
COAXIAL OUTPUT FILTER

Fig. 11—1.25-centimeter converter using a silicon rectifier mounted in a coaxial line.

The rectifier mounting shown in Fig. 5 is not well adapted for use at wavelengths below 3 centimeters, due to its size. For operation at a wavelength of 1.25 centimeters a new type of mounting has been developed and the necessary improvements made in the silicon and the point contact. In this mounting the rectifier is located at the end of a coaxial line. An early form is shown in Fig. 11, together with the matching circuits to form a 1.25-centimeter converter. Since the rectifier is in coaxial and the signal in wave guide, a coaxial-to-wave-guide circuit is required which will also provide a means for connecting the rectifier to the intermediate-frequency output. The coaxial-to-wave-guide circuit shown in Fig. 11 is a supported probe which matches the guide to a 65-ohm coaxial line over a 10 per cent frequency band. Its electrical characteristics are practically identical to those of an open probe, since the supporting member is in a neutral position with respect to the waves in the guide and its length from the side wall of the guide to the probe is approximately one-quarter wavelength. This supporting rod is shorted to the side walls of the guide at the input frequencies by the coaxial filters, which also allow the intermediate frequency to be taken out.

The coaxial-to-wave-guide circuit matches the guide to a 65-ohm coaxial line, but, since the rectifier does not match this impedance, a transformer formed by an enlargement of the coaxial inner conductor is required. The proper transformation is obtained by adjusting the length, diameter, and position of this element. The bandwidth of this transformer, however, is considerably less than that of the coaxial-to-wave-guide circuit, with the result that the converter matches the line over about a 4 per cent frequency band. The beating-oscillator input is not shown in Fig. 11, but could, of course, be accomplished in the same manner as shown in Figs. 7 or 10.

Wide-Band Converter

All of the converters described so far were designed for use in applications where the input impedance was required to match the line from the antenna only sufficiently well to avoid undue reflection loss, where the use of an input-frequency-selecting network was optional, and where only moderately uniform response over a comparatively narrow band of frequencies was required. As a consequence, these converters are not especially satisfactory for use in modern wide-band communication systems. The final converter to be described was designed to meet all the requirements of wide-band applications, and in order to do this it has been found necessary to control the impedance of the input network at the signal frequency, the image frequency, and some frequency near the signal and beating-oscillator second harmonic, and also to take account of the interaction effects that exist between the input and output networks.

The additional specifications set down for this converter before the design work was started were that it was to have an input standing-wave ratio of less than 1 decibel, an input filter to select a band of frequencies anywhere within the 6.9- to 7.5-centimeter wavelength range, and have a transmission band 15 megacycles wide flat to less than 0.1 decibel. The completed converter (shown in Fig. 16) is similar to the one shown in Fig. 10 in that it makes use of a wave-guide hybrid junction, but differs from it in that the rectifiers are mounted at the end of coaxial lines which are coupled to the wave guide by means of probes. The impedance transformation necessary to make the rectifier terminate the line was obtained by adjusting the length and diameter of the cavity in which the rectifier is mounted. With this method of matching, the maximum standing-wave ratio for a group of twenty rectifiers measured over the 6.9- to 7.5-centimeter wavelength range was found to be about 4 decibels.

The output filter is in the form of a quarter-wave stub connected across the coaxial line, followed by a trap. The trap consists of a quarter wavelength of coaxial line followed by a cylindrical polystyrene-filled resonant cavity in the form of a disk transmission line[5] shorted at its outer edge, and is arranged so that the short circuit at the outer edge of the cavity is transferred to the gap at the open end of the quarter-wave stub. The loss through this filter is in excess of 25 decibels throughout the 6.9- to 7.5-centimeter wavelength range, and thus the loss of signal power through it is negligible.

In Fig. 12 is shown an unbalanced converter using these components, which was used to investigate the effect of input-network impedance variations and the interaction effects between the input and output networks. It has an input filter consisting of two inductive irises with a capacitive tuning plug between them, and the beating oscillator is connected in the same manner as that shown in Fig. 7. The remaining equipment consists of an intermediate-frequency amplifier and output meter and a transformer to match the converter output impedance to the amplifier. This transformer is of the variable-impedance-transformation type mentioned earlier, and with it the 76-ohm input impedance to the amplifier may be transformed to any value between 80 and 600 ohms. C_2 is large enough to be an effective short circuit, and C_1 is used to tune the line to antiresonance. Thus both the resistive and reactive components of the converter output impedance may be matched.

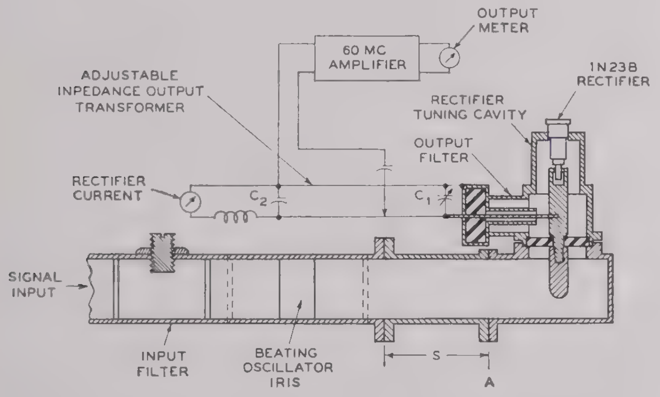

Fig. 12—7.2-centimeter converter arranged for investigating the effect of the input-filter position on the output impedance and conversion loss.

The procedure for the tests, using the equipment shown in Fig. 12, was simply to apply a constant signal at the input and measure the output power and the output impedance as a function of the length S of an added section of wave guide. The reflection coefficient of the filter at the signal frequency was very small, so that the signal power and the signal-frequency impedance at A is independent of the added line length S. However, at frequencies different from the signal frequency the reflection coefficient of the filter is large, and variations in S will cause its phase angle to change in accordance with length of S. Hence, any change in the conversion loss or output impedance as a result of variations in S must be due to changes in the impedance of the input network at frequencies different from the input frequency.

Curves showing the variations in conversion loss and output impedance as a function of the line length S are shown in Fig. 13. At the top is shown the variation in conversion loss in decibels. Below that is the variation in shunt reactance as measured by the dial reading of the capacitor C_1 required to tune the output transformer. At the bottom is the shunt-resistance variation as indicated by the position of the output-transformer tap required to give a maximum output. These are plotted against the value of S in inches. Two things are immediately apparent from these curves. First, the top curve shows that the conversion loss is influenced primarily by the input-network impedance at some frequency much higher than the input frequency. Second, the bottom curve shows that the output impedance is influenced primarily by the input-network impedance at some frequency near the input frequency. Further interpretation of these curves is complicated by the fact that some of the frequencies involved are sufficiently high to excite more than one mode in both the coaxial and the wave guide, and these modes could be expected to produce rather complicated effects.

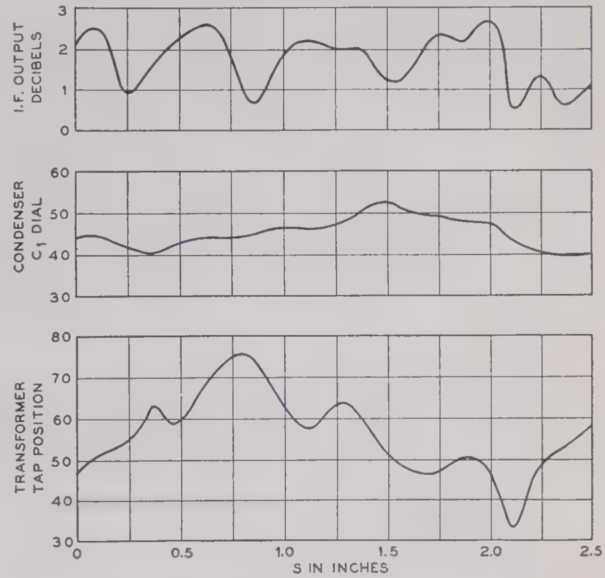

Fig. 13—Variation in output impedance and conversion loss with input filter position.

From the rate at which the conversion loss varies as S is changed, it is evident that the length of line between the rectifier and the filter is sufficient to restrict the frequency range over which a uniform conversion loss can be obtained. In order to eliminate this effect the frequencies involved in the conversion-loss variation must be reflected from a point much nearer the rectifier. This reflection was accomplished by means of a low-pass filter located in the coaxial line near the rectifier, as is shown in Fig. 14.

---

[5] S. A. Schelkunoff, "Electromagnetic Waves," D. Van Nostrand Co., New York, N. Y., 1943; pp. 260–272.

From the results obtained with the converter shown in Fig. 8, it is apparent that the frequencies responsible for the conversion-loss variation shown in Fig. 13 are those in the vicinity of the signal and beating-oscillator second harmonic. For input wavelengths between 6.9 and 7.5 centimeters, these lie in the range between 3.4 and 3.8 centimeters. The filter shown in Fig. 14 was designed to have a large reflection coefficient in this latter wavelength range. It consists of a polystyrene-filled resonant cavity which is the inverse of the cavity used in the output filter, being in the form of a disk transmission line shorted at its inner edge, and forms an antiresonant circuit in series with the coaxial line. This is represented by the inductance L and the capacitance C_b in the equivalent circuit. The diameter required to form the disks is greater than that of the coaxial inner conductor, so that the two disks form capacitances in shunt with the coaxial line represented by the capacitors C_a. In order that the filter match the coaxial line at wavelengths between 6.9 and 7.5 centimeters, the inductance L must have the correct value, and this is accomplished by adjusting the thickness of the polystyrene disk which controls the characteristic impedance of the disk line.

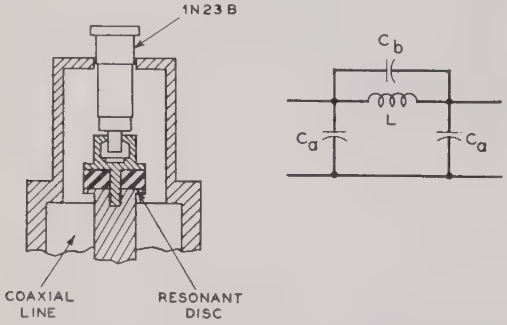

Fig. 14—Coaxial low-pass filter used to stabilize the impedance at higher frequencies, and its equivalent circuit.

Measurements of the standing-wave ratio introduced by this filter were made. At wavelengths between 3.4 and 3.8 centimeters it was above 30 decibels, and between 6.9 and 7.5 centimeters it was below 0.5 decibel. With this filter installed in the converter shown in Fig. 12, the effect of the input-filter position was measured again. The results are shown in Fig. 15. The effect of the coaxial filter is quite pronounced, and it is seen that with it the conversion loss is very nearly independent of S, and uniform operation over a wide frequency band should be readily feasible. The output impedance curve is sufficiently uniform to permit a measurement of the change in S required to vary the resistance through a complete cycle. In Fig. 15 this distance is 2.30 inches, corresponding to a guide wavelength of 4.60 inches or a frequency of 4060 megacycles. This is quite close to 4040 megacycles, which is the calculated image frequency.

An important consideration, but one which has not yet been investigated, is the effect of the position of the low-pass filter on the conversion loss. Presumably, from the curve in Figs. 13 and 15, this alone could cause a change of about 1.5 decibels. However, measurements of the minimum conversion loss obtainable with and without the low-pass filter indicated that the amount to be gained by selecting a better position would be less than 0.5 decibel.

Harmonic filters have been incorporated in the completed converter shown in Fig. 16, with the result that an input filter may now be used without causing variations in conversion loss over the transmission band. In order that the converter output impedance have the correct value to match the intermediate-frequency transformers, the filter position S must be properly chosen. The converter output impedance at the terminals A was measured as a function of the filter position S, using the second method mentioned earlier which makes use of a three-tap transmission line. Curves very much like those in Fig. 15 were obtained, the capacitance varying between 1.6 and 5.5 micromicrofarads, and the resistance varying between 350 and 940 ohms. The position giving the highest impedance was found to give a somewhat lower conversion loss, so that the intermediate-frequency transformers were designed to match this higher value. Two transformers were actually used, each having an impedance-transformation ratio of 470 to 152 ohms, with the primary windings connected in series to give the 940-ohm impedance and the secondaries, one of which has the direction of its winding reversed, connected in parallel to give an output impedance of 76 ohms.

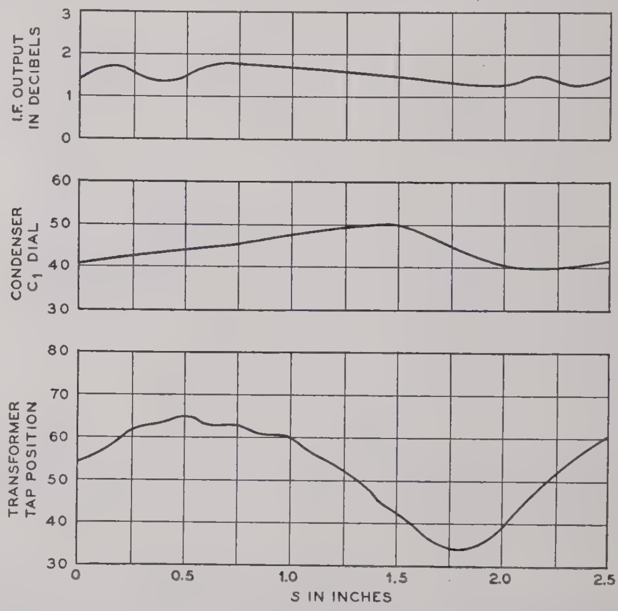

Fig. 15—Variation in output impedance and conversion loss with input-filter position after the addition of the low-pass coaxial filter.

The input tuner shown is necessary to reduce the input standing-wave ratio to less than 1 decibel as required in the original specifications, since without it the standing-wave ratio may be as much as 4 decibels, as stated above. Rather stringent requirements are placed on this tuner by virtue of the fact that ideally it should match the converter to the wave guide at the input frequency and at the same time introduce no phase shift in the wave reflected from the filter at the image frequency, since this is equivalent to a change in the filter position. Furthermore, the tuner must be between the filter and the converter in order that the filter work between the proper impedances. The tuner of the type shown approximates this ideal much better than a conventional two-plug tuner. It consists essentially of two parallel-tuned circuits spaced one-eighth wavelength, the inductances being formed by the rods across the wave guide and the capacitances by the adjustable plugs. A value of inductance has been selected such that the tuner will correct a standing-wave ratio of not more than 4 decibels of any phase. The variation in the susceptance of the tuner over the input frequency band is negligible, while at the image frequency the phase change introduced is much less than that of a two-plug tuner. By locating the tuner effectively one-half wavelength from the filter at the image frequency (dimension D), the phase change may be reduced to a negligible value.

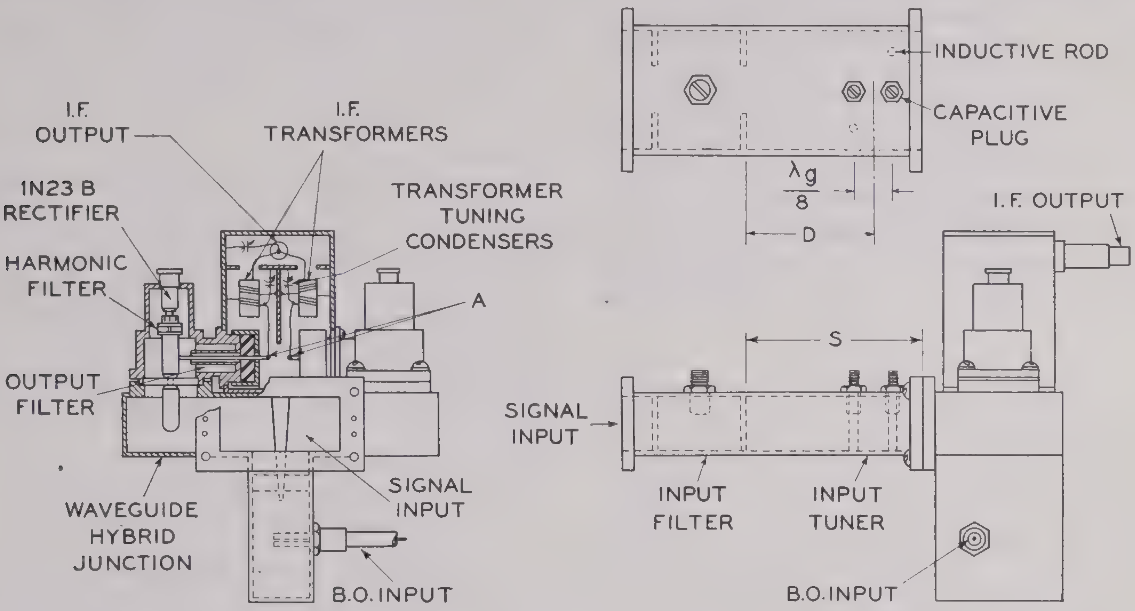

Fig. 16—Wide-band balanced converter using a wave-guide hybrid junction with input filter and matching circuit.

TABLE I

Conversion Loss (decibels)	F_a (decibels)	F (decibels)	Noise Ratio
5.1	9.1	13.1	2.5
5.6	10.1	13.8	2.8
6.4	10.4	14.3	2.5

The final measurements made on this converter were the conversion loss, noise figure, noise ratio, and bandwidth. Three pairs of a group of twelve 1N23B rectifiers were selected as representative of the best, the average, and the poorest, from the standpoint of conversion loss. For the noise-figure measurements an intermediate-frequency amplifier having a noise figure of 6.7 decibels was used. The results are shown in Table I. These results, with the exception of the noise ratio, are all expressed in decibels and were determined by the methods described earlier, using the relations given in (1) to (3). The transmission band was measured by varying the frequency of the signal oscillator and measuring the power in a 76-ohm load resistor. Using intermediate-frequency transformers having a coupling coefficient of 0.5, transmission variations of less than 0.1 decibel were observed over a band 20 megacycles wide.

CONCLUSIONS

The purpose of this paper has been to discuss the problem of the design and construction of microwave converters using point-contact rectifiers as the nonlinear element, with the main emphasis on the networks used between the input and output terminals and the rectifier. The approach has been largely practical, since a complete and rigorous mathematical analysis of the problem is generally so complex as to provide the designer with little more than a broad outline of the requirements. The results obtained indicate that, when uniform conversion efficiency over a wide band of frequencies is required, close attention must be paid to the network-impedance versus frequency characteristics.

ACKNOWLEDGMENTS

The writer wishes to acknowledge the material contributed by co-workers of the Holmdel laboratory who have been intensively engaged in the development of microwave converters for the past several years, and who supplied much of the material presented here. He is particularly indebted to A. B. Crawford and W. M. Sharpless, who provided all the material on the 3-, 10-, and 30-centimeter converters, and to G. E. Mueller, who provided the material on the 1.25-centimeter converter.

Fluctuation Noise in Pulse-Height Multiplex Radio Links*

LAWRENCE L. RAUCH†

Summary—**The choice of a method of multiplex synthesis and analysis will depend on (1) the distortion and noise characteristics of the link connecting the synthesizer and analyzer, and (2) the type of intelligence and tolerable distortion and noise in each channel. Among the various methods of multiplexing adaptable to transmission over radio links is the pulse-height or commutation method. The question of interchannel cross talk has already been solved quantatatively for this multiplex method, and it is the purpose of this paper to solve the associated problem of channel fluctuation noise in a precise manner. Expressions are obtained for the channel fluctuation noise of pulse-height multiplex systems used over f.m. and a.m. radio links. A comparison shows the f.m. channel fluctuation-noise improvement to be 4.15 times the deviation ratio, in contrast to the familiar $\sqrt{3}$ times the deviation ratio for single-channel radio links.**

INTRODUCTION

IT IS GENERALLY recognized that time-division multiplex methods are best for transmission over radio links, particularly when the number of channels to be multiplexed is large, due to the relatively wide bandwidth and large nonlinear distortion offered by radio links. Subcarrier multiplex methods are better adapted for transmission over wire links, where it is easier to obtain the small nonlinear distortion necessary to avoid interchannel cross talk.

The wide bandwidths required by pulse-position multiplex methods make them well adapted to u.h.f. and microwave radio links. Where reduced bandwidths are necessary, such as in the v.h.f. range, the pulse-height multiplex method provides a solution which, at the same time, maintains the general advantages of time-division multiplexing. Various commutator tubes and circuits have been developed to provide pulse-height synthesis and analysis.[1–8]

The method of synthesis consists of taking short samples of several items of intelligence (usually appearing as voltages) in a regular time sequence at a uniform rate. If it is desired to sample a given item at a rate of F times per second and there are n items, a single sample can be no longer than $1/Fn$ second. The principle of analysis for a given item of intelligence consists of observing the synthesized signal during an interval of $1/Fn$ second or less at a rate of F times per second, in such a manner that only the original samples, or portions of them, are obtained. The analyzed samples may be integrated into a "smooth" signal by methods discussed later. It will be shown later that, if the maximum frequency of components appearing in an item of intelligence is less than f, the original intelligence may be perfectly reproduced if a repetition rate of $F=2f$ or greater is used.

The principal type of noise encountered in the output of a v.h.f. radio receiver is fluctuation noise. Pulse noise is either man-made and near by, or else the result of a near-by electrical storm. The analysis of this paper is for fluctuation noise only and, unless modified, the term "noise" will be understood to mean fluctuation noise. Before proceeding, however, we shall review certain characteristics of the multiplex method.

CHARACTERISTICS OF DISTORTION IN RADIO LINKS AND DISTORTION AND CROSS TALK IN INDIVIDUAL CHANNELS

The distortion characteristics (noise included) of a radio link will produce quite different effects in the output of the channels of a pulse-height system. Here we shall treat these effects in a descriptive manner.

A little thought will show that the transient response of the radio link completely determines the cross-talk characteristics. A good transient response will be insured by a uniform amplitude versus frequency characteristic and a fairly proportional phase-shift versus frequency characteristic. By good transient response in a radio link we mean that, after the constant time delay is taken into account, there is very little correlation between the instantaneous signal at time t and the discrepancy between the output and input signals at time $t+\Delta t$, as long as Δt is larger than a certain minimum value determined in part by the upper limit of the frequency response. In other words, a disturbance at time t shall not be unduly prolonged (not to be confused with delay) by transmission through the radio link. The signal in each channel of a commutator system may be considered as a disturbance which should not be prolonged into the next channel as cross talk. If the channels were exactly adjacent almost no prolongation could be tolerated, and a very wide and uniform amplitude versus frequency response and proportional phase characteristic would be required of the link. This difficulty is overcome by inserting "blanking" spaces between adjacent channels so that a certain amount of prolongation can occur without carrying into the next channel. This is the meaning of α in (2).

If the frequency response falls off at the high end, the cross talk in the following channel will be in phase;

---

* Decimal classification: R460×R361.211. Original manuscript received by the Institute, March 29, 1945; revised manuscript received, November 29, 1945, and March 7, 1947.

† Palmer Physical Laboratory, Princeton, N. J.

[1] A. M. Skellett, "The magnetically focused radial beam vacuum tube," *Bell. Sys. Tech. Jour.*, vol. 23, pp. 190–202; April, 1944. And also the subsequent development of the electrostatically focused and rotated radial-beam vacuum tube.

[2] D. D. Grieg, J. J. Glauber, and S. Moskowitz, "The Cyclophon: a multipurpose electronic commutator tube," PROC. I.R.E., this issue, page 1251–1258.

[3] L. L. Rauch, "Electronic commutation for telemetering," *Electronics*, vol. 20, pp. 114–120; February, 1947.

while if the frequency response rises, the cross talk will be out of phase. In fact, it is a fairly simple matter to adjust the frequency response by one or two variables, manually or automatically, to obtain a null in the following-channel cross talk. All channels are equally and simultaneously corrected and the correction can be made at one location to take into account any changes in frequency-response characteristics of terminal equipment or repeaters distributed along the radio link. In practice, it is not difficult to obtain sufficiently good frequency response in the radio link to reduce cross talk between adjacent commutator channels 50 to 60 db below maximum signal.[4]

It is clear that the nonlinear characteristic of the radio link has no connection with cross talk. The nonlinear characteristic of the link is transferred exactly to each channel where it introduces the usual "harmonic" distortion in the signal of the channel. A relatively large percentage of this type of distortion can be tolerated in telephone speech channels and, therefore, in the radio link itself. An excessively large signal applied to one channel will result in a distorted signal in that channel due to the finite extent of the linearity of the radio link, but there will be no disturbances in the remaining channels. If it is desired to prevent overmodulaiton of the radio link, any method of limiting applied to the synthesized signal will produce the same results as applying it to the individual channels before synthesis.

In this section, the nonlinear characteristic and frequency-response characteristics of radio links have been treated as unrelated phenomena. This is by no means always the case. It is easy to think of circuits providing isolated examples of each characteristic, such as a series resistance and shunted high-vacuum diode for the nonlinear case, and a series resistance and shunted capacitance for the frequency-response case. But in all types of radio links, the nonlinear distortion usually increases at the high end of the modulation-frequency range when a constant degree of modulation is maintained.

In amplitude-modulated links the nonlinear distortion at low modulation frequencies is due entirely to tube characteristics in the modulator, modulated-radio-frequency amplifier stages, and detector. As the modulation frequency is increased, the percentage of modulation in the initial stages must be increased to compensate for attenuation of side bands by the reduced load impedance of the tuned circuits in the modulated-radio-frequency amplifiers. This results in operating the tubes into the more nonlinear parts of their characteristics. A similar phenomenon occurs at higher frequencies in audio amplifiers and wide-band amplifiers. The various types of distortion can be reduced[5] to very low levels by application of large amounts of inverse feedback, but such large amounts of inverse feedback increase the size and cost of small radio links considerably.

Frequency-modulated radio links have a reputation for low distortion. This is, in part, because the tube characteristics of the modulated-amplifier stages are eliminated as a source of distortion; all of the troubles are concentrated in the modulator and detector stages. This statement is true for frequency-modulated radio links of large deviation ratio, but the fact is sometimes overlooked that, for small deviation ratios not much greater than unity, the frequency-dependent phase shift in the tuned circuits in the modulated-radio-frequency amplifier stages can introduce large amounts of nonlinear distortion at high-modulation frequencies. To keep distortion at a low level in this circumstance, the tuned circuits must be very carefully designed. This is pointed out because the tendency in multiplex systems is often to use a greater modulation band without increasing the frequency deviation, which results in a reduced deviation ratio.

CHARACTERISTICS OF FLUCTUATION NOISE

Fluctuation noise, or smooth hiss, as it is sometimes called, has a constant amplitude versus frequency spectrum over the range of the r.f. pass band of a radio receiver, but the phase distribution is random. However, the amplitude of the noise-frequency spectrum over the modulation-frequency pass band of a radio-receiver output varies with frequency in a manner which depends on the type of modulation used, although the phase distribution remains random. This results in two important characteristics of the final noise output. For any type of noise with a continuous spectrum, the power in a frequency band of small width $\Delta\omega$ is proportional to $\Delta\omega$. Thus the r.m.s. noise voltage is proportional to $\sqrt{\Delta\omega}$. Due to the random phase distribution of fluctuation noise, the crest voltage (height of the larger peaks)[6,7] is proportional to the r.m.s. voltage, and therefore to $\sqrt{\Delta\omega}$. (This is not true in the case of pulse noise, where the height of the pulse is proportional to $\Delta\omega$.) It follows that, if the noise components over several narrow frequency bands $\Delta_1\omega$ at ω_1, $\Delta_2\omega$ at ω_2, $\cdots$, $\Delta_n\omega$ at ω_n in the modulation pass band are selected by filters and added, the resultant r.m.s. noise voltage will be

$$\sqrt{A^2(\omega_1)\Delta_1\omega + A^2(\omega_2)\Delta_2\omega + \cdots + A^2(\omega_n)\Delta_n\omega} \quad (1)$$

---

[4] W. R. Bennett, "Time division multiplex systems," *Bell. Sys. Tech. Jour.*, vol. 20, pp. 199–221; April, 1941. This paper is fundamental and will repay careful reading. Wire links instead of radio links are considered, and so emphasis is placed upon conditions requiring minimum bandwidth of the link.

[5] Charles R. Burrows and Alfred Decino, "Ultra-short-wave multiplex," PROC. I.R.E., vol. 33, pp. 84–94; February, 1945.

[6] V. D. Landon, "A study of the characteristics of noise," PROC. I.R.E., vol. 24, pp. 1514–1521; November, 1936.

[7] V. D. Landon, "The distribution of amplitude with time in fluctuation noise," PROC. I.R.E., vol. 29, pp. 50–55; February, 1941. For a rigorous definition of crest-noise voltage, some distribution function must be assumed for the instantaneous noise voltage. Many writers, for good reason, assume the normal law as a basis for theoretical investigations. This law offers a finite probability for arbitrarily high noise voltages, but in practice nonlinear circuit elements bring the probability distribution function to unity for finite values of the instantaneous noise voltage. For example, if we assume the crest voltage is attained when the instantaneous voltage is greater than or equal to four times the r.m.s. value, the normal law provides the result that during a sufficiently long period the crest value will be reached a fraction of the time equal to 63×10^{-6}. More can be said if the amplitude versus frequency distribution of the noise is taken into account.

where $A(\omega)$ is the r.m.s. value of the noise voltage in a unit frequency interval at angular frequency ω.

The above relation concerning fluctuation noise is the only one of which explicit use is made in the analysis of the pulse-height system.

In the case of amplitude modulation, $A(\omega)$ is a constant over the modulation pass band. In the case of frequency modulation with deviation ratio greater than unity, $A(\omega)$ is not constant. Analysis shows $A(\omega)$ to be proportional to ω over the modulation pass band of a frequency-modulation receiver (the familiar triangular spectrum). In this and all further discussions involving f.m. receivers, we asume the signal strength remains above the improvement threshold.

In Part I, following, we shall assume a certain f.m. radio link with sufficiently large maximum frequency deviation to provide a deviation ratio greater than unity for all modulating signals discussed. A signal of r.m.s. value S will be produced at the receiver output by a sinusoidal signal modulating the link to maximum frequency deviation. There is a r.m.s. fluctuation-noise voltage of $A(f)=k_1 f$ per unit bandwidth at cyclic frequency f at the receiver output. The value of S/k_1 will be determined by the maximum frequency deviation and by the r.f. signal-to-noise ratio at the discriminator and is easily calculated for any case. We then connect an n-channel pulse-height synthesizer to the transmitter input and an n-channel analyzer to the receiver output, and calculate the maximum signal-to-noise ratio R_{fm} for a particular channel. In Part II the same procedure is followed for an a.m. radio link with a r.m.s. fluctuation-noise voltage of k_2 per unit bandwidth at the receiver output.

In the rest of the paper, the term "noise" is understood to mean r.m.s. fluctuation-noise voltage, and the term "signal" is understood to mean the maximum signal r.m.s. voltage.

PART I—FREQUENCY-MODULATION LINKS

An n-channel commutator synthesizer and analyzer are connected to the f.m. radio link. The analyzer samples each channel with an individual repetition rate of F times per second, each channel being on during a fraction $1/\alpha$ of its alloted interval $1/nF$. The intervals of duration $(\alpha-1)/\alpha nF$ between channels are for blanking. Each channel at the receiver is connected by the analyzer to the radio-link output for an interval of duration $1/\alpha nF$ coinciding with the "on" interval of the respective channel at the synthesizer. In other words, each receiving channel "looks" at the output of the radio link for $1/\alpha nF$ second every $1/F$ second. This causes very definite changes in the radio-link noise and in the original signal, when viewed at the output of a receiving channel. This is determined by the following analysis.

The output of the commutator analyzer for some channel will be $s(t)\cdot c(t)$ where $s(t)$ is the signal on the channel and $c(t)$ is the commutation function:

$$c(t) = 1, \quad \frac{j}{F} - \frac{1}{2\alpha nF} \leq t \leq \frac{j}{F} + \frac{1}{2\alpha nF} \qquad (j = -\infty, \cdots, \infty)$$

$$c(t) = 0, \text{ elsewhere.}$$

A Fourier series representation of $c(t)$ is valid[8] and is

$$c(t) = \frac{1}{\alpha n} + \frac{2}{\pi}\sum_{m=1}^{\infty}\left(\frac{1}{m}\sin\frac{m\pi}{\alpha n}\right)\cos 2\pi mFt.$$

Assume a single-component signal $s(t)=a \cos 2\pi ft$. Then

$$\begin{aligned} s(t)\cdot c(t) &= \frac{a}{\alpha n}\cos 2\pi ft \\ &\quad + \frac{a}{\pi}\sum_{m=1}^{\infty}\left(\frac{1}{m}\sin\frac{m\pi}{\alpha n}\right)[\cos 2\pi(mF+f)t \\ &\quad + \cos 2\pi(mF-f)t]. \end{aligned} \tag{2}$$

The output of each commutator channel passes through a low-pass filter whose pass band has a width

$$f_{\max} < \frac{F}{2} \tag{3}$$

where $f_{\max}$ is the maximum channel signal-frequency component. Observation will show that the right member of (2) represents the signal fundamental plus its a.m. side bands around suppressed carriers at harmonics of the sampling frequency F. In this case we have chosen to recover the signal from its fundamental, but it is a simple matter to add the suppressed carriers by adding a d.c. component to the signal, and then recover the original signal by selecting and demodulating any one of the resulting a.m. signals at harmonics of F. If this is done, the signal-to-noise ratio will in general depend on the harmonic of F used, and in no case is it appreciably better than for the choice of the fundamental. Moreover, the filter problem becomes more difficult. If the transmitted signal has no components above $f_{\max}$, the low-pass filter for the fundamental case is required to go from pass to reject in the interval from $f_{\max}$ to $F-f_{\max}$ in order to avoid the lower side band at $F-f_{\max}$ of the suppressed carrier at F. In case the p^{th} harmonic is selected, the band-pass filter must go from pass to reject in the intervals from $pF-f_{\max}$ to $(p-1)F+f_{\max}$, and from $pF+f_{\max}$ to $(p+1)F-f_{\max}$. Thus, the filter requirements become more exacting. We note that insufficiently sharp filters cannot cause cross talk but only distortion in the individual channels.

If $s(t)=a \cos 2\pi ft$ is viewed as a single component of the radio-link noise, it is apparent from the expansion for $s(t)\cdot c(t)$ in (2) that only the noise in the frequency intervals $mF \pm f_{\max}$ $(m=0, 1, \cdots, r$ depending on the required limit $F_c=rF$ of the radio-link-modulation pass band) will appear in the channel after passing through the low-pass filter. The r.m.s. fluctuation-noise voltage in the frequency interval $mF\pm f_{\max}$ is $k_1 mF\sqrt{2f_{\max}}$ approximately[9] and the noise in any channel due to the noise in this frequency interval is, by (2),

---

[8] G. H. Hardy and W. W. Rogosinski, "Fourier Series," Cambridge Tracts in Mathematics and Mathematical Physics, no. 38, theorem 57, p. 42.

$$\frac{k_1 F}{\pi}\sqrt{2f_{\max}}\sin\frac{m\pi}{\alpha n}\cdot$$

Then by (1), the noise voltage in any channel due to that in all of the intervals $m=1,\cdots,r$ (r being the number of side-band pairs in (2) transmitted by the link) is

$$\frac{k_1 F\sqrt{2f_{\max}}}{\pi}\sqrt{\sum_{m=1}^{r}\sin^2\frac{m\pi}{\alpha n}}\cdot \tag{4}$$

If $s(t)$ is now viewed as a component of a channel signal, it is seen that the maximum channel signal before commutation is S. The first term in the right member of (2) shows that each component of the signal is reduced by a factor of $1/\alpha n$. Therefore, the signal is reduced by the same factor and at the output of the receiving-channel low-pass filter this signal value is

$$\frac{S}{\alpha n}\cdot \tag{5}$$

This, together with (4), determines a signal-to-noise ratio of

$$R_{fm}=\frac{S}{k_1}\cdot\frac{\pi}{\alpha nF\sqrt{2f_{\max}}\sqrt{\sum_{m=1}^{r}\sin^2\frac{m\pi}{\alpha n}}}\cdot \tag{6}$$

When r is large, the evaluation of the sum under the radical becomes laborious. In Appendix 1 it is shown that, when $\alpha n\geqq 20$ and $r/\alpha n\geqq 1$ ($F_c/\alpha nf\geqq 1$), the radical of the sum is approximated by $\sqrt{r/2}$ with an error less than 10 per cent. This provides an approximation R_{fm}^* for R_{fm},

$$R_{fm}^*=\frac{S}{k_1}\cdot\frac{\pi}{\alpha nF\sqrt{rf_{\max}}},\qquad\left\{\begin{array}{l}\alpha n\geqq 20\\ \dfrac{r}{\alpha n}\geqq 1.\end{array}\right. \tag{7}$$

If it is desired to transmit intelligence over the channels with frequency components, including zero, it will be necessary for the radio link to transmit components including zero. This is apparent from an inspection of (2). If it is not convenient to supply the extreme low-frequency response in the link, the necessity can be avoided by the use of a method of sampling different from that in (2). In this method $c(t)$ is replaced by $c^*(t)$ defined by

$$c^*(t)=1,\qquad \frac{j}{F}-\frac{1}{2\alpha nF}\leqq t\leqq\frac{j}{F}+\frac{1}{2\alpha nF}$$

$$(j=\text{even integers }-\infty,\cdots,\infty)$$

$$c^*(t)=-1,\quad \frac{j}{F}-\frac{1}{2\alpha nF}\leqq t\leqq\frac{j}{F}+\frac{1}{2\alpha nF}$$

$$(j=\text{odd integers }-\infty,\cdots,\infty)$$

$c^*(t)=0$, elsewhere.

Amplitude-modulated signals with suppressed carriers appear at frequencies $(m+1/2)F$, $(m=0,1,\cdots,\infty)$. For example, the signal around $F/2$ may be selected and demodulated.[8] A noise analysis similar to the above may be carried out with only minor changes.

PART II—AMPLITUDE-MODULATION LINKS

Following the procedure of Part I, the r.m.s. fluctuation-noise voltage in the frequency interval $mF\pm f_{\max}$ is $k_2\sqrt{2f_{\max}}$ and the noise voltage in any channel due to the noise in this interval is, by (2),

$$\frac{k_2}{m\pi}\sqrt{2f_{\max}}\sin\frac{m\pi}{\alpha n}\cdot$$

Then, by (1), the noise in any channel due to that in all of the intervals $m=1,\cdots,r$ (r being the number of sideband pairs in (2) transmitted by the link) is

$$\frac{k_2}{\pi}\sqrt{2f_{\max}}\sqrt{\sum_{m=1}^{r}\frac{1}{m^2}\sin^2\frac{m\pi}{\alpha n}}\cdot \tag{8}$$

The signal at the output of any channel is, as in (5),

$$\frac{S}{\alpha n}\cdot \tag{9}$$

This, together with (8), gives a signal-to-noise ratio of

$$R_{am}=\frac{S}{k_2}\cdot\frac{\pi}{\alpha n\sqrt{2f_{\max}}\sqrt{\sum_{m=1}^{r}\frac{1}{m^2}\sin^2\frac{m\pi}{\alpha n}}}\cdot \tag{10}$$

In Appendix II it is shown that, when $\alpha n\geqq 20$ and $r/\alpha n\geqq 5/4$ ($F_c/\alpha nF\geqq 5/4$), the radical of the sum is approximated by $\pi/\sqrt{2\alpha n}$ with an error less than 8 per cent. This provides an approximation

$$R_{am}^*=\frac{S}{k_2}\cdot\frac{1}{\sqrt{\alpha nf_{\max}}},\qquad\left\{\begin{array}{l}\alpha n\geqq 20\\ \dfrac{r}{\alpha n}\geqq\dfrac{5}{4}\cdot\end{array}\right. \tag{11}$$

PART III—COMPARISON

To obtain the signal-to-noise improvement of a f.m. radio link over an a.m. radio link for pulse-height multiplexing, we divide (7) by (11) to obtain

$$\frac{R_{fm}^*}{R_{am}^*}=\frac{k_2}{k_1}\cdot\frac{\pi}{F\sqrt{\alpha nr}}\cdot$$

The well-known f.m. interference reduction factor gives, for the same r.f. signal-to-noise ratio,

$$\frac{k_2}{k_1}=F_cD \tag{13}$$

---

[9] The exact value obtained by integration over the interval $mF\pm f_{\max}$ is $k_1\sqrt{2m^2F^2f_{\max}+2/3\,f^3_{\max}}$. The approximation, which improves rapidly as mF increases, is always less than this by not more than 4 per cent for $mF\geqq 2f_{\max}$ which is, by (2), true for all intervals except $0\leqq f\leqq f_{\max}$. But the noise from this interval can be neglected relative to the remainder.

where F_c is the modulation pass band of the radio links, and D is the deviation ratio of the f.m. radio link. Thus,

$$\frac{R_{fm}^*}{R_{am}^*} = \frac{F_c}{F} \cdot \frac{\pi}{\sqrt{\alpha n r}} \cdot D = \pi \sqrt{\frac{r}{\alpha n}} \cdot D, \tag{14}$$

since $F_c/F = r$. Now r depends upon α and n for a given value of adjacent-channel cross talk.

It was pointed out in an earlier section that if F_c ($F_c = rF$) is not great enough the cross talk between certain channels will be intolerable. If F_c is infinite there will be no cross talk. The matter has been treated at length in a paper by Bennett[4] where the quantitative relations giving the cross talk in terms of the quantities n, α, and r are obtained and studied. It can be shown on the basis of Bennett's work that a cross-talk level between adjacent channels of 55 db below the maximum signal is obtained with

$$\begin{aligned} \alpha &= 2 \\ r &= 3.5n. \end{aligned} \tag{15}$$

Under these conditions, cross talk between channels separated by one or more channels is down more than 55 db. Substituting (15) in (14) we obtain

$$\frac{R_{fm}^*}{R_{am}^*} = \frac{\sqrt{7}\,\pi}{2} \cdot D = 4.15D, \quad n \geqq 10, \tag{16}$$

compared to the familiar value of $\sqrt{3}D$ for a single channel obtained by integrating (13). This of course assumes the f.m. signal is maintained above the improvement threshold.

APPENDIX I

To simplify notation, let $\pi/\alpha n = x$. Now

$$\sin^2 mx = \tfrac{1}{2} - \tfrac{1}{2} \cos 2mx.$$

Therefore,

$$\sum_{m=1}^{r} \sin^2 mx = \frac{r}{2} - \frac{1}{2} \sum_{m=1}^{r} \cos 2mx.$$

Now

$$2 \cos 2mx \sin x = \sin (2m+1)x - \sin (2m-1)x.$$

Therefore,

$$\begin{aligned} \frac{1}{2} \sum_{m=1}^{r} \cos 2mx &= \sum_{m=1}^{r} \frac{\sin (2m+1)x - \sin (2m-1)x}{4 \sin x} \\ &= \frac{\sin (2r+1)x - \sin x}{4 \sin x}. \end{aligned}$$

$$\begin{aligned} \sum_{m=1}^{r} \sin^2 mx &= \frac{r}{2} - \frac{\sin 2rx \cos x + \cos 2rx \sin x - \sin x}{4 \sin x} \\ &= \frac{r}{2} - \frac{1}{4} \cot x \sin 2rx + \frac{1}{4} \cos 2rx - \frac{1}{4} \\ &= \frac{r}{2} \left(1 - \frac{1}{2r} \cot x \sin 2rx - \frac{1}{r} \sin^2 rx \right). \end{aligned}$$

$$\sum_{m=1}^{r} \sin^2 \frac{m\pi}{\alpha n} = \frac{r}{2} \left(1 - \frac{1}{2r} \cot \frac{\pi}{\alpha n} \sin \frac{2\pi r}{\alpha n} + \frac{1}{r} \sin^2 \frac{\pi r}{\alpha n} \right). \tag{17}$$

If $\alpha n \geqq 20$, an approximation for the second term in parentheses, with an error less than 1 per cent, is

$$-\frac{\alpha n}{2\pi r} \sin \frac{2\pi r}{\alpha n}.$$

If $r/\alpha n \geqq 1$, the absolute value of the above term cannot be greater than $1/2\pi$, and the value of the last term in parentheses cannot be greater than $1/20$. Therefore, the value in parentheses differs from unity at most by 0.21. Upon taking the square root, this amounts to a maximum error of 10 per cent in the right member of the identity when the value in parentheses is taken as unity. Thus,

$$\sqrt{\sum_{m=1}^{r} \sin^2 \frac{m\pi}{\alpha n}} = \lambda \sqrt{\frac{r}{2}},$$

$$0.9 \leqq \lambda \leqq 1.1 \text{ when } \begin{cases} \alpha n \geqq 20 \\ \dfrac{r}{\alpha n} \geqq 1. \end{cases} \tag{18}$$

APPENDIX II

To obtain an approximation for the finite sum

$$\sum_{m=1}^{r} \frac{1}{m^2} \sin^2 \frac{m\pi}{\alpha n} \tag{19}$$

we first obtain the limit of the convergent infinite series

$$\sum_{m=1}^{\infty} \frac{1}{m^2} \sin^2 \frac{m\pi}{\alpha n} \tag{20}$$

by an application of Parseval's theorem[10] concerning expansion of functions in the space L^2 in a series of complete orthonormal functions in L^2. The set of functions $\sqrt{F}$, $\sqrt{2F} \cos 2\pi mFt$, $\sqrt{2F} \sin 2\pi mFt$ $(m = 1, \cdots, \infty)$ in the interval $-1/2F \leqq t \leqq 1/2F$ is a complete orthonormal set belonging to L^2. We may write the Fourier series for the commutator function $c(t)$ in the form

$$c(t) = \frac{1}{\alpha n \sqrt{F}} [\sqrt{F}] + \frac{2}{\pi \sqrt{2F}} \sum_{m=1}^{\infty} \left(\frac{1}{m} \sin \frac{m\pi}{\alpha n} \right) [\sqrt{2F} \cos 2\pi mFt].$$

---

[10] See theorem 13 of footnote reference 8.

Parseval's theorem provides the relation (sum of squares of orthogonal components = square of norm)

$$\frac{1}{\alpha^2n^2F}+\frac{2}{\pi^2F}\sum_{m=1}^{\infty}\frac{1}{m^2}\sin^2\frac{m\pi}{\alpha n}=\int_{-1/2F}^{1/2F}|c(t)|^2dt=\frac{1}{\alpha nF}$$

$$\sum_{m=1}^{\infty}\frac{1}{m^2}\sin^2\frac{m\pi}{\alpha n}=\frac{\pi^2}{2\alpha n}\left(1-\frac{1}{\alpha n}\right). \qquad (21)$$

Since (19) is monotone increasing with r, (21) is an upper bound. It remains to establish a lower bound on (19).

$$\sum_{m=1}^{r}\frac{1}{m^2}\sin^2\frac{m\pi}{\alpha n}=\frac{1}{2}\sum_{m=1}^{r}\frac{1}{m^2}+\frac{1}{2}\sum_{m=1}^{r}\frac{-1}{m^2}\cos\frac{2\pi m}{\alpha n}\cdot \qquad (22)$$

We consider the first term in the right member. It is easy to show

$$\sum_{m=1}^{\infty}\frac{1}{m^2}=\frac{\pi^2}{6}\cdot \qquad (23)$$

Therefore,

$$\sum_{m=1}^{r}\frac{1}{m^2}=\frac{\pi^2}{6}-\sum_{m=r+1}^{\infty}\frac{1}{m^2}\cdot \qquad (24)$$

Now the function $1/x^2$ is monotone decreasing to zero and concave upward. Therefore,

$$\sum_{m=r+1}^{\infty}\frac{1}{m^2}\leqq\int_{r+1}^{\infty}\frac{dx}{(x-1)^2}=\frac{1}{r}\cdot$$

Substituting in (23) gives

$$\frac{1}{2}\sum_{m=1}^{r}\frac{1}{m^2}\geqq\frac{\pi^2}{12}-\frac{1}{2r} \qquad (25)$$

which is a lower bound for the first term in the right member of (22).

We now consider the remaining term. Substituting (21) and (23) in (22) gives

$$\frac{1}{2}\sum_{m=1}^{\infty}\frac{-1}{m^2}\cos\frac{2\pi m}{\alpha n}=-\frac{\pi^2}{2}\left(\frac{1}{6}-\frac{1}{\alpha n}+\frac{1}{\alpha^2n^2}\right) \qquad (26)$$

which is negative for $\alpha n\geqq 6$. The terms of the second sum of the right member of (22) form the partial sum for r terms of the infinite series of (26). The terms of the series converging to the negative limit ($\alpha n\geqq 6$) of (26) can be grouped in the intervals $1\leqq m\leqq\alpha n/4$ and $(2q-1)\alpha n/4\leqq m\leqq(2q+1)\alpha n/4$, $q=1, 2, \cdots$, to form a series of alternating terms converging to the same negative limit. Each term after the first is

$$\sum_{(2q-1,\alpha n/4}^{(2q+1)\alpha n/4}\frac{1}{m^2}\cos\frac{2\pi m}{\alpha n}\cdot$$

The partial sum consisting of the first three alternating terms has $q=2$ and $r=5\alpha n/4$. The fourth term

$$\sum_{m=5\alpha n/4}^{7\alpha n/4}\frac{-1}{m^2}\cos\frac{2\pi m}{\alpha n} \qquad (27)$$

is positive. A well-known characteristic of alternating series is that a partial sum ending in a negative term is exceeded by the limit by an amount no greater than the value of the next term (27). Thus

$$\sum_{m=1}^{5\alpha n/4}\frac{-1}{m^2}\cos\frac{2\pi m}{\alpha n}\geqq\sum_{m=1}^{\infty}\frac{-1}{m^2}\cos\frac{2\pi m}{\alpha n}-\sum_{m=5\alpha n/4}^{7\alpha n/4}\frac{-1}{m^2}\cos\frac{2\pi m}{\alpha n}\cdot \qquad (28)$$

The inequality can be maintained if the positive last sum is replaced by an upper bound.

It is easy to show in the case of any function $f(x)$, positive and concave downward between two adjacent zeros at integer values x_1 and x_2, that

$$\sum_{m=x_1}^{x_2}f(m)\leqq\int_{x_1}^{x_2}f(x)dx.$$

Now the function $-(1/x^2)\cos 2\pi x/\alpha n$ has zeros at $x_1=5\alpha n/4$ and $x_2=7\alpha n/4$ and in this interval it is positive and concave downward. Therefore

$$\begin{aligned}\sum_{m=5\alpha n/4}^{7\alpha n/4}\frac{-1}{m^2}\cos\frac{2\pi m}{\alpha n}&\leqq-\int_{5\alpha n/4}^{7\alpha n/4}\frac{1}{x^2}\cos\frac{2\pi x}{\alpha n}dx\\&=-\frac{2\pi}{\alpha n}\int_{5\pi/2}^{7\pi/2}\frac{1}{y^2}\cos y\,dy\\&=\frac{2\pi}{\alpha n}\left[\frac{\cos y}{y}\right]_{5\pi/2}^{7\pi/2}+\frac{2\pi}{\alpha n}\left[Si(y)\right]_{5\pi/2}^{7\pi/2}\\&=\frac{2\pi}{\alpha n}\left[Si(7\pi/2)-Si(5\pi/2)\right].\end{aligned}$$

Evaluating the last term provides the result

$$\sum_{m=5\alpha n/4}^{7\alpha n/4}\frac{-1}{m^2}\cos\frac{2\pi m}{\alpha n}\leqq\frac{0.147}{\alpha n}\cdot$$

Substituting this and (26) in (28) gives

$$\frac{1}{2}\sum_{m=1}^{5\alpha n/4}\frac{-1}{m^2}\cos\frac{2\pi m}{\alpha n}\geqq-\frac{\pi^2}{12}+\frac{4.86}{\alpha n}-\frac{\pi^2}{2\alpha^2n^2}\cdot$$

Substituting this and (25) in (22) gives

$$\sum_{m=1}^{r\geqq\alpha n/4}\frac{1}{m^2}\sin^2\frac{m\pi}{\alpha n}\geqq\frac{4.46}{\alpha n}-\frac{\pi^2}{2\alpha^2n^2}\cdot$$

Combining this with (21), we have

$$\begin{aligned}\frac{\pi^2}{2\alpha n}\left(1-\frac{1}{\alpha n}\right)\geqq\sum_{m=1}^{r\geqq 5\alpha n/4}\frac{1}{m^2}\sin^2\frac{m\pi}{\alpha n}\\ \geqq\frac{\pi^2}{2\alpha n}\left(0.904-\frac{1}{\alpha n}\right).\end{aligned}$$

Therefore, when $\alpha n\geqq 20$ and $r/\alpha n\geqq 5/4$

$$\sqrt{\sum_{m=1}^{r}\frac{1}{m^2}\sin^2\frac{m\pi}{\alpha n}}$$

is never less than $\pi/\sqrt{2\alpha n}$ by more than 8 per cent.

Propagation of Radio Waves in the Lower Troposphere*

J. B. SMYTH†, AND L. G. TROLESE†, ASSOCIATE, I.R.E.

Summary—**The effect of tropospheric layers on the propagation of high-frequency radio waves has been experimentally investigated. A theory is proposed which is in agreement with the salient propagation characteristics observed on a nonoptical link. Fields beyond the optical horizon are governed by the layer height and the refractive index change through the layer. For low layers the higher frequencies have the advantage because of height gain, whereas for higher layers the lower frequencies have the advantage of higher reflection coefficients.**

I. INTRODUCTION

ELECTROMAGNETIC waves transmit energy into the shadow region beyond the optical horizon by several different processes: first, the longer waves are diffracted around the earth; second, a small band of intermediate frequencies is effectively reflected from the ionosphere; and third, refraction and reflection in the lower troposphere frequently make it possible to establish communication on the higher frequencies over distances many times the optical line of sight. This paper is a summary of some of the facts about this latter type of propagation.

The immediate problem is quite clear. How is electromagnetic energy, radiated from a source near the earth's surface, distributed throughout a volume enclosed between the earth and a concentric sphere of sufficient radius to include all practical applications of the energy? If the atmosphere were homogeneous, the problem would be one of diffraction alone.[1–4] However, over most areas of the earth the atmosphere in juxtaposition with the ground is seldom homogeneous; air masses are continually being modified by the surface over which they pass, and frontal activities produce elevated transition regions between air masses. Relatively large changes in temperature and water-vapor pressure through these regions produce index-of-refraction gradients that markedly affect the propagation of high-frequency radio waves. Typical index distributions under different atmospheric conditions are shown in Fig. 1, and will be more fully discussed in Section II.

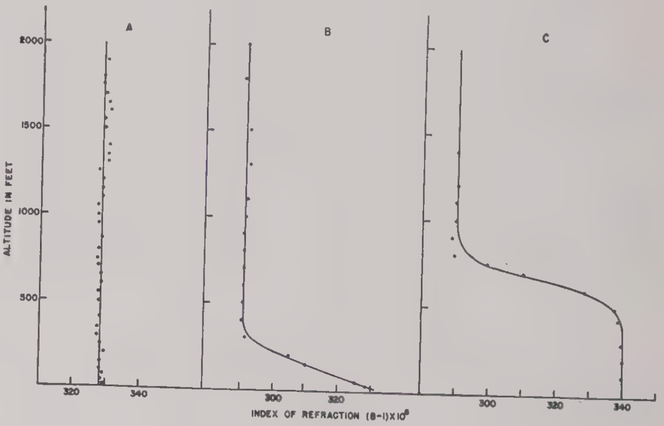

Fig. 1—Typical index-of-refraction distributions.

The effect of the lower atmosphere on radio wave propagation was not fully appreciated until higher frequencies came into general use. Several experimental investigations[5–12] during the middle 1930's qualitatively indicated that field strengths beyond the optical horizon could be quite different on different days, and the effect was correctly attributed to variations in atmospheric refraction. It was not until high-frequency radars came into use during the war that a concentrated effort was made to investigate quantitatively the effect of meteorological conditions on transmission beyond the line of sight.

At the higher microwave frequencies attenuation of energy by rain[13,14] and water vapor becomes a serious problem, and in many cases overshadows the advantage

---

* Decimal classification: R112.2. Original manuscript received by the Institute, November 5, 1946; revised manuscript received, December 26, 1946.

† United States Navy Electronics Laboratory, San Diego 52, Calif.

[1] K. A. Norton, "The calculation of ground-wave field intensity over a finitely conducting spherical earth," PROC. I.R.E., vol. 29, pp. 623–639; December, 1941.

[2] B. van der Pol and H. Bremmer, "The diffraction of electromagnetic waves from an electric point source round a finitely conducting sphere, with applications to radiotelegraphy and the theory of the rainbow," *Phil. Mag.*, vol. 24, part I, pp. 141–176; July, 1937; part II, pp. 825–864; November, 1937.

[3] T. L. Eckersley, "Ultra-short-wave refraction and diffraction," *Jour. I.E.E.* (London), vol. 80, pp. 286–304; March, 1937.

[4] G. N. Watson, "The diffraction of electric waves by the earth," *Proc. Roy. Soc.* (London), vol. 95, pp. 83–99; October 7, 1918; and pp. 546–563; July, 1919.

[5] C. R. Englund, A. B. Crawford, and K. W. Mumford, "Further results of a study of ultra-short-wave transmission phenomena," *Bell Sys. Tech. Jour.*, vol. 14, pp. 369–387; July, 1935.

[6] R. A. Hull, "Air mass conditions and the bending of ultra-high-frequency waves," *QST*, vol. 19, pp. 13–18; June, 1935.

[7] R. A. Hull, "Air-wave bending of ultra-high-frequency waves," *QST*, vol. 21, pp. 16–18; May, 1937.

[8] W. Ochmann and H. Plendl, "Experimentelle untersuchungen über die ultrakurzwellen," *Hochfrequenz. und Elecktroakustik*, vol. 52, pp. 37–44; August, 1938.

[9] R. L. Smith-Rose and J. S. McPetrie, "Ultra-short radio wave refraction in the lower atmosphere," *Wireless Eng.*, vol. 11, pp. 3–11; January, 1934.

[10] C. D. Thomas, and R. C. Colwell, "Wave reflections from diffuse boundaries," *Phys. Rev.*, vol. 52, pp. 1214–1216; December, 1939.

[11] A. W. Friend, and R. C. Colwell, "Measuring the reflection regions in the troposphere," PROC. I.R.E., vol. 25, pp. 1531–1541; December, 1937.

[12] A. W. Friend and R. C. Colwell, "The heights of the reflecting regions in the troposphere," PROC. I.R.E., vol. 27, pp. 626–634; October, 1939.

[13] S. D. Robertson and A. P. King "The effect of rain upon the propagation of waves in the 1- and 3-centimeter regions," PROC. I.R.E., vol. 34, pp. 178P–180P; April, 1946.

[14] G. E. Mueller, "Propagation of 6-millimeter waves," PROC. I.R.E., vol. 34, pp. 181P–183P; April, 1946.

gained by atmospheric refraction. This effect is of minor importance at frequencies discussed in this paper, i.e., below 1000 megacycles. Consequently, attention will be focused on index-of-refraction distributions which occur in the lower troposphere, and their effects on the propagation of high-frequency radio waves.

II. INDEX-OF-REFRACTION DISTRIBUTIONS

At the present time there appears to be no satisfactory method for measuring directly the index-of-refraction gradients in the lower troposphere. The index of refraction is a function of pressure, temperature, and water-vapor content; in practice these parameters are measured and the refractive index calculated from the empirical relationship[5]

$$(n-1) \times 10^6 = \frac{78.5}{T}\left(P + \frac{4800e}{T}\right), \qquad (1)$$

where n is the index of refraction, P is the barometric pressure in millibars, e the water vapor pressure in millibars, and T the absolute temperature.

In a well-mixed atmosphere the index of refraction decreases almost linearly with increasing elevation. It has been shown[3,15] for this case that the problem of refraction may be replaced by a problem in diffraction of radio waves around a sphere of radius approximately equal to 4/3 times the actual earth's radius and surrounded by a homogeneous atmosphere of index of refraction B.[16] With this transformation, typical indices of refraction most generally encountered are shown in Fig. 1. Fig. 1(a) shows the ideal case of a well-mixed atmosphere; 1(b) is an example of modification produced by adding water vapor or subtracting heat from the air near the earth; and 1(c) is a common type of index variation through the interface between two air masses, where the underlying mass is colder and has a higher water-vapor content than the over-riding air. This latter type of index distribution is the one of main interest in this paper.

In the summer season, San Diego lies within the belt of the subtropical anticyclones and, with the absence of surface frontal activity, a stagnant circulation exists. Because of the persistence of high-level anticyclonic circulation aloft, pronounced subsidence is maintained throughout this season. By subsidence aloft a thermal inversion exists over a large maritime area, and thus forms the boundary between the lower maritime polar and the continental tropical or superior air aloft. Variation in the height and the magnitude of the inversion are the governing factors in daily weather phenomena.

The index of refraction variation through the transition region between these two air masses, modified as indicated above, can be represented very closely by[17,18]

$$[B_{(z)}]^2 = \frac{B_3^2 + B_1^2}{2} + \frac{B_3^2 - B_1^2}{2} \tanh u/2 \qquad (2)$$

where B_1 and B_3 are the values of the index of refraction in medium I and medium III, respectively, and $u = kz/p$, p being a parameter which determines the thickness of the transition region, z is the altitude, and $k = 2\pi/\lambda$ as usual. In the case of an elevated layer, Fig. 1(c) shows the agreement between the theoretical curve given by (2) and a typical set of experimental data.

III. REFLECTION FROM ELEVATED LAYERS

Ignoring the earth for the moment and assuming a horizontally stratified atmosphere, it has been found[17,18] that the wave equation may be solved in closed form for the index-of-refraction distribution given by (2). The intensity reflection coefficient for this type of transition layer is given by

$$R = \frac{\sinh^2 \pi(\alpha - \beta)}{\sinh^2 \pi(\alpha + \beta)} \qquad (3)$$

where

$$\alpha = pB_1 \cos \theta_1$$
$$\beta = pB_3 \cos \theta_3.$$

θ_1 is the angle at which the radiation is incident upon the transition stratum, and θ_3 is the refracted angle above the layer.

Fig. 2 gives the reflection coefficient in decibels below the intensity of the incident radiation, for several angles of incidence, as a function of the ratio of stratum thickness to wavelength. The change in index through the layer is taken to be 60×10^{-6}, which is in the range observed over the San Diego area during the summer season. At incident angles equal to or greater than the critical angle,[19] reflection is complete. For a given index change and transmitter elevation there will be a layer height such that all the radiation will be incident upon this layer at angles slightly less than the critical angle. We shall call this the critical height. For layer heights greater than this critical height, the lower frequencies will be reflected more strongly than the higher frequencies. In addition, any deviation of the layer from the horizontal plane will affect the higher-frequency radiation more than the lower frequencies. As the layer rises above the critical height, the incident angles become smaller, and consequently the effect of the reflection diminishes with increase in frequency.

Continuous measurements made on a 90-mile nonoptical link over water offer data that can be compared with the above theory. Fig. 3 shows a condensed log

---

[15] J. C. Schelleng, C. R. Burrows, and E. B. Ferrell, "Ultra-short-wave propagation, "Proc. I.R.E., vol. 21, pp. 427–463; March, 1933.

[16] $B = n + \alpha h$, where $\alpha = 1.18 \times 10^{-8}$/feet.

[17] P. S. Epstein, "Reflection of waves in an inhomogeneous absorbing medium," *Nat. Acad. Sci.*, vol. 16, pp. 627–637; October, 1930.

[18] C. Eckart, "The penetration of a potential barrier by electrons," *Phys. Rev.*, vol. 35, pp. 1303–1309; June, 1930.

[19] $\theta_c = 89° 22.5'$ for $\Delta B = 60 \times 10^{-6}$.

of the field strengths received during a period when considerable meteorological data were taken. Maximum and minimum field strengths during successive two-hour intervals are plotted in decibels below the free-space level at the receivers, thus showing the general signal level and the fading range for each of the three frequencies used. The elevation of the base of the temperature inversion, which is approximately the bottom of the transition layer (Fig. 1 (c)), is shown by the discrete points in the upper part of the figure. As the elevation of the layer increases above the critical height, i.e., the height at which the radiation is incident on the layer at angles less than the critical angle, the higher frequencies decrease more rapidly than the lower frequencies and the fading range is correspondingly greater. This is in qualitative agreement with the theoretical curves of Fig. 2.

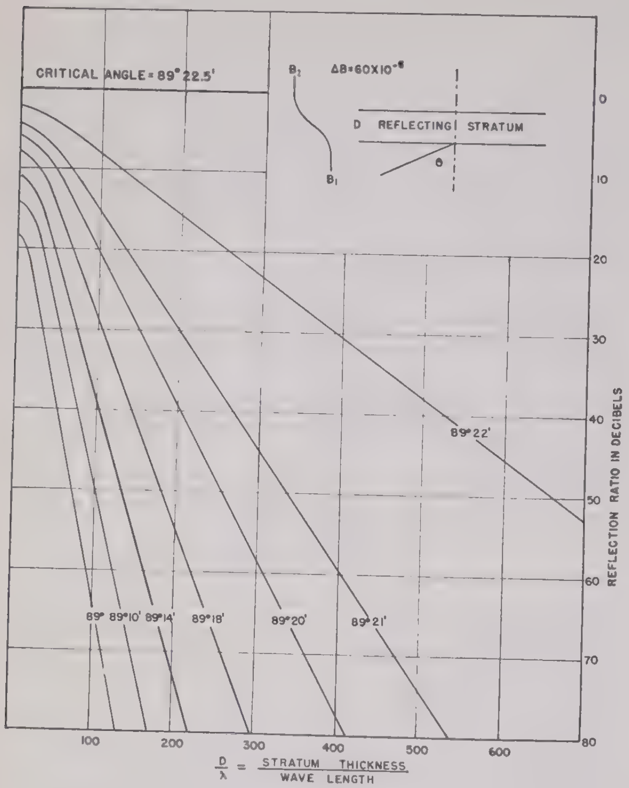

Fig. 2—Reflection coefficient in decibels below the intensity of the incident radiation.

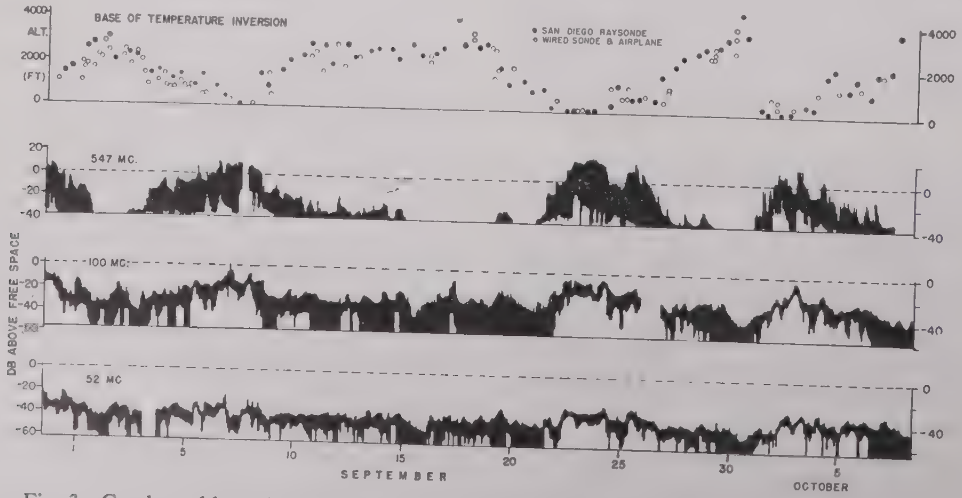

Fig. 3—Condensed log of field-strength records over the 90-mile link from San Pedro to San Diego. Transmitter and receiver at 100 feet altitude, horizontal polorization.

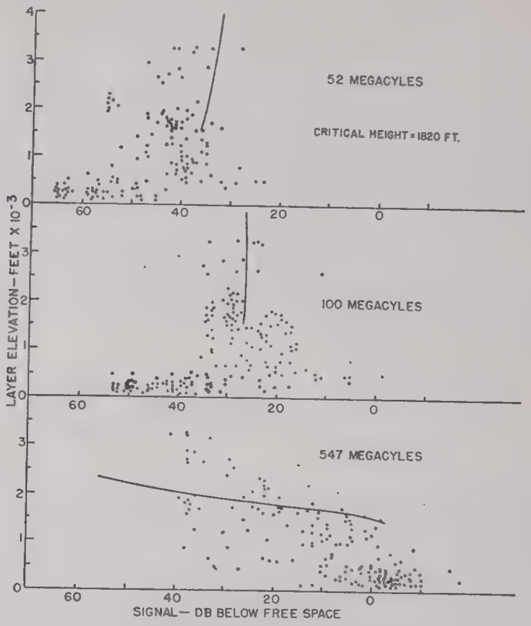

Fig. 4—Maximum fields compared with theory.

It will be observed that for low layers, where part of the radiation is incident at angles greater than the critical angle, the lower-frequency fields do not increase to the free-space level, whereas the higher-frequency fields increase above this level. In fact, if the layer height decreases below a certain height the lower-frequency signals decrease. This apparent discrepancy is closely

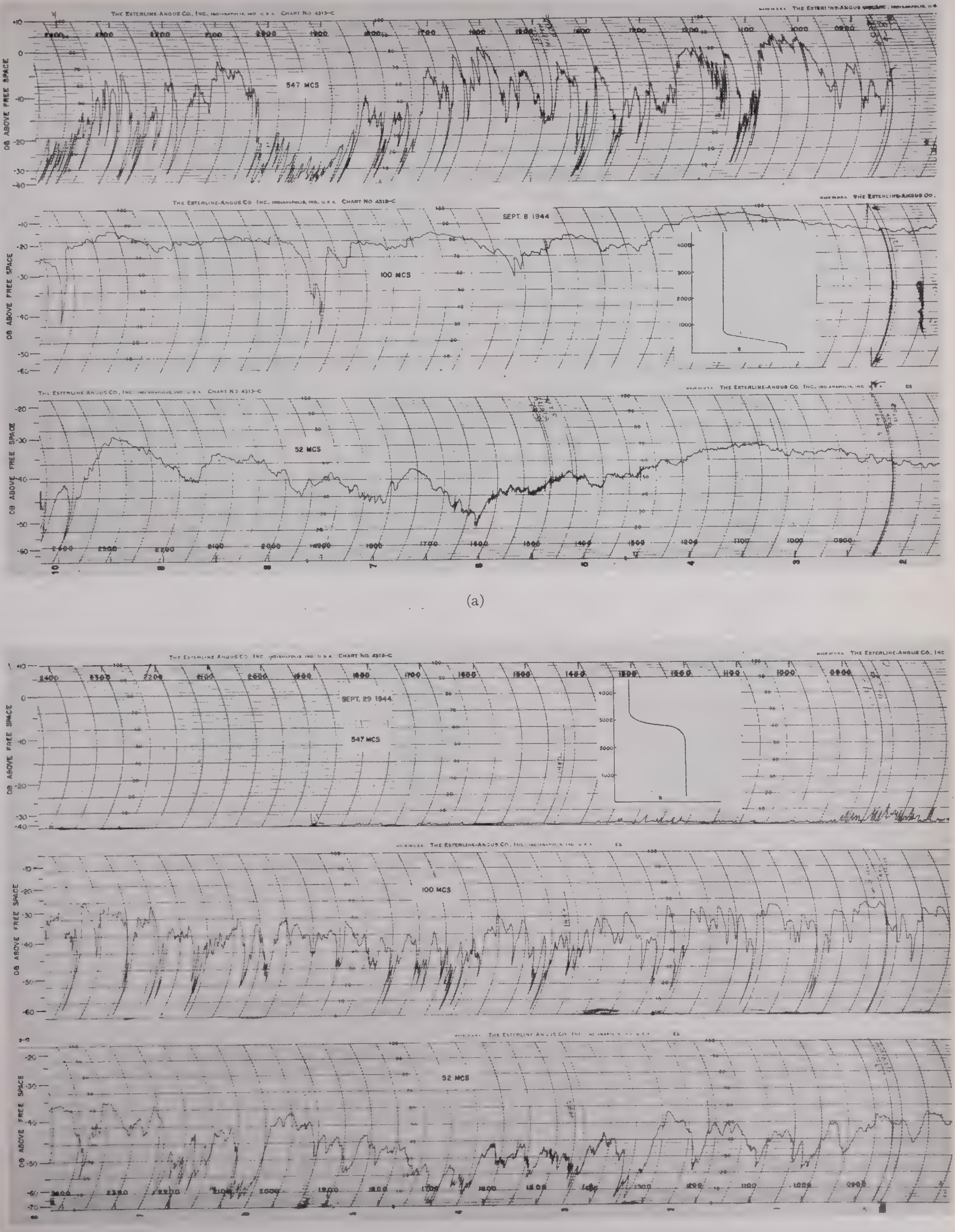

(a)

(b)

Fig. 5—Typical signal records. (a) Low-based reflecting layer. (b) High-based reflecting layer.

connected with the fact that the boundary condition at the earth's surface has been ignored.

For layer elevations greater than the critical height, the middle of the path may be assumed the point of reflection from the elevated stratum. Assuming complete reflection from the sea surface, optical height-gain calculations[1] show that the energy incident upon the layer is less for the lower frequencies than for the higher frequencies. Using this concept, together with the reflection coefficients from the layer, gives the theoretical curves shown in Fig. 4. The discrete points give the maximum field received during the hours in which meteorological data were taken. A mean value of layer thickness was assumed in the calculations and consequently a point-to-point agreement should not be expected. However, the general level of the fields and the variation with layer elevation are quite definite.

For low layers the above simple method yields values for the fields which are too small. This indicates that the center of the path is no longer the controlling point for reflection. For low layers an exact solution of the wave equation satisfying the boundary conditions[20] should yield correct results.

The diffracted field is below detection for all the frequencies used on the 90-mile nonoptical link. During the winter, on occasions when frontal activity dissipates all low-level inversions, all the fields decreased below detection.

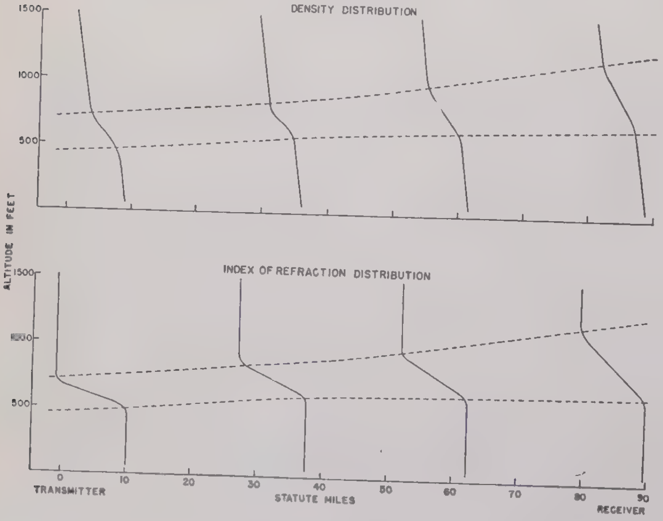

Fig. 6—Typical index and density distributions along propagation path.

IV. Fading

Fig. 5 is a photograph of the receiver recording-tape plot for conditions of a low and a moderately high temperature inversion. When the layer is low the variation in field strength is relatively slow in time, and the variations are smaller for the lower frequencies. The intensity variation is greater when the layer is higher.

Fig. 6 shows a typical distribution of index of refraction along the transmission path. In addition to this space variation, the index distribution on the vertical plane changes with time. It should be noted that the largest change in density takes place through the transition layer, and this provides the possibility of Helmholtz waves[21] in the reflecting stratum. These small interface waves are evident by the undulations on the top surface of the stratus cloud deck which forms the lower boundary of the transition layer between the two air masses.

The transition layer is a warped surface upon which is superimposed small interface waves. The shape of the surface and the characteristics of these waves vary both in space and time, and possibly contribute a great deal to the complexity of signal fading beyond the optical horizon. In addition, turbulence in the atmosphere may contribute to high-frequency scintillations.

V. Conclusion

Treating the elevated refracting stratum as a plane reflecting layer seems to agree in general with experience in that the observed frequency dependency of the reflecting layer is predicted; the observed fading characteristics of the different frequencies are in the right direction, i.e., the higher the frequency the greater the fading; and, under conditions of high layers, strong fields well beyond the horizon cannot be explained on the basis of refraction alone.

The height of the layer above the earth introduces another factor which depends on the frequency. For layers greater than the critical height, height-gain calculations in the optical region, together with reflection coefficients, give the fields to be expected beyond the optical horizon. Agreement between measured and calculated fields is fair.

* * *

---

[20] C. L. Pekeris, "Perturbation theory of the normal modes for an exponential *M*-curve in nonstandard propagation of microwaves," *Jour. Appl. Phys.*, vol. 17, pp. 678–684; August, 1946.

[21] H. Lamb, "Hydrodynamics," Dover Publications, New York, N. Y., 1945; p. 363.

The Determination of Ionospheric Electron Distribution[*]

LAURENCE A. MANNING[†], ASSOCIATE, I.R.E.

Summary—The virtual height versus frequency integral is derived, neglecting absorption and the earth's magnetic field. It is shown how solution of this integral equation can be obtained using the Laplace transformation, and how true height versus frequency can be determined graphically from virtual height versus frequency curves. Application of the method is made to some typical nighttime and daytime ionosphere records.

INTRODUCTION

PROBABLY the most important method of ionospheric investigation is the pulse technique originated by Breit and Tuve. In this method short pulses of radio-frequency energy are directed vertically upwards, and the time required for them to travel to the ionosphere and return is recorded oscillographically. By measuring this delay time as a function of frequency, curves are obtained which are of great value in deducing many of the properties of the upper atmosphere. It is the purpose of this paper to show how these records may be used to calculate the distribution of ionization in the ionosphere by a direct and rigorous method. It is not a new problem. Appleton[1] and de Groot[2] showed the essentials of its solution a good many years ago, but applications of the method seem to have been few. More recently, Rydbeck[3] has treated the question, as has Pekeris,[4] although without laying much stress on application of the procedure. Here we shall demonstrate the method of solution of the equations involved and then present a number of illustrations of actual determination of the electron distribution.

PART I—THEORY

Basic Relations

As a starting point for the analysis three fundamental relations are needed, of which the first is that for the refractive index μ of the ionosphere. The form to be used here neglects the earth's magnetic field, and assumes no absorption. It is

$$= \left(1 - \frac{KN}{f^2}\right)^{1/2} \tag{1}$$

where N is the number of electrons per volume unit, f is the frequency, and K is a constant.

The second fundamental equation is a direct result of (1) and of the definition of refractive index. It is quite easy to show that whenever refractive index is given by an equation of the form $(1+C/\omega^2)^{1/2}$, with C a constant, the group and phase velocities are related by the equation $v_g \cdot v_p = c^2$. Combining this relation with the definition of refractive index $\mu = c/v_p$, we have

$$\mu = v_g/c. \tag{2}$$

The third fundamental equation is simply the definition of velocity as the time derivative of position,

$$v = dz/dt. \tag{3}$$

Here z is taken to be a variable co-ordinate above the earth's surface.

From (3) the time taken by a wave of velocity $v(z)$ to reach a height z is $t = \int_0^z dz/v$. Noting that a pulse of energy travels at approximately the group velocity rather than the phase velocity, (2) gives us $1/v = 1/\mu c$, so that, with the aid of (1), $1/v = f/c(f^2 - KN)^{1/2}$. Making this substitution in the integral,

$$t = \frac{f}{c} \int_0^z \frac{dz}{(f^2 - KN)^{1/2}}.$$

The functions $t(f)$ defined by this integral correspond to the experimental time-delay versus frequency curves, and may be computed if $N(z)$ are known. Our problem is to work backwards and see if we can find $N(z)$, given the experimental curves $t(f)$.

Virtual Height

We now define virtual height z_v as the product of c and the time taken by the wave to reach its maximum height z_m.

$$z_v = f \int_0^{z_m} \frac{dz}{(f^2 - M)^{1/2}} \tag{4}$$

where for the simplicity KN has been replaced by M, so M represents the electron density in units of megacycles squared. It is common practice to scale the experimental ordinates directly in terms of virtual height, rather than time delay.

The preceding expression is the basis of most ionospheric path calculations. The integral, however, is extremely unpleasant to deal with. There are two reasons why this form is awkward to handle. The first reason is that M, which varies with z in a rather involved manner, appears in the integral in an equally involved manner. The second reason is that z_m, the true height to which a wave of frequency f ascends, is a complicated

---

[*] Decimal classification: R113.602.3. Original manuscript received by the Institute, October 28, 1946.

[†] Stanford University, Calif.

[1] E. V. Appleton, "Some notes on wireless methods of investigating the electrical structure of the upper atmosphere, II," *Proc. Phys. Soc.*, vol. 42, pp. 321–339; June 15, 1930.

[2] W. de Groot, "Some remarks on the analogy of certain cases of propagation of electromagnetic waves and the motion of a particle in a potential field," *Phil. Mag.*, vol. 10, pp. 521–540; October, 1930.

[3] O. Rydbeck, "The propagation of electromagnetic waves in an ionized medium and the calculation of the true heights of the ionized layers in the atmosphere," *Phil. Mag.*, vol. 30, pp. 282–293; October, 1940.

[4] C. L. Pekeris, "The vertical distribution of ionization in the upper atmosphere," *Terr. Mag.*, vol. 42, pp. 205–211; June, 1940.

function of f. Actually, it is the inverse of the function $M(z)$, since a wave of frequency f goes to a height $z_m(f)$ where $\mu=0$, so $f^2=M(z_m)$, and hence $z_m=M^{-1}(f^2)$. Considering the difficulties presented by (4), it is fortunate that by a simple change of variables they can all be disposed of.

This manipulation demands a certain readjustment in viewpoint. Equation (4) contends that to each height above the earth there is a definite electron density M corresponding; $M(z)$ is the curve of electron distribution. But it is equally logical, and for many calculations simpler, to consider that for each value M of the electron density a certain height Z corresponds; then $Z(M)$ is the curve of electron distribution. The only drawback to use of this concept is that, although $M(z)$ is necessarily single-valued, $Z(M)$ is not necessarily so.

Since the analysis which follows does not hold unless $Z(M)$ is single-valued, it might be thought that by introducing the function $Z(M)$ to our equations we are unnecessarily restricting the validity of our results. This is not the case, however, since from physical considerations it can be shown that it is impossible to determine exactly the electron distribution beyond the first maximum of the $M(z)$ function in any event. Recalling that a wave of frequency f is turned back at a height such that $M=f^2$, it is evident that the single-valued function formed by taking the least value of $Z(f^2)$ is the true-height function.

Change of Variables and Transformation

In actually transforming (4) to a workable form it is convenient to introduce a number of changes of notation. Instead of f^2, let us write g. Then, for $z_v(f)/f$, write $P(g)$. Now introduce the new variable of integration M, so that $z=Z(M)$, and $dz=Z'(M)dM$. With this substitution the limits are changed; when $z=z_m$, $M=g$, and when $z=0$, $M=0$. Putting all of these substitutions in (4), we obtain

$$P(g) = \int_0^g \frac{Z'(M)}{(g-M)^{1/2}}\, dM \tag{5}$$

a special case of Abel's integral equation.[5] Examination of the integral reveals a number of pleasing characteristics. First, the involved function in the integrand $Z'(M)$ enters in a linear manner into the integral. Second, the upper limit of the integral is not a function, but an independent variable. Another fortunate characteristic of (5) will become more evident upon a further change of variables. Let $1/g^{1/2}=P_1(g)$, and $Z'(M)=P_2(M)$. Then (5) becomes

$$P(g) = \int_0^g P_1(g-M)\cdot P_2(M)\cdot dM. \tag{6}$$

This is seen to be a real convolution, or Faltung,[5–7] integral. Taking the Laplace transform, we obtain

$$\rho(s) = \rho_1(s)\cdot\rho_2(s) \tag{7}$$

where, by definition, $\rho(s)=L[P(g)]$, $\rho_1(s)=L[g^{-1/2}]$, $\rho_2(s)=L[Z'(g)]$. The Laplace transform $f(s)$ of $F(t)$ is defined by $f(s)=L[F(t)]=\int_0^\infty F(t)\epsilon^{-st}dt$. Hence we have $\rho_1(s)=\Gamma(1/2)/s^{1/2}=(\pi/s)^{1/2}$ by direct integration, where $\Gamma()$ is the gamma function. Also, as a result of integration by parts, $\rho_2(s)=sL[Z(g)]-Z(0)=s\zeta(s)-Z(0)$. Combining, we have

$$\rho(s) = (\pi/s)^{1/2}[s\zeta(s) - Z(0)]. \tag{8}$$

In terms of these transforms, then, our integral equation has become a mere algebraic equation. Solving it for $\zeta(s)$,

$$\zeta(s) = [\rho(s)/\pi][\pi/s]^{1/2} + Z(0)/s. \tag{9}$$

We may now reverse the procedure whereby we went from (6) to (7), and so obtain

$$Z(M) = \frac{1}{\pi}\int_0^M [P(g)/(M-g)^{1/2}]dg + Z(0). \tag{10}$$

Here we have the desired result, an explicit expression for electron distribution in terms of known functions. It will clarify matters to return to the original notation. Using $P(g)=z_v/f$, $g=f^2$, $dg=2f\cdot df$, and noting that when $g=M$, $f=\sqrt{M}$, there results

$$Z(M) = \frac{2}{\pi}\int_0^{\sqrt{M}} [z_v/(M-f^2)^{1/2}]df + Z_0 \tag{11}$$

where $Z_0=Z(0)$. The above equation gives the electron-distribution function as a functional transformation of the virtual-height function. The only necessary caution is to remember that we have assumed $M(z)$ to be single-valued. In terms of the experimental data, this condition means that the virtual-height versus frequency function must be bounded, if we maintain the fundamental assumptions of the analysis. For purposes of comparison it is interesting to put (5) in the usual notation, too.

$$z_v = \int_0^{f^2} [Z'(M)/(1-M/f^2)^{1/2}]dM. \tag{12}$$

Equation (11) can be written in a slightly different way so as to give true height as a function of the vertical incidence frequency f_v involved.

$$Z(f_v) = \frac{2}{\pi}\int_0^{f_v} [z_v/(f_v^2-f^2)^{1/2}]df + Z_0. \tag{13}$$

It is interesting to note that (12) and (13) form a function transform pair. Equation (12) transforms the distribution function into the virtual-height function, while (13) does just the converse.

Simplified Form

For use in determining the electron distribution or true height experimentally, (13) can be advantageously transformed. As it stands, the process of determinining the true height corresponding to a given frequency (electron concentration) f_v is to plot a curve derived from the $z_v(f)$ curve by dividing at each point by the value of the radical, and finding the area under this curve up to the frequency f_v. At f_v, however, the radical becomes zero, so that it is necessary to find the area of a curve with a singularity. The simpler procedure is a result of making in (13) the substitution $f=f_v \sin\theta$, $df=f_v \cos\theta d\theta$. When $f=0$, $\theta=0$. When $f=f_v$, $\theta=\pi/2$. Hence,

---

[5] G. Doetsch, "Laplace Transformation," Dover publications, New York, N. Y.; 1943. Text in German.

[6] R. V. Churchill, "Modern Operational Mathematics in Engineering," McGraw-Hill Book Co., New York and London; 1944.

[7] M. F. Gardner and J. L. Barnes, "Transients in Linear Systems," vol. 1, John Wiley and Sons, Inc., New York, N. Y.; 1942.

$$Z(f_v) = (2/\pi)\int_0^{\pi/2} z_v(f_v \sin\theta)\cdot d\theta + Z_0. \tag{14}$$

Using (14), the process of finding the height corresponding to a given electron density or vertical-incidence frequency is very simple.

Technique of Analysis

The given datum is a curve of virtual height z_v versus frequency f. Choose $f_v=\sqrt{M}$, M being the electron concentration whose height is desired. Replot z_v as a function of θ, θ going from zero to $\pi/2$ (90 degrees). This is most easily done with a slide rule in accordance with the relation $f=f_v \sin\theta$, where it is to be noted that f_v is for the time being fixed. The frequency f is entered on the experimental curve to find the virtual height z_v corresponding to θ on the derived curve. To determine $Z(f_v)$ it is necessary to integrate the derived curve from 0 to $\pi/2$, and multiply by $2/\pi$. This integration and multiplication is performed with a planimeter which is calibrated so that the area within the rectangle bounded by $z_v=100$ kilometers and $\theta=90$ degrees is 100 kilometers.

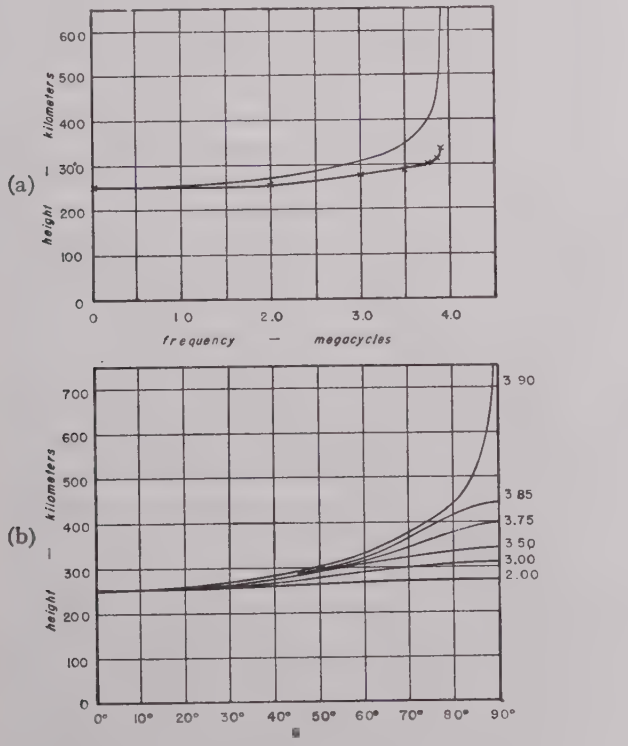

Fig. 1—Analysis of the ionospheric electron distribution for June 2, 1944, 2300 local time, at Stanford University, Calif. (a) Virtual and true height versus frequency. (b) Derived curves used in computing true height.

To determine complete curves of electron distribution, it is necessary to compute point by point the true heights corresponding to given frequencies f_v. For each of these true heights it is necessary to draw a derived curve and find the area with a planimeter, but the work involved is not great, especially as the derived curves tend to form a family, so that not many points need be used except on the first few.

Fig. 1 shows a sample analysis. The upper curve in (a) is the experimentally determined virtual-height function. In (b) are shown six derived curves obtained from the virtual-height curve by warping the frequency scale in accordance with the relation $f=f_v \sin\theta$. The area under one of the derived curves gives the true height corresponding to the value of f_v used in its construction. These true heights have been plotted as the lower curve in Fig. 1(a).

PART II—APPLICATION

Nighttime Records

Nighttime records are generally characterized by much greater simplicity than are daytime records. Ionization in the E layer decreases to such an extent that it is ordinarily not possible to observe any regular refractive effects other than that of the F layer, using multifrequency recorders of usual design. For the purposes of analyzing electron distribution, however, it is necessary that the virtual-height curve be extended all the way to zero frequency. In the case of the records analyzed here, no data were available for frequencies below 0.8 megacycle, and the virtual-height curves were consequently extrapolated to zero as if no lower-layer ionization existed. If an appreciable E-layer ionization does exist at frequencies below 0.8 megacycle, the true height found should be decreased somewhat, especially at the lower frequencies.

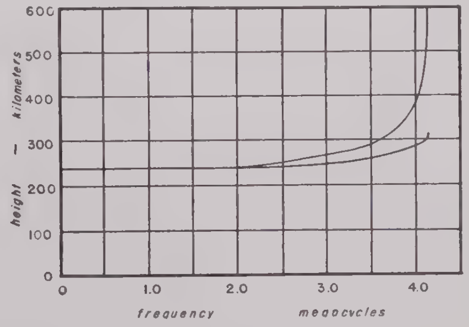

Fig. 2—Virtual and true height versus frequency for June 2, 1944, at 2030, local time.

Figs. 1 and 2 show typical nighttime virtual-height records. Fig. 2 represents conditions in the early evening, and Fig. 1 shows conditions two and one-half hours later. In Fig. 3 are shown the electron distributions corresponding to these records. The distribution for 2030 is interesting in that it is almost precisely elliptical. At 2300 of the same day, however, the distribution shows no such unexpected shape. If there is any arrangement of electrons that can be considered normal, and which will occur whenever extraneous influences are not at play, an analysis covering a much larger number of cases will be needed to determine it.

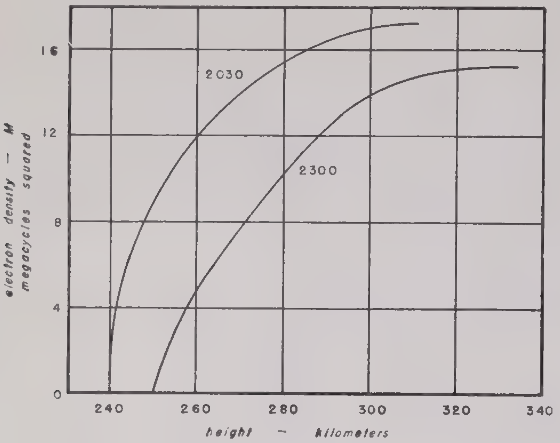

Fig. 3—Ionospheric electron distribution on June 2, 1944, at 2030 and 2300, local time.

Daytime Records

Daytime records are characterized by the existence of a number of layers of relatively high ionization, and by the variety observed in the nature of the virtual-height functions. In Fig. 4 is shown a record of a very commonly occurring form. The E-layer critical frequency is sharp, and because of both the speed of motion of the oscillograph trace and of the relatively great absorption at a critical frequency, it almost appears on an actual record as if there is a discontinuous jump between the E- and F_1-layer virtual heights. But because an ideal lossless ionosphere having the same electron distribution as the actual one would produce an infinite virtual height on each side of the critical frequency, we must assume the experimental curve to do so, too, and thus assist our hypothesis of (1). On the far side of the E-layer critical frequency two virtual-height traces are observed. The upper trace is caused by the presence of the separate F_1 layer shown by the true-height curve. The lower trace is caused by a reflection from the far side of the E-layer maximum, and is hence a sporadic-E trace. Since the reflection occcurs above the height of maximum E-layer ionization, the wave is refracted as well as reflected, and consequently the virtual height becomes infinite as the E-layer critical frequency is approached from above.

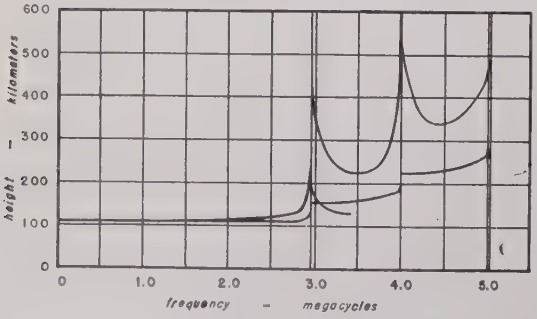

Fig. 4—Virtual and true height versus frequency for June 2, 1944, at 1530, local time.

In addition to explaining the tail dangling from the E-layer critical frequency, analysis of the record of Fig. 4 gives a good illustration of the existence of distinct E, F_1, and F_2 layers. It might be well here to say that, subject to the hypothesis of (1), the necessary and sufficient condition that $dN/dz=0$ is that z_v become infinite. With this necessity in mind, it becomes evident on examining many records with pronounced variations in virtual height that only flexures will occur in the true-height curves.

In analyzing the record of Fig. 4 we have simply ignored the restriction placed upon the solution that the virtual height must never become infinite. As a result, the true-height curve is not rigorous for frequencies beyond the E-layer maximum and, of course, it is not really rigorous near the bottom of the E-layer, either, since we merely assumed that the virtual-height curve could be extended all the way to zero frequency at exactly 110 kilometers. A consideration of the graphical process of finding the true height for a frequency somewhat above that at a previous layer maximum shows, however, that the virtual height near the critical frequency plays a relatively minor role in determining the true height. Physically, note that, for these higher frequencies, the transit time is little influenced by the retardation of the wave in the region of lower electron density where a relative maximum may have occurred, so that in considering virtual height for, say, the F layer, the existence or nonexistence of an E-layer maximum is not important. Now it was seen graphically that the virtual height at a lower frequency, even though it may go to infinity for an earlier maximum, does not contribute greatly to the final determination of height. We conclude, therefore, that analysis of true height is of value for frequencies above those for which the virtual height becomes infinite, and that the true-height curve becomes increasingly accurate as the frequency is raised above these critical values. In drawing true-height curves in the neighborhood of a relative minimum of ionization there is no mathematical guide, and physical reasoning and extrapolation must be employed to estimate the true distribution. A slight warping of such curves as are shown in Fig. 4 may be made as they emerge from the ionization minimum if it seems reasonable, since the analysis is here least accurate.

An illustration of a transition record in which the F_1 layer is disappearing is given in Fig. 5. Only a sag in the true-height curve remains where there were once distinct layers. A considerable insight into the significance of virtual-height curves can be obtained without actual analysis by merely considering the graphical process of obtaining the true height. It is obvious that there cannot be much of an F_1 layer at 3.5 megacycles in Fig. 5 because in the graphical analysis there is no means by which a small change in f_v can appreciably alter the area of the derived curve. This situation is different from that at a critical frequency where the virtual height becomes infinite. If f_v is chosen just above such a critical frequency, the sinusoidal co-ordinate of the derived curve spreads out the region of high virtual heights over a considerable area. But if f_v is chosen just slightly below the critical frequency, the virtual height co-ordinates are bounded, and a considerably smaller area is obtained.

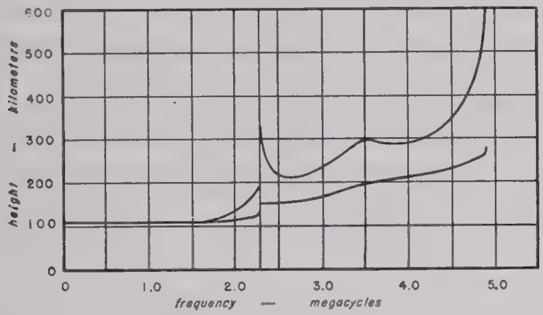

Fig. 5—Virtual and true height versus frequency for May 27, 1944, at 1730, local time.

Fig. 6 provides a most striking illustration of the fact that it is impossible to have a maximum of electron density unless there is a frequency of infinite virtual height. In this figure what appears at first glance to be indicative of a good E layer turns out to represent merely a tendency towards a leveling off in electron density. Of course, if we thought that the virtual height was limited here by absorption or by the assumption of the validity of geometrical optics,[8] we should extend the traces to infinity for the sake of the analysis, but even so only a very slight maximum could exist with this record.

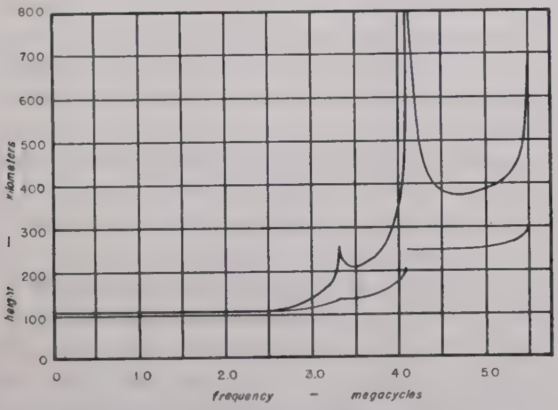

Fig. 6—Virtual and true height versus frequency for May 31, 1944, at 1330, local time.

Electron Distribution

Figs. 7, 8, and 9 show the electron distributions corresponding to the daytime records just discussed. These distributions are surprising, both because of their variety in shape, and because of certain points of similarity between them. The most striking point of similarity is that the true heights of the layers remain relatively constant in time, irrespective of either the electron distribution or virtual height. The height of the F_1-layer maximum remains at 200 kilometers in all three analyses, and the maximum height of the E layer seems fixed at about 130 kilometers.

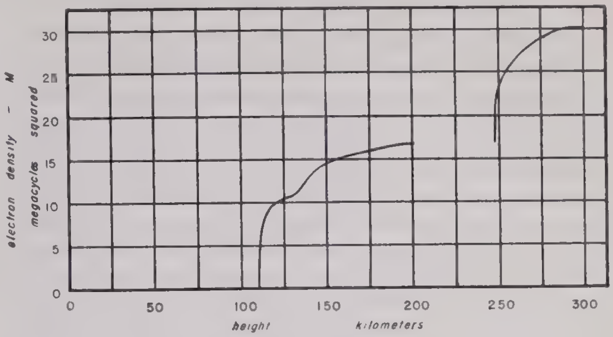

Fig. 7—Ionospheric electron distribution for May 31, 1944, at 1330, local time.

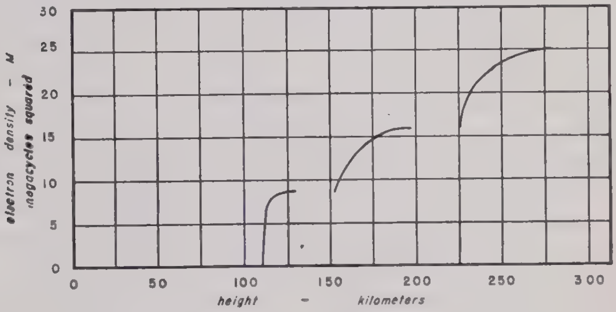

Fig. 8—Ionospheric electron distribution for June 2, 1944, at 1530, local time.

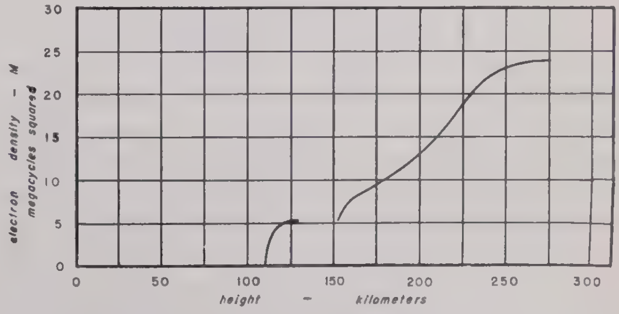

Fig. 9—Ionospheric electron distribution for May 27, 1944, at 1730, local time.

ACKNOWLEDGMENT

The author wishes to express his gratitude to Robert A. Helliwell, whose stimulating comments and frequent encouragement have been essential to the progress of this work. The author is also grateful to Frederick E Terman and to Felix Bloch for their interest.

---

[8] O. E. H. Rydbeck, "Reflection of electromagnetic waves from a parabolic friction-free ionized layer," *Jour. Appl. Phys.*, vol. 13, pp. 577–581; September, 1942.

Considerations in the Design of a Radar Intermediate-Frequency Amplifier*

ANDREW L. HOPPER†, MEMBER, I.R.E., AND STEWART E. MILLER†, MEMBER, I.R.E.

Summary—**The intermediate-frequency amplifier of a microwave radar receiver is commonly required to provide approximately 100 decibels amplification in a bandwidth of 1 to 10 megacycles, centered at frequencies in the 30- and 60-megacycle regions. Meeting such requirements involves the use of five to ten amplifier stages of the highest efficiency that can be suited to production methods. In addition, the noise figure of the radar intermediate-frequency amplifier is a significant contributor to the over-all radar receiver noise figure, and must therefore be maintained at an absolute minimum. By examining a particular intermediate-frequency-amplifier design (one providing an over-all bandwidth of 10 megacycles centered at 60 or 100 megacycles), this paper discusses qualitatively the theoretical problems involved in such a design and gives data of practical importance to the engineer attempting to build a similar amplifier. Measured characteristics of approximately fifty amplifiers are summarized to illustrate the end results achieved.**

I. Introduction

Microwave radar receivers developed during the war are of the superheterodyne form, wherein the received signal is immediately converted to an intermediate frequency and there amplified to a magnitude of the order of a volt. The intermediate-frequency amplifier required in such a receiver is a very specialized device, as will be indicated in the requirements to be listed presently.

During the war a vast amount of development effort has been applied to various aspects of the radar intermediate-frequency-amplifier problem. A number of parallel developments have resulted in more than one method of accomplishing essentially the same result. This paper does not presume to be a comprehensive review of such work, nor is it intended as an intense theoretical discussion of particular circuit arrangements or of the interrelation between the various design factors. Rather, a review of a specific intermediate-frequency-amplifier development will be given, together with a brief indication of the theoretical and practical factors involved.

II. Design Objectives

The microwave radar transmitter-receiver, for which this intermediate-frequency amplifier has been developed, is required in a service application where space and weight are at a premium. This means that all of the components of the transmitter-receiver must be as small and light as possible; in addition, the packaging of all the components should be arranged so as to minimize the size and weight of the over-all unit, at the same time maintaining its serviceability. The result of these requirements in the case of the intermediate-frequency amplifier is that three individual chassis contain intermediate-frequency amplifying tubes.

The requirements just stated, together with other objectives which are self-explanatory, are given in the following list.

(1) The best possible signal-to-noise performance must be maintained at all times, because the intermediate-frequency amplifier is a significant contributor to the over-all radar receiver noise figure.

(2) The amplifier gain must always be sufficient to bring input circuit noise up to about one volt at the second detector output.

(3) Approximately 10 megacycles bandwidth is required.[1]

(4) The center frequency shall be either 60 or 100 megacycles.

(5) Since service use of the equipment involves maintenance by relatively unskilled personnel without the aid of a signal generator, satisfactory operation must be assured when defective tubes are replaced by *randomly selected* stock tubes. No compensating adjustments are permissible.

(6) At least 60 decibels of manual or automatic gain control must be available.

(7) Recovery of normal gain after a severe overload (large signal) should occur within one or two microseconds.

(8) Size and weight shall be held to a minimum.

(9) The packaging arrangement shall fit the needs of the over-all transmitter-receiver unit.

(10) The mechanical layout shall be suitable for manufacture in quantity.

(11) The band-pass characteristics and noise figure shall be reproducible in manufacture.

It might be well to point out that one requirement which is not imposed on the radar intermediate-frequency amplifier is linearity of the phase-versus-frequency characteristic. Faithful pulse reproduction is a desirable feature which can be dispensed with if necessary so long as the signal-to-noise ratio is not appreciably affected. The shape of the gain versus frequency characteristic should be single-peaked at approximately the center of the pass band to facilitate receiver tuning, but in general it may have an irregular shape in the vicinity of maximum gain.

---

* Decimal classification: R363.13. Original manuscript received by the Institute, August 2, 1946; revised manuscript received, November 15, 1946.

† Bell Telephone Laboratories, Inc., New York, N. Y.

[1] All bandwidths mentioned herein refer to the frequency interval between points 3 decibels down from maximum gain.

III. CHOICE OF THE MIDBAND INTERMEDIATE FREQUENCY

In outlining the requirements on the intermediate-frequency-amplifier development above, the question of the choice of the midband intermediate frequency was avoided. This problem is somewhat involved, but it is important enough to warrant a brief digression.

In low-frequency receivers the intermediate frequency is often chosen in conjunction with the selectivity of the radio-frequency section which precedes the converter to eliminate interference due to another signal at the image frequency. In the microwave radar receiver, for reasons too lengthy to be discussed here, great effort is expended to enlarge the band width of the radio-frequency section. In the absence of preselection, interference may be reduced by the proper choice of intermediate frequency. If the intermediate frequency is greater than one-half of the total band of frequencies in which the desired signal and interfering signals may occur, image interference will also be eliminated. However, in the microwave radar receiver this would require an intermediate frequency so high as to be almost impractical, and the noise figure of the intermediate-frequency section would be so poor as to materially degrade the over-all performance of the receiver. Therefore, it is necessary to compromise between (a) elimination of interference, and (b) quality of performance in the condition where no interfering signal is present. The tendency, based on the above reasoning, is to make the intermediate frequency as high as possible consistent with good receiver noise figure.

The location of the image response on the radar's own transmitter (the case where the local oscillator is tuned to the opposite side of the transmitter frequency compared to the desired operating condition) is a factor in the design of automatic tuning systems. Again the preference is for the highest possible intermediate frequency to obtain the widest possible separation between the desired tuning point and the image tuning point.

It has been implied that lower intermediate frequencies result in better intermediate-frequency noise figures. This is a general truism, but the difference in the intermediate-frequency noise figure for a low and somewhat higher intermediate frequency depends on the bandwidth required. The noise-figure advantage of the lower intermediate frequency decreases as the intermediate-frequency bandwidth is increased.

In some radar systems the sideband noise of the local oscillator is an important contributor to the over-all receiver noise figure. During the major part of the war, the only practical way of reducing local-oscillator noise was to use a higher intermediate frequency, thereby placing the signal at a frequency further removed from the local-oscillator carrier.[2] (The output of a reflex-klystron oscillator contains less noise at frequencies further removed from the oscillator frequency.) This aspect of the problem may be summarized by saying that there is an optimum intermediate frequency from the standpoint of over-all receiver noise figure alone.

Finally, there is a very important factor which suggests making the intermediate frequency just as low as possible: The bandpass circuits of the intermediate-frequency amplifier are tuned entirely by stray circuit capacitance and vacuum-tube interelectrode capacitance. This influences the choice of midband intermediate frequency because the number of megacycles misalignment of cascaded tuned circuits caused by a given amount of capacitance variation is made smaller by reducing the intermediate frequency. Using a low midband intermediate frequency to minimize the effect of capacitance variations is therefore most important in narrow-band (1 megacycle, for example) intermediate-frequency amplifiers, and less important in wide-band amplifiers.

Most microwave radar receivers developed in the United States have used midband intermediate frequencies of 30 and 60 megacycles, whereas the British have used 45 megacycles.

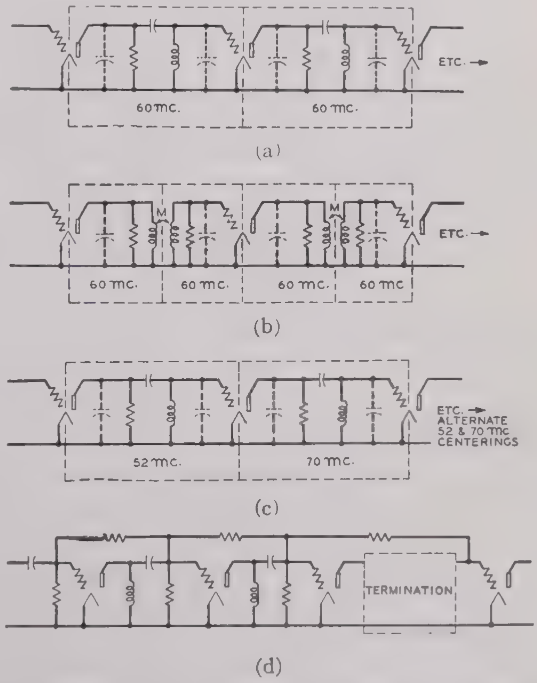

Fig. 1—Typical interstage circuits: (a) synchronous single-tuned; (b) double-tuned, equal Q's; (c) staggered single-tuned (pair); and (d) feedback triple.

IV. THE BASIC AMPLIFYING UNIT: THE INTERSTAGE CIRCUITS

The amount of gain required can be roughly estimated by noting that the objective is 1 volt output in 820 ohms, corresponding to a power level of 0.00122 watt or +0.9 decibel above 1 milliwatt. Thermal noise power *KTB* in a 10-megacycle band is 103.9 decibels below 1 milliwatt. Therefore as a first approximation, 105 decibels over-all gain is required to bring input-circuit noise up to 1 volt output from the second detector.

---

[2] Recent advances in wave-guide circuit design allow for elimination of the major portion of local-oscillator noise without raising the intermediate frequency.

Four commonly used types of interstage circuits are shown in Fig. 1. A careful comparison of these four types of interstage designs is beyond the scope of this paper. However, it is possible to point out the criteria which might be used in such a comparison:

(1) Circuit efficiency—defined as the product of gain times bandwidth.

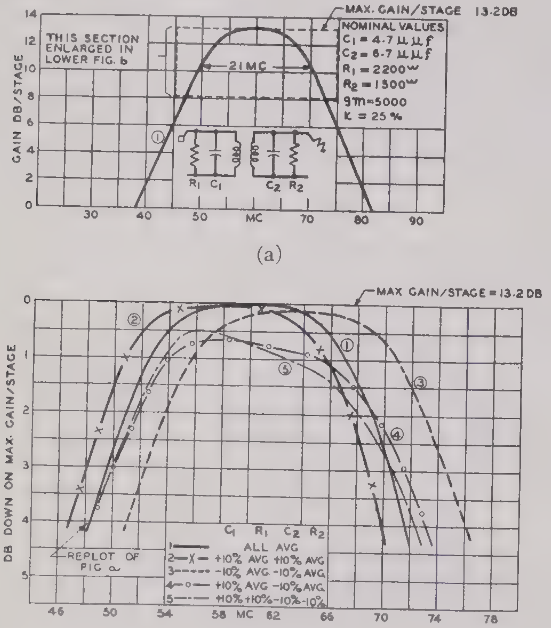

(a)

(b)

Fig. 2—Calculated 60-megacycle gain characteristics: (a) no mistuning, and (b) effect of mistuning when *C*'s and *R*'s vary by ±10 per cent.

(2) Criticalness—defined as the change in the gain versus frequency characteristic due to changes in tube capacitance, circuit capacitance, or damping-resistor values.

(3) Ease of construction—a measure of the practicality of putting the design into production.

An evaluation of the available data on the criteria indicated above led to the choice of the double-tuned interstage circuit for the intermediate-frequency amplifier to be described.

Maximizing the product of gain and bandwidth is the dominant factor in selecting the best tube. A survey of the tubes available led to the selection of the 6AK5 miniature pentode.[3] Among the characteristics which make the 6AK5 an excellent intermediate-frequency amplifier tube are: (a) its small size, (b) its high ratio of transconductance to input and output capacitance, (c) its low active grid-circuit conductance (about 30 micromhos at 60 megacycles), and (d) its low power consumption.

Having selected the tube and the type of interstage network, the undetermined factor in the interstage design is the bandwidth of each interstage network. Although some improvement in efficiency can be achieved by assigning different gain versus frequency characteristics to succeeding double-tuned circuits (giving an over-all characteristic which is the result of adding several nonflat gain-frequency curves), the design to be described is based on maintaining equal *Q*'s on both sides of the double-tuned transformer, and on designing all stages of the amplifier with identical gain versus frequency characteristics. By so doing the amplifier is made less sensitive to parameter variations. In order to obtain a tolerable design the interstage capacitance is held as low as possible; the tuned circuits are resonant with stray-circuit capacitance and tube interelectrode capacitance. Therefore the circuit must be engineered on the basis that ±10 per cent capacitance variations will be experienced in the individual interstage circuits in an uncontrolled manner. Similarly, variations of ±5 to 10 per cent must be expected in the values of damping resistors used in the tuned circuits.

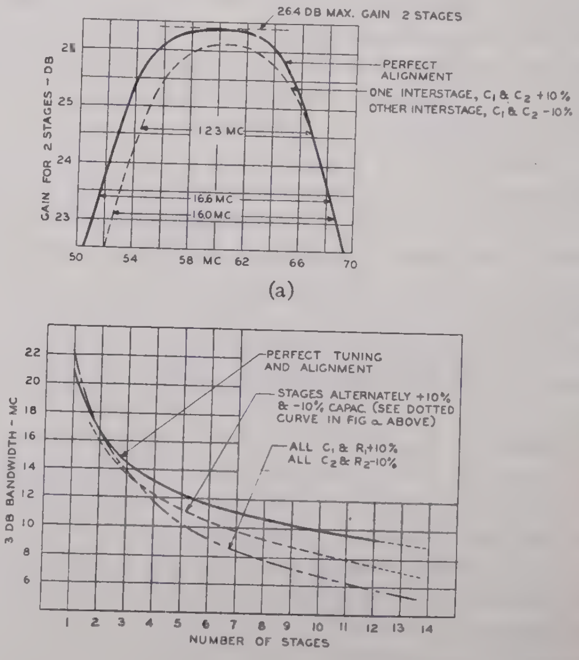

(a)

(b)

Fig. 3—(a) Effect of misalignment of cascaded stages. (b) Bandwidth versus number of stages.

For the amplifier under consideration it was found *necessary* to use ten stages, each having a 3-decibel bandwidth of 21 to 22 megacycles, and a calculated nominal gain of 13+ decibels (based on a g_m of 5000 micromhos). An eleventh stage was added for margin.

The calculation of the interstage gain for a midband intermediate frequency of 60 megacycles is given in Fig. 2. The upper half of this figure shows the characteristic when all parameters are nominal. The lower half shows the effects of capacitance and resistance variations in some of the many combinations of such effects which are possible. Fig. 3 helps to show the way individual interstage misalignment reacts on the bandwidth of a multistage amplifier. The upper half of Fig. 3 shows the gain shape of two stages: (a) with nominal capacitance and resistance values, and (b) with nominal resistance values but one stage high capacitance and one stage low capacitance. The latter case is a severe one with respect to band narrowing. The lower half of Fig. 3 shows the multistage-amplifier bandwidth as a function of the number of stages using (a) the nominal case, (b) the case noted above of capacitance staggering, and (c) the case in which the capacitance and resistance are assumed, to have their most unfavorable values in successive stages simultaneously. (The latter case is not apt to occur in practice, but it does show a limiting condition.)

---

[3] G. T. Ford, "Characteristics of vacuum tubes for radar intermediate-frequency amplifiers," *Bell Sys. Tech. Jour.*, vol. 25, pp. 385–407; July, 1946.

Before curves like those of Fig. 2 can be computed it is necessary to determine the magnitudes of C_1 and C_2, which are composed of circuit and tube capacitances. The active value of C_1 will be very close to its "cold" value (that with no power on the tube); however, the value of C_2 will increase when the tube is turned on due to the presence of the electron cloud between the grid and the cathode. The increase of tube input capacitance may be of the order of 1.0 micromicrofarad. Consequently, the following apportionment of the nominal interstage capacitance may be made:

	Input (micromicrofarads)	Output (micromicrofarads)
Tube capacitance (cold)	3.90	2.85
Tube capacitance increase when hot	1.0	
Socket capacitance	0.95	0.9
Stray circuit capacitance	0.95	0.95
Total	6.7	4.7

Knowing the capacitance distribution of the interstage, conventional network theory may be applied to determine the remaining element values for the desired shape of band-pass characteristic.

Building the double-tuned transformer involves a certain amount of empirical work to obtain the desired coupling coefficient and self inductances. The physical configuration of the transformer used in this amplifier is shown in Fig. 4. The mutual inductance between primary and secondary is almost all due to flux linking the two or three turns of each winding nearest the dielectric fin in the center of the transformer form. Therefore the coupling coefficient may be determined by the thickness of the fin, provided that both windings are wound close to the fin. The outer end turns of the primary and secondary (shown spaced) do not link flux with the other winding and therefore do not contribute to the mutual inductance. However, spacing these end turns in various ways will change the self inductance of the winding considerably. Use is made of this fact to adjust the self-inductance of the primary and secondary independently to the exact design value by comparison to a standard inductance.

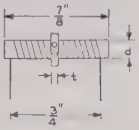

	100 MC.		60 MC.	
COIL DIAMETER (d)	$\frac{3}{16}$ IN.		$\frac{1}{4}$ IN	
FIN THICKNESS (t)	0.035 IN.		0.028 IN	
APPROX. "K"	16 %		23 %	
WIRE SIZE	NO. 30 B.E.		NO 33 B.E	
NO. OF TURNS	PRI.	SEC.	PRI.	SEC.
BALANCED			18¾	18¾
INPUT			18¾	19¼
INPUT	13¾	10¾	11¾	12¾
INTERSTAGE	12¾	10¾	15¾	12¾
OUTPUT	12¾	12¾	16¾	12¾
DETECTOR	12¾	13¾	16¾	16¾

Fig. 4—Transformer data.

The curves of Fig. 5 show the relation between coupling coefficient and transformer fin size for several diameters of forms. These curves are useful in estimating the proper dimensions for a new transformer design. The data for building the transformers used in this amplifier design have been tabulated in Fig. 4.

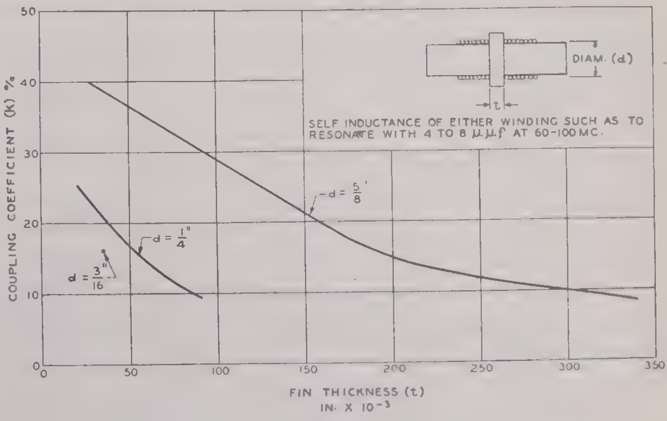

Fig. 5—Coupling coefficient versus fin size.

V. Mechanical Design

As previously mentioned, the packaging of the transmitter-receiver brought about a breakdown of the intermediate-frequency amplifying system into three chassis: (a) amplifier No. 1, containing the input circuit and two intermediate-frequency-amplifier stages; (b) amplifier No. 2, containing six amplifier stages; and (c) amplifier No. 3, containing three intermediate-fre-

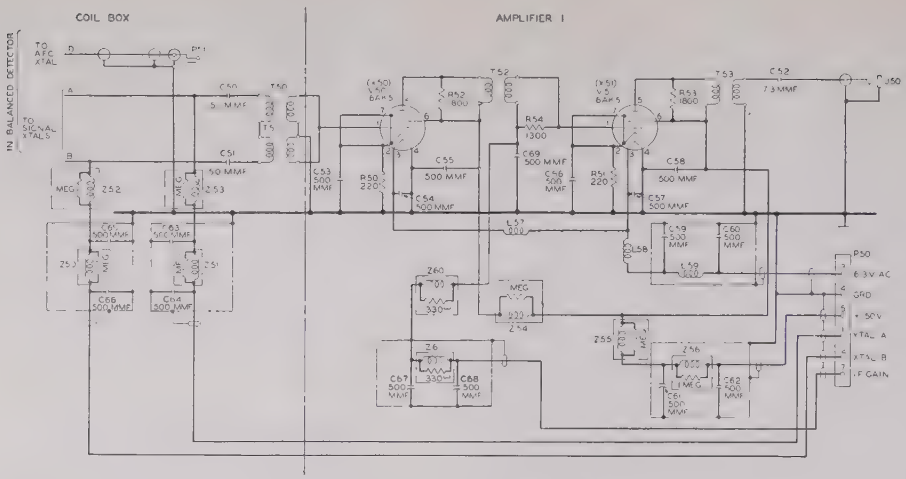
COIL BOX
AMPLIFIER I
IN BALANCED DETECTOR
TO AFC XTAL
TO SIGNAL XTALS
C50 5 MMF
C51 50 MMF
T50
(X50) V50 6AK5
R52 800
T52
R54 1300
(X51) V51 6AK5
R53 1800
T53
C52 7.3 MMF
J50
C53 500 MMF
R50 220
C54 500 MMF
C55 500 MMF
C69 500 MMF
C56 500 MMF
R51 220
C57 500 MMF
C58 500 MMF
L57
C59 500 MMF
C60 500 MMF
L58
L59
Z52
Z53
Z60
330
Z54
Z55
Z56
Z61
C67 500 MMF
C68 500 MMF
C62 500 MMF
P50
6.3 V AC
GRD
+ 50 V
XTAL A
XTAL B
I.F GAIN

Fig. 6—Schematic of amplifier No. 1.

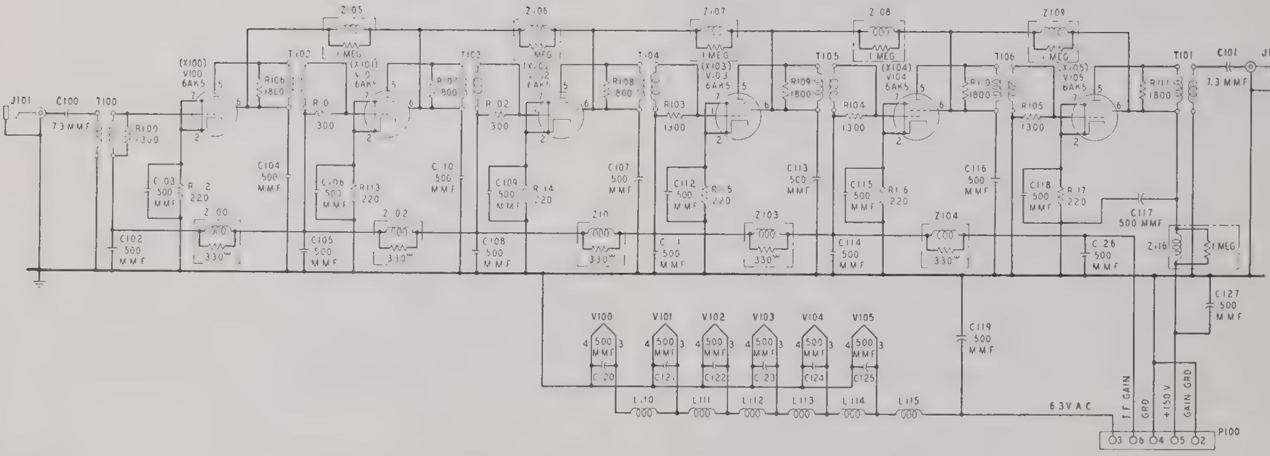
J101
C100 7.3 MMF
T100
R100 1300
(X100) V100 6AK5
R106 1800
T102
(X101) V101 6AK5
T103
(X102) V102 6AK5
R108 1800
T104
(X103) V103 6AK5
R109 1800
T105
(X104) V104 6AK5
T106
(X105) V105 6AK5
R111 1800
T101
C101 7.3 MMF
J100
Z105
Z106
Z107
Z108
Z109
1 MEG
R103 1300
R104 1300
R105 1300
C104 500 MMF
C107 500 MMF
C113 500 MMF
C116 500 MMF
C117 500 MMF
C102 500 MMF
C105 500 MMF
C108 500 MMF
C114 500 MMF
C126 500 MMF
Z100
Z102
Z103
Z104
Z116
330
C127 500 MMF
C119 500 MMF
V100
V101
V102
V103
V104
V105
C120
C122
C124
C125
L110
L111
L112
L113
L114
L115
6.3 V AC
I.F. GAIN
GRD
+150 V
GAIN GRD
P100

Fig. 7—Schematic of amplifier No. 2.

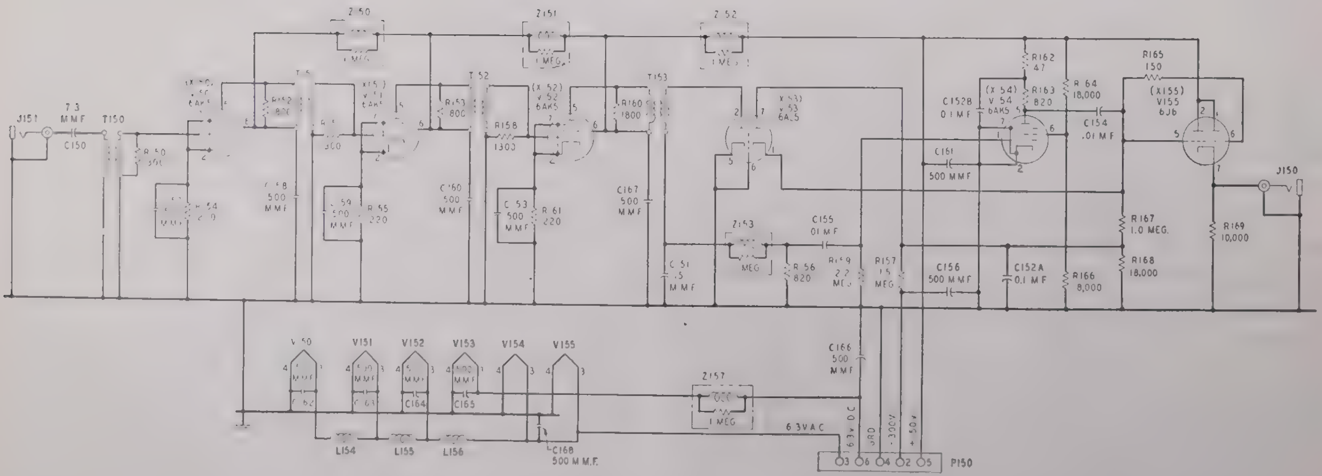
J151
7.3 MMF
C150
T150
Z150
Z151
Z152
1 MEG
T152
T153
(X152) V152 6AK5
R158 1300
R160 1800
(X153) V153 6AK5
R162 47
R163 820
R164 18,000
(X154) V154 6AK5
C152B 0.1 MF
C154 .01 MF
R165 150
(X155) V155 6J6
J150
C161 500 MMF
C157 500 MMF
Z153
C155 .01 MF
R156 820
R159 2.2 MEG
R157 1.5 MEG
C156 500 MMF
C152A 0.1 MF
R166 8,000
R167 1.0 MEG
R168 18,000
R169 10,000
C166 500 MMF
V150
V151
V152
V153
V154
V155
C164
C165
L154
L155
L156
C168 500 MMF
Z157
6.3 V AC
GRD
-300 V
+ 50 V
P150

Fig. 8—Schematic of amplifier No. 3.

quency-amplifier stages, a diode second detector, a video amplifier-limiter, a diode providing direct-current reinsertion in the grid of the output stage, and a cathode-follower video output stage.

The schematic circuit diagrams of amplifiers Nos. 1, 2, and 3 are shown in Figs. 6, 7, and 8, respectively.

Because the physical arrangement of parts is part of the electrical interstage design, it is appropriate to review this aspect of the problem. External and internal views of amplifier No. 2 are shown in Figs. 9 and 10.

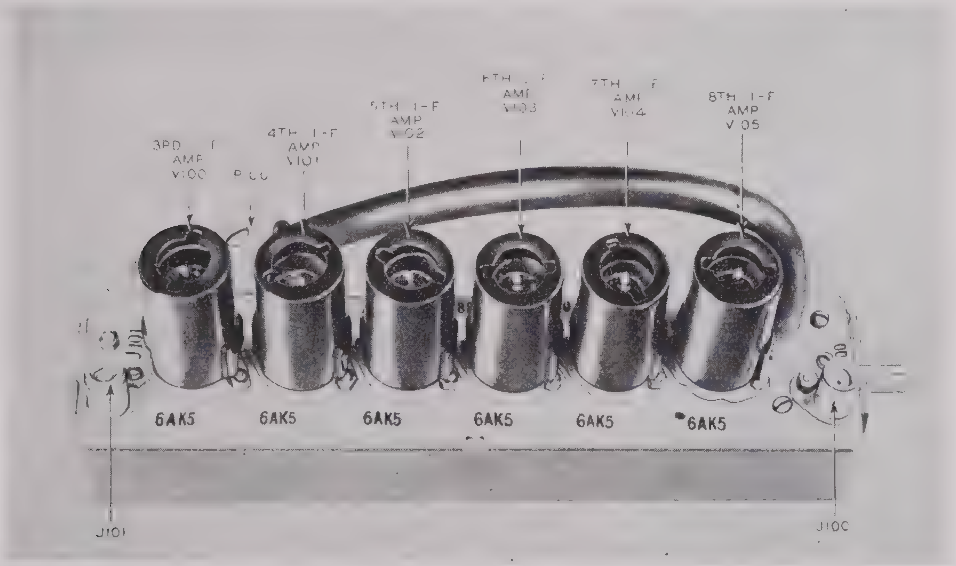

Fig. 9—Top view of amplifier No. 2.

The layout of parts in Fig. 10 may be reviewed as follows: The intermediate-frequency signal is brought to this chassis by means of a low-impedance cable which terminates in the jack at the upper right-hand corner of the photograph. From there the signal is stepped up in a double-tuned circuit to the first tube grid, amplified in a series of identical interstages, and stepped back down to a low impedance at the output jack in the lower right corner of the chassis. The seven double-tuned transformers lined up in the center of the chassis are at an angle, to save space and to minimize mutual-inductance coupling between transformers. Heater decoupling filters (very necessary at these frequencies) in the form of a ladder structure are located on the right-hand side of the unit. Also on the right-hand side of the chassis, the series elements of the grid-circuit gain-control decoupling filters are designated *Z100* to *Z104*. The transmission circuit has just one point ground per stage, achieved by mounting the "button"-type capacitors used for by-passing the grid, cathode, and plate-screen circuits on a grounded rod. This gives a structure resembling a totem pole, with the three disk-type capacitors parallel to each other and mounted on the same axis. Six such by-passing assemblies are shown in Fig. 10 on the left side of the chassis. The outer rims of the capacitors are off ground, and are soldered directly to the tube socket pin to be by-passed. The cathode by-pass capacitor is in the center of the totem pole, with the plate and grid by-pass capacitors above and below it; this aids in minimizing feedback due to cathode impedance common to the input and output circuits.

Finally, a nonstandard method of making circuit connections has been employed to reduce the interstage capacitance variations from amplifier to amplifier in manufacture. For example, in Fig. 10 the circuit connection between *Z105*, socket terminal No. 6, *R106*, and the lower primary terminal of *T102* is made by means of a single strip of brass. This strip is preformed and drilled so as to serve as a mounting support for *T102*, *R106*, and *Z105* as well as to make the electrical connection. These preformed brass strips are made by a punching process, which is rendered economical by using the same preformed part in every interstage of the amplifier. Similarly, a punched, preformed part is used to serve as a mechanical support for *T102*, *R101*, *Z100*, and *Z102*, as well as to make the electrical connections between these elements. Again, the same preformed part is used in corresponding positions of every interstage. The use of these two preformed parts assures better uniformity in circuit capacitance by taking out of the hands of the wireman the decision as to the length and path the various connections will have.

Use of the above-described method of construction contributes to the success of building the amplifier without adjustments. The assembly and test procedure is as follows:

(1) The chassis is wired complete except for transformers.

(2) The transformers are wound and adjusted on a Q meter (by moving the spaced turns) so that the primary and secondary self inductances are the same as those of standard inductances within a tolerance equivalent to ±0.04 micromicrofarad at the mid-band intermediate frequency. The transformers are then coated with a coil cement to hold the turns firmly in place.

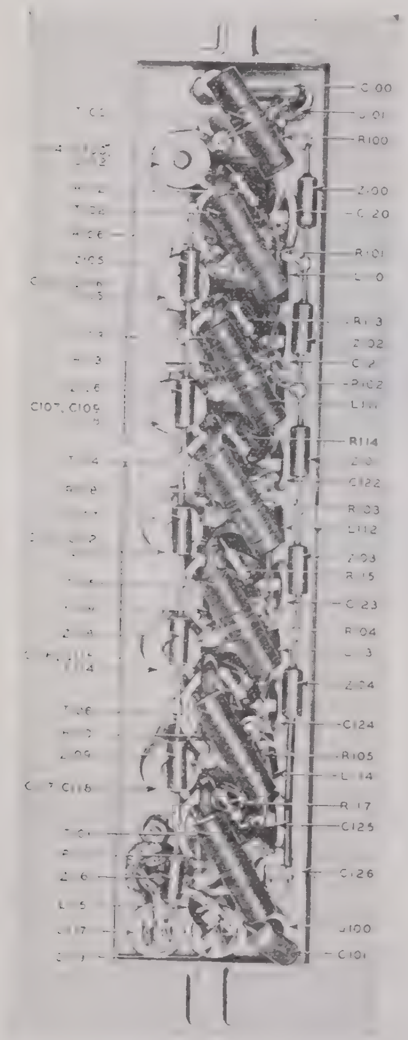

Fig. 10—Bottom view of amplifier No. 2.

(3) The transformers are assembled in amplifiers, and over-all checks of gain, bandwidth, and other electrical characteristics are made. At this point no tuning adjustments are available or necessary. The electrical test procedure involves no adjustments.

The results of this procedure are covered in the section on over-all amplifier characteristics.

VI. Input-Circuit Design

The objective in the design of the input circuit is to obtain the best noise figure achievable in the bandwidth required.[4] Previous publications[5] have treated the input-circuit problem analytically, and the discussion here will be confined to a review from the viewpoint of the present design.

The tube for the first intermediate-frequency-amplifier stage should be chosen for (a) low plate-screen noise, (b) low input and output capacitances, (c) high transconductance, and (d) low input (grid) circuit conductance. Again, the 6AK5 has been found superior to other available tubes, and therefore is used in this amplifier.

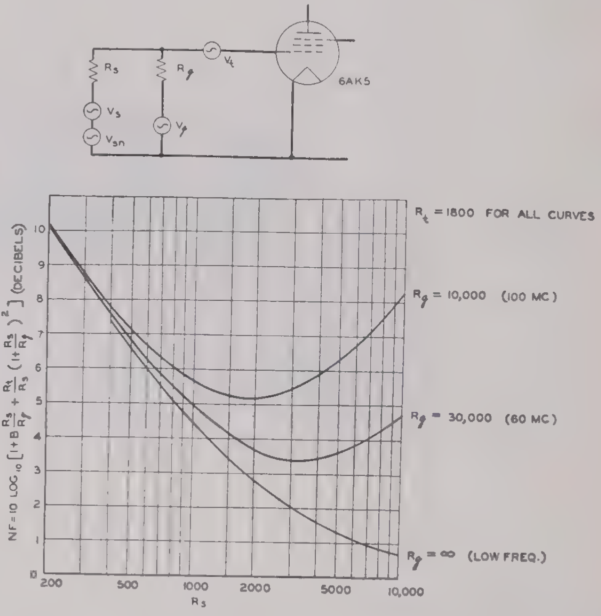

Fig. 11—Calculated noise figure versus source resistance for 6AK5 tube.

The variation of noise figure with input-circuit step-up (ignoring stray capacitance for the moment) may be observed with reference to Fig. 11. The expression for noise figure

$$NF = 10 \log_{10}\left[1 + B\frac{R_s}{R_g} + \frac{R_t}{R_s}\left(1 + \frac{R_s}{R_g}\right)^2\right] \text{(decibels)}$$

follows directly from Friis' definition of noise figure and the equivalent circuit of Fig. 11. The symbols in this equivalent circuit have the following meanings:

---

[4] H. T. Friis, "Noise figures of radio receivers," Proc. I.R.E., vol. 32, pp. 419–422; July, 1944.

[5] E. W. Herold and L. Malter, "Some aspects of radio reception at ultra-high frequency," Proc. I.R.E., vol. 31, pp. 491–510; September, 1943.

R_s and V_s are the internal impedance and the voltage of the source of signal

$V_{sn}=\sqrt{4KT\Delta fR_s}$ is the thermal noise of the signal source

$V_t=\sqrt{4KT\Delta fR_t}$ is an equivalent generator representing shot noise, referred back to the grid of the tube

R_g = is the vacuum-tube loading due to transit time and lead-inductance effects

$V_g=\sqrt{BKT\Delta fR_g}$ where B is a constant introduced to properly represent the noise effect of active grid loading.[6]

The calculations represented in Fig. 11 are only approximately applicable to a complete intermediate-frequency amplifier, because it has been assumed (a) that the first tube of the amplifier is the sole contributor to amplifier noise figure (a good assumption in many cases where pentode first-stage tubes are used), (b) that input-circuit transformer losses are negligible, and (c) that $B=5$, the value North[7] suggests for the grid-conductance effect of electronic transit time only. Nevertheless, Fig. 11 does show the first-order effects of changing source impedance, level, or midband intermediate frequency. At low frequencies where $R_g\rightarrow\infty$, shot noise is the only tube-noise contribution, and the optimum source impedance approaches an open circuit. At higher midband frequencies active grid loading becomes appreciable and there is an optimum source impedance from the noise-figure viewpoint. The optimum source impedance may be obtained by differentiation of the expression for noise figure, and it is

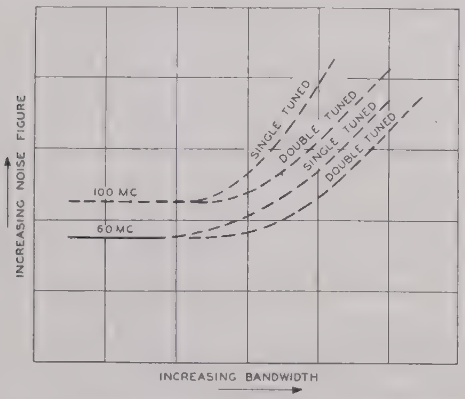

Fig. 12—Optimum noise figure versus bandwidth.

$$R_s\text{ (optimum)} = \sqrt{\frac{R_tR_g}{\left(B+\dfrac{R_t}{R_g}\right)}}. \tag{2}$$

The difference between the curve for $R_g=\infty$ and the curve for $R_g=30{,}000$ or $R_g=10{,}000$ in Fig. 11 represents the noise penalty due to active grid loading. Observe that this penalty becomes small at low source impedances.

Consider now the practical case where grid-circuit capacitance places an upper limit on the impedance which can be built up in a given bandwidth. From this viewpoint the optimum noise figure is related to bandwidth as shown in Fig. 12. (This discussion assumes that the grid-circuit capacitance is held constant at the minimum obtainable value.) When the required bandwidth is small, grid-circuit capacitance is no limitation, and the noise figure is limited by the tube's plate-screen noise and active grid-loading effects. Under this condition the input-circuit step-up should be such as to present the grid with the optimum source impedance. For such narrow bands the noise-figure versus bandwidth relation is a straight line, as shown in Fig. 12. However, when wider bands are required it may prove impossible to build up to the optimum impedance across the grid-circuit capacitance, due to basic network limitations. As shown in Fig. 11, this means degrading the noise figure to a higher value than the best attainable at the given frequency. We may call this condition bandwidth or capacitance limited, because either less bandwidth required or less circuit capacitance will make possible a better noise figure. Bandwidth-limited noise figures are indicated by the rising curves at the right in Fig. 12. Improved circuit efficiencies (which make possible higher impedances in a given bandwidth across a given capacitance) will improve the noise figure when bandwidth or capacitance is limiting. This is represented in Fig. 12 by different curves for single-tuned and double-tuned types of networks.

Another limitation experienced in practical circuits is loss in the network which transforms the source resistance to the resistance R_s which is presented to the grid of the tube. Losses in this transforming network absorb signal energy, but do not change the thermal noise level; therefore, input-circuit losses degrade the amplifier's noise figure. A good general design criterion is that the resistance R_s presented to the tube grid should be due only to the resistance R of the generator and not due to network dissipation. (It might be added that R_g of Fig. 11 is a representation of vacuum-tube grid-circuit conductance; no circuit resistor should be placed in the position occupied by R_g for the reason just given.)

The source of intermediate-frequency signal in the radar for which this amplifier has been designed consists of two 1N26 crystals used in a balanced converter circuit. The intermediate-frequency output of the two crystals is of the same polarity for noise components from the radar's local oscillator, and of the opposite polarity on one crystal relative to the other for desired signal energy. One function of the intermediate-frequency input circuit is to combine the desired signal outputs of the two crystals to produce aiding signal components at the input-tube grid (see Figs. 6 and 13). This involves a phase reversal in one of the transformers (*T50* of Fig. 6). At the same time it is desired that the local-oscillator intermediate-frequency noise components from the two crystals combine to produce zero local-oscillator noise voltage at the input-tube grid. This noise cancellation will take place in the circuit of Fig. 13 if the two source voltages are equal (crystal losses equal) and if the crystal intermediate-frequency resistances are equal. When the crystal intermediate-frequency resistances are unequal, the suppression of local-oscillator noise can be improved by adding an additional impedance Z_2 as shown in Fig. 13. A series of calculations has been made to show the effect of Z_2 on

---

[6] The expression "active grid loading" as used in this paper represents the effects of electronic transit time and lead-inductance feedback effects.

[7] D. O. North and W. R. Ferris, "Fluctuations induced in vacuum-tube grids at high frequencies," Proc. I.R.E., vol. 29, p. 49, February, 1941.

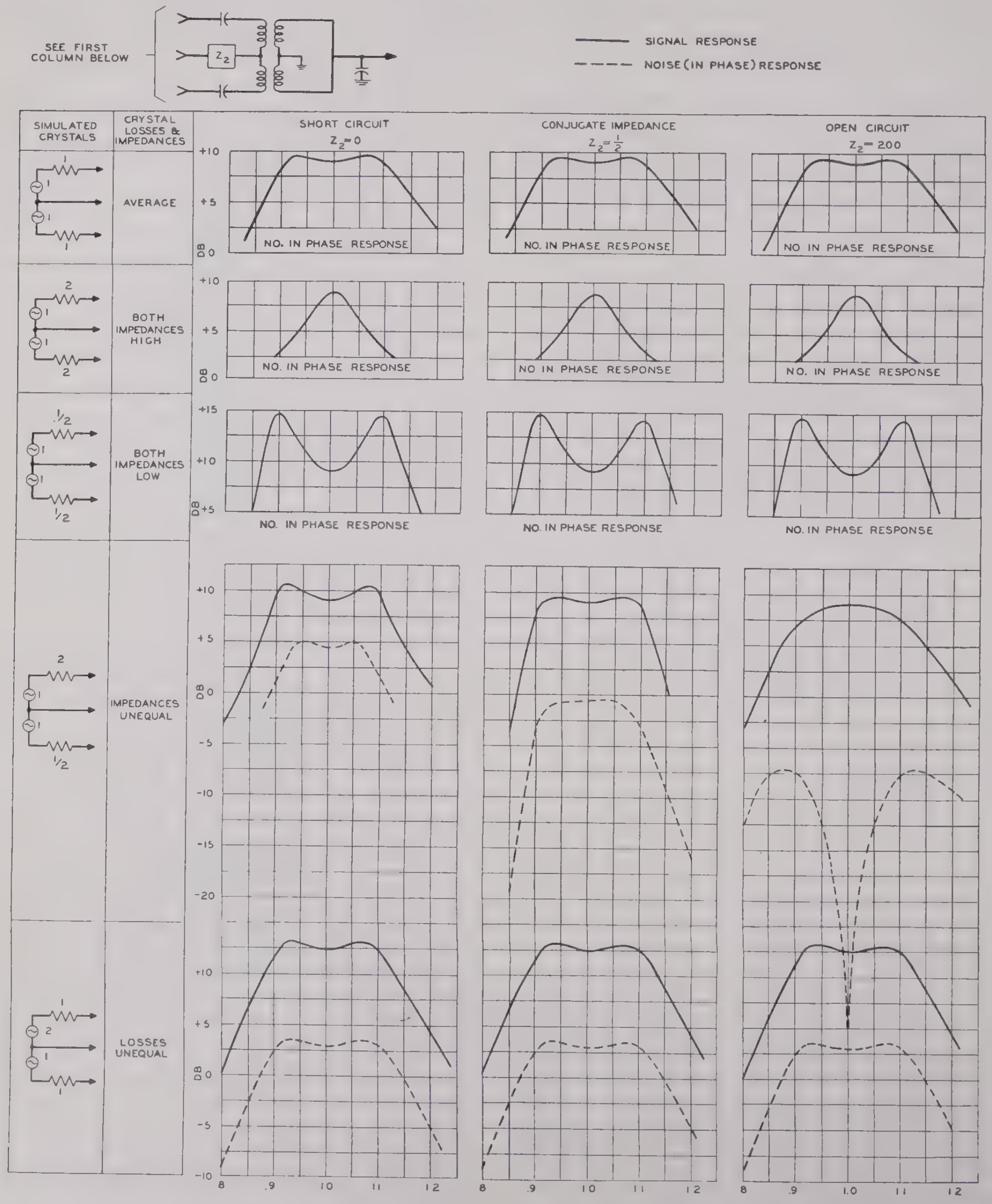

Fig. 13—Balanced-input-circuit signal and noise outputs, effects of Z_2 and crystal variations.

the transmission of the desired signal and on the transmission of undesired noise component. The results are shown in Fig. 13,[8] using unit-impedance and unit-frequency scales. A value of $Z_2 = 200$ is to be interpreted physically as 200 times the source impedance (i.e., essentially an open circuit). Fig. 13 shows that Z_2 has no effect on the circuit performance when the two crystal impedances are equal to each other, even though they may not be equal to the design center value. When two crystal impedances are not equal, a Z_2 approaching an open circuit will best suppress the undesired noise components (in phase on the two crystals). The fact that Z_2 has no degrading effect on signal transmission means that the added protection against local-oscillator noise afforded by Z_2 can be obtained at no expense of signal-to-noise ratio in the intermediate-frequency amplifier.

Viewing the input-circuit design in its entirety, the following series of steps may be considered:

(1) The input-circuit capacitance is minimized by properly arranging the circuit elements and by using inductors with low distributed capacitance.

(2) The losses associated with input-circuit reactance elements or dielectric supports (such as tube sockets) are minimized.

(3) Experimentally, the optimum grid-circuit impedance level is determined for the particular midband intermediate frequency to be used. This may be done by measuring the noise figure of the amplifier at a number of values of input-circuit impedance (R_s of Fig. 11) and plotting the results to estimate the optimum point. The effect of shot noise on amplifier noise figure decreases as the input-circuit impedance level is raised, whereas the effect of active grid loading on noise figure increases as the input impedance is raised. The optimum point is where the ratio of total tube noise to thermal noise is a minimum.

(4) If step 3 results in a bandwidth equal to or greater than the required input-circuit bandwidth, the optimum noise figure for the particular intermediate frequency can be realized in the final design. If the bandwidth is less than that required, the impedance level will have to be reduced, with a consequent degradation in noise figure.

Laboratory measurements of the type outlined above indicate that the optimum impedance level for the 6AK5 pentode is approximately 2000 ohms at 60 megacycles midband, and 1000 to 1500 ohms at 100 megacycles midband.

With the desired input-circuit impedance level established, the problem has been reduced to one of straightforward network design. The impedance of the source in the case of 1N26 crystal is about 450 ohms shunted by a capacitance of about 7 micromicrofarads due to the physical arrangement of parts used to direct the microwave energy into the crystal. Two such crystal sources are used in a push-pull arrangement, with the over-all circuit as shown in Fig. 13 (Z_2 made as large as possible). The arrangement of Fig. 13 can be simplified for the purposes of gain versus frequency calculation by assigning one-half of the grid-circuit capacitance to each of the crystal transformers. When all the dissipation is located at one end of the network, as is approximately the case in the input circuit, a further simplification can be introduced by using the relation

$$\text{Voltage step-up} = 20 \log (R/450)^{1/2} \text{ (decibels).} \qquad (3)$$

Since two networks are to be placed in parallel, the ideal value of R for optimum noise figure (6AK5) at 60 megacycles is 4000 ohms. The ideal input step-up is, therefore, 10 log (4000/450) or 9.5 decibels. Furthermore, an input-circuit bandwidth of about 15 megacycles is desirable in order to allow the over-all amplifier (including band narrowing in all the other tuned circuits) to have a bandwidth of 10 megacycles. Calculations show that these objectives cannot be achieved simultaneously with the network selected.[9] It is necessary to reduce the impedance level slightly and to accept a somewhat narrower bandwidth. The best compromise has been taken as a coupling capacitor of 5 micromicrofarads and a transformer coupling coefficient of 0.2 to 0.25. This results in about 9 decibels voltage step-up from crystal to grid, and a grid-circuit impedance level (including both source impedances) of about 1800 ohms. The resultant circuit arrangement is shown schematically in Fig. 6.

VII. Gain-Control Design

One requirement on the radar intermediate-frequency amplifier not commonly encountered elsewhere is extremely rapid recovery from large overload signals. This means that all grid and cathode circuits must have very short time constants compared to a microsecond to assure rapid decay of self-bias voltages brought on by the flow of grid current under overload conditions. Another requirement on the gain-control design is the large ratio of maximum gain to minimum gain which must be provided in the basic design. In normal operation of the radar it is desirable to be able to reduce the intermediate-frequency gain by as much as 80 decibels, still maintaining a reasonably linear input versus output characteristic.

It is also required, of course, that the bandwidth of the amplifier remain large enough to pass the signal, and in order to permit automatic tuning of the radar local oscillator the midband intermediate frequency must not shift more than a small percentage of the total bandwidth. The change in "hot" capacitance of the grid circuit as the tube's operating point is changed tends to change the tuning of the interstages as the gain control is varied, making the requirements just mentioned difficult to meet in narrow-band amplifiers. Fortunately, in wide-band amplifiers these problems are not serious as long as no attempt is made to hold too much loss in a single gain-controlled stage.

---

[8] The authors are indebted to R. L. Dietzeld of the Bell Telephone Laboratories for deriving an equivalent network and formulas suitable for calculation of this circuit performance.

[9] Double peaking of the gain versus frequency characteristic is considered unsatisfactory because of severe distortions which result from slight mistuning in such a network.

The 6AK5 is a sharp-cutoff pentode, so in order to maintain linearity of response over the large gain-control range required, six tubes have been controlled beginning with the second intermediate-frequency stage. The first intermediate-frequency stage always operates at full gain, in order to prevent degrading the intermediate-frequency noise figure when the gain is reduced to accommodate tube variations. The time constant in each cathode circuit is only 0.11 microsecond, a figure which provides satisfactory decay of overload self biases. The grid-circuit time constant is kept low by providing the gain-control voltage from a cathode follower, thereby maintaining a low resistance from the gain lead to ground. The gain-lead decoupling filters, *Z100*, *Z101*, etc., in Fig. 10, offer low impedance to video frequencies; these filters are wound on 330-ohm resistors in order to keep their *Q*'s low in the video-frequency range.

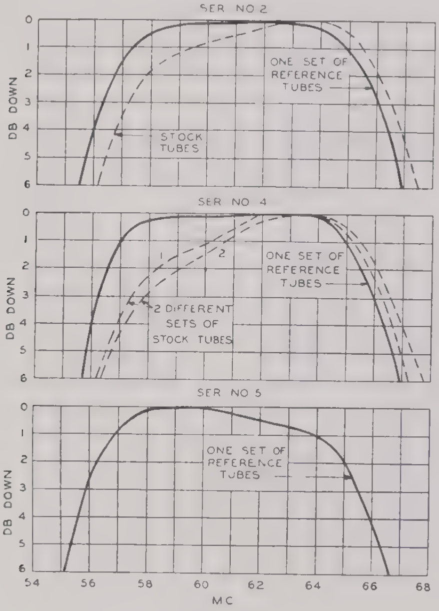

Fig. 14—Measured over-all 60-megacycle gain shapes.

VIII. Detector-Video Circuits

The requirements and reasons for the general design methods employed in the detector and video-circuit design are more closely related to the design of the indicating circuits than to the design of the intermediate-frequency amplifier. However, in practice it is usually convenient to convert to video by the second-detection process and to provide a certain minimum amount of video amplification at the intermediate-frequency amplifier before sending the signal on to the indicator chassis where it is mixed with other voltages for presentation on the radar indicator.

As shown in Fig. 8, the first three tubes of amplifier No. 3 are conventional intermediate-frequency amplifiers using the design previously discussed. The last three tubes perform the functions of second detection, video amplification and limiting, direct-current reinsertion, and cathode-follower output.

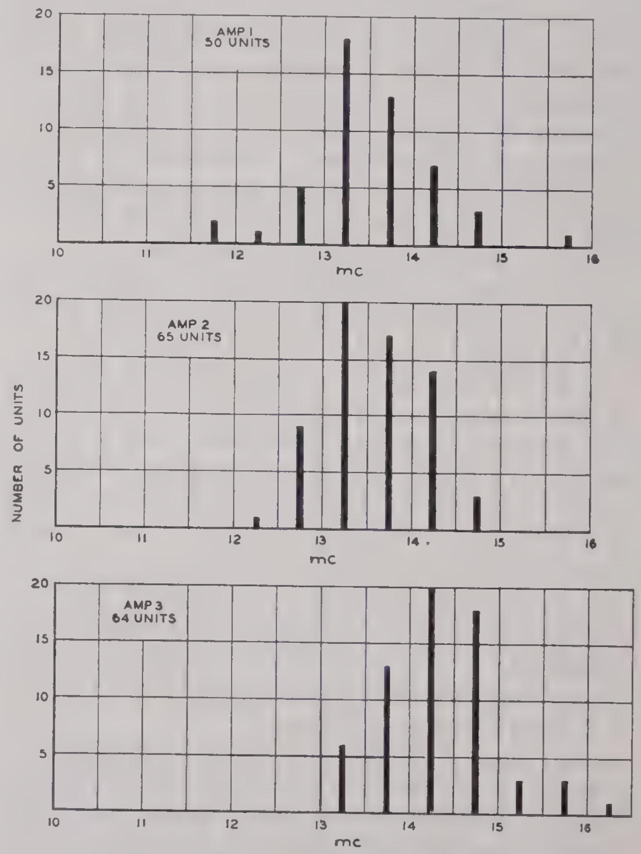

Fig. 15—Bandwidth with stock tubes—60-megacycle preproduction amplifiers.

A conventional diode detector is used because of its excellent linearity over a wide range of signal amplitudes. The output of the diode detector is poled negative with respect to ground so that the following tube, *V154*, may act as a limiter as well as a video-frequency amplifier.

The other half of the double diode, *V153*, is used in the grid circuit of the cathode-follower output tube, *V155*, to provide direct-current reinsertion.

The circuit constants shown in Fig. 8 provide a video output signal limited at about 1.0 to 1.5 volts in an impedance of 72 ohms. Video-amplifier circuits in other parts of the radar are used to further amplify this signal and to present it in a form usable to the radar operator.

IX. MEASURED PERFORMANCE

The over-all gain versus frequency characteristic for the 60-megacycle amplifier is shown in Fig. 14; three typical amplifiers are represented, one with reference tubes only (tubes having input and output capacitances of nominal value ±0.1 micromicrofarads), and the other two with both reference tubes and stock tubes (input and output capacitance tolerances of ±0.5 and ±0.4 micromicrofarads, respectively). Because of the variation in gain versus frequency characteristics possible with different stock tubes, two sets of manufacturing limits are placed on the amplifier performance. A set of narrow limits is used for amplifier test purposes, using reference tubes selected as noted above. Once the amplifier has passed the first set of limits, a set of stock tubes is placed in the amplifier and another recheck made using wider limits. From the standpoint of radar system operation, all of the gain versus frequency characteristics of Fig. 14 (bandwidth 9 to 10 megacycles) are probably indistinguishable in practice.

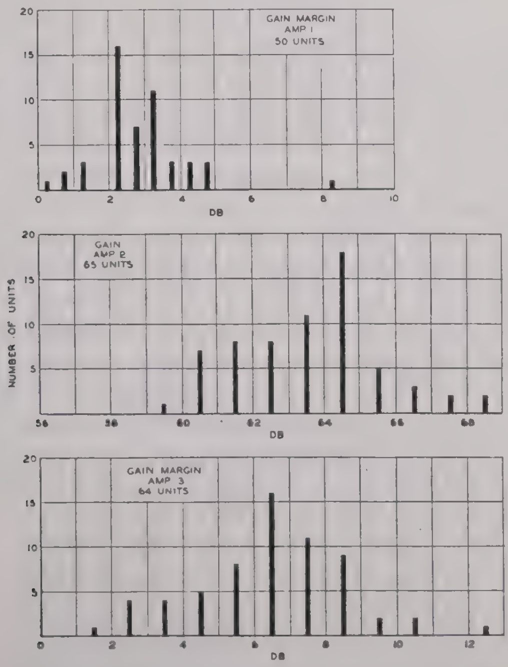

Fig. 16—Gain with stock tubes—60-megacycle preproduction amplifiers.

A summary of the characteristics of the first fifty sets of 60-megacycle amplifiers is given in Figs. 15, 16, and 17. Fig. 15 shows the distribution of bandwidths (3 decibels down from peak gain) for amplifiers Nos. 1, 2, and 3 (intermediate-frequency portion only). The tubes used in these units are unselected stock tubes, made under the JAN specification for the 6AK5.

Fig. 16 shows a similar set of distribution charts, this time with reference to the gains of amplifiers Nos. 1, 2, and 3. In the case of amplifiers Nos. 1 and 3 the term "gain margin" refers to the gain of the unit over and above a minimum acceptable value. The gain of amplifier No. 2 refers to the insertion gain of the unit between 70-ohm source and load impedances.

Fig. 17 shows the distribution of center frequencies for amplifiers Nos. 1, 2, and 3. The center frequency is taken as the average of the frequencies at which the gain is 3 decibels down from maximum. Once again the data shown represent the performance obtained with stock tubes.

As discussed previously, the noise figure is principally determined by the input-circuit design and the first intermediate-frequency tube. For the balanced input circuit already described and a group of seven 6AK5 tubes selected at random, the noise figures measured between 4.3 and 4.9 decibels at 60 megacycles. A similar series of measurements made on the 100-megacycle amplifier, using a single-tuned input circuit having a bandwidth of about 8 megacycles, yields an average noise figure of 5.6 decibels, with a spread from 5.3 to 5.8 decibels on twelve randomly selected tubes.

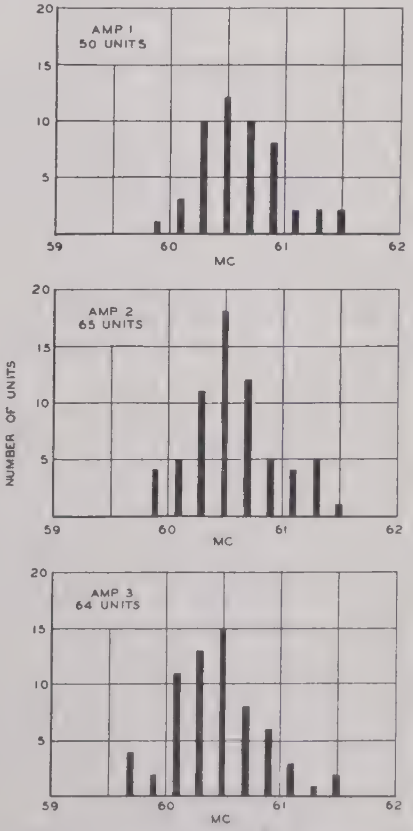

Fig. 17—Center frequency with stock tubes—60-megacycle preproduction amplifiers.

Detectability and Discriminability of Targets on a Remote Projection Plan-Position Indicator[*]

W. R. GARNER[†], AND FERDINAND HAMBURGER, JR.[†], SENIOR MEMBER, I.R.E.

Summary—Quantitative results were obtained on minimum detectable signals and minimum separation between two targets as a function of the following variable factors: video gain, c.r.t. bias, signal clipping, light-source intensity, type of diffraction screen, and position of the operator. The projection (PPI), using a dark-trace tube, appeared to be 1 db worse than a standard 5-inch PPI, when each instrument was operated under its optimal conditions.

INTRODUCTION

A RADAR RECEIVER normally delivers its video output signal to some type of cathode-ray-tube (c.r.t.) indicator. This indicator may be immediately adjacent to the radar receiver or may be remotely located, and, in certain radar systems, several radar indicators may be operated from the same receiver. These remote indicators may take the form of direct repeaters providing, for example, plan-position indication (PPI) or A- or B-scope presentations at a remote location.

In a series of studies recently reported, Haeff[1] studied the effect of several parameters of a radar system on detectability on an A-scope. The factors studied and reported by Haeff are primarily parameters of the radar transmitting and receiving units, and A-scope presentation was used only because it was the most common form of presentation at the time those studies were conducted. Since that time, however, the PPI-type of presentation has become more widely used, and in recent years a projection-type PPI has been developed. This type of indication does not present the c.r.t. picture directly, but rather the picture on a relatively small PPI is reflected and magnified by means of a mirror system so that the picture as it is actually presented to the observer is considerably larger than it is on the c.r.t. face. The development of the projection-type PPI was prompted by the desirability of the larger screen for use where several targets must be tracked simultaneously.

The present investigations were designed to determine the effect of several parameters of the indicating system on the operation of PPI indicators, particularly indicators of the projection type. An attempt has been made to provide answers to the following two questions:

(1) What are the optimum operating conditions for the projection PPI as now constructed?

(2) Is the projection plan inherently satisfactory, or should some other method of obtaining a large presentation be developed?

EXPERIMENTAL SETUP

Radar System

In the studies of detectability, simulated targets were delivered to the radar system from the signal source described below. This signal source consisted of five video-pulse generators whose output was used to pulse a 30-Mc. oscillator. This i.f. signal was attenuated by means of an attenuator calibrated in decibels, and then fed into a mixer stage, as shown in Fig. 1. Simulated noise was also fed into the system at the mixer stage, since with the signals introduced into the second i.f. stage of the radar, the radar noise level was reduced to a negligible value. This noise was generated by simply using a tuned i.f. stage equivalent to the first i.f. stage of the radar receiver.

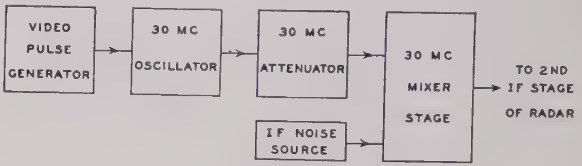

Fig. 1—Block diagram of signal generator.

The radar system used was a long-range ground-search radar system normally operating in the 10-centimeter band. The specifications concerning the microwave characteristics of this system are unimportant for the present purposes since simulated targets were used, and the only characteristics of the particular radar system which have a bearing upon the results of this investigation are those of the radar receiver itself.

The radar receiver used an intermediate frequency of 30 Mc. with an i.f. bandwidth of approximately 1.6 Mc. and a video bandwidth of 1.5 Mc. The receiver consisted of six i.f. stages (of which only five were used, as noted above) plus two video stages. The output of the receiver was fed to the remote PPI's under investigation.

In the studies of discriminability a double-pulse generator was used to pulse the i.f. signal generator. The two pulses were controlled independently and each pulse length could be varied from 1 to 20 microseconds. In addition, the time interval between the two pulses was adjustable.

Plan-Position Indicators

The video output of the radar receiver, together with the necessary synchro and trigger information, was fed simultaneously to three remote PPI units. Two of the three units consisted of the projection-type PPI units to be studied, and the third was a normal 5-inch PPI used as a standard of comparison.

---

[*] Decimal classification: R537. Original manuscript received by the Institute, October 1, 1946; revised manuscript received, January 6, 1947. This research was started under terms of Contract No. OEMsr-658 between the Office of Scientific Research and Development and Harvard University, under the supervision of the National Defense Research Committee. The research was continued under Task Order No. 1 of Contract N5ori-166 between the Office of Naval Research of the Navy Department and The Johns Hopkins University.

[†] The Johns Hopkins University, Baltimore 18, Md.

[1] Andrew V. Haeff, "Minimum detectable radar signal and its dependence upon parameters of radar systems," PROC. I.R.E., vol. 34, pp. 857–861; November, 1946.

The projection PPI units made use of a dark-trace c.r.t. (4AP10) on which targets appear as dark purple marks against a milk-white background. The light from a 1000-watt projection bulb is focused onto the tube face, and this light is in turn reflected onto a concave mirror. The concave mirror projects the light onto a second mirror, which in turn projects it onto the viewing surface. This viewing surface is composed merely of some sort of diffracting material, so that the image appears to be on the surface of the viewing area. The surface is either a flashed-opal screen, or a clear-glass screen covered with a white paper which acts as the diffracting agent. The arrangement described provides a viewing screen 25 inches in diameter, on which targets appear as dark spots against a fairly bright white background. The original tube-face diameter in this instance is 4 inches, which means that the system provides an area magnification of approximately 39 times. The remote PPI used as a standard of comparison consists of a 5-inch c.r.t. (5FP7).

EXPERIMENTAL METHOD

Observers

Six trained radar operators were used as subjects in the experiments. Three men served as operators while three served as recorders, and a rotation of positions occurred every 30 minutes. The rotation was so planned that each of the six men served as operator on each instrument for each experiment.

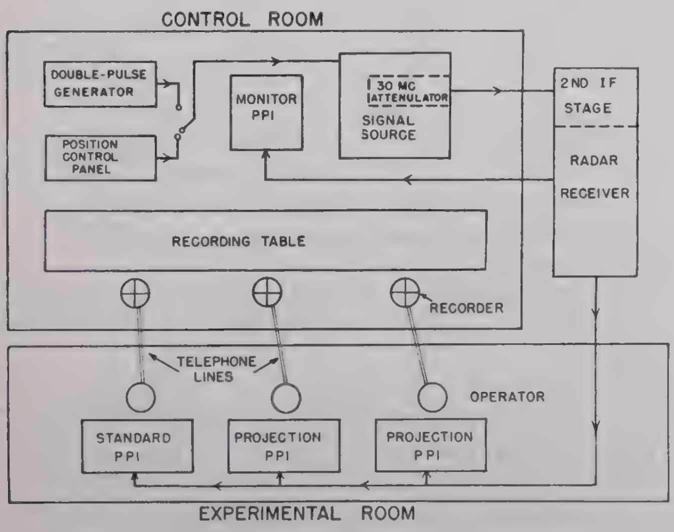

Fig. 2—General experimental equipment and layout.

Each operator was connected by a telephone circuit to a recorder. The recorder was provided with a check sheet indicating the pre-planned positions of the targets, and when an operator identified a target the recorder noted the target conditions for that target at the time of observation. The target condition was made known to the recorders by the experimenter who controlled the targets throughout the experiment. The general layout of the equipment is shown in Fig. 2.

Target Conditions

Detectability Tests: Five targets were presented simultaneously but were so controlled in intensity that the five targets were successively 1 db weaker. The over-all intensity of the targets was increased 1 db for each revolution of the antenna, so that each target would appear in a successive revolution if all targets became visible at the same intensity.

Each operator searched for targets in a clear field. Initially, no targets would be visible, and gradually the targets would increase in strength until located by the operator. When all operators had reported all five targets, the targets were removed and a new series begun. At no time would the operators know where the targets were to appear; it was necessary for them to search continuously over the PPI screen.

Discriminability Tests: Targets were presented as two continuous lines following the sweep around the c.r.t. These lines were produced by the double-pulse generator, and before each run the two pulses were adjusted for the proper range and pulse length. When the pulses were first turned on they coincided and as the sweep continued around the tube the pulses were moved farther and farther apart by the experimenter. As soon as each observer saw the pulses separate on the c.r.t. he called that information to the recorder at the other end of the telephone circuit, and the recorder was then able to indicate the actual separation of the two pulses at the time they were observed to separate. The separation was measured by means of a calibrated oscilloscope. Each run was repeated at four different ranges.

Test Constants

Detectability Tests: Background noise level was adjusted by means of the noise generator at half the value required to saturate the receiver at full gain. In other words, signals were twice as high as the noise-peaks when the signal saturated the receiver. This is the condition which is arbitrarily referred to as a detectability level of zero decibels throughout this investigation.

Antenna rotation rate, lobe width, and pulse length were maintained constant throughout the experiment at the following values: antenna rotation rate, 5 revolutions per minute; lobe width, 20 degrees; and pulse length, 1.5 microseconds.

The antenna rotation rate was controlled by the radar system, which provided the synchro information for the remote PPI's. This same synchro signal was used to control the lobe width of the targets, by means of a gradual gating system. The targets were thus turned on and off gradually in a manner characteristic of real radar targets. The pulse length was determined by the characteristics of the signal generator. The experiments were also conducted at constant cathode-ray sweep time corresponding to the twenty-mile range of the PPI, and at a constant pulse repetition frequency of approximately 500 pulses per second.

Discriminability Tests: Preliminary studies indicated that only one factor had any serious effect upon discriminability. Thus, the only factor reported here is that of pulse length. All other factors were held constant.

Compilation of Data

Detectability Studies: In the curves to follow, each plotted point represents the average of at least thirty observations. Each operator made at least five observations for each condition studied, which means that a minimum of thirty observations was available for each point on the curve. Whenever any condition was changed, another thirty observations was made. In many cases certain duplications of conditions existed, making sixty or ninety observations available for averaging at a given point. The maximum available number of observations for averaging was always used in computing average detectability scores.

Discriminability Studies: A total of twenty-four observations was made for each condition, and all were used in computing the average discriminability score.

Measurements

The two most important measurements of the system during the present investigation are those of cathode-ray-tube bias and video gain.

The cathode-ray-tube bias was measured by means of a calibrated DuMont type 208 oscilloscope. The grid and cathode of the cathode-ray tube of the PPI were connected directly to the vertical plates of the oscilloscope. The generated sweep of the PPI was used to provide the horizontal deflection of the oscilloscope. Thus a trace appeared on the oscilloscope only when the unblanking voltage was applied to the cathode-ray tube of the PPI, giving a reading on the oscilloscope of the grid-to-cathode voltage of the PPI during its "on" period. The oscilloscope showed not only the bias voltage but also the video signal (and video gain, as well).

The video gain measurement was based on the position of the linear input potentiometer of the video system of the PPI. Full gain corresponds to maximum input voltage from this potentiometer to the video amplifier, and this setting corresponds to zero decibels video gain as defined later.

RESULTS

Studies of Detectability

Detectability is that property of a target on a radar indicator which enables it to be seen by an operator. If, for example, a target may be seen at a lower signal intensity (video input to the indicator) under condition "A" than under condition "B," then under condition "A" the targets are more detectable. Thus, if under condition "A" targets are 3 db more detectable than under condition "B," the signal intensity under condition "A" may be 3 db less than under "B," but the targets would still be detectable. It should be remembered that all these measurements were made with a fixed noise level, so that the detectability scores are, in effect, measures of a signal-to-noise ratio. Furthermore, when reference is made to an increase in the gain of the video signal, it should be remembered that the increased gain occurs for the noise as well as the signal, which means that there is no necessary increase in detectability, since if the noise increases proportionately with the signal the ratio of the signal energy to the noise energy has remained constant. However, as we shall see later, the signal-to-noise ratio required for a just-detectable signal can be changed by a change in the over-all video signal level.

The reference level for the decibel scale of detectability used throughout this study was defined in the following manner. A detectability of zero db represents a signal strength just large enough to saturate the radar receiver at full gain. For example, if a target can be observed when the signal intensity is just sufficient to saturate the receiver, the detectability score would be zero db. If, however, the target was visible with a signal 6 db lower than necessary to saturate the receiver, the detectability score would be +6 db.

Before proceeding to an actual investigation of detectability of the PPI an analysis was made of those factors that might be expected to have an influence on detectability. Certain of these factors were selected for this investigation, leaving others for future study. The factors investigated were:

(a) Video gain of the projection-PPI video system.
(b) Bias of the signal grid of the cathode-ray tube.
(c) Clipping of the video signal prior to its input to the PPI video system.
(d) Type of viewing screen.
(e) Intensity of light reflected from face of the cathode-ray tube.
(f) Target position on the viewing screen.

Factors not studied in this investigation, all of which may have an effect on detectability, are:

(a) Pulse-repetition frequency.
(b) Sweep length.
(c) Pulse length.
(d) Antenna rotation rate.

Detectability Study Results

(a) *Effect of Video Gain:* Since a specific remote projection PPI was under study, the video gain of the system is expressed in db with a reference of zero decibels corresponding to full gain of the PPI video-amplifier system, without regard to the actual voltage gain of the video amplifier itself. With respect to the noted arbitrary reference, other values of gain are expressed in terms of the change in input voltage to the video amplifier of the PPI system. Thus a video gain of −6 db means that the input voltage to the amplifier itself is one-half the value required for zero db gain.

The results of this study are shown in Fig. 3. It will be noted that, for the two larger values of cathode-ray-tube signal-grid bias, detectability improves with increased video gain. For the smaller value of bias, video gain in excess of −9 db fails to improve detectability. With fairly large values of bias, however, detectability improves with increasing video gain up to the point of maximum gain.

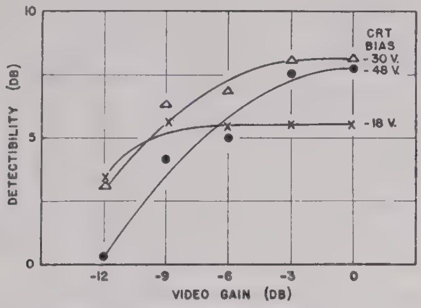

Fig. 3—Effect of video gain on detectability with projection PPI: opal viewing screen, unclipped signal, normal light intensity.

The results just referred to were obtained with signal levels so adjusted that no limiting took place prior to the introduction of the signal to the video input of the projection PPI. The video system of the projection PPI itself incorporates limiting which prevents the grid-to-cathode signal of the cathode-ray tube from becoming positive by more than a few volts. Under the conditions studied here, the best detectability was obtained only when the grid of the cathode-ray tube was actually being driven positive a slight amount, which means that the limiting level of the projection PPI had been reached.

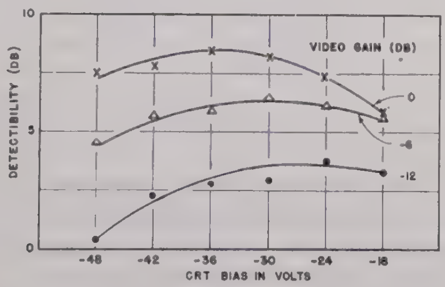

Fig. 4—Effect of cathode-ray-tube bias on detectability with projection PPI: opal viewing screen, unclipped signal, normal light intensity.

(*b*) *Effect of Cathode-Ray-Tube Bias:* The effect of the cathode-ray-tube (signal-grid) bias for several values of video signal level is shown in Fig. 4. There is some change in detectability with bias, leading to the conclusion that for each value of video signal there is an optimum value of bias. This optimum value of bias becomes smaller as the video signal becomes weaker. It should be further observed that the effect of bias on detectability is not nearly so great as the effect of video gain.

An examination of Figs. 3 and 4 indicates that a small value of bias can increase detectability for low values of video gain, and that high values of gain can increase detectability for large values of bias. This general "compensation" effect is never perfect, and consequently there is always an optimum gain and an optimum bias for that gain. Detectability is always greatest under this combined optimum condition.

(*c*) *Effect of Clipping the Video Signal:* A limiter is sometimes inserted between the radar receiver and the remote PPI. In this study of the effect of limiting, the peak-to-peak input signal to the PPI was limited to 2.5 volts. Thus the top clipping that could be achieved was when the gain of the radar receiver was increased to maximum. The effect of limiting is to flatten the top of both signal and noise peaks, to make the signal steadier by elimination of the random fluctuation of the peak of the signal, and to slightly widen the signal pulse.

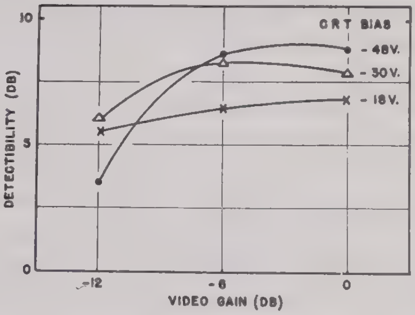

Fig. 5—Effect of video gain on detectability with projection PPI: opal viewing screen, clipped signal, normal light intensity.

A comparison of the detectability for clipped and unclipped signals can be made by an examination of Figs. 3 and 5, which show detectability scores for the two conditions. The effect of video gain on detectability is observed to be less pronounced in the case of the clipped signals. The curves for all three values of cathode-ray-tube bias are flatter for the clipped signals, and it is particularly apparent that there is practically no change in detectability for an increase in video gain beyond −6 db.

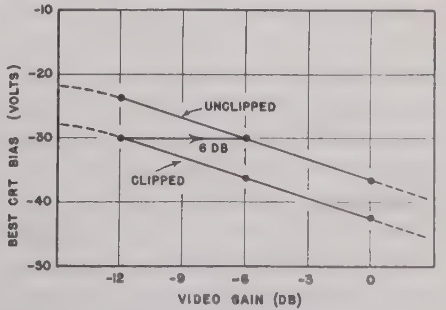

Fig. 6—Effect of video gain on optimal cathode-ray-tube bias with clipped and unclipped signals on projection PPI.

A study of the relationship between video gain and cathode-ray-tube bias for the clipped and unclipped signal is shown in Fig. 6. These curves show the relation between optimal bias and video gain, and also that a lower value of bias is required for lower video gain in both cases but that, for a given bias, less gain (by 6 db) is required for the clipped signals.

The data thus far presented would indicate advantages in the use of clipped signals. On the other hand, certain disadvantages were apparent in the actual study that make clipping of doubtful value. When the video signal is clipped, the peak of the signal never exceeded the peak of the noise for the level used, so that no great contrast is possible between signal and background (noise). Even though the detectability is better with clipped signals, the targets never stand out as well against the background, and very strong targets do not appear much differently than do relatively weak targets.

(*d*) *Type of Viewing Screen:* The investigations reported above were all carried out using an opal-glass viewing screen on the projection PPI. A clear-glass viewing screen covered with white paper has also been used with this type of PPI, and a comparison of the detectability with the two types of viewing screen was made.

Experiments similar to those described above were repeated with a paper viewing screen. The results indicated that the effect of the aforementioned factors on detectability was the same with either type of viewing screen, but that the detectability with the paper viewing screen was considerably poorer than with the opal-glass screen. The difference obtained apparently resulted from an increase in glare when the paper screen was used.

(*e*) *Reflected Light Intensity:* In order to investigate the relationship of detectability to the light intensity focused onto the face of the cathode-ray tube, provision was made for control of the lamp voltage from 70 to 130 volts. It is appreciated that this means of control will affect the spectral composition of the light output from the lamp, but for the purposes of this investigation that effect was not considered serious.

The results of this study showed that there was a maximum change in detectability of 1 db over the range studied, and that this much change did not occur until the limits of voltage range were reached. Thus the effect of light intensity on detectability may be considered negligible.

(*f*) *Effect of Target Position:* Under operating conditions of a radar system targets appear at random range and bearing, and this same randomization was maintained throughout these tests. Thus it is interesting to determine the effect of range and bearing on detectability, since this effect is readily determined from an analysis of data obtained for other purposes.

The effect of range is clearly evident in Fig. 7. For the 40,000-yard range used it is evident that detectability is best in the middle of the range from about 10,000 to 30,000 yards, and poorest at the edge or middle of the viewing screen. At the middle or center of the viewing screen the decreased detectability probably results from the increased darkening common at screen centers, together with the fact that, with constant lobe width, targets are smaller at the center of the screen. The decreased detectability at the outer edge of the screen results from weaker targets, due to the increased angular velocity of the sweep. Note that in these experiments the sensitivity time-control circuits were operated so as to have a minimum effect. The explanation of poorer detectability at the edge as a function of angular velocity would lead to the conclusion that progressive improvement in detectability should occur with decreasing range. Since this is not the case, the poor detectability at the screen edge must be partially a result of an "attention factor" on the part of the operator, whose tendency is to watch the sweep more closely at the center than at either edge. This is particularly the case where such a large surface (25 inches diameter) must be kept under observation.

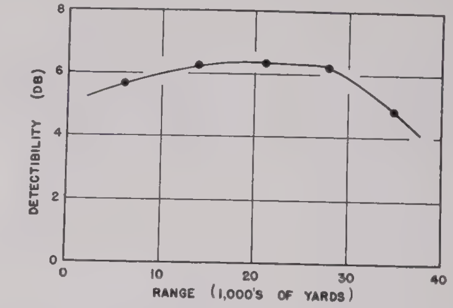

Fig. 7—Effect of range on detectability with projection PPI: opal viewing screen.

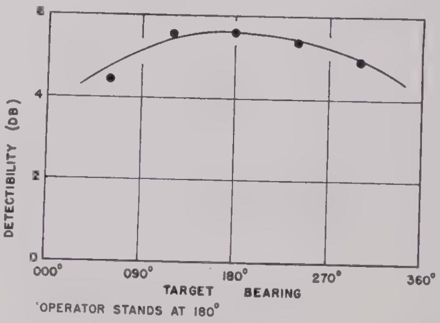

Fig. 8—Effect of bearing on detectability with projection PPI: opal viewing screen.

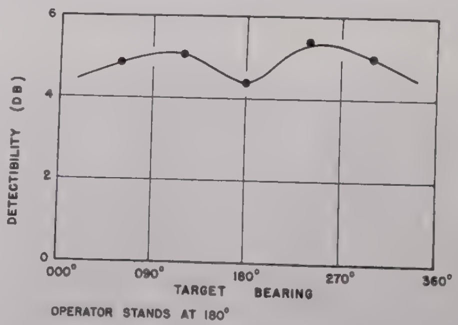

Fig. 9—Effect of bearing on detectability with projection PPI: paper viewing screen.

In considering the effect of azimuth on detectability, both the opal-glass and paper viewing screens were used. The results are given in Figs. 8 and 9, and in examining these figures it should be observed that the operator was always stationed at the 180-degree position. With the opal viewing screen, detectability is best for targets nearest the operators (150 to 210 degrees). Thus, the operator normally finds most easily the targets nearest his position, and most poorly the targets most distant. The differences are not large and may be due in part to "attention factors." With the paper viewing screen, targets are most difficult to detect near the operator (Fig. 9). This striking difference between the two screens is most certainly due to glare. The opal screen is slightly darkened, reducing glare quite effectively; such is not the case with the white screen, and glare is less when the surface is observed at an angle than when viewed directly.

Comparison of Standard and Projection PPI

Detectability has been shown to be a function of cathode-ray-tube bias and video gain for the projection PPI. A similar set of data were taken simultaneously on a standard PPI. These data are shown in Fig. 10 and, as was expected, the variables affect detectability in about the same way for both types of indicators. Actually, when both are operated under their optimum conditions, the standard PPI is about 1 db better than the projection type—not at all a serious difference to pay for the other advantages of the projection device.

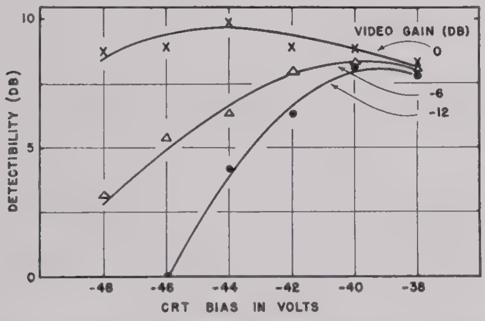

Fig. 10—Effect of cathode-ray-tube bias on detectability with standard PPI.

Studies of Discriminability

In the investigations of discrimination between targets it is necessary to determine the effect upon discriminability of all those factors which were found to have an appreciable effect on detectability. In the preliminary studies the only factor which was found to have a serious effect was that of pulse length, a factor not studied in relation to detectability, and that is the only factor which will be discussed here.

Effect of Pulse Length

Discriminability was measured in terms of the minimum time between pulses necessary for the pulses to be seen as distinct. The measures thus obtained may then be translated into measures of range discrimination, since the smallest range that can be discriminated will be determined by the duration of the pulse, plus the minimum time between successive pulses necessary for them to be seen as distinct. The results are shown in Fig. 11 in this manner.

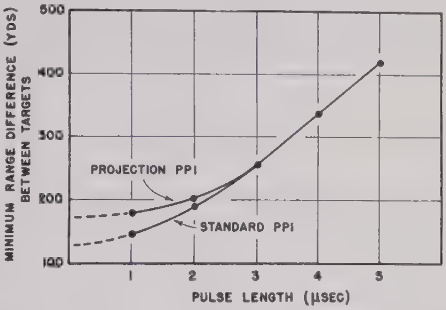

Fig. 11—Effect of pulse length on smallest detectable range difference.

It can be seen that for pulse lengths 3 microseconds and longer, not only is there no difference between the two PPI's, but the slope of the line is linear, indicating that the minimum time separation between pulses is independent of the actual pulse length. In other words, for pulse lengths above 3 microseconds, the minimum range discrimination between targets is dependent almost entirely on the pulse length. For pulse lengths shorter than this, however, the minimum range discrimination does not decrease in proportion to the decrease in pulse length, and the standard PPI becomes better than the projection PPI.

An extrapolation of the two curves would suggest that range discrimination could be improved on the standard PPI if pulse lengths shorter than 1 microsecond were used, although little improvement would result in the case of the projection PPI.

CONCLUSIONS

Detectability of targets on the projection PPI has been shown to be a function of both the cathode-ray-tube bias and the video gain. Increasing the general level of the video signal to the point at which the signal is clipped provides few advantages and some disadvantages.

The use of an opal viewing screen with the projection PPI has been shown to be better than the use of a paper screen over clear glass, primarily because of the glare emitted when the white paper screen is used. The intensity of the reflected light, on the other hand, has practically no effect on detectability over a wide range of intensities.

Testing Repeaters with Circulated Pulses*

A. C. BECK†, SENIOR MEMBER, I.R.E., AND D. H. RING†, ASSOCIATE, I.R.E.

Summary—**An extension of square-wave and pulse-testing techniques is described which permits the signal pulse to be observed after circulating many times through the transmission system under test. This method is particularly useful for measuring the cumulative effect of a number of similar units, such as those used in carrier or microwave-radio-repeater systems, when only one unit is available. Applications to video-frequency, intermediate-frequency, and radio-frequency testing with a.m. or f.m. signals are discussed.**

I. INTRODUCTION

THE ADVENT of television, facsimile, frequency modulation, and pulse modulation has placed new and more stringent distortion requirements on communication systems. For the satisfactory operation of these newer methods of communication, transient signals must be faithfully reproduced. Transient response is a complicated function of the amplitude versus frequency, phase versus frequency, and linearity characteristics of the system. Thus a knowledge of the bandwidth and harmonic distortion of a transmission circuit is inadequate to determine the distortion of transient signals sent through it.

These considerations have led to the development of square-wave and pulse testing techniques with which the transient response may be observed directly. A simple method of observing the transient response of an amplifier or repeater is to connect a pulse-modulated signal source to its input, and an oscilloscope to its output. If the oscilloscope sweep is synchronized with the pulse rate, a stationary picture of the response to pulse signals is obtained on the screen. Since the observed response is a complicated function of what might be called the fundamental steady-state characteristics of the apparatus being tested, such methods are most valuable for comparing different designs and for over-all qualitative tests of complete systems.

In communication systems involving a number of similar repeaters, the distortion permissible in a single repeater is very small, and it is therefore difficult to measure. Furthermore, the chief interest is in the accumulated distortion due to many similar repeaters. G. W. Gilman of Bell Laboratories suggested that information about such systems could be obtained by sending a pulse through one repeater many times before observing it. A method of doing this, which has proved to be very useful in the study of components and repeaters for microwave relay systems, is described in this paper.

II. FUNDAMENTALS OF CIRCULATED-PULSE TESTING

Fig. 1 shows a schematic diagram of a circuit which may be used for circulated-pulse testing. The transmission circuit under test is inserted in a loop consisting of a delay line, an attenuator, and an auxiliary amplifier indicated by the box marked "gated amplifier." The test pulse is introduced into the loop at the input to the equipment under test, and a sample of the output is removed from the loop and connected to the viewing circuit. The major portion of the output is fed through the delay line, attenuator, and gated amplifier back into the input. The delay in the loop circuit is made greater than the duration of the test pulse, and the gain around the loop is made unity. Under these conditions a single pulse inserted in the loop will circulate around the loop indefinitely, and the viewing oscilloscope will show a succession of pulses which are each spaced along the sweep by the total delay time of the loop circuit. Each successive pulse on the oscilloscope shows the original pulse after another trip around the loop and, therefore, another trip through the amplifier or repeater under test.

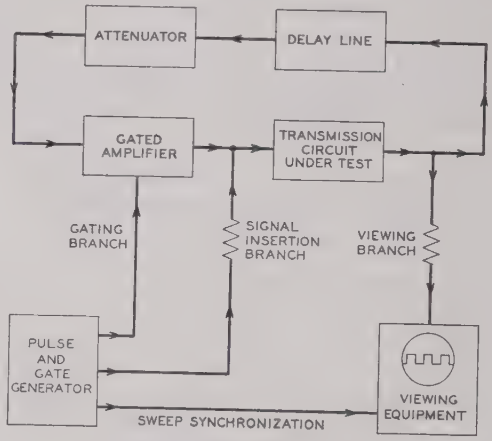

Fig. 1—Block diagram of the fundamental circuit for circulated-pulse testing.

If the test pulse is made recurrent, in order to obtain a stationary picture built up of many superposed traces on the viewing oscilloscope, trouble will be encountered because pulse number one will still be circulating around the loop when pulse number two is inserted. It is the function of the gated amplifier to obviate this difficulty. This amplifier is arranged so that its gain is normally much less than unity. Just before a test pulse is inserted into the loop, a "gate" voltage is applied to the gated amplifier. This gate voltage raises the loop gain to unity and holds it there for a period which is many times greater than the loop delay, but less than the test-pulse repetition time. Thus, the test pulse continues to circulate for the duration of the gate signal. When the gate voltage is removed, the loop gain drops to much less than unity and the circulating pulse is quickly damped out, so that the loop circuit is free from signals when the gate voltage is reapplied and a new test pulse is introduced.

---

* Decimal classification: R200. Original manuscript received by the Institute, October 31, 1946; revised manuscript received, February 14, 1947.

† Bell Telephone Laboratories, Inc., Holmdel, N. J.

The circuit of Fig. 1 will be recognized as a feedback circuit, and, in general, would be expected to break into oscillation as the gain approaches unity. However, oscillations require a building-up process. In the present case, the relatively long delay time of the loop circuit so extends the build-up time that the periodic reduction of gain by the gated amplifier prevents the build-up of any continuous oscillation. In practice it has been found that it is entirely practical to operate the loop at unity or even slightly more than unity gain without any sign of instability or the erratic performance usually associated with circuits operated near the oscillation point.

The transmission circuit under test may include frequency conversion and equipment operating at another frequency, if reconversion to the original frequency is also included.

All the elements of the loop must have negligible distortion compared to that in the transmission circuit under test, since the total distortion of the pulse on each trip around the loop is actually observed on the oscilloscope.

The necessary loop delay may be obtained by inserting a length of transmission line or a radio link. In any case, the phase and amplitude of the delay unit should be equalized over the frequency band used.

The points at which the signal insertion and viewing branches are connected to the loop are arbitrary. As shown in Fig. 1, the signal is inserted at a low-level point in the loop, so that a relatively small pulse voltage is required. The viewing branch is shown connected to a high-level point, so that less amplification is necessary to get a satisfactory oscilloscope deflection. When this is done, the test pulse cannot be observed until it has made one trip through the amplifier or circuit under test. If enough high-quality amplification is provided in the viewing branch, both branches can be connected to the loop at the same point, and one can monitor the test-pulse shape directly.

On the block diagrams, resistors are shown in the test branches to indicate that the connections are made by bridging circuits which do not disturb the impedance terminations of the equipment in the loop.

III. Radio- and Intermediate-Frequency Testing with Amplitude Modulation

A block diagram of the arrangement used at Holmdel for circulated-pulse testing with amplitude modulation at radio and intermediate frequencies, together with a timing diagram for the equipment, is shown in Fig. 2. The circuit under test is connected in a loop with an equalized coaxial or wave-guide delay line, an attenuator, and a gated carrier amplifier. A relaxation oscillator

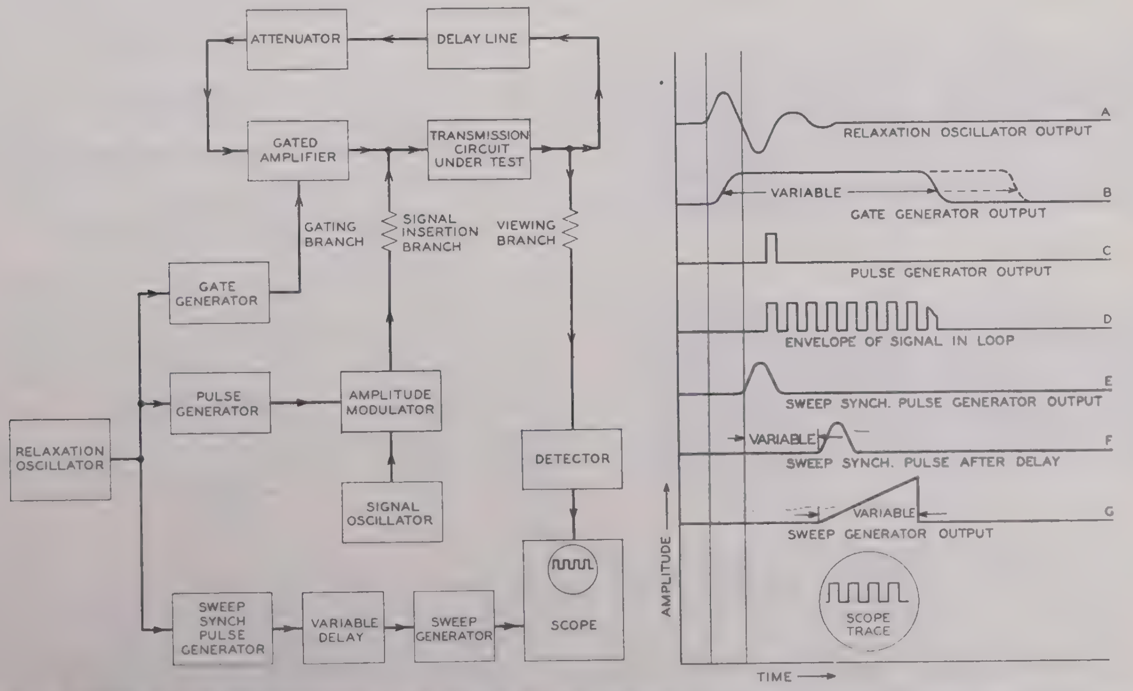
ATTENUATOR
DELAY LINE
GATED AMPLIFIER
TRANSMISSION CIRCUIT UNDER TEST
GATING BRANCH
SIGNAL INSERTION BRANCH
VIEWING BRANCH
GATE GENERATOR
PULSE GENERATOR
AMPLITUDE MODULATOR
RELAXATION OSCILLATOR
DETECTOR
SIGNAL OSCILLATOR
SCOPE
SWEEP SYNCH PULSE GENERATOR
VARIABLE DELAY
SWEEP GENERATOR
A
RELAXATION OSCILLATOR OUTPUT
VARIABLE
B
GATE GENERATOR OUTPUT
C
PULSE GENERATOR OUTPUT
D
ENVELOPE OF SIGNAL IN LOOP
E
SWEEP SYNCH. PULSE GENERATOR OUTPUT
VARIABLE
F
SWEEP SYNCH. PULSE AFTER DELAY
VARIABLE
G
SWEEP GENERATOR OUTPUT
AMPLITUDE
SCOPE TRACE
TIME

Fig. 2—Block diagram and timing arrangement for a method of circulated-pulse testing at i.f. and r.f. using amplitude modulation.

which produces about 3000 damped oscillations per second is shown at the left side of the diagram. This oscillator controls the sequence of operations and triggers the gate, signal pulse, and sweep-synchronizing generators. The output wave form of the relaxation oscillator is shown at A on the timing diagram. The start of each oscillation initiates the gate-generator output voltage pulse shown on line B, which is applied to the gated amplifier, thus raising the loop gain to the operating level. The signal-pulse generator is arranged to produce a rectangular pulse about 1 microsecond in length which starts about 2 microseconds after the relaxation oscillator reversal, as shown on line C. This pulse modulates the r.f. or i.f. signal generator to produce the test signal applied to the loop. A detector is used in the viewing branch to obtain the rectified envelope of the loop signal, as shown on line D. The signal circulates to give successive pulses, each of which represents one more trip around the loop, until the gate generator voltage B drops. The circulating pulses are then quenched by the reduced gain of the gated amplifier. The time at which this happens can be adjusted to suit the number of transits being observed by adjusting the length of the gate pulse. The reversal of the relaxation oscillator also causes the generation of a sweep-synchronizing pulse, shown on line E. A variable delay unit is used to delay this pulse, as shown on line F, when it is desired to view later trips around the loop. A single sweep of variable length is initiated by this pulse.

If the variable delay is set at zero the first signal pulse can be seen, since the 2-microsecond delay shown on line C permits the sweep to get started before the signal appears. The sweep can be made fast enough to show a single signal pulse, and enough delay is available to view it as a single pulse at any time up to 80 transits around the loop. Slower sweeps show several transits at once on the oscilloscope.

In the simplest case the gated amplifier, signal modulator, delay line, and monitoring detector are designed to work at the operating frequency of the circuit under test. This is not essential, however. Complete radio repeaters which include r.f. and i.f. amplification may be tested with equipment designed to operate at either frequency.

When frequency changing is included in the loop, care must be exercised in selecting the beating oscillator frequencies to avoid inversion of the sideband frequencies on successive trips around the loop. If inversion is permitted, certain types of unsymmetrical distortion are canceled out, and an optimistic result is obtained. Intermediate-frequency test equipment may also be used for testing audio or video circuits by providing a detector at the input and a modulator at the output of the low-frequency circuit. One method of doing this will be found in Section V.

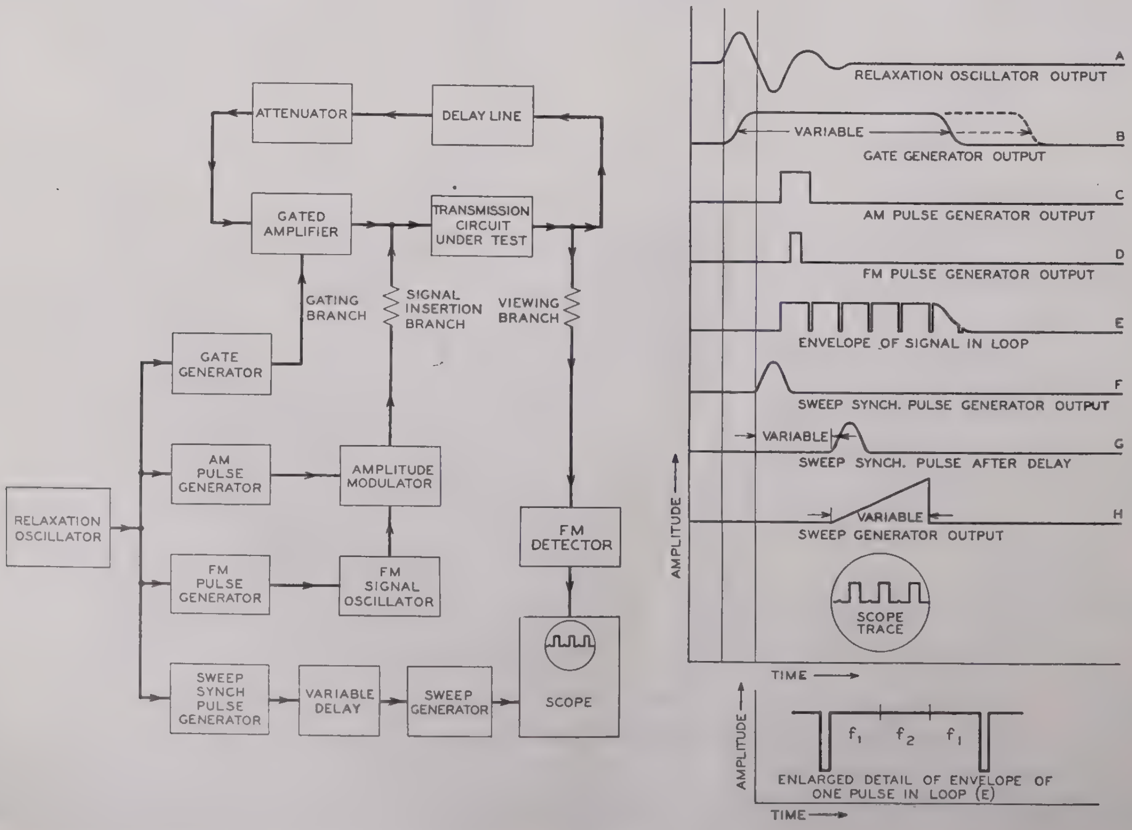
ATTENUATOR
DELAY LINE
GATED AMPLIFIER
TRANSMISSION CIRCUIT UNDER TEST
GATING BRANCH
SIGNAL INSERTION BRANCH
VIEWING BRANCH
GATE GENERATOR
AM PULSE GENERATOR
AMPLITUDE MODULATOR
RELAXATION OSCILLATOR
FM PULSE GENERATOR
FM SIGNAL OSCILLATOR
FM DETECTOR
SWEEP SYNCH PULSE GENERATOR
VARIABLE DELAY
SWEEP GENERATOR
SCOPE
A
RELAXATION OSCILLATOR OUTPUT
VARIABLE
B
GATE GENERATOR OUTPUT
C
AM PULSE GENERATOR OUTPUT
D
FM PULSE GENERATOR OUTPUT
E
ENVELOPE OF SIGNAL IN LOOP
F
SWEEP SYNCH. PULSE GENERATOR OUTPUT
VARIABLE
G
SWEEP SYNCH. PULSE AFTER DELAY
VARIABLE
H
SWEEP GENERATOR OUTPUT
AMPLITUDE
SCOPE TRACE
TIME
AMPLITUDE
f1 f2 f1
ENLARGED DETAIL OF ENVELOPE OF ONE PULSE IN LOOP (E)
TIME

Fig. 3—Block diagram and timing arrangement for a method of circulated-pulse testing at i.f. and r.f. using frequency modulation.

IV. RADIO- AND INTERMEDIATE-FREQUENCY TESTING WITH FREQUENCY MODULATION

Circulated-pulse testing with frequency-modulated pulses has been carried out as shown in Fig. 3. The block diagram is like Fig. 2, except that a box marked "FM Pulse Generator" has been added, and the signal oscillator is arranged so that it can be frequency-modulated by the f.m. pulse. Arrangement and timing of the relaxation oscillator and gating system are the same as for amplitude modulation, and are shown on lines A and B of the timing diagram. The a.m. pulse, which starts 2 microseconds after the relaxation oscillator reversal, has a duration approximately equal to the loop delay in this case, as shown on line C of the timing diagram. The f.m. pulse has a duration about half as long, and is started a little later, so that it coincides with the center of the a.m. pulse, as shown on line D. Thus, the signal which is applied to the loop has its amplitude controlled by the a.m. pulse, and its frequency controlled by the f.m. pulse. The rectified envelope of the loop signal is shown on line E. An enlarged representation of one pulse is shown at the bottom of the timing diagram. A signal of frequency f_1 is introduced into the loop when the a.m. pulse starts. The signal frequency is then suddenly changed by an amount depending on the desired deviation ratio to frequency f_2 when the f.m. pulse is applied to the signal generator. The signal returns to the original frequency f_1 when the f.m. pulse ends, and is turned off when the a.m. pulse ends. Lines F, G, and H show the sweep-circuit timing, which is the same as for amplitude-modulation testing.

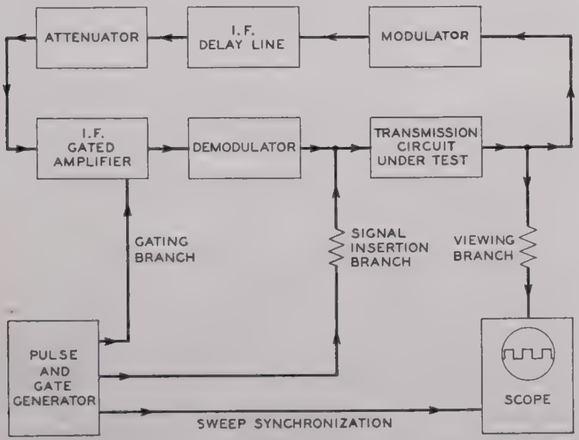

Fig. 4—Block diagram of one method of video-frequency circulated-pulse testing. Modulation and demodulation have been added to simplify delay and gating problems.

The viewing circuit includes an f.m. detector, so that only the frequency changes of the loop signal are observed. However, the sudden application and removal of f_1 by the a.m. modulator does produce a transient in the f.m. detection system, as shown on the oscilloscope trace in Fig. 3. This transient can be somewhat reduced by rounding off the shape of the a.m. pulse rise and fall by appropriate filtering. Sufficient time for the transient to be damped out must be provided before the start of the f.m. pulse. Limiters may be provided in the viewing circuit or the loop circuit or both, as desired.

V. VIDEO-FREQUENCY TESTING

A wide-band video circulating loop requires a high degree of balance in the gated amplifier, in order to avoid transients which circulate with the test pulses. It also requires a precision delay line which has uniform attenuation and delay over the necessary video band. W. M. Goodall of Bell Laboratories has avoided these difficult problems of video testing by using the arrangement of Fig. 4. He used a frequency modulator and discriminator connected to the video system to be tested, with the gating and delay accomplished in the i.f. part of the loop. Amplitude modulation and detection could be used in the same way, as mentioned in Section III.

VI. GENERAL DISCUSSION OF RESULTS

Fig. 5 shows a series of pulses obtained with a wide-band i.f. amplifier under test. The time scale is approximately 0.1 microsecond per division. The deterioration of the original pulse as it is circulated through the amplifier is clearly illustrated. A square-law detector was used in the viewing equipment in this case. This had the

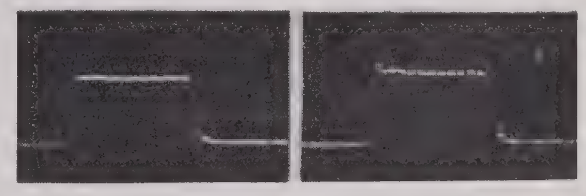
Signal Pulse One Trip

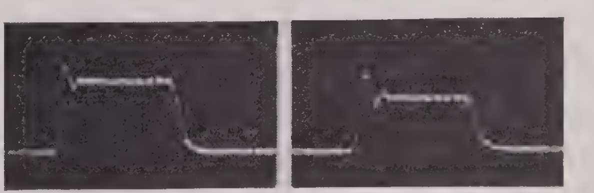
Three Trips Ten Trips

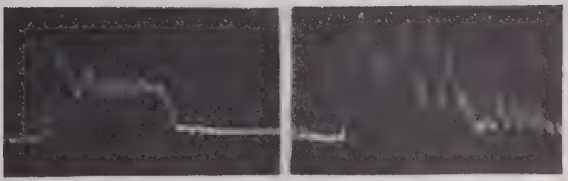
Thirty Trips Eighty Trips

Fig. 5—Photograph of oscilloscope traces showing signal-pulse shape and how it is deteriorated by repeated trips through an amplifier. An expanded sweep is used to show single pulses.

effect of increasing the magnitude of the overshoot and ripples on the top of the pulse, and reducing the corresponding ripples that follow the pulse.

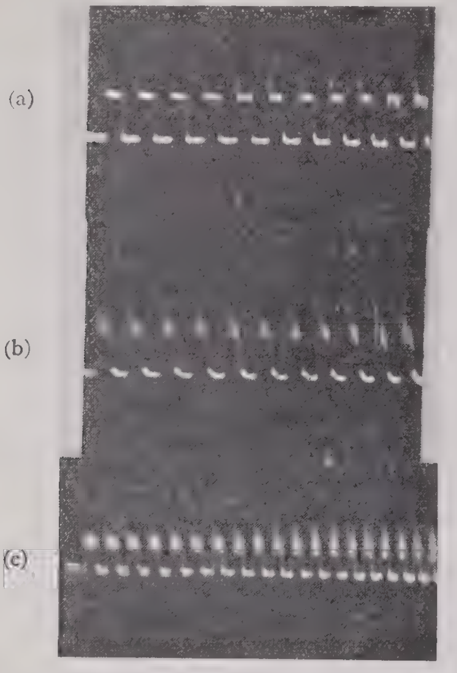

Fig. 6—(a) First 11 trips of a pulse through an i.f. amplifier.
(b) The 30th to the 40th trip through the same amplifier.
(c) First 19 trips of a reduced-amplitude pulse through the same amplifier, showing how noise builds up as the number of transits around the loop increases.

Since there is no simple relation between these pictures and the more familiar amplitude and phase characteristics of the amplifier, one is forced to set up new criteria of amplifier quality for the interpretation of the results. The most significant criteria are the time of rise and the amount of overshoot at the beginning and end of the pulse. This information about a circuit under test is directly applicable to the determination of its performance when it is used with facsimile, television, or any of the various pulse-modulation systems. A short time of rise and a small overshoot are generally desirable.

Fig. 6 shows some pictures taken with a slower sweep, so that a number of successive trips through the amplifier can be observed at one time. The build-up of the overshoot that would occur in a relay system incorporating this amplifier is particularly noticeable in these pictures.

In a relay system of several jumps, the noise power at the output of the nth repeater will be n times as great as the noise output of the first repeater. This can be illustrated and the signal-to-noise ratio can be observed by the circulated-pulse method, if the level of the input signal is reduced to a point where it becomes comparable with the input noise level of the amplifier under test. The lower trace in Fig. 6 was made in this way and illustrates the noise build-up. The thickness of the trace due to poor focus obscures the noise on the first few trips, but the increase after several trips can be seen.

Another characteristic of a transmission system which is of interest is the amount of signal compression, or amplitude nonlinearity. This has been measured as a function of the number of repeaters by using a test pulse with two or more levels arranged like a set of steps. If compression is present, the ratio of the step heights will change as the pulse circulates through the amplifier and suffers additional compression on each trip.

Distortion in Pulse-Duration Modulation*

ERNEST R. KRETZMER†, STUDENT, I.R.E.

Summary—**Pulse-duration modulation inherently gives rise to a certain amount of audio distortion. The analysis presented in this paper relates the distortion to system parameters. The method of analysis is exact, and therefore correct for any degree of modulation. It does not, however, lend itself to periodic sampling. The results are applied to three specific cases.**

I. INTRODUCTION

A SPECTRUM analysis of duration-modulated pulses may be of interest in systems where pulse-duration modulation is used directly, or where pulse-position modulation is converted to pulse-duration modulation for decoding.[1]

The problem investigated here may be classed under the general heading of the analysis of waves derived by sampling a signal wave at discrete intervals. This general problem exists in one form or another in all pulse communication systems, where it is a well-known principle that the sampling rate should be at least twice the highest frequency to be transmitted for faithful reproduction.[2]

Several papers including analyses of pulses with duration or position modulation, as well as comments on these, have recently been published. Most of these,

---

* Decimal classification: R148.6. Original manuscript received by the Institute, September 30, 1946; revised manuscript received, March 20, 1947. The research reported in this document was made possible through support extended the Massachusetts Institute of Technology, Research Laboratory of Electronics, jointly by the Army Signal Corps, the Navy Department (Office of Naval Research), and the Army Air Forces (Air Matériel Command), under the Signal Corps Contract No. W-36-039 sc-32037.

† Research Laboratory of Electronics, Massachusetts Institute of Technology, Cambridge 39, Mass.

[1] "Pulse position modulation technic," *Electronic Ind.*, vol. 4, pp. 82–87, 180–190; December, 1945.

[2] W. R. Bennett, "Time division multiplex systems," *Bell Sys. Tech. Jour.*, vol. 20, pp. 199–221; April, 1941.

however, do not take into account the precise law of modulation, which determines the time instant at which the signal is sampled and used to produce a time shift.[3–6] The analysis presented here applies to that law of modulation which is believed to be most practical.

II. Terminology and Notation

The time function to be analyzed is a sequence of rectangular pulses, for convenience chosen to be of unit amplitude.

The notation used is as follows:

p = angular pulse-repetition frequency
q = angular frequency of modulating signal
d_0 = average or unmodulated pulse duration
d = variable pulse duration
k = modulation index $= \dfrac{d_{\max} - d_{\min}}{d_{\max} + d_{\min}}$
n = harmonic index number of p
m = harmonic index number of q
A_{np+mq} = amplitude of a sinusoidal component of angular frequency $np+mq$
U_{np+mq} = relative intermodulation distortion due to

$$A_{np+mq};\; U_{np+mq} = \frac{A_{np+mq}}{A_q}.$$

Two types of pulse-duration modulation are considered: (a) "symmetrical," and (b) asymmetrical. The former has application primarily to pulse-duration modulation as such[3,7]; the latter has direct application to some present-day pulse-position-modulation systems. In asymmetrical pulse-duration modulation only one of the two pulse edges is time-modulated, while the other one is fixed. In "symmetrical" pulse-duration modulation both edges are modulated. The word "symmetrical" is enclosed in quotation marks because, although both edges move, they do not, in general, move by equal and opposite amounts.

III. Analysis of Actual Modulation Process

In position or duration modulation the pulses or pulse edges are shifted by amounts proportional to the instantaneous signal values sampled at certain instants at approximately the time of the pulse or pulse edge. Before any analysis is made, one must first determine exactly what these certain instants are. In a few instances in the literature[3–5] these instants were assumed to be fixed and equally spaced along the time axis. In other cases, no specification was made.

Most time modulators are based on the principle that the sum of the signal voltage and a linearly rising or falling voltage crosses a given reference voltage at an instant of time which is a function of the signal, a pulse edge being produced at that instant.[4,8–10] It is shown in Fig. 1 that the instant of crossing is a function of the signal value at the instant of crossing only. The linearly changing voltage is here represented by $e_a = a(t_0 - t)$, the signal by $e_s = k \cos qt$, and the reference line by $e = 0$. The time t_m at which the total voltage crosses this line is given implicitly by $[e_a + e_s]_{t=t_m} = 0$:

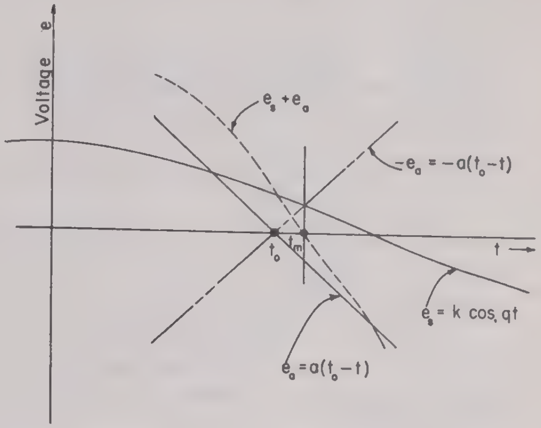

Fig. 1—Illustration of time-position-modulation process.

$$k \cos qt_m + a(t_0 - t_m) = 0 \tag{1a}$$

$$t_m = t_0 + \frac{k}{a} \cos qt_m. \tag{1b}$$

Stated in words, the time shift $(t_m - t_0)$ of a given pulse edge is proportional to the instantaneous modulating signal at the instant t_m at which the pulse edge actually occurs. It should be noted that the condition (1a) can also be written in the form

$$k \cos (qt_m) = -a(t_0 - t_m). \tag{1c}$$

This shows that the pulse edge, i.e., the instant t_m, occurs when the signal voltage and the negative of the linear voltage (indicated by the dot-dash line in Fig. 1) intersect. This idea is useful for graphical construction of modulated pulses (see Figs. 2 and 3).

IV. "Symmetrical" Pulse-Duration Modulation

Consider first the case of "symmetrical" pulse-duration modulation, shown graphically in Fig. 2. The pulses

---

[3] G. L. Fredendall, K. Schlesinger, and A. C. Schroeder, "Transmission of television sound on the picture carrier," Proc. I.R.E., vol. 34, pp. 49–61; February, 1946.

[4] F. F. Roberts and J. C. Simmonds, "Multichannel communications systems. Preliminary investigation based upon modulated pulses," *Wireless Eng.*, vol. 22, pp. 538–549; November, 1945.

[5] R. B. Shepherd, "Letter to the Editor," *Wireless Eng.*, vol. 23, pp. 114–115; April, 1946.

[6] F. F. Roberts and J. C. Simmonds, "Letter to the Editor," *Wireless Eng.*, vol. 23, p. 204; July, 1946.

[7] W. A. Beatty, "Proposals for television and broadcasting systems," *Jour. Instn. Radio Eng.*, vol. 5, pp. 54–78; March–April, 1945.

[8] R. D. Kell, U. S. Patent No. 2,061,734.

[9] W. A. Beatty, British Patent No. 523,575.

[10] D. D. Grieg and A. M. Levine, "Pulse-time-modulated multiplex radio relay system-terminal equipment," *Elec. Commun.*, vol. 23, pp. 159–178; June, 1946.

are so phased that one pulse, in the absence of modulation, is centered at zero time. By ordinary Fourier analysis it is found that the series

$$\frac{pd}{2\pi} + \frac{2}{\pi} \sum_{n=1}^{\infty} \left[\frac{1}{n} \sin \frac{npd}{2} \right] \cos npt \tag{2}$$

represents an unmodulated pulse train with pulse duration d, and with a pulse centered at the origin. Although this has been derived for d constant, d may be made variable in accordance with the modulating signal, and the series will then represent the function generated in the actual modulation process described above.[11] To facilitate an understanding of this, it is helpful to think of d, not as the pulse duration, but as a parameter which determines independently the instants at which the pulse edges occur; the value of d is of importance only at these instants.

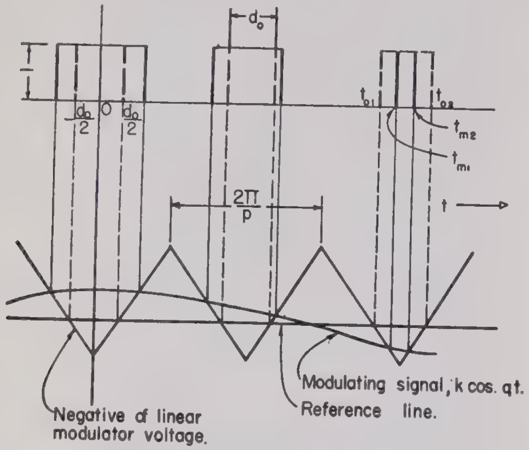

Fig. 2—"Symmetrical" pulse-duration-modulation process.

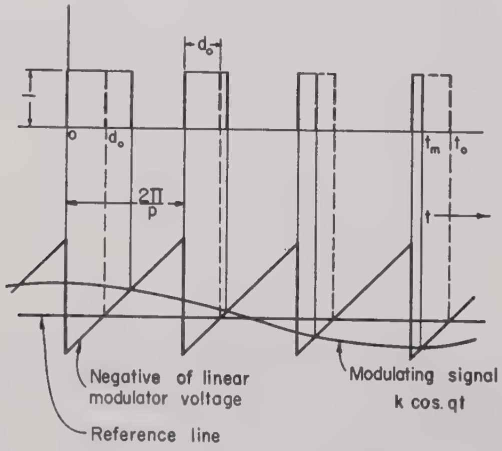

d_o
1
0
d_o
t_m
t_o
$\frac{2\pi}{p}$
t →
Negative of linear modulator voltage
Modulating signal k cos. qt
Reference line

Fig. 3—Asymmetrical pulse-duration-modulation process.

V. Asymmetrical Pulse-Duration Modulation

In analyzing asymmetrical modulation, the leading edges are assumed fixed and the trailing edges modulated as before, which automatically covers also the case of fixed trailing edges. The picture of the modulation process is shown in Fig. 3. One of the fixed leading edges is chosen to coincide with zero time. The Fourier series for the unmodulated pulse train with pulse duration d, phased in this manner, is

$$\frac{pd}{2\pi} + \frac{1}{\pi} \sum_{n=1}^{\infty} \left[\frac{1}{n} \sin npd \right] \cos npt + \frac{1}{\pi} \sum_{n=1}^{\infty} \left[\frac{1}{n} (1 - \cos npd) \right] \sin npt. \tag{3}$$

As in the case of (2), the desired expression for the modulated pulse train is obtained by letting the parameter d vary with the instantaneous signal. This time, the value of d matters only at the instants at which the trailing pulse edges occur.

VI. Spectrum Analyses

(A) "Symmetrical" Modulation[12]

By ordinary Fourier analysis of the wave shown in Fig. 4,

$$f(t) = \frac{pd}{2\pi} + \frac{2}{\pi} \sum_{n=1}^{\infty} \left[\frac{1}{n} \sin \frac{npd}{2} \right] \cos npt. \tag{4}$$

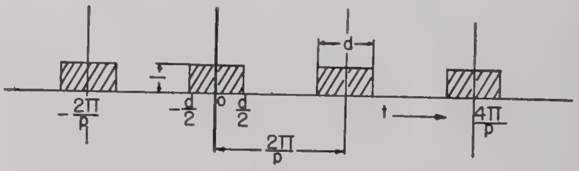

Fig. 4—Pulse train to be modulated "symmetrically."

Letting d become a function of time proportional to the modulating signal, one has

$$d = d_0(1 + k \cos qt), \tag{5}$$

where a cosine wave represents the signal. This step has been discussed in Section IV. The relative phase of the modulating signal affects only the relative phases of the components of the spectrum, not their magnitudes, which are of chief interest here. The relative phases may be important only in the special degenerate cases where p and q are commensurable. Hence, for present purposes, little generality is lost by choosing a fixed-phase sinusoid for modulation. Substitution of (5) into (4) results in

$$f(t) = \frac{pd_0}{2\pi}(1 + k \cos qt) + \frac{2}{\pi} \sum_{n=1}^{\infty} \left[\frac{1}{n} \sin \frac{npd_0}{2} (1 + k \cos qt) \right] \cos npt. \tag{6}$$

---

[11] E. R. Kretzmer, "Letter to the Editor," *Wireless Eng.*, vol. 23. pp. 232–233; August, 1946.

[12] A similar analysis, but more restricted in scope, has been presented by J. L. Callahan, J. N. Whitaker, and H. Shore, "Photo-radio apparatus and operating technique improvements," Proc. I.R.E., vol. 23, pp. 1441–1483; December, 1935.

Using a trigonometric identity, one obtains

$$f(t)=\frac{pd_0}{2\pi}(1+k\cos qt)$$
$$+\frac{2}{\pi}\sum_{n=1}^{\infty}\frac{1}{n}\left\{\sin\frac{npd_0}{2}\cos\left[\frac{nkpd_0}{2}\cos qt\right]\right.$$
$$\left.+\cos\frac{npd_0}{2}\sin\left[\frac{nkpd_0}{2}\cos qt\right]\right\}\cos npt. \qquad (7)$$

But

$$\cos(A\cos qt) = J_0(A) + 2\sum_{m=2,4,\cdots}^{\infty}(-1)^{m/2}J_m(A)\cos mqt$$

$$\sin(A\cos qt) = 2\sum_{m=1,3,\cdots}^{\infty}(-1)^{(m-1)/2}J_m(A)\cos mqt.$$

Substituting these relations in (7) and applying an identity for (cos mqt) (cos npt) yields

$$f(t)=\frac{pd_0}{2\pi}(1+k\cos qt)$$
$$+\frac{2}{\pi}\sum_{n=1}^{\infty}\frac{1}{n}\left\{\left[J_0\left(\frac{nkpd_0}{2}\right)\sin\frac{npd_0}{2}\right]\cos npt\right.$$
$$+\sum_{m=1}^{\infty}J_m\left(\frac{nkpd_0}{2}\right)\sin\left(\frac{npd_0}{2}+\frac{m\pi}{2}\right)$$
$$\left.\cdot[\cos(np+mq)t+\cos(np-mq)t]\right\}. \qquad (8)$$

(B) Asymmetrical Modulation

By ordinary Fourier analysis of the wave shown in Fig. 5,

$$f(t) = \frac{pd}{2\pi}+\frac{1}{\pi}\sum_{n=1}^{\infty}\left[\frac{1}{n}\sin npd\right]\cos npt$$
$$+\frac{1}{\pi}\sum_{n=1}^{\infty}\left[\frac{1}{n}(1-\cos npd)\right]\sin npt. \qquad (10)$$

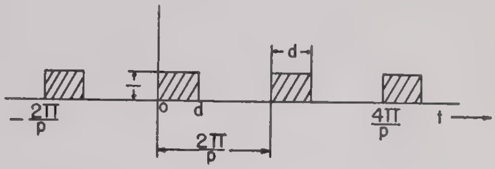

Fig. 5—Pulse train to be modulated asymmetrically.

Letting a cosine wave represent the signal, as before,

$$d = d_0(1+k\cos qt).$$

Substitution of this relation into (10) yields

$$f(t)=\frac{pd_0}{2\pi}(1+k\cos qt)$$
$$+\frac{1}{\pi}\sum_{n=1}^{\infty}\frac{1}{n}[\sin npd_0(1+k\cos qt)]\cos npt$$
$$+\frac{1}{\pi}\sum_{n=1}^{\infty}\frac{1}{n}[1-\cos npd_0(1+k\cos qt)]\sin npt. \qquad (11)$$

By means of the same identities used to obtain (8) from (6), as well as an identity for (cos mqt) (sin npt), one obtains (12) from (11).

$$f(t) = \frac{pd_0}{2\pi}(1+k\cos qt)+\frac{1}{\pi}\sum_{n=1}^{\infty}\frac{1}{n}\left\{[J_0(nkpd_0)\sin npd_0]\cos npt+[1-J_0(nkpd_0)\cos npd_0]\sin npt\right.$$
$$+\sum_{m=2,4,\cdots}^{\infty}(-1)^{m/2}J_m(nkpd_0)\sin npd_0[\cos(np+mq)t+\cos(np-mq)t]$$
$$+\sum_{m=1,3,\cdots}^{\infty}(-1)^{(m-1)/2}J_m(nkpd_0)\cos npd_0[\cos(np+mq)t+\cos(np-mq)t]$$
$$-\sum_{m=2,4,\cdots}^{\infty}(-1)^{m/2}J_m(nkpd_0)\cos npd_0[\sin(np+mq)t+\sin(np-mq)t]$$
$$\left.+\sum_{m=1,3,\cdots}^{\infty}(-1)^{(m-1)/2}J_m(nkpd_0)\sin npd_0[\sin(np+mq)t+\sin(np-mq)t]\right\}. \qquad (12)$$

If the summation over m is extended to cover zero and negative values of m, all components may be covered by $\cos(np+mq)t$ alone. This change requires that the integer m be replaced by its absolute value wherever it appears in the coefficients, as indicated by the magnitude signs in (9).

Finally, this expression can be written more compactly, as follows:

$$f(t) = \frac{pd_0}{2\pi}(1+k\cos qt)+\frac{1}{\pi}\sum_{n=1}^{\infty}\frac{1}{n}[\sin npt]$$

$$f(t) = \frac{pd_0}{2\pi}(1+k\cos qt)+\left[\frac{2}{\pi}\sum_{n=1}^{\infty}\sum_{m=-\infty}^{\infty}\frac{1}{n}J_{|m|}\left(\frac{nkpd_0}{2}\right)\sin\left(\frac{npd_0}{2}+\frac{|m|\pi}{2}\right)\right]\cos(np+mq)t. \qquad (9)$$

$$+\frac{1}{\pi}\sum_{n=1}^{\infty}\sum_{m=-\infty}^{\infty}\frac{1}{n}\left[J_{|m|}(nkpd_0)\sin\left(npd_0+|m|\frac{\pi}{2}\right)\right][\cos(np+mq)t]$$

$$-\frac{1}{\pi}\sum_{n=1}^{\infty}\sum_{m=-\infty}^{\infty}\frac{1}{n}\left[J_{|m|}(nkpd_0)\cos\left(npd_0+|m|\frac{\pi}{2}\right)\right][\sin(np+mq)t]. \tag{13}$$

Several interesting facts are to be noted. The magnitude of a given component, of frequency $np+mq$, is totally independent of p and q, and also of the algebraic sign of m. Further, there are no components of frequency mq,[13] showing that harmonic distortion is not inherent in the modulation process. Finally, an exactly linear relationship exists between the amplitude of the signal-frequency component and the product of duty cycle and modulation index.

These facts follow from the law of modulation assumed, which, as has been shown, corresponds to the law actually governing the modulation process analyzed in Section III.

VII. Numerical Results

It is readily seen that the components of angular frequencies q and $p+mq$ ($n=1$, $m=-1, -2, -3, \cdots$) are of greatest interest from the point of view of audio fidelity. The former is the desired signal and the latter are undesired intermodulation products which may fall within the pass band. The values given by (9) and (13) are peak amplitudes relative to the unit height of the pulses. It is convenient to define a quantity $U_{p+mq}=A_{p+mq}/A_q$, which is the ratio of the undesired component of frequency $p+mq$ to the signal component. The signal amplitude is $A_q=kpd_0/2\pi$ in both cases; the undesired beat amplitudes, divided by A_q, give the following:

"Symmetrical" modulation:

$$U_{p+mq}=\frac{4}{kpd_0}J_{|m|}\left(\frac{kpd_0}{2}\right)\cos\frac{pd_0}{2}\quad(\text{for } m \text{ odd})$$

$$U_{p+mq}=\frac{4}{kpd_0}J_{|m|}\left(\frac{kpd_0}{2}\right)\sin\frac{pd_0}{2}\quad(\text{for } m \text{ even}) \tag{14}$$

Asymmetrical modulation:

$$U_{p+mq}=\frac{2}{kpd_0}\sqrt{J_{|m|}{}^2(kpd_0)\sin^2\left(pd_0+\frac{|m|\pi}{2}\right)+J_{|m|}{}^2(kpd_0)\cos^2\left(pd_0+\frac{|m|\pi}{2}\right)}$$

$$=\frac{2}{kpd_0}J_{|m|}(kpd_0)\qquad(m\neq 0). \tag{15}$$

These expressions contain the essential information for establishing the relations between intermodulation distortion, degree of modulation, and highest signal-to-pulse-frequency ratio.[14] For large degrees of modulation with relatively large average pulse duration, (14) and (15) should be used directly. However, for small degrees of modulation and also for small pulse durations the expressions may be simplified by approximations to the Bessel and trigonometric functions.

Three different cases will be briefly considered:

(1) Average pulse duration equals the average time between pulses; high degree of modulation.

(2) Average pulse duration in the order of 3 per cent of the pulse-repetition period; high degree of modulation.

(3) Average pulse duration anything from 5 to 95 per cent of the pulse-repetition period. Duration variation small in all cases, in the order of 1 per cent of the pulse repetition period. (Asymmetrical modulation only.)

Case 1

The first case is chiefly of academic interest, especially with regard to a comparison between "symmetrical" and asymmetrical modulation. Since $d_0=\pi/p$, U_{p+mq} is zero for m odd in the "symmetrical" case, since $\cos pd_0/2$ in (14) is zero; more generally, for $d_0=\pi/p$, all $np+mq$ components with n odd and m even, or n even and m odd, are zero. No such phenomenon exists in the asymmetrical case. Table I gives the distortion U_{p+mq} expressed in per cent, for $k\leq 1$ chosen so as to give maximum distortion for each component. Maximum distortion does not always occur for $k=1$. It is true, in the

TABLE I

Per Cent Distortion (100 U_{np+mq}) (Case 1)

$d_0=\pi/p$; $k=1$ or as stated, so as to make U_{np+mq} a maximum

Angular Frequency of Undesired Component	"Symmetrical" Modulation Per Cent Distortion	Asymmetrical Modulation Per Cent Distortion
$p-q$	0	65 ($k=0.57$)
$p-2q$	32	32 ($k=0.95$)
$p-3q$	0	21
$p-4q$	1.9	9.5
$p-5q$	0	3.4
$p-6q$	0.04	1*
$2p-3q$	21	21 ($k=0.68$)
$2p-5q$	3.4	12*
$3p-4q$	15.7	15* ($k\approx 0.5$)

* Order of magnitude only.

---

[13] Except, of course, for $m=1$.

[14] For components with n other than 1, n will multiply the letter p wherever it appears in the above equations.

present case of deep modulation, that components with n other than 1, e.g., $2p-3q$ and $3p-4q$, are also very large; but if the audio pass band does not extend to over half the pulse frequency these components will fall outside the pass band, as will the p-q component. On the other hand a component such as that of frequency $2p-5q$ will fall within the audio pass band, but will be completely masked by the $p-2q$ component.

Table I shows superiority on the part of "symmetrical" pulse-duration modulation. It should be remembered, however, that the zero values in the symmetrical case hold only for the particular case where $d_0=\pi/p$ precisely, and cannot exactly be attained in practice.

Case 2

The second case may be of interest because of its proposed use in television sound channels.[8] The average pulse duration d_0 is chosen 3.0 per cent, and d will be varied from 0.5 to 5.5 per cent of a period, corresponding to $k=0.83$. Since d_0 is small, the trigonometric and Bessel functions in (14) and (15) may be approximated as follows with not more than 1 per cent error.

$$J_1(x) \approx 0.50x$$

$$J_2(x) \approx 0.125x^2 \qquad \cos\left(\frac{pd_0}{2}\right) \approx 1$$

$$J_3(x) \approx 0.021x^3 \qquad \sin\left(\frac{pd_0}{2}\right) \approx \frac{pd_0}{2}.$$

If these approximations are substituted, (14) and (15) become

$$\begin{array}{ll} \text{"Symmetrical"} & \textit{Asymmetrical} \\ U_{p-q} = 1.0 & U_{p-q} = 1.0 \\ U_{p-2q} = 0.062k(pd_0)^2 & U_{p-2q} = 0.25(kpd_0) \\ U_{p-3q} = 0.010(kpd_0)^2 & U_{p-3q} = 0.042(kpd_0)^2. \end{array} \qquad (16)$$

TABLE II

PER CENT DISTORTION (100 U_{p+mq})—(CASE 2)

Angular Frequency of Unwanted Component	"Symmetrical" Modulation Per Cent Distortion	Asymmetrical Modulation Per Cent Distortion
$p-q$	100	100
$p-2q$	0.18	3.9
$p-3q$	0.024	0.10

These are general relations which hold whenever the above approximations are justified. For the specific numerical example chosen, the duty cycle $pd_0/2\pi=0.03$, and the modulation index $k=0.83$. Substituting these values in (16) yields the results listed in Table II.

"Symmetrical" pulse duration modulation is seen again to be superior in this case. The ratio of p to the highest value of q should be at least two in order to prevent the p-q component from falling within the pass band, or three if the p-$2q$ component is also to be excluded.

Case 3

The third case may have direct bearing on multichannel pulse-position-modulation systems. This is so because a conventional method of demodulation consists of generating asymmetrically duration-modulated pulses, one edge being formed by the synchronizing pulse and the other by the information-carrying pulse of the channel in question.

The quantity $kpd_0/2\pi$ is the ratio of maximum time shift to pulse-repetition period and may be about 0.01 or 0.02, regardless of the average pulse duration. The same approximation to the Bessel functions as in Case 2 may be used here, and the results are identical to those given by (16) for the asymmetrical case.

For a ten-channel system, using "1 per cent" pulses, a reasonable time-shift amplitude might be 2 per cent of the repetition period, so that each channel pulse covers a range of 5 per cent. Table III gives the inherent distortion for all channels.

TABLE III

PER CENT DISTORTION (100 U_{p+mq})—(CASE 3)

Angular Frequency of Undesired Component	100 U_{p+mq}
$p-q$	100
$p-2q$	3.15
$p-3q$	0.067

These results lead to the following conclusions, if one assumes that ideal low-pass audio filters are used. In Case 2 (asymmetrical) and in Case 3, the ratio of pulse-repetition frequency to the highest audio frequency can be as low as two for low distortion, and three for negligible distortion. In Case 2 ("symmetrical"), the distortion is negligible even for a ratio of only two, the theoretical limit mentioned in the introduction. Case 1, on the other hand, may call for somewhat higher ratios. Some of these results have been checked experimentally.

◆

A Method of Virtual Displacements for Electrical Systems with Applications to Pulse Transformers*

PRESCOTT D. CROUT†

Summary—**A method of virtual displacements is developed for obtaining the transient behavior of electrical systems with distributed constants. This method involves the association of a number of assumed "current modes" with generalized co-ordinates, and gives a set of equations which duplicates the mesh equations of a corresponding equivalent lumped network. The procedure developed is applicable to many different types of problems. Here, however, it is applied to the pulse transformer, the result being equivalent networks and procedures for calculating the constants in these networks.**

I. Introduction

THE PURPOSE of this paper is to develop a method of virtual displacements for obtaining the transient behavior of electrical systems with distributed constants. In using this method certain assumed "current modes" are associated with generalized co-ordinates, the result being a set of equations, one for each mode, which duplicates the mesh equations of a lumped network. The procedure thus gives an equivalent lumped network, which has a number of meshes equal to the number of assumed modes.

The method devised is applied to the pulse transformer. Because the phenomena in question occur during extremely small time intervals, the distributed inductance and capacitance are important factors in the operation of these transformers. The results obtained consist of equivalent networks and procedures for calculating the constants in these networks.

Because there are many kinds of electrical systems which have distributed constants, and because many problems involving other kinds of systems—thermal, for example—may be solved by treating equivalent electrical systems, it appears that the method of virtual displacements is applicable to a wide variety of problems. It can also be applied to find the approximate behavior of certain electrical systems which are lumped, but which have so many meshes that it is not feasible to solve the systems exactly. Specific applications of the method have been made, and experimental data confirming calculated results have been obtained.[1–3]

II. Current Modes[4]

The basic assumption that will be made is that the actual system of displacement and conduction currents in the given electrical system can at each instant be approximated with sufficient accuracy by a linear combination of a few suitably chosen current modes. A current mode is merely a flow pattern, the geometric picture of a current field, together with a magnification factor which for the present we leave unspecified. We shall now consider a few specific cases which, to fix ideas, are applicable to pulse transformers.

TABLE I

Data Defining Modes A, B, and C

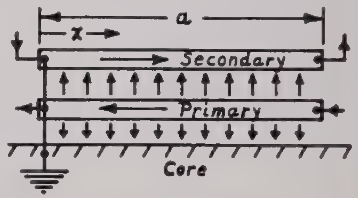

Mode designation	A	B	C
Primary current outside of winding	$\dot{q}_A$	$\dot{q}_B$	$\dot{q}_C$
Primary current in winding	$\dot{q}_A$	$\frac{\dot{q}_B}{2}\left[3\left(\frac{x}{a}\right)^2-1\right]$	$\frac{\dot{q}_C}{2}\left[3\left(\frac{x}{a}\right)^2-1\right]$
Displacement current from primary to core per unit axial length winding	0	$\frac{3x}{a^2}\dot{q}_B$	0
Secondary current outside of winding	$\left(\frac{N_p}{N_s}\right)\dot{q}_A$	0	$\dot{q}_C$
Secondary current in winding	$\left(\frac{N_p}{N_s}\right)\dot{q}_A$	0	$\frac{\dot{q}_C}{2}\left[3\left(\frac{x}{a}\right)^2-1\right]$
Displacement current from primary to secondary per unit axial length of winding	0	0	$\frac{3x}{a^2}\dot{q}_C$

The modes shown schematically in Table I pertain to a transformer having a single-layer primary of N_p turns over which is wound a single-layer secondary of N_s turns, the same end of both being grounded to the core as shown.[5] The modes are designated by letters, the q's are unknown functions of time, a dot indicates dif-

---

* Decimal classification: R140×R143.5. Original manuscript received by the Institute, April 10, 1946; revised manuscript received, April 4, 1947.

This paper is based on work done for the Office of Scientific Research and Development under Contract OEMsr-262 with the Massachusetts Institute of Technology.

† Massachusetts Institute of Technology, Cambridge, Mass.

[1] F. E. Bothwell, "Equivalent network for the 232-BW pulse transformer based on the method of virtual displacements," M.I.T. Rad. Lab. Rep. 734–778; July, 1945.

[2] F. Assadourian, "Theoretical current pulses in magnetron and resistance loads at secondary of pulse transformer driven by line-type modulator," Westinghouse Research Report R-94410-20-A. October, 1945.

[3] The author has successfully used the equivalent networks here described on two specific jobs involving the suppression of oscillations in pulse transformers.

[4] The name "charge mode" (charge in the sense of time integral of current) is more accurate than "current mode" because of the manner in which these modes will be used. The latter name was used because of the physical picture it gives. The charge modes are obtained simply by removing the dots, which indicate differentiation with respect to time, from the q's in the expressions for the current modes.

[5] This simple construction is chosen because it is entirely adequate for explaining the methods which will be developed. These methods are applicable to all designs, including those which involve the use of shields.

ferentiation with respect to time, and the positive directions of the currents are given by the arrows in the diagram. The entries in the table are easily determined from the following specifications:

1. For each mode the corresponding $\dot{q}$ is the external primary current, and the total ampere-turns linking the core is zero.

2. Mode A contains no displacement current, mode B contains only primary-to-core displacement current, and mode C contains only primary-to-secondary displacement current. Each nonvanishing displacement current density varies linearly along the winding starting at zero at the grounded end.

3. In mode B and mode C, the primary ampere-turns and the secondary ampere-turns are both zero.

These specifications are not necessary, but are convenient. The vanishing of the various m.m.f.'s prevents the core from being excited, and simplifies the nature of the leakage fluxes. The linear distribution of the displacement current densities is suggested by the linear voltage distribution obtained if leakage flux is neglected.[6]

None of the above modes produces any excitation of the core. We therefore add a current distribution M comprising a primary magnetizing current I_M, and the actual eddy currents induced in the core. This is not a mode, since the geometric shape of the current field changes with time. Evidently, I_M is determined by the core specifications, the core flux-time curve, and the fact that $0.4\pi I_M N_p$ is the total core m.m.f.[7]

By superimposing the above modes (with suitably determined q's) and the current distribution M, we approximate the actual behavior of the transformer.

III. DETERMINATION OF THE q'S—VIRTUAL DISPLACEMENTS OF CHARGE

Although we may conceivably devise an infinite number of current modes which together are capable of representing the behavior of the electrical system exactly, we shall use only a few of the more important of these, the number being such that a sufficient approximation of this behavior is obtained, and such that the required work is held within tolerable limits. Let the q's of the chosen modes be numbered, thus $q_1, q_2, \cdots, q_n$. These quantities will now be used as generalized co-ordinates in procedures which are analogous to those used in mechanics.

It is evident that all charges arising from the k^{th} mode are proportional to q_k; all currents and magnetic field intensities, to $\dot{q}_k$; and all induced voltages arising from the rate of change of the magnetic field, to $\ddot{q}_k$. Let us consider the transformer in operation, the various q's being suitable but unknown functions of time; and at time t let the system be given a virtual displacement δq_k. By this we mean that at time t time is stopped, in the sense that all voltages and electric field intensities which existed at time t are considered as persisting unchanged, and that q_k is increased by an infinitesimal amount δq_k. The variation δq_k causes a field of flow of charge in the k^{th} mode, which field may be considered as made up of an infinite number of closed, elementary infinitely thin tubes of flow, the charge flowing in each of these being proportional to δq_k. Let us determine the virtual work—the word "virtual" being used to emphasize the fact that the procedure is entirely artificial and can exist only in one's imagination—that is required to produce the motion of charge associated with the virtual displacement δq_k through the voltage differences and electric fields which are persisting from time t, as stated above. The total virtual work is evidently the sum of the virtual works required by all of the elementary tubes of flow. For a single tube, however, the virtual work is merely the product of the elementary charge associated with the tube, which charge is proportional to δq_k, and the quantity

$$[\text{induced back voltage} + \text{total impedance drop} - \text{total source voltage}]. \quad (1)$$

Here the first term is the back voltage due to the rate of change of the magnetic flux which links the tube, the second term consists of all capacitance and resistance drops, the former being composed of back voltages across electric fields; and the last term consists of the total e.m.f. contributed to the tube by external sources —for example, primary and secondary terminal voltages. The quantity (1), however, is zero; hence the virtual work required by any single tube and hence by the entire field of flow is zero. We have thus shown that *the virtual work required by a virtual displacement δq_k is zero, providing induced voltages are included as well as impedance drops and voltage sources (such as terminal voltages).* This is equivalent to saying that *the virtual work required by impedance drops and induced voltages in a virtual displacement δq_k is equal to that provided by voltage sources.* All expressions for virtual work have δq_k as a factor. Dividing these by δq_k gives corresponding expressions for what we define as "generalized voltages." For example if

δW_C = virtual work *required by* capacitances

δW_R = virtual work *required by* resistances

δW_L = virtual work *required by* induced voltages (2)

---

[6] The difference between this linear distribution and the actual one is a distribution which varies with time, vanishes at both ends of the winding, and can be represented exactly by a Fourier sine series. Each sinusoidal distribution in this series can be made the basis of a mode just as the linear distribution was above, the result being an infinite number of modes which can be used with those above to give exact results. These modes are treated in M.I.T. Radiation Laboratory Report 618, which has the same title and author as the present paper, and on which the present paper is based.

[7] I_M can be determined approximately by calculation or by experiment from the fact that the primary voltage *with I_M, acting alone*, minus the primary resistance drop, gives the rate of change of the core flux, plus the average primary leakage flux.

δW_E = virtual work *supplied by* one or several specified sources,

then

generalized capacitance voltage

$$= \frac{\delta W_C}{\delta q_k} = \frac{1}{C_{k1}} q_1 + \frac{1}{C_{k2}} q_2 + \cdots + \frac{1}{C_{kn}} q_n - v_{Ck},$$

generalized resistance voltage

$$= \frac{\delta W_R}{\delta q_k} = R_{k1}\dot{q}_1 + R_{k2}\dot{q}_2 + \cdots + R_{kn}\dot{q}_n - v_{Rk}, \tag{3}$$

generalized inductance (induced) voltage

$$= \frac{\delta W_L}{\delta q_k} = L_{k1}\ddot{q}_1 + L_{k2}\ddot{q}_2 + \cdots + L_{kn}\ddot{q}_n - v_{Lk}; \text{ and}$$

$$\text{generalized source voltage} = \frac{\delta W_E}{\delta q_k} = E_k,$$

where the C's, R's, and L's are constants, and where $-v_{Ck}$, $-v_{Rk}$, and $-v_{Lk}$ are from the virtual works required by the capacitance and resistance drops and the induced voltages due to currents not given by the q's, in the present case the current distribution M.

In order to see that these generalized voltages have the forms indicated, we need only recall that all capacitance drops are proportional to charges, all resistance drops are proportional to currents, and all induced voltages are proportional to the rates of change of currents. Our fundamental relation for virtual work can now be stated in the form of a generalized Kirchoff's law as follows: *For any* $1 \leqq k \leqq n$ *the generalized source voltage is equal to the sum of the generalized impedance drops*. Noting (3), this gives

$$\begin{aligned} Z_{11}I_1 + Z_{12}I_2 + \cdots + Z_{1n}I_n &= E_1 + v_1 \\ Z_{21}I_1 + Z_{22}I_2 + \cdots + Z_{2n}I_n &= E_2 + v_2 \\ \cdots\cdots\cdots\cdots &\cdots\cdots \\ Z_{n1}I_1 + Z_{n2}I_2 + \cdots + Z_{nn}I_n &= E_n + v_n, \end{aligned} \tag{4}$$

where the I's are generalized currents defined by

$$I_i = \dot{q}_i, \qquad i = 1, 2, \cdots, n,$$

where the Z's are generalized impedances defined by

$$Z_{ij} = L_{ij}\frac{d}{dt} + R_{ij} + \frac{1}{C_{ij}}\int_{\text{time when charges}=0}^{t} dt, \qquad i, j = 1, 2, \cdots, n,$$

as in circuit theory; and where

$$v_i = v_{Ci} + v_{Ri} + v_{Li}, \qquad i = 1, 2, \cdots, n.$$

If we can show that the system of (4) is symmetrical, or that $Z_{ij} = Z_{ji}$, and that certain quadratic forms analogous to the usual expressions for energy and dissipation are positive definite, then a lumped network exists in which the I's are the mesh currents, the Z's the impedances, and the E's plus the v's the mesh voltages, and which gives this set of equations when Kirchoff's laws are applied. The network is equivalent to the actual system to the degree of approximation permitted by the choice of modes.[8] The conditions which must be satisfied are the following.

$$L_{ij} = L_{ji},\ C_{ij} = C_{ji},\ R_{ij} = R_{ji},\ i, j = 1, 2, \cdots, n;$$

$$\frac{1}{2}\sum_{i=1}^{n}\sum_{j=1}^{n} L_{ij}x_ix_j, \quad \frac{1}{2}\sum_{i=1}^{n}\sum_{j=1}^{n}\frac{1}{C_{ij}}x_ix_j, \quad \text{and} \tag{5}$$

$$\sum_{i=1}^{n}\sum_{j=1}^{n} R_{ij}x_ix_j$$

must all be positive definite quadratic forms. These conditions are satisfied, which fact will now be proved.

A. Proof that $C_{ij} = C_{ji}$.

If $q_1, q_2, \cdots, q_n$ are increased by amounts $dq_1, dq_2, \cdots, dq_n$, the increase in the electric energy of the system without the current distribution M is

$$\left(\sum_{j=1}^{n}\frac{1}{C_{1j}}q_j\right)dq_1 + \left(\sum_{j=1}^{n}\frac{1}{C_{2j}}q_j\right)dq_2 + \cdots + \left(\sum_{j=1}^{n}\frac{1}{C_{nj}}q_j\right)dq_n. \tag{6}$$

Since the electric energy exists and is a function of only the charges, this expression must be a total differential, the test of which is that the partial derivative of the coefficient of dq_i with respect to q_j must equal the partial derivative of the coefficient of dq_j with respect to q_i. Applying this test gives immediately

$$\frac{1}{C_{ij}} = \frac{1}{C_{ji}}, \quad \text{or} \quad C_{ij} = C_{ji}, \qquad i, j = 1, 2, \cdots, n. \tag{7}$$

---

[8] Regardless of the number of modes used, the nature of the approximate result given by (4) can be obtained as follows. Let there be added to the given electrical system a continuous distribution of (source) constraining voltages such that the approximate result given by (4) without these voltages is the exact solution of the problem with them. These constraining voltages contribute a voltage term to (1) and the terms $\delta W_E'/\delta q_1, \delta W_E'/\delta q_2, \cdots, \delta W_E'/\delta q_n$ to the right-hand sides of (4), respectively. Denoting the modified equations by (4′), we note that (4) is approximate for the case of no constraining voltages, whereas (4′) is exact for the case where constraining voltages are included. Subtracting each equation of (4) from the corresponding equation of (4′) noting that both systems of equations have the same solution, it follows that

$$\frac{\delta W_E'}{\delta q_k} = 0, \qquad k = 1, 2, \cdots, n;$$

hence the constraining voltages do no work in any virtual displacement δq_k, $k = 1, 2, \cdots, n$. We have now shown that *the approximate solution given by (4) is the exact solution of the problem obtained by superimposing on the given electrical system a suitable system of constraining voltages which do no work for any virtual displacement* δq_k. We have also obtained the following result. *Let there be added to the given system a set of constraining voltages which force the solution of the problem to be given exactly (at each instant) by a linear combination of the assumed modes; then (4) gives the one and only such combination that does not require the constraining voltages to do work under any virtual displacement* δq_k *(and, hence, any virtual displacement permitted by the chosen modes).*

B. *Proof that* $R_{ij}=R_{ji}$.

Let F_k be a vector function whose direction at any point is the direction in which charge would flow if q_k were increased, and whose magnitude is the charge per unit cross section of path that flows at this point for unit increase of q_k. We shall now compute δW_R for the virtual displacement δq_k without the current distribution M. The contribution of the resistance drop to the electric intensity vector is (see Fig. 1)

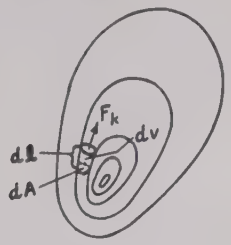

Fig. 1—Current-flow pattern.

$$\rho\sum_{i=1}^{n}F_i\dot{q}_i$$

where ρ is the resistivity of the material at the point. We consider the field of flow arising from δq_k to be made up of elementary tubes of flow. The energy loss in a length dl of such a tube at a point where the cross section is dA is

(voltage component along tube times dl)$(|F_k|\delta q_k dA)$,

the second factor being the charge which moves in the elementary tube. Replacing $dA\ dl$ by dv and integrating over all space (all pieces of all tubes), we have

$$\delta W_R=\int_V\left(\rho\sum_{i=1}^{n}F_i\dot{q}_i\right)\cdot F_k\delta q_k dv$$

$$\frac{\delta W_R}{\delta q_k}=\sum_{i=1}^{n}\dot{q}_i\int_V\rho F_i\cdot F_k dv.$$

Comparing this expression with (3), we see that

$$R_{ki}=\int_V\rho F_i\cdot F_k dv,\qquad k,\ i=1,2,\cdots,n.$$

It follows that

$$R_{ij}=R_{ji}=\int_V\rho F_i\cdot F_j dv,\qquad i,\ j=1,2,\cdots,n.\tag{8}$$

C. *Proof that* $L_{ij}=L_{ji}$.

Let q_i and q_j be taken as arbitrary functions of time, the only condition being that these functions are analytic (smooth) and have time derivatives which vanish at $t=0$; also let all the other q's be put equal to zero, and the current distribution M removed. The work put into the magnetic field as time increases from 0 to t is

$$W_L=\int_0^t[(L_{ii}\ddot{q}_i+L_{ij}\ddot{q}_j)\dot{q}_i+(L_{ji}\ddot{q}_i+L_{jj}\ddot{q}_j)\dot{q}_j]dt.\tag{9}$$

Since this magnetic energy is completely determined by the currents that are flowing at the final time t, this expression can depend only upon the final values of $\dot{q}_i$ and $\dot{q}_j$, and must be the same for all chosen functions which have these same final values. If, then, we give q_i an infinitesimal variation δq_i which is analytic and whose time derivative $d/dt\ \delta q_i=\delta\dot{q}_i$ vanishes at time 0 and t, the integral (9) must remain unaltered, or

$$\delta W_L=0.$$

It follows that

$$\delta W_L=\int_0^t[(L_{ii}\ddot{q}_i+L_{ij}\ddot{q}_j)\delta q_i+(L_{ii}\dot{q}_i+L_{ji}\dot{q}_j)\delta\ddot{q}_i]dt=0.$$

Integrating the second term of the integrand by parts gives

$$[(L_{ii}\dot{q}_i+L_{ji}\dot{q}_j)\delta\dot{q}_i]_0^t$$
$$+\int_0^t(L_{ii}\ddot{q}_i+L_{ij}\ddot{q}_j-L_{ii}\ddot{q}_i-L_{ji}\ddot{q}_j)\delta\dot{q}_i dt=0.$$

But $\delta\dot{q}_i$ vanishes at times 0 and t; hence, the first term is zero; also two terms in the integrand cancel, leaving

$$(L_{ij}-L_{ji})\int_0^t\ddot{q}_j\delta\dot{q}_i dt=0.$$

By choosing a δq_i whose slope $d/dt\ \delta q_i=\delta\dot{q}_i$ is always of the same sign as $\ddot{q}_j$ we obtain a situation where the integral is positive. In such a case the integral is not zero; hence its coefficient must vanish, giving

$$L_{ij}=L_{ji},\qquad i,\ j=1,2,\cdots,n.\tag{10}$$

We have thus established the desired symmetry of the system of equations (4).

D. *Calculation of Electric and Magnetic Energies, and Dissipation. Proof that the Quadratic Forms in* (5) *are Positive Definite.*

We shall finally determine the electric energy, the magnetic energy, and the power loss due to resistance for the fields and currents due to the q's alone (no current distribution M). The expression (6) for the increase in the electric energy has been shown to be a total differential, and can therefore be integrated immediately. Noting that the electric energy vanishes when the q's are all zero, we thus have

$$\text{electric energy due to } q\text{'s alone}=\frac{1}{2}\sum_{i=1}^{n}\sum_{j=1}^{n}\frac{1}{C_{ij}}q_iq_j.\tag{11}$$

The energy given to the magnetic field during increases $dq_1, dq_2, \cdots, dq_n$ is given by an expression similar to (6), namely,

$$\left(\sum_{j=1}^{n}L_{1j}\ddot{q}_j\right)dq_1+\left(\sum_{j=1}^{n}L_{2j}\ddot{q}_j\right)dq_2+\cdots$$
$$+\left(\sum_{j=1}^{n}L_{nj}\ddot{q}_j\right)dq_n$$

$$= \sum_{i=1}^{n}\sum_{j=1}^{n} L_{ij}\ddot{q}_j dq_i.$$

Since $L_{ij}=L_{ji}$, this may be written

$$\frac{1}{2}\sum_{i=1}^{n}\sum_{j=1}^{n} L_{ij}(\ddot{q}_j dq_i + \ddot{q}_i dq_j) = \frac{1}{2}\sum_{i=1}^{n}\sum_{j=1}^{n} L_{ij}(\dot{q}_i d\dot{q}_j + \dot{q}_j d\dot{q}_i)$$

$$= d\left[\frac{1}{2}\sum_{i=1}^{n}\sum_{j=1}^{n} L_{ij}\dot{q}_i\dot{q}_j\right].$$

Integrating this expression while noting that the magnetic energy is zero when the $\dot{q}$'s, and hence all currents, are zero, we obtain finally

$$\text{magnetic energy due to } q\text{'s alone} = \frac{1}{2}\sum_{i=1}^{n}\sum_{j=1}^{n} L_{ij}\dot{q}_i\dot{q}_j. \quad (12)$$

The energy dissipated in the resistances in time dt is given by

$$\left(\sum_{j=1}^{n} R_{1j}\dot{q}_j\right)dq_1 + \left(\sum_{j=1}^{n} R_{2j}\dot{q}_j\right)dq_2 + \cdots$$

$$+ \left(\sum_{j=1}^{n} R_{nj}\dot{q}_j\right)dq_n.$$

Dividing by dt, it follows that

power loss in resistances due to q's alone

$$= \sum_{i=1}^{n}\sum_{j=1}^{n} R_{ij}\dot{q}_i\dot{q}_j. \quad (13)$$

Since the electric and magnetic energies and the dissipation are intrinsically positive quantities, and since the expressions (11), (12), and (13) are measures of the quadratic forms in (5), it follows that these quadratic forms are positive definite.

We now have shown that the conditions in (5) are satisfied, and hence that a lumped network exists which has the system of equations (4) as its mesh equations. It follows that the various theorems and procedures of circuit theory are applicable. For example, it is evident that equivalent networks can be devised which are the duals of those just considered, and in which the q's are node voltages instead of mesh charges.

Although the pulse transformer is being considered at present, *it is evident that the above theory is perfectly general, and can be applied to many different kinds of problems involving distributed constants. In such applications the current distribution M, if necessary at all, will probably differ from that used above with the pulse transformer.*

IV. DETERMINATION OF THE GENERALIZED NETWORK CONSTANTS

We shall now consider the procedures used in calculating the generalized capacitances, resistances, inductances, and voltages; and shall illustrate these using the modes devised in Section II.

A. Calculation of the Capacitances C_{ij}

It is evident that the C's of any mode which does not contain an electric field all vanish. More specifically, if a virtual displacement δq_k does not involve a flow of displacement charge, then $1/C_{ik}=1/C_{ki}=0$ for any i. Furthermore, if the i^{th} and j^{th} modes have electric fields, but if these fields do not overlap in space, then $1/C_{ij}=1/C_{ji}=0$, since a virtual displacement δq_i does not cause displacement charge to move in the electric field due to q_j, and vice versa. The truth of these statements is also evident from the form of the expression (11) for the electric energy.

In computing C_{ki}, we see from (3) that the only part of $\delta W_C/\delta q_k$ that is needed or that can be used is that which remains when the v's and all of the q's except q_i are put equal to zero. We therefore compute the virtual work $\overline{\delta W_C}$ for the flow of charge given by δq_k and the voltage distribution given by q_i alone, after which we have

$$\frac{1}{C_{ki}} = \frac{\overline{\delta W_C}}{q_i\delta q_k}. \quad (14)$$

As examples, we see that modes A, B, and C have no mutual capacitances, and that mode A has no self-capacitance; thus, $1/C_{AB}=1/C_{BC}=1/C_{AC}=1/C_{AA}=0$. Also placing

a = length of winding
x = distance from grounded end of winding
c_{pc} = core-to-primary capacitance per unit length of winding
$C_{pc}=ac_{pc}$ = total core-to-primary capacitance
c_{ps} = primary-to-secondary capacitance per unit length of winding
$C_{ps}=ac_{ps}$ = total primary-to-secondary capacitance,

the procedure in computing C_{BB} may be outlined as follows:

$$\text{primary-to-core voltage due to } q_B = \frac{3x}{a^2 c_{pc}}\, q_B$$

displacement charge per unit length of winding due to δq_B

$$= \frac{3x}{a^2}\,\delta q_B$$

$$\overline{\delta W_C} = \int_0^a \left(\frac{3x}{a^2 c_{pc}}\, q_B\right)\left(\frac{3x}{a^2}\,\delta q_B\right) dx = \frac{3}{ac_{pc}}\, q_B\delta q_B$$

$$C_{BB} = \frac{ac_{pc}}{3} = \frac{1}{3}C_{pc}.$$

The last expression follows from (14). In the above calculation, fringing of the electric field at the ends of the winding was neglected. If desired this can be included using flux plotting methods.[9–11]

In calculating a mutual capacitance two modes are involved, one of which is arbitrarily chosen to be given a virtual displacement. If the roles of these modes were interchanged so that the other is varied, it is evident that the only effect is to take the δ from one q and place it with the other, the integral on x being unaltered. Since both q and δq are divided out, we see clearly how

$$\frac{1}{C_{ij}} = \frac{\overline{\delta W_{Cj}}}{q_j \delta q_i} = \frac{\overline{\delta W_{Ci}}}{q_i \delta q_j} = \frac{1}{C_{ji}},$$

which relation was proved in Section III.

B. Calculation of the Resistances R_{ij}.

In calculating R_{ki} we see from (3) that the only part of $\delta W_R/\delta q_k$ that is needed or that can be used is that which remains when the v's and all of the $\dot q$'s except $\dot q_i$ are put equal to zero. We therefore compute the virtual work $\overline{\delta W_R}$ for the flow of charge given by δq_k and the voltage distribution given by $\dot q_i$ alone, after which we have

$$R_{ki} = \frac{\overline{\delta W_R}}{\dot q_i \delta q_k}. \qquad (15)$$

As an example, let us place

r_p = resistance per unit length of primary winding
R_p = resistance of primary winding
r_s = resistance per unit length of secondary winding
R_s = resistance of secondary winding;

then the procedure in computing the mutual resistance R_{BC} may be outlined as follows:

$$\text{Volts per unit length of primary} = \frac{r_p}{2}\left[3\left(\frac{x}{a}\right)^2 - 1\right]\dot q_B$$

$$\text{Virtual charge that passes any point of primary due to } \delta q_C = \frac{1}{2}\left[3\left(\frac{x}{a}\right)^2 - 1\right]\delta q_C$$

$$R_{BC} = \frac{\overline{\delta W_R}}{\dot q_B \delta q_C} = \frac{r_p}{4}\int_0^a \left[3\left(\frac{x}{a}\right)^2 - 1\right]^2 dx = \frac{1}{5} R_p.$$

In the above calculation, skin effect was not considered explicitly; however, its effect can be included approximately by assigning suitable values to r_p and r_s.

In calculating a mutual resistance two modes are involved, one of which is arbitrarily chosen to be given a virtual displacement. If the roles of these modes were interchanged so that the other were varied, it is evident that the only effect would be to take the δ from one q and place it with the other, the integral on x being unaltered. Since both the $\dot q$ and the δq are divided out, we see clearly how

$$R_{ij} = \frac{\overline{\delta W_{Rj}}}{\dot q_j \delta q_i} = \frac{\overline{\delta W_{Ri}}}{\dot q_i \delta q_j} = R_{ji},$$

which relation was proved in Section III.

C. Calculation of the Inductances L_{ij}.

In calculating L_{ki} we see from (3) that the only part of $\delta W_L/\delta q_k$ that is needed or that can be used is that which remains when the v's and all the $\ddot q$'s except $\ddot q_i$ are put equal to zero. We shall therefore compute the virtual work $\overline{\delta W_L}$ for the flow of charge given by δq_k and the voltage distribution given by $\ddot q_i$ alone, after which we have

$$L_{ki} = \frac{\overline{\delta W_L}}{\ddot q_i \delta q_k}. \qquad (16)$$

In the case of the transformer, the procedure is as follows. Let us consider the distribution of currents given by $\dot q_i$ to be flowing. These give rise to a magnetic field which is proportional to $\dot q_i$, which field must be determined. From it, the flux linkages per unit length of the primary and secondary windings are obtained in the following form:

$$\left.\begin{aligned}&\text{Flux that passes through the primary at any point} = f_p(x)\dot q_i\\ &\text{Flux that passes through the secondary at any point} = f_s(x)\dot q_i\end{aligned}\right\} \qquad (17)$$

where $f_p(x)$ and $f_s(x)$ are known once the magnetic field has been obtained. The corresponding voltage distributions are, therefore,

$$\text{Volts per unit length of primary opposing a current in the positive direction} = \frac{N_p 10^{-8}}{a} f_p(x)\ddot q_i$$

$$\text{Volts per unit length of secondary opposing a current in the positive direction} = -\frac{N_s 10^{-8}}{a} f_s(x)\ddot q_i.$$

But the virtual flow of charge is given by expressions of the form

$$\left.\begin{aligned}&\text{Virtual charge that passes any point of primary in the positive direction} = g_p(x)\delta q_k\\ &\text{Virtual charge that passes any point of secondary in the positive direction} = g_s(x)\delta q_k,\end{aligned}\right\} \qquad (18)$$

as is evident from Table I; hence,

$$\overline{\delta W_L} = \frac{10^{-8}}{a}\ddot q_i \delta q_k \int_0^a \left[N_p f_p(x) g_p(x) - N_s f_s(x) g_s(x)\right] dx$$

$$L_{ki} = \frac{\overline{\delta W_L}}{\ddot q_i \delta q_k} = \frac{10^{-8}}{a}\int_0^a \left[N_p f_p(x) g_p(x) - N_s f_s(x) g_s(x)\right] dx. \qquad (19)$$

---

[9] H. Poritsky, "Graphical field-plotting methods in engineering," *Trans. A.I.E.E.* (*Elec. Eng.*, Supplement, 1938), vol. 57, pp. 727–732; Supplement, 1938.

[10] A. D. Moore, "Fundamentals of Electrical Design," McGraw-Hill Book Co., New York, N. Y.

[11] P. D. Crout, "The determination of fields satisfying Laplace's, Poisson's, and associated equations by flux plotting," M.I.T. Rad. Lab. Rep. 1047, January, 1946.

It has already been shown in Section III that the L's are symmetrical; hence, the roles of the two modes just used may be interchanged.

In actually carrying out the above procedure the integration in (19) is, at worst, a simple numerical integration in which Simpson's rule can be used; hence, practically all of the work lies in determining the magnetic field from the given current distribution corresponding to $\dot{q}_i$. Of the techniques available for solving this type of problem, perhaps the simplest is flux plotting. By means of flux plotting the magnetic fields can be determined to an accuracy depending largely upon the amount of time available for making such plots.[7] We shall now apply (19) to modes A, B, and C; however, in order to avoid becoming involved with the details of flux plotting, we shall make certain approximations as follows.

1. Self-inductance of mode A

Let us suppose that the field due to the current distribution given by mode A passes axially down the space occupied by the primary-to-secondary insulation, with negligible leakage through the windings themselves. The flux passing down this space is, thus,

$$\phi = \frac{.4\pi\alpha N_p\dot{q}_A}{\mathcal{R}} = A\dot{q}_A,$$

where $\mathcal{R}$ is the reluctance of this space, and α is the fraction of the total m.m.f. which appears across it. It may be noted that, for this mode, the primary and secondary both produce the same m.m.f. $\mathcal{R}$ can be obtained to sufficient accuracy for most purposes by computing the reluctance of the space occupied by the primary-to-secondary insulation (including the wire insulation). α can be taken as the ratio of the coil length to this length increased by twice the primary-to-secondary insulation thickness. Of the flux ϕ, let a fraction σ return through the core, and a fraction $(1-\sigma)$ return through the space outside of the secondary. We then have

Volts per unit length of primary opposing a current in the positive direction $= \left(10^{-8}\dfrac{N_p}{a}\sigma\right)\left(\dfrac{0.4\pi\alpha N_p}{\mathcal{R}}\right)\ddot{q}_A$

Virtual charge that passes any point of primary $=\delta q_A$

Volts per unit length of secondary opposing a current in the positive direction $= \left[10^{-8}\dfrac{N_s}{a}(1-\sigma)\right]\left[\dfrac{0.4\pi\alpha N_p}{\mathcal{R}}\right]\ddot{q}_A$

Virtual charge that passes any point of secondary $=\dfrac{N_p}{N_s}\delta q_A$

$$\overline{\delta W_L} = \int_0^a \frac{10^{-8}0.4\pi\alpha N_p}{a\mathcal{R}}\left[N_p\sigma + N_s(1-\sigma)\frac{N_p}{N_s}\right]\ddot{q}_A\delta q_A dx$$

$$L_{AA} = \frac{\overline{\delta W_L}}{\ddot{q}_A\delta q_A} = \frac{4\pi 10^{-9}\alpha N_p^2}{\mathcal{R}}. \tag{20}$$

2. Mutual inductance between mode A and any one of the other modes

Referring to (19), let mode A be taken as the basis of $f_p(x)$ and $f_s(x)$, and let one of the other modes be taken as the basis of $g_p(x)$ and $g_s(x)$. Since ϕ does not vary with x, it follows that $f_s(x)$ and $f_p(x)$ are both constants; hence, (19) becomes

$$L_{kA} = \frac{\overline{\delta W_L}}{\ddot{q}_A\delta q_k} = 10^{-8}[N_p f_p(\text{average value of } g_p(x)) - N_s f_s(\text{average value of } g_s(x))].$$

But the average value of $g_p(x)$ and of $g_s(x)$ is zero for each of the modes in question; hence,

$$L_{kA} = 0,$$

and there is no mutual inductance between mode A and any of the other modes.

3. Self-inductance of mode B

In obtaining the field due to the current distribution given by $\dot{q}_B$, we shall replace the winding by a current sheet and place this against the core, the assumption being that the field so obtained is a sufficient approximation to the actual field, in so far as the determination of flux linkages per unit length of primary is concerned. The current at any point of the primary is, noting Table I,

$$\frac{1}{2}\left[3\left(\frac{x}{a}\right)^2 - 1\right]\dot{q}_B. \tag{21}$$

The average value of this current along the winding is zero; hence it exerts no net m.m.f. on the core. The current at one end of the winding opposes that at the other end, and the magnetic field is in a sense "squirted" out into the region outside of the winding. The total m.m.f. of the current flowing in the region between 0 and x is

$$\frac{0.4\pi N_p\dot{q}_B}{2a}\int_0^x\left[3\left(\frac{x}{a}\right)^2 - 1\right]dx = 0.2\pi N_p\dot{q}_B\left[\left(\frac{x}{a}\right)^3 - \frac{x}{a}\right].$$

By plotting a curve of

$$\left[\left(\frac{x}{a}\right)^3 - \frac{x}{a}\right]$$

and from it obtaining the values of x/a corresponding to equal increments of the ordinates, the location of the equipotential lines on the flux plot for the chosen number of such increments is determined.[9–11] It may be noted that the number of such lines per unit distance along the winding is proportional to the derivative of the m.m.f. with respect to x, or the current. It may also be mentioned that the lines of force do not enter the current sheet at right angles, since there must be a tangential component of magnetic field intensity given by 0.4π times the current per unit length of winding. From such a plot $f_p(x)$ of (17) is obtained directly, after which (19) gives

$$L_{BB} = \frac{10^{-8}N_p}{2a}\int_0^a \left[3\left(\frac{x}{a}\right)^2 - 1\right] f_p(x)dx, \qquad (22)$$

the integration being carried out numerically using Simpson's rule.

4. Self-inductance of mode C

The primary and secondary currents are

$$\frac{1}{2}\left[3\left(\frac{x}{a}\right)^2 - 1\right]\dot{q}_C. \qquad (23)$$

Since the average current in each winding is zero, neither produces any net m.m.f. on the core; also, the secondary produces no net m.m.f. on the space occupied by the primary-to-secondary insulation. Here, as in Part 3, we assume that a sufficient approximation to the actual field can be obtained by replacing the secondary winding by a current sheet on the core. Because of the identity of (21) and (23), we see that the flux plot obtained in Part 3 may be used here. Denoting the function $f_p(x)$ obtained in Part 3 by $F_p(x)$, it follows that in the present case

$$f_p(x) = \frac{N_p - N_s}{N_p}F_p(x), \qquad g_p(x) = \frac{1}{2}\left[3\left(\frac{x}{a}\right)^2 - 1\right],$$

$$f_s(x) = \frac{N_p - N_s}{N_p}F_p(x), \qquad g_s(x) = \frac{1}{2}\left[3\left(\frac{x}{a}\right)^2 - 1\right];$$

hence (19) gives

$$L_{CC} = \frac{10^{-8}}{2a}\int_0^a \left(3\left(\frac{x}{a}\right)^2 - 1\right]$$

$$\left[\frac{(N_p - N_s)(N_p - N_s)}{N_p}\right] F_p(x)dx,$$

or, comparing this expression with (22),

$$L_{CC} = \left(\frac{N_p - N_s}{N_p}\right)^2 L_{BB}.$$

5. Mutual inductance between mode B and mode C

Proceeding as before, we consider both the primary and the secondary as current sheets on the core. Allowing the currents corresponding to $\dot{q}_B$ to flow, and giving q_C a virtual displacement, we have

$$f_p = f_s = F_p$$

$$g_p = \frac{1}{2}\left[3\left(\frac{x}{a}\right)^2 - 1\right]$$

$$g_s = \frac{1}{2}\left[3\left(\frac{x}{a}\right)^2 - 1\right],$$

where, as in Part 4, $F_p(x)$ is the function obtained for $f_p(x)$ in Part 3. Equation (19) now becomes

$$L_{BC} = \frac{10^{-8}}{2a}\int_0^a \left[3\left(\frac{x}{a}\right)^2 - 1\right][N_p - N_s]F_p(x)dx$$

or, comparing this expression with (22),

$$L_{BC} = \frac{N_p - N_s}{N_p}L_{BB}.$$

The above picture can evidently be refined by a more exact treatment of skin effect, and, in the case of small wire sizes, by a separate consideration of the flux which links the individual turns.

D. Calculation of the Source Voltages E_k

The generalized voltages E_k are given by (3), thus

$$E_k = \frac{\delta W_E}{\delta q_k}. \qquad (24)$$

It should be noted that δW_E is the virtual work *supplied by* the various sources, whereas δW_C, δW_R, and δW_L are the virtual works *required by* the various impedances, respectively.

As an example, the procedure used in calculating E_A may be outlined as follows:

$$\delta W_E = E_p\delta q_A - E_s\frac{N_p}{N_s}\delta q_A$$

$$E_A = \frac{\delta W_E}{\delta q_A} = E_p - \left(\frac{N_p}{N_s}\right)E_s.$$

E. Calculation of the Residual Voltages v_k

As described in connection with (3) the residual voltages are obtained by dividing certain virtual works by δq_k. In the transformer the only current distribution that we have that is not included in the various modes, and hence given by the q's, is the current distribution M, comprising the magnetizing current and the eddy currents in the core. We shall now calculate the three component parts of v_k, namely, v_{Ck}, v_{Rk}, and v_{Lk}.

1. Residual voltages v_{Ck}

The weak electric field which links the core and gives rise to the "volts per turn" of the winding is at right angles to the direction of flow of the displacement charge due to δq_k in the core-to-primary or primary-to-secondary insulation. It follows that the corresponding virtual work is zero, and the v_{Ck}'s all vanish.

2. *Residual voltages v_{Rk}*

The only place where the various mode currents and the currents of distribution M follow common paths is in the primary winding. It follows that

$$-v_{Rk} = \frac{\overline{\delta W_R}}{\delta q_k} \tag{25}$$

where $\overline{\delta W_R}$ is the virtual work required by the virtual displacement δq_k due to the primary voltage $I_M R_p$ caused by distribution M. In obtaining the self- and mutual-resistances involving mode A, the virtual work required by δq_k due to the primary voltage $R_p \dot{q}_A$ was calculated; hence, by replacing $\dot{q}_A$ by I_M in these expressions, we obtain the corresponding expressions for the present case. Noting (25), it follows that the v_{Rk}'s all vanish except that for mode A, which is

$$-v_{RA} = I_M R_p.$$

3. *Residual voltages v_{Lk}*

In order to determine the v_{Lk}'s we must determine the virtual work $\overline{\delta W_L}$ required by a virtual displacement δq_k due to the induced voltages arising from the distribution M; then

$$-v_{Lk} = \frac{\overline{\delta W_L}}{\delta q_k}. \tag{26}$$

The magnetic field due to this distribution is made up of two parts; the large circulating flux which is confined to the core, and the small leakage flux whose path lies part in the core and part in the air. We shall consider these two parts separately, as follows.

a. Circulating flux confined to core

The volts per turn opposing a positive primary current and aiding a positive secondary current due to this flux at any instant is independent of x, and will be denoted by $H(t)$. Noting (18), we see that the contribution of the voltage due to this flux to $\overline{\delta W_L}$ is

$$\int_0^a \left\{\left[\frac{N_p}{a} H(t)\right][g_p(x)\delta q_k] - \left[\frac{N_s}{a} H(t)\right][g_s(x)\delta q_k]\right\} dx$$
$$= \{N_p[\text{Average value of } g_p(x)] - N_s[\text{Average value of } g_s(x)]\}H(t)\delta q_k = 0$$

since the average values of $g_p(x)$ and $g_s(x)$ along the windings are zero for all modes except mode A, and since for mode A the two terms in the brace cancel. The circulating flux which is confined to the core therefore contributes nothing to the v_{Lk}'s.

b. Leakage flux

Let us assume that for any I_M the shape of the external leakage field would be altered negligibly if the material of the core were changed to one which is electrically nonconducting (no eddy currents), and which has a suitable, high, constant permeability. With such a core, let us consider a mode

$$\begin{aligned} \text{primary current} &= \dot{q}_0 \\ \text{secondary current} &= 0. \end{aligned} \tag{27}$$

The virtual work required by a virtual displacement δq_k because of the induced voltage due to $\dot{q}_0$ is, noting (3),

$$L_{k0}\ddot{q}_0\delta q_k.$$

But $L_{k0} = L_{0k}$ due to (10), and I_M and the current corresponding to $\dot{q}_0$ follow the same path; hence, noting (26) and (27), it follows that

$$-v_{Lk} = L_{0k}\dot{I}_M. \tag{28}$$

L_{0k} is $1/\ddot{q}_k\delta q_0$ times the virtual work required by δq_0 due to the induced voltages corresponding to $\ddot{q}_k$; hence, the L_{0k}'s can be determined using the same fields required in Part C.[12] More explicitly, we may apply (19) placing $g_p(x) = 1$, $g_s(x) = 0$, thus

$$\begin{aligned} L_{0k} &= \frac{10^{-8}}{a} N_p \int_0^a f_p(x)dx \\ &= 10^{-8}N_p \text{ Average value of } f_p(x)] \end{aligned} \tag{29}$$

where $f_p(x)$ is the same function defined in (17), used in Part C, and therefore available with no further calculation. Proceeding as in division 5 of this part, we obtain

$$L_{0C} = \frac{N_p - N_s}{N_p} L_{0B}. \tag{30}$$

If we make the same assumptions concerning the nature of the field due to mode A that were made in division 1 of this part, and proceed as with (20), we have

volts per unit length of primary

$$= \left(10^{-8}\frac{N_p}{a}\sigma\right)\left(\frac{0.4\pi\alpha N_p}{\mathcal{R}}\right)\ddot{q}_A$$

virtual charge that passes any point of primary $= \delta q_0$

$$L_{0A} = \frac{4\pi 10^{-9}\alpha N_p{}^2\sigma}{\mathcal{R}},$$

or, comparing this result with (20),

$$L_{0A} = \sigma L_{AA}.$$

This in (28) gives[7]

$$-v_{LA} = \sigma L_{AA}\dot{I}_M.$$

---

[12] The inductances L_{0k} could also be obtained from a plot of the leakage field due to I_M alone. Since this plot is simpler than those of the leakage fields of the various modes, greater accuracy would probably be obtained using it than would be obtained using those required in Part C of Section IV.

V. SUMMARY OF GENERALIZED NETWORK CONSTANTS

The results of calculations carried out in accordance with Section IV are contained in the following matrices (Table II). Here C_{pc} and C_{ps} are the total core-to-primary and primary-to-secondary capacitances, R_p and R_s are the total primary and secondary resistances, E_p and E_s are the primary and secondary voltages, N_p and N_s are the primary and secondary turns, and L_{AA} and L_{BB} are given by (20) and (22), respectively; also L_{0B} and L_{0C} are given by (29) and (30). σ is given in division 1 of Part C in Section IV, and $K=(N_p-N_s)/N_p$.

TABLE II

Matrix of Values of $1/C_{ij}$

Mode Mode	A	B	C
A	0	0	0
B	0	$\frac{3}{C_{pc}}$	0
C	0	0	$\frac{3}{C_{ps}}$

Matrix of Values of R_{ij}

Mode Mode	A	B	C
A	$R_p+\left(\frac{N_p}{N_s}\right)^2R_s$	0	0
B	0	$\frac{1}{5}R_p$	$\frac{1}{5}R_p$
C	0	$\frac{1}{5}R_p$	$\frac{1}{5}(R_p+R_s)$

Matrix of Values of L_{ij}

Mode Mode	*A*	*B*	*C*
A	(20)	0	0
B	0	(22)	KL_{BB}
C	0	KL_{BB}	K^2L_{BB}

Table of Values of E_k and $-v_k$

Mode	E_k	$-v_k$
A	$E_p-(N_p/N_s)E_s$	$R_pI_M+\sigma L_{AA}\dot{I}_M$
B	E_p	$L_{0B}\dot{I}_M$
C	E_p-E_s	$L_{0C}\dot{I}_M$

The data given above are exactly those required to set up the equations (4). If the solution of these equations is to be entirely mathematical there is no particular object in looking for an equivalent network, since such a network is by definition one whose mesh equations duplicate (4). If, however, the solution is to be obtained using a network analyzer (phantom circuit or "model"), then an equivalent network must be devised *which can be realized physically.* Aside from such a use, however, an equivalent network gives one an intuitive feeling for the significance of the various modes and design constants of the transformer that is not given by the impedance matrix $\|Z_{ij}\|$; also, it enables one to estimate the behavior of a transformer as a component part of a larger network or system, and hence the behavior of the system as a whole. Because of this, the equivalent network is useful in guiding certain types of experimental work; for example, that having to do with the suppression of high-frequency oscillations.

VI. EQUIVALENT NETWORKS

In devising an equivalent network the entire objective is to locate the various meshes relative to each other and include the right circuit elements, so that the various self- and mutual-capacitances, resistances, and inductances, and the various source and residual voltages take the values given in the matrices in Table II. Before considering any specific networks, it will be well to specify what is meant by an ideal transformer and also by a change of impedance level.

An ideal transformer is a fictitious transformer with no leakage, no resistance, and zero magnetizing current It has the following properties: it supplies or dissipates no energy, there is no electrical connection between the primary and the secondary windings, voltage ratio = 1/current ratio = turn ratio = constant. The impedance level of any mesh in a network is said to be increased in the ratio ρ^2, if the following alterations are made in the quantities associated with that mesh: all self-impedances are increased in the ratio ρ^2, all mutual impedances and voltages are increased in the ratio ρ, and the mesh current is decreased in the ratio ρ. That the network so altered is in equilibrium follows from the fact that its network equations are satisfied, for these equations can be obtained from those for the original network simply by multiplying the one equation corresponding to the given mesh through by ρ, and by replacing the given mesh current by ρ times the altered mesh current in all the equations. If desired, the impedance levels of several meshes can be similarly raised or lowered.

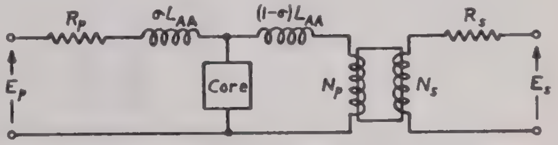

Fig. 2—Equivalent network using mode A and current distribution *M*.

We shall now obtain equivalent networks for a number of progressively more difficult cases, as follows.

A. Equivalent Network Using Mode A and Current Distribution M

In the network of Fig. 2 the fundamental mesh or mode currents are as follows:

1. I_M flows clockwise around through E_p, R_p, σL_{AA}, and the box marked "core."

2. $\dot{q}_A$ flows clockwise around through E_p, R_p, σL_{AA}, $(1-\sigma)L_{AA}$ and N_p; and $(N_p/N_s)\ \dot{q}_A$ flows clockwise around through N_s, R_s, and E_s.

The directions of the turns in the windings of the ideal transformer are such as to enforce the current mode just described in 2. The box marked "Core" is a fictitious impedance which requires the proper magnetizing current I_M.[13] It is evident by inspection that the various resistances, inductances, source voltages and residual voltages duplicate the values specified in Section V for mode A alone; also, the currents flowing through E_p and E_s are the actual primary and secondary currents $\dot{q}_A+I_M$ and $(N_p/N_s)\ \dot{q}_A$, respectively; hence, the four-terminal network Fig. 2 can replace the transformer in any network in which the transformer is a component part. If the impedance level of the part of this network that is associated with the secondary is reduced in the ratio $(N_p/N_s)^2$, the ideal transformer may be omitted, and the equivalent network of Fig. 2 reduces to Fig. 3.

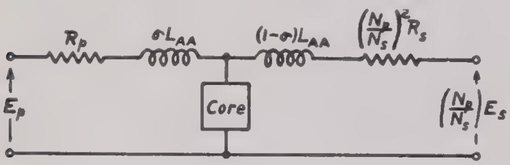
R_p
σL_{AA}
$(1-\sigma)L_{AA}$
$\left(\frac{N_p}{N_s}\right)^2 R_s$
E_p
Core
$\left(\frac{N_p}{N_s}\right)E_s$

Fig. 3—Equivalent network using mode A and current distribution *M*.

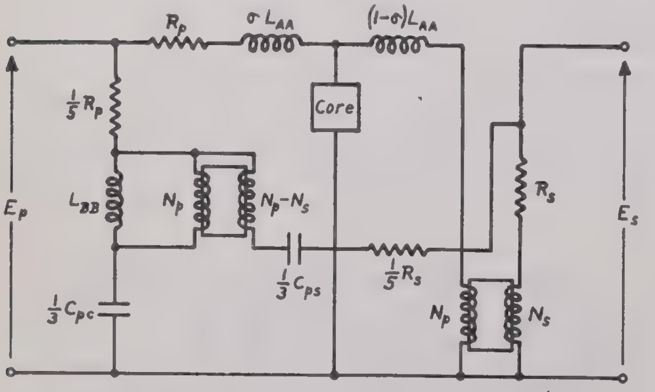
R_p
σL_{AA}
$(1-\sigma)L_{AA}$
$\frac{1}{5}R_p$
Core
E_p
L_{BB}
N_p
N_p-N_s
R_s
E_s
$\frac{1}{3}C_{ps}$
$\frac{1}{5}R_s$
$\frac{1}{3}C_{pc}$
N_p
N_s

Fig. 4—Equivalent network using modes A, B, and C, and current distribution *M*.

B. Equivalent Network Using Modes A, B, and C, and the Current Distribution M

In the network of Fig. 4[14] the fundamental mesh or mode currents are as follows:

1. I_M flows clockwise around through E_p, R_p, σL_{AA}, and the box marked "Core."

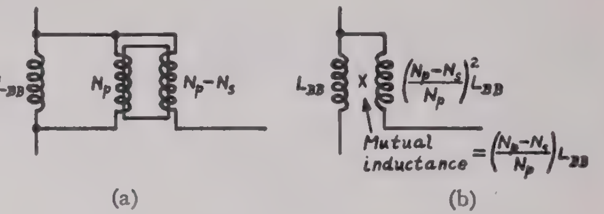
L_{BB}
N_p
N_p-N_s
L_{BB}
x
$\left(\frac{N_p-N_s}{N_p}\right)^2 L_{BB}$
Mutual inductance $=\left(\frac{N_p-N_s}{N_p}\right)L_{BB}$

(a) (b)

Fig. 5—Inductance combination and the part of Fig. 4 which it can replace.

2. $\dot{q}_A$ flows clockwise around through E_p, R_p, σL_{AA}, $(1-\sigma)L_{AA}$, and N_p; and $(N_p/N_s)\ \dot{q}_A$ flows clockwise around through N_s, R_s, and E_s.

3. $\dot{q}_B$ flows clockwise around through E_p, $(1/5)R_p$, L_{BB}, and $(1/3)C_{pc}$.

4. $\dot{q}_C$ flows around through E_p, $(1/5)R_p$, N_p-N_s, $(1/3)C_{ps}$, $(1/5R_s)$, and E_s; and $[(N_p-N_s)/N_p]\ \dot{q}_c$ flows counterclockwise around through L_{BB} and N_p.

The directions of the turns in the windings of the two ideal transformers are such as to enforce the current modes just described in 2 and 4. The box marked "Core" is a fictitious impedance which requires the proper magnetizing current I_M and which has the proper mutual inductances with modes B and C.[7,13] It is easily verified that the various capacitances, resistances, inductances, and source and residual voltages have the values specified in Section V; also, the currents flowing through E_p and E_s are the actual primary and secondary currents $\dot{q}_A+\dot{q}_B+\dot{q}_C+I_M$ and $(N_p/N_s)\ \dot{q}_A+\dot{q}_C$, respectively; hence, the four-terminal network Fig. 4 can replace the transformer in any network in which the transformer

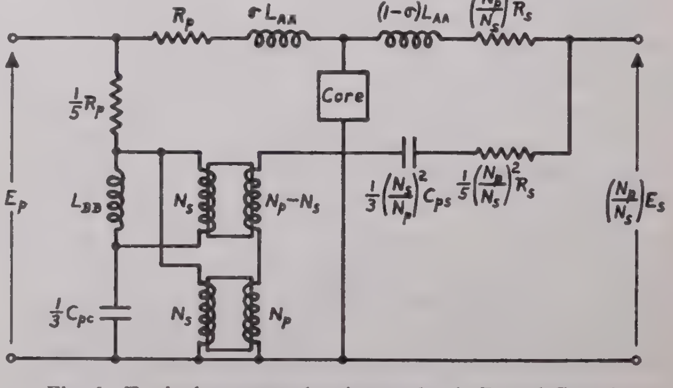
R_p
σL_{AA}
$(1-\sigma)L_{AA}$
$\left(\frac{N_p}{N_s}\right)^2 R_s$
$\frac{1}{5}R_p$
Core
E_p
L_{BB}
N_s
N_p-N_s
$\frac{1}{3}\left(\frac{N_s}{N_p}\right)^2 C_{ps}$
$\frac{1}{5}\left(\frac{N_p}{N_s}\right)^2 R_s$
$\left(\frac{N_p}{N_s}\right)E_s$
$\frac{1}{3}C_{pc}$
N_s
N_p

Fig. 6—Equivalent network using modes A, B, and C, and current distribution *M*.

---

[13] The inductances due to the leakage fields are evidently small compared with an inductance associated with the main circulating flux in the core. Of the mutual inductances given by the v_k's of Section V, only that due to v_A is shown in the diagrams.

[14] Instead of using the combination of Fig. 5(a), the combination of Fig. 5(b) could be used. This combination does not require an ideal transformer, but does require a coefficient of coupling of unity between the two coils.

is a component part. If the impedance level of the part of this network that is associated with the secondary, and also of part of the mesh described first under 4 above is reduced in the ratio $(N_p/N_s)^2$, the equivalent network becomes Fig. 6.

Here the fundamental mesh or mode currents are as follows:

1. I_M flows clockwise around through E_p, R_p, σL_{AA}, and the box marked "core."
2. $\dot{q}_A$ flows clockwise around through E_p, R_p, σL_{AA}, $(1-\sigma)\,L_{AA}$, $(N_p/N_s)^2\,R_s$, and $(N_p/N_s)E_s$.
3. $\dot{q}_B$ flows clockwise around through E_p, $(1/5)R_p$, L_{BB}, and $(1/3)C_{pc}$.
4. $\dot{q}_C$ flows clockwise around through E_p, $(1/5)R_p$, and N_s of the lower ideal transformer; $[(N_p-N_s)/N_p]\,\dot{q}_c$ flows counterclockwise around through L_{BB} and N_s of the upper ideal transformer; and $(N_s/N_p)\,\dot{q}_C$ flows clockwise around through N_p, (N_p-N_s), 1/3 $(N_s/N_p)^2\,C_{ps}$, 1/5 $(N_p/N_s)^2R_s$, and $(N_p/N_s)E_s$.

The directions of the turns in the windings of the ideal transformers are such as to enforce the current mode just described in 4. The current through E_p is the actual primary current $\dot{q}_A+\dot{q}_B+\dot{q}_C+I_M$, and the current through $(N_p/N_s)E_s$ is the actual secondary current $(N_s/N_p)\,([N_p/N_s]\dot{q}_A+\dot{q}_C)$ corresponding to the new impedance level.

VII. Simplification of Equivalent Networks

The complexity of the equivalent network to be used in solving a particular problem is determined by the nature of the problem and the accuracy of the desired results. For example, in problems involving low-frequency power transformers where distributed capacitance is unimportant, mode A and the current distribution M are sufficient, the resulting equivalent network being Fig. 7. If resistance and magnetizing current are unimportant in a particular application, this degenerates to Fig. 8.

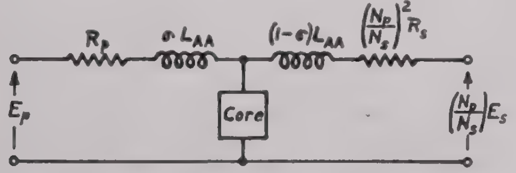
R_p
σL_{AA}
$(1-\sigma)L_{AA}$
$\left(\frac{N_p}{N_s}\right)^2 R_s$
E_p
Core
$\left(\frac{N_p}{N_s}\right)E_s$

Fig. 7—Simplified network based on mode A and current distribution M.

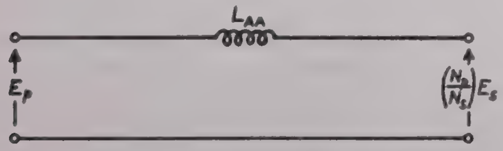

Fig. 8—Simplified network based on mode A.

Again, in solving certain specific problems in suppressing oscillations in pulse transformers, modes A, B, and C were used, the current distribution M being omitted. Resistances were found to be of negligible effect; also, L_{BB} when calculated was found to be very small and was neglected. Noting Fig. 6, it is evident that Fig. 9 is a corresponding equivalent network.

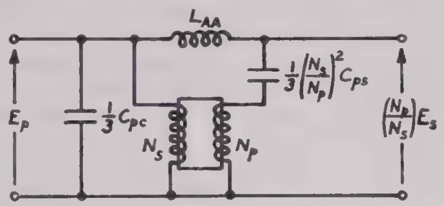
L_{AA}
$\frac{1}{3}\left(\frac{N_s}{N_p}\right)^2 C_{ps}$
E_p
$\frac{1}{3}C_{pc}$
N_s
N_p
$\left(\frac{N_p}{N_s}\right)E_s$

Fig. 9—Simplified network based on modes A, B, and C.

Finally, in investigating the relatively long-time backswing phenomena of a pulse transformer after the pulse is over, modes A, B, and C, and the current distribution M were used. Resistances and inductances were found to be small; hence, noting Fig. 6, it is evident that Fig. 10 is a corresponding equivalent network. However, since the middle branch comprising the ideal transformer and capacitor is equivalent to a capacitor, this network reduces to Fig. 11.

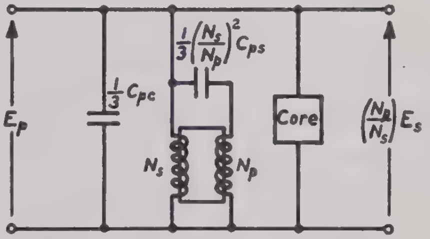
$\frac{1}{3}\left(\frac{N_s}{N_p}\right)^2 C_{ps}$
$\frac{1}{3}C_{pc}$
E_p
Core
$\left(\frac{N_p}{N_s}\right)E_s$
N_s
N_p

Fig. 10—Simplified network based on modes A, B, and C, and current distribution M.

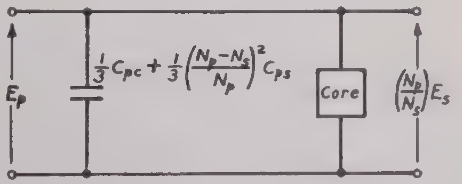
$\frac{1}{3}C_{pc}+\frac{1}{3}\left(\frac{N_p-N_s}{N_p}\right)^2 C_{ps}$
E_p
Core
$\left(\frac{N_p}{N_s}\right)E_s$

Fig. 11—Network further simplifying Fig. 10.

In any specific problem, only as many modes are used as are necessary to explain the particular phenomena under investigation. When the numerical values of the various circuit constants of the equivalent network are calculated, it is likely that certain of these will be seen to be negligible, in which case corresponding simplifications in the network are automatically suggested.

Transadmittance and Input Conductance of a Lighthouse Triode at 3000 Megacycles*

NORMAN T. LAVOO†, MEMBER, I.R.E.

Summary—**Measurement of the transadmittance and input conductance of a lighthouse triode at 3000 Mc. as a function of the cathode-to-grid transit angle θ_1 are described, and results are given. These measurements indicate that, for small values of θ_1 (that is, for close spacings and high current densities), transadmittances of 50 to 70 per cent of the low-frequency values can be obtained even with relatively coarse grids. On such tubes, however, the input conductance is about two to three times as high as might be expected. When θ_1 becomes of the order of 10 radians, the transadmittance falls to about 20 per cent of its low-frequency value. The input conductance falls off considerably for large θ_1, but there is no indication of negative input conductance. A discussion is given of the conspicuous discrepancy between the experimental results and the results predicted for an "ideal" tube.**

INTRODUCTION

THE LIGHTHOUSE TUBES[1] find many applications in the frequency range of a few hundred to a few thousand megacycles. At frequencies above a few thousand megacycles the lighthouse tube loses its high efficiency, and other tubes designed to capitalize on transit time replace it in many applications. This paper deals with the measurement of some tube parameters at a frequency in the upper useful range. Specifically, the input conductance and transadmittance will be given for a lighthouse triode of the 2C40 type at a frequency of 3000 megacycles. The first part of the paper will give the results of this investigation and the latter part will be devoted to a brief discussion of the apparatus and technique used.

This paper will deal only with small signals. It was found that the signal level could be increased so that the signal peak was equal to the bias before the characteristics described in this paper were appreciably affected. The alternating components of plate and grid currents may be expressed in the following way:

$$i_p = y_1 e_g + y_2 e_p \tag{1}$$

$$i_g = y_3 e_g + y_4 e_p. \tag{2}$$

At frequencies where transit time is not important, in a grid-return circuit $i_p = i_g$ and, therefore, $y_1 = y_3$ and $y_2 = y_4$. Hence, under these conditions, we recognize y_1 as the transconductance (at low frequencies the transconductance and transadmittance are identical) and y_2 as the plate conductance With the onset of appreciable transit time, however, the plate current is not identical with the grid current and y_1 and y_3 are no longer equal. The transadmittance y_1 may be measured by causing the alternating plate voltage e_p to be zero by detuning the output cavity and determining the ratio i_p/e_g In like manner y_3, the input admittance, may be determined by making e_p zero and measuring the ratio i_g/e_g.

INPUT CONDUCTANCE

The lighthouse tube, as normally used in a cavity, employs a grid-return type of circuit. Such a grid-return circuit results in a low input impedance to the tube even at the lowest frequencies.[2] If the output impedance be low by detuning of the output cavity, the input conductance is given by the transconductance of the tube. For example, at low frequencies a tube having a transconductance of 5000 micromhos would have an input conductance of 5000 micromhos. In terms of impedance this tube would have an input resistance of 200 ohms.

The more important data describing the tubes are these: (1) cathode diameter, 0.186 inch; (2) grid mesh, 0.002-inch wires spaced 100 per inch; (3) bias derived from 250-ohm cathode resistor; (4) oxide emitter, thickness 0.001 to 0.0015 inch.

The following data refer only to Figs. 1 and 2:

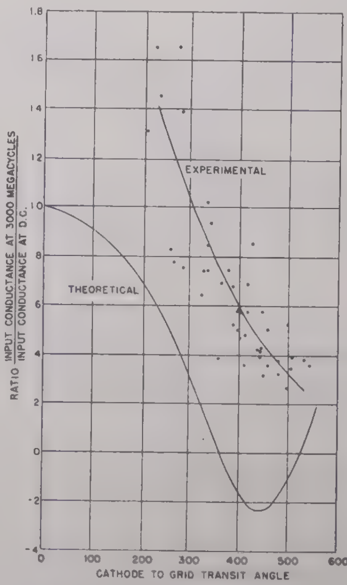

Fig. 1—Effect of cathode-to-grid transit angle on the ratio of high-frequency input conductance to the low-frequency input conductance taken on a number of parallel-plane triodes at 3000 megacycles. Included for comparison is the theoretical curve for an ideal tube.

---

* Decimal classification: R252×R262. Original manuscript received by the Institute, June 27, 1946; revised manuscript received, August 22, 1946.

† Research Laboratory, General Electric Co., Schenectady, N. Y.

[1] E. D. McArthur, "Disk-seal tubes," *Electronics*, vol. 18, pp. 98–102; February, 1945.

[2] M. Dishal, "Theoretical gain and signal-to-noise ratio of grounded-grid amplifier at ultra-high frequencies," PROC. I.R.E., vol. 32, pp. 276–284; May, 1944.

(5) plate voltage, 250; (6) grid-to-plate transit angle, roughly 100 degrees for each tube; (7) direct-current plate current, 8 to 30 milliamperes, depending on grid-to-cathode spacing.

If the triode had an infinitely fine grid, and if the cathode and grid were absolutely parallel and the electrons had zero initial velocities, the input conductance should fall off from the low-frequency value as frequency increases. It should actually go through zero, periodically yielding negative conductance at certain combinations of operating parameters. Fig. 1 shows how the input conductance varies with the cathode-to-grid transit angle in such an ideal tube.[8] In addition, Fig. 1 shows how the input conductance varies with cathode-to-grid transit angle in about forty parallel-plane triodes at 3000 megacycles. Each point represents a different tube.

It can be seen that increasing transit time does result in a decrease of conductance. The predicted decrease to zero does not occur, however. One factor that prevents this is the losses in the input circuit. These losses, as evaluated by taking a measurement with the tube biased considerably beyond cutoff, amount to approximately 1000 micromhos in the average tube. This loading is primarily caused by losses in rare-earth oxides used for the emitter, glass seals, and to a lesser extent by the thin fernico foil used in the cathode post, and by other loss sources. Were these losses not present one might expect the wide-spacing tubes to behave much as theory predicts.

Very-close-spacing tubes seem to suffer from a tremendous amount of input loading. For instance, the high-frequency input loading with the closer-spacing tubes is up to fifty per cent greater than the low-frequency value. One of the main contributing factors, in addition to those previously mentioned, is the effect of electrons within the potential minimum.

The potential minimum is a result of the electrons being emitted from the cathode with a finite initial velocity. This emission velocity causes all emitted electrons, even those that never get to the plate, to travel at least part way to the grid. As a result, there is a potential minimum between grid and cathode which is lower than cathode potential, and a good deal more current may be circulating aimlessly between cathode and potential minimum than actually moves on to be useful plate current. These potential minimum effects are especially pronounced at high frequencies and with close-spacing tubes. Actually the potential minimum may be located practically at grid plane in certain close-spacing tubes. The electrons making up the going and return current in the potential-minimum region will have appreciable transit angles in the microwave region. They are thereby capable of taking up power from the source by repeated accelerations. Though they induce current in, and therefore load down, the input cavity, they fail to contribute anything to the transadmittance.

TRANSADMITTANCE

This section is captioned transadmittance rather than transconductance because at the highest frequencies this parameter is no longer a real quantity but a complex one. Hereafter, the term "transadmittance" will be used to designate the magnitude of this quantity. No attempt was made to measure the phase angle of the transadmittance because of the complexity of the equipment thought necessary for this measurement.

For this measurement, the output circuit was again detuned and sufficient measurements were taken to obtain the output current and input voltage. Fig. 2 shows the results plotted as a ratio of the high-frequency transadmittance to the low-frequency transadmittance versus the cathode-to-grid transit angle. Each of the points on the experimental curve represents a different tube having a somewhat different spacing and current. Fig. 2 also shows a plot of an ideal parallel-plane triode whose spacing from grid to cathode varies in the same manner as the experimental tubes. The tubes having transit angle of 200 degrees correspond to a grid-to-cathode spacing of about 0.0015 inch. As the transit angle of the tubes shown in Fig. 2 increases the spacings vary more or less smoothly, so that at 500 degrees the spacing is

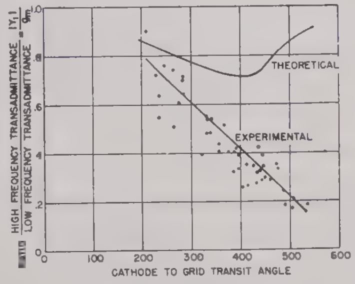

Fig. 2—Effect of cathode-to-grid transit angle on the ratio of high-frequency transadmittance to the low-frequency transadmittance. Each point represents one of the forty parallel-plane triodes operating at a given spacing and current density at 3000 megacycles. Also presented is the curve for an ideal tube.

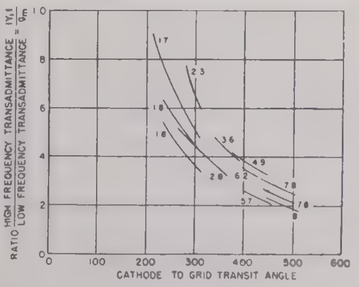

Fig. 3—Ratio of high-frequency transadmittance to the low-frequency transadmittance as a function of cathode-to-grid transit angle with cathode-to-grid spacing (given on the graph in mils) as a parameter. Each curve represents measurements on a parallel-plane triode with a given spacing at 3000 megacycles.

---

[8] The performance of an ideal tube is calculated from equations adapted from F. B. Llewellyn, "Electron Inertia Effects," Cambridge Physical Tracts, Macmillan Co., New York, N. Y., 1941.

about 0.008 inch. It is interesting to note that the experimental curve shows no upward trend at the longer transit angles as does the theoretical curve. Fig. 3 extends the usefulness of Fig. 2 by showing separately the effects of current and spacings.

This departure from the theoretical performance cannot be explained with any degree of certainty. One is tempted to ascribe the discrepancy to the coarseness of the grid mesh. However, for a given grid mesh the widest-spacing tube will approach the more closely to the ideal tube. That is to say, the tube with the widest spacing has effectively a finer grid mesh; and if the grid mesh were at fault, then this tube should approach more nearly to the ideal. If the trouble were that the elements of the tubes were nonparallel, this again could go a long way towards the explanation. However, it is hardly conceivable that all of the tubes would suffer from this defect to an equal extent. Furthermore, the tilt should become less significant with the wider-spaced tubes.

Another trouble with these tubes could be the nonuniformity of emission from the cathode. Certain areas that are more active than others have higher current density, which results in transit angles different from those in other less-active areas. There are many factors that enter into this uniformity problem. Not only is there the technique of preparation of the oxides but also the method of application, degassing of metals within the tube, activation method of cathode, and other processes difficult to control.

Still another possible factor is the influence of edge effect. A considerable portion of the total current is emitted by the area near the outer edge of the cathode. The discontinuity caused by the cathode post results in a nonuniform electric field in the outer areas of the emitter. This nonuniform field causes different transit times over the face of the cathode and would be more pronounced in the wider-spaced tubes.

APPARATUS

The cavity used for the measurements is shown in Fig. 4. There are several reasons for the use of such an unorthodox cavity. To simplify the calculations necessary to transform a measured impedance in region *III* of the grid-cathode cavity to the edge of the electron stream within the tube, it is desirable that the local waves generated by the discontinuity introduced by the cathode post attenuate to a negligible amount before reaching the corner *IV*. This then determines the minimum value for the inner diameter of section *III* (this dimension was 6.36 centimeters in the actual cavity). However, a choice of such large diameters makes it possible for circumferential modes to propagate in this region. The grid-cathode cavity is excited by a loop in section *I*, where there is high attenuation of higher-order waves. Section *I* then symmetrically excites section *III* (where measurements are taken) through the section of radial line *II*. An equivalent four-terminal network was calculated and then checked experimentally for section *IV* and the radial section *V* connecting the corner network to the tube.[4,5]

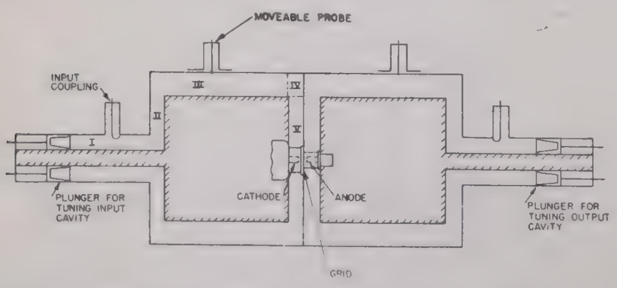
MOVEABLE PROBE
INPUT COUPLING
III
IV
II
I
V
PLUNGER FOR TUNING INPUT CAVITY
CATHODE
ANODE
PLUNGER FOR TUNING OUTPUT CAVITY
GRID

Fig. 4—Coaxial cavity used for measurement of 3000-megacycle transadmittance and input conductance.

It is convenient to construct charts so that, as soon as the measurements of standing-wave ratio and mode position are taken in section *III*, the real and imaginary components of the input impedance to the tube can be obtained immediately. If, in addition to the above information taken on both the input and output of the tube, one also takes a reading of the magnitude of the voltage maximum in both cavities, then with some simply constructed graphs the radio-frequency components of the plate current and grid voltage of the tube are easily obtained.

The numerical value of the cathode-to-grid transit angle for a particular tube was calculated by the use of the following formula[3]:

$$\theta_1 = \frac{126}{\lambda}\left(\frac{x}{I_0}\right)^{1/3}$$

where

θ_1 = the cathode-to-grid transit angle in radians
λ = the wavelength in centimeters
x = the cathode-to-grid spacing in centimeters
I_0 = the current density in amperes per square centimeter.

In all the measurements λ was fixed at 10 centimeters. The spacing was deduced from a knowledge of the high-frequency capacitance and previous studies of models. There are several assumptions that tend to make the transit angle, as calculated by the use of the above formula, incorrect. For example, there must be complete space-charge limitation at the cathode so that the electric field is zero at that plane. In addition, the assumption is inherent that the electrons are emitted with zero velocity and that the grid is very fine. The conditions in the experimental tubes depart sufficiently from these assumptions so that the results should be taken only to indicate trends. It is thought the accuracy of the transadmittance is within ±10 per cent; but the cathode-to-grid transit angle associated with this transad-

---

[4] W. C. Hahn, "A new method for the calculation of cavity resonators," *Jour. Appl. Phys.*, vol. 12, pp. 62–68; January, 1941.

[5] J. R. Whinnery and H. W. Jamieson, "Equivalent circuits for discontinuities in transmission lines," Proc. I.R.E., vol. 32, pp. 98–114; February, 1944.

mittance may be in error more than this, especially in the case of the closely spaced tubes.

Despite many precautions in the design of the cavity, considerable trouble was experienced with higher-order waves distorting the principal wave in the measurement zone. Some of this was eliminated by redesign of tube contacts; but in other instances, where the trouble originated within the tube from such things as a tilted or eccentric cathode, nothing could be done but reject that tube for testing purposes.

ACKNOWLEDGMENT

The writer wishes to acknowledge the contributions of S. Ramo and J. R. Whinnery to the theoretical analysis of the problem, and of J. E. Beggs for the many sample tubes which were used.

The Cyclophon: A Multipurpose Electronic Commutator Tube*

D. D. GRIEG†, SENIOR MEMBER, I.R.E., J. J. GLAUBER†, SENIOR MEMBER, I.R.E., AND S. MOSKOWITZ†, MEMBER, I.R.E.

Summary—**Electronic switching or commutation provides an inertialess mechanism for precise high-speed operation, and permits a multiplicity of circuits to be controlled by relatively small voltages such as are encountered in radio reception. The Cyclophon tube is one particular form of electronic switch which provides for the control of twenty-five separate circuits. This control is so precise that it can be used as a modulator and demodulator for pulse-time-modulation transmission and reception. Some further applications are in the fields of telemetering, pulse generation, phasing, frequency multiplication, counting of electric impulses, monitoring, and synchronizing-wave-form generation in television.**

THE NAME "Cyclophon" is given to a generic type of tube utilizing a beam of electrons as a switching or commutating element. The application of an inertialess switching device of this nature to a variety of problems has been long recognized and many references to it can be found in the literature.

As far back as 1906, Diekmann and Glage applied for a patent on a cathode-ray relay which was claimed to be capable of performance substantially equivalent to that achieved with a metallic switch.[1] More recently, radial types of commutating tubes have been described which are applicable to signaling and control systems.[2]

The Cyclophon may take a variety of forms utilizing various types of construction and methods of control. These include the cathode-ray-oscilloscope type, the aforementioned radial type, forms involving linear construction, or a combination of any of these. The electron beam may consist of a fine beam of electrons or, alternatively, a flat sheet capable of large current capacity. Control of the beam may also be accomplished in a variety of fashions including both electric and magnetic means. Whatever the form utilized, however, the functional characteristics are similar, in that results equivalent to those obtained with a moving metallic contactor are achieved.

I. THEORY OF OPERATION

A. General Description

The component parts of a typical Cyclophon tube are shown schematically in Fig. 1. The portions labeled 1 to 4 comprise a cathode-ray gun consisting of a cathode (1), control grid (2), electrostatic focusing element (3), accelerating anode (4), and electric-field deflection system (5). This gun produces a sharply defined beam of electrons, which may be deflected in any direction by impressing proper voltages on the deflection plates. Thus, in the tube illustrated, the beam is caused to describe a circular path in the plane of the target. Other types of deflection paths, and deflection and focusing systems, may of course be utilized.[3]

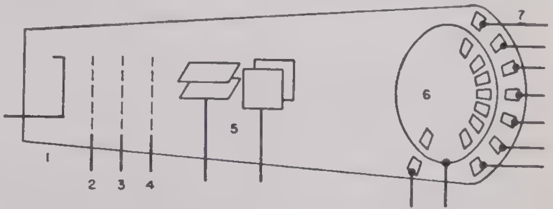

Fig. 1—Schematic representation of a Cyclophon tube, consisting of (1) cathode, (2) control grid, (3) electrostatic focusing element, (4) accelerating anode, (5) electric-field deflection system, (6) aperture plate, and (7) collector or secondary-emitting elements.

The gun structure is followed by a "stopper" or aperture plate, containing as many apertures as there are channels or circuits to be controlled. A series of targets (7), which may be current collectors or secondary-emitting dynodes, are placed directly behind the aperture-plate openings.

B. Secondary Emission

The current output of each channel may be increased several times by the use of secondary emission from the

---

* Decimal classification: R257.2. Original manuscript received by the Institute, August 26, 1946. Revised manuscript received, October 25, 1946. Presented, New York Section, I.R.E., New York, N. Y., April 6, 1946.

† Federal Telecommunication Laboratories, Inc., New York, N. Y.

[1] M. Diekmann and G. Glage, "Continuously quantitatively acting relay employing the electrical deflecting power of cathode rays," D.R.P. No. 184710, Klasse 21g, Gruppe 4, application date, Oct. 10, 1906, publication date, April 7, 1907.

[2] A. M. Skellet, "The magnetically focused radial beam vacuum tube," *Bell Sys. Tech. Jour.*, vol. 23, pp. 190–202; April, 1944.

[3] O. S. Puckle, "Time Bases," John Wiley and Sons, Inc., New York, N. Y., 1943; p. 9.

target anodes (dynodes). To obtain such a secondary current flow, the aperture plate is maintained at a higher positive potential than the dynodes. The dynode current then is a function of primary beam current, secondary-emission ratio, and aperture-plate-to-dynode voltage.

C. Dynode Characteristics and Equivalent Circuits

A typical dynode volt-ampere characteristic is shown in Fig. 2 for several values of primary beam current.

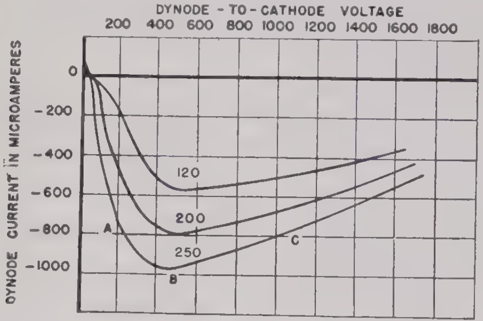

Fig. 2—Dynode volt-ampere characteristic for the three indicated values of primary beam current in microamperes.

The forms of these curves suggest three modes of operation and equivalent circuits. If the operation is such that the quiescent operating point is at A and assuming an output voltage which is small compared to the dynode voltage, the equivalent circuit may be represented by a current generator whose current is equal to $(N-1)i_pf(t)$, a switch or commutator, each contact having a negative resistance $-R$ and a load impedance Z. Such an equivalent circuit is shown in Fig. 3. The switching function $f(t)$ is derived from the geometric configuration of the apertures and from the type of cyclic variation of the sweep used. The internal contact resistance corresponds to the slope of the dynode characteristic at the operating point. Analysis then shows that the output-voltage function e_0 (i.e., the voltage appearing across the load impedance Z) may be written as

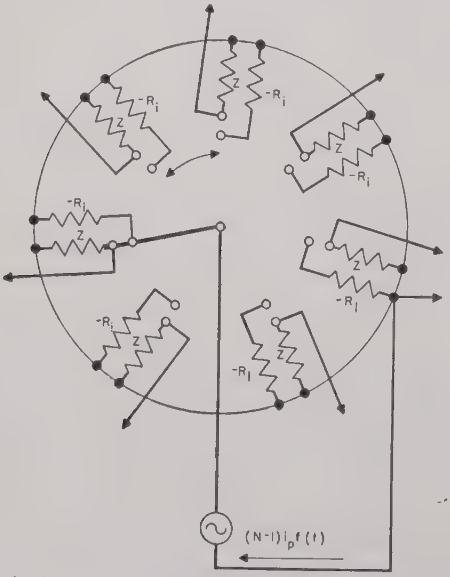

Fig. 3—Equivalent circuit of the Cyclophon tube. The tube may be represented by a rotating switch having a contact resistance $-R$.

$$e_0 = \frac{(N-1)i_pf(t)ZR}{(Z-R)}. \tag{1}$$

This equation shows that, with the described mode of operation, the output voltage may become exceedingly large if Z is a positive resistance[4] and almost equal or equal to R. Since for normal operation it is stipulated that the output voltage is small with respect to the dynode voltage, linear conditions prevail. Examination of the curves of Fig. 2 shows that a large increase in dynode voltage will bring the internal resistance into a positive region, thus causing the output voltage to reach equilibrium. This effect of secondary emission may be regarded as regenerative and thus must be carefully considered when using reactive loads. Under these conditions, where the output dynode voltage is large, nonlinear operation results and the equations indicated hold only for operation over the limited linear portion of the curves.

If the quiescent operating point is at C, Fig. 2, the equivalent circuit is similar to that described above, with the contact resistance replaced by a positive resistance. Thus the output voltage may be written as

$$e_0 = \frac{(N-1)i_pf(t)ZR}{R+Z}. \tag{2}$$

However, if the operating point is at B, the internal contact resistance is much greater than any normal load impedance, so that the load current becomes substantially independent of the load impedance. Hence, the output voltage becomes

$$e_0 = (N-1)i_pf(t)Z. \tag{3}$$

The above equations are useful in the analysis of the operation of Cyclophon tubes utilizing secondary emission. It should be noted that Z is in the form of a differential operator, since $f(t)$ may not necessarily be a simple sinusoidal function. Of course, the tube operation may be suitably analyzed by the usual graphical method using the characteristic curves.[5] These analyses are simplified if the load is a pure resistnace.

D. Cross Talk

An important characteristic of any type of commutating tube is cross talk, the interference obtained in one channel when a signal appears in another channel. It is obvious that the dynode circuits most affected are those which are physically adjacent in the tube.

Cross talk may be encountered for several reasons. Circuits in physical proximity may affect each other by either magnetic or electric induction. Thus cross talk may originate in the Cyclophon by electric induction through the capacitance between dynodes or dynode leads. Two dynode circuits are shown schematically with their interdynode capacitances and resistance loads in Fig. 4.

---

[4] A. W. Hull, "The dynatron, a vacuum tube possessing negative resistance," PROC. I.R.E., vol. 6, pp. 5–36; February, 1918.

[5] A Preisman, "Graphical Construction for Vacuum Tube Circuits," McGraw-Hill Book Co., Inc., New York, N. Y., 1943; p. 130.

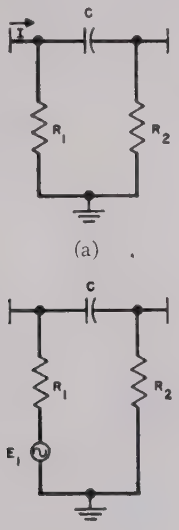

(a)

(b)

Fig. 4—Dynode circuits, including source of voltage or current and interdynode capacitances.

Assume that a sinusoidal current I flows as shown in Fig. 4(a). Then the voltage across R_1 is

$$E_1 = \frac{IR_1(jX_c + R_2)}{R_1 + jX_c + R_2}, \tag{4}$$

and the voltage across R_2 is

$$E_2 = \frac{IR_2R_1}{R_1 + jX_c + R_2}. \tag{5}$$

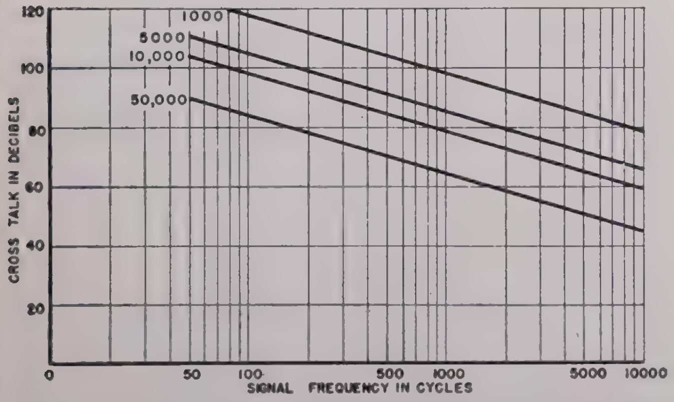

Fig. 5—Curves of cross talk as a function of signal frequency for the several specified values of load resistance (ohms). The cross talk indicated is caused by the interdynode capacitance of 2 micromicrofarads.

The cross-talk ratio is usually expressed in decibels, so that:

$$\text{db cross talk} = 20 \log_{10} \frac{(jX_c + R_2)}{R_2}. \tag{6}$$

An alternate condition arises when a signal is impressed in the dynode circuit as shown in Fig. 4(b). For this case the cross talk is similarly derived as

$$\text{db cross talk} = 20 \log_{10} \frac{R_1 + R_2 + jX_c}{R_2}. \tag{7}$$

Curves of cross talk as a function of frequency for several values of load resistance and assuming a total interdynode capacitance of 2 micromicrofarads are shown in Fig. 5.

Cross talk may also arise if more than one dynode is switched at one time. To minimize this effect, the electron beam must have a sharply defined boundary and must have a diameter consistent with the operational requirements.

II. CONSTRUCTION

The design considerations, construction, and processing vary only in detail for different types of tubes, and hence the following description is confined to one typical design of Cyclophon, designated as the Type X153C.

In the construction of the Cyclophon, four main objectives had to be realized, namely, maximum output, minimum interchannel cross talk, uniformity, and long life.

Preceding the construction of actual tubes, tests were conducted on models in an electrolytic tank and rubber-membrane apparatus to determine the optimum relations between various elements which would insure minimum cross talk and stable operation. These tests were also supplemented by experiments with tubes built in a demountable fashion.

The high secondary-to-primary-emission ratio and the uniformity desired required considerable experimentation before satisfactory results were achieved. It must be realized that, with 25 dynodes in one tube, one inoperable or low-output dynode will considerably decrease the usefulness of the tube. A reliable material capable of uniform secondary-emission yield must be used. Beryllium copper was chosen, although other alloys may be employed.

The target end of the cyclophon is a single assembly consisting of a metallic disk (aperture plate) with 25 accurately and uniformly spaced sectoral apertures and shields arranged in a circle. The 25 dynodes and support wires are assembled to two eyeleted mica disks and a 26-lead stem. When the aperture plate is assembled to the dynode assembly, each dynode is automatically aligned behind each aperture. The dynode is slightly larger than the corresponding aperture. The various components are shown in Fig. 6.

The dynodes undergo special processing before the aperture plate is attached. The active faces are carefully surfaced and degassed, and the dynodes are then oxidized. The entire dynode assembly receives identical treatment; thus great uniformity exists among the dynodes of any one structure. While the tube is on final exhaust the dynodes are bombarded, producing a higher and more uniform secondary-emission yield.

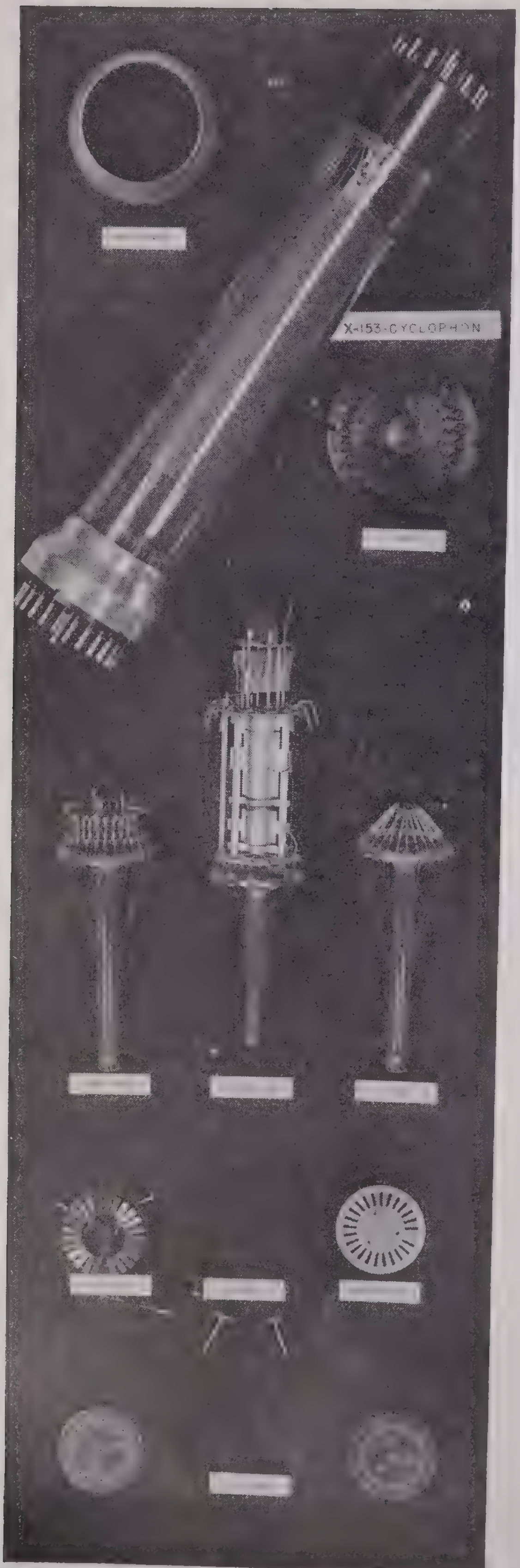

Fig. 6—The various components of a Cyclophon tube, illustrating its form of assembly.

The shortness of the target assembly and the large number of lead wires supporting it produces an extremely rugged structure. Life tests indicate that the cathode emission fails before any decrease in secondary-emission yield manifests itself, and it may be concluded that tube life is dependent only on the cathode.

Table I gives the operating characteristics of two types of Cyclophon tubes which have been manufactured. The X153C is a low-current, high-impedance type, while the X153G can operate with approximately 30 times the current and a corresponding reduction of dynode-aperture impedance. Fig. 7 illustrates representative type of Cyclophon tubes.

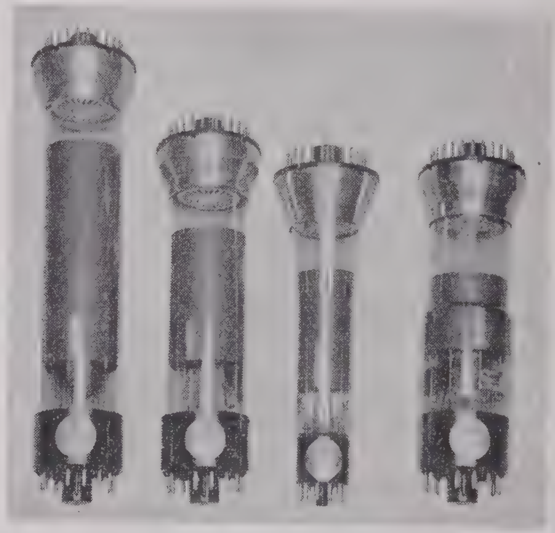

Fig. 7—A group of representative Cyclophon tubes. The three tubes on the left are high-impedance tubes, whereas the tube on the right is capable of supplying a dynode current of 30 milliamperes.

III. Application

The characteristics of Cyclophon tubes are such that a variety of applications is possible. These applications cover a range of subjects, including switching, separation and demodulation for systems of communication, telemetering, generation of pulse wave forms, phasing, frequency multiplication, and counting, to mention a few.

A. Switching

The limitations of mechanical switching are those of speed, accuracy, and mechanical wear. The Cyclophon tube, being an electronic device, finds application where either high speed, accuracy, or both characteristics, without variation because of inertia or wear, are necessary. The limitation of speed of operation of the Cyclophon is of the order of megacycles per second, and for normal speeds of operation the limitation is not in the tube itself but in the type of output circuits used. The fundamental accuracy is a function of the inherent rsistance noise, which is made up of a combination of the shot effect, secondary-emission noise, and thermal-agitation noise. Measurements have indicated that the total noise power is of the same order as that of a pentode amplifier, and these limitations can therefore be determined in the same manner as for this type of device. For some applications, of course, the accuracy is determined not by the noise power but by variation of physical dimensions with temperature, changes in beam cross section due to external fields, and fluctuating supply voltages. These variations can be reduced to an acceptable value by control of the external parameters of operation, however. Two basic types of switching can be distinguished: low-impedance switching and high-impedance switching. The Cyclophon tubes of the X153C type are essentially high-impedance devices, and to obtain extremely low impedances auxiliary tubes must be used. For example, thyratron tubes can be controlled by the output of the Cyclophon and this latter tube used only to switch from one thyratron to the next. In this manner the internal impedance of the X153C, which is of the order of thousands of ohms, can be effectively reduced to that determined by the controlled tube, which may be a few hundred ohms or less.

TABLE I

Cyclophon Characteristics

	X153C	X153G	
Heater			
Voltage (alternating or direct)	6.3	6.3	
Current (amperes)	0.6	1.5	
Interelectrode capacitances			
Dynode to dynode (micromicrofarads), approximate	2.0	2.0	
Dynode to aperture plate (micromicrofarads), approximate	2.0	2.0	
Focusing	Electrostatic	Electrostatic	
Deflection	Electric field	Electromagnetic	
Over-all length (inches)	12 11/16	7½	
Diameter of bulb (inches)	2	2¼	
Mounting position	Any	Any	
Gun base	Medium shell Diheptal 12-pin	Medium shell Diheptal 12-pin	
Target base	Special 26-pin	Special 26-pin	
Number of dynodes	25	25	
Type of sweep	Circular	Circular	
Typical Operation:			
Accelerating anode volts	2000	2000	1000
Focusing anode volts, approximate	200	—	—
Focusing cup No. 1 volts	—	+10	+10
Focusing cup No. 2 volts	—	−90	−90
Aperture anode volts	2000	2000	1000
Dynode volts	500	500	500
Deflection factor	135–170 (volts per inch)	70 (gauss per inch)	50
Dynode current (milliamperes)	1	30	12
Dynode load resistance (ohms)	50,000	1000	5000

Fig. 8(a) illustrates the use of the Cyclophon tube in a switching circuit. The tube voltages are those for normal operation. The signal source to be commutated is applied to the aperture plate through impedance Z and the signals are obtained from the dynode outputs labeled 1, 2, n. The speed of commutation is determined by the source applied to the deflection plates. Of course, in the example shown the source must be arranged so that two quadrature voltages are obtained to cause the beam to rotate across the apertures.

With this switching arrangement, two types of operating characteristics can be obtained: a variable-resistance characteristic, or one possessing a constant resistance. The former characteristic is obtained by operating the Cyclophon tube over the range OCD indicated by Fig. 8(b), which shows the aperture-dynode transfer characteristic, while linear operation is achieved by limiting the tube swing to the region OB. By proportioning the voltage E, the proper quiescent conditions can be obtained for either type of operation.

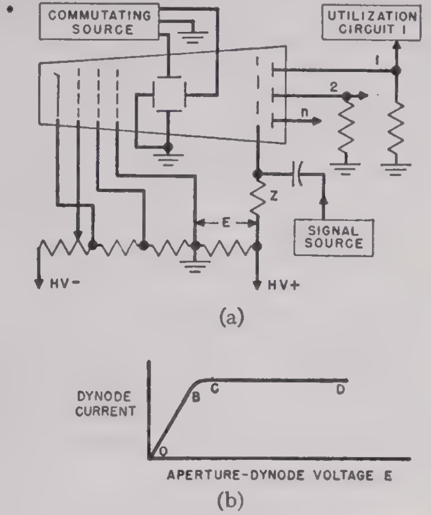

(a)

(b)

Fig. 8—(a) Switching circuit: The signal to be switched is applied to the aperture plate while the output signal is obtained at the dynodes 1, 2, n. (b) Cyclophon transfer characteristics. A constant-impedance characteristic is obtained by operation over the region OB. Variable impedance is obtained by extending operation to include CD.

Since switching covers a large range of functions, only a few such applications need be mentioned. These properties have been used for telemetering purposes and switching between various instruments at a rapid rate. Other applications have been in telephone circuits for accomplishing several of the functions previously obtained with mechanical switching.

B. Pulse-Time Modulation

An important use of the Cyclophon is found in its application to voice multiplexing by means of pulse-time modulation.[6] In fact, the term Cyclophon is derived from the Greek form "kyklos" (circle) and "phone" (speech), or "speech in a circular sequence," denoting the original multiplex application for which the tube was constructed. The Cyclophon is utilized both in the modulator unit for generating the required pulse series and also in the demodulator which separates the various channels and translates the time-modulation displacement into the normal voice currents.[7]

---

[6] E. M. Deloraine and E. Labin, "Pulse time modulation," *Elec. Commun.*, vol. 22, pp. 91–98; February, 1944.

[7] D. D. Grieg and A. M. Levine, "Pulse-time-modulated multiplex radio relay system-terminal equipment," *Elec. Commun.*, vol. 23, pp. 159–178; June, 1946.

In an application such as pulse-time demodulation, where use is made of the variation of output current as the beam is varied in position with respect to the aperture, the transfer characteristic is a function of the electron-beam cross section. For example, if the beam is circular, the variation in position across the aperture dynode elements will give a functional output-current variation represented by the expression (see Appendix)

$$i_d = \frac{4I}{\pi D^2}\left[\frac{D^2}{4}\sin^{-1}\frac{2(d - d^2)^{1/2}}{D} - \left(\frac{D}{2} - d\right)(dD - d^2)^{1/2}\right] \quad (8)$$

where I is the effective beam current, D is the beam diameter, and d is the displacement relative to the fixed apertures.

This expression is derived on the basis of the geometric variation of the sector area of a circular beam passing a straight-line barrier, and assumes constant beam-current density. Fig. 9 shows a plot of this function with the aperture-plate dimensions corresponding to the X153C type tube.

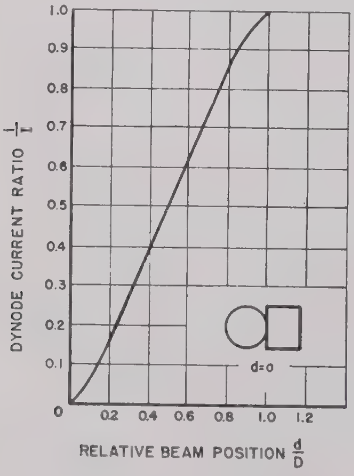

Fig. 9—Cyclophon demodulation characteristic. D = beam diameter, and I = beam current.

It should be noted that a linear function may be obtained by varying either the aperture shape, beam geometry, or the duration of the grid keying pulse.

C. Pulse Generation

By causing the beam to pass the aperture-plate openings, a pulse of current is caused to flow in the output dynode load circuits. This property can therefore be utilized for pulse generation. The build-up time of the pulse thus obtained, assuming that the impedance characteristics of the output load circuits are sufficient to pass the required band of frequencies, is given for tubes of the X153C type by the expression

$$t = \frac{D}{\pi L f_c} \quad (9)$$

where D is the beam diameter, L is the mean diameter of aperture plate, and f_c is the frequency of switching.

If the beam is of circular cross section, the build-up characteristic of the pulse is of the same shape as that shown in Fig. 9. The width of the pulse is determined by the duration of time the beam is within the aperture windows and is given by

$$w = \frac{(A + D)}{\pi L f_c}. \quad (10)$$

The decay time is similar to that of the build-up time. Since the shape of the pulse is thus a function of the frequency of commutation f_c, beam width, and aperture dimensions, a large variety of wave shapes can be obtained by manipulating these characteristics. Fig. 10 shows an oscillogram of the pulse wave forms obtained by utilizing the Cyclophon as a pulse generator. The repetition rate of the pulses thus derived is likewise a function of the frequency of commutation as well as the number of aperture dynode elements utilized.

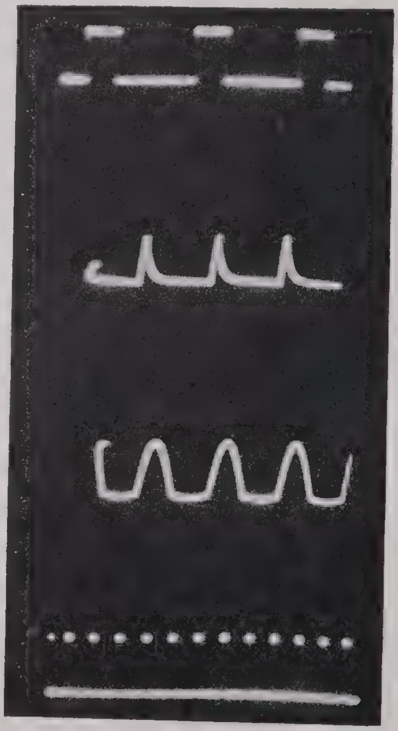

Fig. 10—Several wave forms obtained by using the Cyclophon as a pulse generator.

D. Pulse Delay and Phasing

Since the pulses derived at each aperture dynode element are generated in sequence, a division of the output pulse of the Cyclophon tube can be made in such a manner as to obtain sets of pulses with each pulse series delayed from the previous one by a given amount. This delay is dependent on the number of dynode aperture elements M, as well as the frequency of commutation, and is given by the expression

$$T = \frac{1}{Mf_c}. \tag{11}$$

If, in place of pulses, phased sinusoids are required, tuned circuits responding to a single frequency may be substituted for the dynode output resistance. In this case the angle of phase delay is given by the mechanical angle between the adjacent dynode aperture elements. For example, for the X153C, the angular delay is approximately 14.4 degrees, although any multiple of this delay may be obtained by grouping the elements.

E. Frequency Multiplication

The tuned dynode circuits may, of course, be tuned to a harmonic of the pulse-repetition rate. Alternatively, all dynode elements may be connected in parallel and fed to a common load impedance which is tuned to nM times the commutation frequency, where n is the harmonic multiple chosen. Fig. 11(a) illustrates the circuit diagram for a Cyclophon used in this manner. For each passage of the beam across the aperture dynode element a pulse of current is injected into the tuned circuit, and thus a frequency multiplication is obtained.

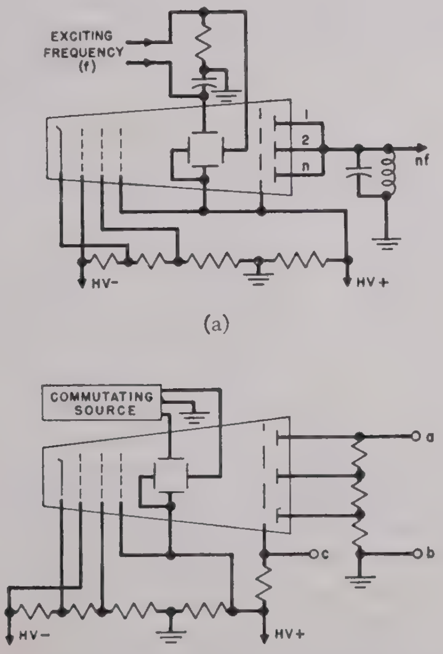

Fig. 11—(a) The Cyclophon is used as a frequency multiplier. An output corresponding to nf is obtained across the tuned circuit. (b) High-speed potentiometer. The terminals are labeled a and b with c as the common contactor.

F. Voltage Divider

An interesting application of the Cyclophon tube is its use as a high-speed voltage divider. In this case resistances are connected to each dynode with the aperture plate serving as the common contractor. The resulting configuration may be used in the manner normal to any voltage divider. A representative circuit arrangement for this application is shown in Fig. 11(b).

In place of the resistances, other circuit elements such as inductances may be used, or a capacitance voltage divider may be constructed provided the resistance return for each dynode element is included in the circuit.

G. Miscellaneous Applications

Other applications include counting of electrical impulses, blanking for noise reduction in pulse systems, monitoring and control, and synchronizing-wave-form generation in television. These constitute only a few of the possibilities, and many more applications utilizing Cyclophon characteristics can of course be envisaged.

IV. ACKNOWLEDGMENT

Acknowledgment is due to E. Labin, who with the authors conducted the original research on the tubes described. Mention should also be made concerning the contributions of A. M. Levine, M. Arditi, and other research engineers of the Federal Telecommunication Laboratories.

V. APPENDIX

If the total current in a circular homogeneous beam is I, the current i contained in a section A bounded by the aperture edge is

$$i = \frac{4I}{\pi D^2}(A)$$

where A is the area of the section.

The area A may be found by subtracting the triangular area aob from the sectoral area defined by the angle d, so that

$$A = \frac{d}{2}\frac{D^2}{4} - \left(\frac{D}{2} - d\right)(dD - d^2)^{1/2}$$

where

$$\frac{d}{2} = \sin^{-1}\frac{2(dD - d^2)^{1/2}}{D}.$$

So that

$$i = \frac{4I}{\pi D^2}\left[\left(\frac{D^2}{4}\sin^{-1}\frac{2(dD - d^2)^{1/2}}{D}\right) - \left(\frac{D}{2} - d\right)(dD - d^2)^{1/2}\right].$$

Writing d in terms of D so that $d = XD$,

$$\frac{i}{I} = \frac{4}{\pi}\left[\frac{1}{4}\sin^{-1} 2(X - X^2)^{1/2} - (1/2 - X)(X - X^2)^{1/2}\right]. \tag{12}$$

A curve of i/I versus $X = d/D$ is shown in Fig. 9.

Video Storage by Secondary Emission From Simple Mosaics*

ROBERT A. McCONNELL†, SENIOR MEMBER, I.R.E.

Summary—It has been found that the derivation of a video signal in an iconoscope by scanning does not involve bringing each element of the mosaic into an electron-exchange equilibrium while under the beam. Consequently, the mosaic charge is erased, not at the instant of passage of the beam, but continuously by the rain of low-velocity electrons. An output-signal attenuation of less than 1 per cent per scan has been observed. A factor of 10 increase in the number of removal scans per unit time after the creation of the original stored signal has yielded no observable change of attenuation per unit time. Only for storage tubes having a beam-density to capacitance ratio at least 100 times that of the iconoscope can a scanning-exchange equilibrium with charge obliteration be observed. In general, the mosaic escape current constituting the signal can be represented as a linear function of both the beam current and the potential of the mosaic element. The complex stored signals resulting from square-wave grid modulation of an ordinary oscilloscope used as a storage tube are explained in terms of electron loss at the instant of scan, preceded and followed by the gain of secondary electrons from the near-by beam.

I. INTRODUCTION

THE TELEVISION ICONOSCOPE is the first and most successful of storage tubes. There are many storage problems, however, which have nothing to do with a light image, but which might be solved by a cathode-ray beam in conjunction with a mosaic. The most important of these arises in radar moving-target indication where it is desired to store the video echo pattern following a transmitted pulse so that it may be subtracted from the pattern following the succeeding transmitted pulse. In this way, fixed targets may be canceled and moving targets retained. Other applications have been suggested in the field of supercalculating machines (for the storage of large numbers), in television (for the superposition of the pictures from unsynchronized cameras), and in communication service (for multiplexing and bandwidth changing).

A wartime attempt to use a storage tube similar to the iconoscope led to the discovery of certain effects which had not been anticipated from the literature.[1] The present investigation was then undertaken to obtain a more precise picture of what happens when a cathode ray scans a thin dielectric sheet backed by a metallic electrode at beam velocities yielding a secondary-emission ratio greater than 1.

If one subjects an insulated metal target to continuous bombardment by 1000-volt electrons, the target assumes a potential within several volts of the neighboring collector electrode, so that the number of secondary electrons escaping to the collector exactly equals the number of arriving primaries. If the target is initially too negative, it will repel secondaries and will shift positively. If the target is initially too positive, the low-velocity secondaries will fail to escape to the collector, and the target will shift negatively until equilibrium is reached.

The extension of this idea of an electron-exchange equilibrium to the scanning of an insulated surface, only one point of which is under the beam at any instant, is a plausible but inaccurate procedure. Following this procedure, one might predict, among other things, the possibility of storage by modulation of the collector electrode.[2] As the beam progressed across the mosaic it would discharge each point to an equilibrium potential determined by the modulation signal on the collector at that instant. The subsequent recovery of such a stored signal might be accomplished by discharging the mosaic, as in the case of television, by scanning without collector modulation. Since the total variation of potential over the face of the mosaic is not more than several volts in television usage, collector modulation of only several volts should be adequate to accomplish storage.

Collector modulation was tried unsuccessfully. It can be stated with certainty that storage of this class does not appreciably occur for modulation signals less than 50 volts. Above that level it was difficult to eliminate extraneous storage caused by deflection, intensity modulation, etc.

Thus, a pointwise exchange equilibrium does not occur between a simple mosaic and its collector. The actual behavior of such a mosaic, when under bombardment, has been analyzed qualitatively in the present paper.

II. EXPERIMENTAL PROCEDURES

The general method of this investigation was to apply a video pulse to a storage tube and to observe the resulting mosaic electrode signal at the time of this application and upon subsequent scans.

The modulating pulse was variable in length from one-half to four microseconds and in amplitude from zero to plus or minus 250 volts. The pulse rise was about

---

* Decimal classification: R583.1. Original manuscript received by the Institute, November 6, 1946; revised manuscript received, February 17, 1947.

This paper is based on work done for the Office of Scientific Research and Development under contract OEMsr-262 with the Radiation Laboratory of the Massachusetts Institute of Technology. By prior arrangement, it has been submitted to the Graduate School of the University of Pittsburgh in partial fulfillment of the requirements for the degree of doctor of philosophy in physics.

† Formerly, Radiation Laboratory, Massachusetts Institute of Technology; now, University of Pittsburgh, Pittsburgh 13, Pa.

[1] R. A. McConnell, A. G. Emslie, and F. Cunningham, "A moving target selector using deflection modulation on a storage mosaic," M.I.T. Rad. Lab. Rep. 562; June, 1944.

[2] G. Krawinkel, W. Kronjäger, and H. Salow, "On the question of electrical picture storage," *Telegraph., Fern., Funk und Fernseh-Tech.*, vol. 27, pp. 527–533; November, 1938.

one-tenth microsecond and the top was flat as delivered by the pulse generator. However, in some of the work a modulating amplifier was interposed which had an equivalent low-frequency time constant of less than 10 microseconds.

The modulating pulse was applied separately to the grid, deflection system, and secondary-electron collector of the storage tubes. Parameters varied from one experiment to the next included focus, astigmatic focus, and scanning-pattern geometry. Parameters variable from one scan to the next included average beam density, collector potential, scanning-pattern position, and modulation position.

Three storage tubes used at approximately 1000 volts are shown in Fig. 1. The 5-inch storage tube was a modified iconoscope constructed for this research. Its mosaic was similar in size and preparation to that of a type 1848 tube, except that low photosensitization was employed. The second tube was an ordinary Dumont type 3BP1 oscilloscope tube with a partially silvered exterior face. The third tube was an experimental 3-inch iconoscope loaned by RCA. In it a fully sensitized transparent mica mosaic was mounted normal to an electrostatic gun.

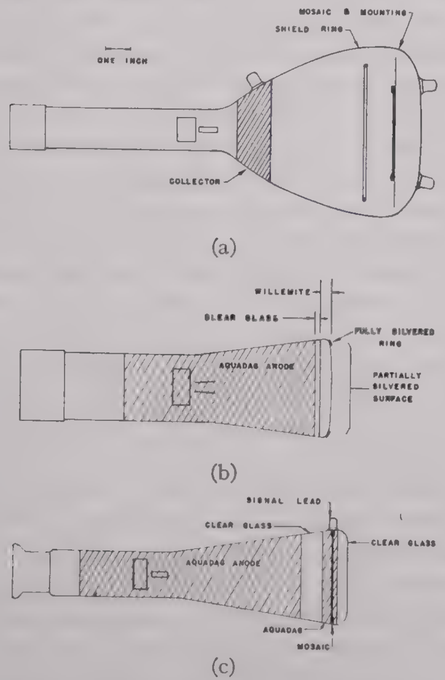
MOSAIC & MOUNTING
SHIELD RING
ONE INCH
COLLECTOR
(a)
WILLEMITE
CLEAR GLASS
FULLY SILVERED RING
AQUADAG ANODE
PARTIALLY SILVERED SURFACE
(b)
SIGNAL LEAD
CLEAR GLASS
CLEAR GLASS
AQUADAG ANODE
AQUADAG
MOSAIC
(c)

Fig. 1—Cathode-ray storage tubes. (a) Experimental 5-inch storage tube. (b) Type 3BP1 with half-silvered face. (c) Experimental iconoscope.

A standard test procedure is shown schematically in Fig. 2. A master trigger operating at 800 cycles per second fed a "three-step pedestal generator." This generator divided its input by three, and thereby determined the sequence of operations. The modulation pulse was applied during step one, i.e., within the interval following the first of three triggers. The mosaic electrode signal could be observed independently during steps one, two, and three. The mosaic signal occurring at modulation has been termed the "put-on" signal. The mosaic signals occurring upon subsequent scans have been termed "take-off" signals.

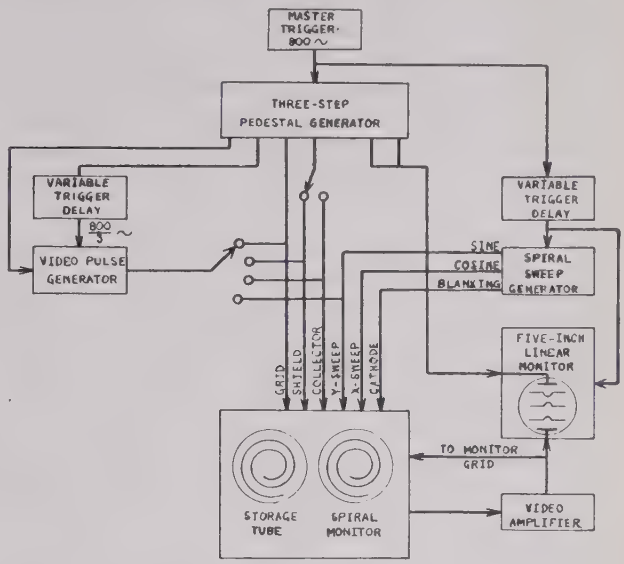
MASTER TRIGGER 800 ~
THREE-STEP PEDESTAL GENERATOR
VARIABLE TRIGGER DELAY
800/3 ~
VIDEO PULSE GENERATOR
VARIABLE TRIGGER DELAY
SINE
COSINE
BLANKING
SPIRAL SWEEP GENERATOR
FIVE-INCH LINEAR MONITOR
GRID
SHIELD
COLLECTOR
Y-SWEEP
X-SWEEP
CATHODE
TO MONITOR GRID
STORAGE TUBE
SPIRAL MONITOR
VIDEO AMPLIFIER

Fig. 2—Functional block diagram of the three-step process.

In addition to dividing by three, the three-step modulator generated as many as six independent pedestals, or voltage steps, each of which lasted for 1/800 second. The six pedestals could be distributed to occur among the three time steps in any combination, could be independently and continuously adjusted as to amplitude and polarity, and could be combined in any sequence. Thus, the pedestal generator allowed all possible combinations of potentials to be applied to the various electrodes of the storage tube.

For most of the work, a spiral sweep was used. The following features of this sweep were continuously variable at will: x and y position, over-all size, ellipticity, number of turns, and the spiral Q. Available values of turning rate ranged from 24 to 244 microseconds per turn. The value of 61 microseconds per turn was used except as noted. The number of turns varied from one to ten. At the typical spiral diameter of one and one-quarter inches, the linear spot speed was 1.6×10^5 centimeters per second, a value commonly used in television camera service.

The signal generated by the mosaic electrode was amplified by a high-gain video amplifier and fed simultaneously to two monitoring oscilloscopes. The first, a grid-modulated spiral-sweep oscilloscope, duplicated the scanning pattern of the storage tube. The second, a deflection-modulated linear-sweep oscilloscope, allowed the observation of mosaic-electrode signal shapes.

The over-all bandwidth of the monitoring circuits exceeded 700 kilocycles to half-power. The mosaic load resistor was 4700 ohms. Uncompensated circuits were employed throughout to minimize transient effects. The over-all equivalent low-frequency time constant most frequently used was 15 microseconds from mosaic to monitor screen.

III. The Mosaic Secondary-Escape Ratio

A. The Escape Process

The time changes of voltage which make up a "signal" can be stored as line changes of potential on the path of the scanning beam. Once created, these potential patterns cannot be examined directly, but must be studied by the effect they produce when subsequently scanned.

This "effect" is the video signal derived from the mosaic signal plate during the scanning process. Such a video signal is a measure of the net number of electrons reaching and leaving the mosaic *as a whole.* When a high-velocity beam impinges upon a mosaic, the resulting secondary electrons may return to the mosaic or may escape to a collector electrode. Those which do not escape make no contribution to any change of the mean mosaic potential, i.e., to the mosaic output signal. (The charge redistribution is, for all practical purposes, instantaneous.)

In the past it was believed that the charge which escaped from the mosaic while scanning a mosaic element corresponded to that required to discharge the intelligence stored on the element. Thus, it was *a priori* clear that the signal-plate (escape) current was a linear replica of the surface-potential pattern along the scanning path. It has now been discovered that an iconoscope television image is not destroyed by scanning. Such being the case, one may ask: "What factors do control the escape current? How is the output signal related to the stored signal?"

It has been found that the secondary-escape current I_m can be expressed in terms of the primary beam current I_b, according to the following equation:

$$I_m = kI_b.$$

The proportionality constant k will be called the "mosaic secondary-escape ratio," as distinct from the secondary-emission ratio.

During step one of the three-step test procedure described earlier, I_b is pulse-modulated. During steps two and three I_b remains constant, but k varies at video frequency as the moving beam crosses any previously stored signal.

B. The Mosaic Signal at Put-On

Neglecting the frequency-discriminatory effect of stray capacitance, the output signal developed by the mosaic is proportional to its net gain of electrons, i.e., to $I_b - I_m$. If I_b is modulated, the output signal will be proportional to $(1-k)$.

Suppose a small positive pulse is applied to the grid of a storage tube. The signal which is simultaneously observed at the mosaic (the put-on signal) may have either polarity, depending upon whether the mosaic as a whole gains or loses electrons by reason of the modulation pulse. If the escape ratio k is greater than one, the mosaic signal is positive, and vice versa.

It has been found that k is independent of instantaneous beam current, but that it can be readily controlled by the application of a several-volt pedestal to the collector electrode throughout the put-on sweep, as well as by other factors such as average beam current, scanning duty cycle, local shading gradients, and illumination. These factors are interrelated by the requirement that the mosaic must seek a mean potential relative to its surroundings so that the gain of electrons will equal the loss by all possible mechanisms, when averaged over the period of the slowest mechanism involved.

C. The Mosaic Signal at Take-Off

When the beam current is constant, the only change in mosaic output is that caused by changes in k. Any previously stored point-to-point fluctuations in mosaic potential cause a corresponding change in k at the moment of scanning, and thereby generate the video output signal.

If the point under the beam is more positive, fewer electrons escape to the collector and the mosaic signal plate shows a negative shift. This does not imply that the electron increment which just fails to escape must return to the spot under scan, but only that it must return to the mosaic as a whole.

It has been found that the relationship between k and the potential of the point which will be scanned is roughly linear over a wide range of beam currents. This implies that a constant-density scanning beam will faithfully reproduce the mosaic potential fluctuations over the scanning path. Consequently, any qualitative difference between a take-off signal and the corresponding original modulating signal is to be explained in terms of a put-on, rather than a take-off, mechanism.

IV. Electron Behavior in Scanning

Because it has been found by experiment that individual path segments do not seek an exchange equilibrium potential at the instant of scan, it is necessary to re-examine all of the older ideas of electron behavior which were tied to the notion of a pointwise equilibrium. Many of the statements which follow conform entirely to earlier concepts, and only a few are wholly unexpected.

Secondary electrons return to the mosaic more densely in the vicinity of their origin than elsewhere. This effect may be greatly accentuated within a few beam widths at high beam currents. Included in the more distant return are most of those electrons which did not quite surmount the potential grade to the collector. The most direct method used to study electron redistribution was to scan at a low constant beam current while applying a strong positive grid pulse at some particular point on the mosaic. The drift of the resulting excess electrons over the surface of the mosaic could be seen at a glance on the spiral monitor.

Those areas which are not scanned have no means of losing electrons in the absence of light. Consequently, after a short interval such areas become highly negative and repel additional electrons. In proof of this, the former spiral position could be seen for about one second as a strong, sharply defined "television" image, when the monitor and storage-tube spirals were suddenly subjected to a simultaneous oscillatory displacement.

Under television scanning conditions the scanning paths are contiguous, and the secondary electrons are free to travel in any direction. With an open spiral, the negative interturn barrier inhibits electron travel normal to the path of scan. Under this condition many secondaries which would otherwise have crossed to another turn or line are channeled onto their own line, and collect before and after the beam. The diminution or disappearance of before-and-after-collection signals was clearly noted as the scanning pattern was adjusted continuously from an open spiral to a spiral with contiguous turns.

At television beam densities, the electrons whose mosaic escape is controlled by stored signals are drawn from electrons which would otherwise rain uniformly over the mosaic. The number of those electrons which return to the vicinity of the scanning beam is not influenced by the potential discontinuities which constitute the stored signal. These conclusions result from the experimental observation that stored signals are not moved, blurred, or appreciably diminished by uniform scan at low beam currents (in darkness, of course). When, with the iconoscope, the number of take-off scans per unit time was increased from 2 to 29 by converting the spiral to a circle, the attenuation per unit time remained unchanged, being less than 1 per ecnt per scan for the circle.

Only with the 3BP1 and at beam densities at least ten times those of the iconoscope and 5-inch tube was it possible completely to eradicate the stored signal by a single scan. This effect might be explained by the formation of a localized space charge made possible by the small capacitance of the 3PB1 (about 4 $\mu\mu$fd. per square centimeter as compared with 100 $\mu\mu$fd. per square centimeter for television mosaics).

At low beam currents the 3BP1 gave a response like that of the iconoscope and the 5-inch storage tube. On the other hand, when the beam current of either of the latter was raised above several tenths of a microampere, the storage take-off signals were lost in scanning noise and shading signal well before the high attenuation ratios of the 3BP1 could be reached—a fact reflecting the difference in secondary-emission ratio and surface uniformity of the willemite screen versus the caesiated-silver mosaic.

Most experiments were carried out by means of the repetitive three-step procedure described earlier. The possibility of integration effects extending over several cycles was checked as follows. By shifting the modulation-pulse delay at a suitable rate, the individual put-on signals could be completely separated as seen on the linear monitor. With this arrangement, each stored pulse was the result of a single scan. No limit was placed upon the number of take-off signals—these appearing on the linear monitor directly beneath their associated put-ons. The ratio of step two to step three take-off signals was found independent of integration, although a function of beam current as already indicated. Moreover, integration was found to give negligible take-off signal increase for high beam currents, and not more than a factor-of-two increase for low beam currents.

That the difference in behavior between the 3BP1, on the one hand, and the iconoscope and 5-inch tube, on the other, was not caused by surface leakage was shown by an experiment in which the 5-inch tube was able to store a signal for at least ten seconds in darkness with the beam current off. The 3BP1 could, of course, do likewise.

The proper interpretation of grid-modulation take-off patterns was verified by numerous other auxiliary experiments, such as those in which a focused image of a small lamp filament was allowed to fall near or upon the iconoscope spiral path for various spiral spacings. It may be remarked in this connection that the signals stored by the light image were of the same order of magnitude as those stored by grid modulation of that tube.

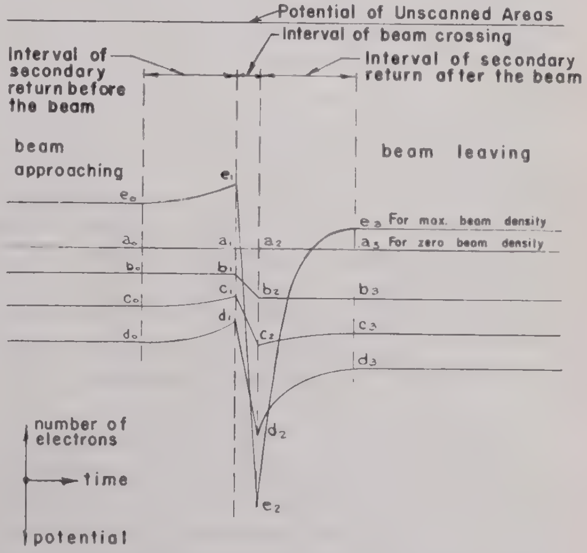

Fig. 3—Potential of a mosaic point as a function of time during step one of a three-step process: step 1 at the indicated beam densities; steps 2 and 3 at one fixed nominal beam density.

V. Mosaic Potential Under a Uniformly Scanning Beam

Fig. 3 represents in qualitative fashion the potential of a particular point on a mosaic as a function of time during step one of a three-step process while that point is being repeatedly scanned by a high-velocity electron beam traveling at a uniform speed in the absence of modulation or stored signals in the vicinity thereof. Fig. 3 was induced to explain the experimental findings reported in Section VII.

Only the time interval in the vicinity of scan is shown in Fig. 3. During perhaps 95 per cent of the time the mosaic point is remote from the beam and slowly drifts down in potential while gathering secondary electrons at a relatively uniform rate. The several curves of Fig. 3 correspond to several beam currents. However, these are the beam currents only in the vicinity of the time interval which is represented and only during step one of a three-step process. The average beam current is the same for all curves. The curves of Fig. 3 are based upon the further approximating assumptions that the beam has a uniform cross-sectional density, and that secondary electrons return in excess above a uniform areal rate only in a well-defined region before and after the beam.

The salient features of Fig. 3 are these: At all beam currents the mosaic point while beneath the beam is driven positive as a result of secondary emission. At low beam currents (curve *b*), the secondary electrons fall uniformly upon the mosaic. At a somewhat higher beam current (curve *c*), electrons collect equally before and after the beam. Television scanning conditions are represented by curves *b* and *c*. At still higher beam currents (curves *d* and *e*), secondary collection behind the beam predominates. For increasing beam current up to a certain point (*a*, *b*, *c*, *d*) the final mosaic potential after the the passage of the beam is increasingly positive. Above a certain beam current (*d*, *e*) there is a reversal of final potential.

It might be added that, in the case of a nonuniformly scanning beam, e.g., in the case of deflection modulation, an increased spot velocity for tubes operating in the region of curves *a* to *d* should be equivalent to a decrease in beam density. Such a decrease should give rise to a decreased mosaic point potential, to an increased secondary-escape ratio, and to a positive mosaic signal. A strong positive put-on "spike" at the rise and fall of a square-wave, deflection-modulation pulse was found experimentally under the specified conditions.

VI. The Storage of Signals by Grid Modulation

Fig. 4 shows the types of potential patterns which can be stored upon a mosaic by applying a square positive video pulse of several microseconds length to the grid of a storage tube. These curves are derived graphically and exactly to scale from Fig. 3, according to the following method and assumptions.

Curve *cdc* represents the stored pattern which results if the beam current of the storage tube is increased from that of curve *c* of Fig. 3 to curve *d* and back to curve *c* by means of the above-mentioned video pulse. The potentials of those points which are well removed from the rise and fall of the video pulse can be read directly as the number 3 potentials of Fig. 3. Potentials in the vicinity of the step points are derived upon the assumption that potential is determined primarily by the beam current at time of scan, and that the effect of the near-by transient is to cause an electron excess or shortage for which correction can be made.

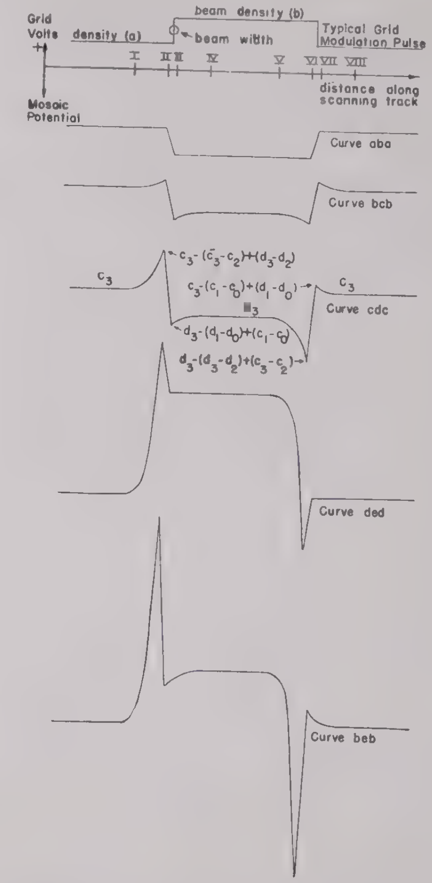
Grid Volts
+
density (a)
beam density (b)
beam width
Typical Grid Modulation Pulse
I
II
III
IV
V
VI
VII
VIII
distance along scanning track
Mosaic Potential
Curve aba
Curve bcb
c_3
$c_3-(c_3-c_2)+(d_3-d_2)$
$c_3-(c_1-c_0)+(d_1-d_0)$
c_3
3
Curve cdc
$d_3-(d_1-d_0)+(c_1-c_0)$
$d_3-(d_3-d_2)+(c_3-c_2)$
Curve ded
Curve beb

Fig. 4—Theoretical forms of potential variations stored on a mosaic by grid modulation. Direction of scan is to the right; letter designations refer to Fig. 3.

As an example, consider point *II* of curve *cdc*. This point received its prebeam electrons and its scanning from a beam of density *c*. Point *II* is defined as that point which the back edge of the beam was leaving at the instant modulation was applied. Hence, point *II* received all of its post-beam electrons from a beam of density *d*. Therefore, the potential of point *II*, after the passage of the beam, may be calculated from

$$II = c_3 - (c_3 - c_2) + (d_3 - d_2)$$

because $(c_3 - c_2)$ of Fig. 3 represents the potential change that did not occur but which would have brought point *II* to potential c_3, whereas $(d_3 - d_2)$ represents the potential change that did result owing to electrons arriving from a beam of density *d*.

VII. The Comparison of Theoretical and Experimental Wave Forms

The theoretical curves of Fig. 4 may be compared with the typical experimentally observed curves of Figs. 5

and 6. The experimental wave forms are tracings of freehand sketches from an oscilloscope made a year before the theory and curves of Figs. 3 and 4 were conceived.

Figs. 5 and 6 show wave forms in groups of three. Each group consists of the mosaic put-on and take-off signals of the three-step process in their relative positions, as displayed upon the linear monitor oscilloscope. The significance of the put-on signals has been discussed in Section III-B. Directly beneath each put-on signal are the second- and third-step take-off signals, respectively. Dotted lines indicate exact time coincidence between put-on and take-off. Both figures show modulation amplitude increasing to the right and average beam current increasing progressively downward.

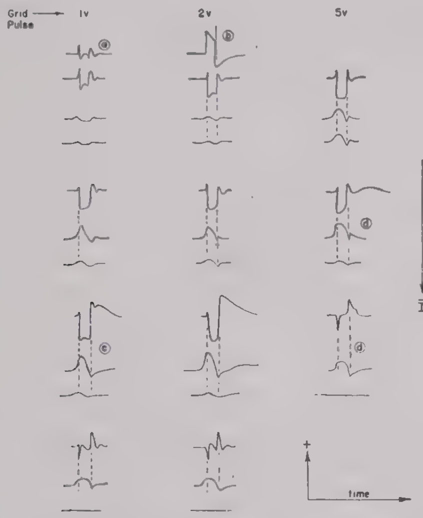

Fig. 5—3BP1 mosaic signals for positive grid modulation. Modulation pulse voltage and average beam current variable; five spiral turns, well spaced; spiral rate: 61 microseconds per turn; pulse length: $3\frac{1}{2}$ microseconds.
(a) Mosaic electrostatic pickup at 1 volt with beam biased off.
(b) Pulse shape as applied to grid.
(c) Average beam current set to give maximum step two take-off.
(d) Preamplifier gain cut by one-half to avoid saturation.

With the iconoscope and the 5-inch tube, the only patterns obtainable were very similar to those shown in the upper left-hand corner of Figs. 5 and 6. Curve *cdc* of Fig. 4 may be compared with the upper left-hand curve of Fig. 5. Notice that each take-off consists of a negative pulse preceded and followed by positive humps. The negative pulse represents positive storage caused by loss at put-on of secondary electrons. The positive humps represent secondary electrons which have collected in excess before and behind the modulation. The corners are rounded by the limited bandwidth of the beam and amplifiers.

The second row, pattern *d* of Fig. 5, may be compared to curve *ded* of Fig. 4. Note that secondary-electron collection precedes the modulation segment on the curves of both figures. However, the positive spike of Fig. 4 is missing from Fig. 5. This departure from theory was found generally and proves that highly negative mosaic points repel additional electrons which would otherwise land. The take-off pulse is not flat because of droop of the modulation pulse, as shown at *b* of Fig. 5. The downward spike at the end of the same signal represents positive storage on a point which lost electrons by scanning at a high beam current but which, with sudden collapse of modulation, was given no opportunity to recoup its losses. The positive take-off following the end of modulation represents secondary collection ahead of the scanning beam, as seen on curve *cdc* of Fig. 4. This suggests that a curve *cec* (not drawn) would provide a better fit than curve *ded*.

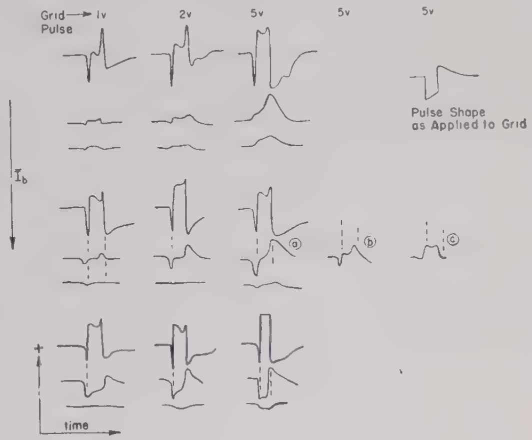

Fig. 6—3BP1 mosaic signals for negative grid modulation. Modulation pulse and average beam current variable; four spiral turns spaced six line widths; spiral rate, 61 microseconds per turn; pulse length, 4 microseconds. (a) becomes (b) with defocus. (b) becomes (c) with further defocus to four normal line widths.

Curve *cdc* of Fig. 4 may be compared with the first take-off curves of Fig. 6. Since negative modulation is used in Fig. 6, the comparison is made by dividing curve *cdc* at its midlength and inverting the order of the halves. The 5-volt curve of the top row of Fig. 6 exhibits the effect of the modulation-pulse overshoot, and is not readily comparable with Fig. 4.

Curves *a*, *b*, and *c* of Fig. 6 are especially significant because they show reversion to the low-beam-current pattern of the upper left-hand corner brought about by beam defocus. With defocus, the beam area increases and the beam density must drop. All of the second- and third-row patterns of Fig. 6 match excellently with properly split and inverted patterns of Fig. 4.

The analysis of the development of experimental waveshapes by means of Figs. 3 and 4 must not be pushed too far. It will be recalled that these curves assume a constant average beam current. This condition was not met experimentally. The data at hand are insufficient to pursue the matter in greater detail. It is certainly safe to say that the same electron transfer mechanisms will be in operation. Indeed, as can be seen from the experimental figures, the wave forms have readily identifiable features over the gamut of average beam current and modulation amplitude.

ACKNOWLEDGMENT

The three-step pedestal generator used in this work was developed by G. M. Nonnemaker. The spiral sweep central and variable trigger delay were developed by V. A. Olson. The author is grateful to F. Cunningham, A. G. Emslie, E. C. Pollard, and C. A. Whitmer for their encouragement and criticism.

ADDITIONAL REFERENCES

1. V. K. Zworykin, "The Iconoscope—A modern version of the electric eye," PROC. I.R.E., vol. 22, pp. 16–32; January, 1934.
2. V. K. Zworykin, "Iconoscopes and kinescopes in television," *RCA Rev.*, vol. 1, pp. 60–84; July, 1936.
3. M. Knoll and F. Schroter, "Electron image transmission with insulating and semi-conducting layers," *Phys. Zeit.*, vol. 38, pp. 330–333; May, 1937.
4. H. Iams and A. Rose, "Television pickup tubes with cathode-ray beam scanning," PROC. I.R.E., vol. 25, pp. 1048–1070; August, 1937.
5. V. K. Zworykin, G. A. Morton, and L. E. Flory, "Theory and performance of the iconoscope," PROC. I.R.E., vol. 25, pp. 1071–1092; August, 1937.
6. M. von Ardenne, "On experiments with light-sensitive semi-conducting layers in cathode-ray tubes," *Hochfrequenz. u. Elektroakustic*, vol. 50, pp. 145–149; November, 1937.
7. W. Heimann and K. Wemheuer, "Contribution on the manner of operation of the cathode-ray picture scanner," *Elek. Nach. Tech.*, vol. 15, pp. 1–9; January, 1938.
8. G. Krawinkel, W. Kronjäger, and H. Salow, "On a storing television camera tube with semi-conducting dielectric," *Zeit. für Tech. Phys.*, vol. 19, pp. 63–73; March, 1938.
9. G. Krawinkel and H. Salow, "On the potential rise and efficiency of television tubes with semi-conducting dielectrics," *Telegraph., Fern., Funk und Fernseh-Tech.*, vol. 27, pp. 285–290; August, 1938.
10. M. Knoll, "Significance of the 'stray electron effect' in the operation of picture scanning tubes," *Zeit. für Tech. Phys.*, vol. 19, pp. 307–313; October, 1938.
11. M. Knoll and R. Theile, "Capacitance controlled scanning tubes," *Telegraph., Fern., Funk und Fernseh-Tech.*, vol. 27, pp. 538–540; November, 1938.
12. W. Heimann and K. Wemheuer, "On the cause of the shading signal in picture pickup tubes," *Zeit. fur Tech. Phys.*, vol. 19, pp. 451–454; November, 1938.
13. J. D. McGee and H. G. Lubszynski, "EMI cathode ray television transmission tubes," *Jour. I.R.E.* (London), vol. 84, pp. 468–475, 480–482; April, 1939.
14. V. K. Zworykin and G. A. Morton, "Television," John Wiley and Sons, New York, N. Y., 1940.
15. I. G. Maloff, "Electron bombardment in television tubes," *Electronics*, vol. 17, pp. 108–111, 327–331; January, 1944.

Space-Charge and Transit-Time Effects on Signal and Noise in Microwave Tetrodes*

L. C. PETERSON†, ASSOCIATE, I.R.E.

Summary—**Signal and noise in microwave tetrodes are discussed with particular emphasis on their behavior as space-charge conditions are varied in the grid-screen, or drift, region. The analysis assumes that the electron-stream velocity is single-valued. For particular conditions the noise figure may be substantially improved by increasing the space-charge density in the grid-screen region until an entering electron encounters a field of a certain magnitude. The noise reduction is largely due to the cancellation in the output of the noise produced by the random cathode emission. The method of noise reduction described is applicable only when the transit angles of both input and drift regions are fairly long.**

In a forthcoming paper, H. V. Neher describes experimental results which broadly agree with the theory.

INTRODUCTION

THIS PAPER presents a theoretical investigation of the effect of space charge in the drift (grid-screen) regions on noise and signal behavior of long-transit-angle microwave tetrodes.

The theory involves the use of "single-valued-velocity" equations derived on the assumption that all electrons leaving the cathode at any instant have the same velocity. Although this is not in accord with the Maxwellian velocity distribution of the electrons actually leaving the cathode, it seems expedient at the present time to use the single-valued-velocity theory since to the author's knowledge there is no theory for multivalued-velocity electron streams. Furthermore it seems justifiable on the basis of some experimental evidence.

The analysis predicts that the noise figure of a tube of the sort considered has a minimum value with respect to the degree of space charge in the drift region. The control of the degree of space charge may be assumed to occur by changing the screen voltage. In a forthcoming paper, H. V. Neher describes experimental results on tetrodes specially constructed to have a uniform electron stream. These results show that whenever the transit angles in the input and drift regions are large, minimum noise figures can be achieved by proper adjustment of the space charge in the drift region. It can thus be said that the theoretical prediction of the existence of minimum noise figures for the long-transit-time tetrode at microwave frequencies has been confirmed qualitatively. Moreover, on the basis of reasonable assumptions a quantitative agreement has also been obtained. Dr. Neher has further found that when the transit angle in the input region was decreased so that it was no longer large, there was no reduction of noise by space charge. This result also can be explained on the basis of single-valued velocity theory.

There is insufficient data for a thorough going and critical correlation between theory and experiment. However, it seems fair to say that there are indications that the single-valued electron-velocity theory can be

---

* Decimal classification: R138×R339.2. Original manuscript received by the Institute, November 8, 1946; revised manuscript received, December 31, 1946. Presented, I.R.E. Electronics Conference, New Haven, Conn.; June 27 and 28, 1946.

† Bell Telephone Laboratories, Inc., Murray Hill, N. J.

expected to serve as a fairly reliable guide in predicting the signal and noise performance of devices so constructed as to minimize nonuniformities introduced by the structure.

The geometrical structure treated in the analysis is shown schematically in Fig. 1. *C* represents the cathode, *G* the control grid, *S* the screen, and *P* the plate. The input cavity 1 is connected between grid and cathode and the output cavity 3 between screen and plate. It will be assumed that both grids are of very fine mesh so that the individual diode regions are completely shielded from each other. The structure as a whole we shall take to be planar with all electrodes parallel, and we also take the electron stream to be such that at any point in a given plane parallel to the electrodes, the electron velocity is single valued. This latter assumption is essential at present since as already stated there is no theory available for multivalued electron streams. Its justification can only be determined from experiments such as those of Neher, made on tetrodes whose geometry approximates the ideal assumed here.

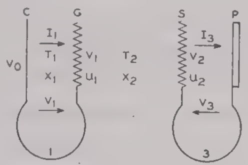

Fig. 1—General diagram of tetrode.

In using this single-valued velocity idealization, the various fluctuations leading to noise in the output (fluctuations in convection current and mean speed of electrons emitted by the cathode and fluctuations due to the irregular interception of electron current at the grids (partition noise)) will be replaced by fluctuations of the single-valued velocity stream, fluctuations uniform over a plane normal to the flow, which have the same mean square values as the fluctuations in the actual multi-velocity stream.

Some further assumptions will be made concerning the single-valued velocity flow on which calculations are based. In the first place, it will be assumed that space charge is complete in the input region between the cathode and grid and that the potential minimum coincides with the cathode. Secondly, it will be assumed that space charge may develop freely in the drift space between grid and screen, but not to an extent which would result in a virtual cathode, since this would violate the assumption of a single-valued velocity. This necessitates that in general both grid and screen be at positive d.c. potentials with respect to the cathode. It will also be assumed that space charge in the output region is sufficiently small to be disregarded.

ANALYSIS

The starting point in the analysis to follow is furnished by the small-a.c.-signal theory of the general diode. This theory finds its essential expression in the so-called electronics equations. These equations are the result of a study of electron motion between two parallel planes, with general initial boundary conditions at one of the planes which may or may not coincide with an emitting cathode. These equations, together with several applications to signal properties of multigrid amplifier tubes, have been published in a recent paper to which the reader is referred for some of the fundamental concepts.[1]

Since the tetrode can be imagined as composed of cascade-connected component diodes, we shall, as an introduction to the analysis of the tetrode in Fig. 1, first study some broad features of fluctuation properties of diodes. Imagine a diode composed of parallel planes *a* and *b* as indicated in Fig. 2. An electron stream having an initial fluctuation component v_a in its velocity and q_a in its convection current at the *a* plane is injected perpendicularly through the plane *a* into the diode space between *a* and *b*. Knowing this, we are interested in determining how these fluctuation variables v_a and q_a become modified in passing through the diode to the plane *b*. In other words, how are the fluctuations at the plane *b* related to those at plane *a*? If a small frequency interval Δf is considered, the electronics equations state that:

$$
\begin{aligned}
I &= (V_b - V_a)a_{11} + a_{12}q_a + a_{13}v_a \\
q_b &= (V_b - V_a)a_{21} + a_{22}q_a + a_{23}v_a \\
v_b &= (V_b - V_a)a_{31} + a_{32}q_a + a_{33}v_a
\end{aligned}
\qquad (1)
$$

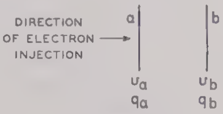

Fig. 2—General diode.

where $V_b - V_a$ is the fluctuation in potential across the diode, *I* is the fluctuation in the total current (convection plus displacement current) through the diode, q_b is the fluctuation in convection current at plane *b*, and, finally, v_b is the fluctuation in velocity at plane *b*. These fluctuations arise as the result of the impressed fluctuations q_a and v_a. The coefficients appearing in (1) (of which a_{11} represents the diode admittance) are functions of frequency as well as of the space-charge conditions prevailing in the diode, but if the frequency interval Δf is small they may be regarded as the same for all frequency components involved. Their exact values may be found from the literature.[1]

For small signals, these equations contain all the space-charge and transit-time effects which can occur in a stream having a single-valued velocity. Several of these coefficients are familiar under other names; among these are the diode admittance a_{11}, the beam-coupling or modulation coefficient a_{12}, and the drift-bunching parameter a_{23} of velocity-modulation theory. Other coefficients are ordinarily treated in the simple forms which they take in the absence of space charge, e.g., in that case the coefficient a_{22} becomes a simple phase shift $e^{-\beta}$. Still others take care of effects which are usually neglected; for instance, "space-charge debunching" is described by the coefficients a_{22} and a_{32}.

---

[1] F. B. Llewellyn and L. C. Peterson, "Vacuum-tube networks," Proc. I.R.E., vol. 32, pp. 144–166; March, 1944.

Among effects not included in the equations are those arising from large signals, dual or multiple-valued velocities, and the Maxwellian distribution at the cathode; however, there will be attempted here a computation of noise effects due to the Maxwellian distribution.

It is immediately clear that the fluctuations at plane b are determined to a large extent by the values of the coefficients in (1); that is to say, by the location of the small frequency interval Δf in the spectrum and by space-charge conditions in the diode. Let us first consider the case of complete space charge, a condition which exists in the tetrode input region. We then identify plane a with a cathode. When the initial d.c. acceleration and velocity are very small it follows that the coefficients a_{12}, a_{22} and a_{32} are nearly zero, so that for conditions of complete space charge (1) assumes the approximate form:

$$\begin{aligned} I &= (V_b - V_a)a_{11} + a_{13}v_a \\ q_b &= (V_b - V_a)a_{21} + a_{23}v_a \\ v_b &= (V_b - V_a)a_{31} + a_{33}v_a. \end{aligned} \tag{2}$$

According to (2), a fluctuation in the emitted current (q_a in (1)) does not contribute to the fluctuation q_b in the convection current at the plane b. But, we notice that the fluctuation v_a in the velocity of emission does produce a fluctuation in q_b. The same holds also for the fluctuation v_b in velocity at plane b.

Moreover, it is seen from (2) that the original velocity fluctuation v_a gives rise to two fluctuation components, namely, q_b and v_b. Although the two components are not independent of each other it will nevertheless be useful to consider them as separate fluctuation variables, and we will think of q_b as resulting from drift action and accompanying bunching.

Now, it is well to recall that D. O. North, A. J. Rack, and several others have made accurate calculations of diode noise at low frequencies such that the effect of transit time could be disregarded.[2,3] Moreover, Rack also showed that by using the diode equations in a form equivalent to (2) and by letting the fluctuation in velocity v_a at the cathode correspond to the mean-square fluctuation in velocity of a stream which is emitted randomly from a cathode, the same low-frequency fluctuation calculated by the more elaborate and exact method is obtained. The idea, due to Rack, of extending this method to long transit time thus presents itself. But we must keep clearly in mind the approximations involved. They are: (a) uniform transit time, and (b) no electron leaving the cathode ever returns to it. Thus, if the spread in transit angle is small and if also the transit time of electrons returning from the potential minimum is small, we do expect the single-valued velocity equations (1) or (2) to give a good approximation to the actual state of affairs. From now on this situation will be postulated.

Consider now the general diode between the grid and screen in Fig. 1. The fluctuation behavior is then described by the general diode equations (1). We now consider q_a and v_a as the fluctuations which are present in the electron stream as it enters the diode through the grid. How the fluctuation components have arisen is at the moment of no particular significance. The main thing is that the diode between grid and screen can be broadly pictured as constituting within itself a drift space in which q_b, the convection current fluctuation at the screen, can be thought of as resulting from the action of the drift space upon the initial convection current q_a and velocity v_a.

Employing the commonly used terms of bunching and debunching, we can also say that q_b is established both as a result of bunching due to the impressed velocity fluctuation v_a and debunching of the impressed convection fluctuation q_a. Thus we think of a_{22} in (1) as expressing debunching and of a_{23} as bunching. We shall now point out some interesting properties of the coefficient a_{22} in the high-frequency region where the transit angle of the drift space is large. First it will be shown that a_{22} can be made to vanish, from which it follows that by selecting the d.c. operating condition so that a_{22} vanishes it is possible to nullify the effect of the initial convection-current fluctuation. What characterizes this space-charge condition? To find this we have to look at the high-frequency asymptotic expression for a_{22} which is,

$$a_{22} = \left(1 - \frac{\eta}{\epsilon} I_D \frac{T^2}{2u_b}\right) e^{-\beta} \tag{3}$$

where

$\eta = (e/m)\ 10^7 = 1.77 \times 10^{15}$ is the ratio between electron charge and mass

$\epsilon = 1/36\pi \times 10^{11}$ is the dielectric constant of vacuum

I_D=d.c. current density through the diode in amperes/cm^2

T=d.c. transit time through the diode in seconds

μ_b=d.c. electron velocity at the b-plane (screen) in centimeters per second

β=complex transit angle of the diode of drift space.

Now we observe that the amplitude factor in the high-frequency asymptotic expression (3) depends only upon the d.c. space-charge conditions prevailing in the drift space. It vanishes when

$$\frac{\eta}{\epsilon} I_D \frac{T^2}{2u_b} = 1$$

---

[2] A. J. Rack, "Effect of space charge and transit time on the shot noise in diodes," *Bell Sys. Tech. Jour.*, vol. 17, pp. 592–619; October, 1938.

[3] D. O. North, "Fluctuations in space-charge limited currents at moderately high frequencies. Part II—Diodes and negative grid triodes," *RCA Rev.*, vol. 5, pp. 106–124; July, 1940.

or

$$u_b = \frac{\eta}{\epsilon} I_D \frac{T^3}{2}. \tag{4}$$

In general we have the d.c. relation

$$u_b = u_a + a_a T + \frac{\eta}{\epsilon} I_D \frac{T^2}{2} \tag{5}$$

where u_a is the d.c. electron velocity at the a-plane and a_a the d.c. acceleration at the a-plane of the diode. Thus, in order that (4) may be satisfied, we must also according to (5) require that

$$u_a + a_a T = 0. \tag{6}$$

Since u_a and T are both positive quantities it follows that the space-charge condition formulated by (4) requires a negative acceleration, that is to say, a retarding field following the plane a of injection. Moreover, if we imagine a space-charge-free diode of transit time T the condition (6) also tells us that the retarding field a_a is equal to that required to turn back a single electron at the b-plane when it is injected with an initial velocity u_a. We may in addition also note that the final speed u_b required by (4) corresponds to that acquired by an electron in a space-charge-limited diode with d.c. current I_D and transit time T. Finally, it may be noted that if the initial retarding field as given by (6) is further increased, the amplitude factor in a_{22} becomes negative and may under certain circumstances exceed unity in magnitude.

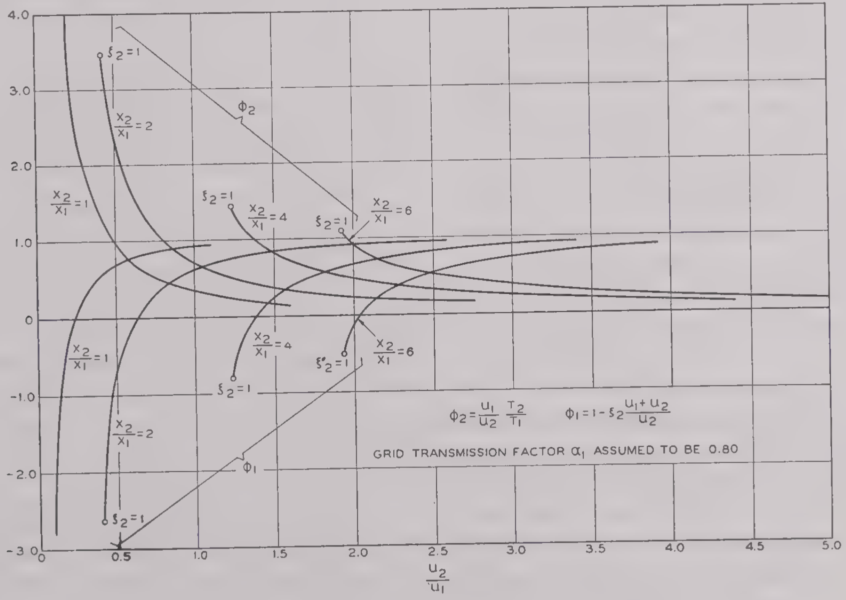

Fig. 3—Magnitudes of space-charge functions ϕ_1 and ϕ_2.

Let us write (3) as

$$a_{22} = \Phi_1 e^{-\beta}$$

where

$$\Phi_1 = 1 - \frac{\eta}{\epsilon} I_{D_2} \frac{T^2}{u_b}$$

or, in terms of the space-charge factor ζ, defined in the literature[1]

$$\Phi_1 = 1 - \zeta \frac{u_a + u_b}{u_b}.$$

This factor ζ varies from a value of zero for no space charge to a value of unity for "complete" space charge.

The function ϕ_1 has been plotted on Fig. 3 for the drift region of a tetrode for several values of the grid-screen and cathode-grid distance ratio x_2/x_1 on the assumption that the emission at the cathode is space-charge-limited. For very small space charge (ζ small) in the grid-screen region Φ approaches unity, and as space charge increases it decreases monotonically, passes through zero, and takes on negative values until space charge is complete at $\zeta=1$. The domain where Φ_1 exceeds unity in magnitude is to be noted. We cannot at present give a satisfactory physical picture of this behavior of the function Φ_1.

The practical importance, if any, of the zero points lies, of course, in the fact that for such a space-charge condition the part of the fluctuation q_b caused by q_a vanishes.

The foregoing discussion on fluctuations, though incomplete, is intended to aid in understanding the more detailed tetrode discussion which now follows.

Consider now the tetrode arrangement schematically indicated in Fig. 1. In regard to notation, the following rules will be adapted. Subscripts 1, 2, and 3 will in general be used on quantities referring to input, drift, and output space respectively. T represents d.c. transit time, x the distance between electrodes. u_1 and u_2 represent the d.c. electron velocities at the grid and screen planes respectively. The corresponding a.c. quantities are v_1 and v_2. The total current between electrodes is I, and its positive direction is in the direction of the arrows.

The electron emission from a real cathode occurs in a random manner and as already mentioned we take this into account by assuming that there is superimposed upon the steady electron stream an alternating velocity component v_0. Moreover, by virtue of the assumption of complete space charge this is the only fluctuation component introduced in region 1.

As we proceed further along the electron stream and as the control grid G is passed, a new fluctuation component is introduced in the stream, namely, that arising from the capture of electrons by the positive grid. This component is taken into account by supposing that a convection current N' is superimposed upon the already existing convection current at that point. As pointed out previously, this new fluctuation component is statistically independent of the fluctuations already present. We have thus, all in all, three fluctuation components to consider for the initial conditions of the general diode composing the drift region between grid and screen. First, there is a fluctuation component in a.c. velocity v_1 caused by the velocity fluctuation v_0 at the cathode. Second, there is a convection-current fluctuation resulting from drift action in the input region, and finally there is the convection-current fluctuation caused by the capturing of electrons by the positive grid.

Still further along the stream, the screen S is passed, and here again a statistically independent convection current N'' is superimposed upon the stream, so that in the output region the fluctuations in the total current arise from the statistically independent fluctuation sources of random electron emission and two random positive-grid electron selections.

From the previous discussion of the generalized diode we can now get a broad picture of the action of the drift space. Depending upon the degree of space charge present in the drift region, the initially impressed velocity and convection-current fluctuations may become considerably modified. In fact, we saw that space charge may exercise such a debunching action on the initial convection fluctuation as to completely nullify its effect. This debunching effect is, of course, counteracted in greater or lesser degree by the bunching effect resulting from the impressed velocity fluctuation. However, we may at this point perceive somewhat vaguely that an optimum fluctuation condition may be obtained by the judicious combination of bunching and debunching effects.

Making repeated applications of (1) and (2) to the successive diode regions of the tetrode with due regard to the various boundary conditions, we get the following four-pole equations for the fluctuation behavior of the tetrode.

$$\left.\begin{aligned} I_1 - b_{11}v_0 &= y_{11}V_1 \\ I_3 - (b_{31}v_0 + c_{32}N' + c_{33}N'') &= -\, y_{31}V_1 - y_{33}V_3 \end{aligned}\right\} \qquad (7)$$

where V_1 is the fluctuation potential across the input and V_3 the fluctuation potential across the output, and I_1 and I_3 are the corresponding fluctuations in the total input and output currents.

The quantities

$$\text{and} \qquad \left.\begin{aligned} I_{i1} &= -\, b_{11}v_0 \\ I_{i3} &= b_{31}v_0 + c_{32}N' + c_{33}N'' \end{aligned}\right\} \qquad (8)$$

from (7) are seen to be in the nature of impressed noise currents, I_{i1} being impressed across the input and I_{i3} across the output terminals.

The coefficients appearing in the impressed noise currents (8) have the values

$$\left.\begin{aligned} b_{11} &= -\, (a_{13})_1 \\ b_{31} &= -\, (a_{12})_3\alpha_2\left[(a_{33})_1(a_{23})_2 + \alpha_1(a_{23})_1(a_{22})_2\right] \\ c_{32} &= -\, (a_{12})_3\alpha_2(a_{22})_2 \\ c_{33} &= -\, (a_{12})_3 \end{aligned}\right\} \qquad (9)$$

where $(a_{12})_3$ is the modulation factor of the output gap and α_1 and α_2 the transmission factors of grid and screen, respectively, so that $(1-\alpha_1)$ and $(1-\alpha_2)$ represent the captured fraction of the electron currents. The quantities a_{33}, a_{23}, and a_{22} are the electronic functions appearing in (1) and, as has been remarked, the index refers to a particular region of the tetrode.

In (7) y_{11} is the input admittance, $-y_{31}$ the transadmittance, and y_{33} the output admittance of the tetrode. The latter quantity can usually be taken as that of a pure capacitance.

The transadmittance has the value

$$-\, y_{31} = (a_{12})_3\alpha_2\left[\alpha_1(a_{21})_1(a_{22})_2 + (a_{31})_1(a_{23})_2\right] \qquad (10)$$

where again the electronic functions are defined by (1).

Before we proceed to a more detailed discussion of the coefficients involved, let us first make some general observations concerning the four-pole equations (7).

Using the definitions (8), the tetrode equations (7) can be written in the form

$$\left.\begin{aligned} I_1 + I_{i1} &= y_{11}V_1 \\ I_3 - I_{i3} &= -\, y_{31}V_1 - y_{33}V_3 \end{aligned}\right\} \qquad (11)$$

which is a special case of the more general four-pole equations

$$\left.\begin{aligned} I_1 + I_{i1} &= \beta_{11}V_1 + \beta_{13}V_3 \\ I_3 - I_{i3} &= \beta_{31}V_1 + \beta_{33}V_3 \end{aligned}\right\}. \qquad (12)$$

The feedback term corresponding to β_{13} V_3 in (12) is missing in (11), reflecting the fact that the grids were assumed to be infinitely fine, corresponding to very large μ-factors.

From (11) or (12) it follows that, in so far as the external tetrode terminals are concerned, the tetrode noise performance can be dsecribed by assuming the tefrode itself to be noiseless and by assigning one impressed-noise-current generator I_{i1} to the input and one impressed-noise-current generator I_{i3} to the output terminals of the tube. These noise generators depend only upon conditions within the tetrode, and it is to be particularly noted that they are independent of any terminal impedances to which the tetrode might be connected. This representation can be shown to be valid for any four-terminal network.

Equations (11) and (12) also show that noise analysis may proceed in much the same manner as signal analysis, the main difference being that in noise analysis one needs to know, in addition to the signal parameters β_{ij}, the noise parameters I_{i1} and I_{i3} and their statistical correlation.

The noise performance of the tetrode will be discussed in terms of Friis's noise-figure concept F, which compares the total noise output from the tetrode with the part which arises from Johnson noise in the signal-generator impedance.[4] The noise figure F may readily be expressed in terms of the impressed noise currents I_{i1} and I_{i3} in the form:

$$F = 1 + \frac{\overline{\left| I_{i1} + I_{i3}\frac{\beta_{11} + Y_s}{\beta_{31}} \right|^2}}{4KTg_s} \tag{13}$$

where Y_s is the admittnace of the signal source and g_s its real part. K is Boltzman's constant and T the absolute temperature of the source admittance. It is seen that, in addition to being a function of I_{i1} and I_{i3}, the noise figure also depends on the signal-generator admittance Y_s and the coefficients β_{11} and β_{31}. The noise figure, on the other hand, is not a function of the load admittance or the coefficients β_{13} and β_{33}.

After these general remarks, let us return to the tetrode equations (11) and give a physical interpretation of the quantities involved in the noise-figure expression (13).

Consider first the noise parameters. We observe from (8) that the impressed noise currents I_{i1} and I_{i3} are statistically dependent since v_0 occurs in both. The impressed noise current I_{i1} corresponds to that of the space-charge-limited diode formed by the input region. The impressed-noise generator I_{i3} contains three statistically independent parts. The first term $b_{31}v_0$ results from the impressed velocity variation v_0 at the cathode. The value of b_{31} is given in (9) and, although not dimensionally a transadmittance, it acts essentially as one. It is composed of two terms each of which contains two factors. All these factors may be given a physical interpretation. The factor $(a_{33})_1$ expresses a change which velocity fluctuation v_0 experiences as the stream passes through the input region. The velocity fluctuation thus present in the grid plane will give rise in the following drift region to electron bunching; $(a_{23})_2$ is a measure of this effect. The first term in b_{31} can thus be thought of as produced essentially by bunching in the drift region between grid and screen. In the second term of b_{31} the factor $(a_{23})_1$ expresses the fact that bunching also occurs in the input region because of the impressed velocity variation v_0. The factor $(a_{22})_2$ gives the effect of debunching caused by the drift space. Thus it is seen that the coefficient b_{31} expresses a combination of the physical phenomena of bunching and debunching.

The next term in I_{i3} is $c_{32}N'$ and from the value of c_{32} given in (9) and the explanation of $(a_{22})_2$ given just above it follows that c_{32} gives the effect of the drift space upon the impressed convection-current fluctuation N'. The last term of I_{i3}, $c_{33}N''$ may be seen from (9) to be unaffected by the drift space and is therefore not directly influenced by conditions prevailing there.

Finally, a few words about the signal parameters are appropriate. The transadmittance $-y_{31}$ is given by (10) Except for the multiplying modulation factor it is seen that it is made up of two terms each of which is composed of two factors. From the general diode discussion the following broad physical interpretation may be obtained. The factor $(a_{21})_1$ represents the convention current in the grid plane resulting from an impressed potential across the input, and the factor $(a_{22})_2$ expresses the effect of the drift space upon this convection current which enters through the grid. This component of the transadmittance may be referred to as the convection-current-variation component. In the second term the factor $(a_{31})_1$ gives the alternating velocity component in the grid plane produced by an impressed potential across the input, and the factor $(a_{23})_2$ gives the bunching action of the drift space. We may refer to this component as the velocity-variation component of the transadmittance. Hence, it follows that the total transadmittance can be thought of as being established through the combined action of convection-current variation and velocity variation, and as will be shown can become larger than the low-frequency transconductance. Or, if we prefer, we can of course also say that the transadmittance arises as a net result of both bunching and debunching.

With these general physical pictures as a background, we are now ready to take up the detailed study of the noise figure F. Let us introduce an auxiliary quantity I_{ie} defined by

$$I_{ie} = I_{i1} + I_{i3}\frac{\beta_{11} + Y_s}{\beta_{31}} \tag{14}$$

which quantity may be referred to as the total equivalent impressed noise current of a linear four-terminal network. In terms of I_{ie} we have

$$F = 1 + \frac{\overline{I_{ie}{}^2}}{4KTg_s} \tag{15}$$

---

[4] H. T. Friis, "Noise figures of radio receivers," Proc. I.R.E., vol. 32, pp. 419–423; July, 1944.

and we now propose to investigate how F varies with the space charge in the drift region when the frequency is so high that the transit angles in the input and the drift region are large enough to permit asymptotic expansions of the electronic functions to be made. In the preceding discussion where a physical picture was attempted there was no need to refer to a particular frequency range. It is in the very-high-frequency regions, however, that bunching as well as debunching effects are most pronounced and it is there also that interesting phenomena occur.

By introducing the values of I_{i1} and I_{i3} from (8) and by using (9) and (10), it follows by straightforward algebra that the total equivalent noise current I_{ie} can be written:

$$I_{ie} = (y_{11} + Y_s)\left[\frac{\alpha_2(a_{12})_3[(a_{33})_1(a_{23})_2 + \alpha_1(a_{23})_1(a_{22})_2]}{y_{31}} v_0 + (a_{12})_3 \frac{\alpha_2(a_{22})_2 N'}{y_{31}} + \frac{(a_{12})_3}{y_{31}} N''\right]$$

if terms which become small at large transit angles are ignored, or, if the values of y_{31} from (10) is introduced,

$$I_{ie} = (y_{11} + Y_s)\left[\frac{(a_{33})_1(a_{23})_2 + \alpha_1(a_{23})_1(a_{22})_2}{-[(a_{31})_1(a_{23})_2 + \alpha_1(a_{21})_1(a_{22})^2]} v_0 + \frac{(a_{22})_2}{-[(a_{31})_1(a_{23})_2 + \alpha_1(a_{21})_1(a_{22})_2]} N' + \frac{1}{-\alpha_2[(a_{31})_1(a_{23})_2 + \alpha_1(a_{21})_1(a_{22})_2]} N''\right] \quad (16)$$

from which incidentally, it may be noted that the impressed noise current I_{ie} and thus also the noise figure F are independent of the modulation factor of the output gap.

The asymptotic expansions of the various electronic functions may now be introduced into (16). The needed expansions are:

$$\left.\begin{aligned}
&(a_{21})_1 \to -g_0 e^{-\beta_1}\\
&(a_{31})_1 \to \frac{3\eta}{u_1}\frac{e^{-\beta_1}}{\beta_1}[1+e^{\beta_1}]\\
&(a_{22})_2 \to \Phi_1 e^{-\beta_2} \text{ where } \Phi_1 = 1 - \frac{\eta'}{\epsilon}\frac{I_D T^2}{u_2} = 1 - \zeta_2 \frac{u_1+u_2}{u_2}\\
&\text{where } \zeta_2 \text{ is the space-charge factor for the drift region}\\
&(a_{23})_2 \to \frac{\alpha_1 I_D \beta_2}{u_2} e^{-\beta_2}\\
&(a_{33})_1 \to -e^{-\beta_1}\\
&(a_{23})_1 \to \frac{I_D \beta_1 e^{-\beta_1}}{u_1}.
\end{aligned}\right\} \quad (17)$$

In these expressions:

g_0 = d.c. conductance of the input region in mhos/cm.²

β_1, β_2 = complex transit angles of input and drift regions respectively

I_D = d.c. current density at the cathode in amps./cm.²

u_1, u_2 = d.c. electron velocities in the planes of the grid and screen respectively in cm./sec.

We thus get:

$$-[(a_{31})_1(a_{23})_2 + \alpha_1(a_{21})_1(a_{22})_2] \to \alpha_1 g_0 e^{-(\beta_1+\beta_2)}[\Phi_1 - \Phi_2(1 + e^{\beta_1})] \quad (18)$$

where Φ_1 is given by (17),

$$\Phi_2 = \frac{u_1}{u_2}\frac{T_2}{T_1} \quad (19)$$

and

$$(a_{33})_1(a_{23})_2 + \alpha_1(a_{23})_1(a_{22})_2 \to \frac{\alpha_1 I_D \beta_1}{u_1} e^{-(\beta_1+\beta_2)}(\Phi_1 - \Phi_2). \quad (20)$$

It is well to examine these expressions somewhat more closely. Equation (18) represents essentially the transadmittance of the tetrode for large transit angles. From the previous discussion it may also be recalled that Φ_1 gives the effect of the drift space upon the entering convection current. For an applied signal of 1 volt this convection current equals (for large transit angle)

$$-(a_{21})_1\alpha_1 = \alpha_1 g_0 e^{-\beta_1}$$

thus explaining the physical meaning of the first term of the right side in (18). The second term involving the function Φ_2 arises from bunching action of the drift space arising from the alternating velocity component $(a_{31})_1$. For large transit angles $(a_{31})_1$ is inversely proportional to frequency, while the bunching factor $(a_{23})_2$ is directly proportional to frequency. The net bunching effect is thus independent of frequency.

The functions Φ_1 and Φ_2 have been plotted on Fig. 3 against the variable u_2/u_1, where u_1 and u_2 are the d.c. electron velocities in the grid and screen plane respectively. As parameters the distance ratio x_2/x_1 between drift and input region has been used.

For very small space charge (u_2/u_1 large) we note again that the value of Φ_1 approaches unity, which is its asymptotic value at zero space charge. Under the same condition the function Φ_2 approaches zero. As space charge increases (u_2/u_1 decreases) Φ_1 decreases, passes through zero, and becomes negative until the Kipp point is reached, where ζ_2 equals unity. The function Φ_2 on the other hand increases steadily towards the limiting value reached at the Kipp point. Regarding the function Φ_1, we note again that a domain of the distance parameter x_2/x_1 exists within which the absolute value of Φ_1 exceeds unity.

The points where the functions equal each other should also be noted. Within the range shown for the distance ratio x_2/x_1 it is seen that the points of intersection occur in a domain for which both functions have values falling between 0 and 1.

Returning now to the transadmittance (18), we see that its magnitude is largely independent of frequency, which essentially enters as rotation of the phase. We also note that when space charge in the drift region is very small, $\Phi_1 \doteq 1 \Phi_2 \doteq 0$, the magnitude of the high-frequency transadmittance is the same as the low-frequency one.

Let us now investigate the effect of space charge, and in so doing let it be assumed that the transit angle in the input region has been so adjusted that $\cos \theta_1 = 0$. The magnitude Γ of the quantity within the square bracket in (18) then becomes:

$$\Gamma = \sqrt{(\Phi_1 - \Phi_2)^2 + \Phi_2^2} \tag{21}$$

From Fig. 3 we can infer that as space charge increases there is at first a slow decrease in the magnitude of Γ until a minimum is attained. As a space charge is further increased the point $\Phi_2 = 0$ is reached. Here Γ equals $\Phi_2\sqrt{2}$, and since here x_2/x_1 can be so chosen that Φ_2 is in the neighborhood of unity, we see that space charge has caused an enhancement of the low-frequency transadmittance. At this point the transadmittance is established purely by means of bunching in the drift space. As space charge is further increased Γ increases monotonically until at the Kipp point, it reaches its maximum. As a numerical illustration of the maximum Γ, consider the case $x_2/x_1 = 2$. From Fig. 3 we find for this case $\Gamma_{\max} \doteq 6$ or 10 db. above the low-frequency value. Thus, we have found that space charge also may be utilized for gain enhancement in the microwave region. We shall shortly see, however, that such an operating condition results in poor noise performance.

Consider now the expression (20) which acts essentially as a transadmittance from the fluctuation in velocity of emission to the output. First we note that it is directly proportional to frequency. The effect of space charge is expressed by the factor $\Phi_1 - \Phi_2$. For very small space charge this factor is nearly unity and as space charge in the drift region increases the factor decreases, passes through zero at $\Phi_1 = \Phi_2$, and as space charge is further increased it increases rapidly until a maximum is reached at the Kipp point. Now the space-charge condition required for equality in Φ_1 and Φ_2 corresponds to zero noise contribution from the cathode. We can also say that the cathode noise disappears when the combined bunching and debunching effects in input and drift region cancel each other.

Consider finally $(a_{22})_2$ in (17). As may be recalled, it gives the effect of the drift space upon the impressed fluctuation due to grid noise and it vanishes when Φ_1 equals zero.

We have thus shown that, among the three statistically independent terms of which the total equivalent noise current (16) is composed, two can be made to vanish at different values of space charge in the drift region. The third component arising from screen noise is not directly influenced by conditions in the drift region. It might thus be expected that the total impressed noise current and hence also the noise figure F will have a minimum somewhere between the values u_2/u_1 at which $\Phi_1 = \Phi_2$ and $\Phi_1 = 0$. Since the noise performance is to be measured in terms of the noise figure, let us consider this quantity. From (13), (16), (17), (18) and (20):

$$F = 1 + \frac{|y_{11} + Y_s|^2}{4KTg_s}\left[\frac{I_D^2}{g_0^2 u_1^2}\theta_1^2\left|\frac{\Phi_1 - \Phi_2}{\Gamma}\right|^2 \overline{v_0^2} + \frac{1}{\alpha_1^2 g_0^2}\left|\frac{\Phi_1}{\Gamma}\right|^2 \overline{N'^2} + \frac{1}{\alpha_1 \alpha_2 g_0^2 |\Gamma|^2}\overline{N''^2}\right]. \tag{22}$$

Regarding (22), we note first that the presence of minimum values of F for particular conditions of space charge depends only upon the behavior of the space-charge functions involved and of course also upon the way the fluctuation sources have been taken into account. However, to locate these minima and to find their magnitudes we must also know the mean square values of the impressed fluctuation sources.

Secondly, it is seen that the high-frequency or asymptotic expression (22) for the excess noise figure F-1 is composed of two factors. The first factor involves the source admittance Y_s while the second factor depends only upon the electronic properties of the tetrode. It is readily established that the first factor has a minimum occurring for tuned and matched input-circuit conditions. The minimum value is found to be $4g_{11}$ where g_{11} is the real part of the input admittance.

Finally, it may be observed that the frequency enters (22) through both factors in (22). Thus it is expected that, in general, the asymptotic noise figure F will behave as a polynomial of even degree equal to or higher than the second.

As already remarked, for the mean-square fluctuation $\overline{v_0^2}$ in velocity we shall take the value given by Rack, which is, per unit frequency interval

$$\overline{v_0^2} = \frac{4}{3I_D}\eta K 0.644 T_C \tag{23}$$

where T_C is the cathode temperature is absolute degrees, K is Boltzman's constant, I_D is the d.c. current in amps./cm.^{2} leaving the cathode and $\eta = e10^7/m$.

For the impressed partition fluctuations we take the value

$$\overline{N^2} = 2e\alpha(1 - \alpha)I_D \tag{24}$$

per unit frequency interval. In (24) e is the electron charge, α is the transmission factor of the grid in question, and I_D is the d.c. current density in the region preceding the grid. Expression (24) assumes that the grid is so fine that the probability of an electron hitting it is the same regardless of the position on the cathode from which it leaves.

Introducing (23) and (24) into (22) and taking the typical value

$$\frac{0.644 T_C}{T} = 2.4$$

and

$$\frac{e}{2KT} = 19.3,$$

we finally get for the asymptotic value of the noise figure

$$F = 1 + \frac{|y_{11} + Y_s|^2}{g_s}\left[\frac{0.267}{g_0}\theta_1^2\left|\frac{\Phi_1 - \Phi_2}{\Gamma}\right|^2 + \frac{19.3(1-\alpha_1)I_D}{\alpha_1 g_0^2}\left|\frac{\Phi_1}{\Gamma}\right|^2 + \frac{19.3(1-\alpha_2)I_D}{\alpha_1\alpha_2 g_0^2|\Gamma|^2}\right]. \quad (25)$$

In order to illustrate the general behavior of F as a function of space charge, let us take the following numerical values:

$\theta_1 = 8$ radians corresponding to a cathode-grid spacing $x_1 = 13 \times 10^{-3}$ cm. and a wavelength $\lambda = 10$ cm.
$g_0 = 3000$ micromhos
$I_D = 0.8$ milliampere.
$\alpha_1 = \alpha_2 = 0.80$.

With these values the second factor which we shall denote by M becomes

$$M = 5696\left|\frac{\Phi_1 - \Phi_2}{\Gamma}\right|^2 + 429\left|\frac{\Phi_1}{\Gamma}\right|^2 + 515\frac{1}{|\Gamma|^2}. \quad (26)$$

The function M is plotted on Fig. 4 with the ratio between screen and equivalent grid d.c. potentials as abscissa and with the distance ratio x_2/x_1 as parameter. The minimum points are seen to occur very nearly for a value of d.c. screen potential which results in $\Phi_1 = \Phi_2$, reflecting the fact that in the example chosen the cathode noise contribution is by far the largest. Thus it follows that for this particular case minimum noise figure occurs when the bunching and debunching effects through the tube just about equal each other.

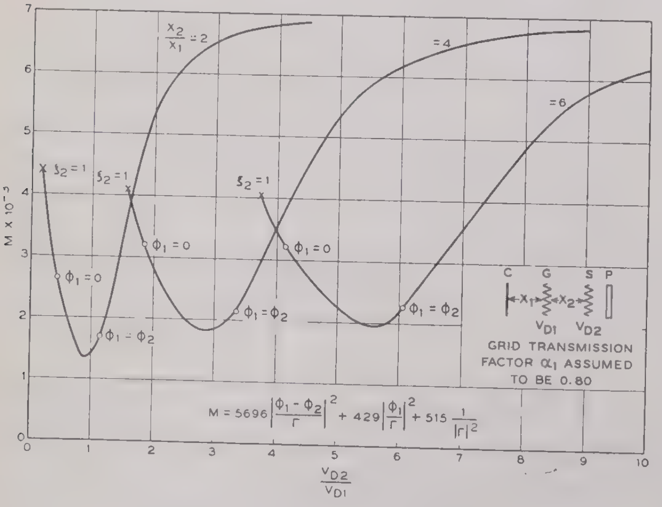

Fig. 4—Magnitude of factor M.

It also appears that the magnitudes at the minimum points are fairly independent of the distance ratio. However, the minimum broadens with increasing grid-screen distance.

Let us also estimate the magnitude of optimum noise figure. Suppose we take $x_2/x_1 = 2$ and $g_{11} = 1/200$.[5] We then have

$$F_{\text{min.}} = 1 + \frac{4}{200}0.135 \times 10^3 = 28 \text{ or } 14 \text{ db.}$$

if optimum input circuit conditions also are assumed.

From the discussion of the general behavior of the transadmittance it follows that this improved noise performance has been accomplished with a certain amount of sacrifice in transadmittance which may be estimated to equal about 30 per cent of the low-frequency value.

The method of noise reduction which has been described is of course independent of frequency as long as it is high enough to justify the use of the asymptotic values for the electronic functions. It does not work if, for example, the transit angle of the input region is small. This can easily be proved analytically and has also been confirmed experimentally by Neher.

The general ideas developed in this paper have also been applied to velocity-variation tubes, but this is beyond the scope of the paper.

CONCLUSION

In conclusion, while the limitations of the assumption of a single-valued-velocity electronic stream are recognized, nonetheless the broad effects predicted in signal and noise behavior have been experimentally confirmed. This experimental confirmation is recorded in a forthcoming paper by Neher. Signal enhancement alone as a result of space-charge effects was first confirmed at Bell Telephone Laboratories by experimental work carried out by F. B. Llewellyn and J. A. Morton. Experimental data avilable at present are too meager for more critical correlation with theory. What is needed most at present is a more systematic experimental study of the effects of space charge and transit angle upon signal and noise. Exact experimental agreement with theory is not to be expected until a multivalued-velocity electron-stream theory is developed. Initial efforts along this line, which should contribute much to a more complete understanding of microwave tubes, have been made by both Frank Gray of these Laboratories and R. Q. Twiss in England.

ACKNOWLEDGMENT

I want to express my gratitude to F. B. Llewellyn, W. E. Kirkpatrick, J. A. Morton, J. R. Pierce, and R. M. Ryder, with whom the writer has had numerous helpful discussions. Also, I want to thank Miss M. Packer, who has made the numerical calculations.

---

[5] The theory allows g_{11} to be calculated neglecting the effect of returning electrons. However, the calculated value is greatly in error because of this neglect. Accordingly we use an experimental value of g_{11} which may be regarded as an empirical parameter designed to take account of the circuit effects principally caused by returning electrons. (This does not, however, take into account noise from the returning electrons.)

The Motion of Electrons Subject to Forces Transverse to a Uniform Magnetic Field*

PAUL K. WEIMER†, ASSOCIATE, I.R.E., AND ALBERT ROSE†, SENIOR MEMBER, I.R.E.

Summary—The paths of electrons in a uniform magnetic field, under the influence of forces transverse to the magnetic field, are of interest in a variety of vacuum tubes. In general, the force experienced by the electron varies with time. The time variation may arise from motion of the electron through an electrostatic field, from motion of the electron along the lines of a curved magnetic field (inertial forces), or from the deliberate application of a time-varying electric field. A graphical method for obtaining the electron paths is described as follows; the given transverse-field versus time curve is approximated by tangent sections; the complete analytic solution is obtained for any tangent section; the analytic solution is interpreted graphically; and a method for joining graphical solutions of neighboring sections is developed. Emphasis is placed on the resultant velocity components and displacement after the field has ceased to act. The graphical method is used to analyze the motion of electrons in the orthicon and image orthicon, television pickup tubes in which the velocity components of the scanning beam critically affect performance. Problems considered are: magnetic and electrostatic deflection in a magnetic field, an electrostatic lens immersed in a magnetic field, the effect of "tapering" the applied forces, and the possibility of canceling unwanted velocity components introduced in one part of the tube by equal and opposite components introduced in another part.

I. INTRODUCTION

A UNIFORM magnetic field has been used for controlling the paths of electrons in several types of television pickup tubes.[1-3] In these tubes the motion of the electron is sufficiently constrained by the field that the resulting path lies approximately along a magnetic line. The uniform field is particularly useful in the orthicon[2] and image orthicon[3] where the electron beam approaches the target with an energy of several hundred volts and must be decelerated to strike the target with less than a volt energy. Care must be taken, however, in the design of the tube that the beam does not acquire velocity components transverse to the magnetic field at the expense of its velocity parallel to the field. If such a transfer of energy does take place the beam will not possess sufficient longitudinal energy to reach the target. The loss of as little as a few tenths of a volt longitudinal energy in the scanning beam of the image orthicon is objectionable.

The necessity for reducing the transverse motion of electrons in the image orthicon has prompted a more general study of helical motion in a uniform magnetic field. The following problems were considered:

1. Motion of an electron along a uniform magnetic field and subject to perturbing transverse electrostatic fields.
2. Motion of an electron along a curved magnetic field.
3. Two-dimensional motion of an electron in a uniform magnetic field and subject to a time-varying transverse electric field.

The solution of the two-dimensional problem specified in 3 may be shown to be an approximate solution of the apparently diverse problems listed in 1 and 2. The approximation involved in this procedure is that the transverse velocity in problems 1 and 2 be sufficiently small compared to the longitudinal velocity that the variations induced in the transverse velocity may be considered to have negligible effect on the longitudinal velocity. Accordingly, a time may be assigned at the outset to each point along the prescribed path of the electron. Thus, in problem 1, the spatial variation of the perturbing electrostatic field along the path may be converted into a time variation of the field, and the solution of 3 applied.

In problem 2 the electron moves along the lines of a curved magnetic field and experiences an inertial force given by mv^2/r where v is the velocity of the electron and r is the radius of curvature of the field lines at each point. The inertial force, to the approximation considered here, is the equivalent of an electric field transverse to a uniform magnetic field. Owing to the motion of the electron and the spatial variation in curvature of the lines, the transverse field experienced by the electron varies with time. By first calculating the transverse field as a function of time the solution of 3 may be applied directly. This method of solving the motion of an electron in a curved magnetic field has been found to give results equal in accuracy to the mathematically more direct but physically less revealing method of obtaining an approximate solution to the three-dimensional equation of motion.[4]

In general, the transverse electric field may vary with time in any arbitrary manner, as shown by the solid curve of Fig. 1. A convenient graphical procedure for solving these problems was developed and will be described below. Application of the graphical method will be made to problems of the types 1 and 2 as they occur in the orthicon and the image orthicon.

---

* Decimal classification R138×R583.6. Original manuscript received by the Institute, June 20, 1946; revised manuscript received, October 7, 1946.

This paper is based in part on work done for the Office of Scientific Research and Development under Contract No. OEMsr-441 with the Radio Corporation of America.

† RCA Laboratories, Princeton, N. J.

[1] P. T. Farnsworth, "Television by electron image scanning," *Jour. Frank. Inst.*, vol. 218, pp. 411–444; October, 1934.

[2] A. Rose and H. Iams, "Television pickup tubes using low-velocity electron beam scanning," PROC. I.R.E., vol. 27, p. 547; September, 1939.

[3] A. Rose, P. K. Weimer, and H. B. Law, "The image orthicon, a sensitive television pickup tube," PROC. I.R.E., vol. 34, pp. 424–432; July, 1946.

[4] Albert Rose, "Electron optics of cylindrical electric and magnetic fields," PROC. I.R.E., vol. 28, pp. 30–40; January, 1940.

II. Two-Dimensional Motion of an Electron in a Magnetic Field Subject to a Time-Varying Transverse Electric Field

Starting with the well-known cycloidal motion of an electron in crossed electric and magnetic fields, the curve representing the transverse field as a function of time might well be represented by a series of steps, as shown by the dashed lines of Fig. 1. The solution for the first step would provide the initial conditions for the second step, and so on. The objection to this procedure is the number of steps required to attain a prescribed degree of approximation. Greater accuracy can be obtained in fewer steps if the curve of Fig. 1 is approximated by straight-line tangents, as shown in Fig. 2 (solid lines).

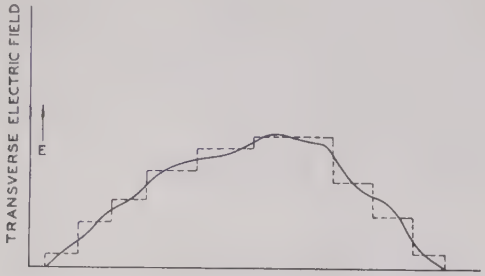

Fig. 1—A stepped approximation to a transverse-field versus time curve.

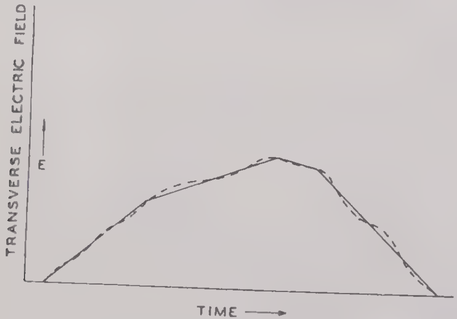

Fig. 2—A tangential approximation to a transverse-field versus time curve.

Furthermore, the procedure can be greatly simplified if the analytical solutions for the successive linear sections are replaced by a single graphical construction. It has been found that by using compasses and a protractor one may quickly find the final phase and magnitude of the circular motion acquired by an electron subjected to a time-varying electric field consisting of many linear sections. (See Figs. 5 and 7.) The same construction gives information about the path of the electron *while* the field is acting. By supplementing the construction with a simple formula the complete paths may be plotted if required.

In the following description, the analytic solution of the motion for a single linear section will be derived first to form a basis for the graphical construction.

A. Analytical Solution for a Linear Section

The solution of the equations of motion for a single tangent section (Fig. 2) is the solution for an electron in a uniform magnetic field subject to a transverse electric field that varies linearly with time. The equations of motion of an electron for any one section in electromagnetic units are

$$
\begin{aligned}
m\ddot{x} &= -eH\dot{y} \\
m\ddot{y} &= -e(E_0 + \dot{E}t) + eH\dot{x}
\end{aligned}
\tag{1}
$$

where E and H are directed positively along the Y and Z axes, respectively, in a right-handed co-ordinate system, and all derivatives are with respect to t. Taking the initial conditions for the section considered as $t=0$, $E=E_0$, $x=x_0$, $y=y_0$, $\dot{x}=\dot{x}_0$, $\dot{y}=\dot{y}_0$, the solution of (1) is

$$
\begin{aligned}
x - x_0 = \frac{T}{2\pi}\Bigg[&\left(\dot{y}_0 + \frac{m\dot{E}}{eH^2}\right)\cos 2\pi\frac{t}{T} \\
&+ \left(\dot{x}_0 - \frac{E_0}{H}\right)\sin 2\pi\frac{t}{T} - \dot{y}_0 - \frac{m\dot{E}}{eH^2}\Bigg] \\
&+ \frac{E_0}{H}t + \frac{\dot{E}t^2}{2H}
\end{aligned}
\tag{2}
$$

$$
\begin{aligned}
y - y_0 = \frac{T}{2\pi}\Bigg[&\left(\dot{y}_0 + \frac{m\dot{E}}{eH^2}\right)\sin 2\pi\frac{t}{T} \\
&- \left(\dot{x}_0 - \frac{E_0}{H}\right)\cos 2\pi\frac{t}{T} + \dot{x}_0\Bigg] \\
&- \frac{m}{eH^2}(E_0 + \dot{E}t)
\end{aligned}
\tag{3}
$$

where

$$
T = 2\pi\left(\frac{m}{eH}\right). \tag{4}
$$

For convenience in applying and demonstrating the graphical construction, these equations will be modified as follows:

1. The independent variable is changed[5] from t to τ

---

[5] The principal advantage of this change of variable is the generalization of the graphical solution. One construction may then apply for more than one value of magnetic field and of beam voltage. Also it provides a convenient measure of electron velocity and period, two quantities which are of inconvenient magnitude when expressed in centimeters per second and seconds, respectively. For example, the velocity of an electron in centimeters per second is

$$v = 5.93 \times 10^7\sqrt{V}$$

where V is the energy of the beam in volts. When T is taken as the unit of time, the velocity in centimeters per electron period is

$$v = \frac{21.2\sqrt{V}}{H}$$

where H is the magnetic field in gausses. Thus, in the new units the velocity of the beam is numerically equal to the distance between successive nodes in the beam. This distance in the image orthicon is about 4 centimeters for the scanning beam. Another advantage of the change of variable is the simple relation between transverse velocity and the radius of the motion in the magnetic field alone. This is

$$v = 2\pi R.$$

where τ is the nondimensional measure of time in units of the electron period T.

2. The origin is chosen so that $x_0=\dot{y}_0/2\pi$ and $y_0=-(\dot{x}_0/2\pi)$, where the velocities $\dot{x}_0$ and $\dot{y}_0$ are in centimeters per electron period. This places the origin at the initial center of rotation of the electron in the magnetic field alone.

The complete solution with all derivatives taken with respect to τ, E expressed in volts per centimeter, H in gausses, and with the constants evaluated is

$$\begin{aligned} x = \frac{1}{2\pi}\Bigg[\left(\dot{y}_0+\frac{5.69\dot{E}}{H^2}\right)\cos 2\pi\tau \\ +\left(\dot{x}_0-\frac{35.7E_0}{H^2}\right)\sin 2\pi\tau\Bigg] \\ -\frac{5.69\dot{E}}{2\pi H^2}+\frac{35.7}{H^2}\left(E_0\tau+\frac{\dot{E}\tau^2}{2}\right) \end{aligned} \tag{5}$$

$$\begin{aligned} y = \frac{1}{2\pi}\Bigg[\left(\dot{y}_0+\frac{5.69\dot{E}}{H^2}\right)\sin 2\pi\tau \\ -\left(\dot{x}_0-\frac{35.7E_0}{H^2}\right)\cos 2\pi\tau\Bigg] \\ -\frac{5.69}{H^2}(E_0+\dot{E}\tau) \end{aligned} \tag{6}$$

$$\begin{aligned} \dot{x}(cm/T) = -\left(\dot{y}_0+\frac{5.69\dot{E}}{H^2}\right)\sin 2\pi\tau \\ +\left(\dot{x}_0-\frac{35.7E_0}{H^2}\right)\cos 2\pi\tau \\ +\frac{35.7}{H^2}(E_0+\dot{E}\tau) \end{aligned} \tag{7}$$

$$\begin{aligned} \dot{y}(cm/T) = \left(\dot{y}_0+\frac{5.69\dot{E}}{H^2}\right)\cos 2\pi\tau \\ +\left(\dot{x}_0-\frac{35.7E_0}{H^2}\right)\sin 2\pi\tau-\frac{5.69\dot{E}}{H^2}. \end{aligned} \tag{8}$$

Inspection of these equations shows that the actual motion of the electron is the resultant of two simpler motions. The harmonic terms indicate that one motion consists of a uniform velocity in a circle of constant radius R where

$$R=\frac{1}{2\pi}\left[\left(\dot{x}_0-\frac{35.7E_0}{H^2}\right)^2+\left(\dot{y}_0+\frac{5.69\dot{E}}{H^2}\right)^2\right]^{1/2}. \tag{9}$$

The other motion is that of the center of this circle. It follows a parabolic path in space resulting from a constant velocity in the y direction given by $\dot{y}=-(5.69\dot{E}/H^2)$, and a uniformly accelerated velocity in the x direction given by $\dot{x}=(35.7/H^2)(E_0+\dot{E}\tau)$. The breakdown of the actual motion into circular and translational components greatly simplifies the problem.

B. Graphical Method for Calculating the Circular Motion

The aim of this section is to derive from the above equations a graphical construction which will yield the magnitude and direction of circular motion that an electron has after being acted upon by an electric field whose variation with time has been approximated by linear sections. In the constructions which follow, the instantaneous circular motion is represented by a radius vector drawn outward from the center of the circle to the electron. The circumferential velocity is perpendicular to this vector and has a magnitude proportional to the length of the vector. In (5) to (9) the velocity is expressed in centimeters per electron period and is very simply related to the length of the corresponding radius vector by the proportionality factor 2π. The magnetic field is always assumed to be directed out of the paper and the radius vectors rotate counterclockwise through 360 degrees in the time interval $\tau=1$.

The final construction arrived at will become clear if a complete picture of the electron path is first considered. By way of illustration, the simple transverse-field versus time curve shown in Fig. 3 will be treated. The initial conditions are taken to be $\dot{x}_0=\dot{y}_0=E_0=0$. The origin of the co-ordinate system for (5) and (6) is at the center of the circle in which the electron moves at $\tau=0$ by virtue of its initial velocity. In this instance, the initial velocity is zero and the origin and the initial electron position coincide. From (5) and (6) the complete path is made up of two parts, motion of the electron on a circle and motion of the center of the circle.

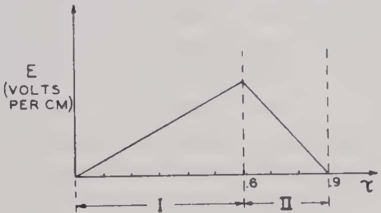

Fig. 3—A simple transverse-field versus time curve consisting of two linear sections.

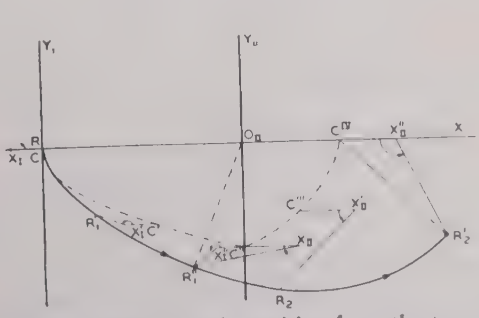

Fig. 4—Complete electron path resulting from the transverse-field versus time curve of Fig. 3. The magnetic field is directed toward the reader.

It is convenient for purposes of the final method of construction to consider the constant term $5.69\dot{E}/2\pi H^2$ of (5) independently of the other terms representing the motion of the center of the circle. The remaining nonperiodic terms are called the "translational terms" and are plotted in Fig. 4 as the dotted curve $C\ C'\ C''$. The constant term of (5), defines a point X_{I} displaced by the constant amount $-(5.69\dot{E}_1/2\pi H^2)$ from the dotted curve. ($\dot{E}_1$ is the slope of the first section of the force field when E is plotted against τ.) The center of the circle while the field is changing at the rate $\dot{E}_1$ is at X_{I} and moves along a parabolic path displaced at the constant distance $X_{\text{I}}C$ from the dotted curve. The electron itself is on the periphery of the circle and rotates around the center of the circle as the center slides along its parabolic path. The circular motion of the electron is represented by the rotation of the radius vector $X_{\text{I}}C$ about its center X_{I}. The complete path of the electron is shown as the solid curve. Three positions, initial, intermediate, and final, of the rotating vector in the first section are shown. At R_1'' the rotating vector, by Fig. 3, has completed 0.6 of a revolution. At R_1'', also, the electron has a total velocity, given by (7) and (8), which constitutes the initial velocity for the second section. It may be shown from (7) and (8) that the radius vector giving the total velocity of the electron at R_1'' is $R_1''O_{\text{II}}$. With O_{II} as the new origin, the translational terms of (5) and (6) furnish the parabolic curve $C^{\text{II}}C^{\text{III}}C^{\text{IV}}$. The center X_{II} of the new circle is displaced from the curve by the constant term $-(5.69\dot{E}_2/2\pi H^2)$. In this section $\dot{E}_2$ is negative and the displacement is to the right. The radius vector of the new circle must have a magnitude and direction such as to make the electron position (as well as total velocity) continuous across the boundary of the two sections. This means that it must extend from its center at X_{II} to the final position of the electron at the end of the first section, namely, R_1''. Again, the radius vector $X_{\text{II}}R_1''$ rotates about its center X_{II}, as its center slides along a parabolic curve displaced from the dotted curve. The total rotation, according to Fig. 3, is 0.3 of a revolution, and the final position is $X_{\text{II}}''R_2'$. At R_2' the force field has ceased to act and the electron continues to rotate about the center C^{IV}, its motion being described by the radius vector $C^{\text{IV}}R_2'$.

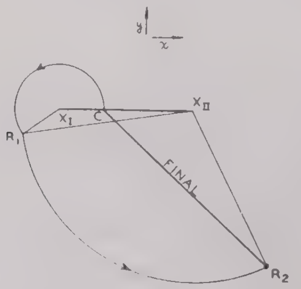

Fig. 5—The graphical construction giving the circular motion produced by the transverse field of Fig. 3. The radius vector CR_2 indicates the phase and magnitude of the motion at the instant the electric field ceases to act.

Fig. 5 shows the simple graphical construction required to obtain the same information about the final circular motion as found in Fig. 4. The translational terms have been dropped since they may be conveniently treated independently. The point C represents the center of rotation of the electron before and after the application of the transverse force. During the application of the force this point follows the parabolic paths indicated by the dotted curve of Fig. 4, and its total translation may be readily calculated as described in the following section.

Fig. 7 is the graphical construction applied to the more complex force field of Fig. 6. For generality it is assumed that the electron has an initial velocity represented by the radius vector CR_0. The fulcrum of the rotating vector in the first section is displaced from C a distance $-(5.69\dot{E}_1/2\pi H^2)$ and CX_{I} is drawn proportional to this distance. The initial position of the rotating vector is then $X_{\text{I}}R_0$. During the time interval of section I, given by $\tau=0.2$, $X_{\text{I}}R_0$ rotates through 0.2 of a revolution or 72 degrees. At the end of the interval the vector has the position $X_{\text{I}}R_1$.

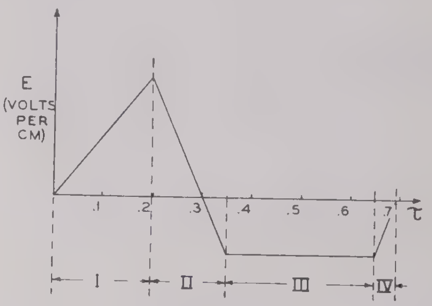

Fig. 6—A transverse-field versus time curve consisting of four linear sections.

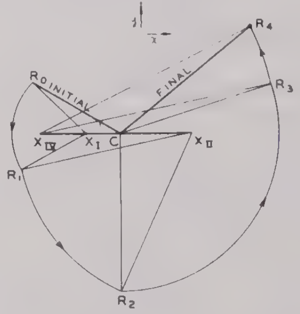

Fig. 7—The graphical construction for the transverse field of Fig. 6. The radius vector representing the initial circular motion is CR_0, its magnitude being drawn proportional to the actual radius in centimeters, determined by

$$R=\frac{3.3\sqrt{V}}{H}$$

where V is the transverse energy of the circular motion in volts. The vectors CX_{I}, CX_{II}, and CX_{IV} are drawn in the same proportion to the distance $-(5.69\dot{E}/2\pi H^2)$ calculated for each section. The final vector CR_4 gives the phase and magnitude of the final circular motion and may be converted to volts by the relation

$$V=\frac{H^2R^2}{3.3^2}.$$

CX_{II} is then drawn proportional to $5.69\dot{E}_2/2\pi H^2$, giving $X_{\text{II}}R_1$ as the initial value of the rotating vector in the second section. $X_{\text{II}}R_1$ rotates into $X_{\text{II}}R_2$.

In the third section $\dot{E}_3=0$ and the center of the rotating vector is C. The rotating vector is CR_2 and rotates into CR_3.

CX_{IV} is drawn proportional to $-(5.69\dot{E}_4/2\pi H^2)$, locating the fulcrum of the vector in the fourth section. $X_{IV}R_3$ rotates into $X_{IV}R_4$. CR_4 represents the radius vector corresponding to the total motion of the electron at the instant the field ceases to act.

C. Complete Electron Paths in Transverse Fields

Reference to (5) and (6) shows that a transverse force field produces a net translation of the center of rotation along the X axis by an amount proportional to the area under the curve of E plotted against τ. Thus

$$x = \frac{35.7}{H^2}\int_0^\tau E\,d\tau. \qquad (10)$$

The translation in the y direction parallel to the electric field occurs only while the field is acting, and is proportional to the instantaneous value of E. Thus, after the field has dropped to zero we have

$$y = 0. \qquad (11)$$

The complete electron paths while the field is acting may be conveniently plotted by using only the translational terms of (5) and (6) combined with a graphical construction of the type illustrated in Figs. 5 and 7.

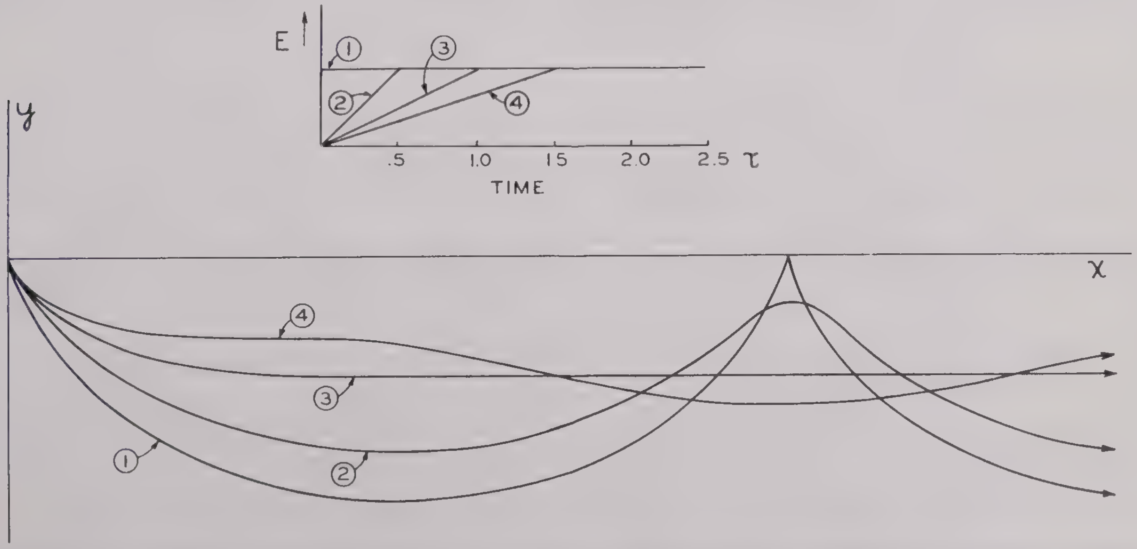

Fig. 8—Electron paths for different rates of application of a transverse electric field. The magnetic field is directed toward the reader.

In Fig. 8 the paths between two plates are plotted for several cases in which the field is applied at different rates. The maximum circular motion occurs in case *1* where sudden application of the field gives the familiar cycloidal paths. As the field is applied more and more gradually the resulting circular motion is reduced. For those particular cases where the time for the field to reach its final value is an integral number of periods, the resultant circular motion between the plates is zero. The fact that an electric field introduces less circular motion when applied gradually is utilized in the orthicon, as will be described in the next section.

It is interesting to note from (5) to (8) that if an electron is introduced to an electric field E_0 in a time of τ electron periods, the amplitude of circular motion during the rise time of E_0 is reduced by the factor $1/2\pi\tau$ and the corresponding energy of circular motion by the factor $1/4\pi^2\tau^2$ relative to the amplitude and energy it would have if introduced suddenly to the same field. This would suggest that the starting electrons in a diode magnetron describe smooth paths concentric with the cathode. The anode field of the magnetron is applied in a time of many electron periods. Pulse rise times of one-half microsecond, for example, in combination with magnetic fields of a thousand gausses attenuate the energy of circular motion by a factor of the order of 10^{-8}.

III. Electrostatic Deflection Plates Immersed in a Magnetic Field

In the 1840-type orthicon, electrostatic plates within the magnetic focusing field are used for the horizontal scanning of the target. The net displacement is parallel to the plane of the plates and can be calculated from (10). The plates are curved so that they are closely spaced at the center and flared out at the ends where the electron enters and leaves the deflecting field. The purpose of this shape is to reduce the helical motion produced in the beam by the transverse field. It is of interest to apply the graphical method to determine the conditions for which the flaring of the plates is advantageous.

The curvature of the plates is such that an electron passing between them at constant velocity experiences a transverse field whose time variation[6] is similar to that shown in Fig. 3, except that now the maximum occurs at the midpoint in time. If the plates had been flat and so closely spaced that the fringe field were of negligible extent, the transverse field would, of course, have been constant with an abrupt rise and fall. The helical motion acquired by the electron in both of these cases has been calculated by the graphical method and plotted in Fig. 9 for various lengths of plates. It is noted that the curved plates actually introduce more helical motion for the same deflection than the flat plates if the plates are shorter than 1.4λ. (λ is the distance apart of successive nodal planes in the beam.) With longer lengths, both types of plates introduce less helical motion and the advantage in flaring the plates is apparent.

---

[6] The periodic variation of the electric field owing to the scanning process is so slow compared to the transit time of the electron that the field may be considered stationary for any one electron.

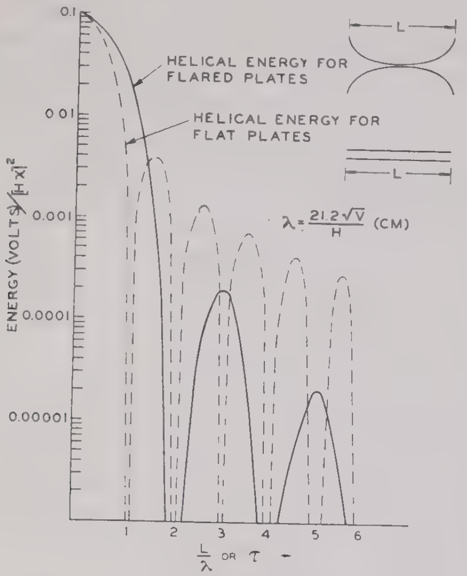

Fig. 9—Helical energy introduced by electrostatic deflection plates plotted as a function of the length of the plates. The abscissa represents the number of orders of focus within the plates and is also equal to the transit time in units of τ. The translation x is perpendicular to E and H.

IV. Electrostatic Lens Immersed in a Magnetic Field

The deceleration field in front of the target in the image orthicon forms an electrostatic lens immersed in a uniform magnetic field (see the dotted lines of Fig. 10). An electron path of special interest is the one approaching the edge of the target along the magnetic line indicated. Along this path the transverse electric field is larger than for paths near the axis of the tube. From the equipotential plot the transverse-field versus time curve has been calculated for the portion of the path from F to G. This curve is shown in Fig. 11.

By use of (10) and Fig. 11, the translation of the electron in the deceleration lens may be computed. This translation, at right angles to the electric and magnetic fields, appears as a slight rotation of the scanning pattern as a whole on the target.[7]

The helical motion acquired by the electron has been computed by a graphical construction similar to Fig. 7. For the relatively small transverse motions involved here the electric field may be assumed to be uniform across the path. It was found that several volts of helical energy are acquired by an electron deflected toward the edge of the target.

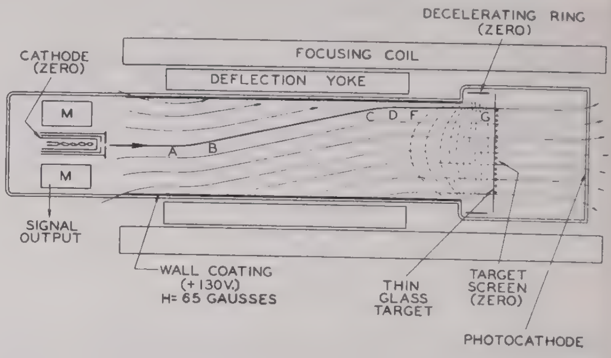

Fig. 10—Cross-sectional diagram of the image orthicon. The dotted lines in front of the target represent the equipotential surfaces of the electrostatic field. The curved lines within the deflection coil indicate the direction of the magnetic field resulting from the combined effects of the deflection and focusing coils. An electron path of particular interest is shown by the heavy line.

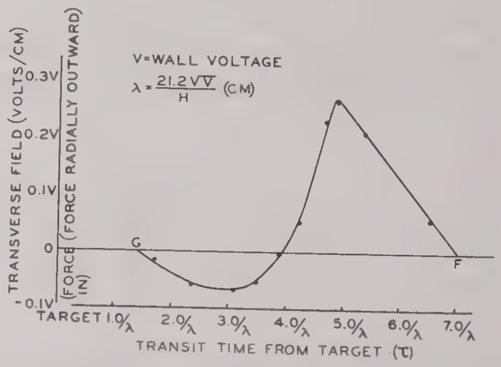

Fig. 11—Plot of transverse field versus time for an electron approaching the target along the path indicated from F to G in Fig. 10.

V. Curved Magnetic Field

A deflection coil immersed in a uniform magnetic field causes the resultant field lines to bend as shown in Fig. 10. An electron whose principal motion is along the magnetic lines experiences at each bend an mv^2/r force which may be expressed as an equivalent transverse electrostatic field. The value of this field in volts per centimeter is

$$E = \frac{2V_p}{r} \tag{12}$$

where V_p is the longitudinal energy of the beam in volts, and r is the radius of curvature of the magnetic lines at each point. By use of this equation, transverse-field versus time curves may be plotted for the bends AB and CD.

---

[7] This translation is also the chief reason why the electron on its return from the target does not retrace its initial path. The lack of retrace gives rise to a scanning pattern on the first stage of the electron multiplier. This pattern is oriented approximately 90 degrees to the scanning pattern on the target.

The effect of each bend is to produce a translation perpendicular to the plane of the curve as well as to introduce helical motion. The translation, whose magnitude is given by (10), is usually not significant in the image orthicon since that occurring at the first bend is equal and opposite to that produced by the second. The helical motions, however, introduced by the two bends usually do not cancel. Their magnitudes are not in general equal and their vectorial summation may vary depending on their relative phase as determined by the transit time between bends. The net helical energy impressed on the electron in passing through the deflection coil varies from zero for zero deflection to as much as several volts for maximum deflection.

Higher wall voltages and decreased magnetic field strengths tend to increase the helical energy acquired by the electron in passing through either the deflection coil or the deceleration lens. In the image orthicon, where zero helical motion at the target is desired, it has been found advantageous to balance the helical motion introduced by the deceleration lens against that produced by the deflection coil. The proper phase for cancellation can readily be obtained by sliding the deflection coil along the axis of the tube.

An Oscillographic Method of Presenting Impedances on the Reflection-Coefficient Plane*

A. L. SAMUEL†, FELLOW, I.R.E.

Summary—**A method is described which permits the direct presentation of the reflection-coefficient plane on an oscillograph. The theory is briefly outlined and photographs reproduced showing one simple form of equipment and the results which it yields. Mention is made of more elaborate arrangements which increase the accuracy of the method.**

AN EXPERIMENTAL study at ultra-high frequencies of the input impedance as a function of frequency for any given circuit element requires measurements of the complex impedance at a number of different frequencies over a prescribed frequency range. The usual method involves (1) observations of the standing-wave ratio along a uniform transmission line which is terminated by the unknown impedance, (2) the computation from these data of the input impedance or of the reflection coefficient at a number of different frequencies, and (3) the presentation of these data on a transmission-line chart, usually of the reflection-coefficient-plane type. The oscillographic method, which is to be described, offers a convenient and rapid method of presenting the data directly in the desired form without computation. The principal advantage of this method over the conventional point-by-point method is one of speed. Results may be obtained in a very few minutes which otherwise would require hours or even days of work. In fact, it is possible to observe the variations in the input impedance of devices under transient conditions, something that is not possible using more conventional methods. The variations in impedance produced by rotating joints, and even random variations in the input impedance of an antenna produced by reflections, are examples of time-varying impedances which can be observed in this way.

One common usage of such a device is that of observing the effects of adjustments made on a circuit in an attempt to match impedances. When so used, inaccuracies for large values of reflection coefficient are of no concern; therefore, the simplest possible system is indicated, as long as it is capable of giving good indications when the reflection coefficient approaches zero. Fortunately, this requirement is easy to meet.

Another usage is that of measuring Q. Here accuracy is of some concern, so that one of the more elaborate methods to be described is indicated. For devices having large negative out-of-tune reflection coefficients, it is possible to construct a transparency for the oscilloscope screen containing curves giving the loci of the reflection coefficients at frequencies displaced from resonance by amounts which are simply related to the Q. A frequency marker in the form of a dotting circuit enables one to measure the frequency difference ΔF between such pairs of points (one on each side of resonance), so that Q can be computed from the relationship

$$Q = \frac{f}{\Delta f}.$$

The required loci for the intrinsic Q, (Q_0), for the loaded Q, (Q_L) and for the external Q, (Q_{EXT}) are shown on Fig. 1. The Q_0 loci are circles of radius 1.414 going through the $R=0$ and $R=00$ points (with centers at $X=\pm 1$). The Q_L loci are straight lines (circles of infinite radius) going through $R=0$, one going through $X=1$ and the other through $X=-1$. The Q_{EXT} loci are circles of unit radius through these same points. Similar loci exist for the more general case, although different curves are obviously needed for each value of the out-of-tune reflection coefficient.

---

* Decimal classification: R244.3. Original manuscript received by the Institute, September 25, 1946; revised manuscript received, December 6, 1946. Presented, Second Annual National Electronics Conference, Chicago, Ill., October 5, 1946.

† Formerly, Bell Telephone Laboratories, Inc., New York, N. Y.; now, University of Illinois, Urbana, Ill.

Perhaps a word might be in order regarding the choice of the reflection-coefficient plane as a medium for presenting impedance data. As is now generally known, the Smith chart[1] is obtained by a bilinear transformation to the reflection-coefficient plane of the co-ordinate system on the impedance plane. Since the reflection coefficient is always less than unity (that is, for passive circuits) the plane is bounded by a unit circle, the reflection coefficient being given by the vector distance from the origin to any point on the plane. The impedance co-ordinates are transformed into orthogonal families of circles, and the bilinear nature of the transformation requires that circles remain circles and that angles be preserved. Distance along a lossless transmission line appears on the chart as distance along the circumference of a circle coaxial with the center of the chart; the absolute magnitude of the reflection coefficient remains constant under these conditions.

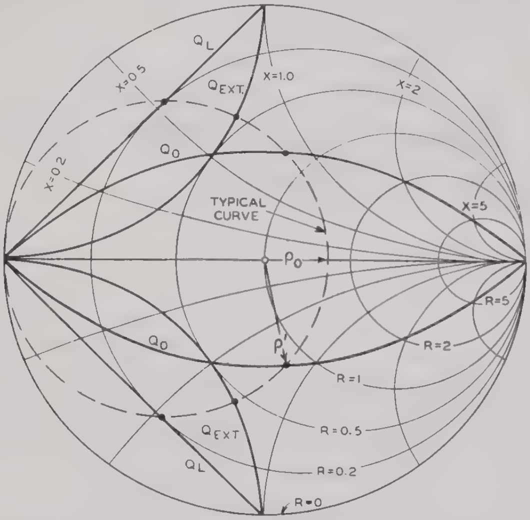

Fig. 1—The loci of the Q points on the reflection plane. The reflection coefficient p is the vector from the center of the plot to the point in question.

The simplest scheme by which the necessary information can be obtained to supply the oscilloscope is shown in Fig. 2, and schemetically in Fig. 3. Four probes are used to sample the waves existing in the transmission line, which may be either a wave guide or a coaxial line. These probes are in pairs, the two probes of each pair being spaced along the line by a quarter wavelength, while the two sets are staggered by an eighth wavelength. The output from each probe goes directly to a crystal detector. The two crystals of one pair of probes are balanced, the difference in their outputs being impressed on one pair of deflection vanes in the oscilloscope. The difference in the outputs from the second pair is impressed in a like manner on the other pair of deflecting vanes in the oscilloscope. If, then, the input to the transmission line is varied in frequency but not in amplitude, and if the crystals follow a square law, the oscilloscope spot will trace a path representing the desired curve on the reflection-coefficient plane. The center of the reflection-coefficient plane is located by interrupting the output of the driving oscillator at the end of each frequency excursion.

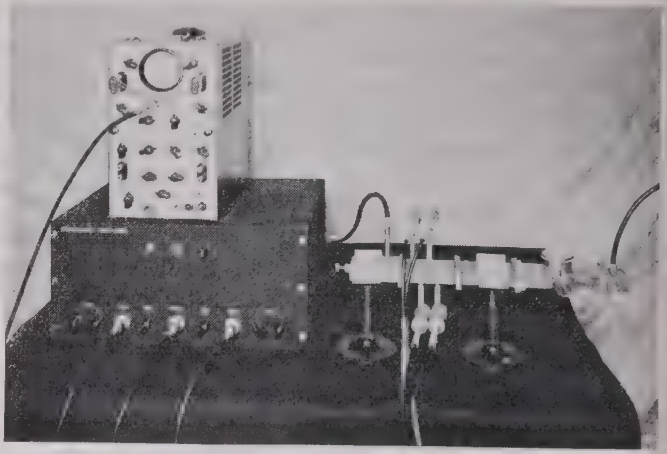

Fig. 2—The simple experimental equipment used to obtain the photographic records of Figs. 10 and 11.

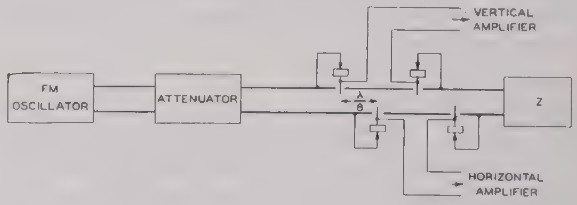

Fig. 3—Schematic drawing of the simple four-probe method.

The mathematical verification for this result is extremely simple. If the incident wave, as seen by crystal (1), is constant at an amplitude V_i and the reflected wave is V_r at an angle θ for some fixed angular frequency ω, then the output from this crystal is

$$[V_i \cos \omega t + V_r \cos (\omega t + \theta)]^2$$
$$= \frac{V_i^2}{2} + \frac{V_r^2}{2} + V_i V_r \cos \theta + \text{radio-frequency terms.} \quad (1)$$

At crystal (2) the incident wave will be delayed by $\pi/2$ and the reflected wave will be advanced by $\pi/2$, corresponding to the time required by the wave to traverse the quarter-wavelength section of transmission line separating the two probes. The output from this crystal will then be

$$[V_i \cos (\omega t - \pi/2) + V_r \cos (\omega t + \theta + \pi/2)]^2$$
$$= \frac{V_i^2}{2} + \frac{V_r^2}{2} - V_i V_r \cos \theta + \text{radio-frequency terms.} \quad (2)$$

---

[1] P. H. Smith, "Transmission line calculator," *Electronics*, vol. 12, pp. 29–33; January, 1939.

The difference in the outputs which appears between the abscissa vanes of the oscilloscope is

$$2V_iV_r \cos \theta. \qquad (1)-(2)$$

Crystal (3) will have an output of

$$[V_i \cos (\omega t - \pi/4) + V_r \cos (\omega t + \theta + \pi/4)]^2$$

$$= \frac{V_i^2}{2} + \frac{V_r^2}{2} - V_iV_r \sin \theta + \text{radio-frequency terms.} \qquad (3)$$

Similarly, crystal (4) will have

$$[V_i \cos (\omega t - 3\pi/4) + V_r \cos (\omega t + \theta + 3\pi/4)]^2$$

$$= \frac{V_i^2}{2} + \frac{V_r^2}{2} + V_iV_r \sin \theta + \text{radio-frequency terms.} \qquad (4)$$

The difference for this pair, which will be

$$2V_iV_r \sin \theta, \qquad (4)-(3)$$

can be impressed on the ordinate vanes of the oscilloscope. If V_i is constant, the position of the spot will then be given by

$$X = V_r \cos \theta$$

$$Y = V_r \cos \theta$$

so that the spot will lie at a distance V_r from the origin and at an angle θ. When the frequency is varied over a a restricted range, the spot will trace the value of V_r in magnitude and phase. The proper scale factor for the oscilloscope and its accompanying amplifier can readily be obtained by terminating the transmission line in a short circuit, so that $(V_r) = (V_i)$, and calling the accompanying deflection unity. Since, by definition, V_r for unity V_i is the reflection coefficient, the desired relationship has been verified.

The four-probe method just outlined is subject to a number of limitations and errors. Since use is made of fixed spacings in the transmission line, the method is limited in its frequency range if reasonable accuracy is to be expected. The maximum percentage error in position of the spot, with fixed probes in a coaxial line, is shown in Figs. 4 and 5 as a function of the departure in frequency from the value for which the spacings are correct. The data were computed in terms of the reflection coefficient as referred to the mid-plane of the probe system. The errors will be somewhat greater for a waveguide system because of the more rapid variation in guide wavelength with frequency. Care must be taken to insure that the probes are not large enough to produce noticeable distortions in the standing-wave pattern which is being sampled.[2]

A third type of error is introduced if the crystals do not follow a square law, as assumed in the above analysis. This imparts a nonlinear radial scale to the oscilloscopes. This error will be largest for large values of the reflection coefficient. It will decrease as the reflection coefficient approaches zero, in just the same way that a converter becomes linear for signals that are small compared to the beating-oscillator level. A fourth type of error arises from any lack of balance in the system. Provision must be made to adjust the gain of the two amplifiers to equality. Variations in crystal sensitivity can be compensated by varying the probe length or by means of potentiometers. However, it is not sufficient to adjust the crystals to the same sensitivity at a single level only. If the crystals do not follow the same law, the V_r^2 terms in the above analysis will not cancel. These last two types of error can be greatly reduced by some alternative circuits which will be described later.

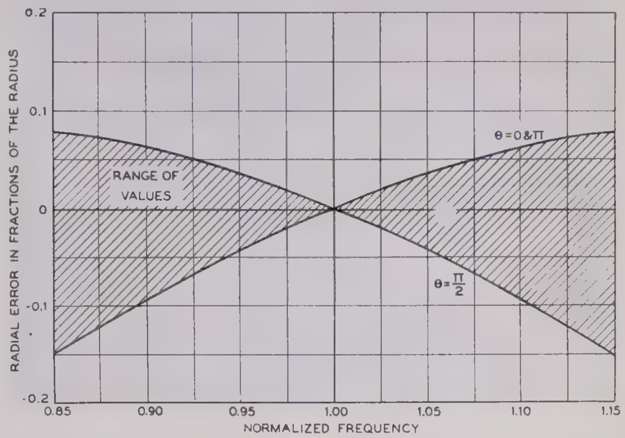

Fig. 4—The maximum radial error in the oscilloscope spot position as a function of frequency using the four-probe method.

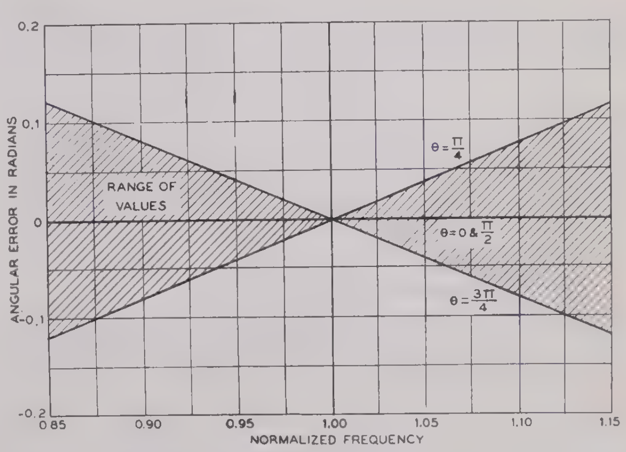

Fig. 5—The maximum angular error in the oscilloscope spot position for a unit signal as a function of frequency using the four-probe method.

It should also be noted that care must be exercised in the design of the crystal circuits to make them sufficiently broad in their frequency-response characteristic so that their outputs remain level over the band.

---

[2] William Altar, F. B. Marshall, and L. P. Hunter, "Probe errors in standing-wave detectors," Proc. I.R.E., vol. 31, pp. 33–44; January, 1946.

Variations in input-power level with frequency will introduce yet another error. However, it is possible to adjust the mechanically modulated oscillator shown in Fig. 6 so that the output is constant to better than ½ decibel over a 5 per cent frequency band; therefore, this error is not too serious.

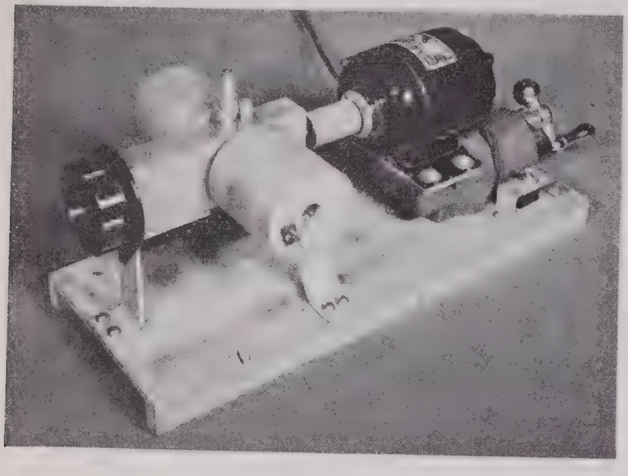

Fig. 6—The mechanically swept oscillator used to obtain the constant-amplitude, variable-frequency power source.

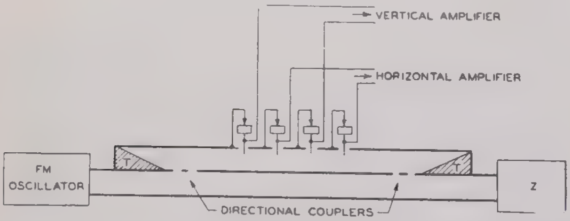

Fig. 7—The basic directional-coupler method of sampling the incident- and reflected-wave components to permit the independent adjustment of their levels.

With suitable attention to detail, the four-probe method has been found to yield results which are accurate to the order of 5 per cent over a 5 per cent frequency band.

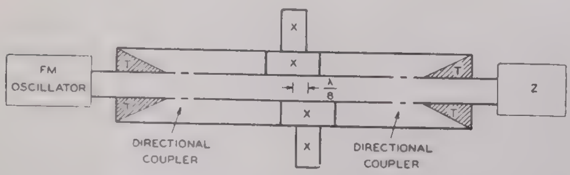

Fig. 8—A circuit employing hybrid junctions to perform the required additions and subtractions.

The crystal-law errors can be substantially eliminated by any arrangement which attenuates the reflected-wave component so that it is always small compared with the direct-wave component. The direct wave then takes the place of the beating oscillator in the conventional converter, and the reflected wave takes the place of the signal. This results in a linear signal-response characteristic. It does not modify the requirements that the input-power level be constant, since the magnitude of reflected wave will still vary with the magnitude of the incident wave. A variety of different circuits have been suggested which permit the separation of the incident-wave and reflected-wave components so that one can be attenuated relative to the other. Some of these circuits are shown in Figs. 7, 8, and 9. These circuits are shown in terms of wave guides, although they are equally well adapted to coaxial-line systems.

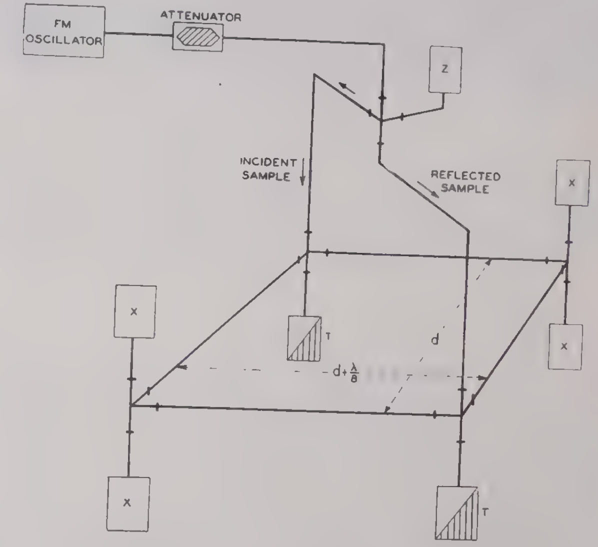

Fig. 9—An all-hybrid-junction circuit which provides the desired information.

In the circuit of Fig. 7, two directional couplers[3] are used to sample the incident and reflected waves. The coupler which samples the reflected wave may be constructed to have a greater coupling attenuation than the coupling attenuation of the coupler sampling the incident wave, or a resistive attenuator may be used to provide the desired difference in level. The probes in the secondary line then measure a reflection coefficient which is reduced by some desired factor with respect to the reflection coefficient of the impedance under test. Suitable allowance for this can then be made in the calibration of oscilloscope so that the device is still direct-reading. It is, of course, possible to dispense with one of the directional couplers, but the use of a single coupler to sample both wave components is not recommended because of the severe requirements on impedance matching which this usage imposes.

The use of directional couplers to sample the waves makes it possible to dispense with the use of probes and use hybrid junctions[4] to obtain the necessary additions and subtractions. Such a circuit using wave guides is shown in Fig. 8. Two input couplers and two output couplers are shown. The output from one incident-wave coupler and one reflected wave coupler are added and subtracted by one hybrid tee with a crystal on each of the two remaining arms. The second hybrid tee is displaced by an eighth wavelength to obtain the necessary phase difference. The balanced crystal outputs go to the oscillograph amplifiers as before. The sensitivity of the directional coupler and hybrid junction method can be made somewhat greater than that of the simple probe method, since it is possible to obtain much larger samples of the incident wave without serious error by these means.

---

[3] W. W. Mumford, "Directional couplers," Proc. I.R.E., vol. 35, pp. 160–166; February, 1947.

Some improvement in the frequency characteristic can be obtained by using hybrid junctions throughout, as shown in Fig. 9, although the mechanical complexity of the scheme becomes formidable. A 3-decibel difference in level between the incident and reflected wave samples is automatically supplied by this arrangement. Since the hybrid junctions are inherently less frequency-sensitive than are directional couplers, this scheme has perhaps the broadest band of any of the various schemes suggested.

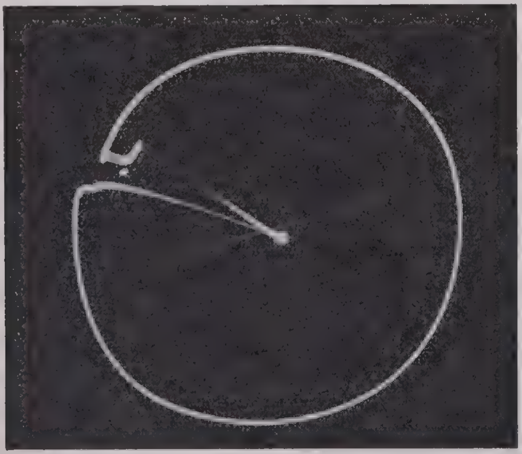

Fig. 10—Oscilloscope picture of the reflection coefficient of a 1-meter length of wave guide terminated in a short circuit with a frequency excursion of 100 megacycles.

As experimental proof of the usefulness of the impedance viewer, Figs. 10 and 11 are offered. Fig. 10 is a photograph of the oscilloscope pattern when a long line is terminated by a short circuit. This should, of course, be an arc of the unit circle, the length of the arc depending upon the length of the line and upon the frequency excursion. The departure from a true circle is a measure of the errors of the system. The irregularities at the ends of the circular arc in the picture are due to variations in input power level and a reversal in the direction of the frequency sweep during the switching period which are associated with the transient behavior of the power supply and switching circuits. Fig. 11 shows the input impedance of an over-coupled double-tuned circuit adjusted to match the line at two different frequencies.

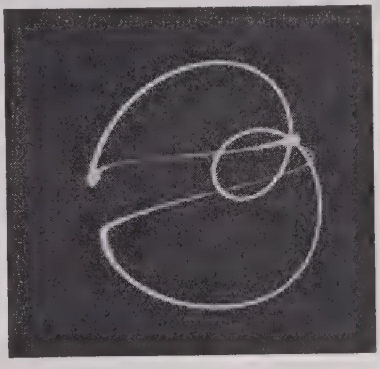

Fig. 11—The reflection coefficient of an over-coupled double-tuned circuit adjusted to match the line at two different frequencies.

Although somewhat outside the scope of the present paper, it may be well to point out that similar schemes exist for measuring the transmission properties of four-terminal impedances. One possible circuit is shown in Fig. 12. This circuit is analogous in every way to those already discussed, except that it presents the transfer impedance (or admittance) in phase and amplitude.

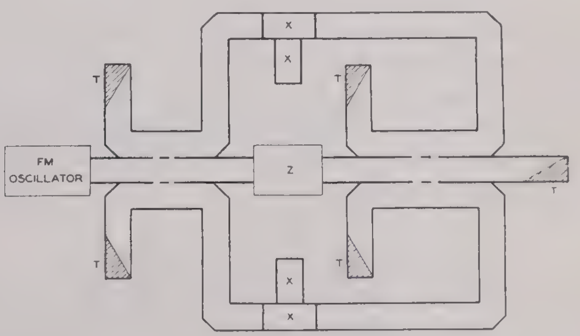

Fig. 12—Transmission-measuring circuit based on the same principles.

ACKNOWLEDGMENT

The assistance and co-operation of C. F. Crandell in constructing and demonstrating the experimental equipment is gratefully acknowledged. In spite of the simplicity of the ideas on which the impedance viewer is based, the author has been unable to find any published references to previous suggestions along these lines.[5]

---

[4] W. A. Tyrrell, "Hybrid circuits for microwaves," PROC. I.R.E., vol. 35, pp. 1294–1307; this issue.

[5] N. I. Korman, "The theory and design of several types of wave selectors," *Proc. N.E.C.*, vol. 2, pp. 404–423; 1947.

Parabolic-Antenna Design for Microwaves*

C. C. CUTLER†, ASSOCIATE, I.R.E.

***Summary*—This paper is intended to give fundamental relations and design criteria for parabolic radiators at microwave frequencies (i.e., wavelengths between 1 and 10 centimeters). The first part of the paper discusses the properties of the parabola which make it useful as a directional antenna, and the relation of phase polarization and amplitude of primary illumination to the over-all radiation characteristics. In the second part, the characteristics of practical feed systems for parabolic antennas are discussed.**

I. Introduction

THE USE OF radio waves in the wavelength range between 1 and 10 centimeters has resulted in many innovations in directional-antenna design. In particular, it has become a common practice to focus microwave energy into a desired directional beam by the use of a metallic reflecting surface excited by radiation from a small, relatively nondirectional source. Where maximum directivity of the antenna is desired, the reflector shape is usually parabolic, with a primary source located at the focus and directed into the reflector area. The reflector may be a section of a surface formed by rotating a parabola about its axis (circular paraboloid), a parabolic cylinder, or a parabolic cylinder bounded by parallel conducting planes. Also, there is a choice of how much, and what part, of the parabolic curve is used for the reflector. It is the purpose of this paper to discuss the design of such antennas, particularly the paraboloid and associated wave-guide-feed radiators. In this discussion, where the subject matter applies to a general characteristic, the word parabola will refer to either a paraboloid, a parallel-plate parabola, or a parabolic cylinder. The word paraboloid will be used only where subject matter refers specifically to the circular paraboloid, which is the surface generated by rotating a parabolic curve about its axis.

II. Fundamental Relations

The following equations describe a parabolic curve and are useful in determining its properties. See Fig. 1 for the meaning of the symbols.

Cartesian co-ordinates:

$$y^2 = 4Fx. \tag{1}$$

Polar co-ordinates:

$$r = \frac{F}{\cos^2 \dfrac{\theta}{2}}. \tag{2}$$

Parametric equations:

$$\left| \begin{aligned} y &= 2F \tan \theta/2 & (3) \\ x &= F \tan^2 \theta/2. & (4) \end{aligned} \right.$$

The properties of the parabola which make it particularly useful for focusing radiant energy into a directional beam are characterized by two ray considerations: First, any ray from the focus is reflected in a direction parallel to the axis of the parabola; and second, the distance traveled by any ray from the focus to the parabola and by reflection to a plane perpendicular to the parabola axis is independent of its path, and therefore such a plane represents a wave front of uniform phase.

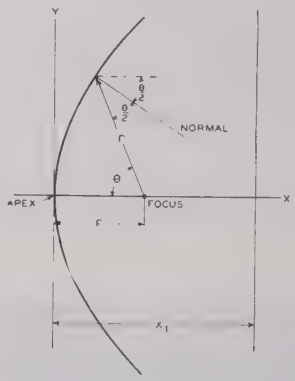

Fig. 1—The parabola.

The analysis of microwave antennas by consideration of geometrical rays may serve to give a crude picture, but generally it is necessary to use diffraction theory to obtain accurate results. In the discussion that follows both methods of attack are found useful.

III. Design Considerations

To obtain maximum efficiency from the paraboloid antenna requires a close control of amplitude, phase, and polarization of the field incident to the reflector. This puts rather strict requirements on the primary source of radiation, or the parabola "feed." In the first place, the feed must be small and of such configuration that it gives a spherical phase front; that is, from a distance it must appear as though the energy were radiated from a point. The amplitude of the radiation from the feed must be directed uniformly over a wide angle, to illuminate adequately the entire reflector area. Also, the field should be of such a nature that after reflection the waves will be properly polarized.

---

* Decimal classification: R326.8. Original manuscript received by the Institute, July 24, 1946; revised manuscript received, November 15, 1946.

† Bell Telephone Laboratories, Inc., New York, N. Y.

A. Phase

The phase of the field radiated from an antenna depends on the electrical distance the wave has traveled to arrive at the point under consideration. This in itself is of no great significance, but if we measure the phase at all points in a field at a distance of several wavelengths from the source and connect points of equal phase we get a curve or surface representing the wave front from which we may draw certain conclusions. The direction of propagation of energy in the wave is perpendicular to the surfaces of constant phase. From one such surface we can project forward to find the destination of the wave, and we can project backward to locate the effective source and analyze its properties. On the basis of geometrical ray construction, we see that the deviation of such a surface from a sphere will cause a deviation of the wave front from a plane, after reflection from an ideal paraboloid. Similarly, we may find by projecting back that the apparent source is not a point, but is instead a line or some peculiar surface. Such an apparent source does not necessarily have a significant relation to the physical size and shape of the radiator, but it does give a basis for comparing various feeds, and often suggests methods of correction. If the phase front from a feed is not spherical, the phase in the aperture can be corrected by changing the shape of the reflector. For a small phase deviation Φ, the compensating correction to r of (2) is

$$\Delta r = \frac{\lambda}{2\pi}\,\frac{\Phi}{1+\cos\theta}. \qquad (5)$$

If the phase front is not spherical, or is not corrected for, the radiation pattern will be distorted and the gain reduced. The effect on the pattern depends upon a number of factors, so it is difficult to generalize. However, a widening of the main lobe at low levels, or a filling-in of the nulls between minor lobes, usually indicates deviations of phase.

It is a fallacy to attribute the limitation of directivity of a parabolic antenna to phase deviations because of the physical size of the feed. Both the half-wave doublet, with or without a reflector, and an open-ended wave guide give very good phase distributions in spite of their relatively large physical size. The ultimate limitation to the sharpness of the beam is the diffraction at the paraboloid aperture and is due to the limited size of the effective area in wavelengths.

B. Amplitude

To make effective use of the area of the paraboloidal reflector, the energy must be distributed over the surface with some degree of uniformity. However, it is important to avoid loss of energy by waves radiated from the feed which fail to strike the reflector. This energy is called "spill-over," and to obtain the optimum gain efficiency from a paraboloid it is necessary to design the combination of reflector and feed to compromise between the loss due to spill-over and the loss due to nonuniformity of illumination. There is a direct relationship between the directivity of the feed and the angle subtended at the focus by the paraboloid for optimum gain. Furthermore, if a circular section of a paraboloid is used, it is important that the feed should radiate energy with circular symmetry. With the assumption of circular symmetry of feed pattern and reflector, and ideal phase and polarization conditions, the relationship between the feed directivity and the subtended angle of the reflector may be determined as follows:

The amplitude of the field at a distant point on the paraboloid axis is the sum of the contributions from all elementary areas of a plane through the circular aperture of the reflector.

$$E_p \sim \int_0^{y_1} yV(y)dy \int_0^{2\pi} d\Psi = 2\pi \int_0^{y_1} yV(y)dy \qquad (6)$$

where

$V(y)$ = amplitude of the incident field at any point on the surface of the reflector

$= (1/F)\,U(\theta)\cos^2\theta/2$ (from 2)

$U(\theta)$ = relative amplitude of field radiated from the feed where $U(\theta)=1$ when $\theta=0$

Ψ = the angle describing rotation about the axis

y_1 = radius of reflector.

Other symbols are indicated in Fig. 1. The power gain of the antenna is proportional to $E_p{}^2$.

$$G_a = \Omega\left[\int_0^{y_1} yU(\theta)\cos^2\frac{\theta}{2}\,dy\right]^2 \qquad (7)$$

where the proportionality function Ω may be obtained by comparing this to the gain of a system consisting of a circular area illuminated by the same primary source at a great distance. For such a system the gain is

$$\lim_{y_1/F\to 0} G_a = G_hG_t\,\frac{\text{Area of circle of radius } y_1}{\text{Area of sphere of radius } F} \qquad (8)$$

where

G_h = gain of the primary source or feed illuminating the reflector

G_t = theoretical gain of uniformly excited circular area, which is[1]

$$G_t = \frac{4\pi A}{\lambda^2} = \left(\frac{2\pi y_1}{\lambda}\right)^2 \quad \text{if} \quad \frac{y_1}{\lambda} \gg 1. \qquad (9)$$

From (8),

$$\lim_{y_1/F\to 0} G_a = G_h\left(\frac{\pi y_1{}^2}{\lambda F}\right)^2. \qquad (10)$$

---

[1] J. C. Slater, "Microwave Transmission," McGraw-Hill Book Co., New York, N. Y., 1942; p. 260.

Also, from (7),

$$\lim_{y_1/F\to 0} G_a = \frac{1}{4}\Omega y_1^4. \tag{11}$$

Equating (10) and (11),

$$\Omega = 4G_h\left(\frac{\pi}{\lambda F}\right)^2 \tag{12}$$

and therefore, from (7),

$$G_a = 4G_h\left(\frac{\pi}{\lambda F}\right)^2\left[\int_0^{y_1} yU(\theta)\cos^2\frac{\theta}{2}\,dy\right]^2. \tag{13}$$

From (3),

$$y = 2F\tan\frac{\theta}{2}; \quad \text{and} \quad dy = \frac{F\,d\theta}{\cos^2\dfrac{\theta}{2}} \tag{14}$$

and

$$G_a = 16G_h\left(\frac{\pi F}{\lambda}\right)^2\left[\int_0^{\theta_1} U(\theta)\tan\frac{\theta}{2}\,d\theta\right]^2. \tag{15}$$

Now, G_h may be obtained from $U(\theta)$:

$$G_h = \frac{2}{\displaystyle\int_0^{\pi}[U(\theta)]^2\sin\theta\,d\theta} \tag{16}$$

and

$$G_a = 32\left(\frac{\pi F}{\lambda}\right)^2\frac{\left[\displaystyle\int_0^{\theta_1} U(\theta)\tan\frac{\theta}{2}\,d\theta\right]^2}{\displaystyle\int_0^{\pi}[U(\theta)]^2\sin\theta\,d\theta}. \tag{17}$$

The efficiency of a radiator is taken as the ratio of its gain to that of a uniformly illuminated aperture of the same area (see (9)).

$$\text{Efficiency} = 2\cot^2\frac{\theta_1}{2}\,\frac{\left[\displaystyle\int_0^{\theta_1} U(\theta)\tan\frac{\theta}{2}\,d\theta\right]^2}{\displaystyle\int_0^{\pi}[U(\theta)]^2\sin\theta\,d\theta}. \tag{18}$$

With a given feed-radiation characteristic $U(\theta)$, the integrals can be evaluated by graphical methods, or by using a Fourier analysis, and the relationship of the subtended angle of the reflector to the efficiency can be obtained. Fig. 2 shows a typical plot of such a calculation for the radiation from a circular wave guide 0.84 wavelength in diameter whose radiation characteristic is shown in Fig. 3. The broad maximum of efficiency indicates that the subtended angle is not critical. It can be seen that the greatest efficiency is obtained with a reflector subtending an angle such that the radiation toward the edges is between 8 and 12 decibels below that at the center. In other words, the intensity of the energy radiated toward the edge of a parabolic reflector usually should be about one-tenth of the maximum intensity. It should be noted that the value "one-tenth" relates to the energy per unit solid angle in the primary pattern, taken at a constant distance from the feed. The intensity at the edge of the reflector is further reduced because of the increased space attenuation in the longer path.

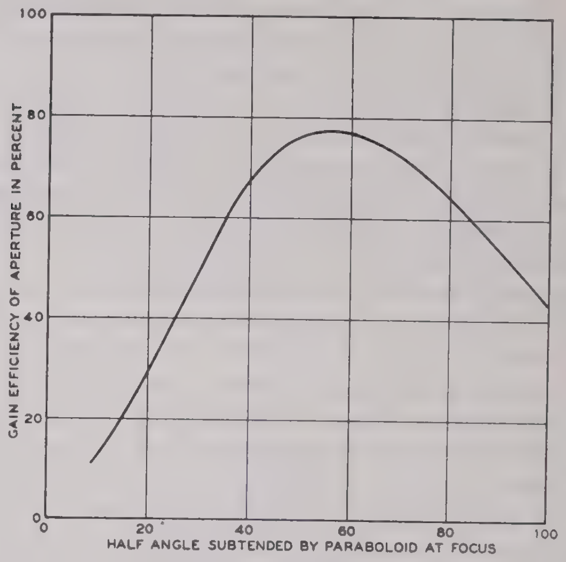

Fig. 2—Area efficiency of a paraboloid as a function of its proportions.

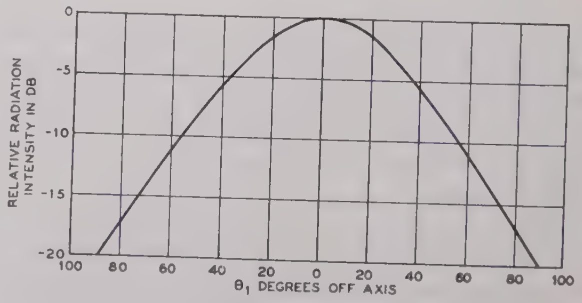

Fig. 3—Radiation pattern of 0.84-wavelength-diameter circular wave-guide aperture.

Calculations of the type given above indicate a theoretical gain efficiency of about 80 per cent for paraboloidal antennas, but because of defects in the phase and polarization characteristics and certain sources of interference to be discussed later, an efficiency much higher than 65 per cent is rarely obtained.

The effect of the amplitude distribution on the radiation pattern is very direct; but usually it is not an important factor in determining the desired illumination characteristic provided that sharp variations in intensity are avoided, and that the illumination is suitable from the point of view of gain. The diffraction pattern of a circular aperture, uniformly illuminated, has minor lobes 17 decibels below the maximum, and any tapering of illumination toward the edge of the aperture will reduce the lobes still further. A smooth reduction of intensity (of 10 decibels or more) towards the edge of the aperture results in a pattern with minor lobes 25 decibels or more below the major lobe. (This is usually less than minor lobes from other causes.) Where low side lobes are of paramount importance it may be desirable to use a deeper paraboloid, or, if beam sharpness is more important, a more shallow paraboloid than the gain criterion would indicate.

It should be noted here that the "spill-over" radiation mentioned above is the main source of wide-angle lobes from parabolic antennas, i.e., lobes at 90 degrees or further from the beam. The paraboloid is apt to be worse in this regard than other structures. This undesired radiation can be reduced (but only at the expense of gain or size) by using more directive feeds, or by extending the reflector sufficiently to intercept the energy.

C. Polarization

The radiation characteristic of the feed should be of such a nature that all the waves will be polarized in the same direction after reflection from the paraboloid surface. All field components which emerge from the aperture with polarization perpendicular to the average are wasted and contribute to minor-lobe radiation. This requirement will be satisfied if at any point the direction of polarization of the wave makes the same angle with a plane through the feed axis of symmetry and the point as does the average polarization of the feed. This may be seen by examination of such a wave after reflection, or, conversely, by imagining a polarized plane wave incident to the paraboloid, and analyzing the reflected wave over a sphere surrounding the focus. This required field is markedly different from that of a doublet, as may be seen by examining Figs. 4 and 5. The doublet has two poles (or points of indeterminate polarization and zero field strength) opposite each end of the antenna. The desired plane-polarized circularly symmetric feed has one pole directly behind the source. Lines indicating the desired polarization of the electric vector on a spherical surface around the feed, describe circles tangent to one another at a point on the surface of the sphere directly behind the feed. This specifies the polarization in all directions from the feed, but it is of significance only in the field radiated in the direction of the paraboloid surface.

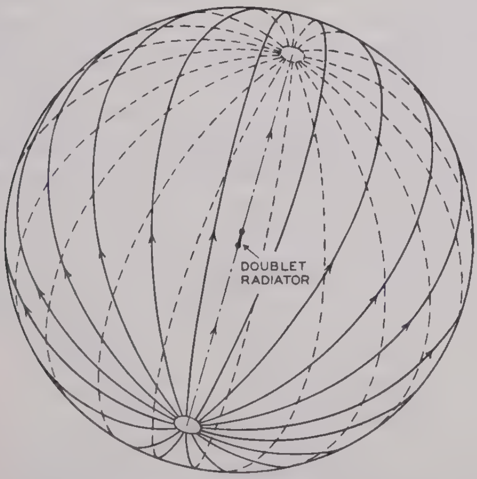

Fig. 4—Polarization for a dipole radiator field (lines indicate direction of *E* vector).

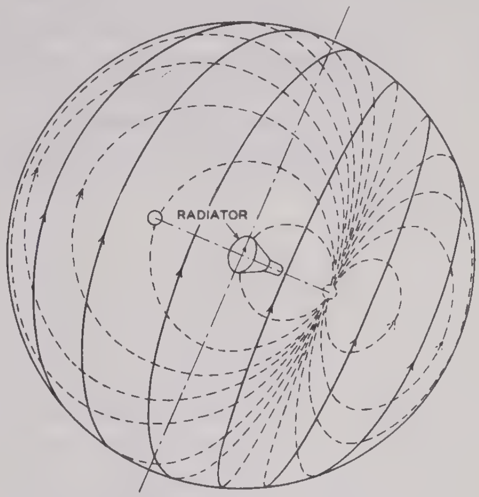

Fig. 5—Polarization of spherical wave front of field from an ideal paraboloidal feed (lines indicate direction of *E* vector).

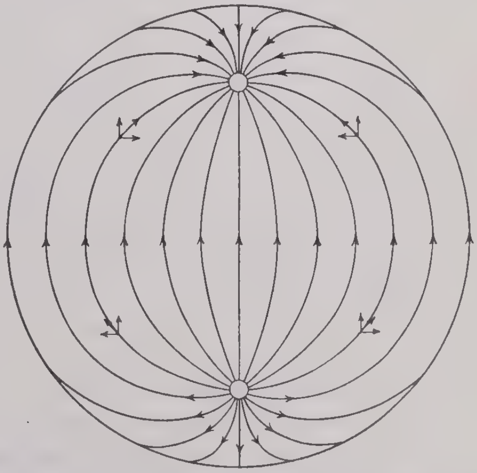

Fig. 6—Polarization of field in the aperture of a deep paraboloid fed from a dipole radiator.

If a feed having a poor polarization characteristic is used in a paraboloid, the resulting radiation pattern will contain regions where the polarization is perpendicular to that of the feed. Generally this energy is concentrated in four minor lobes, located in the quadrants between the plane of polarization and a perpendicular plane intersecting the axis of the paraboloid. For instance, consider a paraboloid excited by a feed having a polarization characteristic as shown in Fig. 4. After reflection from a deep paraboloid, the energy emerging through a plane across the aperture of the paraboloid will be polarized approximately as shown in Fig. 6. The component of field perpendicular to the feed polarization is called the "cross-polarized" field, and the resulting distant radiation, the "cross-polarized" radiation. The cross-polarized field for the case being considered has a maximum in each of the four quadrants of the reflector, as can be seen in Fig. 6. The resulting radiation pattern (Fig. 7) has cross-polarized lobes appearing in planes at 45 degrees to the axes of symmetry. Nearly all radiators have some cross-polarized radiation, but it is often undetected because of measurement techniques which discriminate against it.

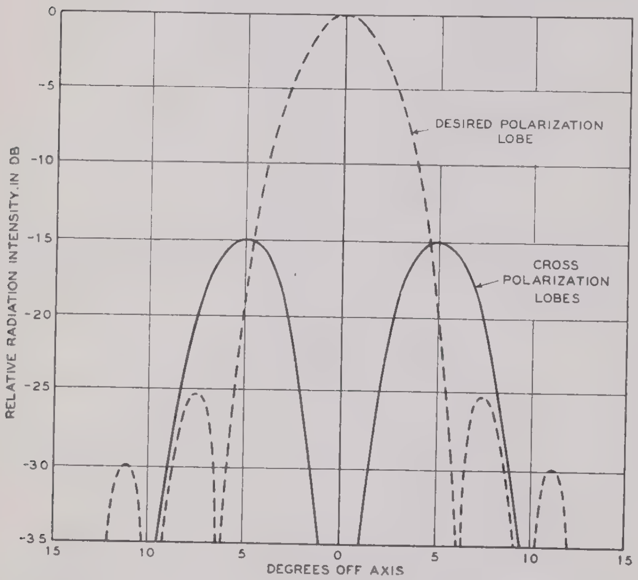

Fig. 7—Radiation pattern illustrating cross-polarized lobes.

D. Interference of Feed with Reflected Beam

The effect of the rearward radiation from a feed is indicated by a plot of gain against feed position. (See Fig. 8.) As the feed (wave guide in this case) is moved along the axis, the gain oscillates as the field radiated directly from the feed adds at various phases to that reflected from the paraboloid. To obtain optimum gain, the position of the feed should coincide with the focal point of the reflector. This requires that (for small antennas) the focal length shall be co-ordinated with the wavelength to assure proper phase of the rearward radiation from the feed.

The beam is deflected if the feed is moved laterally away from the focal point, and the defocusing loss does not take place as rapidly as it does for longitudinal motion. For the usual paraboloid proportions, by moving the feed the beam can be shifted about twice the half-power beam width with only $\frac{1}{2}$ decibel loss in gain. The beam shift can be doubled if the feed is fixed and the reflector is tilted.

A defect in many parabolic radiator designs is the fact that the feed obstructs the path of the reflected field. This creates a region of low intensity (or shadow) at the center of the aperture. The effect on the radiation pattern can be approximated by taking the difference of the radiation from the aperture and from the shadow area located at the feed position. This second hypothetical radiator is a small, relatively nondirectional source the same size and shape as the shadow, and acts on the resulting pattern to reduce the main lobe somewhat and raise the side lobes at least to the level of the radiation from the second source. This is illustrated in Fig. 9. The shadow effect may be reduced somewhat by "streamlining" the back of the feed by tapering it in the E plane.

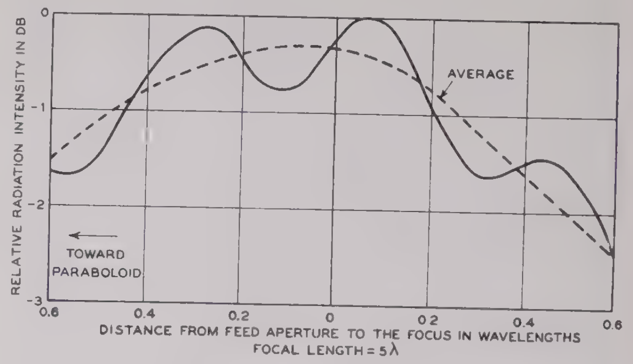

Fig. 8—Effect of rearward radiation on paraboloid gain as a function of axial feed position.

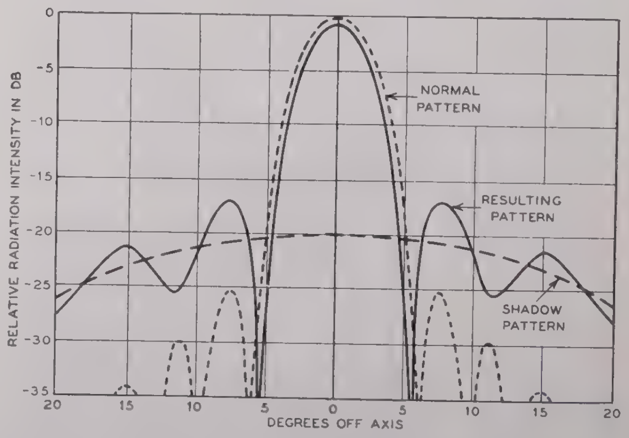

Fig. 9—Effects of a shadow on a paraboloid radiation pattern.

Another effect of the feed being in the path of the reflected wave is that some of the energy from the reflected wave returns to the feed system, producing an impedance mismatch. The absolute value of this impedance is fairly constant as a function of frequency or of feed position, but varies rapidly in phase because of the long round-trip path length of the reflected wave.

The mismatch may be corrected in the feed with an iris (or a stub line) over a narrow bandwidth, but inevitably this results in a more serious impedance mismatch at a frequency such that the focal length has changed by one-quarter wavelength. Moreover, if it is required that the feed be moved with respect to the reflector (in order to direct the beam) the impedance of the feed will change in phase and magnitude, making it impossible to match at a fixed point in the feed system. Thus, for conditions that require relative motion of the feed it may be desirable to match the feed to free space and tolerate the impedance change resulting from the reflector.

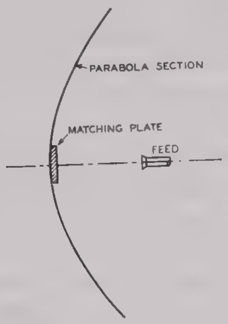

Fig. 10—Apex-matching plate for improving the impedance at the feed.

There are other ways of avoiding the effect of the reflector on the impedance of the feed. One method is to raise a portion of the reflecting surface to produce a reflected signal in the feed, equal and opposite to that received from the remainder of the reflector, thus canceling the reflected signal at the focus. This apex-matching plate is illustrated in Fig. 10. Since the two sources of reflection, namely, the undisturbed part of the reflector and the apex-matching plate, are at nearly the same distance from the focus, this impedance correction is effective over a very wide frequency band. Of course, the energy reflected from the raised surface is scattered widely and reduces the gain somewhat and increases the minor-lobe level of the radiation pattern.

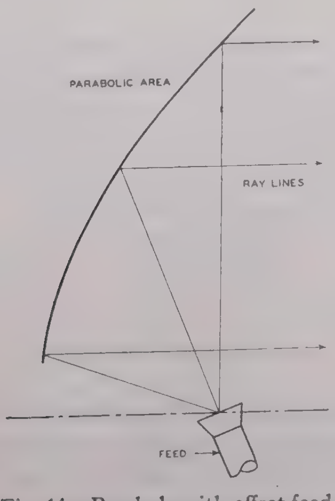

Fig. 11—Parabola with offset feed.

A method of avoiding the above-mentioned impedance problem, and also the shadow interference, is to use an off-set feed with a parabolic area (cylindrical or paraboloidal) located at one side of the apex, as shown in Fig. 11. In this type of antenna the feed is, for all practical purposes, clear of the reflected energy, and the bandwidth is limited only by the properties of the feed employed.

IV. Feed Systems

A. Half-Wave-Doublet Feeds

The earliest parabolic antennas evolved from attempts to increase the directivity of the half-wave doublet antenna by using sheet reflectors. However, as the art progressed and higher-gain antennas were required, it became apparent that the simple half-wave doublet was an ineffective source for exciting large parabolas.

The doublet antenna radiates uniformly in a plane perpendicular to its length. If a paraboloid is made to subtend a solid angle of 180 degrees at the focus, half of the energy will be radiated into space without striking the reflector. If this "lost energy" is properly phased with that of the reflected beam, it contributes to the gain of the antenna, as was discussed in connection with rearward radiation, and therefore the loss is not serious, provided that the aperture area is only a few square wavelengths. However, for large antennas most of the energy which does not strike the reflector is wasted. To reduce this loss and increase the radiating efficiency of the over-all system, it is necessary to direct most of the energy from the feed into the paraboloid.

The half-wave-doublet feed can be made more directive by using techniques familiar in wire antennas at lower frequencies, but the simple parasitically excited reflector appears to be the most practical. The reflector can be another doublet, a plane sheet, a half cylinder, or a hemisphere. The disk and the half cylinder appear to give best operation, but the other reflectors also have been used in specific applications.

The doublet antenna is at a disadvantage for feeding paraboloids in that the polarization characteristic is poor, as was discussed earlier. Beyond 90 degrees in the E plane, the polarization actually reverses, and extending the paraboloid beyond 90 degrees in this plane would result in a decrease in gain. To obtain minimum cross-polarization effects, and best distribution of illumination from a doublet radiator, a relatively shallow reflector should be used, as is indicated by the fact that the paraboloid which gives best efficiency with most of these feeds subtends only 140 degrees at the focus.

B. Wave-Guide Feeds

At centimeter wavelengths it is practical to feed the parabola with the radiation from an open-ended wave guide. The radiation characteristic of a wave-guide aperture is dependent upon the size and shape of the aperture and the mode or modes of propagation within the guide. Where a circular paraboloid is used, a circular $TE_{1,1}$ wave guide may be used for a feed, and indeed gives almost the ideal phase and polarization characteristics with suitable directivity. A fairly nondirective source for illuminating a deep paraboloid may be obtained by loading a small-diameter guide with a dielectric. A more directional source of illumination for a shallow paraboloid may be obtained by using a larger-diameter wave-guide aperture or by flaring the aperture into a small conical horn.

A rectangular $TE_{1,0}$ wave guide does not generally give a circularly symmetric radiation pattern, but it is suitable for feeding a paraboloidal section which is cut to subtend a wide angle in the E plane and a narrow angle in the H plane. A contour of uniform intensity in the pattern of such a feed is approximately elliptical, so the most efficient reflector area should be nearly elliptical, although sometimes it is mechanically more practical to use a rectangular shape. The directivity in the electric and magnetic planes can be controlled more or less independently by the corresponding aperture dimensions. The phase characteristic of a rectangular wave-guide aperture used as a radiator is very good, provided only the dominant mode is transmitted to the aperture. The measured polarization characteristic is usually deformed somewhat from the ideal, but it is still very good in the useful part of the amplitude pattern.

Where more directivity is required in the feed than can be obtained with a simple aperture, some form of wave-guide horn may be used. However, the phase characteristics of horn feeds should be examined carefully. In particular, the rectangular sectoral horn, which is often used for feeding elliptical paraboloid sections having large ratios of major-to-minor axes, has a poor phase characteristic. For instance, if the front of constant phase is measured for a sectoral horn of optimum flare,[2] it is found to be circular in the plane of flare, with the phase center near the apex of the angle of flare. In the other plane the phase front is also circular with the center at the horn aperture. Since these centers may be several wavelengths apart, the phase front is far from spherical, and may deviate a large fraction of a wavelength over the paraboloid surface. Acceptable operation is usually obtained for such a horn if the aperture is located at the focus, but better efficiency can be obtained by altering the shape of the reflector or by using a feed with more desirable phase characteristics.

There are many ways of obtaining a feed pattern for an elliptically cut paraboloid which will have more desirable phase characteristics than the sectoral horn with optimum flare. Some improvement may be had by using a flare angle somewhat smaller than that for optimum gain, but this requires a much longer horn for relatively small improvement. For reflectors with a major-to-minor-axis ratio of from 3 to 5, a "two-mode" or "box" type of horn has been found to give very good results.

The "two-mode" horn is simply a wide rectangular wave-guide aperture which is excited with both the $TE_{1,0}$ and the $TE_{3,0}$ modes of propagation. It can be shown that if both these modes are present in the aperture in the proper amplitude ratio and relative phase, the resulting aperture field approaches the desirable condition of uniform amplitude and phase. The two modes are set up in the guide by exciting it abruptly from a smaller guide which carries only the dominant ($TE_{1,0}$) mode. (See Fig. 12.) Since the large guide is wide enough to propagate the $TE_{1,0}$, $TE_{2,0}$, and the $TE_{3,0}$ modes, a discontinuity at the junction will tend to excite all three modes. However, if symmetry about a central plane is maintained, the $TE_{2,0}$ mode is not set up, and only the first and third modes are excited. At the junction, of course, many odd-order modes must be present in order to satisfy the boundary conditions presented by the walls of the guide, but if the larger guide is not wide enough to propagate modes higher than the third, they may for the sake of this discussion be ignored. At the junction the two modes add to approximately the field distribution of the original wave. However, since the two waves propagate with different velocities, their relative phases vary along the length of the guide, and at any other section the resultant amplitude will be different. When the length of the large guide is such that the relative phases of the two waves has changed by 180 degrees, they will add to give a uniphase field across the aperture with a nearly uniform amplitude. The superposition of these waves is shown in Fig. 12.

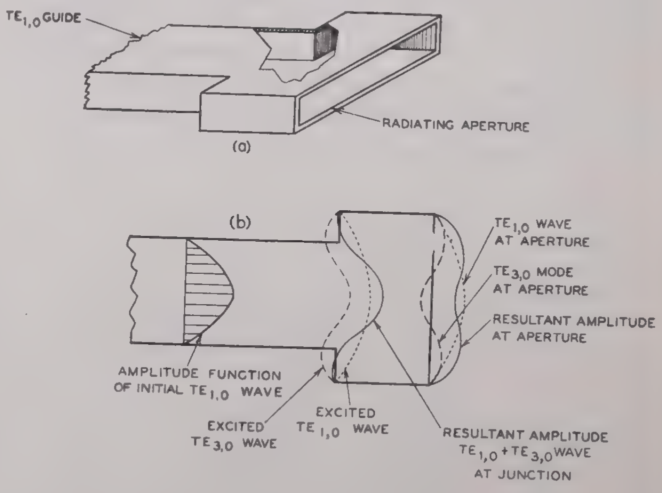
$TE_{1,0}$ GUIDE
RADIATING APERTURE
(a)
(b)
$TE_{1,0}$ WAVE AT APERTURE
$TE_{3,0}$ MODE AT APERTURE
RESULTANT AMPLITUDE AT APERTURE
AMPLITUDE FUNCTION OF INITIAL $TE_{1,0}$ WAVE
EXCITED $TE_{3,0}$ WAVE
EXCITED $TE_{1,0}$ WAVE
RESULTANT AMPLITUDE $TE_{1,0}+TE_{3,0}$ WAVE AT JUNCTION

Fig. 12—Two-mode feed horn.

---

[2] S. A. Schelkunoff, "Electromagnetic Waves," D. Van Nostrand Co., Inc., New York, N.Y., 1943; pp. 363–365.

The relative amplitudes of the $TE_{1,0}$ and $TE_{3,0}$ waves can be obtained by making a Fourier analysis of the incident field at the junction, taking into consideration only the first two terms of the series. The field at the junction may be expressed as

$$f(x) = A_1 \cos x + A_3 \cos 3x + A_h \cos 5x + \cdots + A_p \cos px \tag{19}$$

where p is any odd integer. The constants A_p may be found from

$$A_p = \frac{4}{\pi} \int_0^{\pi/2} f'(x) \cos (px) dx \tag{20}$$

where $f'(x)$ is the field incident to the junction, and is equal to $f(x)$. It may be taken as

$$f'(x) = \cos \frac{x}{b} \Big]_{x=0}^{x=(\pi/2)b}, \tag{21}$$

and

$$f'(x) = 0 \Big]_{x=(\pi/2)b}^{x=\pi/2}$$

where b is the ratio of the smaller to the larger guide widths. With values of 1 and 3 for p, the values of A_1 and A_3 may be obtained, and since higher-order waves are not propagated, the first two terms of the series (19) give the field propagated in the large guide.

In analyzing this field at any point it is necessary to know the relative amplitude of the two modes. This is given by

$$\frac{A_3}{A_1} = \frac{b^2 - 1}{9b^2 - 1} \frac{\cos \frac{3\pi}{2} b}{\cos \frac{\pi}{2} b} \tag{22}$$

which is plotted as a function of b in Fig. 13.

To phase the two modes properly, the large guide must be of such a length as to cause 180 degrees relative phase shift between the two components. This requires a length equal to

$$\frac{L}{\lambda} = \frac{1}{2} \frac{\lambda_1 \lambda_2}{\lambda_1 - \lambda_2} \tag{23}$$

where λ_1 and λ_2 are the guide wavelengths for the two modes. Substituting for these, we get

$$\frac{L}{\lambda} = \frac{1}{\sqrt{4 - \left(\frac{3\lambda}{w}\right)^2} - \sqrt{4 - \left(\frac{\lambda}{w}\right)^2}} \tag{24}$$

where λ is the air wavelength, and w the guide width.

The impedance presented to the guide by the two-mode feed horn has about the same magnitude as that of an open-ended wave guide, and can be easily matched over a fairly wide band of frequencies. For some applications it has been matched by adding a dielectric plate (of appropriate thickness) over the aperture, which also seals the guide from the weather. The impedance has also been matched by exciting the horn directly from a wave-guide elbow, and matching both elbow and horn simultaneously at the corner. A horn of this type is show in the photograph, Fig. 14.

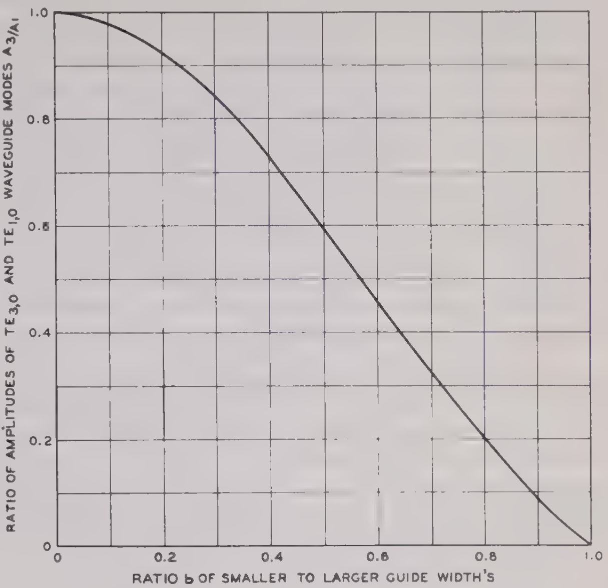

Fig. 13—Relative amplitudes of modes in a two-mode horn.

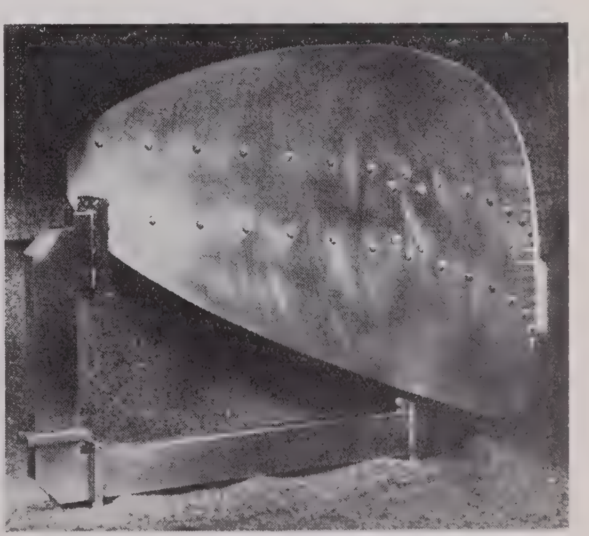

Fig. 14—Paraboloidal antenna with two-mode feed horn.

In spite of the fact that the wavelength appears critically in the dimensioning of this horn, it has been found to give acceptable operation over a bandwidth of at least 10 per cent.

Where still more directivity in the feed is desired, other types of antennas (such as lenses, and even small parabolas) may be used as paraboloid feeds.

C. Rear Wave-Guide Feeds

The wave-guide feeds discussed so far are all directive along the axis of the paraboloid and away from the feed mounting, and as a result they all require mechanical support and a source of power in front of the reflector. It is desirable, in most applications, to avoid the interference of the feeding guide and supporting structure with the reflected beam and, therefore, a number of rear feeds, or feeds supported and fed from the apex of the parabola, have been developed.

An early attack on this problem was to use a round wave-guide aperture, supported at the paraboloid apex and lying along the axis, opening toward the focus, with a metallic reflector to direct the energy back into the paraboloid. However, the simple geometric image picture of the field is not accurate, and we are not aware of any success in attempts to reshape the reflecting plate so as to produce a good over-all pattern. Finally, it was discovered that the phase front of this feed, instead of being spherical as desired, is toroidal with an apparent center in a ring lying between the circumference of the disk reflector and the wave guide, as shown in Fig. 15. For that reason, feeds with this type of phase characteristic are called "ring-focus" feeds. An empirical equation for the phase front in cylindrical co-ordinates is:

$$x^2 + (\rho - a)^2 = r^2, \text{ (independent of } \Phi). \qquad (25)$$

The reflecting surface for such a source should be

$$(\rho - a)^2 = -4Fx, \text{ (independent of } \Phi). \qquad (26)$$

which is the surface generated by a parabola rotated about a line parallel to its axis and displaced a distance a from the axis. Such a surface is called a "ring-focus" paraboloid.

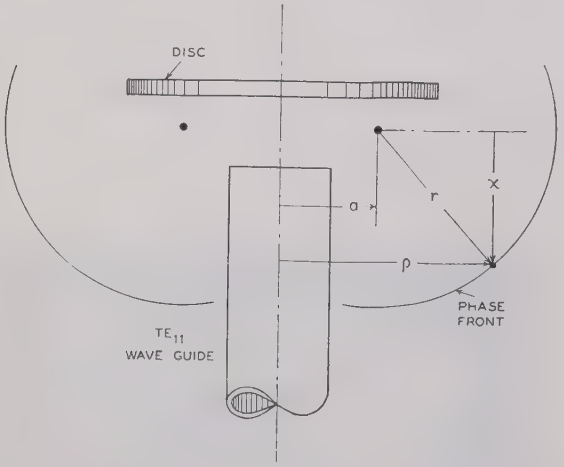

Fig. 15—Ring-focus-feed phase front is $x^2=(p-a)^2=r^2$. Ring-focus parabola contour is $(f-a)^2=-4fx$.

The cirular symmetry of the amplitude characteristic of a ring-focus feed becomes somewhat better when a cup, instead of the disk, is used to direct the energy from the feed into the paraboloid, as shown in Fig. 16. The amplitude characteristic of this feed is shown in Fig. 17. The distribution is more nearly uniform and covers a wider angle than that for other feeds. The optimum angle subtended by the paraboloid is about 160 degrees and consequently the reflector is much deeper than that required by most feeds.

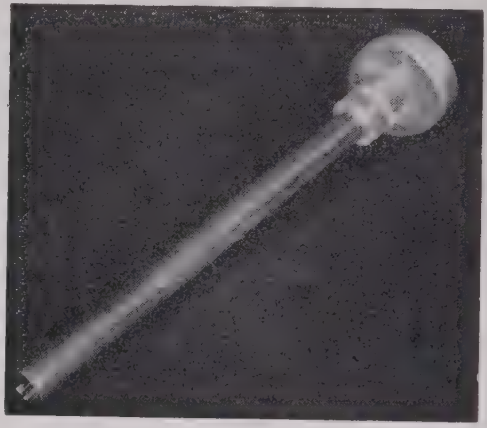

Fig. 16—Ring-focus feed.

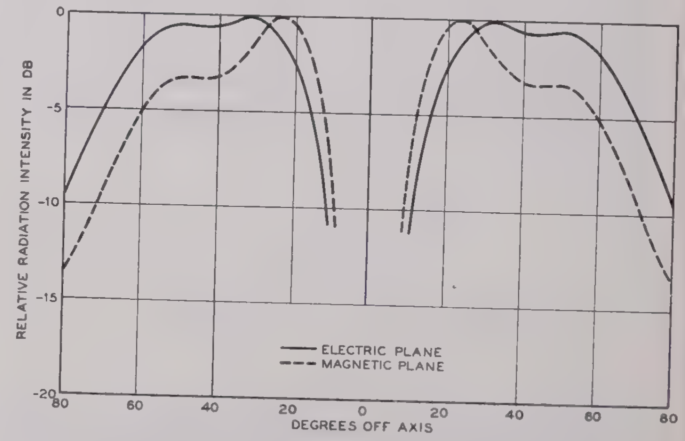

Fig. 17—Radiation pattern of ring-focus feed.

A picture of the field in the aperture of the ring-focus feed may be obtained by sampling the energy with a small probe. If the rim of the cup is extended, the part of the structure outside of the feeding wave guide comprises a large-diameter coaxial line. Because of the size of the line a great many modes of propagation may be supported, but only two modes can be initiated because of symmetry in the system. They are analogous to the $TE_{1,1}$ and the $TE_{1,2}$ modes in a circular guide. These modes are sketched in Fig. 18. By adjusting the dimensions of a ring-focus feed, it has been possible to set up either of these modes, and combinations of the two, with

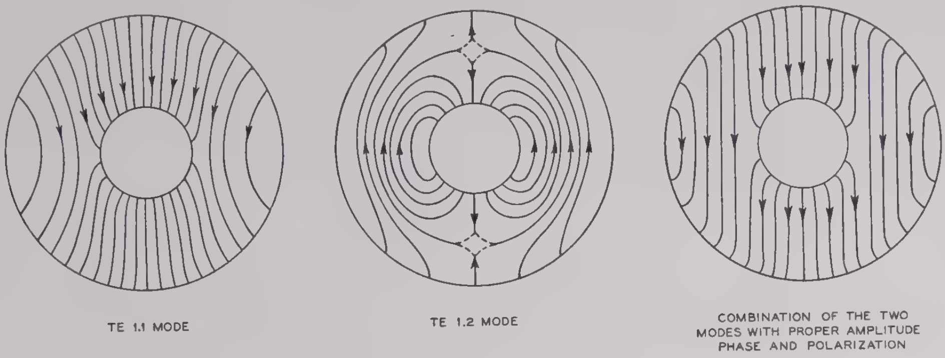
TE 1.1 MODE
TE 1.2 MODE
COMBINATION OF THE TWO MODES WITH PROPER AMPLITUDE PHASE AND POLARIZATION

Fig. 18—$TE_{1,1}$ and $TE_{1,2}$ modes of propagation in coaxial, as combined in the ring-focus feed.

various amplitudes and phases. Usually such combinations give very uneven amplitude and polarization distributions at the aperture, but when the dimensions are chosen to give the proper amplitudes and phases in the two waves, the amplitude at the aperture becomes very uniform and the lines of polarization are nearly parallel. It is this condition that accounts for the uniformity of the amplitude and phase characteristics of the ring-focus feed. Of course, there is not enough length of coaxial line to justify analyzing the field wholly in terms of these modes, but adding a length of line indicates that the fields present are closely related to these modes of propagation.

The impedance match of this feed is poor, and when matched by an iris in the wave guide the bandwidth is very narrow. Attempts to match impedance by changing the shape of the cup or disk have been unsuccessful because of the undesirable effects on the radiation pattern. Ring-focus antennas have given about 0.4 decibel more gain than the other paraboloid antennas described because of the closer approach to uniformity in the amplitude distribution of this type of feed.

Another method of feeding a paraboloid is by dividing the power in a rectangular guide, by providing two exit apertures symmetrically disposed with respect to the median magnetic plane, as shown in Figs. 19 and 20. Here the radiation is from two apertures which, to give a smooth amplitude pattern, should be less than a half-wavelength apart. It is also important that the apertures should not be too close to the guide wall; therefore, the guide must not be wider than about one-quarter wavelength. The phase front on either side appears to be coming from the nearer aperture and its image reflected in the adjacent side of the wave guide, thus resulting in phases in the E and H planes at the edge of the reflector which differ by about 30 degrees. The polarization shows a tendency to depart from the ideal similarly to a "magnetic dipole" (a loop antenna or a narrow slot in a conducting plane), but this is not serious. This feed has several advantages over many other rear feeds in that the directivity is directly dependent on the dimensions of the aperture; the impedance may be matched by properly dimensioning the cavity; and the structure can be easily weatherproofed by incorporating windows across the apertures.

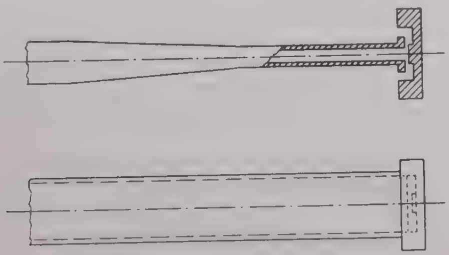

Fig. 19—Dual-aperture rear-feed horn.

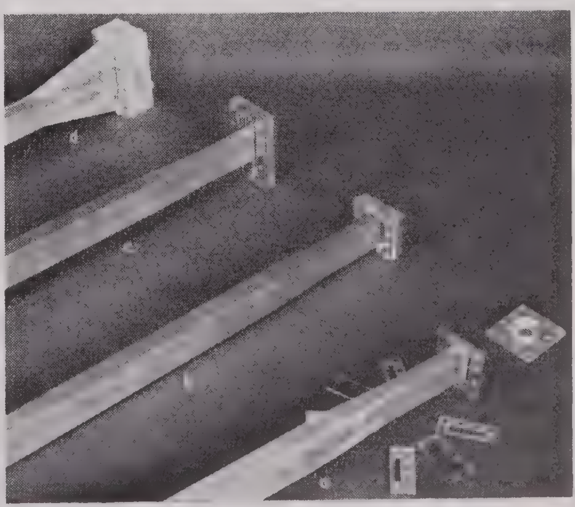

Fig. 20—Dual-aperture rear feeds.
(a), (b) Feed for circular paraboloids.
(c) Feed for elliptical paraboloids.
(d) Two-mode rear-feed horn.

The directivity of the feed in the E plane can be controlled, within limits, by the separation of the slot from the wave-guide wall and somewhat by the width of the slot. The directivity in the H plane is roughly inversely proportional to the length of slot from a length of one-half to three half-wavelengths, as shown in Fig. 21. For greater directivity a slot longer than 3 half-wavelengths may be used applying the principles of the "two-mode" horn previously described and shown in Fig. 12. The rear-feed, dual-aperture, two-mode horn [Fig. 20(d)] has the junction between the wide and narrow guides at the cavity where the energy is divided between the two radiating apertures. Thus the transmission in the head of the horn consists of two modes ($TE_{1,0}$ and $TE_{3,0}$) and the length of the path necessary to properly phase the modes is built into the head.

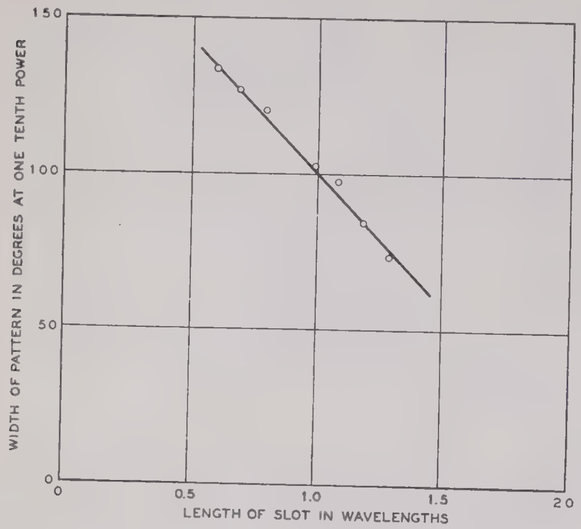

Fig. 21—H-plane directivity as a function of the length of the openings in the dual-aperture feed horn.

If the wave guide is not changed as the slots are lengthened, it soon ceases to adequately shield the radiating openings from one another, with the result that the E-plane pattern becomes sharper. Where it is desired to have the E plane broad, the outside wall of the wave guide should be extended in width to at least equal the length of the slots, also shown in Fig. 20(d). The size of the flat surface in the plane of the apertures is not critical, but some advantage in uniformity of illumination (and reduction of rearward radiation) is obtained if it extends at least one-quarter wavelength from the slots. There are three basic dimensions of the cavity which affect the impedance, namely, the width and depth, and an indentation at the center of the cavity as shown in Fig. 19. The feed for a circular paraboloid having slots about 0.7-wavelength long and a circular cavity is shown in Figs. 20(a) and (b). In this case the diameter, the depth, and the indentation at the center of the cavity may be controlled to match almost any impedance condition. For horns with longer slots a rectangular cavity is usually used and the impedance is controlled by the depth and the indentation at the center of the cavity. The relation of the cavity dimensions to the impedance is not simple and usually requires an experimental determination for each new application.

ACKNOWLEDGMENT

The development of the ideas described in this paper cannot be attributed to any particular time and place, inasmuch as many of the most basic ones may be traced back over several decades. However, most of the recent development described resulted from war-project work during the last six years within the Bell Telephone Laboratories at Deal, N. J., and Holmdel, N. J.

Hybrid Circuits for Microwaves*

W. A. TYRRELL†, MEMBER, I.R.E.

***Summary*—The fundamental behavior of hybrid circuits is reviewed and discussed, largely in terms of reciprocity relationships. The phase properties of simple wave-guide tee junctions are briefly considered. Two kinds of hybrid circuits are then described, the one involving a ring or loop of transmission line, the other relying upon the symmetry properties of certain four-arm junctions. The description is centered about wave-guide structures for microwaves, but the principles may also be applied to other kinds of transmission line for other frequency ranges. Experimental verification is provided, and some of the important applications are outlined.**

I. INTRODUCTION[1]

IN RADIO systems it is often desirable or even mandatory to incorporate means for uncoupling the receiver from the transmitter or for isolating the local beating oscillator from the antenna. There will be described certain passive circuits which perform these and many other important functions with a high degree of efficiency. The description is confined to wave-guide structures[2] suitable for microwaves, although the considerations are general enough to apply to other types of transmission line or even to equivalent networks with lumped constants.

---

* Decimal classification: R118. Original manuscript received by the Institute, August 27, 1946. This paper is based on an investigation of microwave bridge circuits carried on in 1941–1942 at the Bell Telephone Laboratories, Holmdel, N. J. Withheld from publication, the greater part of this material was extensively circulated as an unpublished memorandum dated February 12, 1942, to United States and Allied agencies connected with the war effort. Much work on these circuits has been subsequently done at this and other laboratories. Since the present paper is limited to fundamentals, it does not detail the more recent contributions to the subject.

† Bell Telephone Laboratories, Inc., New York, N. Y.

[1] It is assumed that the reader is familiar with elementary transmission-line theory, as given, for example, in S. A. Schelkunoff, "Electromagnetic Waves," D. Van Nostrand Co., Inc., New York, N. Y., pp. 188–200, 210–221, et passim, and also with wave-guide theory in terms of transmission lines, as developed by Schelkunoff in "Electromagnetic Waves," pp. 242–266, 316–324, 375–390, 480–496.

The performance of these devices is very similar to that of the hybrid coil, long familiar in telephone practice as a means for securing preferential isolation of circuits.[3] On account of this analogy,[4] the term "hybrid" has been selected to describe the present microwave constructions, even though the term may be somewhat foreign to current radio terminology.

A hybrid device is represented schematically in Fig. 1 as an eight-terminal network. When a source of alternating electromotive force is connected across the terminals A, no signal appears at the terminals C, but transmission takes place freely between A and B and between A and D, with the input power thus divided between loads placed at B and D. If the generator is transferred from A to C, no voltage can appear at A, from reciprocity considerations, and again the input power is divided in some fashion between loads at B and D. It is generally desirable, moreover, that the terminals B and D be balanced with respect to each other, so that a generator applied at either of these points delivers power only to loads at A and C. In most cases, the circuit is so proportioned as to bring about equal power division between the driven loads.[5]

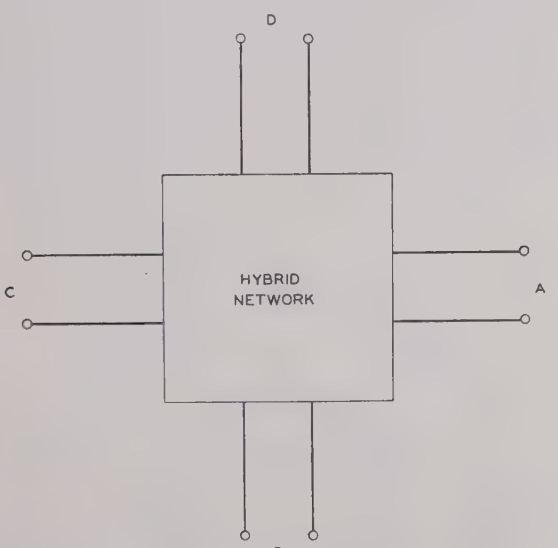

Fig. 1—Schematic representation of a hybrid circuit.

In constructions suitable for use at extremely high frequencies, the terminals correspond to four appropriate transmission lines, not necessarily alike, emerging from the network. It is assumed that the loads or generators which are attached to these lines terminate each arm in its characteristic impedance. If this is not done, reflections from the loads will tend to upset the balance.[5]

The elements comprising the hybrid network are presumed to be primarily reactive, so that internal dissipation is minimized. The resistive component of the impedance viewed at any one of the emerging lines corresponds, therefore, almost solely to the loads in the two adjacent lines, transformed by the network. A properly compensated circuit is one which combines these loads so as to present at any arm an impedance equal as nearly as possible to the characteristic impedance of that arm.[5]

Within the hybrid network, the four emerging lines must be joined in some manner. Two distinct possibilities can be visualized. The terminal lines may all be connected to another transmission line, or they may be joined directly without any intervening medium. Correspondingly, two classes of circuits will be described: hybrid rings, involving a ring or loop of line to which connections are appropriately made, and hybrid junctions, in which the four lines are joined at a common point. In both cases, there can be anticipated a need for compensating reactors to perfect the impedance match to all arms. This will be particularly essential when wave guides are involved, on account of the relatively severe reflections encountered at discontinuities.

In the wave-guide considerations which follow, attention is confined to the most common case of dominant waves in a rectangular pipe so proportioned

$$\frac{\lambda}{2} < a < \lambda, \; b < \frac{\lambda}{2}$$

that only the dominant mode and only one orientation of its polarization can be freely sustained. This choice avoids the effective conversion of wave power into higher-order transmission modes or states of polarization. Such modes and states will exist in the immediate vicinity of discontinuities, but will be rapidly suppressed in propagation away from the discontinuity. Under these conditions, the wave guide acts like a single transmission line, with geometrical discontinuities appearing as reactive elements.

In order to effect the joining of wave guides with each other and with coaxial lines, certain tee junctions are of great importance. These are the two wave-guide junctions and the junction of coaxial line to wave guide which are illustrated in Fig. 2. While a complete understanding of these junctions is not necessary for present purposes, an appreciation of their essential character and phase properties is important. By a simple consideration of wave fronts spreading out in the vicinity of the junctions, this necessary information can be readily obtained, as summarized herewith.[6]

---

[2] Supplemented by coaxial lines in certain cases.

[3] G. A. Campbell and R. M. Foster, "Maximum output networks for telephone substation and repeater circuits," *Trans. A.I.E.E.*, (*Elec. Eng.*), vol. 39, pp. 231–280, February, 1920.

[4] In the present treatment no close connection with the conventional hybrid coil is apparent, other than that of performance as viewed externally. Closer analogies can be established, however, by departing from the usual transmission-line analysis of wave guides to an extent that does not seem justified in a first approach to the subject.

[5] Interesting and important interrelationships among balance, impedance match, and power division are deduced from the laws of reciprocity in Appendix I.

In the electric-plane wave-guide junction the side arm is effectively connected in series with the main guide. When power is sent toward the junction from the side arm, two sets of waves are set up in the main guide, traveling in opposite directions away from the junction. These two sets of waves are 180 degrees out of phase with respect to each other; that is, their polarities are reversed. Conversely, if standing waves are set up in the main guide, the side arm receives maximum power when a voltage minimum of the standing-wave pattern coincides with the center of the junction and minimum power when a voltage maximum is located at the junction If only a pure standing wave is present in the main guide, caused by the interference of waves of equal amplitude traveling in opposite directions, no power appears in the side arm when it is placed at a voltage maximum[6]

In the magnetic-plane wave-guide junction and the junction of coaxial line to wave guide illustrated in Fig. 2, the side arm is effectively connected in parallel across the main guide. When power is sent toward the junction from the side[7] arm, two sets of waves, in phase, are caused to travel away from the junction in the main guide. Conversely, in the presence of standing waves in the main guide, the side arm receives maximum power when a voltage maximum in the pattern is centered at the junction and minimum power when a voltage minimum occurs at the junction. In the latter case, the side arm receives no power if the voltage minimum is zero.[6]

On account of the severe geometrical discontinuities characterizing each of these junctions, marked reflections may be expected when power is sent toward the junction from any of the three arms. These reflections may be reduced or substantially eliminated by the incorporation within the junction of suitable reactors, such as metal rods or plates. If these tuning elements are disposed in a sufficiently symmetrical manner, the original series or shunt character of the junction can be preserved.

II. Hybrid Rings

Principles underlying the construction of a hybrid network from a ring or loop of transmission line can be understood by examination of Fig. 3. This is a cross section in the electric plane of a wave-guide ring with a straight guide connected to it symmetrically from the exterior. The electrical length around the ring is one and one-half wavelengths. Here, as in further references below, it is to be understood that the wavelength corresponds to the increased phase-velocity characteristic of a hollow pipe. It is assumed that the electrical length around the ring is equal to the mean circumference.[8]

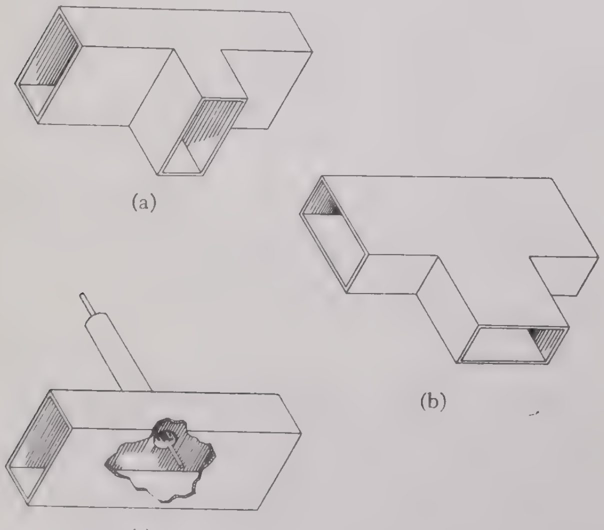
(a)
(b)
(c)

Fig. 2—Three important kinds of wave-guide tee junctions. (a) Electric-plane junction. (b) Magnetic-plane junction. (c) Coaxial-to-wave-guide transformation.

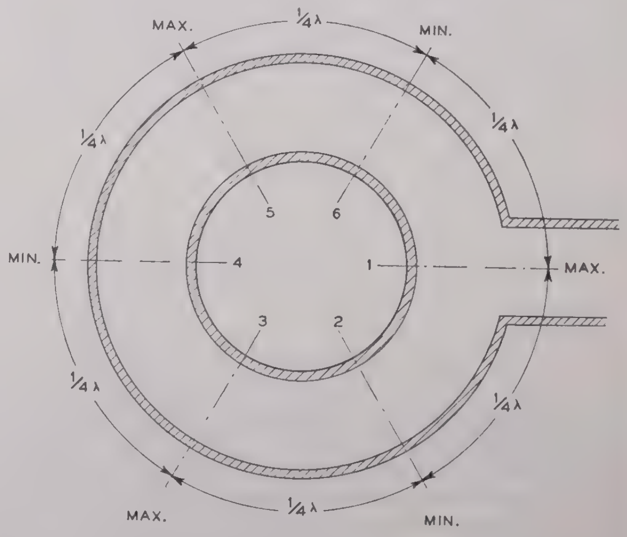

Fig. 3—Wave-guide ring with exterior radial arm, cross-sectional view in the electric plane.

When dominant waves are sent into the ring from the side arm, they will be split at the junction into two sets of waves of equal amplitude traveling around the ring in opposite directions. A pure standing wave will therefore be set up within the ring. This must be the case, for no mechanism has been provided for dissipation within the ring other than the minor ohmic losses associated with wave transmission. The two sets of waves spreading out from the junction are 180 degrees out of phase, on account of the nature of an electric-plane tee junction. When they reach the point diametrically opposite the junction, they have traversed paths of equal length and are still 180 degrees out of phase. This point is therefore a voltage minimum (zero). With this as a starting point, the standing wave within the ring can be mapped by marking off alternate voltage maxima and minima at quarter-wave intervals, as indicated on the figure.

---

[6] These relationships are derived in Appendix II.

[7] In the case of the coaxial-to-wave-guide junction, the coaxial line is the side arm.

[8] See Section IV for experimental verification.

If identical wave guides are connected symmetrically to the ring at points *2* and *4* so as to form additional electric-plane tee junctions and if these side arms are terminated in their characteristic impedance, they will receive equal amounts of power which are large, since they are series connections at voltage minima. The amplitude of waves proceeding past *2* toward *3* will, however, still be equal to the amplitude of waves proceeding past *4* toward *3*, since equal amounts of power are being extracted from two equal sets of waves. The arc $\widehat{234}$ still contains, therefore, a pure standing wave. Since identical phase shifts have been introduced at *2* and *4* by the identical tee junctions, the position of this standing wave is unaltered, and there is still a voltage maximum at *3*. A series connection to the ring at *3* will thus receive no power. Such a connection may be made by introducing a fourth electric-plane junction at *3*.

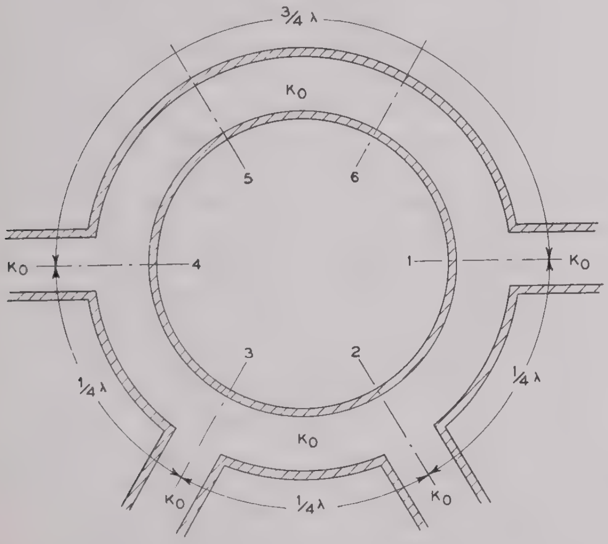

Fig. 4—A wave-guide hybrid ring.

Fig. 4 shows the modified structure, with series connections to the ring at *1*, *2*, *3*, and *4*. Before it can be concluded that this represents a hybrid circuit with bidirectional characteristics, attention must be directed to what happens when the ring is driven by a generator in arm *2*, with appropriate loads in arms *1* and *3*. At *5*, the point diametrically opposite the driving point, the fields will interfere to produce a voltage minimum, and in the absence of arms *1*, *3*, and *4* there will be voltage maxima at *2*, *4*, and *6* and additional minima at *1* and *3*. Arms *1* and *3* will thus receive equal amounts of power without disturbing the position of the standing-wave pattern in the arc $\widehat{153}$, and the arm at *4* receives no power. The construction of Fig. 4 possesses, therefore, the essential properties of a hybrid network.

It is now necessary to consider the improvement of this circuit by the elimination of undesired reflections within the ring. These arise in two ways. First, there are reflections taking place at each tee junction to the ring, due to the abrupt geometry which characterizes these junctions. It has already been suggested that these reflections can be reduced or eliminated by introducing in the vicinity of the junction appropriate reactive elements. If this is done in a sufficiently symmetrical manner, all four junctions of the hybrid ring can be made individually reflectionless. A second source of reflection can be traced to the inherent resistive mismatch which results from using wave guide of approximately the same size for the ring and all the arms. In this case, a generator of impedance K_0 is connected to two loads essentially in series, each of which has an impedance approximately equal to K_0. This mismatch can be readily eliminated by altering the characteristic impedance[9] of one or more of the wave guides involved.

A specific example of impedance proportions suitable to secure a complete resistive match in all directions is shown in Fig. 5. Here the guide used for the ring and for two opposed arms has the impedance K_0, while the remaining arms correspond to $2K_0$. When power is delivered to the ring from arm *1*, a matched condition exists because two K_0 loads in series terminate the $2K_0$ generator. When the ring is driven from arm *2*, matching is secured because each $2K_0$ load is transformed by the intervening quarter wavelength of line into $\frac{1}{2}K_0$, so that two $\frac{1}{2}K_0$ loads in series are driven by the K_0 generator. This set of impedance values is by no means the only one which brings about resistive matching.[10] There is, however, only one other set which employs only two different guide impedances.[11] Not shown in Fig. 5 are the reactors necessary to reduce the reflections from the junction discontinuities.

---

[9] For the dominant mode, the characteristic impedance of a reactangular pipe is linearly proportional to the cross-sectional dimension parallel to the electric intensity. For present purposes, variation of the characteristic impedance is most conveniently accomplished by varying only this dimension.

[10] In general, matching is secured when the characteristic impedance K_i of one series arm is related to the characteristic impedance K_j associated with each of the adjacent series arms as follows: $K_iK_j = 2K_0^2$, where K_0 is the characteristic impedance of the guide composing the ring.

[11] The other set of impedances is: $K_i = K_j = \sqrt{2}K_0$. In this case, the structure is most symmetrical, since all the arms have the same impedance. From the viewpoint of bidirectional characteristics and round-trip performance (cf., Section V), the broadest usable frequency band can be expected from the most symmetrical configuration.

The hybrid ring so far described is by no means the only loop structure which functions as a hybrid circuit. If a series element of impedance Z on a transmission line of characteristic impedance K_0 is replaced by a shunt element of impedance K_0^2/Z, on one side of which is added a quarter wavelength of line and on the other side, a three-quarter wavelength of line, the entire performance of the circuit is unaltered. By means of such replacements, the four series connections to the ring can be replaced, one by one, by shunt connections. This yields five distinctly different hybrid rings in addition to the one already discussed. These six circuits are shown in Fig. 6.[12] They are indicated schematically in order to emphasize the perfect generality of these networks. It has been found convenient to discuss the hybrid ring in terms of a wave-guide structure, but no important feature depends upon characteristics peculiar to wave guides. The circuits of Fig. 6 may be constructed, therefore, from any type of transmission line or from any mixture of types. For any of the six circuits, moreover, it is possible to find sets of impedance values which bring about resistive impedance matching in all directions.[13] This refinement is perhaps of greater importance in constructions with coaxial or parallel-wire lines for longer wavelengths, where the lines impedances are not so much obscured by severe reflections at the junctions.

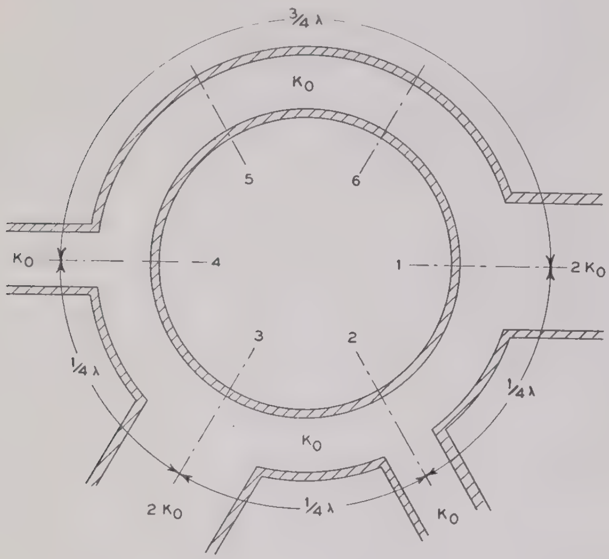

Fig. 5—A wave-guide hybrid ring proportioned for resistive matching.

For microwave frequencies, the practical realization of the circuits shown in Fig. 6 calls for electric-plane wave-guide tee junctions as series connections and magnetic-plane wave-guide tee junctions or transformations to coaxial as parallel connections. In certain combinations, there may be structural advantages in making the plane of the ring the magnetic plane. An interesting situation arises when square or circular wave guide is used, for here the circuits of Figs. 6(a) and 6(f) can be embodied in the same structure. For one orientation of the polarization, the ring lies in the electric plane; for another, the magnetic plane; and for any orientation in general, the input waves may be resolved into components parallel with and perpendicular to the plane of the ring, for each of which a hybrid circuit is provided. In this case, the matching of resistive impedances for both components becomes somewhat more involved.[14]

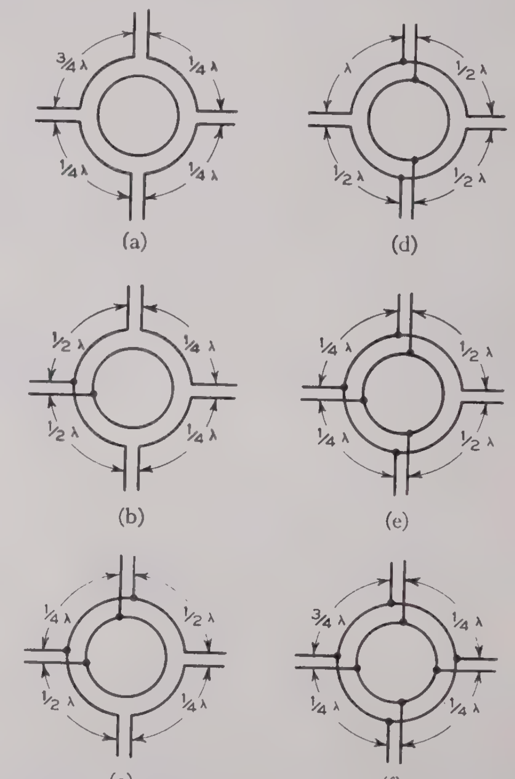

(a) (d)

(b) (e)

(c) (f)

Fig. 6—Schematic representation of the six fundamental hybrid rings.

The circumferential dimensions of hybrid rings can be changed in discrete steps without altering any of the circuit characteristics, by the application of either or both of the following rules:

(a) An integral number of wavelengths may be added to or subtracted from any arc (i.e., portion of ring between centers of adjacent connections).

(b) A pair of half wavelengths may be added to or subtracted from any two arcs.

---

[12] The dimensions shown in Fig. 6 have been obtained by subtracting pairs of half wavelengths.

[13] When only parallel connections are involved, as in Fig. 6(f), the matching condition (see footnote reference 10) becomes $K_iK_j = 1/2\, K_0^2$. Here again there are only two sets of values which involve only two different impedances: either two opposite arms with $K_i = K_0$, the other arms with $K_j = 1/2\, K_0$, or all arms with $K_i = K_j = \sqrt{1/2}\, K_0$ (cf. footnote 11). When both series and parallel connections are present, proper values for matching are derived from simultaneous consideration of the relations above and in footnote 10.

[14] By distorting the cross-sectional shape so that the guide presents different impedances to the two orientations, such matching can be effected.

These rules can be applied when it is desired to simplify the construction or to alter the structure to conform more readily to available space.

These rules, in subtraction, have already been used in arriving at some of the dimensions shown in Fig. 6. As the series connections are progressively replaced by shunt connections with the added quarter wavelength and three-quarter wavelength of line, the ring becomes larger unless a wavelength or pair of half wavelengths is judiciously subtracted at each step in the progression. The proportions indicated in Fig. 6 conform in each case to the smallest ring in which all connections are separated by finite arcs. From each of the circuits of Figs. 6(b) through 6(e), an additional pair of half wavelengths may be removed, but this eliminates the separation between certain adjacent connections. In such instances, care must be taken to preserve connections which are truly adjacent and which are not superposed symmetrically to the same point of the ring, if the properties of the original hybrid ring are to be preserved.[15]

Although such highly condensed circuits appear superficially attractive in general, wave-guide constructions are likely, indeed, to call for an expansion from the dimensions of Fig. 6. The size of rectangular wave guides has become somewhat standardized upon an electric-plane dimension only a little less than a half (free-space) wavelength. Since the wavelength in the guide is seldom as great as twice the free-space wavelength, the quarter (guide) wavelength spacings stipulated in Fig. 6 correspond to extremely close spacings or sometimes even to overlapping of adjacent series connections. Greater difficulties will be experienced with adjacent connections in the magnetic plane. These troubles, when they arise, can be obviated by increasing the size of the ring according to the rules above. For example, the arcs in Fig. 6(a) may be increased to $\frac{3}{4}\lambda$, $\frac{3}{4}\lambda$, $\frac{3}{4}\lambda$, $1\frac{1}{4}\lambda$.

In connection with the wave-guide embodiment of the circuit in Fig. 6(a), it has already been pointed out that the reactances associated with the junctions do not upset the performance because equal phase shifts are introduced as the waves travel past the two driven arms. It is clear that the same argument can be applied to the highly symmetrical circuits of Figs. 6(d) and 6(f). Not so obvious, however, is the situation with regard to the rings involving asymmetrically disposed, mixed connections, since different phase shifts may be expected at series and shunt branches. Consider, therefore, the circuit of Fig. 6(b). When this is driven from the shunt arm or from the opposite series arm, equal phase shifts take place at the two identical, adjacent series arms, and balance is secured with the dimensions as given. If the junction reactances are reduced or eliminated by symmetrical tuning, balance and equal power division will still be retained. General considerations based on reciprocity[16] may now be cited to show that this same tuning automatically brings about balance, equal division of power, and impedance match when the circuit is driven from either of the opposed series arms, even though the connections adjacent to these arms have such a totally different character. The same argument can be applied to Fig. 6(e). The completely asymmetrical circuit of Fig. 6(c) remains, then, as the only one whose dimensions may perhaps require substantial alteration when appreciable phase shifts are involved.

There remains to be discussed the variation of hybrid ring characteristics with frequency. Of the various electrical properties, the balance between opposite arms is the most critical one. Consider what happens when, in Fig. 3, there are sent into the ring waves of a frequency different from that originally considered. There will still be cancellation of fields at point *4*, but now the spacing in the standing-wave pattern is changed, and the voltage maximum is displaced from point *3*. An arm attached at *3* will thus not be completely uncoupled from the arm at *1*. This reasoning can be applied to the circuits shown in Figs. 6(a), 6(d), and 6(f), and also to those pairs of opposite connections in Figs. 6(b) and 6(e) which are balanced by virtue of two paths around the ring which differ by a half wavelength; that is, to all cases in which the opposite connections are both parallel or both series. A different situation exists when balance is obtained between a series connection and a shunt connection located at geometrically opposite points across the ring, since the standing-wave pattern at the point diametrically opposite the feed point does not shift with frequency. This argument applies to Fig. 6(c) and one pair of opposed arms in Figs. 6(b) and 6(e). When a high degree of balance is desired between one particular pair of arms over as broad a band as possible, the circuits of Figs. 6(b) and 6(e) will be preferred, for they offer driven arms which are symmetrically connected.

If the loads attached to the arms of a hybrid ring are maintained nearly reflectionless over a band of frequencies, and if the junction reactances in the ring are effectively canceled throughout this band, important variations in the power division or in the resistive matching ability of the network will not be expected. In general, limits to the usable bandwidth will be set by deviations from balance or by inability to tune out satisfactorily the internal reflections associated with the junctions.

III. HYBRID JUNCTIONS

A hybrid network for microwaves can also be secured in the form of a compound junction comprising a series connection and a parallel connection made to a guide at the same point on its longitudinal axis. One form of such a junction is shown by Fig. 7 as a cross section in the electric plane. Lines of electric intensity in successive positions of a wave front are drawn to indicate what happens when power is introduced from the wave-guide series arm. Equal intensities appear in the collinear guide arms, with a 180-degree phase difference, while the voltages induced in the coaxial line are such as to cancel mutually.[17] If the two ends of the main guide are terminated in characteristic impedance, the power will divide equally between the two loads, and no power will appear in the coaxial line.

---

[15] As will appear in the following section, certain symmetrically superposed connections form compound junctions which are in themselves hybrid circuits. The combination of such a hybrid junction with a ring of guide does not generally constitute a hybrid circuit.

[16] See Appendix I.

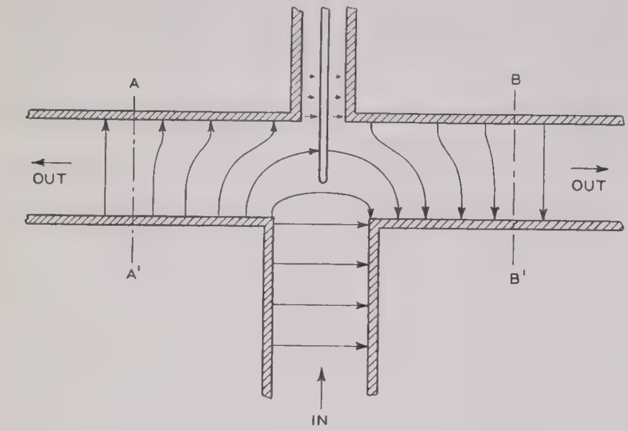

Fig. 7—Spreading of a wave front into a compound junction from the series arm.

The same junction is again shown in Fig. 8, but here the power is introduced from the parallel arm, i.e., from the coaxial line. The two arms of the main guide receive equal intensities in phase, and no net voltage appears across the series branch.[18]

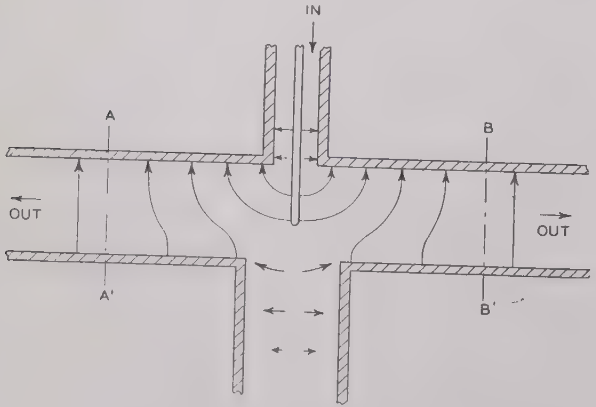

Fig. 8—Spreading of a wave front into a compound junction from the parallel arm.

This compound junction, a clearer view of which is given in Fig. 9, possesses, therefore, the properties required of a hybrid circuit. The series and parallel arms *S* and *P* are balanced with respect to each other, and power delivered from either of them is equally divided between suitable loads attached to arms *1* and *2*. This behavior is brought about by the geometrical symmetry prevailing in the region of the junction, rather than by interference effects between alternative paths as in the case of hybrid rings.

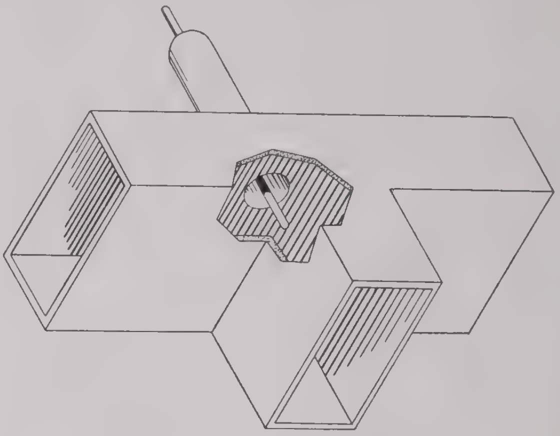

Fig. 9—The wave-guide-to-coaxial hybrid junction.

Another important form of hybrid junction is shown in Fig. 10, where the parallel connection is established by means of a magnetic-plane wave-guide junction. It is not difficult to see that this construction possesses the desired hybrid behavior, and, moreover, that a hybrid junction results from any practical realization of perfectly superposed series and parallel connections to a common transmission line. The illustrations given, however, are sufficiently representative.

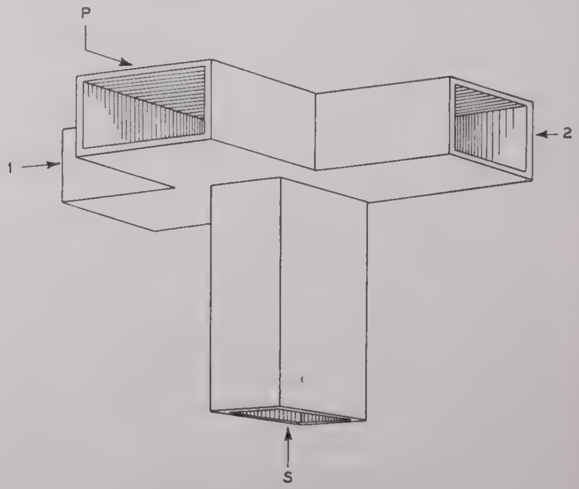

Fig. 10—The wave-guide hybrid junction.

As in the case of hybrid rings, the termination of each arm in a load or generator which matches the line comprising the arm is the most satisfactory condition for straightforward operation as a hybrid network. Here again, however, relatively severe reflections are experienced as the device is driven from any arm, on account of the severe discontinuities at the hybrid junction, unless suitable reactive tuning is associated with the junction. These reflections do not affect the balance between the *S* and *P* arms, which is maintained from symmetry alone. When viewed from arms *1* or *2*, however, the junction does not appear symmetrical. By arguments derived from reciprocity,[19] mismatches to arms *1* and *2* and a lack of balance between *1* and *2* may be inferred from the mismatches presented by the untuned junction to the *S* and *P* branches. Again, the introduction of reactive tuning which improves the match to *S* and *P*[20] without disturbing the balance between these arms and the equal power division between *1* and *2* automatically tends to bring about a balanced condition between *1* and *2*, a matching of the junction to these arms, and equal division between *S* and *P* of power sent toward the junction from *1* or *2*.

---

[17] This will not be true if the coaxial is large enough to support freely the first higher-order transmission mode.

[18] This will not be true if the (rectangular) series arm is large enough to support freely the TM_{11} (coaxial-like) transmission mode.

It is interesting to note that no such conclusion about balance between *1* and *2* would be reached from a naive consideration of the spreading of wave fronts into the junction from *1* or *2*. Indeed, it would be anticipated that power from either of these arms would divide in roughly equal proportions among the other three branches. This indicates the danger latent in the indiscriminate application of Huygens' principle except under conditions of high geometrical symmetry.

Suitable reactive tuning can be accomplished by a variety of metal rods and plates or by tuning stubs appropriately associated with the junction. As in hybrid rings, it is preferable to select these tuning elements so that the impedances presented by the network and its associated loads to the *S* and *P* arms can be adjusted independently. The use of two reactances, one in the *S* arm, the other in the *P* arm, is clearly one solution to this problem, for adjustments in one arm cannot affect the impedance viewed from the other arm, since no power flows between the two arms. In testing a tuned junction, the degree of balance between *1* and *2* is often taken as a convenient measure of the over-all impedance match and symmetry.

The frequency response of hybrid junctions is similar to that of the hybrid rings shown in Figs. 6(b) and 6(e). That is, the balance between *S* and *P* depends only upon the extent to which perfect symmetry is maintained within the junction and in the loads attached to arms *1* and *2*. It is not necessary that these loads be well matched so long as they give rise to equal reflections. Balance between *1* and *2* is, however, critically dependent upon perfection of matching by reactances associated with the junction. Illustrations of what can be accomplished in this regard will be given in the next section. As a general rule, the *S* and *P* arms are preferred for the placement of loads or generators which are to remain uncoupled over as wide a frequency band as possible.

IV. Experimental Results

Verification of the principles discussed in the preceding sections has been provided by the construction and measurement of the hybrid junction illustrated in Fig. 10 and of a representative wave-guide assortment of the hybrid rings indicated schematically in Fig. 6. In all instances, the agreement between expectations and results has been very satisfactory.

All of the hybrid rings constructed have been found to perform well at or near the frequencies for which they were designed. If the electrical lengths of the paths around the ring are taken in accordance with the arithmetic mean circumference, it thus appears that no very large correction is necessary.[21]

In conformity with expectation, all arms of wave-guide hybrid circuits develop standing waves which may run as high as 15 or 18 decibels. It is found, however, that the standing waves can be reduced or essentially eliminated by appropriate reactive tuning associated with the circuit, of which satisfactory examples will be given below. In these and other applications, tolerances of the order of 0.001 to 0.010 inches, for wavelengths from 1 to 10 centimeters, must be placed upon the dimensions and locations of the compensating reactors, or else the results will spread undesirably.

With terminations which have been adjusted by conventional means to match the wave guide closely, the balances observed between opposed connections correspond to losses between 20 and 40 decibels. When it is realized that a load which introduces only 0.25-decibel standing waves reflects power which is about 36 decibels below the level of the incident power, it can be appreciated that an extremely high degree of balance is attainable only by adjustment of the loads in situ so as to reduce the reflections or to alter them to cancel small reflections in other parts of the circuit. In this fashion it is possible to secure losses between opposed connections as high as 60 to 75 decibels, but the balance then becomes so sensitive to changes in frequency or to mechanical distortion of the circuit that it cannot be maintained at this level for many practical purposes.

---

[19] See Appendix I.

[20] Just as for hybrid rings, it would appear that, after the discontinuities have been tuned out, a resistive mismatch should remain, associated, for example, with driving two K_0 loads from a K_0 generator. It turns out that this is not the case (cf. Section IV).

[21] This observation is in agreement with the theoretical analysis of propagation in curved rectangular wave guides as first given by H. Buchholz, "Der Einfluss der Krümmung von rechteckigen Hohlleitern auf das Phasenmass ultrakurzer Wellen," *Elek. Nach. Tech.*, vol. 16, pp. 73–85; March, 1939, and as confirmed by recent unpublished work of S. O. Rice of the Bell Telephone Laboratories, who uses a matrix calculus. It is convenient to interpret these results in terms of an effective circumference, along which the phase velocity is the same as in a straight guide of identical cross-sectional dimensions. From the theory, it can be shown that the effective radius of a guide curved along the arc of a circle may in general be either smaller or larger than the arithmetic mean radius, depending upon the ratios between the operating wavelength and the cross-sectional dimensions of the guide. The magnitude of the departure from the mean not only depends upon these ratios but also varies inversely as the square of the mean radius of curvature of the bend. For the proportions commonly used, the arithmetic mean circumference should be an excellent approximation to the effective circumference. These predictions apply to gentle or even moderately severe bends in either the electric or magnetic plane.

In order to illustrate specific microwave circuits, data will be given for two versions of the hybrid junction shown in Fig. 10. This type of circuit has been more highly developed than the others. The two examples differ only in the relative proportions of the wave guides involved and in the means correspondingly adopted to effect the impedance matching.[22]

Fig. 11 shows the first particular construction, with two metal rods employed for matching purposes.[23] Even though these are located within the junction their action is essentially independent, since the electric intensity lies wholly transverse to the one rod when power enters from the series arm, and wholly transverse to the other rod when the shunt arm is driven. The performance[24] of this hybrid junction is indicated by the data given in Table I. These results were obtained on a particular sample, using wave-guide terminations which were matched within 0.1-decibel standing waves and which therefore reflected power more than 46 decibels below the incident power.[25]

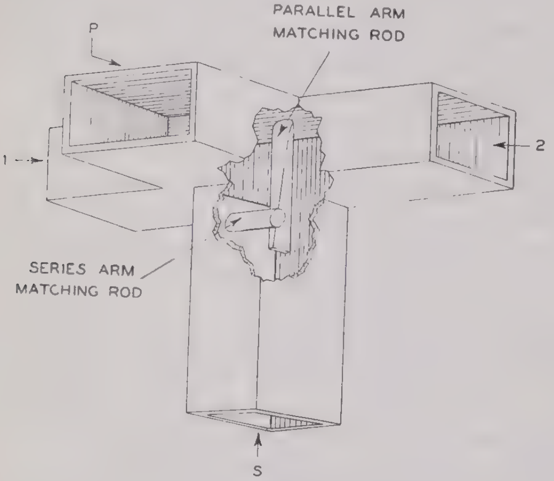

Fig. 11—The wave-guide hybrid junction tuned with two metal rods.

TABLE I

Performance Data on Hybrid Junction of Fig. 11

Free-space wavelength in centimeters	3.13	3.33	3.53
Standing waves in decibels:			
Match to P arm	0.8	0.2	0.8
Match to S arm	2.5	0.6	2.6
Loss in decibels:			
P to S	36	39	38
1 to *2*	21	36	24

The second example is shown in Fig. 12, with two metal plates used for the independent matching reactors. Curves[26] illustrating the impedance matching to the S and P arms as a function of wavelength are given in Fig. 13.

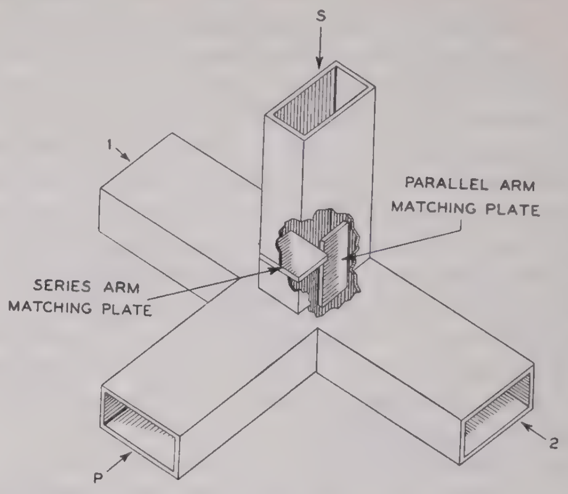

Fig. 12—The wave-guide hybrid junction tuned with two metal plates.

V. Applications

The very nature of a hybrid circuit is such as to suggest immediately numerous applications in duplexing. In Fig. 1, for example, the following connections may be made: at A, a transmitter; at B, a transmission line or antenna; at C, a receiver; at D, a dummy load. Of the power sent into the network from the transmitter, half will be sent out the line or antenna, half will be dissipated in the dummy load, and none will appear in the receiver. Signals entering the network from the line or antenna will be divided equally between the receiver

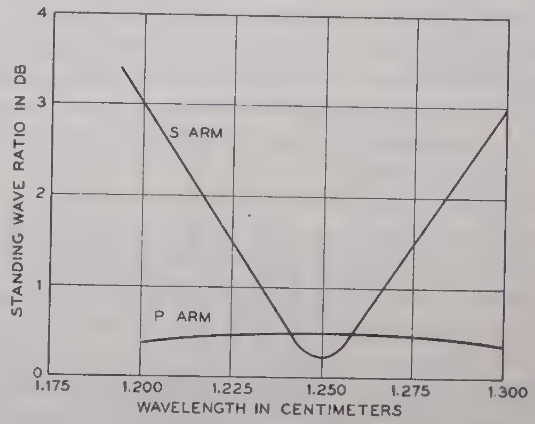

Fig. 13—Frequency variation of impedance match to arms S and P of hybrid junction of Fig. 12.

---

[22] When the cross-sectional dimensions of the guide are varied with respect to each other and with respect to the wavelength, it appears that the general choice and arrangement of tuning reactors leading to broadest-band characteristics will also vary.

[23] This design was originated by C. F. Edwards, Bell Telephone Laboratories.

[24] Data furnished by A. P. King, Bell Telephone Laboratories.

[25] Note that the reactors not only cancel junction reflections but also bring about a resistive match as well. If only the reactance were eliminated, a 6-decibel standing-wave would be expected from the termination of a K_0 generator in two K_0 loads in series or parallel.

[26] Data furnished by S. D. Robertson, Bell Telephone Laboratories. The remarks of the preceding footnote (25) apply also to this second example.

and transmitter.[27] There will therefore be a 3-decibel loss in reception and in transmission, or the total round-trip loss of 6 decibels often associated with hybrid devices.[28] This duplex system still compares favorably with the two simplex systems necessary to accomplish the same result, for the total area of two similar antennas associated with the simplex systems may be devoted to a single antenna with a 3-decibel increase in gain, or, in the case of transmission lines, the two lines needed in simplex operation may be replaced by a single improved line, so that again the 6-decibel round-trip loss is recovered. This loss can also be reduced materially by the appropriate employment of active circuit elements, such as gas-discharge switches.

A second important field of application occurs in connection with balanced mixers and converters. As an interesting preliminary to this subject, consider the following argument. In Fig. 1, let the terminals *B* and *D* be joined externally at a junction *E*. This junction may be so located that when power is introduced at *A* the equal amounts of power delivered to *B* and *D* reach *E* in phase. All of the power from *A* will therefore be developed in the appropriate load at *E*. Since *A* and *E* are completely coupled, the terminals *C*, by reciprocity, have no connection with either *A* or *E* and hence play no part in the circuit. Thus it is not possible to combine the two radio-frequency voltages to drive a single load and to avoid the 3-decibel loss accompanying the use of a dummy load, without at the same time destroying the hybrid properties of the circuit.

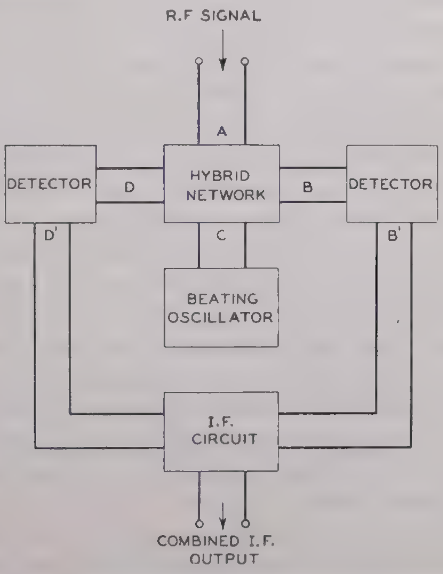

Fig. 14—Schematic representation of a balanced converter.

It is possible, however, to avoid a loss, when detection is involved, by combining detected signals. It is this principle which is involved in the use of a hybrid network for a balanced converter in the manner represented schematically in Fig. 14. The intermediate-frequency voltages appearing at *B'* and *D'* must be combined with due regard for their relative phase. While it is important that there is no loss in signal power over that normally associated with detection, this in itself is scarcely a reason for preferring the balanced converter. Its advantages, however, are numerous, including the isolation between the signal and the local beating oscillator and the elimination of noise contributions from the local oscillator. This has, indeed, been an application in which these hybrid circuits have been extensively used in microwave systems. For this purpose, the hybrid junction of Fig. 10, modified as in Figs. 11 or 12 or in other ways, has been chosen, for reasons of compactness, convenient geometry, and broad frequency response.[29]

Beyond these and other applications for hybrid circuits in microwave systems, there are numerous uses in laboratory measurements.[30–33] These will arise whenever it is necessary to establish directional balance or to make special use of the phase properties[34] which characterize these hybrid circuits.

APPENDIX I

The Application of Reciprocity Theorems to Hybrid Networks

The law of reciprocity for electrical networks may be stated in a variety of ways.[35] A familiar form is: the positions of an impedanceless generator and an impedanceless ammeter may be interchanged without affecting the ammeter reading.[36] From this will now be derived a theorem concerning attenuation between any two points in a transmission network.

Consider Fig. 15(a), which shows two transmission lines connected to an arbitrary network containing only passive linear circuit elements. The characteristic impedances of these lines are K_1 and K_2, both assumed purely resistive for the sake of simplicity. Line 1 is terminated in a characteristic impedance generator, that is, in a resistance R_1 in series with an impedanceless generator *G* whose electromotive force is represented by $V_0e^{j\omega t}$. Line 2 is terminated in a characteristic-impedance recording load, that is, in a resistance R_2 in series with an impedanceless ammeter A. The network is not assumed to provide an impedance match to either line.

---

[27] The power sent toward the transmitter will be so small as not to affect the transmitter appreciably. If the incident power is reflected from the transmitter, it will appear at the line and at the dummy load and will not affect the signal level at the receiver, so long as the dummy is a passive load.

[28] The round-trip loss is minimized at 6 decibels when equal power division both ways is chosen. See Appendix I.

[29] C. F. Edwards, "Microwave converters," presented orally, 1946 I.R.E. Winter Technical Meeting, New York, N. Y., and published in Proc. I.R.E., this issue, pp. 1381–1392.

[30] F. J. Gaffney, "Microwave measurements and test equipment," Proc. I.R.E., vol. 34, pp. 775–794; October, 1946.

[31] A. L. Samuel, "An oscillographic method of presenting impedances on the reflection coefficient plane," Proc. I.R.E., this issue, pp. 1279–1284.

[32] A. F. Pomeroy, "Precision measurements of impedance mismatches in wave guides," *Bell Sys. Tech. Jour.*, vol. 26, July, 1947.

[33] E. W. Houghton, "Electrical Engineers' Handbook," H. Pender and K. McIlwain, 1947 edition; John Wiley and Sons, Inc., New York; N. Y. Section on Microwave Measurements.

[34] See Appendix I for phase properties exhibited by the use of two generators.

[35] See pp. 103, 104, 201, 202, and 476–479 of footnote reference 1.

[36] See page 476 of footnote reference 1.

The power delivered from the generator to the termination of line 2 is $R_2|I_{21}|^2$. The maximum power which can be obtained from the generator with its associated series resistance corresponds to the termination of line 1 in a resistance R_1 and is equal to $V_0^2/4R_1$, with an equal amount of power dissipated in R_1 associated with the generator. The ratio between these expressions,

$$\frac{4R_1R_2|I_{21}|^2}{V_0^2},$$

is the loss between the terminations of the lines. It will be noted that this takes account of reflections at the entrance to the network as well as dissipation within the network. No other expression for the loss would be meaningful from the transmission-line point of view.

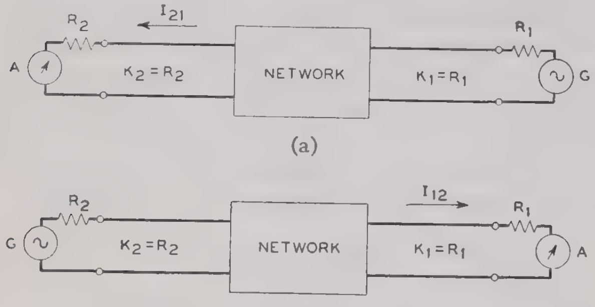

(a)

(b)

Fig. 15—Schematic representation of circuits for application of reciprocity.

In Fig. 15(b), the positions of the generator and ammeter have been interchanged. By similar reasoning, the loss between the terminations of lines 1 and 2 is

$$\frac{4R_1R_2|I_{12}|^2}{V_0^2}.$$

By the theorem of reciprocity[36] quoted above, however, $|I_{12}|^2=|I_{21}|^2$, and the losses in either direction are equal. Thus, the same fraction of the available generator power is transmitted from either point to the other. This, an alternative statement of reciprocity, is the form needed for present purposes. It will be seen later that the interpretation in terms of fractional power is not valid when more than one generator is simultaneously involved.

Certain important deductions can now be made about the balance, power division, and impedance match associated with hybrid circuits. When characteristic impedance loads are externally attached to any three arms, the hybrid network combines them to present a certain impedance to the fourth arm or pair of terminals. Two cases need to be distinguished, depending upon whether this impedance is or is not equal to the characteristic impedance of the transmission line comprising the fourth arm. The former, or matched case, will be considered first.

In Fig. 1, therefore, let appropriate loads be attached to B, C, and D, with a characteristic-impedance generator connected to A. Since it is assumed that the generator works into a matched load, all of its available power is delivered into the network. It is further assumed that this power is equally divided between B and D, with none appearing at C. Thus, exactly half of the power flows from A to B. Let now the generator be replaced by a corresponding load at A and the load at C be replaced by an appropriate generator. By reciprocity, no power can flow from C to A. It is further assumed that the generator works into a matched load at C and that the power is equally divided between B and D. Exactly half of the available power flows from C to B. If the conditions are now changed so that a generator is connected to B, with loads at A, C, and D, the application of reciprocity shows that half of the power flows to the load at A and half to the load at C. There is, therefore, no residual power to appear at D or to be reflected back to the generator. B and D are thus balanced with respect to each other, power sent from either of them is equally divided between A and C, and the network provides a match to both B and D.

It is seen, then, that balance, equal power division, and impedance match for one pair of opposite arms constitute conditions sufficient to insure balance, equal power division, and impedance match for the other arms.

Consider now the mismatched case, in which the network with its associated loads fails to provide an impedance match to some one arm, A, for instance. Standing waves will be set up in the line between the network and the generator terminating this arm. Assuming, as before, equal power division and balance, somewhat less than half of the available power will be delivered to loads at B and D, with the remainder accounted for in reflection back toward the generator. By reciprocity, the same fraction of power, somewhat less than half, will be transmitted from B to A. If equal power division from B is postulated, C also receives somewhat less than half of the power from B. The remainder of the power available at B must appear, therefore, either as reflection back upon the generator, as power developed at D, or in both ways. If equal power division from B is abandoned, on the other hand, it should be generally possible to secure balance between B and D and an impedance match of the network and its associated loads to the arm B. In any case, however, at least one of the three quantities, balance, power division, and impedance match, has been compromised at B by the mismatch at A as a necessary consequence of reciprocity.

The generality of this last conclusion must be tempered to some extent by consideration of the specific network involved. If the network is symmetrically disposed with respect to one pair of opposite arms,[37] the balance between these arms will be independent of impedance matching provided that the other arms are terminated in equal loads, symmetrically disposed, of any character whatsoever. Similarly, if symmetry does not prevail with respect to a pair of opposite arms,[38] all electrical characteristics viewed at these arms will vary concurrently.

---

[37] E.g., the S and P arms of a hybrid junction.

The stress which has been placed upon equal power division deserves explanation. Consider a duplexing system in which a passive hybrid network is employed as the central element.[39] Let this network be so proportioned that a fraction r of the transmitter power is delivered to the antenna or transmission line, the remainder being dissipated in a dummy load. Reciprocity then limits the fraction of the power which is delivered to the receiver from the antenna or line to $1-r$ at the most. The round-trip efficiency is thus $r(1-r)$. This is a maximum for $r=\frac{1}{2}$, and the over-all loss is therefore kept to a minimum of 6 decibels with the network designed for equal power division. In other applications as well, such as balanced converters, the most successful operation is usually obtained with equal power division.

So far, only operation with a single generator has been treated. Another important set of properties of the hybrid network is suggested by the consideration of Fig. 16, which shows two generators of identical frequencies connected to the opposite arms *1* and *3*. It is assumed that balance, equal power division, and impedance match have been secured in all directions. If the peak voltages of G_1 and G_3 are taken as V_0 and

$$V_0\sqrt{\frac{R_3}{R_1}},$$

respectively, they will deliver equal amounts of power to the network, and so $|I_{41}|=|I_{43}|$ and $|I_{21}|=|I_{23}|$. Since the generators are located in balanced arms, they operate independently. The currents in R_2 and R_4 may therefore be combined linearly with due regard for relative phase. Let now G_1 and G_3 be so phased with respect to each other that the currents I_{21} and I_{23} are exactly in phase. The current through R_2 is thereby doubled, and the power developed here is four times the power delivered to R_2 from either generator in the absence of the other. This accounts for all of the available power from both G_1 and G_3. The currents I_{41} and I_{43} must therefore be 180 degrees out of phase, so as to cancel completely so that no power is developed in R_4. It is not difficult to see that the phasing of G_1 and G_3 which brings that about is the same as the phasing of voltages appearing across loads at *1* and *3* when the network is driven from arm *2*.[40] If the phasing between G_1 and G_3 is altered by 180 degrees, all of the total available power will appear in R_4, and R_2 receives none, but this in turn implies the same phasing as that between loads at *1* and *3* driven from arm *4*. With any intermediate phasing of the generators G_1 and G_3, the power will be appropriately divided between R_2 and R_4.

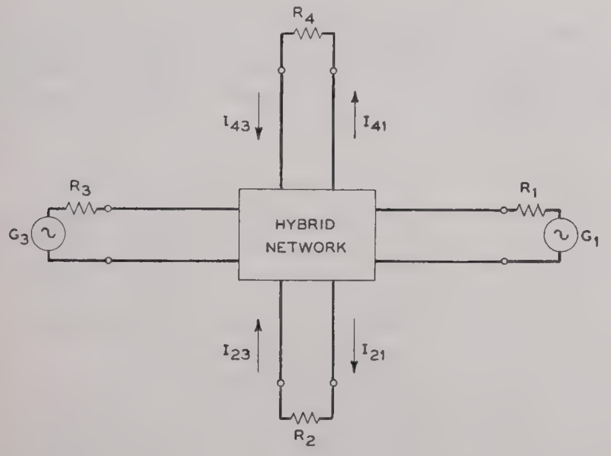

Fig. 16—Hybrid network with opposed generators.

This brings out clearly the close relationship between balance and phasing in the hybrid network. It is also evident that the interpretation of reciprocity in terms of fractional power transmitted is seriously altered when more than one generator is present.

Many other interesting properties and relationships peculiar to the hybrid network can be derived from reciprocity and conservation of energy. The examples given, however, are sufficient to illustrate the general nature of these relationships as well as to illuminate certain statements made in the text.

APPENDIX II

THE PHASE PROPERTIES OF WAVE-GUIDE JUNCTIONS

The principal concern here is to derive phase relationships for the tee junctions illustrated in Fig. 2. This will be done by the qualitative application of Huygens' principle.

A cross-sectional view of an electric-plane wave-guide junction is shown in Fig. 17, with lines of electric intensity drawn in successive positions of the same wave front to indicate what happens when dominant waves

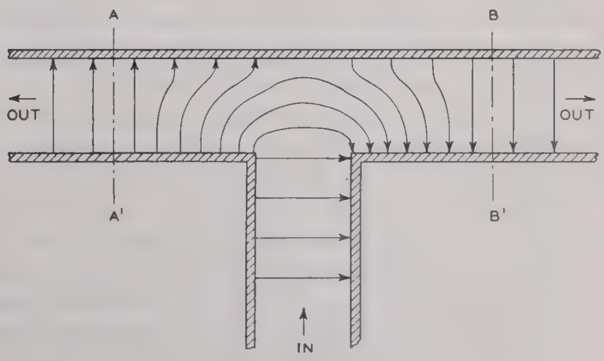

Fig. 17—Spreading of a wave front into an electric-plane junction from the side arm.

---

[38] E.g., the arms *1* and *2* of a hybrid junction.

[39] As described in Section V.

[40] A formal proof of this would involve a restatement of reciprocity so as to show that the electrical length between any two points in a network is the same in either direction.

are sent toward the junction from the side arm. Although at the junction there will usually be some reflection, not indicated, it is clear that the transmitted power tends to be divided equally between the collinear arms and, if the planes AA' and BB' are equidistant from the center of the junction, the waves at AA' are 180 degrees out of phase with the waves at BB'. Fig. 18 shows the same junction, with solid lines to represent electric intensity in successive positions of the same wave front for waves arriving from the left, and with broken lines for waves from the right, in the main guide. If the waves are in phase at AA' and BB', the side arm receives two waves which are 180 degrees out of phase. If the amplitudes of the incoming wave trains are equal, the waves in the side arm cancel completely, and this branch receives no power. Such sets of waves of equal amplitude traveling in opposite directions create pure standing waves in the main guide, with a voltage maximum at the junction. Conversely, the side arm of an electric-plane tee junction receives maximum power when a pure standing wave exists in the main guide with a voltage minimum (current maximum) at the junction. This is precisely the behavior exhibited by a load which has a series connection to a transmission line. From the point of view of phase relationships, therefore, the side arm of the electric-plane tee may be regarded as connected in series with the main guide.

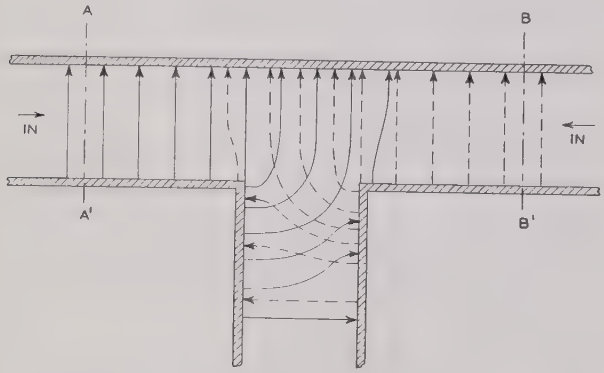

Fig. 18—Spreading of wave fronts into an electric-plane junction from both ends of the main guide.

A cross-sectional view of a magnetic-plane wave-guide tee junction is shown in Fig. 19. Here the electric intensity is perpendicular to the plane of the figure. The situation shown is the case where a wave front approaches the junction from the side arm. Since the geometry does not act here to reverse the polarity of the lines of force, the waves at AA' are in phase with those at BB'. Similarly, if waves of equal amplitude are sent toward the junction from the left and right so as to be in phase at the junction, the side arm receives two sets of waves in phase and therefore maximum power. From the point of view of phase relationships, then, the side arm of the magnetic-plane tee is connected in parallel across the main guide.

A sectional view of a wave-guide-to-coaxial tee junction is given in Fig. 20, with lines of electric intensity shown for successive positions of a wave front which emerges from the coaxial and spreads both directions in the guide. It is seen that the waves crossing AA' are in phase with those crossing BB'. The coaxial line therefore receives maximum power when located at a voltage maximum, and the connection is identified as a parallel connection across the guide.

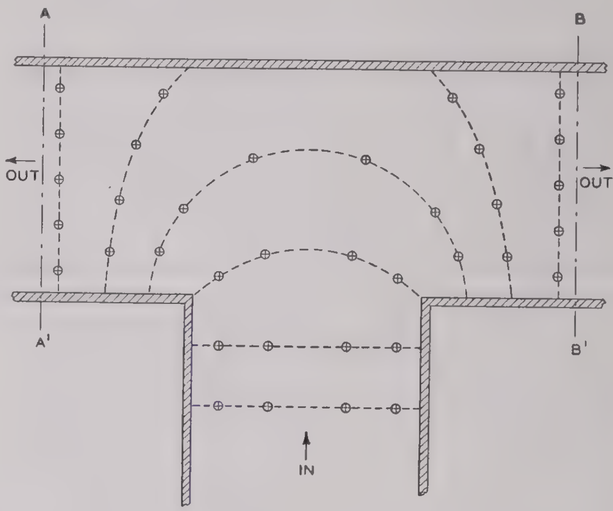

Fig. 19—Spreading of a wave front into a magnetic-plane junction from the side arm.

Only one particular method of coupling the coaxial to the guide has been shown. Many other methods of establishing an abrupt connection are similar in that some portion of the inner conductor of the coaxial is aligned parallel to the electric intensity of the dominant wave in the guide. Any such abrupt connection may therefore be characterized as a shunt connection. By similar reasoning, it is evident that the direct connection of a point-contact rectifier or thermistor to a wave guide, involving a conductor parallel to the electric intensity, is a parallel connection.

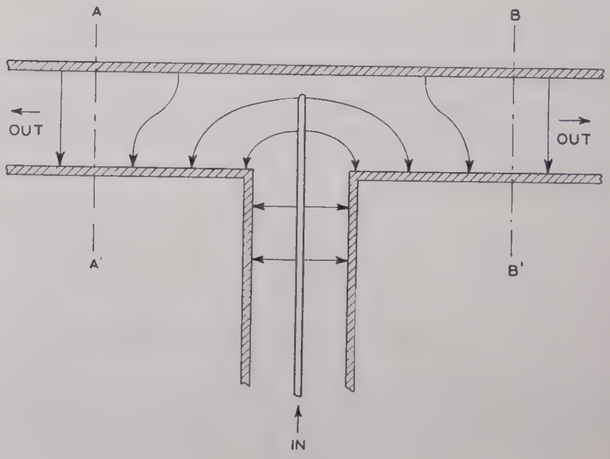

Fig. 20—Spreading of a wave front into a wave guide from a coaxial side arm.

A Mathematical Theory of Directional Couplers*

HENRY J. RIBLET†, ASSOCIATE, I.R.E.

Summary—**Directional couplers are becoming an increasingly important component in microwave radio-frequency circuits. By the suitable generalization of concepts used in discussing the lumped loading of a single transmission line, it is possible to discuss the interaction of the coupling elements of these more complicated circuits in a reasonably complete and elementary manner. Input impedances are analyzed in terms of equivalent tee and pi sections. The transformation of line impedances is shown to commute with similarity transformations, so that the circuit problem is equivalent to one involving independent but properly loaded transmission lines. The behavior of many aperture-coupled directional couplers may be analyzed by the use of a single conventional impedance diagram. A small-hole theory is given which predicts previously unexplained results.**

I. INTRODUCTION

A DIRECTIONAL coupler or wave selector is a passive, linear, four-terminal-pair network such as is shown in Fig. 1, having the property that power fed in at terminal *1* divides in some ratio between terminals *3* and *4* without appearing at terminal *2*, while power fed in at terminal *3* divides between terminals *1* and *2* without appearing at terminal *4*. In the event that power in at *1* divides equally between *3* and *4*, the network is known as a bridge circuit. A familiar type of wave-guide directional coupler is shown in Fig. 2.

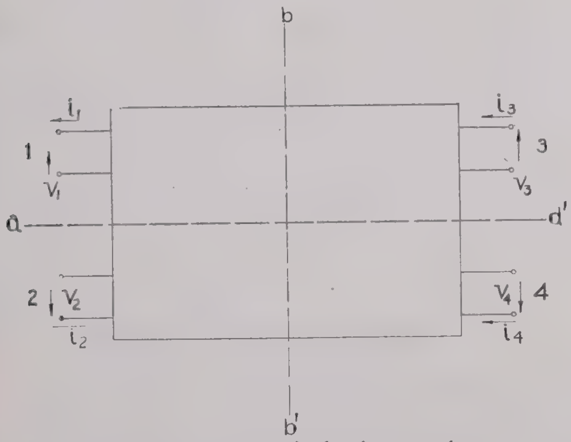

Fig. 1—Four-terminal-pair network.

An indication of the important role played by directional couplers in the microwave field has been given by Mumford.[1] For a description of various directional couplers, together with design and performance data, reference is made to a report by Harrison.[2]

The performance of a directional coupler fed at *1* is usually specified in terms of the directivity, coupling, and input standing-wave ratio. Suppose that terminals *2*, *3*, and *4* are perfectly matched and that power in the amount P_i is incident on 1, then if P_1, P_2, P_3, and P_4 are the powers leaving the directional coupler through terminals *1*, *2*, *3*, and *4*, respectively, we define the directivity to be P_4/P_2 and the coupling to be P_3/P_4. Of course, the input standing-wave ratio may be determined in the usual way from P_i and P_1. The directivity so defined has little practical interest unless the directional coupler is symmetrical end for end. In this case it measures the ability of terminal *2* to discriminate between power incident at *1* and power incident at *3*.

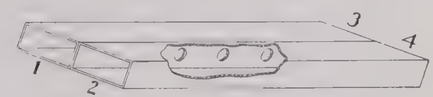

Fig. 2—Wave-guide directional coupler.

Consideration of Fig. 2 shows that our problem is that of a pair of uniform transmission lines coupled together at discrete points. A number of references in the literature treat the matter of multiple-terminal transmission lines. Some of these writers (for example, Pipes)[3] restrict themselves to uniform lines which are coupled by the interaction of their electromagnetic fields, while others (for example, Koizumi)[4] consider the problem of replacing an arbitrary network by a system of isolated uniform lines. Rice[5] has written an extensive monograph analyzing these questions. Lippman[6] has discussed the cascading of branched-guide directional couplers using the directional coupler as the basic unit. For this purpose he has introduced the matrix analogues of the propagation constant and image impedances of a two-terminal-pair network.

The theoretical work referred to above has in common the development of a formalism which is identical with that of the familiar quadripole. This paper will extend this similarity, primarily by treating the coupling elements as lumped loads on a uniform transmission line. It is clear that this underlying point of view may have other applications. For the sake of conciseness, however, the discussion is limited to directional couplers.

---

* Decimal classification: R142. Original manuscript received by the Institute, August 23, 1946; revised manuscript received, November 6, 1946.

† Submarine Signal Co., Boston, Mass.

[1] W. W. Mumford, "Directional couplers," PROC. I.R.E., vol. 35, pp. 160–166; February, 1947.

[2] R. J. Harrison, "Design considerations for directional couplers," M.I.T. Rad. Lab. Rep. 724; December, 1945.

[3] L. A. Pipes, "Matrix theory of multiconductor transmission lines," *Phil. Mag.*, vol. 24, pp. 97–100; 1937.

[4] Shiro Koizumi, "Mehrpolleitungstheorie," *Arch. für Electrotech.*, vol. 33, pp. 171–188, 609–622; 1939.

[5] S. O. Rice, "Steady state solutions of transmission line equations," *Bell Sys. Tech. Jour.*, vol. 20, pp. 131–179; April, 1941.

[6] B. A. Lippman, "Theory of directional couplers," M.I.T. Rad. Lab. Rep. 860, December, 1945.

II. Coupled Lines

Consider the schematic drawing of Fig. 3, which is equivalent to the directional coupler of Fig. 2. It is specifically assumed that the sections of transmission line (*a*) are uniform and isolated from each other so that the only coupling which exists is localized at definite points on the transmission lines. The devices (*c*) which provide this coupling will be referred to as coupling elements, and they may consist of holes in a common wall, complete transmission lines, or loops. It simplifies the discussion to assume that the two transmission lines are identical and that the spacing between the coupling elements in electrical degrees is the same on both transmission lines. Cases where this is not obviously true should be examined individually to see if the methods of this paper are applicable or not.

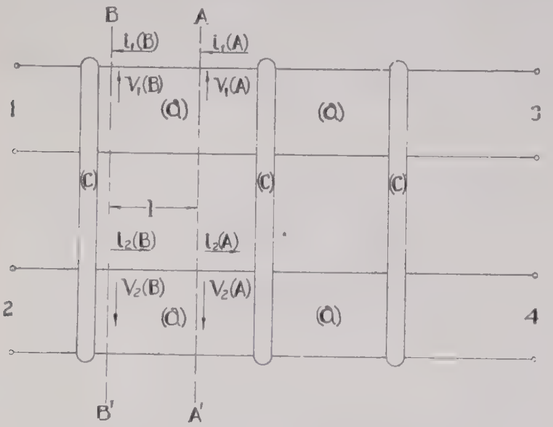

Fig. 3—Lump-coupled transmission lines.

Our immediate program will be as follows:

(a) Definition of the Impedance of the network looking to the right at any point.

(b) Determination of the formula by which this Impedance transforms down the transmission-line portions of the network.

(c) Definition of the parallel Admittance and series Impedance associated with each coupling element.

(d) Determination of rules by which a parallel Admittance or series Impedance combines with the Admittance or Impedance to the right of the terminals of the coupling element.

As we shall see, these generalized Impedances and Admittances are second-order matrices. They may be defined so that the similarity with single-transmission-line procedure is very close.

(a) If a network such as the one shown in Fig. 3 is terminated in any impedances and broken into along the line $A-A'$, we will have

$$\begin{aligned} v_1(A) &= z_{11}i_1(A) + z_{12}i_2(A) \\ v_2(A) &= z_{12}i_1(A) + z_{22}i_2(A). \end{aligned} \tag{1}$$

The matrix

$$Z_A = \begin{pmatrix} z_{11} & z_{12} \\ z_{12} & z_{22} \end{pmatrix} \tag{2}$$

will be defined as the *Impedance to the right* of the generalized transmission line. A similar definition holds for the *Admittance to the right.*

(b) We should now like to determine in Fig. 3 the Impedance to the right at $B-B'$ in terms of the Impedance to the right at $A-A'$. On both lines of Fig. 3 we will have relationships of the form

$$\begin{aligned} v_k(B) &= v_k(A)\cosh\gamma l + z_0 i_k(A)\sinh\gamma l \\ i_k(B) &= \frac{1}{z_0} v_k(A)\sinh\gamma l + i_k(A)\cosh\gamma l \end{aligned} \tag{3}$$

where γ and z_0 are the propagation constant and characteristic impedance, respectively, common to the two lines. We may express this in matrix form:

$$\begin{aligned} V(B) &= \cosh\gamma l I V(A) + \sinh\gamma l Z_0 I(A) \\ I(B) &= \sinh\gamma l Z_0^{-1} V(A) + \cosh\gamma l I I(A), \end{aligned} \tag{4}$$

if we put

$$V(B) = \begin{pmatrix} v_1(B) \\ v_2(B) \end{pmatrix}; \qquad I(B) = \begin{pmatrix} i_1(B) \\ i_2(B) \end{pmatrix}; \quad \text{etc.};$$

$$I = \begin{pmatrix} 1 & 0 \\ 0 & 1 \end{pmatrix}; \qquad Z_0 = \begin{pmatrix} z_0 & 0 \\ 0 & z_0 \end{pmatrix}.$$

By definition, $V(A) = Z_A I(A)$, and we have, on substitution in (4),

$$\begin{aligned} V(B) &= \{Z_A\cosh\gamma l + Z_0\sinh\pi l\} I(A) \\ I(B) &= Z_0^{-1}\{Z_A\sinh\gamma l + Z_0\cosh\gamma l\} I(A). \end{aligned} \tag{5}$$

Then, upon elimination of $I(A)$ from (5), with due regard for the fact that matrices do not commute, we obtain

$$\begin{aligned} V(B) = {} & \{Z_A\cosh\gamma l + Z_0\sinh\gamma l\} \times Z_0 \\ & \times \{Z_A\sinh\gamma l + Z_0\cosh\gamma l\}^{-1} I(B). \end{aligned}$$

Thus the Impedance to the right at $B-B'$, Z_B, can be written as

$$Z_B = Z_0 \frac{Z_A\cosh\gamma l + Z_0\sinh\gamma l}{Z_A\sinh\gamma l + Z_0\cosh\gamma l}. \tag{6}$$

This is a special case of a known formula for multiwire transmission lines.[7] The similarity with familiar single-wire formulas is clear.

(c) Consider a coupling element having the specialized appearance shown in Fig. 4. The relationship between v_a, v_b, i_a, and i_b is given by equations of the form:

$$\begin{aligned} v_a &= z_{aa}i_a + z_{ab}i_b \\ v_b &= z_{ab}i_a + z_{bb}i_b. \end{aligned}$$

The matrix

$$Z_s = \begin{pmatrix} z_{aa} & z_{ab} \\ z_{ab} & z_{bb} \end{pmatrix}$$

---

[7] See page 137 of footnote reference 5.

will be called the *series Impedance* of the coupling element. The reason for the use of the term "series" is clear, since, for the coupling element as shown, the discontinuity seen from any terminal will appear to be an impedance in series with the line. Similarly, a network shunted across both lines will give rise to an admittance matrix,

$$Y_p = \begin{pmatrix} y_{aa} & y_{ab} \\ y_{ab} & y_{bb} \end{pmatrix},$$

which we will call the *parallel Admittance* of the coupling element. Coupling elements of either of these types will be called *simple* coupling elements.

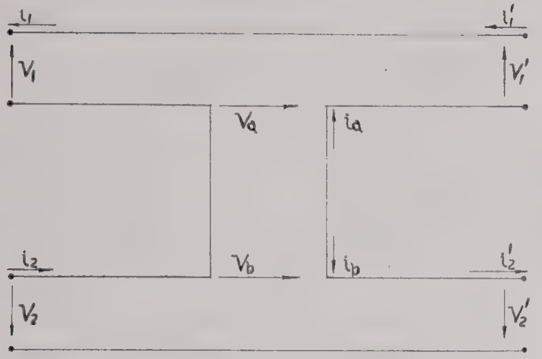

Fig. 4—Simple series coupling element.

(d) From a consideration of Fig. 4, we have the following:

$$\begin{aligned} v_1 &= v_a + v_1' \\ v_2 &= v_b + v_2' \qquad (7) \\ i_1 = i_1 = i_a&; \qquad i_2 = i_2' = i_b. \end{aligned}$$

Thus

$$\begin{aligned} v_1 &= z_{aa}i_1 + z_{ab}i_2 + z_{11}i_1 + z_{12}i_2 \\ v_2 &= z_{ab}i_1 + z_{bb}i_2 + z_{12}i_1 + z_{22}i_2, \end{aligned} \qquad (8)$$

and so $Z_B = Z_S + Z_A$ where Z_B is the Impedance to the right on the left of the coupling element, Z_S is the series Impedance of the coupling element, Z_S is the series Impedance of the network to the right on the right of the coupling element. For parallel coupling elements we must add, to the Admittance to the right, the parallel Admittance of the coupling element.

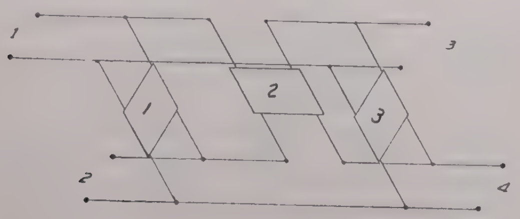

Fig. 5—Generalized pi section.

This completes the analogy between the problem of lump-coupled transmission lines and the lump-loaded uniform line. On the uniform portions of the lines we transform Impedances according to (6), and when we encounter simple coupling elements we add series Impedances and parallel Admittances in a manner completely analogous to the usual treatment of pi and tee sections. Actually, it is not difficult to show that any coupling element having symmetry about $a-a'$ or $b-b'$ of Fig. 1 can be represented as a pi or tee section of simple coupling elements as indicated in Fig. 5.

III. SIMILARITY TRANSFORMATION

If we denote $Z_i = (Z_L \cosh \gamma l + Z_0 \sinh \gamma l)Z_0(Z_L \sinh \gamma l + Z_0 \cosh \gamma l)^{-1}$, we may consider the effect of a similarity transformation[8] on Z_i. Such a transformation may be written AZ_iA^{-1} where A is a nonsingular matrix. We have

$$\begin{aligned} AZ_iA^{-1} &= A(Z_L \cosh \gamma l + Z_0 \sinh \gamma l)Z_0 \\ &\quad \times (Z_L \sinh \gamma l + Z_0 \cosh \gamma l)^{-1}A^{-1} \\ &= A(Z_L \cosh \gamma l + Z_0 \sinh \gamma l)A^{-1}Z_0 \\ &\quad \times A(Z_L \sinh \gamma l + Z_0 \cosh \gamma l)^{-1}A^{-1} \\ &= (AZ_LA^{-1} \cosh \gamma l + Z_0 \sinh \gamma l)Z_0 \\ &\quad \times (AZ_LA^{-1} \sinh \gamma l + Z_0 \cosh \gamma l)^{-1} \qquad (9) \end{aligned}$$

since the unit matrix commutes with all matrices and the inverse of the product of two matrices is the product of the inverses in the reverse order. Now this equation has the consequence that an Impedance may be reduced to diagonal form and then transformed down the line. This materially simplifies the calculations, since these line transformations may be handled independently just as if there were no coupling between the lines.

If all of the Impedances and Admittances of the simple coupling elements comprising the directional coupler are reduced to diagonal form by the same similarity transformation, then our problem is equivalent to that of solving, independently, separate lump-loaded uniform transmission lines. Of considerable practical interest is the case where the coupling elements are symmetrical about line $a-a'$ of Fig. 1. Then the Impedances and Admittances encountered all have the form

$$\begin{pmatrix} \alpha & \beta \\ \beta & \alpha \end{pmatrix}.$$

This is reduced to the diagonal form

$$\begin{pmatrix} \alpha + \beta & 0 \\ 0 & \alpha - \beta \end{pmatrix}$$

by the transformation

$$\begin{pmatrix} 1 & 1 \\ -1 & 1 \end{pmatrix}.$$

This can be seen readily by consideration, for example, of the equations defining the Admittance of a simple parallel coupling element, which are

---

[8] C. C. MacDuffee, "Vectors and Matrices," Opencourt Publishing Co., Menasha, Wis., 1943; pp. 112–148.

$$i_1 = y_a v_1 + y_b v_2$$
$$i_2 = y_b v_1 + y_a v_2.$$

Upon addition and subtraction, we obtain

$$i_1 + i_2 = (y_a + y_b)(v_1 + v_2)$$
$$-i_1 + i_2 = (y_a - y_b)(-v_1 + v_2),$$

so that the equations

$$\begin{aligned} i^+ &= i_1 + i_2; \qquad & v^+ &= v_1 + v_2 \\ i^- &= -i_1 + i_2; \qquad & v^- &= -v_1 + v_2 \end{aligned} \tag{10}$$

relate the voltages and currents on the "diagonal form" transmission lines, called for convenience the "plus" and "minus" lines to those actually observed in the directional coupler. The inverse equations are

$$\begin{aligned} v_1 &= \frac{v^+ - v^-}{2}; \qquad & v_2 &= \frac{v^+ + v^-}{2} \\ i_1 &= \frac{i^+ - i^-}{2}; \qquad & i_2 &= \frac{i^+ + i^-}{2}. \end{aligned} \tag{11}$$

Thus the assumed symmetry of the coupling elements leads to an input Admittance for the coupled lines of the form

$$1/2\begin{pmatrix} y_i^+ + y_i^- & y_i^+ - y_i^- \\ y_i^+ - y_i^- & y_i^+ + y_i^- \end{pmatrix}. \tag{12}$$

Here y_i^+ is the input admittance of a transmission line, called the "plus" line, having the same parameters as each of the coupled lines, with loads $\alpha_k + \beta_k$ spaced on it just as on the coupled lines; and y_i^- is obtained, as above, except that the $\alpha_k + \beta_k$ are replaced by $\alpha_k - \beta_k$,

IV. ILLUSTRATIVE EXAMPLE

In the interest of brevity, this section is limited to the very simple but important practical case where the coupling elements have Admittances and Impedances of the form

$$\begin{pmatrix} \alpha & \alpha \\ \alpha & \alpha \end{pmatrix}.$$

It can be shown without difficulty that any simple coupling element with an Admittance of this form scatters equally into the two transmission lines of Fig. 3, and vice versa. Apertures which are either simple series or simple parallel couplings, cut in the infinitesimally thin wall separating wave guides which have one wall in common as in Fig. 2, will have this property. It will also hold if the holes are of sufficient size so that the attenuation and phase shift passing through them is negligible. Slots longer than resonant in thin walls illustrate this type of coupling.

Let us consider the case where the directional coupler has an even number, n, of simple parallel coupling elements of Admittance

$$\begin{pmatrix} y_a & y_a \\ y_a & y_a \end{pmatrix}$$

equally spaced on two transmission lines with propagation constant γ and characteristic impedance unity. The voltages and currents of the directional coupler are determined from those of the "plus" and "minus" lines by (11). The plus line has n equal shunt loads, $2y_a$, spaced l units apart, while the minus line is unloaded. The lump-loaded line may be readily solved by replacing a typical section of the network, broken, say, midway between the loads by a uniform line having the correct characteristic admittance y^+ and propagation constant γ^+. These are determined from the formulas

$$\begin{aligned} \cosh \gamma^+ l &= \cosh \gamma l + y_a \sinh \gamma l \\ \frac{\sinh \gamma^+ l}{y^+} &= \sinh \gamma l + 2y_a \sinh^2 \frac{\gamma l}{2} \end{aligned} \tag{13}$$

which may be derived exactly like Campbell's formula for the loaded line.[9]

In terms of these quantities, the relationships between the input and output voltages and currents are

$$\begin{aligned} v_i^+ &= v_0^+ \cosh n\gamma^+ l + \frac{1}{y^+} i_0^+ \sinh n\gamma^+ l \\ i_i^+ &= y^+ v_0^+ \sinh n\gamma^+ l + i_0^+ \cosh n\gamma^+ l. \end{aligned} \tag{14}$$

Similar equations relate the "minus" voltages and "minus" currents, except that $y^- = 1$ and $\gamma^- = \gamma$. If the output terminals are assumed to be matched, we will have $i_0^+ = v_0^+$ and $i_0^- = v_0^-$, so that

$$\begin{aligned} v_i^+ &= v_0^+(\cosh n\gamma^+ l + \frac{1}{y^+} \sinh n\gamma^+ l) \\ i_i^+ &= v_0^+(y^+ \sinh n\gamma^+ l + \cosh n\gamma^+ l). \end{aligned} \tag{15}$$

Let us put

$$\begin{aligned} T^+ &= \cosh n\gamma^+ l + \frac{1}{y^+} \sinh n\gamma^+ l \\ S^+ &= y^+ \sinh n\gamma^+ l + \cosh n\gamma^+ l, \end{aligned} \tag{16}$$

with analogous expressions for T^- and S^-.

Then we may write the input admittances to the "plus" and "minus" lines:

$$y_i^+ = \frac{S^+}{T^+}; \qquad y_i^- = 1 = \frac{S^-}{T^-}. \tag{17}$$

In terms of these quantities, the input Admittance to the directional coupler is

$$1/2\begin{pmatrix} y_i^+ + y_i^- & y_i^+ - y_i^- \\ y_i^+ - y_i^- & y_i^+ + y_i^- \end{pmatrix}.$$

If we write $y_{11} = (y_i^+ + y_i^-)/2$ and $y_{12} = (y_i^+ - y_i^-)/2$, we have as a consequence of definition

$$i_1 = y_{11} v_1 + y_{12} v_2$$
$$i_2 = y_{12} v_i = y_{11} v_2.$$

---

[9] W. L. Everitt, "Communication Engineering," McGraw-Hill Book Co., New York, N. Y., 1937; pp. 173–174.

If power is fed into the directional coupler of Fig. 1 through terminal *2*, and terminal *1* is well matched, it can easily be shown that

$$v_1 = \frac{-y_{12}v_2}{1+y_{11}}; \qquad i_2 = \frac{y_{11}^2 - y_{12}^2 + y_{11}}{1+y_{11}} v_2;$$
$$i_1 = \frac{y_{12}}{1+y_{11}} v_2. \tag{18}$$

To determine the voltages at the far end of the wave selector, we first determine v_i^+ and v_i^-, according to our previous rules. From (10) we have

$$v_1^+ = \frac{1+y_{11}-y_{12}}{1+y_{11}} v_2; \quad v_i^- = \frac{1+y_{11}+y_{12}}{1+y_{11}} v_2. \tag{19}$$

From (15),

$$v_0^+ = v_i^+ \frac{1}{T^+}; \qquad v_0^- = v_i^- \frac{1}{T^-}. \tag{20}$$

Now, finally, we determine the output voltages, from (11), to be

$$\begin{aligned} v_3 &= 1/2\left\{\frac{1+y_{11}-y_{12}}{(1+y_{11})T^+} - \frac{1+y_{11}+y_{12}}{(1+y_{11})T^-}\right\} v_2 \\ v_4 &= 1/2\left\{\frac{1+y_{11}-y_{12}}{(1+y_{11})T^+} + \frac{1+y_{11}+y_{12}}{(1+y_{11})T^-}\right\} v_2. \end{aligned} \tag{21}$$

The input admittance is given by

$$\frac{y_{11}^2 - y_{12}^2 + y_{11}}{y_{11}+1}.$$

The condition for perfect directivity is that y_i^+ shall equal 1, and we see that this is the condition for perfect match. Thus, for the class of directional couplers under discussion, we have the interesting property that high directivity is equivalent to low standing-wave ratio. The condition that $y_i^+ = 1$ is, by (17),

$$\frac{y^+ \sinh n\gamma^+ l + \cosh n\gamma^+ l}{\cosh n\gamma^+ l + 1/y^+ \sinh n\gamma^+ l} = 1.$$

For n even, this will happen when $\gamma^+ l = j\pi/2$. The actual spacing on the line is given by the expression,

$$\cosh \gamma l + y_a \sinh \gamma l = 0. \tag{22}$$

Assuming perfect directivity for this type of directional coupler is equivalent to putting $y_{12} = 0$. Hence,

$$v_3 = 1/2\left\{\frac{1}{T^+} - \frac{1}{T^-}\right\} v_2$$
$$v_4 = 1/2\left\{\frac{1}{T^+} + \frac{1}{T^-}\right\} v_2.$$

Thus

$$\frac{v_3}{v_4} = \frac{T^- - T^+}{T^- + T^+} = \frac{\sinh n\gamma l + \cosh n\gamma l - (-1)^{n/2}}{\sinh n\gamma l + \cosh n\gamma l + (-1)^{n/2}}$$
$$= \frac{\cosh \frac{n}{2}\gamma l}{\sinh \frac{n}{2}\gamma l} \quad (n = 4k+2)$$
$$= \frac{\sinh \frac{n}{2}\gamma l}{\cosh \frac{n}{2}\gamma l} \quad (n = 4k). \tag{23}$$

Since l is in the neighborhood of $\lambda_g/4$ for small couplings, the ratio v_3/v_4 increases linearly for small n but deviates from linearity as the directional coupler approaches a bridge. It is clear that the voltages in the two wave guides have a 90-degree phase difference, and that the power can be made to alternate from one guide to the other by the use of a sufficient number of coupling elements.

In the case when $n = 2$, it may be shown that

$$|v_3| = |\cosh \gamma l| = \frac{|y_a|}{\sqrt{1+|y_a|^2}}, \tag{24}$$

whereas the voltage induced in the auxiliary guide by a single coupling element may be obtained from (22) by putting $y_{11} = 1 + y_a$ and $y_{12} = y_a$. Thus

$$v_3' = \frac{-y_a}{2+y_a},$$

so that

$$|v_3'| = \frac{|y_a|}{\sqrt{4+|y_a|^2}}. \tag{25}$$

Hence, for small y_a the voltage is approximately doubled by using two coupling elements. Here we have made use of the fact that y_a is purely imaginary.

For the case when $n = 2$, it may easily be shown that, if terminals *1*, *3*, and *4* are perfectly matched,

$$\begin{aligned} v_1 &= -(2cy_L + sy_L^2) \\ v_2 &= 4c + 4s + 4sy_L + 2cy_L + sy_L^2 \\ v_3 &= -2y_L - \frac{s}{s+c} y_L^2 \\ v_4 &= 4 + 2y_L + \frac{s}{s+c} y_L^2 \end{aligned} \tag{26}$$

where $y_L = 2y_a$, $s = \sinh \gamma l$ and $c = \cosh \gamma l$.

For such a directional coupler, if y_a is independent of frequency, we see that v_3 changes very slowly with frequency, since y_a^2 generally is much smaller than y_a. Hence, for small couplings the change in coupling with frequency is determined primarily by the behavior of y_a.

By careful design it is possible to choose the coupling elements so that y_L changes slowly with frequency. Hence the output voltages are sensibly constant compared with the rate at which the voltage, v_1, changes. Accordingly, once the coupling and directivity at a given frequency have been determined, the principal characteristics of the coupler may be determined by the value of the input Impedance of the network. For the study of this quantity a conventional circle diagram is particularly well suited.

We easily see that the condition when two coupling elements, each with the parallel Admittance

$$\begin{pmatrix} y_a & y_a \\ y_a & y_a \end{pmatrix},$$

have infinite directivity is that they be spaced a distance such that when we add a susceptance of magnitude $2y_a$ to 1 and move along the diagram the prescribed distance, the addition of $2y_a$ will bring us back to 1. For a two-hole coupler of the type shown in Fig. 2, this predicts a spacing between the holes somewhat less than a quarter guide wavelength. This is in good agreement with observed results.[10] The arguments of the previous section show that we also have zero reflection at this point. The rate at which the directivity falls off is clearly indicated by this procedure. The use of binomial distribution of elements has been suggested as a means of increasing the bandwidth of this type of directional coupler. If we use the same spacing but now add $2y_a$ to 1, travel around the diagram as before, then add $4y_a$ and travel around again, the addition of $4y_a$ will bring us back to the center. Thus this arrangement also gives infinite directivity. Consideration of the circle diagram will show, however, that there is a somewhat shorter spacing, or longer wavelength, at which this arrangement of coupling elements again gives infinite directivity. A suggestion of this double-resonance phenomenon is seen in Fig. 7 of the paper by Mumford, referred to previously.[1]

V. SMALL-COUPLING THEORY

The assumption that the coupling between the transmission lines is weak or, what is essentially equivalent, that the elements of the coupling Impedances and Admittances are small, somewhat extends the range of usefulness of the preceding results. We have seen that problems involving directional couplers whose coupling Admittances are of the form

$$\begin{pmatrix} y_a & y_a \\ y_a & y_a \end{pmatrix}$$

can be handled on a single impedance diagram. Now, the same state of affairs is still true for more general symmetric coupling elements of the form

$$\begin{pmatrix} y_a & y_b \\ y_b & y_a \end{pmatrix}$$

if we assume that $y_a^2 - y_b^2$ is small compared with y_a. This assumption is actually weaker than requiring that y_a and y_b be both small, and allows us to extend the analysis in terms of a single circle diagram to the majority of aperture-coupler wave selectors now in use.

In order to show this, consider a pair of elements whose admittances are

$$\begin{pmatrix} y_a & y_b \\ y_b & y_a \end{pmatrix}$$

and which are spaced a distance l apart on transmission lines of propagation constant γ and characteristic impedance unity. The Admittance to the right at a point just to the right of the first element will be, assuming perfectly matched output terminals,

$$\begin{pmatrix} y_{11} & y_{12} \\ y_{12} & y_{11} \end{pmatrix}$$

where

$$y_{11} = 1/2\left\{\frac{c(1 + y_a + y_b) + s}{s(1 + y_a + y_b) + c} + \frac{c(1 + y_a - y_b) + s}{s(1 + y_a - y_b) + c}\right\}$$

$$= \frac{(c + s)^2(1 + y_a) + cs(y_a^2 - y_b^2)}{(s + c)^2 + s(s + c)2y_a + s^2(y_a^2 - y_b^2)}$$

and

$$y_{12} = 1/2\left\{\frac{c(1 + y_a + y_b) + s}{s(1 + y_a + y_b) + c} - \frac{c(1 + y_a - y_b) + s}{s(1 + y_a - y_b) + c}\right\}$$

$$= \frac{(c^2 - s^2)y_b}{(s + c)^2 + s(s + c)2y_a + s^2(y_a^2 - y_b^2)}. \tag{27}$$

Now, from these equations we can easily see that the assumption that $y_a^2 - y_b^2$ is negligible gives the same Admittance on the right of the first coupling element as the assumption that $y_a = y_b$. They also show that $y_{11} = 1 + y_{12}y_a/y_b$, so that an Admittance of the form

$$\begin{pmatrix} 1 + y_a & y_a \cdot y_b/y_a \\ y_a \cdot y_b/y_a & 1 + y_a \end{pmatrix}$$

has the same form after any transformation down the line. Moreover, this form is not changed by the addition of parallel Admittances of the form

$$\begin{pmatrix} y_a' & y_b' \\ y_b' & y_a' \end{pmatrix}$$

so long as $y_b'y_a' = y_b'y_a'$. On the basis of these remarks, we can conclude that the input Admittance of a directional coupler, whose coupling elements can be analyzed as simple coupling elements with Admittances of the form

$$\begin{pmatrix} y_a & y_b \\ y_b & y_a \end{pmatrix}$$

for which $y_a^2 - y_b^2 \ll y_a$ and y_b/y_a is a fixed constant, is determined from that where all the coupling admittances are of the form

$$\begin{pmatrix} y_a & y_a \\ y_a & y_a \end{pmatrix}$$

by multiplying the transfer admittance y_{12} by y_b/y_a. This requires that y_{12} does not gradually become large with the addition of more coupling elements. Actually, we may relax the requirement on the size of y_a and y_b because of cancellation effects between coupling elements approximately one-quarter wavelength apart. Thus the condition for directivity and low standing-wave ratio are the same as in the case $y_a=y_b$, and high directivity implies low standing-wave ratio. The spacing for maximum directivity for two equal coupling elements is given as before by (22). This result differs from what is given by the usual "small-hole theory," which predicts quarter-wavelength spacing for maximum directivity. Of course, we get that result by allowing $y_a \to 0$. However, in this limit the device is a directional coupler only in a trivial sense. From (18) we see that the input voltages and currents differ from what they are in the case where $y_a=y_b$ by a factor of y_b/y_a; and, by consideration of (8), we see that this will be true for all of the voltages and currents of the auxiliary wave guide. Hence the complete solution for the case $y_a \neq y_b$ is obtained from that where $y_a=y_b$ by multiplying the voltages and currents in the auxiliary line by y_b/y_a.

---

[10] See page 19 of footnote reference 2.

If the ratio of y_b to y_a is not the same for all coupling elements, we will have to recalculate it after each coupling element in order to handle the problem on a single circle diagram. For this case, in general the conditions for maximum directivity and minimum input standing-wave ratio do not coincide.

The Equivalent Circuit of a Corner Bend in a Rectangular Wave Guide*

JOHN W. MILES†

Summary—Following the fundamentals set down in an earlier paper, the impedance representation of a right-angle bend in a rectangular wave guide is calculated. Two types of bends are considered, being defined by the polarization of the electric field relative to the plane of the bend. The results are stated in the form of infinite series. Numerical results are given in the form of curves.

NOTATION

a = dimension of wave guide parallel to electric field
b = dimension of wave guide transverse to electric field
a_0 = amplitude of field propagated in positive direction
b_n = amplitude of reflected field due to nth mode
$\bar{i}$ = unit vector along positive x axis
$\bar{j}$ = unit vector along positive y axis
$\bar{k}$ = unit vector along positive z axis
x, y, z = right-handed Cartesian co-ordinates
β_n = amplitude in field expansion
C_{mn} = coefficient of A_n in field matrix
$\bar{E}$ = vector electric field (m.k.s. units)
G = Green's function
$\bar{H}$ = vector magnetic field (m.m.f.) (m.k.s. units)
I_0 = transmission-line current in reference plane
V_0 = transmission-line voltage in reference plane
Y_{ij} = equivalent circuit admittance
Y_n = field admittance
Y_0 = characteristic admittance of transmission line
Z_{ij} = equivalent circuit impedance
$\beta = 2\pi/\lambda$ = phase constant
$\beta_n = [\beta^2-(n\pi)^2]^{1/2}$
$\delta_n^m = 1$ if $m=n$, $=0$ if $m \neq n$ (Kronecker delta)
ϵ = dielectric constant (m.k.s.)
μ = permeability (m.k.s.)
λ = wavelength in medium of ϵ and μ
$\lambda_g = [(1/\lambda)^2-(1/2a)^2]^{-1/2}$ guide wavelength for TE_{10} mode
$\zeta = (\epsilon/\mu)^{1/2}$ characteristic impedance of medium
η = normalized transverse electric field in reference plane
$\bar{\Phi}_n$ = normalized transverse electric field due to nth mode in guide
$\bar{\Psi}_n$ = normalized transverse electric field due to nth mode in corner.

INTRODUCTION

THE ANALOGY between propagation of a single mode in a cylindrical wave guide and the propagation along an ordinary transmission line, wherein the voltage and current on the latter represent, respectively, the transverse electric and magnetic fields in the former, has been considered in an earlier paper.[1] However, the problems solved therein included only the impedance representations of plane discontinuities. The present paper will be concerned with the impedance representation of a right-angle bend in a rectangular wave guide. The assumptions made in the solution and the notation are identical with those advanced in the treatment of plane discontinuities[1]; in particular, it is assumed that only the dominant (TE_{10}) mode is freely propagated, and that all other discontinuities are sufficiently removed from the one under consideration to mitigate the possibility of interaction among the higher-order modes excited by the different discontinuities.

For the bend in a rectangular guide there are two distinct cases to be considered: (1) the bend in the plane of the electric field of the dominant mode (electric field is bent), and (2) the bend transverse to the plane of the

---

* Decimal classification: R118.1. Original manuscript received by the Institute, October 14, 1946; revised manuscript received, January 29, 1947.

† University of California, Los Angeles, Calif.

[1] John W. Miles, "The equivalent circuit for a plane discontinuity in a cylindrical wave guide," PROC. I.R.E., vol. 34, pp. 728–734; October, 1946.

electric field. These two cases are shown in cross section in Figs. 1 and 2.

Equivalent Circuit

If the electric and magnetic fields in the regions of negative co-ordinates (i.e., in the guides proper) are described, respectively, by voltages and currents evaluated in the co-ordinate planes ($x=0$ and $y=0$ for case 1; $x=0$ and $z=0$ for case 2), then the region of positive co-ordinates (i.e., the square bounded by the corners of the bend) may be described by a four-terminal network relating the voltages and currents in the reference planes. It is evident that this network is symmetrical, and, therefore, the equivalent circuit may be reduced to either the symmetrical tee or pi network shown in Figs. 3 and 4.

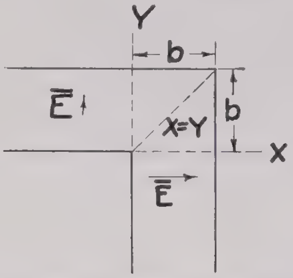

Fig. 1—Bend in plane of electric field.

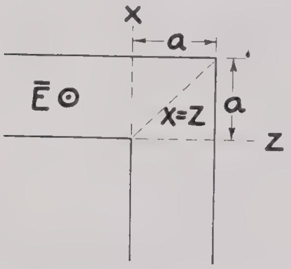

Fig. 2—Bend transverse to plane of electric field.

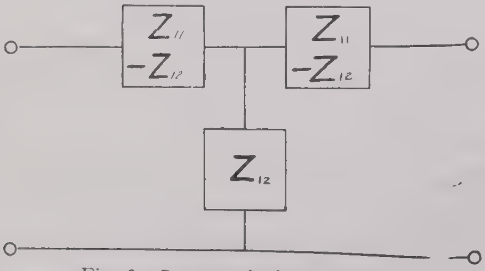

Fig. 3—Symmetrical tee network.

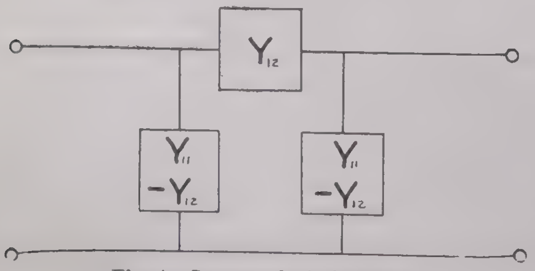

Fig. 4—Symmetrical pi network.

In order to take full advantage of the symmetry of the problem at hand, it is expedient to consider the effect of successively placing a short circuit (corresponding to zero tangential electric field) and an open circuit (corresponding to zero tangential magnetic field) in the plane of symmetry. Dividing the tee and pi networks in their planes of symmetry yields the "semi"-networks shown in Figs. 5 and 6. Hence, the impedances seen at the input of the semi-tee for short and open circuits in the plane of symmetry are

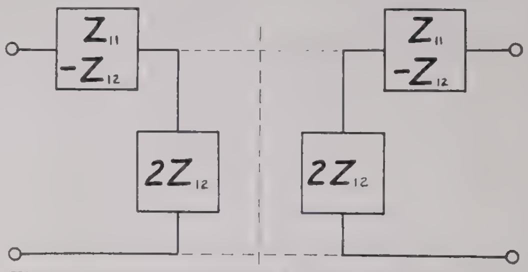

Fig. 5—Tee network divided in plane of symmetry.

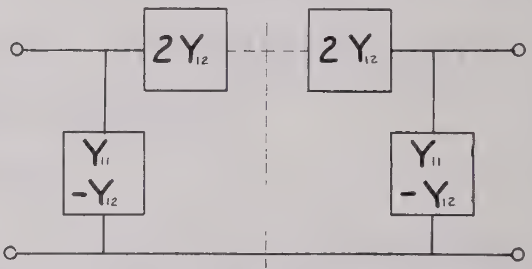

Fig. 6—Pi network divided in plane of symmetry.

$$Z_{sc,oc} = Z_{11} \mp Z_{12}, \tag{1}$$

while for the semi-pi the results are

$$Y_{sc,oc} = Y_{11} \pm Y_{12}. \tag{2}$$

Hence, the problem of the symmetrical corner is deduced in the two problems involving open and short circuits in the plane of symmetry (which is the plane $x=y$ for case 1, and $x=z$ for case 2).

Fields—Electric Field Bent

The bend in the plane of the electric field will be considered first, after which the second problem can be treated by comparison. In the treatments of the change of cross section in the plane of the electric field and of the capacitive window in a rectangular wave guide,[1] it was shown that the results for the parallel-plate guide (where the fields are independent of the z co-ordinate in Fig. 1) may be used if only the wavelength (λ) in these results is replaced by the actual guide wavelength (λg) for the rectangular guide, all impedances being expressed relative to the characteristic impedance. The identical arguments hold for the present case; accordingly, Fig. 1 will be considered as a parallel-plate guide.

A solution to Maxwell's equations for the transverse electric field in the region of negative x (region 1) is given by

$$\overline{E}^1(x, y) = (a_0 e^{-i\beta x} + b_0 e^{i\beta x})\bar{\Phi}_0 + \sum_1^\infty b_n e^{i\beta_n x}\bar{\Phi}_n(y) \tag{3}$$

$$\bar{\Phi}_n(y) = \bar{j}\left(\frac{2 - \delta_n{}^0}{b}\right)^{1/2} \cos\left(\frac{n\pi y}{b}\right) = \bar{j}\phi_n(y) \tag{4}$$[2]

$$(\beta_n)^2 = (\beta)^2 - \left(\frac{n\pi}{b}\right)^2, \quad \beta = \left(\frac{2\pi}{\lambda}\right) \equiv \beta_0 \tag{5}$$

$$b_n = -\delta_0{}^n a_0 + \int_0^b \overline{E}^1(0, y) \cdot \bar{\Phi}_n(y)dy \tag{6}$$

where a_0 is the amplitude of the incident mode, and b_n is the amplitude of the nth reflected mode. The transverse magnetic field is then given by[1] (see also Appendix):

$$\overline{H}^1(x, y) = \bar{k}Y_0(a_0 e^{-i\beta x} - b_0 e^{i\beta x})\phi_0 - \bar{k}\sum_1^\infty b_n Y_n e^{i\beta_n x}\phi_n(y) \tag{7}$$

$$Y_n = \left(\frac{\beta}{\beta_n}\right)\zeta, \tag{8}$$

where Y_n is the "field admittance" for the nth mode, and $\zeta = (\epsilon/\mu)^{1/2}$ is the field admittance of the medium filling the guides.

The electric field in the region 2 (bounded by $x=0$, $x=y$, and $y=b$) is required to satisfy Maxwell's equations (or, more directly, the vector wave equation and the condition of zero divergence), to have its tangential component vanish at $y=b$, and to have its tangential (normal) component vanish on the plane $x=y$ for the short- (open-) circuit case. A field satisfying these conditions and having a tangential component which reduces to $\overline{E}^1(0, y)$ at the plane $x=0$ is

$$\overline{E}^2(x, y) = \sum_0^\infty (\delta_n{}^0 a_0 + b_n)\bar{\Psi}_n(x, y) \tag{9}$$

$$\begin{aligned}\bar{\Psi}_n{}^{sc,oc}(x, y) = {} & \left(\frac{2 - \delta_n{}^0}{b}\right)^{1/2} \csc(\beta_n b) \\ & \cdot\left\{\bar{i}\left[\mp\cos\left(\frac{n\pi x}{b}\right)\sin\beta_n(b - y) + \left(\frac{n\pi}{\beta_n b}\right)\cos\beta_n(b - x)\sin\left(\frac{n\pi y}{b}\right)\right]\right. \\ & + \bar{j}\left[\sin\beta_n(b - x)\cos\left(\frac{n\pi y}{b}\right) \left.\mp\left(\frac{n\pi}{\beta_n b}\right)\sin\left(\frac{n\pi x}{b}\right)\cdot\cos\beta_n(b - y)\right]\right\},\end{aligned} \tag{10}$$

the upper and lower signs corresponding, respectively, to the short- and open-circuit cases. The magnetic field associated with (9) is given by

$$\overline{H}^2(x, y) = j\left(\frac{\zeta}{\beta}\right)\sum_0^\infty (\delta_n{}^0 a_0 + b_n)\nabla x\bar{\Psi}_n(x, y). \tag{11}$$

THE IMPEDANCES

The transmission-line voltage and current, representing the dominant-mode fields in the guide, are defined by

$$V(x) = a_0 e^{-i\beta x} + b_0 e^{i\beta x} \tag{12}$$

$$I(x) = Y_0(a_0 e^{-i\beta x} - b_0 e^{i\beta x}). \tag{13}$$

If the voltage and current in the reference plane $x=0$ are denoted by V_0 and I_0, it is evident from (1) and (2) that

$$\left(\frac{V_0}{I_0}\right)_{sc,oc} = Z_{11} \mp Z_{12} = (Y_{11} \pm Y_{12})^{-1}. \tag{14}$$

Comparing (12) and (6), it is seen that

$$V_0 = \int_0^b \overline{E}(0, y)\cdot\bar{\Phi}_0 dy. \tag{15}$$

To obtain I_0 the continuity of the transverse magnetic field may be invoked at $x=0$. (The transverse electric field is a priori continuous there, since both $\overline{E}^1(0, y)$ and $\overline{E}^2(0, y)$ have been chosen to reduce to the Fourier expansion of $\overline{E}(0, y)$ at $x=0$.) Evaluating (7), (11), and (13) at $x=0$ and invoking this continuity yields

$$I_0\phi_0 = \sum_1^\infty b_n Y_n \phi_n(y) + j\left(\frac{\zeta}{\beta}\right)\sum_0^\infty (\delta_n{}^0 a_0 + b_n)[\bar{k}\cdot\nabla x\bar{\Psi}_n(0, y)], \tag{16}$$

it being evident that the transverse magnetic field for the case at hand is entirely in the z direction (although independent of the co-ordinate z).

To determine the impedances it is expedient to write

$$\overline{E}(0, y) = \bar{j}V_0\eta(y), \tag{17}$$

in which case (15) becomes

$$\left(\frac{I_0}{V_0 Y_0}\right)\phi_0 = \int_0^b G(y, y')\eta(y')dy' = \left(\frac{Y_{11} \pm Y_{12}}{Y_0}\right)\phi_0 \tag{18}$$

$$G(y, y') = \sum_0^\infty\left[(1 - \delta_n{}^0)\left(\frac{Y_n}{Y_0}\right)\phi_n(y) + \left(\frac{j\zeta}{\beta Y_0}\right)\bar{k}\cdot\nabla\bar{\Psi}_n(0, y)\right]\phi_n(y'). \tag{19}$$

In order to satisfy (15), $\eta(y)$ may be expanded as

$$\eta(y) = \phi_0 + \sum_1^\infty A_n\phi_n(y). \tag{20}$$

Now, if (20) is substituted in (18), both sides of the equation multiplied by $\phi_n(y)dy$, and the result integrated between $y=0$ and $y=b$, there result the equations

$$\sum_1^\infty C_{mn}A_n = -C_{m0} \tag{21}$$

---

[2] The $\bar{\Phi}_n$ are normalized so that $\int_0^b \phi_m\cdot\phi_n dy = \delta_n^m$.

$$\left(\frac{Y_{11} \pm Y_{12}}{Y_0}\right) = C_{00} + \sum_1^\infty C_{0n}A_n \tag{22}$$

$$C_{mn} = (1 - \delta_0{}^n)\delta_n{}^m\left(\frac{Y_m}{Y_0}\right) + \left(\frac{j\zeta}{\beta Y_0}\right)\int_0^b \bar{k}\cdot\nabla x\bar{\psi}_n(0,\ y)\phi_m(y)dy. \tag{23}$$

To evaluate the C_{mn} it is found that

$$\left(\frac{\zeta}{\beta Y_0}\right)\bar{k}\cdot\nabla x\bar{\psi}_n(0,\ y) = -\left(\frac{Y_n}{Y_0}\right)[\cot(\beta_n b)\phi_n(y) \pm \csc(\beta_n b)\cos(b - y)\phi_n(0)]. \tag{24}$$

Substituting in (23) yields

$$C_{mn} = \delta_n{}^m[(1-\delta_0{}^m) - j\cot(\beta^2b^2 - m^2\pi^2)^{1/2}](\beta b)(\beta^2b^2 - m^2\pi^2)^{-1/2} \mp j(2-\delta_m{}^0)^{1/2}(2-\delta_n{}^0)^{1/2}(\beta b)[(\beta b)^2 - (n^2+m^2)\pi^2]^{-1}. \tag{25}$$ [3]

(It is evident that $C_{mn} = C_{nm}$.) Thus the first approximations to the desired results are

$$\left(\frac{Y_{11} \pm Y_{12}}{Y_0}\right) = C_{00} = -j(\cot\theta_b \pm \theta_b{}^{-1}), \qquad \theta_b = 2\pi\left(\frac{b}{\lambda_g}\right) \tag{26}$$

while the second approximation is

$$\left(\frac{Y_{11} \pm Y_{12}}{Y_0}\right) = C_{00} - \frac{C_{01}C_{10}}{C_{11}} = -j(\cot\theta_b \pm \theta_b{}^{-1}) - j\left[\frac{2\theta_b{}^2}{(\pi^2 - \theta_b{}^2)^2}\right]\left\{\frac{\theta_b[1 + \coth(\pi^2 - \theta_b{}^2)^{1/2}]}{(\pi^2 - \theta_b{}^2)^{1/2}} \pm \frac{2\theta_b}{(2\pi^2 - \theta_b{}^2)^{1/2}}\right\}^{-1}. \tag{27}$$

Similarly, the $N+1$th approximation is

$$\left(\frac{Y_{11} \pm Y_{12}}{Y_0}\right) = C_{00} - \sum_1^N\sum_1^N C_{0n}C_{m0}(-)^{m+n}\frac{D_{mn}{}^N}{D^N} \tag{28}$$

where D^N is the determinant of (C_{11}, C_{12}, C_{21},—C_{NN}), $D_{mn}{}^N$ is the minor of C_{mn} in D_N, and the upper and lower signs in (28) correspond to the upper and lower signs in (25). As θ approaches π, i.e., as b approaches ($\lambda g/2$), the convergence of (28) is poor, but for the usual values of b found in practice, (27) should be accurate within a few per cent.

A somewhat different approach to the impedance determination is obtained if (18) is multiplied by $\eta(y)dy$, integrated from 0 to b, and the result divided by the square of (15) to obtain

$$\left(\frac{Y_{11} \pm Y_{12}}{Y_0}\right) = \frac{\int_0^b\int_0^b \eta(y)G(y,\ y')\eta(y')dy'dy}{\left[\int_0^b \eta(y)\phi_0 dy\right]^2}. \tag{29}$$

If an approximate form of the field can be guessed, (29) is useful; but since $G(y,\ y')$ is not positive (or negative) definite, it cannot be inferred that (29) is an absolute maximum or minimum, although this has been permissible in other cases.[1]

FIELDS—MAGNETIC FIELD BENT

For case 2, only TE_{m0} modes are excited by the TE_{10} incident mode; accordingly, there is no y-variation of the fields. The electric fields in the region of negative z are then given by

$$\overline{E}^1(x,\ z) = (a_1e^{-j\beta_1 z} + b_1e^{j\beta_1 z})\bar{\phi}_1(x) + \sum_2^\infty b_m e^{j\beta_m z}\bar{\phi}_m(x) \tag{30}$$

$$\bar{\phi}_m(x) = \bar{j}\phi_m(x) = \bar{j}\left(\frac{2}{a}\right)^{1/2}\sin\left(\frac{m\pi x}{a}\right). \tag{31}$$

The a_m, b_m, and β_m are given by (5) and (6) if m is substituted for n, a for b, and x for y. The transverse magnetic field is then given by[1] (or see Appendix):

$$\overline{H}^1(x,\ z) = -\bar{i}Y_1(a_1e^{-j\beta_1 z} - b_1e^{j\beta_1 z})\phi_1(x) + \bar{i}\sum_2^\infty b_m Y_m e^{j\beta_m z}\phi_m(x) \tag{32}$$

$$Y_m = \left(\frac{\beta_m}{\beta}\right)\zeta. \tag{33}$$

The required fields in region 2 are given by

$$\overline{E}^2(x,\ z) = \sum_1^\infty(\delta_m{}^1 a_1 + b_m)\bar{\psi}_m(x,\ z) \tag{34}$$

$$\overline{H}^2(x,\ z) = j\left(\frac{\zeta}{\beta}\right)\sum_1^\infty(\delta_m{}^1 a_1 + b_m)\nabla\times\bar{\psi}_m(x,\ z) \tag{35}$$

$$\bar{\psi}_m{}^{sc,oc}(x,\ z) = \bar{j}\left(\frac{2}{a}\right)^{1/2}\csc(\beta_m a)\cdot\left[\sin\left(\frac{m\pi x}{a}\right)\sin\beta_m(a - z) \mp \sin\left(\frac{m\pi z}{a}\right)\sin\beta_m(a - x)\right]. \tag{36}$$

It is evident from (36) that the electric field is purely transverse and has only a y-component, so that the magnetic field has only x- and z-components; and the transverse magnetic field has only an x-component.

The analysis now proceeds along lines exactly analogous to those of the previous case, and culminates in the equations

$$\left(\frac{Y_{11} \pm Y_{12}}{Y_0}\right) = C_{11} - \sum_2^N\sum_2^N C_{1n}C_{m1}(-)^{m+n}\frac{D_{mn}{}^N}{D^N} \tag{37}$$ [4]

---

[3] λ_g should be used in evaluating β.

[4] Y_1 is implicitly the characteristic admittance (Y_0) in the analysis, but the ratio $(Y_{11} \pm Y_{12})/Y_0$ is independent of the actual definition of Y_0.

$$C_{mn} = \delta_n{}^m[(1 - \delta_1{}^m) + j \cot (\beta_m a)]\left(\frac{\beta_m}{\beta_1}\right)$$

$$\mp 2j \frac{(m\pi)(n\pi)}{(\beta_1 a)} [(m^2 + n^2 - 1)\pi^2 - (\beta_1 a)^2]^{-1}. \quad (38)$$

The second approximation to (7) is

$$\left(\frac{Y_{11} \pm Y_{12}}{Y_0}\right) = - j\left[\cot \theta_a \pm \frac{2}{\theta_a}\left(1 - \frac{\theta_a{}^2}{\pi^2}\right)^{-1}\right]$$

$$+ j\left(\frac{4}{\theta_a}\right)^2\left(4 - \frac{\theta_a{}^2}{\pi^2}\right)^{-1} \left\{\left[1 - \coth\left(1 - \frac{\theta_a{}^2}{\pi^2}\right)^{1/2}\right]\right.$$

$$\left.\cdot\left(\frac{\pi}{\theta_a}\right)\left(3 - \frac{\theta_a{}^2}{\pi^2}\right)^{1/2} \mp \frac{8}{\theta_a}\left(7 - \frac{\theta_a{}^2}{\pi^2}\right)^{-1}\right\}^{-1}$$

$$\cdot\theta_a = \frac{2\pi a}{\lambda_g}\cdot \quad (39)$$

NUMERICAL RESULTS

Curves of $(Y_{11} \pm Y_{12})/Y_0$, computed from (27), are given in Fig. 7 for values of $(b/\lambda g)$ from 0 to 1/2 (0.433 will generally be the upper limit in practice). Curves computed from (39) are given in Fig. 8, for $(a/\lambda g)$ from 0 to 0.866 (cutoff point for E_{20} mode). Along with the results of (27) and (39) are plotted (dashed curves) the susceptances

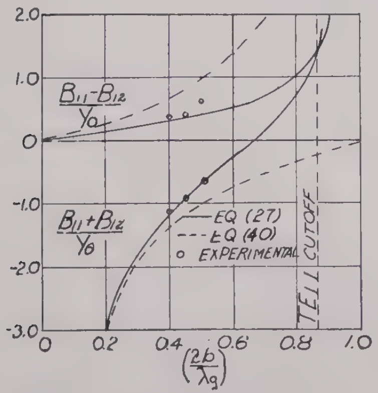

Fig. 7—$Y_{11} \pm Y_{12}$ for E-plane bend as computed from equation (27).

$$(B_{11} \pm B_{12}) = \mp\left(\tan \frac{\theta}{2}\right) \mp 1 \quad (40)$$

for a section transmission line of length b, a, respectively. Evidently, (40) is an excellent approximation to (39), while not very satisfactory for $(B_{11} - B_{12})$ as given by (27).

EXPERIMENTAL CHECKS

Experimental results were available[5] for $\lambda = 3.00$, 3.20, 3.40 centimeters in a guide of $a = 0.9$, $b = 0.4$ inch. While the check on the E-plane bend is quite satisfactory, the check on the H-plane bend is poor; unfortunately, the latter data are near a resonance point where the convergence of (37) is undoubtedly poor, although the implication is that the resonance indicated at $\theta = \pi$ by (37) actually should occur at a somewhat larger value of this parameter.

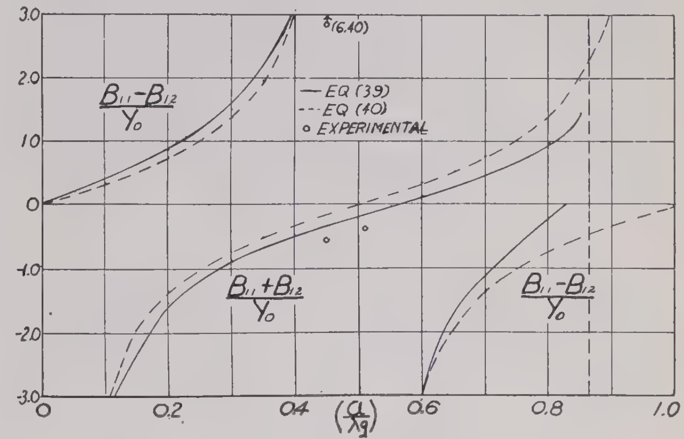

Fig. 8—$Y_{11} \pm Y_{12}$ for H-plane bend as computed from equation (39).

APPENDIX

Maxwell's equations may be written

$$\nabla \times \overline{H} = j\beta\zeta\overline{E} \quad (41)$$

$$\nabla \times \overline{E} = - j\beta\zeta^{-1}\overline{H}. \quad (42)$$

If the transverse (to direction of propagation, z) electric field is written

$$\overline{E}(u, v, z) = \sum_n C_n\Phi_n(u, v)e^{+j\beta_n z} \quad (43)$$

if follows from (41) and (42) and the definition of TE and TM modes that the transverse magnetic field may be written

$$\overline{H}(u, v, z) = \pm Y_n[\bar{k} \times \overline{E}(u, v, z)] \quad (44)$$

$$Y_{n(TE)} = \left(\frac{\beta_n}{\beta}\right)\zeta \quad (45)$$

$$Y_{n(TM)} = \left(\frac{\beta}{\beta_n}\right)\zeta. \quad (46)$$

---

[5] "Wave Guide Handbook," M.I.R. Rad. Lab. Rep. 41, January 23, 1945; available through the Department of Commerce, Washington, D. C., and soon through the McGraw-Hill Publishing Co., New York, N. Y. The measurements cited were made by the author at the California Institute of Technology in 1944, under the direction of W. H. Pickering.

Microwave Filters Using Quarter-Wave Couplings*

R. M. FANO†, ASSOCIATE, I.R.E., AND A. W. LAWSON, JR.‡

Summary—This paper presents a method of designing band-pass and band-rejection microwave filters by appropriately transforming lumped-element filters. Such microwave filters are realized physically as chains of resonant elements (either cavities or irises), coupled by quarter-wave sections of line. A structure of this type has a number of practical advantages over other types of filter structures, such as a chain of directly coupled cavities, because it permits the construction of the resonant elements as separate units, and yields more liberal tolerances on the dimensions of the coupling irises. A comparison is made of the theoretical and measured characteristics of an experimental four-cavity filter.

INTRODUCTION

THE DESIGN of a filter having specified frequency characteristics is a problem of network synthesis. A number of synthesis procedures have been developed in the last two decades[1–3] which are applicable to lumped-element networks, that is, to networks consisting of inductances, capacitances, and resistances. In microwave systems, however, these lumped elements cannot be used, for obvious reasons, and must therefore be replaced by more suitable elements, such as sections of transmission lines or wave guides, cavity resonators, resonant irises, etc. Unfortunately these microwave elements behave with frequency in such a complex manner that the development of direct synthesis procedures applicable to microwave networks seems quite remote. On the other hand, if one is interested in a limited frequency band, the same microwave elements can be made to approximate rather well the frequency behaviors of lumped elements, either alone or in resonant combinations. On this basis, one is led to consider the possibility of designing microwave filters by appropriately transforming lumped-element filters.

In addition to theoretical limitations on filter design, the actual systems applications and the manufacturing techniques available often impose widely varying geometrical and physical requirements. These requirements are largely responsible for the ultimate appearance of microwave filters, and they also determine the practical usefulness of any design procedure. It follows that no single design procedure can be expected to be applicable in all cases, and that the solution of any specific problem depends largely on the ingenuity of the designer. This paper will discuss a particular design procedure which is applicable in a variety of cases, and which meets most of the usual practical requirements. This procedure is limited to the design of band-pass and band-elimination filters; fortunately, however, filters of other types are seldom needed in microwave systems.

GENERAL THEORY OF QUARTER-WAVE COUPLING

The method of design discussed below leads to filters consisting of a chain of resonant elements, such as cavity resonators, linked by quarter-wave sections of line. This chain-like structure is obtained by appropriately transforming a lumped-element ladder structure which is characteristic of most practical low-frequency filters. To understand the mechanism of the transformation, consider first a quarter-wave lossless line terminated in a normalized[4] impedance Z. The normalized input impedance of such a line is

$$Z' = \frac{Z + j \tan \frac{\pi}{2}}{1 + jZ \tan \frac{\pi}{2}} = \frac{1}{Z}. \tag{1}$$

It follows that the circuits of Fig. 1 are equivalent if the normalized impedance Z' is numerically equal to the normalized admittance Y and if both lines are one-quarter of a wavelength long. In fact, the two networks have the same open-circuit and short-circuit impedances.

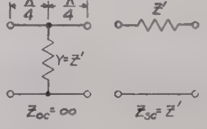

Fig. 1—Transformation of a series branch.

Consider now the structures of Fig. 2, in which Y_2, Y_4, Y_6, etc., are numerically equal, respectively, to Z_2', Z_4' Z_6', etc., and the coupling lines are all identical. These

---

* Decimal classification: R386.1. Original manuscript received by the Institute, October 10, 1946; revised manuscript received, February 17, 1947. Presented, International Scientific Radio Union. Washington, D. C., May, 1946.

The research reported in this paper was made possible in part through support extended the Massachusetts Institute of Technology, Research Laboratory of Electronics, jointly by the Army Signal Corps, the Navy Department (Office of Naval Research), and the Army Air Forces (Air Matériel Command), under the Signal Corp Contract No. W-36-039 sc-30237, and in part through support given the Radiation Laboratory under contract OEMsr 262.

† Massachusetts Institute of Technology, Research Laboratory of Electronics, Cambridge 39, Mass.

‡ Formerly, Massachusetts Institute of Technology, Research Laboratory of Electronics: now, the Institute for the Study of Metals, University of Chicago, Chicago, Ill.

[1] E. A. Guillemin, "Communication Networks," vol. II, John Wiley and Sons, New York, N. Y., 1935.

[2] H. W. Bode, "Network Analysis and Feedback Amplifier Design," D. Van Nostrand Co., New York, N. Y., 1945.

[3] S. Darlington, "Synthesis of reactance 4 poles," *Jour. Math. and Phys.*, vol. 18, pp. 257–353; September, 1939.

[4] The normalized impedance is the ratio of the actual impedance to the characteristic impedance of the line. The normalized admittance is defined in a similar manner. Normalized impedances and admittances are used throughout this paper in connection with microwave structures, although the word "normalized" will be dropped in most instances for the sake of brevity.

two networks are exactly equivalent at the frequency ω_0 for which the coupling lines are one-quarter wavelength long. At other frequencies, however, the equivalence does not hold, but the characteristics of the two networks will not differ appreciably over a frequency band small compared to ω_0. Therefore, in the following discussion, we shall neglect the frequency dependence of the electrical length of the lines and assume that the two structures of Fig. 2 are exactly equivalent. The error introduced by this approximation when the frequency band of interest is relatively large will be discussed later.

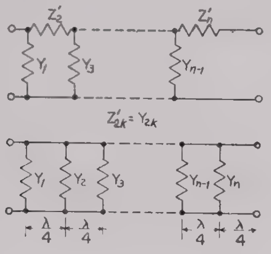
Z_2'
Z_n'
Y_1
Y_3
Y_{n-1}
$Z_{2k}'=Y_{2k}$
Y_1
Y_2
Y_3
Y_{n-1}
Y_n
$\frac{\lambda}{4}$
$\frac{\lambda}{4}$
$\frac{\lambda}{4}$
$\frac{\lambda}{4}$

Fig. 2—Ladder network transformed into a quarter-wave-coupled structure.

To proceed from this point, one must be more specific about the elements of the general structures of Fig. 2. We shall consider the particular case of the ladder structure shown in Fig. 3(a) in which the series branches are series-tuned circuits resonating at the frequency ω_0, and the shunt branches are parallel-tuned circuits also resonating at the frequency ω_0. This structure is characteristic of band-pass filters whose insertion loss in the attenuation band is a monotonic function[3]; for instance, constant-k band-pass filters[1] are of this type. Filters of the m-derived type and band-elimination filters will be considered later.

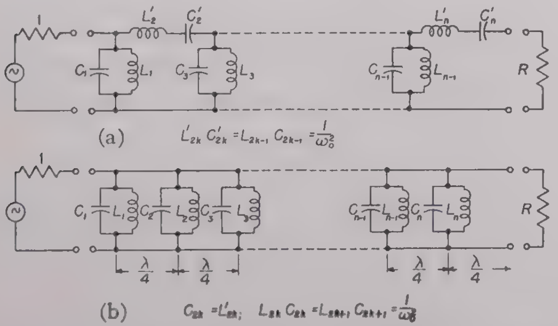
1
L_2'
C_2'
L_n'
C_n'
C_1
L_1
C_3
L_3
C_{n-1}
L_{n-1}
R
(a)
$L_{2k}'C_{2k}'=L_{2k-1}C_{2k-1}=\frac{1}{\omega_0^2}$
1
C_1
L_1
C_2
L_2
C_3
L_3
C_{n-1}
L_{n-1}
C_n
L_n
R
$\frac{\lambda}{4}$
$\frac{\lambda}{4}$
$\frac{\lambda}{4}$
$\frac{\lambda}{4}$
(b)
$C_{2k}=L_{2k}';\quad L_{2k}C_{2k}=L_{2k+1}C_{2k+1}=\frac{1}{\omega_0^2}$

Fig. 3—Band-pass filter and equivalent quarter-wave-coupled filter.

Suppose, then, that a lumped-element filter of the type shown in Fig. 3(a) has been designed following any one of the available methods of network synthesis. The corresponding filter employing quarter-wave coupling lines is shown in Fig. 3(b). The next step in the design procedure is to substitute for each tuned circuit a microwave element which behaves approximately in the same manner over the frequency band of interest. Such an element may be a cavity resonator, a resonant iris, or a shorted section of line, depending on the particular application and on the bandwidth of the filter.

It can be shown[5] that a cavity resonator with an input and an output line can be represented, approximately, in the vicinity of one of its resonant frequencies by the two equivalent circuits of Fig. 4. The reactances X_1 and X_2 are very closely equal to the input and output reactances when the cavity is detuned. In most practical cases they are very small and can be neglected to a first approximation. The other parameters of the equivalent circuits are usually expressed in terms of the "loaded Q's" of the cavity, defined as follows. Q_{L1} is the Q of the cavity when a resistance equal to the characteristic impedance Z_{01} of the input line is connected to the input terminals and the cavity itself is assumed to be lossless; Q_{L2} is defined in a similar manner when a resistance equal to the characteristic impedance Z_{02} of the output line is connected to the output terminals. Finally, Q_L is the Q of the cavity when both pairs of terminals are loaded by the characteristic impedances of the input and output lines. The unloaded Q_0[6,7] is the Q resulting from the losses in the cavity itself. According to these definitions and neglecting X_1 and X_2, one obtains for the Q's of the cavity:

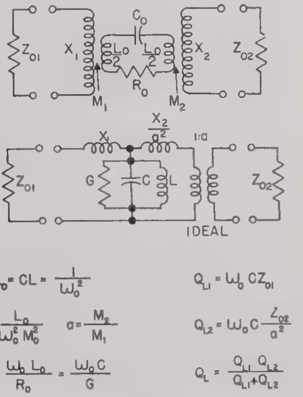
Z_{01}
X_1
C_0
$\frac{L_0}{2}$
$\frac{L_0}{2}$
R_0
X_2
Z_{02}
M_1
M_2
X_1
$\frac{X_2}{a^2}$
1:a
Z_{01}
G
C
L
Z_{02}
IDEAL
$C_0L_0=CL=\frac{1}{\omega_0^2}$
$Q_{L1}=\omega_0CZ_{01}$
$C=\frac{L_0}{\omega_0^2M_0^2}$
$a=\frac{M_2}{M_1}$
$Q_{L2}=\omega_0C\frac{Z_{02}}{a^2}$
$Q_0=\frac{\omega_0L_0}{R_0}=\frac{\omega_0C}{G}$
$Q_L=\frac{Q_{L1}Q_{L2}}{Q_{L1}+Q_{L2}}$

Fig. 4—Approximate equivalent circuit for a cavity resonator.

$$Q_{L1}=\omega_0CZ_{01} \tag{2}$$

$$Q_{L2}=\omega_0C\frac{Z_{02}}{a^2}=\omega_0C\left(\frac{M_1}{M_2}\right)^2Z_{02} \tag{3}$$

$$Q_L=\frac{Q_{L1}Q_{L2}}{Q_{L1}+Q_{L2}}. \tag{4}$$

In the particular case of a symmetrical cavity,

---

[5] S. A. Schelkunoff, "Representation of impedance functions in terms of resonant frequencies," Proc. I.R.E., vol. 32, pp. 83–91; February, 1944.

[6] Staff, M.I.T. Radar School, "Principles of Radar," The Technology Press, Cambridge, Mass., 1944.

[7] R. I. Sarbacher and W. A. Edson, "Hyper and Ultrahigh Frequency Engineering," John Wiley and Sons, New York, N. Y., 1943.

$$Q_{L1} = Q_{L2} = 2Q_L = \omega_0 C Z_0 \tag{5}$$

and the equivalent circuit reduces to a simple parallel-tuned circuit in shunt to the line. Note that CZ_0 is the normalized capacitance of the resonant circuit.

It follows from the above discussion that each resonant branch of the structure shown in Fig. 3(b) can be physically realized by means of a symmetrical cavity resonator whose loaded Q is given by

$$(Q_L)_k = \tfrac{1}{2}\omega_0 C_k \tag{6}$$

where C_k is the normalized capacitance of the resonant branch. The only difficulty which may arise in this transformation concerns the terminating resistance which, in general, is different from the line impedance. Since it is desirable to match the filter to the output line, the last element of the structure is further transformed as shown in Fig. 5 to obtain the proper change of impedance level. The corresponding cavity resonator is then no longer symmetrically coupled, and in this case the loaded Q's are given by

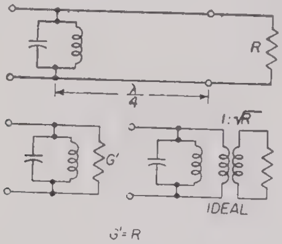

Fig. 5—Impedance-level transformation.

$$Q_{L1} = C_n\omega_0 \tag{7}$$

$$Q_{L2} = \frac{C_n}{R}\,\omega_0. \tag{8}$$

If the last element of the structure of Fig. 3(a) were a shunt branch, one would obtain

$$Q_{L1} = C_n\omega_0 \tag{9}$$

$$Q_{L2} = RC_n\omega_0. \tag{10}$$

Changes of impedance level similar to the one just described can be performed at other points of the structure, if so desired.

In the case of wave-guide filters, resonant irises[6,8] can be used instead of cavity resonators to approximate the behavior of the resonant branches of Fig. 3(b). However, since resonant irises have relatively low unloaded Q's they are not used in connection with narrow-band filters. On the other hand, in the case of bandwidths of a few per cent, the use of resonant irises instead of cavities results in a considerable saving of space and weight. The design procedure for such filters is the same as for cavity filters, although no change of impedance level can be performed in this case because resonant irises are inherently symmetrical.

Filters Employing Identical Elements

The construction of a microwave filter can be considerably simplified by making all the resonant elements identical. Such a design is not optimum in the sense that better filter characteristics could be obtained with the same number of cavities, but very often the resulting simplicity of construction is worth the loss of performance.

The power-loss ratio of a filter consisting of a number of identical resonant elements can be easily computed by noting that such a filter is a cascade connection of n identical sections of the type shown in Fig. 6. The susceptance of the shunt branch can be expressed in terms of the loaded Q, as follows:

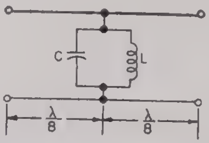

Fig. 6—Section of quarter-wave coupled filter.

$$B = 2Q_L\left(\frac{\omega}{\omega_0} - \frac{\omega_0}{\omega}\right) = 2x \tag{11}$$

where x is a normalized frequency variable which is zero at the resonance frequency and becomes ±1 at the two half-power frequencies. By making use of image-parameter theory[1,9] one obtains for the power-loss ratio

$$\left(\frac{P_0}{P_L}\right)_n = 1 + x^2U_n^2(x) \tag{12}$$

where the function $U_n(x)$ is a Tschebyscheff polynomial of the second kind and order n. The polynomials corresponding to $n=1, 2, 3, 4$ are given below with a recurrence formula from which they may be successively derived.

$$\begin{aligned} U_1(x) &= 1 \\ U_2(x) &= 2x \\ U_3(x) &= 4x^2 - 1 \\ U_4(x) &= 8x^3 - 4x \end{aligned} \tag{13}$$

$$U_{n+1}(x) = 2xU_n - U_{n-1}. \tag{14}$$

Plots of the insertion loss are shown in Fig. 7 for $n=1, 2, 3, 4$. These curves show that the pass-band tolerance increases with n; consequently, values of n larger than 4 are seldom used. For large values of x, the off-band insertion loss becomes approximately

$$L_n \approx 6(n-1) + 20n\log x \text{ db}. \tag{15}$$

---

[8] H. A. Leiter, "A microwave band-pass filter in waveguide," M.I.T. Rad. Lab. Rep. 814.

[9] P. I. Richards, "Applications of matrix algebra to filter theory," Proc. I.R.E., vol. 34, pp. 145P–151P; March, 1946.

When the frequency dependence of the electrical length of the lines is taken into account, one obtains

$$\left(\frac{P_0}{P_L}\right)_n = 1 + x^2 U_n{}^2(kx) \tag{16}$$

where

$$k = 1 + \frac{\pi}{4}\,\frac{1}{Q_L}\left(\frac{\lambda_g}{\lambda}\right)^2. \tag{17}$$

A comparison of this equation with (12) shows that, to a first approximation, the bandwidth of the filter is reduced by a factor equal to k. The pass-band tolerance is also reduced, since x^2 is inversely proportional to k^2 for any given value of $U_n{}^2$. In the particular case of $n=3$ the bandwidth and the maximum pass-band value of

$$\left[\left(\frac{P_0}{P_L}\right)_3 - 1\right]^{1/2}$$

are both reduced exactly by a factor equal to k.

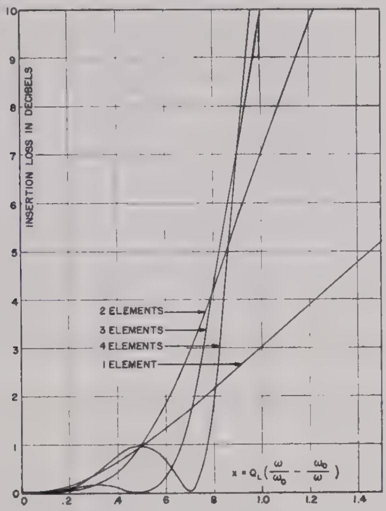

Fig. 7—Theoretical characteristics of filters employing identical elements.

PRACTICAL DESIGN CONSIDERATIONS

The main advantage of quarter-wave-coupled filters is that the resonant elements can be built, tested, and tuned separately. Only minor tuning adjustments are necessary after assembly, since the cavities can be joined to each other by means of standard connectors[6] without need of any further soldering. This great advantage results from the fact that the coupling lines are nonresonant and, therefore, their length is not critical and their continuity can be broken by standard connectors without causing appreciable additional loss. Such a construction would not be possible, on the other hand, if the lines were an integral number of half-waves long.

The structure employing quarter-wave coupling lines is not the only microwave structure equivalent to the lumped-element ladder network. The ladder network of Fig. 3, for instance, can be transformed[1] into a chain of resonant loops tuned to the same frequency and coupled to one another by mutual inductances. The microwave realization of this structure consists of a chain of directly coupled cavity resonators. Filters of this type, however, must be built in a single unit, and, moreover, require closer machining tolerances than the corresponding filters employing quarter-wave coupling lines. It can be shown, in fact, that, in the case of directly coupled cavities, the coupling susceptances are equal to the square of the coupling susceptances required when the cavities are quarter-wave spaced. It must be pointed out, however, that directly coupled filters are superior from the point of view of space and weight requirements. This advantage may outweigh, in some instances, the construction difficulties mentioned above.

In connection with the design of quarter-wave-coupled filters, the determination of the effective location of the terminals of a cavity on the input and output lines requires further explanation, particularly in the case of loop couplings to coaxial lines. Such a determination can be performed experimentally with the help of a standing-wave detector by finding the position of the voltage zero in the line when the cavity is detuned. Under these conditions the input terminals of the cavity are effectively short-circuited, so that their location must be an integral number of half-wavelengths from the position of any voltage zero. This experimental determination may be done in such a way as to include the equivalent line length of whatever fittings are used to connect the cavity to the coaxial line. Moreover, the locations of the terminals are automatically shifted to compensate approximately for the presence of the reactances X_1 and X_2 of Fig. 4, which have been neglected in the theoretical analysis.

The actual characteristics of a number of quarter-wave-coupled filters were found to be very close to those predicted apart from the effect of incidental dissipation, which was neglected in the theoretical analysis. The theoretical and measured characteristics of a four-cavity filter are compared in Fig. 9. The main effect of dissipation is a finite loss in the pass band, approximately equal, in the case of n identical cavities, to n times the loss of one cavity; the insertion loss for a symmetrical cavity ($Q_{L1} = Q_{L2}$) at resonance is given by

$$L_0 = 20 \log\left(1 + \frac{Q_L}{Q_0}\right) \text{db}. \tag{18}$$

In view of the fact that the bandwidth of a filter is inversely proportional to the loaded Q's of the cavities employed, the effect of incidental dissipation becomes increasingly important in narrow-band filters. For detailed computations of the effects of incidental dissipation, the reader is referred to the literature on this subject in the case of lumped-element filters.[1–3]

The value of Q_0 for a cavity is limited, in practice, by space considerations as well as by the requirement that the cavity must approximate the behavior of a simple resonant circuit over a specified frequency band. The unloaded Q_0 is roughly proportional to the ratio of the volume of the cavity to its surface area,[6,7] so that Q_0 increases with the volume. On the other hand, an increase of volume always results in a reduction of the separation between resonance frequencies, and therefore in a reduction of the useful frequency band. In general, this fact sets up an upper limit on the size of the cavity and consequently on the unloaded Q for a given surface material.

A discussion of the design of cavity resonators is beyond the scope of this paper. It will suffice here to describe a type of cavity, shown in Fig. 8, which is particularly suitable for wave-guide filters. The proper distance between the two inductive irises, for a given resonance frequency, depends on the dimensions of the irises, and it is always smaller than one-half of the guide wavelength. In practice, this distance is made a little shorter than required and the cavity is then tuned to the desired frequency by means of the screw shown in Fig. 8. The loaded Q and the length l of a symmetrical cavity of this type can be computed to a good approximation by means of the following equations:

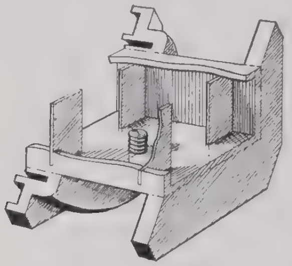

Fig. 8—Cavity resonator suitable for wave-guide filters.

$$Q_L = \frac{1 + b_0^2}{4} \left(\frac{\lambda_g}{\lambda_0}\right)^2 \tan^{-1} \frac{2b_0}{b_0^2 - 1} \qquad (19)$$

$$l = \frac{\lambda_g}{2\pi} \tan^{-1} \frac{2b_0}{b_0^2 - 1} \qquad (20)$$

where b_0, λ_0 and λ_g are, respectively, the normalized susceptances of the irises,[10] the resonance wavelength, and the corresponding guide wavelength.[6,7] The cavity is provided with standard choke and flange connectors[6] spaced a distance equal to $\lambda_g/8$ from the two irises so as to yield the desired quarter-wave coupling when two cavities are connected together.

Fig. 9 presents a comparison of the theoretical and measured characteristics of an experimental filter employing four identical cavities of the type shown in Fig. 8. The theoretical curves have been computed from the physical dimensions of the cavities and the measured value of the transmission loss of one cavity at resonance. The theoretical curve for the insertion loss of the filter, neglecting dissipation, is plotted as curve *B*. The transmission loss of the individual cavities at resonance was found to be approximately 0.44 db; this value yields, according to (18), a ratio $Q_0/Q_L = 20$. It must be pointed out in this connection that the actual Q_0 of a cavity may differ considerably from the theoretical value because of the additional losses resulting from the presence of the coupling irises and of the tuning screw. In this particular case, for instance, the theoretical Q_0 is almost twice the measured value. Curve *A* is a plot of the theoretical insertion loss in the presence of dissipation for a ratio $Q_0/Q_L = 20$. The crosses in the same figure represent measured values of the loss for the whole filter. In considering the rather large effect of dissipation one must remember that no attempt has been made in the design of this filter to reduce the losses. Silver-plating alone would increase Q_0 by a factor of approximately 2, thus reducing the midband loss by approximately the same factor. Further improvement could be obtained by reducing the losses in the tuning device.

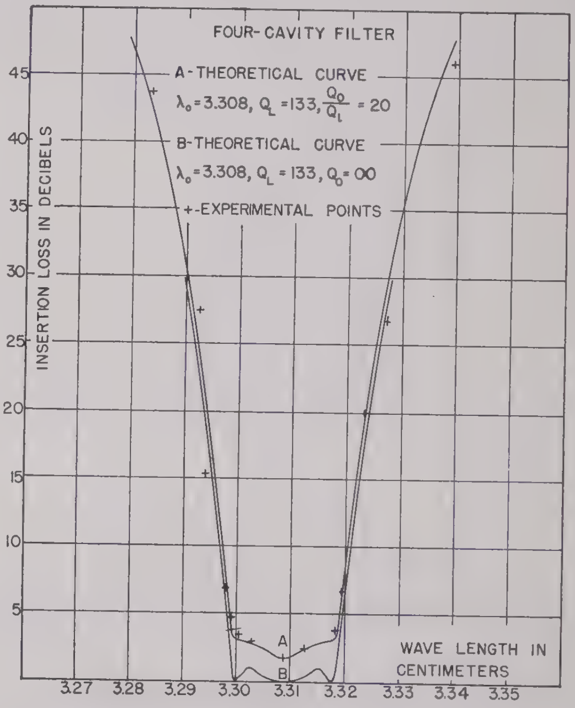

Fig. 9—Theoretical and experimental characteristics of a filter consisting of four identical cavities of the type shown in Fig. 8.

In many cases where loaded Q's of less than 30 to 40 are required, it is possible to reduce the size and weight of a filter by replacing the cavity resonators with resonant irises.[6,8] These irises behave like parallel-tuned circuits in shunt to the line, and, therefore, may be considered as combinations of inductive and capacitive irises. The saving in space and weight resulting when resonant irises are used follows from the fact that the wave guide stores the energy associated with the irises, while still performing its function as a line. However, since the ratio of the effective volume to the surface is always smaller for an iris than for a cavity with the same loaded Q, the unloaded Q of the iris will always be smaller. Thus, the use of resonant irises is restricted to values of loaded Q sufficiently small to keep the transmission loss within reasonable limits. On the other hand, the design of cavities becomes rather difficult when small loaded Q's of the order of magnitude of 50 are desired because the coupling elements become a major portion of the cavity. It follows that resonant irises are complements to cavities, rather than substitutes.

---

[10] "Wave Guide Handbook," M.I.T. Rad. Lab. Rep. 43, February 7, 1944, Sections 2-1, 21-a, 26-a.

One of the outstanding uses of resonant irises is in the construction of broad-band transmit-receive (TR) tubes.[6] The technique of quarter-wave-coupling a number of identical resonant irises was first used by Fiske[11,12] in the design of these tubes before the authors considered its application to cavity resonators and to the design of microwave filters. TR boxes and filters[8] employing identical irises were also designed at the Radiation Laboratory in the section headed by L. D. Smullin.

FILTERS OF THE "*m*-DERIVED" TYPE AND BAND-REJECTION FILTERS

Filters of the m-derived type are used when fast-rising attenuation functions are required.[1,3] No quarter-wave filter of this type has yet been built by the authors, but the design procedure is straightforward. The only difference between the simple band-pass ladder structure and the m-derived structure is the presence of shunt branches of the type shown in Fig. 10(a) or of series branches of the type shown in Fig. 10(c). Since these two types of branches are equivalent when quarter-wave coupling is employed, only the first type will be considered in detail. Foster's reactance theorem[1,2] permits the transformation of the branch of Fig. 10(a) into the network shown in Fig. 10(b), in which the two resonant circuits are tuned at the frequencies $\omega_{\infty 1}$ and $\omega_{\infty 2}$. These frequencies correspond to peaks of infinite attenuation in the characteristics of the filter. A microwave realization of the network of Fig. 10(b) is readily obtained, as shown in Fig. 11(a). One may also consider the network of Fig. 10(a) as a two-element ladder structure with its output terminals open-circuited (see Fig. 11(b)). Its microwave equivalent, shown in Fig. 11(c), is then obtained by quarter-wave-coupling two cavities tuned at the mean frequency ω_0 of the filter. In this case the separation of the frequencies $\omega_{\infty 1}$ and $\omega_{\infty 2}$ is controlled by the ratio of the loaded Q's of the two cavities. In the case of wave-guide filters the same design technique is employed, although the appearance of the final structure might be somewhat different.

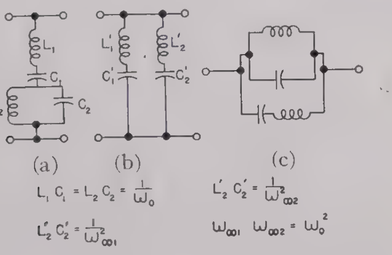
L₁
C₁
L₂
C₂
L′₁
C′₁
L′₂
C′₂
(a)
(b)
(c)
$L_1C_1 = L_2C_2 = \frac{1}{\omega_0}$
$L'_2C'_2 = \frac{1}{\omega^2_{\infty 1}}$
$L'_2C'_2 = \frac{1}{\omega^2_{\infty 2}}$
$\omega_{\infty 1}\,\omega_{\infty 2} = \omega_0^2$

Fig. 10—Typical elements of "*m*-derived" filters.

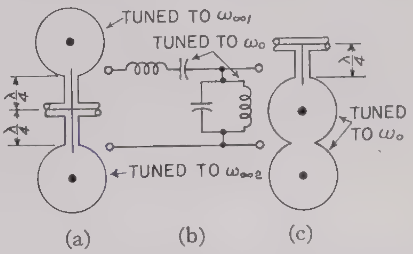

Fig. 11—Transformation and microwave realizations of the elements shown in Fig. 10.

Band-elimination filters can be designed in the same manner, since the lumped-element ladder structure of this type of filter can be obtained from the band-pass structure by the simple process of substituting a series-tuned circuit for any parallel-tuned circuit, and vice versa.[1]

CONCLUSIONS

The quarter-wave-coupled structure has been shown to be a microwave equivalent of the lumped-element ladder structure for the purpose of designing band-pass and band-elimination filters. This structure provides physical spacing between the resonant elements, and at the same time permits the construction and test of these elements as separate units which can be easily assembled afterwards. The method of design discussed in this paper, however, is not necessarily the best method in all cases. For instance, filters consisting of directly coupled cavities may be preferable when space is at a premium. These filters can also be designed by properly transforming lumped-element ladder structures, but they may present serious construction problems when more than two cavities are used. Therefore, in some cases the two methods of design may be effectively combined to satisfy space requirements without introducing excessive construction difficulties. In such instances one may also use special cavities which alone behave like two- or three-element filters. These cavities will be the subject of a future paper.

---

[11] M. D. Fiske, "A broad-band TR switch," General Electric Report, October 18, 1943.

[12] M. D. Fiske, "Characteritsics of the single and multiple tuned circuits," General Electric Report, May 25, 1945.

Broad-Band Noncontacting Short Circuits for Coaxial Lines

Part III—Control of Parasitic Resonances in the S-Type Plunger*

W. H. HUGGINS†, ASSOCIATE, I.R.E.

Summary—It is known that parasitic resonances may occur in the noncontacting plunger of a coaxial-line resonator, when the wavelength is less than the circumference of the outer gap. When it is not possible to select inner and outer diameters such that the parasitic resonances occur at wavelengths outside of the tuning range, these resonances must be controlled by cutting grooves or slots in the plunger.

This paper develops a theory of the resonances in a slotted plunger based upon a loaded-transmission-ring model. The wavelengths at which the parasitic resonances occur as calculated from this model are found to be in satisfactory agreement with experimental measurements made upon a typical plunger. It is concluded that ordinarily an odd number of slots is preferable to an even number, and that the parasitic resonances are more readily controlled in the Z-type than in the British S-type plunger.

I. Parasitic Resonances in a Coaxial Resonator

THE COAXIAL-LINE resonator which may be made to tune over a wide range has rather important application to oscillators and filters operating in the microwave region.[1] One of the principal advantages of a resonator of this type is that it can be tuned with a noncontacting plunger over a tuning ratio as great as 3 to 1.[2]

Unfortunately, parasitic resonances may often exist, and the major problem in the design of a wide-tuning-range resonator is to eliminate the deleterious effect of those resonances that may be caused by higher-order modes in the coaxial cavity, and also by circumferential resonances associated with the noncontacting plunger.[3] Ordinarily, the diameters of the inner and outer coaxial conductors are determined by factors that are independent of the plunger design, and the problem eventually reduces to one of designing a noncontacting plunger for use in a coaxial line of given dimensions and capable of being tuned over a specified tuning range without exhibiting any parasitic resonances.

If parasitic plunger resonances occur within the tuning range, the plunger must be modified in such a way as to suppress or remove them. One method of controlling these resonances is to cut axial slots into the plunger. Since the circumferential currents associated with the parasitic resonances must flow across these irregularities, axial slots will increase the resonant wavelength of the circumferential resonances. On the other hand, the surface currents associated with the *TEM* wave are entirely axial and the slots will have little effect upon the *TEM* currents and, consequently, upon the *TEM* impedance of the plunger.

Because of this "selective-tuning" property, axial slots may be utilized to modify the more harmful resonances so that their wavelengths will lie *outside* of the tuning range. Furthermore, the slots provide a means of introducing selectively sufficient dissipation that those resonances remaining within the tuning range will have negligible effect. These properties will now be examined in greater detail.

II. Resonances in Transmission Rings

Before discussing the slot resonances that occur in a slotted plunger, we shall examine the conditions for resonance in a transmission ring formed by connecting together the output and input terminals of a transmission circuit. For a parallel-strip transmission circuit, the connection could be made as shown in Fig. 1.

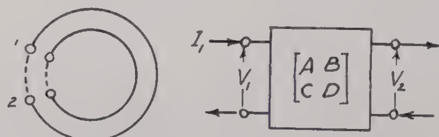

Fig. 1—Parallel-strip transmission ring and network equivalent.

The condition for resonance may be established by breaking the ring at any plane and then considering the resultant structure as a 4-terminal network. Assuming a linear passive network, the currents and voltages appearing at the input and output terminals will be related by the two linear equations

$$
\begin{aligned}
V_1 &= AV_2 + BI_2 \\
I_1 &= CV_2 + DI_2
\end{aligned}
\qquad (1)
$$

where the coefficients A, B, C, and D are commonly known as the *general circuit parameters* and, for all circuits where reciprocity applies, $AD-BC=1$. But, connection of the input and output terminals imposes the conditions that

---

* Decimal classification: R117.112. Original manuscript received by the Institute, February 25, 1947. Presented, Boston Section, I.R.E., February 20, 1947, Boston, Mass.

This paper is based in part upon work done for the OSRD under contract OEMsr-411 with the President and Fellows of Harvard College.

† Communications Laboratory, Cambridge Field Station, Air Matériel Command, Army Air Forces, Cambridge 39, Mass.

[1] Radio Research Laboratory Staff, "Very High Frequency Techniques," McGraw-Hill Book Co., New York, N. Y., 1947; chapters 28 and 32.

[2] W. H. Huggins, "Broad-band noncontacting short-circuits for coaxial lines. Part I—*TEM*-Mode characteristics," PROC. I.R.E., vol. 35, pp. 906–913; September, 1947.

[3] W. H. Huggins, "Broad-band noncontacting short-circuits for coaxial lines. Part II—Parasitic resonances in the unslotted S-type plunger," PROC. I.R.E., vol. 35, pp. 1085–1092; October, 1947.

$$\begin{aligned} V_1 &= V_2 \\ I_1 &= I_2. \end{aligned} \tag{2}$$

Equations (1) and (2) together form a set of four equations in four variables, and if a solution other than the trivial all-zero solution exists, it is necessary that the determinant formed of the coefficients must vanish. Recalling that $AD-BC=1$, this requires that

$$A + D = 2. \tag{3}$$

When the resonance condition (3) is satisfied, the transmission ring may be treated as an *infinite* filter chain. This is an interesting viewpoint which allows the application of microwave filter techniques in studying the effect of axial grooves in the plunger surfaces.

If the four-terminal network shown in Fig. 1 can be decomposed into n identical four-terminal sections connected on an iterative basis, there exists a simple relation between the general circuit parameters of the individual sections and the resonance condition (3). From standard filter theory we know that if $\mathcal{A}$, $\mathcal{B}$, $\mathcal{C}$, $\mathcal{D}$ are the general circuit parameters of the individual section, the propagation parameter per section is

$$\gamma = \cosh^{-1}\left[\frac{\mathcal{A}+\mathcal{D}}{2}\right]. \tag{4}$$

Furthermore, the over-all propagation parameter of n such sections, iteratively cascaded, is simply

$$\Gamma = n\gamma. \tag{5}$$

This relation holds, even though the individual sections are asymmetric (i.e., $\mathcal{A}=\mathcal{D}$).

A relation similar to (4) also holds for the entire transmission ring, so that (5) may be written as

$$\Gamma = \cosh^{-1}\left[\frac{A+D}{2}\right] = 0 + j2\pi k \tag{6}$$

where k is any integer.

Equation (6) simply states that for resonance the attenuation must be zero (or nearly so) and the *total* phase shift around the ring must be some integral multiple of 360 degrees. This conclusion may appear to be self-evident, but it must be appreciated that the phase shift given by (6) is that which occurs in an ideal, iterative filter chain, and that the "electrical length" may differ radically from any measurable physical length associated with the ring. In particular, when there are n sections in the ring, resonance may be expected whenever β, the phase shift per section, is

$$\beta_k = \left(\frac{360^\circ}{n}\right)k. \tag{7}$$

As the simplest illustration of the foregoing, consider the resonant frequencies of the uniform-strip transmission ring shown in Fig. 2(a). The whole length of line forms the basic section, so that $n=1$ in (7) and resonances may be expected when the electrical length $\beta_1=360$ degrees, $\beta_2=720$ degrees, etc.

Consider next the effect of a single lumped discontinuity, such as a shunt susceptance or series reactance as shown in Figs. 2(b) and 2(c). By breaking these rings at any arbitrary plane and applying standard distributed-constant filter theory[4] to the resulting section, is is easily shown that the "loaded phase shift" β for the section is given by

$$\cos\beta = \cos\theta - m\sin\theta \tag{8}$$

where

θ = electrical length of line (without loading)

$m = \dfrac{X}{2Z_0}$ or $\dfrac{BZ_0}{2}$

Z_0 = characteristic impedance of line

X = lumped series reactance

B = lumped shunt susceptance.

Resonance of any of the rings of Fig. 2 will occur when $\beta=360^\circ\ k$ or when

$$\cos\theta - m\sin\theta = 1. \tag{9}$$

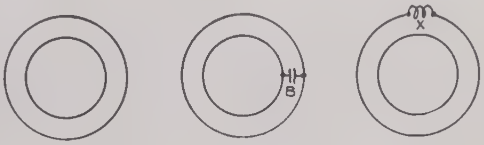

(a) (b) (c)

Fig. 2—Transmission rings. (a) No discontinuity. (b) Shunt discontinuity. (c) Series discontinuity.

It is of interest that (9) has two sets of solutions. The "quadrature-axis" solutions $\theta_{kq}=(360^\circ)k$ are independent of m. Hence, the addition of a single lumped discontinuity to a uniform transmission ring does not alter the original resonant wavelength of that ring. The discontinuity does produce, however, an *additional set* of "direct-axis" resonances at wavelengths differing slightly from those of the original resonances by an amount proportional to the discontinuity. That is, resonances may also occur when the line length is $\theta_{kd}=\theta_{kq}-\Delta_k$ where the Δ_k are the (radian) differences between the electrical line lengths for the quadrature- and direct-axis conditions.

Assuming that the Δ_k are small, the expression $\theta=\theta_{kq}-\Delta_k=2\pi k-\Delta_k$ when substituted in (9) and the resulting expression solved approximately for Δ_k, yields

$$\Delta_k \simeq 0,\ 2m. \tag{10}$$

---

[4] Paul I. Richards, "Applications of matrix algebra to filter Theory," Proc. I.R.E., vol. 34, pp. 145P–150P; March, 1946.

Hence, if l is the mean circumference of the transmission ring, the resonant wavelengths will be approximately

$$\lambda_{kq} = \frac{l}{k}$$
$$\lambda_{kd} \simeq \frac{l}{k}\,\frac{1}{1 - m/\pi k}. \tag{11}$$

It is of interest that when the shunt discontinuity is a lumped capacitance C, the resonant wavelength λ_{kd} may be written as

$$\lambda_{kd} \simeq \frac{l}{k}\,\frac{1}{1 - C/\overline{C}} \tag{12}$$

where $\overline{C}$ is the distributed capacitance of the line alone.

The physical explanation of why the discontinuity produces *pairs* of nearly equal-frequency resonances is that when the standing wave is in such a position that a voltage null appears across the shunt susceptance (or a current null appears at the series reactance) the discontinuity will have no effect. The "quadrature-axis" resonances correspond to this field distribution. On the other hand, when the standing-wave position is such as to give a maximum value at the discontinuity, "direct-axis" resonances at a slightly different wavelength are produced.

III. Transmission-Ring Model of a Slotted Plunger

Fig. 3 shows a cut-away view of a typical plunger, other aspects of which have already been discussed in previous papers.[5] It might appear at first glance that the analytic determination of the wavelengths at which the circumferential resonances occur in a slotted plunger, such as shown in Fig. 3, would be exceedingly difficult. Surprisingly, however, experience has shown that a relatively simple transmission-ring model can be established, the calculated lower-order resonances of which are in excellent quantitative agreement with experimental observations. Since this model is defined by the dimensions of the plunger, it provides a method of predetermining the optimum slotting configuration for a given situation.

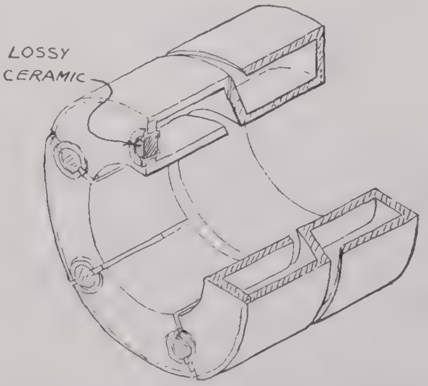

Fig. 3—Slotted plunger showing method of loading slots.

In setting up this model, the narrow gap (L-L-L in Fig. 4(a)) between the front and rear plunger sections is identified with the transmission line forming the transmission ring. Each slot that is cut through into this gap introduces a lumped impedance in series with the transmission ring at the junction d of the slot with the ring.

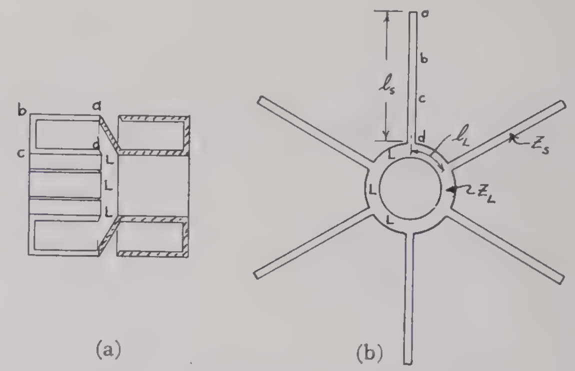

(a) (b)

Fig. 4—Slotted plunger and transmission-ring model for slot resonances.

The lumped impedance introduced in series with the transmission ring is the input impedance of a "stub line" of length l_s equal to the total length of the slot (i.e., $l_s = \overline{ab} + \overline{bc} + \overline{cd}$), and of characteristic impedance Z_s. If the "line" gap is assumed to have a characteristic impedance Z_L, the model shown in Fig. 4(b) may be established by making the mean circumference of the ring equal to that of the line gap L-L-L.

The resonant wavelength of the transmission ring will depend upon the ratio Z_s/Z_L. As a first approximation, this ratio should be equal to the ratio of the widths of "slot" and "line" gaps. Hence, the model is essentially defined by the physical dimensions of the plunger and its slots.

IV. Calculated and Experimental Results

In this section, we shall illustrate the foregoing theory by calculating the resonant wavelengths of a typical plunger similar to that shown in Fig. 3.

The plunger here considered was used in a $1\frac{3}{4}\times 15/16$-inch coaxial-line resonator to tune a 2K28 reflex klystron over a wavelength range of 7 to 14 centimeters. Before slots were added to this plunger, one-cycle parasitic resonances occurred in the outer gap at wavelengths of 13.58 and 12.80 centimeters, and in the inner gap at 7.90, 7.83, and 7.00 centimeters.[3] By slotting the plunger with five slots as shown in Fig. 3, the one-cycle resonances in the inner gap were moved to a wavelength of 20 centimeters, which is well outside the 5- to 14-centimeter tuning range. The three-cycle resonance that remained within the tuning range was suppressed by inserting lossy ceramic disks across the slots in the face of the plunger.[6]

---

[5] See the discussions of experimental results in footnote references 2 and 3.

For the example plunger with six slots, the "slot" length $l_s=4.32$ centimeters, and the "line" length $l_L=1.25$ centimeters. Here, the transmission ring consists of six sections, and by (8) the phase shift per section is

$$\begin{aligned}\beta &= \cos^{-1}\left\{\cos\theta - m\sin\theta\right\}\\ &= \cos^{-1}\left\{\cos(2\pi l_L/\lambda)\right.\\ &\qquad \left. - \frac{Z_s}{2Z_L}\tan(2\pi l_s/\lambda)\sin(2\pi l_L/\lambda)\right\}. \quad (13)\end{aligned}$$

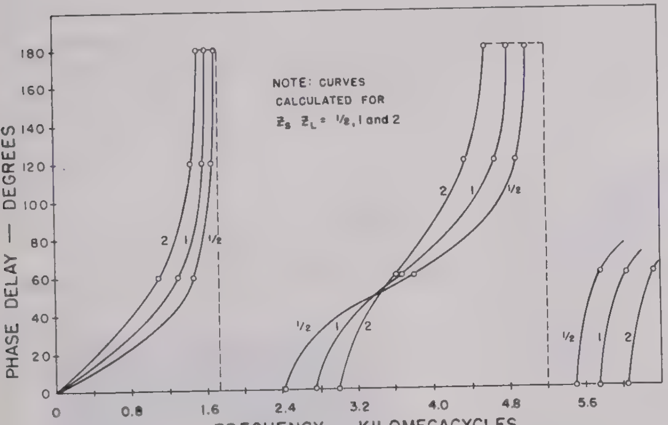

Fig. 5—Calculated phase delay for a 6-slot, Z plunger (per section)

To show the effect of various slot widths, we calculate β from (13) as a function of frequency for $Z_s/Z_L=\frac{1}{2}$, 1, and 2. The results are plotted in Fig. 5. Since these are six sections, resonance can be expected whenever β is an integral multiple of 60 degrees. These eigenvalues are marked by circles in Fig. 5.

Fig. 6 compares experimental data obtained from measurements on an actual plunger with the wavelengths calculated from Fig. 5. This plunger had 1/32-inch slots and a 1/16-inch line gap. Thus, the ratio of $Z_s/Z_L=\frac{1}{2}$ should yield the best model. The data of Fig. 6 are in excellent agreement for the lower-order resonances, but at the higher frequencies a ratio somewhat greater than $\frac{1}{2}$ seems to be required. However, the model holds qualitatively even there.

The small numerals immediately above the plotted data in Fig. 6 refer to the order of the resonance, i.e., the number of complete waves existing around the ring. It is significant that the transmission ring exhibits band-pass filter characteristics. Thus, as shown in Fig. 5, from 1600 to 2800 megacycles the ring is cut off; there is, in filter terminology, a large attenuation and constant phase shift of 180 or 360 degrees per section.[7] From roughly 2800 to 4800 megacycles, the chain is operating in the pass-band with zero attenuation (360 degrees has been repeatedly deducted from the true phase shift for ease in plotting). It should be noted that the resonance occurring at the upper edge of the first pass band is of zero order. That is, all sections are in phase. Also, it is significant that if seven slots had been cut in the plunger, the number of resonances within the tuning range would not have been increased, and the effectiveness of the slots would have been improved. In general, it is concluded that *an odd number of slots is preferable to an even number.*

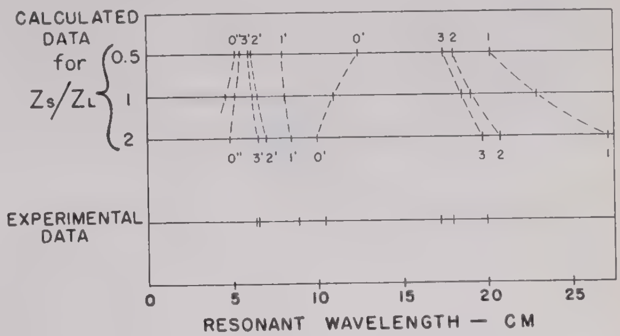

Fig. 6—Comparison of calculated resonance wavelength (based on transmission-ring model of Figs. 4 and 5) with experimental results.

In general, the smaller the circumference of the transmission ring, the fewer will be the resonances lying within a given tuning range. Hence, it is desirable that the slots open into the inner rather than the outer gap of the plunger; that is, *the Z-type plunger is generally to be preferred to the British S-type plunger.*[2]

V. Excitation of Slot Resonances

The excitation of the slot resonances may largely be attributed to slight asymmetries in the plunger segments, or near-by irregularities such as coupling loops, etc. When viewed from the cavity, the delineated plunger would appear somewhat as sketched in Fig. 7. Also shown in Fig. 7 is the *TEM* electric field across the plunger at the instant that the top conductor is positive and the bottom negative.

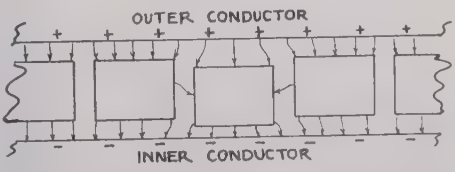

Fig. 7—Slot excitation due to a bent plunger segment.

Because of the displacement of the bent sector, a voltage will be induced across the slot on either side of this sector. These voltages will be *in phase*, but of *opposite sign* with respect to a given direction of propagation around the transmission ring. At resonance, the excitations occurring at the various slots may be combined into a single, equivalent excitation, provided the proper *phase shift* is applied to each of the slot excitations. Thus, suppose that the excitations across the two adjacent slots in Fig. 7 are F_1 and $-F_2$. Since the resonance undergoes a phase-shift of β degrees per section, the *equivalent* excitation acting at the first slot *only* would be

---

[6] Experimental data for this plunger with 3 or 5 slots in both S and Z configurations is given in Table 32-4 of footnote reference 1.

[7] When Z_s becomes infinite, the phase shift abruptly changes from 180 to 360 degrees, as shown by the broken lines in Fig. 5.

$$F = F_1 - F_2 e^{i\beta}. \tag{14}$$

It is apparent that maximum excitation will occur when $\beta = 180$ degrees, and, hence, the third-order resonances of Fig. 6 may be easily excited by a bent plunger sector.

Equation (14) may be generalized to include excitation of all n slots in the plunger. The excitation acting at each slot may be expressed in terms of variations in the plunger gaps. For coupling to the *TEM* wave, the F_k will all be in-phase but of mixed polarity, and the equivalent excitation will be

$$F = \sum_{k=1}^{n} F_k e^{ik\beta}. \tag{15}$$

If a perfectly symmetric plunger is mounted eccentrically in the cavity, the F_k will pass through a single cycle of variation around the plunger. This yields a strong excitation to the first-order resonance (i.e., when $\beta = 360°/n$) but only a slight excitation to higher-order resonances. But it will be noted that *the effect of slots is to greatly lengthen the wavelength at which the first-order resonance occurs.* Consequently, the only slot resonances occurring within the tuning range of a properly slotted plunger are higher-order resonances which have only a slight coupling to the dominant field. These resonances may usually be suppressed by "loading" the slots with some "lossy" dielectric, as shown in Fig. 3.

Contributors to Proceedings of the I.R.E.

Alfred C. Beck

Alfred C. Beck (A'30–SM'46) was born on July 26, 1905, at Granville, N. Y. He received the E.E. degree from Rensselaer Polytechnic Institute in 1927. After two summers in the test department of the New York Edison Company and a year as instructor in mathematics at Rensselaer, he became a member of the technical staff of Bell Telephone Laboratories in 1928. Since then he has been in the radio research department, working chiefly on antennas and microwave equipment. He is a New York State licensed professional engineer and a member of Sigma Xi.

◆

Prescott D. Crout was born in Columbus, Ohio, on July 28, 1907. He received the Ph.D. degree in mathematics from the Massachusetts Institute of Technology in 1930. He was employed by the General Electric Company from 1930 to 1932, and by the Raytheon Manufacturing Company from 1932 to 1934. He has been on the staff of the mathematics department at M.I.T. since that time, and now has the rank of associate professor.

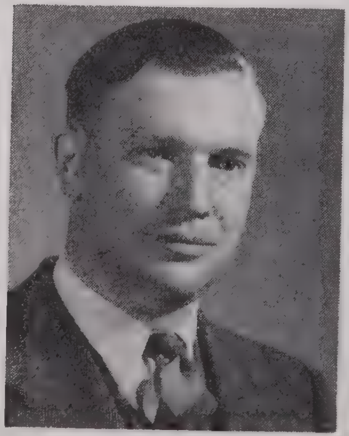

Prescott D. Crout

From 1941 to 1945 Dr. Crout was a staff member in the theoretical group of the M.I.T. Radiation Laboratory. He is a member of Sigma Xi, the American Physical Society, the American Institute of Electrical Engineers, and the American Mathematical Society.

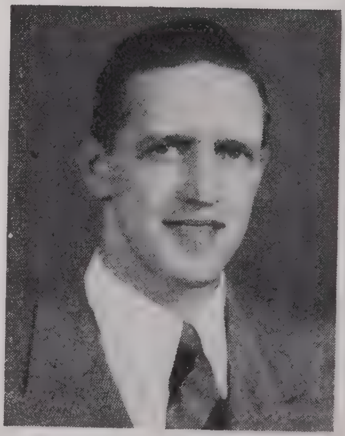

C. Chapin Cutler

C. Chapin Cutler (A'40) was born on December 16, 1914, at Springfield, Mass. He received the B.S. degree from Worcester Polytechnic Institute in 1937. Since 1937 he has been a member of the Technical Staff of the Bell Telephone Laboratories, engaged in radio research in the short-wave and microwave regions. He is a member of Sigma Xi.

◆

C. F. Edwards (A'41) was born at Greenfield, Ohio, on April 21, 1906. He received the B.A. degree in physics from Ohio State University in 1929, and the M.A. degree from the same University in 1930.

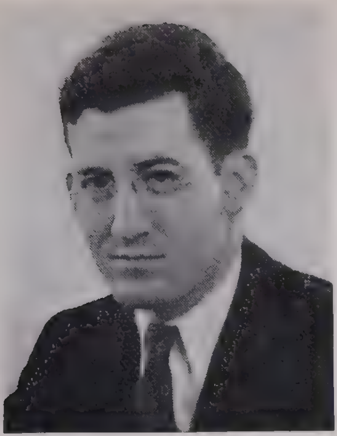

C. F. Edwards

From 1930 to 1934 he was with the American Telephone and Telegraph Company, engaged in short-wave transoceanic transmission studies. Since 1934 Mr. Edwards has been a member of the technical staff of the Bell Telephone Laboratories at Holmdel, N. J.

❖

Roberto M. Fano (S'41–A'45) was born on November 11, 1917, in Torino, Italy. He received the S.B. degree in electrical engineering from the Massachusetts Institute of Technology in 1941, and the Sc.D. degree in 1947. From 1941 until 1944 he was a member of the teaching staff of the electrical engineering department of M.I.T., first as an assistant and later as an instructor. In 1944 he joined the staff of the Radiation Laboratory, where he worked on the design of microwave components. Dr. Fano is co-author of one of the books in the Radiation Laboratory series.

After the war, Dr. Fano became a research associate in the electrical engineering department of M.I.T., and was recently made an assistant professor. He is an associate member of the American Institute of Electrical Engineers, and a member of Sigma Xi.

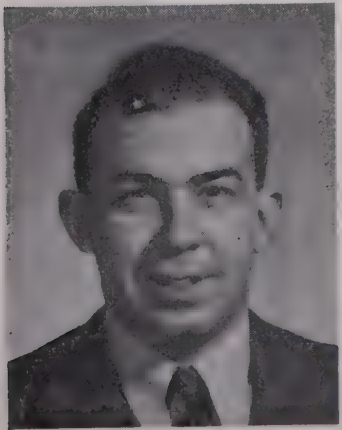

Roberto M. Fano

W. R. Garner was born on January 21, 1921, in Buffalo, N. Y. His formal training was in psychology, receiving the A.B. degree at Franklin and Marshall College in 1942, and the Ph.D. degree at Harvard University in 1946. From 1942 to 1943 he did graduate work, and in 1943 was appointed research associate at Harvard, doing contract research in the Harvard Office of Scientific Research and Development laboratories. He became an instructor in psychology at The Johns Hopkins University in February, 1946. Since that time, he has been teaching in the department of psychology at Johns Hopkins and doing research with Systems Research.

❖

John J. Glauber (A'27–SM'45) was born in New York, N. Y. on July 31, 1903, and received the M.E. degree from Stevens Institute of Technology in 1925. From 1925 to 1927, he was associated with the U. S. Tool Company, Ampere, N. J., engaged in variable-capacitor design. In 1927, he joined the Arcturus Radio Tube Company, Newark, N. J., as laboratory assistant, and was chief engineer from 1933 to 1936. He then joined the Westinghouse Lamp Company, Bloomfield, N. J., as a vacuum-tube development engineer, and in 1939 became development engineer for the National Union Radio Corporation, Newark, N. J.

❖

W. R. Garner

❖

From 1941 to 1947, Mr. Glauber was associated with the vacuum-tube department of the Federal Telecommunications Laboratories, New York. He is now chief engineer of the United Electronics Company, Newark, N. J.

❖

D. D. Grieg (A'41–SM'44) was born on February 26, 1915 in London, England. He received his early schooling in England and the B.S. degree in electrical engineering from the College of the City of New York. He has done graduate work at Columbia and New York Universities.

John J. Glauber

❖

From 1936 to 1940, Mr. Grieg was in charge of the television department of the Davega Radio Company. In early 1941 he taught radio communication in the Brooklyn Technical High School. Since 1941, he has been a research engineer for Federal Telecommunication Laboratories. He is now a division head and has charge of the television and communication departments.

Mr. Grieg is a member of the American Institute of Electrical Engineers. He has served on several technical committees, including the Television Committee of the Radio Technical Planning Board and those on Television Relays and Studio–Transmitter Links of the Radio Manufacturers Association. He is the author of several technical papers and holds many patents in the field of radio.

❖

Ferdinand Hamburger, Jr. (A'32–M'39–SM'43) was born on July 5, 1904, at Baltimore, Md. He received the B.E. degree in electrical engineering in 1924, and the doctorate in engineering in 1931, from The

❖

D. D. Grieg

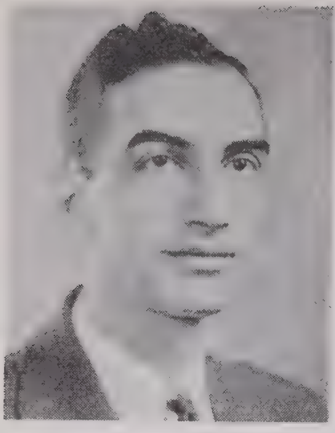

Ferdinand Hamburger, Jr.

Johns Hopkins University. From 1924 to 1925 Dr. Hamburger was with the Consolidated Gas, Electric, Light and Power Company of Baltimore, and from 1925 to 1929 he was a research associate at Johns Hopkins for the Underground Systems Committee of the National Electric Light Association. He was a graduate student at Johns Hopkins from 1929 to 1930; a Charles A. Coffin Fellow from 1930 to 1931; instructor in electrical engineering from 1931 to 1939; associate in electrical engineering from 1939 to 1941; and has been an associate professor in electrical engineering since 1941.

During the war Dr. Hamburger served as chief test engineer, Bendix Radio, Bendix Aviation Corporation; as a consultant to the Research and Standards Branch of the Navy Department; consultant to the National Defense Research Council; and since December, 1945, he has been associate director of Systems Research under contract between The Johns Hopkins University and the Office of Naval Research. He is a member of Sigma Xi, Tau Beta Pi, and the American Institute of Electrical Engineers.

❖

Andrew L. Hopper

Andrew L. Hopper (A'42–M'46) was born on January 11, 1906, at Mahwah, N. J. He received the E.E. degree from Rensselaer Polytechnic Institute in 1928. From 1928 to 1932 he was engaged in the development of machine switching circuits for the Bell Telephone Laboratories. The following four years provided a variety of experience, including electrification inspection for the Pennsylvania Railroad and electroacoustical acceptance testing for the New York Navy Yard.

In 1936 Mr. Hopper returned to Bell Laboratories and until 1942 was engaged in the development of telegraph circuits. From 1942 to 1945 he was concerned with the design of components for a number of microwave radars. He is now engaged in radio and television research.

❖

For a photograph and biography of W. H. Huggins, see page 936 of the September, 1947, issue of the Proceedings of the I.R.E.

❖

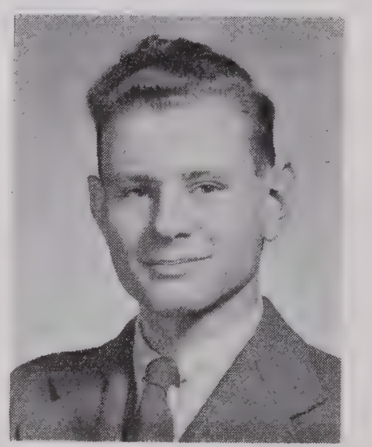

Ernest R. Kretzmer

Ernest R. Kretzmer (S'46) was born on December 24, 1924, in M. Gladbach, Germany, and came to the United States in 1940. He received the B.S. degree in electrical engineering from Worcester Polytechnic Institute in 1944, and the M.S. degree in the same field from the Massachusetts Institute of Technology in 1946. Since 1944 he has held the position of assistant on the electrical engineering staff at the Massachusetts Institute of Technology, being engaged in basic communications research at the present time.

Mr. Kretzmer is a student member of the American Institute of Electrical Engineers, and an associate member of Sigma Xi.

❖

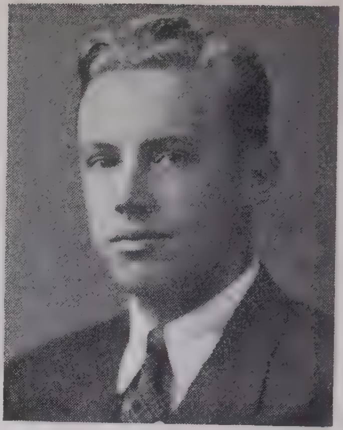

Norman T. Lavoo

Norman T. Lavoo (A'41–M'45) was born in St. Louis, Mo., on October 12, 1918. He received the B.S. degree in electrical engineering from Washington University in 1940. Since that time he has been associated with the General Electric Company, working in several of their development laboratories. He completed the three-year General Electric Advanced Engineering Program in 1943. At present he is in the electronics group of the Research Laboratory.

❖

A. W. Lawson was born in San Francisco, Calif., on March 3, 1917. He received the Ph.D. degree in physics from Columbia University in 1940. From 1940 to 1944 he was first an instructor and later an assistant professor of physics at the University of Pennsylvania. From 1942 to 1944 he served as official investigator on a National Defense Research Council contract concerned with the development on crystal rectifiers. In 1944, Dr. Lawson joined the Radiation Laboratory at the Massachusetts Institute of Technology as a staff member, where he worked variously on the development of transmit-receive tubes, antennas, r.f. filters, and the APS-30 airborne radar series. Since March, 1946, he has been associated with the University of Chicago as assistant professor of physics in the Institute for the Study of Metals.

Dr. Lawson is a Fellow of the American Physical Society, and associate editor of the *Review of Scientific Instruments*.

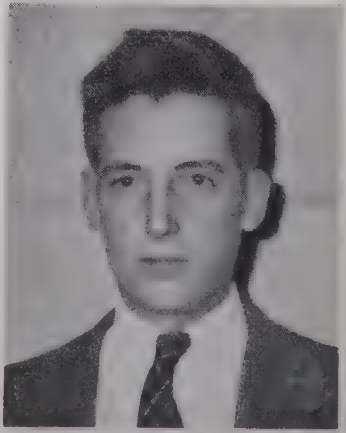

A. W. Lawson

Robert A. McConnell

Robert A. McConnell (S'35-A'38-SM-'47) was born at McKeesport, Pa., on April 6, 1914. He received the B.S. degree in physics from Carnegie Institute of Technology in 1935. Following three semesters of graduate study at the University of Pittsburgh, he devoted two years to petroleum prospecting with the Gulf Research and Development Company, and two years to the flight testing of aircraft at the Naval Aircraft Factory. In 1941 he joined the M.I.T. Radiation Laboratory. There, throughout the last two years of World War II, he supervised research in radar moving-target indication.

Dr. McConnell returned to the University of Pittsburgh in February, 1946, and received the Ph.D. degree in June, 1947. He is now assistant professor of physics at this university.

❖

Laurence A. Manning (S'43-A'45) was born on April 28, 1923, at Palo Alto, Calif. He received the A.B. degree from Stanford University in June, 1944, at which time he joined the microwave oscillator research group at the Office of Scientific Research and Development sponsored Radio Research Laboratory, at Harvard University. During the year prior to his graduation Mr. Manning had been engaged in ionosphere research in connection with the Interservice Radio Propagation Laboratory's activities at Stanford. Late in 1945 he returned to Stanford as a teaching assistant in the physics department.

In July, 1946, Mr. Manning was appointed a research associate in the electrical engineering department, and he has since been in charge of a program of contract research in high altitude propagation undertaken for the Army Air Forces.

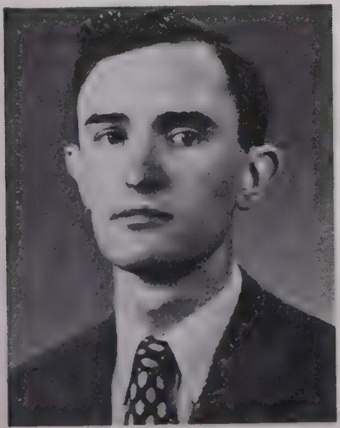

Laurence A. Manning

❖

John W. Miles was born on December 1, 1920, in Cincinnati, Ohio. He received the B.S. degree in electrical engineering in 1942, the M.S. degree in 1943, the aeronautical engineering degree in 1944, and the Ph.D. degree in 1944, from the California Institute of Technology. From 1941 to 1943 he was a teaching fellow there, and from 1943 to 1944, an instructor.

In the summer of 1942, Dr. Miles was employed by the General Electric Research Laboratory; in 1944, he was associated with the Radiation Laboratory of the Massachusetts Institute of Technology; and in 1945 he was with the aerodynamics department of the Lockheed Aircraft Company. He took a leave of absence from the engineering department of the University of California to participate in Operation Crossroads. At present, Dr. Miles is an assistant professor of engineering at the University of California. He is a member of the Institute of Aeronautical Sciences, Tau Beta Pi, and Sigma Xi.

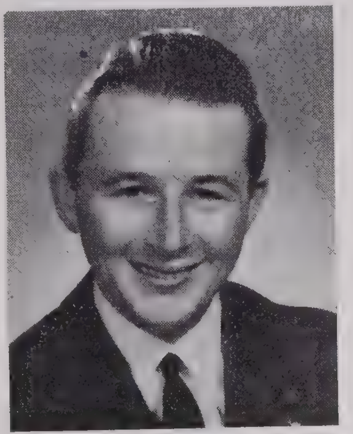

John W. Miles

❖

Stewart E. Miller (M'46) was born at Milwaukee, Wis., in 1918. He attended the University of Wisconsin for three years, and was there elected to Tau Beta Pi and Eta Kappa Nu. At the beginning of the senior college year he transferred to Massachusetts Institute of Technology and studied communications engineering under a joint Massachusetts Institute of Technology–Bell System co-operative plan. Studying under a Tau Beta Pi fellowship during the graduate year, he received the B.S. and M.S. degrees in electrical engineering in 1941, and was elected an associate member of Sigma Xi. Joining the technical staff of the Bell Telephone Laboratories as a member of the systems development department, he became engaged in repeater development for the coaxial-cable carrier system. During the war he was engaged in the design and development of centimeter-wave transmitter-receivers for the United States Army and Navy. When the war ended he became engaged in the development of transmission systems for coast-to-coast relaying of telephone and television.

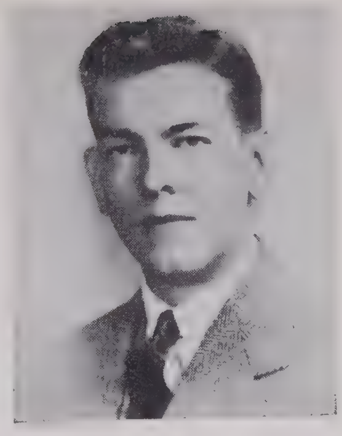

Stewart E. Miller

❖

Sidney Moskowitz (M'45) was born in Brooklyn, N. Y., on February 23, 1919. In 1940 he received the B.E.E. degree from the School of Technology of the College of the City of New York. From 1941 to 1945 he was a member of the evening-session staff at that College.

While teaching evenings, he was also engaged in the development of electronic apparatus for the Industrial Scientific Corpo-

Sidney Moskowitz

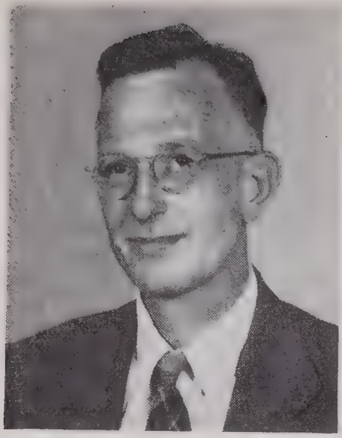

L. C. Peterson

ration in New York. In 1943 Mr. Moskowitz joined the Federal Telecommunication Laboratories, where he has been active in the design and development of pulse-time-modulation systems. He is a member of Tau Beta Pi.

❖

L. C. Peterson (A'32) was born in Varberg, Sweden, on November 8, 1898. He studied at Chalmers Technical University in Gothenberg and took further courses at the Technical Universities in Berlin and Dresden in Germany.

After finishing these studies, Mr. Peterson took the test course at the General Electric Company in Schenectady. A year later he became a member of the development and research department of the American Telephone and Telegraph Company.

In 1931 Mr. Peterson transferred to the Bell Telephone Laboratories as a member of the Technical Staff. Here his work has been largely concerned with the analysis of circuits and with vacuum-tube performance at radio frequencies.

❖

Lawrence L. Rauch

Lawrence L. Rauch was born in Los Angeles, Calif., on May 1, 1919. He received the A.B. degree in mathematics and physics from the University of Southern California in 1940. He was a graduate assistant in physics at Cornell University until 1941, at which time he entered the Graduate School of Princeton University in mathematical physics, where he is at present.

From 1937 to 1940 Mr. Rauch was engaged in broadcast engineering. During 1942 and 1943 he was an instructor in mathematics and a member of a National Defense Research Committee project at Princeton concerned with antiaircraft fire-control problems; during 1944 he lectured to officers of the Armed Forces assigned to the radar school at Princeton. From 1943 through 1946 he has been engaged, under several government contracts, in research and development of radio telemetering systems for flight-testing aircraft and missiles, and at present he is a consultant in this field. During 1946, at the request of the Navy, he organized and took a group to Bikini to do radio telemetering work in connection with Operation Crossroads. He is a member of the American Mathematical Society, Mathematical Association of America, Phi Beta Kappa, and Sigma Xi.

❖

D. H. Ring

❖

For a photograph and biography of Henry J. Riblet, see page 497 of the May, 1947, issue of the Proceedings of the I.R.E.

❖

D. H. Ring (A'30) was born in Butte, Mont., on March 28, 1907. He received the A.B. degree in 1929 and the E.E. degree in 1930 from Stanford University. Since 1930 he has been a member of the technical staff in the radio research department of the Bell Telephone Laboratories, where he has been engaged in research on radio problems in the short-wave and microwave bands. He is a member of Sigma Xi and Phi Beta Kappa.

Albert Rose

Albert Rose (A'36–M'40–SM'43) was born in New York, N. Y., on March 30, 1910. He received the A.B. degree in 1931 and the Ph.D. degree in physics in 1935 from Cornell University. From 1931 to 1934 he was a teaching assistant at Cornell University, and since 1935 he has been a member of the RCA Laboratories. Dr. Rose is a member of the American Physical Society.

❖

For a photograph and biography of Arthur L. Samuel, see the January, 1947, issue of the Proceedings of the I.R.E.

❖

J. B. Smyth was born in Pembroke, Ga., on June 8, 1914. He received the B.S. degree in 1934 and the M.S. degree in 1937 from the University of Georgia, and the Ph.D. degree in 1942 from Brown University. From 1937 to 1938 he was on the technical staff of the Tennessee Eastman Corporation. Since 1942 he has been engaged in electromagnetic-wave propagation studies at the United States Navy Electronics Laboratory, San Diego, Calif.

J. B. Smyth

L. G. Trolese

L. G. Trolese (A'42) was born on July 2, 1908, in Sonora, Calif. He received the B.S. degree in electrical engineering at the University of California in 1930. His engineering experience includes one year with Radio Corporation of America, RCA Victor Division, as a field engineer, and five years with General Air Conditioning and Heating Company, San Francisco, as electrical engineer. Since 1942 he has been with the United States Navy Electronics Laboratory at San Diego, where he is engaged on high-frequency wave propagation.

Warren A. Tyrrell (M'44) was born on October 2, 1914, in St. Louis, Mo. He received the B.S. degree in 1935 and the Ph.D. degree in 1939 from Yale University. Since 1939 he has been a member of the wave-guide research group of the Bell Telephone Laboratories, Holmdel, N. J.

W. A. Tyrrell

❖

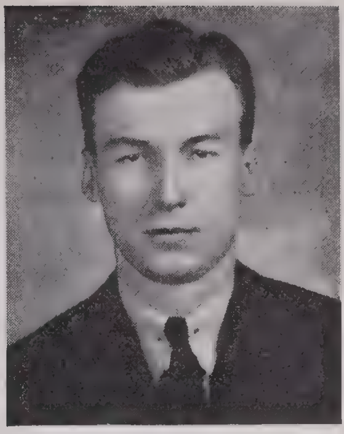

Paul K. Weimer

Paul K. Weimer (A'43) was born at Wabash, Ind., on November 5, 1914. He received the B.A. degree from Manchester College in 1936, the M.A. degree in physics from the University of Kansas in 1938, and the Ph.D. degree in physics from the Ohio State University in 1942.

During 1936 to 1937, he was a graduate assistant in physics at the University of Kansas. From 1937 to 1939, he taught physics and mathematics at Tabor College, Hillsboro, Kan. While at the Ohio State University, he was a graduate assistant in physics. Since 1942, he has been engaged in television research at the RCA Laboratories, Princeton, N. J.

Dr. Weimer is a member of the American Physical Society and Sigma Xi.

Correspondence

Quantitative Radar Measurements*

It is the purpose of this note to describe a method whereby quantitative measurements of radar transmission may be made using only standard radar test instruments. This method has been in use at the Naval Research Laboratory for several years.

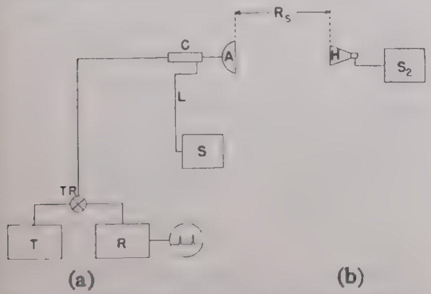

(a) (b)

Fig. 1—Block diagram of measuring arrangement (a), and calibration (b).

Fig. 1 (a) shows a block diagram of the method. To a standard radar there is added a test set S, which combines the functions of a power meter and a signal generator. S measures the average power of the radar through the directional coupler (or similar device) C and line (or wave guide) L. It also generates a synchronized pulse of controllable amplitude at the radar frequency, which appears on the A scope at an apparent range which can be adjusted at will. The "echo" due to the test set S can be adjusted to equal that of any echo it is desired to measure. In the case of rapidly fading echoes the peak value is usually chosen for comparison in measurements of this type.

The ratio of received to transmitted power is given by

$$\frac{P_R}{P_T} = \frac{G^2\lambda^2F^4\sigma}{64\pi^3R^4} \tag{1}$$

where P_R is the echo power delivered by the antenna, P_T is the radar-pulse power delivered to the antenna, G is the gain of antenna A, σ is the *radar area* of the target, F is the *propagation factor*, defined as the ratio of the *field intensity* produced at the target to that which would exist in free space, and R is the range of the target. (1) holds if F is constant over the dimensions of the target.

In the arrangement of Fig. 1 the test set S receives from the transmitted pulse an *average* power

$$P_T' = P_TD/g_Cg_L \tag{2}$$

where D is the duty cycle of the radar (=pulse length×repetition frequency), g_C is the insertion loss of the coupler C, and g_L is the loss in the line L. The pulse power generated by S which produces the same A-scope deflection as the target echo is

$$P_R' = P_Rg_Cg_L. \tag{3}$$

Introducing (2) and (3) into (1), there results

$$F^4\sigma = \frac{64\pi^3R^4D}{\lambda^2G'^2}\cdot\frac{P_R'}{P_T'} \tag{4}$$

where

$$G' = g_Cg_LG. \tag{5}$$

From (4) it follows that the test set need measure only *power ratios*, so that its absolute calibration is unimportant for this purpose. If the factor G' is known, (4) may be used to investigate the propagation factor F if the radar area of the target is known or is constant, or the radar characteristics of the target (σ) if the propagation factor is known.

The factor G' may be determined by measuring separately its constituent factors g_C, g_L, and G. However, G' may be measured directly by the calibration procedure shown in Fig. 1(b). A second test set S_2 transmits a synchronized pulse of peak power P_S through an antenna H (shown here as a horn) of known gain G_H. The location of antenna H and its directivity should be such that propagation over indirect paths makes a negligible contribution to the received signal, and the distance R_S should

---

* Received by the Institute, July 22, 1947.

be great enough to insure plane-wave illumination of the aperture of antenna *A*. An adequate criterion is $R_S > (d_A^2 + d_H^2)/\lambda$ where d_A and d_H are the biggest aperture dimensions of antennas *A* and *H*, respectively. The A-scope signal resulting from P_S is matched by one of power P_R' from test set *S*. Then

$$G' = \frac{1}{G_H}\left(\frac{4\pi R_S}{\lambda}\right)^2 \frac{P_R'}{P_S}. \qquad (6)$$

Here, again, only a power ratio is involved, so that absolute calibration errors can be canceled out simply by an intercomparison (or exchange of positions) of the two test sets.

The above calibration procedure also can be used to determine the gain of the standard antenna *H*. It is necessary to have two *identical* antennas, and determine the transmission loss, P_R/P_S, between them. Then

$$G_H = \frac{4\pi R_S}{\lambda}(P_R/P_S)^{1/2}. \qquad (7)$$

The measurement procedure outlined above may be modified and extended in several ways which need not be described here. An outstanding advantage of the above method of measurement is the fact that only power ratios need be measured. The measurement accuracy thus is essentially the calibration accuracy of the attenuator of the test set *S*.

Martin Katzin
Naval Research Laboratory
Washington 20, D.C.

Ultra-Short-Wave Propagation Studies Beyond the Horizon*

I have read with interest the paper by Wickizer and Braaten.[1] The authors treat, in some detail, the effect of atmospheric refraction on the signals received near the ground beyond the horizon. Their meteorological instruments were mounted within about 100 feet of the ground, and they state: "It may be concluded that the controlling (atmospheric) gradient is more than 100 feet above the ground in about 60 per cent of the cases when unusually strong signals are received beyond the horizon on this particular transmission path."

A somewhat similar study has previously appeared in the Proceedings[2] in which a correlation was noted between day-to-day meteorological conditions and 41.5-Mc. beyond-the-line-of-sight average signals over a transmission path much like that of reference 1. The refractive effects were found to be associated with slow, large-amplitude fading of the received signal which appears to be synonymous with the term "unusually strong signals" as used by the above authors. However, free-air meteorological data were used from which the dielectric constant at the ground and at a height of 0.3 kilometers, the lowest height of observation, were determined.

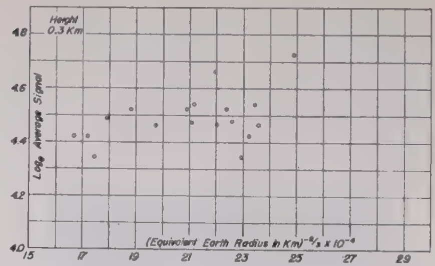

Fig. 1—Check of relation $\log_e$ (average signal) ∝ (equivalent earth radius)$^{2/3}$. 11:00 G.M.T. signal; 12:00 G.M.T. free-air data. Assumes linear e gradient. Height 0.3 kilometers.

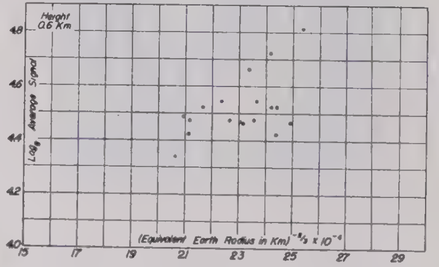

Fig. 2—Similar to Fig. 1, height 0.6 km.

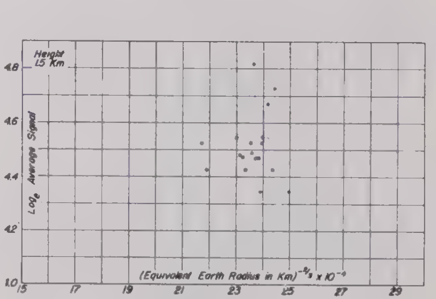

Fig. 3—Similar to Fig. 1, height 1.5 km.

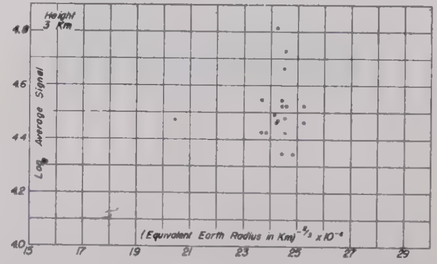

Fig. 4—Similar to Fig. 1, height 3.0 km.

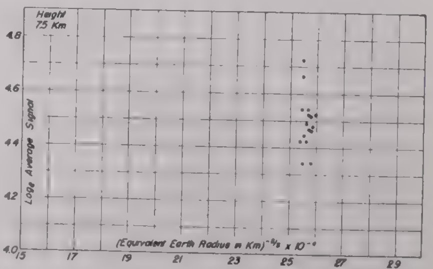

Fig. 5—Similar to Fig. 1, height 7.5 km.

In view of the interesting question as to what height above the earth's surface meteorological conditions are effective in returning such signals toward a receiving point near the ground, the data of reference 2 were re-examined as follows: The free-air data for the days of interest were determined for heights of 0.6, 1.5, 3, and 7.5 kilometers. Noon data is involved and no inversions were noted. From these observations the equivalent earth radiuses, assuming a linear dielectric-constant gradient, were calculated. The results appear in the figures below.

Fig. 1 is equivalent to Fig. 8 of reference 2 and is for a height of 0.3 kilometers. These data, for reasons discussed in reference 2, are considered a definite check on the effect of refraction since theory predicts a linear variation, with positive slope, for the variables noted when plotted as in this figure. Fig. 2, 3, 4, and 5 are similar to Fig. 1 but for heights of 0.6, 1.5, 3, and 7.5 kilometers, respectively. It will be noted that the correlation between variables begins to break down at a height of 1.5 kilometers.

The data presented are believed to: (a) verify the statements of the authors of reference 1 to the effect that atmospheric heights greater than about 100 feet are effective in returning signals of these frequencies back towards the earth; and (b) indicate that the portion of the atmosphere so effective is the region below about 1.5 kilometers for the experimental conditions involved.

A. H. Waynick
The Pennsylvania State College
State College, Pa.

---

* Received by the Institute, August 7, 1947.

[1] G. S. Wickizer and A. M. Braaten, "Propagation studies on 45.1, 474, and 2,800 megacycles within and beyond the horizon," Proc. I.R.E., vol. 35, pp. 670–680; July, 1947.

[2] A. H. Waynick, "Experiments on the propagation of ultra-short radio waves," Proc. I.R.E., vol. 28, pp. 468–475; October, 1940.

Scalar and Vector Potential Treatment*

Smith and Shulman[1] have recently applied a variational method to the calculation of the change in the resonant frequency of a cavity due to the introduction of an electron beam. The derivation of the result (74) can be somewhat simplified by a so-called gauge transformation.

As noted on page 651 of Smith and Shulman's paper, the scalar and vector electromagnetic potentials are not completely defined by (55a) and (55b) but may be subjected to one additional condition. They choose this condition to be div $A=0$, but an equally acceptable (and more usual) choice is div $A+\mu\epsilon\dot{\phi}=0$. Equations (55a) and (55b) then take the form:

$$\nabla\cdot\nabla A - \mu\epsilon\ddot{A} = -\mu J$$
$$\nabla^2\phi - \mu\epsilon\ddot{\phi} = -\rho/\epsilon.$$

Thereafter, the argument of Smith and Shulman may be carried through with the following simplifications:

(a) Omit all equations in ϕ and ρ.

(b) Omit all terms in ϕ and ψ in the remaining equations.

(c) Omit the remark just before (74). It will be seen that this reduces both the explicit and implied mathematical manipulations by about half, and avoids one use of

---

* Received by the Institute, July 17, 1947.

[1] Lloyd P. Smith and Carl I. Shulman, "Frequency modulation and control by electron beams," Proc. I.R.E., vol. 35, pp. 644–657; July, 1947. Equation numbers refer to those in this paper.

the convenient, if rather annoying, phrase "it can be shown."

I feel that the authors are to be congratulated on both the use and dissemination of these powerful methods. It is unfortunate that there is so little literature in English on the expansion, completeness, and orthogonality theorems on which these arguments depend.

Paul I. Richards
Brookhaven National Laboratory
Upton, L. I., N. Y.

Selective Demodulation*

In the June issue of your journal you published a paper by D. B. Harris.[1] You may be interested to know that the proposed method of demodulation was checked experimentally by me in 1934, and a patent covering the method was granted to the State Telecommunication Works in Warsaw in June, 1939 (first application made in August, 1934).

The main points contained within that patent are as follows:

(a) The demodulation is being obtained by "multiplying" the incoming signal by the locally generated signal synchronized to the frequency of the incoming carrier.

(b) The generation of the local oscillations, as well as the synchronization and modulation, can be performed by the same multielectrode tube of a proper design.

(c) In the example given in the description, the tube used was an early Philips hexode (EH1), where the local oscillator was working in a transitron circuit. The anode-current signal-grid-voltage characteristic was linear. This tube was showing a particularly strong pulling effect between the input signal and the local oscillator. This effect was, of course, detrimental from the point of view of the normal use of the tube as a frequency converter in superhetrodyne receivers, and it caused the withdrawal of the tube from the market. The behavior of the tube, however, was ideal for a "selective-demodulation" circuit, and several receivers built by me with this tube were working quite well and strictly in accordance with theoretical considerations.

B. Starnecki
Ministry of Supply
Signals Research and
Development Establishment
Hants, England

---

* Received by the Institute, August 11, 1947.

[1] D. B. Harris, "Selective demodulation," Proc. I.R.E., vol. 35, pp. 565–572; June, 1947.

Resonant Frequencies of n-Meshed Tuned Circuits*

In his letter Philip Parzen[1] has gone to some pains to show that "In an n-meshed coupled tuned circuit multiplying all inductances, both self and coupled, by a factor A^2, and all capacitances, both self and coupled, by a factor of B^2, the resonance frequencies of the circuit are multiplied by a factor $1/AB$."

The above property is nothing but a particular case of the following, well-known theorm: If a network N' is a model of N and the model factors of L, C, and ω are, respectively, k_L, k_C, and k_ω then,

$$k_\omega = \frac{1}{\sqrt{k_L k_C}}.$$

Thus, if

$$k_L = A^2, \qquad k_C = B^2$$

then

$$k_\omega = \frac{1}{\sqrt{A^2B^2}} = \frac{1}{AB}.$$

Lotfi A. Zadeh
Columbia University
New York, N. Y.

---

* Received by the Institute, March 30, 1947.

[1] P. Parzen, "On the resonant frequencies of n-meshed tuned circuits," Proc. I.R.E., vol. 35, pp. 284–285; March, 1947.

Nodal Method of Circuit Analysis*

I have noted with interest the articles and comments on the nodal method of circuit analysis, particularly the communication by William H. Huggins.[1] It seems to me that the choice of the nodal or mesh method of analysis depends fundamentally upon the following factors:

1. If the nullity is less than the rank, the mesh method is preferable; and
2. If the rank is less than the nullity, the nodal method is preferable.

The reason is that, by proper choice of method, a lesser number of simultaneous linear equations have to be solved, and the order of the resultant determinant is less.

As a simple example, in Fig. 1(a) the nullity N is 3 and the rank R is 4; hence the mesh equations would be preferred. In Fig. 1(b) the nullity is 4 and the rank is 1; hence the nodal equations would be employed. The definitions of rank and nullity are evident from the figure.

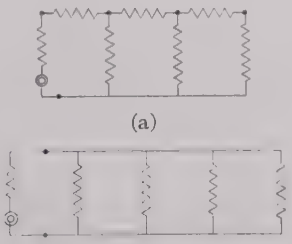

(a)

(b)

Fig. 1—Examples of two networks having different ranks and nullities. Let B = number of branches, V = number of vertices or nodes, and P = number of separate parts in a circuit. Then $N = B - V + P$ and $R = V - P$.
(a) $N = 3$ and $R = 4$.
(b) $N = 4$ and $R = 1$.

The remarks made by Mr. Huggins would therefore appear to be of secondary importance; nevertheless, they are very interesting.

Albert Preisman
Capitol Radio Engineering Institute
Washington 10, D.C.

---

* Received by the Institute, July 16, 1947.

[1] W. H. Huggins, "Node-pair method of circuit analysis," Proc. I.R.E., vol. 34, pp. 661–662; September, 1946.

Federal, Elwell, and Stone*

Although I have not received my copy of the August, 1947, issue of the Proceedings of the I.R.E., I am informed that it carries a statement on page 804 stating *inter alia* that I had "organized the Federal Telegraph Company on the Pacific Coast." This statement is not correct. I was President of Federal Telegraph Company of California from 1924 to 1931, but since the Federal Telegraph Company was incorporated in 1911, and its predecessor, the Poulsen Wireless Telegraph and Telephone Company, was organized in 1909, it should be clear that I was in no way connected with the original organization of either company.

The Poulsen Wireless Telegraph and Telephone Company was actually organized through the efforts of Cyril F. Elwell, who deserves the credit for bringing the Poulsen arc to the United States.

Out of fairness to Mr. Elwell, I shall be grateful if you will publish this letter in the next issue of the Proceedings.

Ellery W. Stone
P.O.B. 2034
Cairo, Egypt

---

* Received by the Institute, September 9, 1947.

Attention, Authors

PAPERS DESIRED FOR 1948 I.R.E. NATIONAL CONVENTION

Outstanding papers on timely subjects are desired for the technical program of the I.R.E. National Convention scheduled for March 22, 23, 24 and 25, 1948. All of the radio and electronic fields will be included to make the program truly representative of the interests of the Institute. It will be possible to accept only a limited number of papers. To receive consideration, the following rules must be followed:

1. The title and a brief abstract of the paper, similar to the summaries published at the beginning of the papers in the Proceedings of the I.R.E. but not more than 75 words in length, should be submitted as soon as possible. No abstracts can be considered which are received after November 30, 1947.
2. Correspondence should be addressed to Chairman, Technical Program Committee, Dr. Charles R. Burrows, Director, School of Electrical Engineering, Cornell University, Ithaca, New York.
3. The length of the paper should be such that oral presentation can be made within 20 minutes, in order to allow adequate time for general discussion.
4. Authors are responsible for obtaining military clearance where required.
5. Submission of the papers for publication in the Proceedings of the I.R.E. is desired, but is not a necessary requirement for acceptance.
6. Papers published in any journal prior to the date of the Convention necessarily will be withdrawn from the program.
7. A condensed 750-word summary of the paper must be prepared by the authors whose papers are accepted, and must be available by January 15, 1948.

Institute News and Radio Notes

REVISED CONSTITUTION APPROVED

The Tellers Committee has reported the following results of balloting on the Revised Constitution: 6143 ballots mailed; valid ballots received, 3074, or 50 per cent of those mailed; 2753 (88.1 per cent) for, 321 (10.2 per cent) against. The Revised Constitution has therefore been adopted as of July 15, 1947.

NUCLEONICS

The Executive Committee, at its August 5, 1947, meeting, agreed on the following bases for procurement of papers on nucleonics for publication in the PROCEEDINGS OF THE I.R.E.

(1) The Institute's contribution in this field will be to further the development of "electronic aids to nucleonics." (2) Such aids are, for the present, primarily in the nature of electronic instruments, control devices, and special arrangements whereby any of the necessary conditions can be brought about or maintained during nucleonic processes using electronic means or devices to produce or to control such conditions. (3) A new special Group of the I.R.E. Papers Procurement Committee shall carry out the proposed program.

NUCLEAR SUBJECTS DISCUSSED

Representatives of The Institute of Radio Engineers have been meeting with officials of the Atomic Energy Commission in a series of conferences designed to implement organizational liaison in the electronic instrumentation aspects of nuclear research.

The interest of I.R.E. in the field of nuclear studies, as outlined by President W. R. G. Baker, is primarily in electronic instrumentation and electronic processes of control of the production and utilization of nuclear energy.

JOINT TECHNICAL COMMITTEE

The Executive Committee, at its August 5, 1947, meeting, approved on behalf of the Board of Directors, the formation of a Joint A.I.E.E., I.R.E., and NEMA Co-ordination Committee on Commercial Induction and Dielectric Heating Apparatus. G. P. Bosomworth, Chairman of I.R.E. Industrial Electronics Committee, was elected I.R.E. representative on the joint committee.

STUDENT BRANCH

The Board of Directors, at its September 10, 1947, meeting, approved the petition for the formation of a Student Branch at Kansas State College.

ABBREVIATIONS

A list of approved abbreviations, as used by the Editorial Department of the Institute, has been made available to authors, technical committee personnel, and others who might be interested, in order to secure as nearly uniform practice as possible. Its use is urged. Copies are available on request.

BUENOS AIRES SECTION "ENGINEERING WEEK"

The Buenos Aires Section is holding another "Engineering Week," November 9 through 14, 1947. President W. R. G. Baker will address the meeting by means of a recording.

PRINCETON SECTION INAUGURAL MEETING

The inaugural meeting of the Princeton Section, on the occasion of its change-over from a subsection, was held October 9, 1947 Dr. Alfred N. Goldsmith, Editor of I.R.E., was invited to present an address. He expressed the good wishes and felicitations of the Institute and its Board of Directors to the new Section on that occasion.

NEW STANDARD

The Executive Committee approved, at its September 9, 1947, meeting, the official I.R.E. adoption of the Standard on "Methods of Testing F.M. Broadcast Receivers."

MATHEMATICAL ASSOCIATIONS MEETINGS

The American Mathematical Society, the Institute of Mathematical Statistics, and the Mathematical Association of America, met in New Haven, Conn., from September 1 to 5, 1947.

An outstanding feature of the meeting of the Mathematical Association of America was the symposium or round-table discussion on mathematical problems at the college level. Mathematicians from various institutions formulated procedures, on the basis of their personal experience in research and teaching, which they found particularly useful in handling and solving problems.

Those who delivered addresses at the symposium of the Institute of Mathematical Statistics were: Churchill Eisenhart, "Tests of Significance," C. P. Winsor, "Estimation," and Joseph Berkson, "Non-Standard Cases." There was also an address by the noted statistician, R. A. Fisher; and, by invitation of the program committee, Professor Abraham Wald of Columbia University delivered an address on "Sequential Estimation and Multi-decisions."

For the American Mathematical Society this was its fifty-third summer meeting. A series of four colloquium lectures on Abstract Algebraic Geometry were given by Professor Oscar Zariski of Harvard University. Professor S. S. Wilks of Princeton University, who was a special guest speaker, addressed the group on "Sampling Theory of Order Statistics." In addition, there were over 100 contributed papers in various fields of pure and applied mathematics.

ELECTRONICS RESEARCH FELLOWSHIPS

The Radio Corporation of America Fellowship Board of the National Research Council has announced the first series of awards to five young scientists. These fellowships for the academic year 1947–1948 provide for advanced graduate study and research in the broad field of electronics. The successful candidates for these awards are:

Arnold S. Epstein, B.S. in electrical engineering, Lehigh University, for continuation of graduate study at the University of Pennsylvania with special reference to selenium and other rectifiers as variable capacitors.

Willis W. Harman, B.S. in electrical engineering, University of Washington, for continuation of graduate study at Stanford University with special reference to the use of microwaves in certain cavity oscillators

Arnold E. Moore, B.S. in chemistry, Polytechnic Institute of Brooklyn, for continuation of graduate study at Cornell University with special reference to electronic properties of semiconductors.

Sol Raboy, A.B. in physics, Brooklyn College, for continuation of graduate study at Carnegie Institute of Technology with special reference to the properties of semiconductors and their use as crystal counters.

H. Gunther Rudenberg, S.B. and M.A. in physics, Harvard University, for continuation of graduate study at Harvard University with special reference to operation and design of wide-band pulse amplifiers.

These fellowships have been made possible by a grant to the National Research Council from the Radio Corporation of America, Inc., for the purpose of increasing the number of trained scientific personnel and for the furtherance of electronics and closely related fields. The selection of the fellows and the administration of the fellowship program are under the direction of the RCA Fellowship Board of the National Research Council, the members of which are Frederick E. Terman, chairman; C. C. Chambers, W. G. Dow, Frederick M. Feiker, R. Clifton Gibbs, I. I. Rabi, and Lloyd P. Smith.

Applications for the next series of awards for the academic year 1948–1949 must be filed before February 1. Stipends will be from $1600 to $2100 a year and an added amount, not to exceed $600, may be provided annually to the institution to which the fellow is assigned for tuition or necessary equipment.

Further information concerning these fellowships and application blanks may be secured from the Secretary of the RCA Fellowship Board, National Research Council, 2101 Constitution Avenue, Washington 25, D. C.

PUBLICATION OF AUTOMATIC COMPUTING MACHINERY DATA

The quarterly journal, *Mathematical Tables and Other Aids to Computation*, will publish a new feature section, "Automatic Computing Machinery," designed to disseminate information and news on research and development in the field of high-speed automatic calculating machinery, beginning with the October issue. The journal can be obtained from the National Academy of Sciences, 2101 Constitution Avenue, Washington, D. C.

Industrial Engineering Notes[1]

DIAMONDS AS ATOMIC RADIATION DETECTORS

Testing of diamonds for detection and counting of gamma radiation has revealed, according to the National Bureau of Standards, that they are at least one thousand times more sensitive, size for size, than any man-made counter. To the advantages of high sensitivity and long life is added smallness of size which permits use of such counters inside the human body or in small openings in industrial equipment.

RESEARCH ON ELECTRON TUBES

The National Bureau of Standards is making a study of vacuum tubes in collaboration with industry in its new tube laboratory. The research, which is both basic and applied, deals with the study of electron emission from cathodes and other elements in the tube envelope, the prevention of "gas clean-up," the gradual absorption of gas in high-current relay and rectifier tubes used in industry, finding and eliminating the causes for mechanical tube noise, the development, improvement, comparison, and standardization of test methods and equipment for evaluating tube performance. One of the developments which is expected to have a profound effect in industrial and commercial fields will be tubes with a life expectancy of from 15,000 to 20,000 hours, or ten to twenty times the life of the present-day computer tubes.

The National Bureau of Standards *Technical News Bulletin* for October, which gives a thorough description of this program, may be obtained by sending 10 cents to the Superintendent of Documents, Government Printing Office, Washington 25, D. C.

VISIBILITY MEASURING DEVICE

An electronic instrument for measuring atmospheric visibility which promises to be an important addition to airport safety equipment has been developed by government scientists. The new device, called a transmissometer, was designed in the National Bureau of Standards' airport lighting laboratory to reduce the human factor in visual estimates of distance, particularly in foggy weather. A complete description was published in the September issue of the Bureau's *Technical News Bulletin;* copies may be obtained from the Superintendent of Documents, Washington 25, D. C. at $.10 a copy.

GERMAN CERAMIC PRESSES

The Office of Technical Services has issued a report on two novel German machines: an automatic mechanical press for dry pressing steatite ceramics, and a combination spot-welding and impact press for fastening metal parts to ceramics. The report (PB-6494: photostat, $3.00; microfilm, $.50), describing the two machines in detail, is available through the Office of Technical Services, Department of Commerce, Washington 25, D. C. Checks should be made payable to the Treasurer of the United States.

DEVELOPMENT OF MICROTUBE

The Bureau of Standards has announced the development in its laboratories of the microtube, or "rice-grain" tube, which is a trifle larger than a grain of rice and not quite the size of an average pencil eraser. The tube was originally one-quarter inch in diameter, but design simplifications which had been introduced facilitated a further reduction in size. No other details are available as the microtube has various military applications.

NATIONWIDE-SCALE RESEARCH URGED BY SCIENCE BOARD

A proposal was recently set before President Truman by his Scientific Research Board recommending expenditures of at least one per cent of the country's annual income by 1957 for the expansion of scientific research. This would mean expenditures of more than two billion dollars a year, or about twice the amount that is being spent now. Half the money, the board said, should be provided by the Federal Government and the rest by industry, education, and privately financed research organizations. Due to the present shortage of trained scientists, a completely balanced program of expansion would be impossible before 1957.

The report, which is the first of five on "Science and Public Policy," was submitted by John R. Steelman, assistant to the President and board chairman. The document stressed the need for American accomplishments in "basic research."

NEW ELECTRONIC COMPUTER

One of the giant high-speed electronic computing machines, now under development by the Bureau of Standards, will be installed at the Bureau's newly established Institute of Numerical Analysis, University of California, Los Angeles, Calif., when completed.

"These computers will solve problems in minutes that now take days to work out, and will solve in days problems that are now out of the reach of scientists," the Bureau has announced. "Design specifications call for high memory capacity and automatically sequenced mathematical operations from start to finish at speeds attainable only with electronic equipment."

NEW INDEX TO TECHNICAL REPORTS

The third volume of a comprehensive index to reports on wartime technological developments in the United States, and in Germany and other foreign countries, was recently released for sale by the Office of Technical Services.

The index is intended for use with the OTS *Bibliography of Scientific and Industrial Reports*, which has been published weekly since January, 1946, and which lists all reports acquired by the Office with a brief abstract of each. The new index is available from the Superintendent of Documents, United States Government Printing Office, Washington 25, D. C., at 35 cents a copy.

WAR TECHNICAL REPORTS AVAILABLE

Approximately 2500 reports of research on wartime technical problems sponsored by the Office of Scientific Research and Development, and now released from security restrictions, are now available to the public, according to a *Bibliography and Index* recently published by the Office of Technical Services, United States Department of Commerce.

Orders for the *Bibliography and Index* (PB-78000; *OSRD Reports—Bibliography and Index;* multilith, $.75; 109 pages) should be addressed to the Office of Technical Services, Department of Commerce, Washington 25, D. C., and should be accompanied by check or money order, payable to the Treasurer of the United States.

NEW TECHNICAL SUBJECT LIST

A new list of scientific and technical subject headings, designed for the use of librarians and scientific research workers, and covering the latest advances in the fields of electronics, explosives, ordnance, tropicalization, aeronautics, photography, metallurgy, nuclear physics, and others, has been released by the Office of Technical Services. The document (PB-79322, *Subject Headings for Technical Libraries*, multilith, $1.50, 167 pages) is available through the Office of Technical Services, Department of Commerce, Washington 25, D. C., and should be accompanied by check or money order, payable to the Treasurer of the United States.

F.C.C. PROPOSES ABOLITION OF SHARING OF TELEVISION CHANNELS

The F.C.C. has issued a formal notice of a proposed amendment in its rules and regulations to abolish the sharing of television channels with other radio services, and to assign non-government fixed and mobile radio services, which were to share certain channels with television, to the 44–50-Mc. band. As a result of comprehensive studies on the subject, the Commission is of the opinion that there is no practicable sharing arrangement which will not cause serious interference to television reception.

F.C.C. EXTENDS LICENSES OF GENERAL MOBILE STATIONS

The F.C.C. has extended to November 1, 1948, the license term of all General Mobile Class 2 Experimental licenses which normally would have expired November 1, 1947, if not renewed by application before September 1, 1947.

"It is contemplated that the General Mobile hearing set for October 27, 1947, will result in the establishment of a regular service for which many licensees of Experimental General Mobile Systems will be eligible," the F.C.C. said. "In this event it will be necessary for eligible experimental licensees to apply for authority to operate in such a service, and the extension will serve to avoid a duplication of work involved in the submission and processing of applications for renewals as well as new licenses."

EXPERIMENTAL AMATEUR F.M. AUTHORIZED BY F.C.C.

Under F.C.C. Order 130-P, the Commission has authorized the use of narrow-band f.m. for radiotelephony in the bands of 3850–3900 kc. and 14,200–14,250 kc. by Class A amateur radio operators. In addition, the holder of any class of amateur radio operator license is authorized to use narrow-band f.m. radiotelephony at any licensed amateur radio station on frequencies from 28.8 to 29 Mc. and from 51 to 52.5 Mc. This authorization is on an experimental basis until further order of the Commission, but in no event beyond August 1, 1948. The order also included authorization for use of the band 5650–5925 Mc., which the F.C.C. recently allocated to replace the amateur band 5650–5850 Mc.

---

[1] The data on which these NOTES are based were drawn, by permission, from "Industry Report," issues of August 8, 15, 22, and 29, and September 5, 1947, published by the Radio Manufacturers' Association, whose courteous co-operation in this matter is gratefully acknowledged.

RAILROAD USE OF RADIO GROWS

The F.C.C. has called attention to the inauguration of public radiotelephone service on moving trains, and the growing uses of radio communications facilities by the railways. About 100 authorizations, representing 75 land stations and 700 mobile units, contribute to the safety and efficiency of rail operation. It is believed that this latter type of radio service, designed to aid train operation and yard and terminal traffic control, will become the most important adaptation of radio by the railroad industry.

NEW OPERATOR LICENSE PLAN

The F.C.C. has announced the first step in its plan to place the commercial radio operator examinations and licenses in step with the advancements that have been made in the industry. The plan provides, in part, for three classes of broadcast operator licenses authorizing operation of Standard, International, Frequency Modulation, Facsimile, Television, Development, and Auxiliary Broadcast stations.

F.C.C. PRIMER ON RADIO

The F.C.C. has recently issued *Radio—A Public Primer*, a 25-page mimeographed report containing a review of the various radio services, a brief history of broadcasting, and a short explanation of how the Commission "polices the ether." Published by the Government Printing Office, copies of the report are available from the Superintendent of Documents.

NEW F.M. STATIONS

The F.C.C. approved two new conditional grants for new f.m. stations and authorized construction permits for eight other f.m. outlets on August 22, 1947. As of September 4, 1947, 276 f.m. stations were in operation with 14 new stations having gone on the air during August and eight during the first week of September.

SURPLUS ELECTRONIC EQUIPMENT TO SCHOOLS

War Assets Administrator Robert M. Littlejohn has announced a plan whereby surplus electronic equipment which would otherwise have to be scrapped because of the lack of commercialized markets, will be allocated to schools for training programs. Major engineering schools will receive equipment on contract for research and development work on its adaptation to training purposes. The Federal Works Agency will have equipment transferred to it without charge for use in schools having veteran training programs. Equipment will be made available at 5 per cent of fair value to state educational agencies for distribution to their schools.

NEW RADAR SYSTEM INSTALLED

Two new devices, a separate v.h.f. radio-identification indicator and a radar height-finding antenna, have been installed as part of a new radar all-weather landing and traffic system at the Naval Air Station, Quonset Point, R. I.

SIGNAL CORPS CONTRIBUTES TO SCHOOL EQUIPMENT

During the past year approximately 3,500 schools and educational institutions have received donations of surplus equipment from the Signal Corps. This represents over $6,000,000 in material. Additional requests are being filled.

ARMY SIGNAL ASSOCIATION APPOINTMENTS

Frederick R. Lack was recently appointed chairman of a general committee on manufacturing by the Army Signal Association. Mr. Lack is a director of The Institute of Radio Engineers and a member of its Executive Committee. Major General G. L. Van Deusen, (ret.) was named chairman of the military training committee.

NEW CHIEF OF SIGNAL CORPS BRANCH

Colonel F. W. Kunesh has been designated Chief, Industrial Mobilization Branch Office of the Chief Signal Officer, succeeding Colonel J. H. B. Bogman, who has retired.

AERONAUTICAL RADIO EQUIPMENT TO BE STANDARDIZED

At the suggestion of the Civil Aeronautics Administration, an all-industry conference was held in Washington on September 18. RMA has arranged to co-operate with the CAA and aircraft industry organizations in the standardization of aeronautical radio equipment.

V.H.F. REQUIREMENTS WAIVED

All airdrome control stations operated under the authority of the F. C. C. have been granted exemption, until further notice, from the requirements for installation of very-high-frequency service. This is due to difficulty in obtaining material.

JULY EXCISE TAXES

Collections of excise taxes on radio sets, phonographs, and their component parts totalled $6,450,451.19 for July, 1947; the comparative figure for July, 1946, was $2,799,751.53.

TUBE PRODUCTION

Production of radio receiving tubes totalled 15,057,109 items in June, 1947, a slight gain over the 14,575,237 produced in May, but was reduced by the usual seasonal slump to 11,244,202 in July. The accumulated production for the first seven months of 1947 was thus 114,606,634 tubes.

RADIO AND TELEVISION RECEIVER PRODUCTION

July production of all types of radio receivers by RMA member-companies dropped, in a regular seasonal decline, to 1,155,456 sets, as compared to June's total of 1,213,142. However, a sharp increase in total set production occurred during the last week of July.

Television receiver production, including radio table models, radio consoles, radio-phonograph combination consoles, and television converters, was 10,007 sets, slightly below the record of 11,484 produced in June but well above the total of any other month reported this year.

F.m. and a.m. receiver production, including table models, consoles, radio-phonograph combination consoles, and table-model radio-phonograph combinations, was 70,649 sets, also below that of 76,624 in June.

Total radio set production by RMA member-companies for the first seven months of 1947 was 9,766,100 sets, of which 516,212 were a.m. and f.m. receivers.

Production of phonographs for July totalled 11,924 items, and of record players as radio attachments, 13,107.

PARTS PRODUCTION

Statistics on parts production show the usual seasonal decline, with 58 companies reporting on deliveries to manufacturers and 26 on deliveries to jobbers. July, 1947, deliveries to manufacturers averaged 89.01 per cent of the total for July, 1946; while June, 1947, figures were 110.99 per cent of those for June, 1946. Deliveries to jobbers for July were 64.25 per cent of those for the same month last year; in June the percentage was 76.20.

RADIO EXPORTS

Exports of radio equipment and parts for June, 1947, totalled 6,335,260 units with a value of $11,087,200, bringing the cumulative figures for the first six months of 1947 to 48,348,494 units valued at $60,186,964.

NEW RMA AMPLIFIER AND SOUND EQUIPMENT DIVISION CHAIRMEN

Chairman F. D. Wilson of RMA's Amplifier and Sound Equipment Division has organized three new project and service sections with the following chairmen: Commercial Sound Equipment, A. K. Ward; Intercommunication Equipment, A. V. Samuelson; Recording Equipment, H. A. Crossland.

NEW RMA TRANSMITTER SECTION CHAIRMAN

M. R. Briggs has been appointed chairman of the transmitter section, RMA engineering department, by Director W. R. G. Baker, president of The Institute of Radio Engineers.

RMA MEETINGS

The following RMA engineering meetings have been held:

Sub-committee on Fixed Paper Dielectric Capacitors—August 25 and 26, 1947
Committee on Dry Disc Rectifiers—August 26, 1947
Subcommittee on Antennas and R.F. Lines—September 10, 1947
Executive Committee, Receiver Section—September 10, 1947
Broadcast Transmitter Section—September 16, 1947
Subcommittee on Transformers and Reactors, September 19, 1947
Subcommittee on Gas-filled Microwave Transmission Lines—September 26, 1947.

RMA MEETING

A meeting of the RMA School Committee was held on October 27 and 28, 1947.

Books

Klystron Tubes, by A. E. Harrison

Published (1947) by McGraw-Hill Book Company, Inc., 330 W. 42 St., New York 18, N. Y. 246 pages+3-page index+22 pages of appendixes+x pages. 155 illustrations. 6×9 inches. Price, $3.50.

Most microwave engineers are familiar with the "Klystron Technical Manual," prepared by Harrison for the Sperry Gyroscope Company and distributed in 1944. The book, "Klystron Tubes," is in a sense an extension of that publication, but most sections have been rewritten, all subjects have been expanded, and a number of new subjects have been added. Most important of these are the sections on klystron modulation and multiple-resonator klystrons. The theoretical sections on all types of tubes have been greatly expanded. In conformity with the use of the name klystron as a generic description of the class of tubes sometimes known as velocity-modulation or velocity-variation tubes, some material on tubes developed in other companies has been included, but the book is primarily concerned with principles and not tube types.

The book begins with two introductory chapters on klystron construction and cavity resonators. There is then a chapter on electron-bunching theory, in which the basic processes of velocity-modulation of the beam, bunching by drifting, and induction of current in the output gap are described and analyzed from the electron-ballistic point of view. The results from this electron-ballistic approach are then combined in succeeding chapters with basic circuit theory to give the behavior and analysis of klystron amplifiers, frequency multipliers, reflex oscillators, two-resonator oscillators, oscillator-buffer tubes, cascade amplifiers, amplifier-multiplier tubes, and the derivation of modulation characteristics. Although frequency, phase, amplitude and pulse modulation of klystrons are discussed, much of this last material is only qualitative. There are chapters on klystron tuners, klystron power supplies, and klystron operation discussed with reference to the theoretical principles developed earlier in the book. A final section gives a concise general survey of certain microwave measurement techniques.

The book is advertised on the jacket as an introduction to klystron tubes, and as such it can be criticized little. It mentions most of the important effects and characteristics of this class of tubes, gives some discussion of most of these, and provides analyses for many. The mathematical developments are short and for the most part relatively simple, and the author makes a point of discussing the physical significances of derivations wherever possible. Perhaps even for an introductory book there should have been more complete quantitative discussions, even if to order of magnitude only, of certain effects only cited, such as the limitations placed on drift length by space-charge debunching, the effects of transit times and secondary electrons on beam loading, etc. Certainly the reviewer feels that there should have been at least a qualitative description of the Hahn-Ramo space-charge-wave approach to the analysis of this class of tubes as an important extension to the electron-ballistic approach. Nevertheless, the book will prove invaluable to engineers beginning work on klystron applications or design, and to students studying the general subject of microwave tubes.

The book will also be useful for engineers who have considerable experience with klystron design or applications because of the large amount of useful reference material which it contains, but this group will find the above-mentioned omissions more disappointing. To make the book of optimum usefulness for this group, another edition should contain more material of an advanced nature, such as a discussion of the sources of noise and the fundamental limits on improving noise properties, gain-bandwidth limitations in power-amplifier applications, advantages and disadvantages of many-gap tubes as compared with the few-gap tubes discussed, the effects of multiple-transit electrons in reflex tubes, the Pierce theory of gun design for beam tubes, and the theoretical limits on transadmittance in klystron tube types.

J. R. Whinnery
University of California
Berkeley 4, Calif.

Antennae: An Introduction to Their Theory, by J. Aharoni

Published (1946) by Oxford University Press, 114 Fifth Ave., New York 11, N. Y. 254 pages+3-page index+6-page appendix+2 page bibliography+viii pages. 145 figures. 6¾×9 inches. Price $8.50.

This volume contains a comprehensive account of mathematical developments in antenna theory made in the half-century preceding the date of publication (1946), with particular emphasis on the work done during the last decade. It is an advanced book. The author assumes that the reader is familiar with mathematical methods needed in the development of this subject and wastes no space on details and collateral explanations. However, the readers with a proper mathematical background will find the exposition remarkably clear. The book is addressed to the applied mathematician rather than to the average engineer.

The contents of the book are subdivided into three chapters according to the methods of mathematical analysis. The first chapter, entitled "Antennae and Boundary-Value Problems," begins with Maxwell's equations, boundary conditions, and a general statement of the antenna problem. This chapter contains an account of those solutions which may be obtained by the method of separation of independent variables. Thus it includes plane, cylindrical, and spherical waves in free space; spherical waves along coaxial cones; free and forced oscillations on spherical and spheroidal conductors. The second chapter, entitled "Antennae and Integral Equations," is the longest. It begins with a derivation of the low-frequency circuit theory from Maxwell's equations. Next come integral equations, at first exact and then approximate. This is followed by an exposition of an approximate method for solving one of the approximate integral equations and by a discussion of some of the numerical results obtained by this method. The remainder of the chapter is devoted to circuit relations in antennas, to radiation patterns, and to ground effects. The third and last chapter contains a brief but exceptionally clear exposition of the wave-guide theory of antennas.

The book should make it easy for the research worker to learn what has been done in the field of fundamental antenna theory, which problems are still unsolved, and what questions remain as yet unanswered.

S. A. Schelkunoff
Bell Telephone Laboratories, Inc.
New York 14, N. Y.

Vector and Tensor Analysis, by Louis Brand

Published (1947) by John Wiley and Sons, Inc., 440 Fourth Ave., New York, 16 N. Y. 429 pages +8-page index +xvi pages. 59 figures. 5½×8¾ inches. Price, $5.50.

In this, the first of two volumes, Professor Brand has constructed an exceptionally systematic and lucid account of the closely related subjects of vector and tensor analysis. The greater part of the book is devoted to the algebra and the differential-integral calculus of vectors, dyadics, triadics, etc. (tensors of valence 1,2,3, etc.). The subject of tensor analysis per se is treated in a single chapter. Although not primarily intended as a text, the fundamental nature of the presentation and the inclusion of many problems well adapts this book to a course in vector analysis and a short course in tensor analysis. Despite the preponderance of applications to the fields of mechanics, differential geometry, and hydrodynamics, this book should nevertheless appeal to the mathematically inclined electrical engineer. A second volume is intended to cover applications of tensor analysis to relativity, electrodynamics, and electrical machines.

The initial chapters are concerned with vector algebra and include as well a treatment of the algebra of dual vectors and motors which are of importance in mechanics. Vector functions of a single variable are introduced as a preliminary to the discussion of linear vector functions of a vector. The associated concepts of dyadic operators, their scalar and vector invariants, their eigenvector properties, and the related Hamilton-Cayley equation are well presented.

Particularly noteworthy are the chapters on the differential and integral properties of vectors, dyadics, etc. With the general concept of derivative as a basis, the invariant forms and integral transformations of the gradient of a tensor point function are developed. Volume and surface divergence and curl operations on vectors, together with their integral transformations, appear as special invariant forms. Surface operators, too often neglected, are of particular interest to electrical engineers because of recent developments in wave-guide theory. In addition to a generous sprinkling of applications of vector analysis throughout the book, complete chapters are devoted to hydrodynamics and surface geometry.

Tensor analysis, rephrasing many of the developments of the preceding chapters in the new notation, is relegated to a single chapter. Transformation theory is discussed first in 3-space and later extended to N-space. The distinction of the invariant tensor from its components leads to simple treatments of the metric properties of various geometries.

The book concludes with a chapter on quaternions, their relation to vectors, and applications to rotations.

Considered as a whole, this is a well-planned book which represents a welcome addition to the literature on the subject.

NATHAN MARCUVITZ
Polytechnic Institute of Brooklyn
Brooklyn, N. Y.

The Strange Story of the Quantum, by Banesh Hoffmann

Published (1947) by Harper & Brothers, 49 East 33rd Street, New York 16, N. Y. 232 pages+7-page index+xiv pages. 15 figures. $5\frac{1}{2}\times 8$ inches. Price $3.00.

To those who may have a speaking acquaintance with the frontier developments of theoretical physics during the last half century, the book under review offers an excellent summary, in nontechnical terms, of the steps leading to the present quantum-mechanical picture of matter and radiation. In a manner both novel and entertaining, Dr. Banesh Hoffmann has marshalled in appropriate sequence the ideas which have been offered as interpretation of the ever-expanding experimental knowledge of atoms and associated radiations. More than this, he has provided the connective tissue by which these ideas are bound one to the other and also the matrix whence new speculations have sprung. To the present reviewer, who has lived only on the periphery of these revolutionary developments of atomic theory during the past quarter century, Dr. Hoffmann has been eminently successful in collating the seemingly diverse hypotheses and molding them into a clear and continuously unfolding picture.

"The Strange Story of the Quantum" embraces fifteen chapters, one each devoted to a "Prologue," an "Intermezzo," and an "Epilogue." The remaining twelve chapters are grouped into "Act I" and "Act II." A very complete and commendable "Index" provides means for reference.

The Prologue outlines the early explanations of human vision and the theories of the corpuscular and wave nature of light championed by Newton and Huygens, ending with an account of Faraday's concept of "tubes of force" and Maxwell's electromagnetic theory. Act I commences with Planck's hypothesis of the "quantum of energy" and Einstein's subsequent application of this entity to the concept of light, culminating in an excellent exposition of Bohr's fundamental ideas of the quantum relations of permissible energy states in the hydrogen atom.

Following a word of warning in the "Intermezzo" that the reader proceeds at his own risk, the author continues the story in Act II with de Broglie's association of wave packets with particles of matter, thus initiating the dual picture of particles as waves and waves as particles (photons). From here the going is difficult, as we are led through the maze of give-and-take theories of Heisenberg, Dirac, and Schrödinger. The curtain falls on Act II with the wave and particle, like Dr. Jekyll and Mr. Hyde, being but two aspects of the same thing; and their existence in time and space being without meaning except as a matter of calculable probability.

The "Epilogue" consists of an evaluation of the finally developed quantum mechanics in opening up new lines of progress in physical science. One such avenue of progress has been the recent discovery of elementary particles in nuclear structures: the positron, the neutron, the neutrino, and the meson.

"The Strange Story of the Quantum" bears on its title page the statement: "An account for the general reader of the growth of ideas underlying our present atomic knowledge." The "general reader" cannot mean, surely, the lay reader. Only one interested in the constitution of matter and having at least a genuine desire to understand physics can reap full enjoyment from the reading of this book. As expressed in the statement just quoted, the story offers the *growth of ideas*. One will not find, regrettably, much reference to the experimental foundations of our present atomic knowledge. It is also regrettable to find an almost complete lack of biographical information on these great promoters of the subject at hand, whose role in the family of scientists is an integral and often fascinating part of "The Strange Story of the Quantum."

As regards the style of presentation, I do not subscribe to the opinion of a previous reviewer that this book is "in the same class with Popular Science Classics of Jeans, Eddington, and E. T. Bell." The author has of necessity resorted to explanations by analogies; this is all right. But his long drawn-out metaphors and ubiquitous rhetorical questions I find diverting. Just one example of each. On page 229: "It matters not that our theories are but temporary shelters from those icy winds of doubt and ignorance that chill the stoutest heart." On page 164: "Do we still wish to cling to the twirling? Do we think there is no other possible explanation that would make sense? Does it seem that we have been splitting philosophical hairs to pretend the twirling might be illusory?" These forms of expression in moderation make excellent seasoning, but in quantity they are hard to stomach. Otherwise, the fine choice of words, the nicely balanced sentences, and the well chosen bits of humor (including even the puns) leave little to be desired.

All in all, the author has accomplished with distinction his stated purpose of establishing a "guide to those who would explore the theories by which the scientist seeks to comprehend the mysterious world of the atom." To those so minded and who are not without some experience in the field of modern physics, this book is recommended.

WILLIAM H. CREW
Rensselaer Polytechnic Institute
Troy, New York

Electronic Engineering Patent Index, 1946, edited by Frank A. Petraglia

Published (1947) by Electronics Research Publishing Company, 2 W. 46 Street, New York 19, N. Y. 476 pages+viii pages. 1677 figures $6\frac{1}{2}\times 10$ inches. Price, $14.50.

The compiler of this book states in his preface that this is the first of a proposed annual series which is designed to provide engineers with a convenient guide to new electronics patents issued during the year by the U. S. Patent Office, and that he believes it will serve as a valuable reference. He further states that the compilation reproduces in full, from the 1946 file of the Gazette of the U. S. Patent Office, circuit diagrams and descriptions of patents, so that they are identical with those of the original source and, hence, provide all the information necessary to facilitate further search where such is desired.

The preface and the table of contents are the only original subject matter introduced by the compiler over that given by the Official Gazette. The patents listed under each of the ninety subject classifications, which appear to be rather arbitrarily selected by the compiler, are incomplete because no cross references are given. For example, Seismic Surveying Systems and Prospecting Apparatus must be examined to find even the primary patents used in the geophysical field, which at this date enjoys the status of a well-defined branch of the electronic art.

This book is neither convenient, nor a guide, nor a reference. Had the compiler given some attention to classification, some definition of the ninety subject classifications; given complete references under each classification, including cross references, headings on each page indicating the classification, an index of the numerical patents, their inventors and assignees; and a brief description of the invention in addition to the printed claim; then a constructive step would have been taken which could have some value to the engineer. As it is, however, the engineer who wants to familiarize himself with the patents issued in this field, or who wishes to refer to certain patents, will find the Official Gazette of the U. S. Patent Office with its annual index more useful.

ALOIS W. GRAF
120 South La Salle St.,
Chicago 3, Illinois

Sections

Chairman		Secretary
P. H. Herndon c/o Dept. in charge of Federal Communication 411 Federal Annex Atlanta, Ga.	Atlanta November 21	M. S. Alexander 2289 Memorial Dr., S.E. Atlanta, Ga.
F. W. Fischer 714 Beechfield Ave. Baltimore 29, Md.	Baltimore	E. W. Chapin 2805 Shirley Ave. Baltimore 14, Md.
W. H. Radford Massachusetts Institute of Technology Cambridge, Mass.	Boston	A. G. Bousquet General Radio Co. 275 Massachusetts Ave. Cambridge 39, Mass.
A. T. Consentino San Martin 379 Buenos Aires, Argentina	Buenos Aires	N. C. Cutler San Martin 379 Buenos Aires, Argentina
R. G. Rowe 8237 Witkop Avenue Niagara Falls, N. Y.	Buffalo-Niagara November 19	R. F. Blinzler 558 Crescent Ave. Buffalo 14, N. Y.
J. A. Green Collins Radio Co. Cedar Rapids, Iowa	Cedar Rapids	Arthur Wulfsburg Collins Radio Co. Cedar Rapids, Iowa
Karl Kramer Jensen Radio Mfg. Co. 6601 S. Laramie St. Chicago 38, Ill.	Chicago November 21	D. G. Haines Hytron Radio and Electronics Corp. 4000 W. North Ave. Chicago 39, Ill.
J. F. Jordan Baldwin Piano Co. 1801 Gilbert Ave. Cincinnati, Ohio	Cincinnati November 18	F. Wissel Crosley Corporation 1329 Arlington St. Cincinnati, Ohio
W. G. Hutton R.R. 3 Brecksville, Ohio	Cleveland November 27	H. D. Seielstad 1678 Chesterland Ave. Lakewood 7, Ohio
C. J. Emmons 158 E. Como Ave. Columbus 2, Ohio	Columbus November 14	L. B. Lamp 846 Berkeley Rd. Columbus 5, Ohio
L. A. Reilly 989 Roosevelt Ave. Springfield, Mass.	Connecticut Valley November 20	H. L. Krauss Dunham Laboratory Yale University New Haven, Conn.
Robert Broding 2921 Kingston Dallas, Texas	Dallas-Ft. Worth	A. S. LeVelle 308 S. Akard St. Dallas 2, Texas
E. L. Adams Miami Valley Broadcasting Corp. Dayton 1, Ohio	Dayton November 20	George Rappaport 132 E. Court Harshman Homes Dayton 3, Ohio
P. O. Frincke 219 S. Kenwood St. Royal Oak, Mich.	Detroit November 21	Charles Kocher 17186 Sioux Rd. Detroit 24, Mich.
N. J. Reitz Sylvania Electric Products, Inc. Emporium, Pa.	Emporium	A. W. Peterson Sylvania Electric Products, Inc. Emporium, Pa.
F. M. Austin 3103 Amherst St. Houston, Texas	Houston	C. V. Clarke, Jr. Box 907 Pasadena, Texas
R. E. McCormick 3466 Carrollton Ave. Indianapolis, Ind.	Indianapolis	M. G. Beier 3930 Guilford Ave. Indianapolis 5, Ind.
C. L. Omer Midwest Eng. Devel. Co. Inc. 3543 Broadway Kansas City 2, Mo.	Kansas City	Mrs. G. L. Curtis 6003 El Monte Mission, Kansas
R. C. Dearle Dept. of Physics University of Western Ontario London, Ont., Canada	London, Ontario	E. H. Tull 14 Erie Ave. London, Ont., Canada
C. W. Mason 141 N. Vermont Ave. Los Angeles 4, Calif.	Los Angeles November 18	Bernard Walley RCA Victor Division 420 S. San Pedro St. Los Angeles 13, Calif.
O. W. Towner Radio Station WHAS Third & Liberty Louisville, Ky.	Louisville	D. C. Summerford Radio Station WHAS Third & Liberty Louisville, Ky.
E. T. Sherwood Globe-Union Inc. Milwaukee 1, Wis.	Milwaukee	J. J. Kircher 2450 S. 35th St. Milwaukee 7, Wis.
R. R. Desaulniers Canadian Marconi Co. 211 St. Sacrement St. Montreal, P.Q., Canada	Montreal, Quebec December 10	R. P. Matthews Federal Electric Mfg. Co. 9600 St. Lawrence Blvd. Montreal 14, P.Q., Canada
J. E. Shepherd 111 Courtenay Rd. Hempstead, L. I., N. Y.	New York December 3	I. G. Easton General Radio Co. 90 West Street New York 6, N. Y.
L. R. Quarles University of Virginia Charlottesville, Va.	North Carolina-Virginia	J. T. Orth 4101 Fort Ave. Lynchburg, Va.
K. A. Mackinnon Box 542 Ottawa, Ont. Canada	Ottawa, Ontario November 20	D. A. G. Waldock National Defense Headquarters New Army Building Ottawa, Ont., Canada
P. M. Craig 342 Hewitt Rd. Wyncote, Pa.	Philadelphia December 4	J. T. Brothers Philco Radio and Television Tioga and C Sts. Philadelphia 34, Pa.
E. M. Williams Electrical Engineering Dept. Carnegie Institute of Tech. Pittsburgh 13, Pa.	Pittsburgh December 8	E. W. Marlowe 560 S. Trenton Ave. Wilkinburgh PO Pittsburgh 21, Pa.
Francis McCann 4415 N.E. 81 St. Portland 13, Ore.	Portland	A. E. Richmond Box 441 Portland 7, Ore.
N. W. Mather Dept. of Elec. Engineering Princeton University Princeton, N. J.	Princeton	A. E. Harrison Dept. of Elec. Engineering Princeton University Princeton, N. J.
A. E. Newlon Stromberg-Carlson Co. Rochester 3, N. Y.	Rochester November 20	J. A. Rodgers Huntington Hills Rochester, N. Y.
E. S. Naschke 1073-57 St. Sacramento 16, Calif.	Sacramento	G. W. Barnes 1333 Weller Way Sacramento, Calif.
R. L. Coe Radio Station KSD Post Dispatch Bldg. St. Louis 1, Mo.	St. Louis	N. J. Zehr Radio Station KWK Hotel Chase St. Louis 8, Mo.
Rawson Bennett U. S. Navy Electronics Laboratory San Diego 52, Calif.	San Diego December 2	C. N. Tirrell U. S. Navy Electronics Laboratory San Diego 52, Calif.
W. J. Barclay 955 N. California Ave. Palo Alto, Calif.	San Francisco	F. R. Brace 955 Jones San Francisco 9, Calif.
J. F. Johnson 2626 Second Ave. Seattle 1, Wash.	Seattle December 11	J. M. Patterson 7200—28 N. W. Seattle 7, Wash.
C. A. Priest 314 Hurlburt Rd. Syracuse, N. Y.	Syracuse	R. E. Moe General Electric Co. Syracuse, N. Y.
C. A. Norris J. R. Longstaffe Ltd. 11 King St., W. Toronto, Ont., Canada	Toronto, Ontario	C. G. Lloyd 212 King St., W. Toronto, Ont., Canada
O. H. Schuck 4711 Dupont Ave. S. Minneapolis 9, Minn.	Twin Cities	B. E. Montgomery Engineering Department Northwest Airlines Saint Paul, Minn.
L. C. Smeby 820—13 St. N. W. Washington 5, D. C.	Washington December 8	T. J. Carroll National Bureau of Standards Washington, D. C.
	Williamsport December 3	R. G. Petts Sylvania Electric Products, Inc. 1004 Cherry St. Montoursville, Pa.

SUBSECTIONS

Chairman		Secretary
J. D. Schantz Farnsworth Television and Radio Company 3700 E. Pontiac St. Fort Wayne, Ind.	FORT WAYNE (Chicago Subsection)	S. J. Harris Farnsworth Television and Radio Co. 3702 E. Pontiac Fort Wayne 1, Ind.
F. A. O. Banks 81 Troy St. Kitchener, Ont., Canada	HAMILTON (Toronto Subsection)	E. Ruse 195 Ferguson Ave., S. Hamilton, Ont., Canada
A. D. Emurian HDQRS. Signal Corps Engineering Lab. Bradley Beach, N. J.	MONMOUTH (New York Subsection)	Ralph Cole Watson Laboratories Red Bank, N. J.
A. R. Kahn Electro-Voice, Inc. Buchanan, Mich.	SOUTH BEND (Chicago Subsection) October 16	A. M. Wiggins Electro-Voice, Inc. Buchanan, Mich.
W. M. Stringfellow Radio Station WSPD 136 Huron Street Toledo 4, Ohio	TOLEDO (Detroit Subsection)	M. W. Keck 2231 Oak Grove Place Toledo 12, Ohio
W. A. Cole 323 Broadway Ave. Winnipeg, Manit., Canada	WINNIPEG (Toronto Subsection)	C. E. Trembley Canadian Marconi Co. Main Street Winnipeg, Manit., Canada

I.R.E. People

A. W. MARRINER

A. W. Marriner (A'29), formerly director of the aviation department of International Telecommunication Laboratories, has been named assistant technical director for the International Telephone and Telegraph Corporation.

General Marriner has been the Air Force's oldest communications officer, having pioneered air communications for the Air Corps shortly after the first World War. During World War II he organized the Directorate of Communications, which was responsible for the inauguration of Air Force communications and navigation services. This included the organization of the Army Airways Communications System. Later, General Marriner went to foreign duty as Senior American Air Communications Officer in England during the preparations for the Normandy invasion. Subsequently he served as American Air Signal Officer-in-Chief in the Mediterranean Theater.

General Marriner joined the I.T.&T. System on May 1, 1946, having retired from the regular Army after more than twenty-eight years of continuous service in the Air Forces. During that service he advanced through all grades from second lieutenant to brigadier general. He is the possessor of the Legion of Merit with Oak Leaf Cluster, the Citation Ribbon, and is Honorary Commander of the Order of the British Empire (Military Division), and Commendatore of the Order of the S.S. Maurizio and Lazzaro.

◆

DR. W. L. BARROW

RUDOLF FELDT

Rudolf Feldt (M'44), who has been connected with the Allen B. Du Mont Laboratories, Inc., of Passaic, N. J., since 1935, has been recently appointed head of its cathode-ray oscillograph manufacturing department in Clifton, N. J.

Mr. Feldt was graduated as an electrical engineer from Technische Hochschule in Berlin, Germany, and worked in the plants of the A.E.G. and C. Lorenz Companies. In 1931 he became research engineer for the Compagnie Lignes Telegraphiques et Telephoniques in Conflans Ste. Honorine.

He has several important developments and refinements to his credit in the field of cathode-ray oscillographs and tubes. One of his first assignments at the Du Mont Laboratories was the compilation of a bibliography on the cathode-ray art.

During World War II he volunteered and served with the French Foreign Legion in North Africa.

◆

W. L. BARROW

W. L. Barrow (A'28–M'40–F'41) was recently appointed chief engineer of the Sperry Gyroscope Company, Inc. Dr. Barrow was born in Baton Rouge, La., on October 25, 1903. He received the B. S. degree in electrical engineering from Louisiana State University in 1926, and the M. S. degree from Massachusetts Institute of Technology in 1929. He was a Redfield Proctor Fellow in physics at the Technische Hochschule in Munich, Germany, where, in 1931, he received the Sc. D. degree in physics. Serving from 1931 to 1936 as an instructor in the communications division of Massachusetts Institute of Technology and as a member of the Round Hill research group, Dr. Barrow was appointed professor of electrical communications in 1936. In 1943 he joined Sperry as full-time director of armament engineering, following several years of serving as consultant.

ARTHUR DORNE
JOSEPH MARGOLIN

Arthur Dorne (A'47–M'47) supervising engineer, and Joseph Margolin (M'47), engineer, of the antenna-design section of Airborne Instruments Laboratory, Mineola, N. Y., have established their own antenna consulting firm, Dorne and Margolin, Antenna Consultants, in Freeport, L. I. Both Mr. Dorne and Mr. Margolin have done important work in faired-in, dragless antenna designing groups for Airborne Instruments Laboratory. They anticipate enlisting the assistance of A.I.L. for measurement and field-pattern work.

◆

DONALD A. QUARLES

Donald A. Quarles (M'41–SM'43), director of apparatus development of Bell Telephone Laboratories, has been elected a vice-president of the organization. Associated with Bell System since 1919, he previously served as outside-plant-development director and transmission-development director.

Mr. Quarles is vice-chairman of the committee on electronics of the Joint Research and Development Board of the federal government. He is also a member of the board of directors of the American Institute of Electrical Engineers.

DONALD A. QUARLES

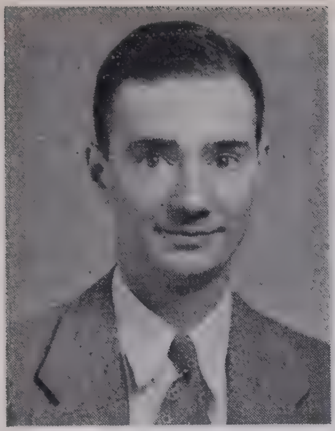

GROTE REBER

GROTE REBER

Grote Reber (A'33–SM'44) was recently appointed to the staff of the National Bureau of Standards. His investigation will center on the study of cosmic and solar radio noise.

Mr. Reber was born on December 22, 1911. He received the B.S. degree from Armour Institute of Technology in 1933, after which he did graduate work at the University of Chicago in physics. He was a radio engineer for General Household Utilities in 1933 and 1934, and was with the Stewart-Warner Corporation from 1935 to 1937. In 1939 he was associated with the Research Foundation of Armour Institute of Technology. In 1941 he returned to Stewart-Warner to aid the war program. During 1946 he joined the Belmont Radio Corporation as a radio engineer.

Mr. Reber is the author of a number of technical papers in the fields of interstellar static and electrical engineering. He is an associate member of the American Institute of Electrical Engineers and the American Rocket Society, a member of the Chicago Astronomical Society, the American Association for the Advancement of Science, the Astronomical Society of the Pacific, and the Franklin Institute.

❖

ROBERT J. GLEASON

ROBERT J. GLEASON

Robert J. Gleason (A'36–M'39–SM'43), communications superintendent of the Pacific-Alaska Division of Pan American World Airways, was recently awarded the Bronze Star medal by the United States War Department for outstanding work in establishing communications networks in the China-Burma-India theater of war.

"Colonel Gleason's zealous devotion to duty," the War Department citation states, "led him to removed and virtually inaccessible areas in China to supervise personally the installation of radar beacons and radio ranges, in many instances disregarding prevalent enemy activity. Working in direct support of tactical and transport units, Colonel Gleason handled special emergency missions of furnishing communications for entire networks to support operations involving the movement of thousands of troops to forward areas to halt the Japanese advances in China.".

❖

JOHN H. BATTISON

John H. Battison (M'47) has joined the general engineering department of the American Broadcasting Company as assistant to John G. Preston (S'35–A'37), A.B.C.'s chief allocations engineer.

Mr. Battison graduated from the City and Guilds of London, England, in 1936 with a B.S. degree in radio communication. From 1934 to 1937 he was a research engineer for the EKCO Radio Company of London, and from 1937 to 1939 was supervisor of radio equipment production for the Air Ministry. During the war years he served the Royal Air Force as an acting squadron leader.

Following the war, Mr. Battison came to the United States as a research engineer for the Midland Broadcasting Company in Kansas City, Missouri, and later became technical director for that company. He resigned this post to become transmitter development engineer for the Federal Radio and Telephone Company.

❖

F. M. SLOAN

F. M. Sloan (A'41) formerly assistant general manager of Westinghouse Radio Stations, Inc., has recently been appointed manager of the Westinghouse Home Radio Division, Sunbury, Pa.

Mr. Sloan has been associated with Westinghouse radio activities for more than 15 years in both technical and administrative positions. During the latter part of the war he was manager of the Field Engineering Service Department for the Industrial Electronics Division at Baltimore. In this capacity he developed and supervised a world-wide engineering service organization that included operations in the distant theaters of operation where radar and electronic equipment were installed for the Navy.

❖

A. C. KRUEGER

A. C. KRUEGER

A. C. Krueger (M'46) has joined the staff of the Airborne Instruments Laboratory, Mineola, N. Y., to assume the administrative direction of the antenna-design section.

Dr. Krueger received the B.A. degree from Westminster College in Missouri in 1925, the M.A. from the University of Missouri in 1927, and the Ph.D. from the University of Wisconsin in 1930. From 1930 to 1942 he served as professor of physics and applied mathematics at Westminster College. He lectured at Culver-Stockton College in 1942 and at the University of Wisconsin in 1943. From September, 1943, to July, 1945, he worked on the Manhattan Project at the University of Chicago, making contributions in nuclear physics and in nuclear and radiation chemistry. He then served as engineer in charge of research and development for the Allen D. Cardwell Company until February, 1946, when he went to Republic Aviation Corporation as development engineer on a guided-missiles project.

Dr. Krueger is a member of the Electrochemical Society, the American Chemical Society, the Association of New York Scientists, the American Association of Physics Teachers, the Missouri Academy of Science, Alpha Chi Sigma, and the American Radio Relay League.

❖

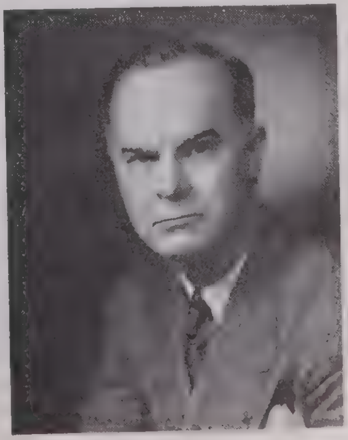

F. M. SLOAN

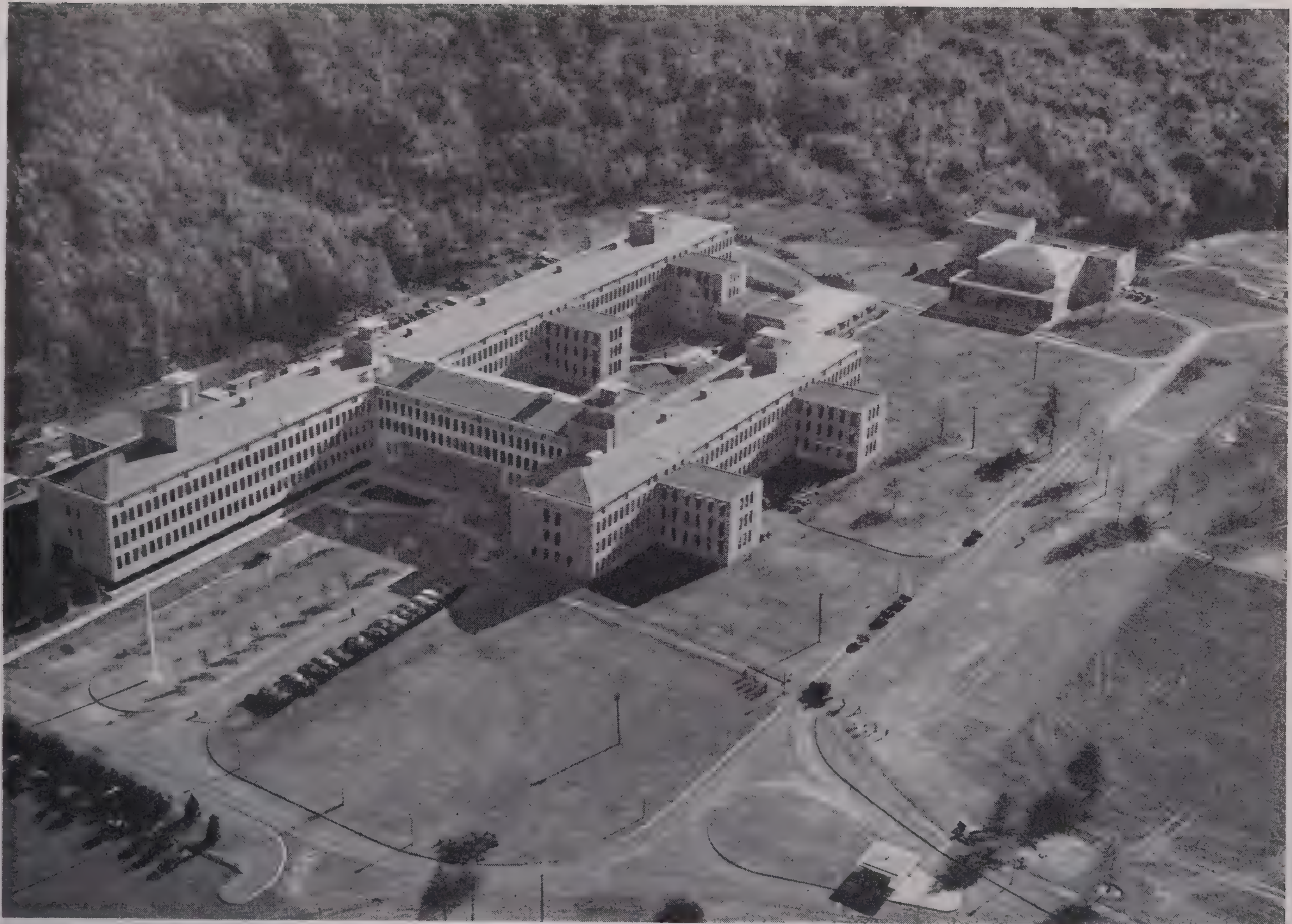

Fairchild Aerial Surveys, Inc.

THE MURRAY HILL, N. J., FACILITIES OF THE BELL TELEPHONE LABORATORIES

The Bell Telephone Laboratories, research and development organization of the Bell System, has established this Laboratory near Summit, N. J. An adjoining unit, comparable in size to the one shown, which was completed before the war, is now under construction and is expected to be ready for occupancy by 1948.

John E. Keto

Chairman, Dayton Section, May 1946-May, 1947

John E. Keto was born on June 9, 1909, in Maynard, Mass. He received his E.E. degree in 1932 after completing the five-year co-operative engineering course at the University of Cincinnati. In 1935, he obtained his M.S. degree in physics from the same university.

From 1927 through 1935, Mr. Keto was employed by various electrical and product industries in Cincinnati, Ohio, and Detroit, Mich., as part of his training course. The last three years were with the Detroit Edison Company, as a member of its research staff.

For the next two years, Mr. Keto instructed in the electrical engineering department of the University of Cincinnati as a teaching fellow. During this period he continued his research activity in connection with his graduate thesis.

Association in the field of radio engineering and development began in 1935 with the appointment as physicist to the Aircraft Radio Laboratory, Wright Field. The period of 1935 through 1939 was spent in research and development on high-frequency compasses, instrument-landing aids, and radio altimeters. In 1940, Mr. Keto was assigned as project engineer in charge of initiating and conducting the development of airborne radar equipment for the Army Air Forces, and became chief engineer of the Radar Laboratory in 1943. He continued in this position until early 1946, when he assumed the position of chief engineer of the newly established Radiation Laboratory; in June, 1946, he was appointed chief of the laboratory.

In February of 1946 Mr. Keto received the Medal for Merit for his outstanding services in the development of airborne radar equipment for the Armed Services during the war.

Mr. Keto joined The Institute of Radio Engineers as an Associate Member in 1936 and became a Senior Member in 1945. He is a member of Sigma Xi, Tau Beta Pi, Eta Kappa Nu, and the American Association of Commons Clubs.

Postwar Curriculum Emphasis*

OTTO J. M. SMITH†, MEMBER, I.R.E.

The qualifications of an engineer are, among other factors, a complex function of his natural intelligence and resourcefulness, personality and physical vigor, and his training. It is timely in this turbulent and changing period to re-evaluate current methods of professional engineering training and to suggest constructive changes and useful improvements, as has here been done by a Member of the Institute who has had experience both in professional instruction, and in research as Chief Electrical Engineer of the Summit Corporation.—*The Editor*.

RECENT TECHNOLOGICAL advances have greatly increased the amount of material which every engineering graduate should know. Engineering schools are striving towards maximum teaching efficiency. More efficient teaching methods are necessary for students to cover the increased material available, and also to relieve the load on overworked faculties.

Many engineering schools are expanding the scope of their curriculums. There is more fundamental material to be taught than can be adequately covered in four years. Some schools are stressing a five-year course, while others have increased the requirements per semester until many students need five years to complete a four-year course. The latter is discouraging to the student, and a headache to the adviser who must arrange the nonstandard programs. This evades the problem. To recognize part of the problem and require all engineers to take five years, or more, is to overlook the fact that industry has positions for men who do not have a master's or professional engineer's degree, but yet have had more than a technical-high-school education or a mechanics course. The four-year man will continue to be the main product of the majority of our universities, and the first four years in engineering should be designed to fulfill the needs of the man who intends to go no further, and at the same time form a solid basis for graduate work.

The purposes of this paper are to present a four-year curriculum that satisfies the above conditions, and to describe a few methods of increasing the amount of material which can be presented in a limited time. Of course, a great deal depends upon the *caliber* of the teachers. Properly, a discussion of the personality, characteristics, and method of selection of professors should be included. But the assumption will be made that the faculty is fixed, and that the variables are the curriculum and teaching methods. The development of considerable student responsibility and the use of "problem-technique" teaching was found by the author to be very successful at Tufts College and Denver University.

The conventional engineering curriculum contained a sequence of courses that was semihistorical. The advanced and special courses usually were centered around the study of particular types of equipment. This method of "product-centered" organization was satisfactory until it was hard-pressed by the exigencies of the present situation. A school now may find it necessary to increase its teaching efficiency by shifting from "product-centered" thinking to "problem-technique" thinking. Combined with psychologically superior teaching methods, this will allow them to graduate four-year men with better training than their prewar graduates.

The beginning courses should present the physical fundamentals in a logical mathematical sequence. This need have no correlation with the historical development of the ideas. The material in the advanced courses should be chosen with reference to the method of solution of the problems involved, rather than the type of equipment in which the problem occurs. This has been recognized in the past in such courses as transients, design, and thermodynamics, but not in d.c. machines or internal-combustion engines.

This shift of emphasis tends toward higher teaching efficiency, and produces the most desirable thinking patterns in the students. It leads immediately to electromechanical analogies, generalized circuit theorems applicable to hydraulic, electrical, or mechanical servomechanisms, the laws of thermodynamics in a form as useful to the physical chemist or electrical engineer as to the steam-power man, and an application of basic design philosophies to all engineering problems.

A teacher is a salesman. He must interest the students by his opening statements, give them the facts, and sell them on the idea of outside study. The most effective teaching starts with a practical problem to introduce each new mathematical or engineering tool. The student should be sold on the usefulness of the mathematical tool to him, personally, and he should study with a specific problem uppermost in his mind. This, it has been proved, produces the highest rate of learning and the greatest retention, and we engineers should not condone anything less than the maximum possible efficiency.

The student is able to cover not only more fundamentals, but also more equipment examples with "problem-technique" teaching, because of the reduction in the amount of wasted classroom and study time. The professors, too, find their time more productive.

Initiative and responsibility on the part of the students has to be developed in the laboratory sessions. To be certain, it is easier on an instructor's nerves and disposition for him to take all of the responsibility in a sophomore laboratory, but then his students will still lack initiative when they are seniors. The saving in time in a senior laboratory where all of the students competently assume responsibility more than makes up for the extra time that it takes to start them right as sophomores. Prospective employers are seriously concerned with an engineer's approach to laboratory work. This is so important that it can warrant the department's best man teaching the first course in a student's major field.

As an example of a unified course, Table I gives an electrical engineering curriculum designed primarily for four-year students, but applicable to the first four years of a five-year program. Appendix I is a description of the important courses. There is a general orientation program which presents the fields of engineering, evaluates the student's abilities and desires, and offers technical and psychological guidance. The few basic courses emphasize those elements which are applicable in all fields of electrical engineering. The multitude of little courses which many undergraduate curriculums accumulate upon the request of new teachers or industrial men with limited interests has been omitted. Since all of the courses listed here are intended to be practical, there is no need for the special so-called practical courses.

Direct-current machinery illustrates the reasoning in determining the correct placement of a subject in a curriculum of this type: it is taught in the general machinery course in the senior year because it is not a prerequisite for any junior subject, and it is easier to teach d.c. after synchronous machinery than before it. Electromagnetic theory is a basic course which precedes circuit theory (which is derived from it), and follows calculus, which is used extensively in it. Attention should be directed to the

---

* Decimal classification: R070. Original manuscript received by the Institute, August 5, 1947.

† Summit Corporation, Scranton 2, Pa.

TABLE I

ELECTRICAL ENGINEERING CURRICULUM

		Hours Laboratory	Hours Credit
	First Year		
Math 1	General Mathematics		6
Chem 1	Inorganic I	1	4
CE 1	Engineering Lectures		1
CE 2	Engineering Drawing	2	2
Engl 1	Exposition and Business English		3
		3	16
Math 2	Differential Calculus		6
Chem 2	Inorganic II	1	4
CE 3	Descriptive Geometry	2	3
Engl 2	Composition		3
		3	16
	Second Year		
Math 3	Integral Calculus		5
Physics 1	General Physics I	1	5
Chem 3	Engineering Materials	1	3
EE 1	Orientation		1
CE 4	Statics		2
		2	16
Math 4	Advanced Engineering Mathematics		4
Physics 2	General Physics II	1	5
EE 2	Electromagnetic Theory	1	6
Shop 1	Fabrication	1	1
		3	16
	Third Year		
EE 3	Linear Circuits	2	7
CE 5	Dynamics		2
CE 6	Strength of Materials	1	3
Shop 2	Machine Shop	1	1
Acct 1	Engineering Accounting		3
		4	16
EE 4	Transients and Nonlinear circuits	1	5
EE 5	Distributed Constants	1	3
CE 7	Surveying	1	2
CE 8	Hydraulics		3
ME 1	Thermodynamics		3
		3	16
	Fourth Year		
EE 6	Electrical Machinery I	1	6
EE 8	Radio I	1	4
ME 2	Power Plants	1	4
Speech 1	Public Speaking		2
		3	16
EE 7	Electrical Machinery II	1	6
EE 9	Seminar		1
EE	Elective	1	3
EE	Elective	1	3
	Liberal Arts elective		3
		3	16

fact that calculus is completed in the middle of the second year, supplying the student with his most important tool at the time he is starting his fundamental major work. This was made possible by consolidating all noncalculus items into two courses: general mathematics and advanced engineering mathematics.

It is best for a student to have only a few professors each semester. Most one-hour one-semester courses should be compressed into two and one-half weeks of a six-hour course. Such a change increases the teaching efficiency by several hundred per cent, because each subject is hit hard, rather than spread thin. This desirable reduction in the number of courses has been accomplished in the given curriculum by scheduling subjects in succession in a few main courses. For example, linear circuits and its laboratories (EE3) includes the usual courses in measurements and symmetrical components. Occasionally, engineering students have too many laboratories and too many reports. Then there is competition between different classes for a student's study time. This is another reason for reducing the number of contact professors per semester. The usual congestion of laboratories in the junior year has been dissolved by the careful selection of the material that should come in the sophomore and senior years. There are never more than five courses a semester, and only once are there as many as four laboratory sessions a week in this sample curriculum.

A reorganization of courses and course material initially places added responsibilities upon the professors, but the hard work is like planting a garden—there are rewards. A program of this type also requires the co-operation of other departments. Courses in mathematics, physics, and chemistry should be tailored specifically for engineers. Instructors for these courses should be skilled in "problem-technique" teaching, preferably having had engineering experience. The content of the important service courses is given in Appendix I. Notice that calculus is started in the freshman year so that it can be used as a tool in all engineering courses. Advanced engineering mathematics replaces the classical differential equations.

TABLE II

CREDIT HOURS SUMMARY

Year	Fundamentals			Major	Other Engineering			Liberal
	Math	Physics	Chem	EE	CE	ME	Shop	
1	12		8		6			6
2	9	10	3	7	2		1	
3				15	10	3	1	3
4				23		4		5
Totals	21	10	11	45	18	7	2	14
Per Cent	16.4	7.8	8.6	35.2	14.1	5.5	1.5	10.9

	Hours	Per Cent
Fundamentals	42	32.8
Major	45	35.2
Other Engineering	27	21.1
Liberal	14	10.9
	128	100.0

Table II is a summary of the curriculum emphases in hours and per cent. The balance is good when the student's time is equally divided between fundamentals, his major, and all other courses. This program bears heavily enough upon the technical side that the substitution of business or liberal arts courses for the senior major electives is not only permissible, but advisable. There should be available, for seniors, courses in business management, advanced accounting, statistics, psychology, education, history of civilization, law, and economic geography. One can find a champion of each of these courses among our engineering schools today, and with respect to what the engineer needs when he becomes a part of management ten years after graduation, these champions are right. There are some students mainly interested in business, and these should enroll in the business school and take only an engineering minor.

A student who intends to go on for a master's, engineer's, or Ph.D. degree should take his advanced work in engineering, mathematics, and physics in the graduate school. He should not take undergraduate electives of poorer quality covering the same subjects, but instead should emphasize liberal arts courses. The undergraduate senior electives are for the man who finishes his formal education in four years.

APPENDIX I

Description of courses: (Numbers in parentheses indicate hours credit):

EE 1 Orientation (1). Training, experience, and duties of the various grades and classes of engineers in power, design, manufacturing, control, communications, research, etc., and equipment and problems encountered in these fields.

EE 2 Electromagnetic Theory (6). Electric, magnetic, and dielectric phenomena, units, space vector, field theory, Maxwell's equations, derivation of circuit equations, permeability, permitivity, resistivity, water-table studies.

EE 3 Linear Circuits (7). Computation of capacitance, inductance, voltage, and force, complex notation, a.c. and d.c. steady-state response of n-loop and n-node networks, meters, standards, bridges, measurements, impedance charts, 3-phase, symmetrical components.

EE 4 Transients and Nonlinear Circuits (5). Transient solutions of linear networks, coupled circuits, electromechanical systems, network analyzers, repeated transients, glow tubes, lightning arresters, iron, Fourier analysis, thermionic emission, electronic tubes and circuits, differential analyzer.

EE 5 Distributed Constants (3). Transmission lines, cables, filters, transducer theorems, nomographs, antennas, heat flow, radiation and wave guides, Bessel functions, generalized circle diagrams, Riecke charts.

EE 6 Electrical Machinery I (6). Power and audio transformers, synchronous generators, d.c. machines.

EE 7 Electrical Machinery II (6). Induction motors, synchronous motors, single-phase machines, rototrol, amplidyne, control equipment, rectifiers, inverters, special machines.

EE 8 Radio I (4). Amplifiers, coupled circuits, detectors, oscillators, a.m. and f.m. receivers, rectifiers.

EE 9 Seminar (1). Student papers based upon library research.

Electives, given upon demand:

EE 10 Radio II (4). Transmitters, antennas, ultra-high-frequency techniques, pulsed circuits, television, radar.

EE 11 Advanced Circuit Analysis (3). LaPlacian transform, operational methods, matrices, boundary problems, n-winding transformer.

EE 12 Power Systems (3). Generation, transmission, distribution, protection, steady-state and transient stability.

EE 13 High Voltage (3). Gaseous discharge, dielectrics, insulation co-ordination, impulse testing, circuit breakers, relaying, corona loss.

EE 14 Design (3). Elements of transformer, machinery, relay, and meter design.

EE 15 Illuminations (3). Photometry; industrial, display, theater, and home lighting, photocell applications, optical systems.

EE 16 Industrial Electronics (3). Control and signaling equipment, timers, counters, dielectric and induction heating, d.c., a.c., and r.f. welding, arc furnaces, electrolysis, X-rays, gauges.

EE 17 Servomechanisms (3). Control and positioning apparatus, stability problems, gyropilots, lathe controls, turbine exciters and governors.

Description of important service courses:

Math 1 General Mathematics (6). Advanced algebra, trigonometry, and analytics, consolidated and taught simultaneously.

Math 2 Differential Calculus (6). A standard course.

Math 3 Integral Calculus (5). A standard course including complete solution of linear differential equation and power-series method for any differential equation.

Math 4 Advanced Engineering Mathematics (4). Determinants, n-mesh linear networks, series, Fourier analysis, selected differential equations, Bessel's functions, dimensionless solutions, cubic and quartic, indicial admittance, partial differentiation, vector algebra, space vectors, field equations, probability.

Physics 1 General Physics I (5). Mechanics, heat, sound.

Physics 2 General Physics II (5). Electricity and magnetism, light. Both of the above would use calculus and differential equations extensively. Physically incorrect concepts, such as that of the "unit magnetic pole," would be revised.

Chem 1 Inorganic I (4). Semi-micro laboratory methods.

Chem 2 Inorganic II (4). Semi-micro laboratory methods.

Chem 3 Engineering Materials (3). Water, gas, and ore analyses, photomicroscopy, mass spectrograph, steels, alloys, eutectic solders, lubricants, dielectrics, porcelains, industrial hazards and poisons, etc.

Dynamic Performance of Peak-Limiting Amplifiers*

DONALD E. MAXWELL†, SENIOR MEMBER, I.R.E.

Summary—Dynamic requirements for peak-limiting amplifiers are discussed briefly with respect to such factors as attack time, signal-to-thump ratio, gain-reduction characteristics, and recovery time. There is described a novel measurement technique and apparatus for the visual analysis of the dynamic performance of peak-limiting amplifiers.

The dynamic characteristics of several typical commercial peak-limiting amplifiers are individually analyzed by a series of cathode-ray oscillograms. These amplifiers exhibit various short-comings of a dynamic nature. As an example of the practical improvement which is obtainable, there is shown the dynamic performance of an experimental peak-limiting amplifier developed by the Columbia Broadcasting System.

I. INTRODUCTION

ALTHOUGH the use of peak-limiting amplifiers in radio broadcasting and recording systems has become very general, the actual dynamic performance of these amplifiers is often a matter of considerable conjecture. Most users know from their own experiences that the action which occurs in a peak-limiting amplifier under actual operating conditions frequently has little correlation to that which is indicated by steady-state sine-wave measurements. Overmodulation "splatter," audible "thump," and "motorboating" are among the more familiar operational defects due to dynamic deficiencies in these amplifiers. Manufacturer's specifications on commercial peak-limiting amplifiers usually include little or no information on dynamic performance, and in the past there has been no available measuring technique or equipment by means of which the user could reliably judge the dynamic merits or defects of a particular amplifier.

It is one object of this paper to describe a measuring technique which provides a means for evaluating the transient characteristics of peak-limiting amplifiers. A second object of this paper is to describe the results of the above measurements as applied to several peak-limiting amplifiers. By way of background, there will first be presented a discussion of some of the dynamic requirements of peak-limiting amplifiers.

II. DYNAMIC REQUIREMENTS FOR PEAK-LIMITING AMPLIFIERS

The essential function of a peak-limiting amplifier[1] is to provide an automatic means of gain control, such that no audio peak amplitude at the input of the amplifier will produce an output level in excess of a predetermined maximum value. A peak-limiting amplifier has an automatically controlled gain characteristic such that its gain is essentially constant for all peak signal amplitudes below the predetermined maximum output value, and is approximately inversely proportional to the input peak signal amplitude for all values in excess of that corresponding to the predetermined maximum output value. A peak-limiting amplifier is usually characterized by a rapid reduction of gain at the onset of a high signal peak, and a relatively slow restoration of gain after the peak has subsided. The time required for gain restoration is usually long, compared to any signal-frequency variations. The minimum time required for gain reduction is commonly known as "attack" time, and the time required for gain restoration as "recovery" time.

Since broadcast program material by nature consists of a series of non-sustained and rapidly recurring signal peaks, a peak-limiting amplifier which does not have a sufficiently short attack time will permit the occasional passage of short signal bursts having amplitudes in excess of that corresponding to 100 per cent modulation of the associated transmitter. If each of the resulting periods of overmodulation does not persist for more than a few milliseconds, it is probable that few listeners will be able to detect the serious wave-form distortion which occurs during these short periods before the gain-reducing action of the peak-limiting amplifier has taken place. However, such occasional bursts of overmodulation in an amplitude-modulated transmitter can set up the well-known and undesirable phenomena of adjacent-channel "splatter." Due to the very steep wave fronts characteristic of many signal peaks, it has been observed experimentally by the Columbia Broadcasting System that the effective attack time of a peak-limiting amplifier should be on the order of 100 microseconds or less, if part or all of these peaks are not to be transmitted at a level in excess of the predetermined maximum.

Most commercial peak-limiting amplifiers on the market today effect the required gain reduction by automatic variation of either a circuit resistance or the signal transconductance of a vacuum tube. In either case, the actual resistance or transconductance variation is usually accompanied by a comparatively large change in the d.c. potential across the variable element. Since this change in d.c. operating values, commonly referred to as "control voltage," occurs at a very rapid rate, it will appear at the output of the amplifier along with the desired signal, unless special means are provided to balance it out. It is, therefore, a fundamental dynamic requirement of a satisfactory peak-limiting amplifier that a high signal-to-control-voltage ratio be maintained at the output terminals throughout each gain-reduction cycle. One audible effect of an insufficient degree of con-

---

* Decimal classification: R363.2×R255.1. Original manuscript received by the Institute, December 20, 1946; revised manuscript received, April 30, 1947.

† Columbia Broadcasting System, Inc., New York, N. Y.

[1] F. E. Terman, "Radio Engineers' Handbook," McGraw-Hill Book Co., New York, N. Y. 1st edition, 1943, p. 413.

trol-voltage balance is a pronounced and disagreeable "thump" or "click" every time the signal reaches a peak amplitude sufficient to produce limiting.

In some cases the thump component may be so large and the nature of the control circuit such that over-control occurs, i.e., the output signal voltage decreases to a very small value immediately after the onset of an input signal peak. In the most extreme cases of unbalance the thump component may be so heavy as to produce sustained low-frequency oscillations ("motorboating") at the output terminals.

Another requirement of a peak-limiting amplifier is that the slope of the output-signal versus input-signal curve be as close to zero as possible for all input signal levels in excess of that corresponding to the threshold of gain reduction. This is equivalent to saying that the gain of the amplifier should be inversely proportional to the input level for all increases of input level above the threshold point. While this requirement is not in itself a dynamic one, it frequently has a direct bearing on the dynamic stability of the amplifier, since in the majority of commercial peak-limiting amplifiers available today a flat output-level characteristic can be obtained only by an increase of the sensitivity of the signal-control circuit. It is a fundamental relationship[2] that, the greater the sensitivity of the signal control circuits of these amplifiers, the more susceptible the amplifiers are to "thumping" and instability.

The "recovery time" of a peak-limiting amplifier is also an important dynamic characteristic. Optimum recovery time is a combined function of the characteristics of the input signal and the personal preferences of the individual user. The longer the recovery time, the less noticeable is the effect of the automatic gain-reducing action on the dynamic range and balance of the program material. In general, the shorter the recovery time which can be tolerated from a listening standpoint, the higher will be the average signal level at the output terminals. If the recovery time is much shorter than 0.2 second, the gain of the amplifier will change appreciably between successive cycles of low-frequency signal voltages, resulting in severe wave-form distortion. With the exception of a few cases where the amplifier design is such that a change in recovery time also changes the attack time, there are usually no instability problems associated with the recovery-time circuits.

III. Dynamic-Measurement Technique

The basic technique of the dynamic measurements to be described consists of suddenly applying a sustained signal of high peak amplitude to the input terminals of the peak-limiting amplifier and analyzing the resulting voltage at the output terminals, from the instant the peak signal is applied until the output voltage reaches a steady-state condition. A sine-wave voltage of a known frequency is perhaps the most significant signal wave form which can be used for such transient analysis, since any distortion of the output voltage due to transient effects is readily detectable. A sinusoidal wave form also provides a convenient time base when measuring the elapsed time from the instant of its application to the amplifier to the time when the output voltage reaches a steady-state condition.

The following dynamic-measurement technique was employed in obtaining the results described in this paper. With reference to Fig. 1, the measurement technique consists of:

1. The application of a sinusoidal signal voltage e of a predetermined frequency f to the input terminals of the peak-limiting amplifier, the amplitude a of the signal voltage being of such a value that the peak-limiting amplifier is on the threshold of gain-reducing action.

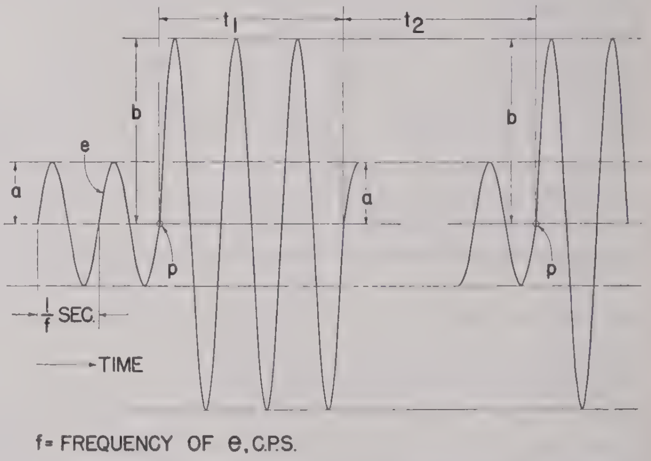

Fig. 1—Wave form applied to input of peak-limiting amplifiers for analysis of dynamic performance. The sine-wave amplitude a i adjusted so that the amplifier is on the verge of gain-reducing action. Amplitude b is any desired higher amplitude. The shift from amplitude a to amplitude b is made at a point p when the sine wave is crossing the axis of zero amplitude.

2. The effectively instantaneous increase of the amplitude of the input signal voltage e to a greater predetermined value b at a time phase when e is crossing the axis of zero amplitude (point p of Fig. 1) in either the positive or negative direction, as desired.

3. The maintenance of amplitude b of the input signal for a predetermined time interval t_1, and at the end of that interval the restoration of the input signal level to amplitude a for a predetermined time t_2.

4. The connection of a cathode-ray oscillograph to the output terminals of the peak-limiting amplifier, and the initiation and synchronization of a linear-time-base sweep voltage in the oscillograph, so as to display visually on the cathode-ray tube a predetermined number of cycles of the output signal voltage immediately before and after the application of signal amplitude b to the input of the amplifier.

5. At the end of time t_2, the repetitive re-application

---

[2] W. L. Black and N. C. Norman, "Program-operated level-governing amplifier," Proc. I.R.E., vol. 29, pp. 573–578; November, 1941.

for times t_1 of the increased amplitude b to the input of the peak-limiting amplifier. Time t_2 may or may not bear a fixed periodic relationship to t_1. It is required only that time (t_1+t_2) be an integral multiple of $1/f$, and that the sweep voltage of the oscillograph be so initiated and synchronized that successive traces of the electron beam across the cathode-ray-tube screen are exactly superimposed on one another to produce a stationary visual pattern of the output signal voltage for the predetermined number of cycles before and after the application of the increased amplitude b to the input of the peak-limiting amplifier.

6. The graphical analysis of the amplitude and wave form of the cathode-ray-tube pattern, and comparison of this pattern with the applied input voltage to the peak-limiting amplifier.

In a study of peak-limiting-amplifier performance, the time t_1 of Fig. 1 is an arbitrary value sufficiently long to allow complete gain reduction of the amplifier to take place. For the specific measurements described and illustrated below, the time t_1 was chosen to be approximately 10 milliseconds. It was subsequently found, however, as will be illustrated, that few if any of the current commercial peak-limiting amplifiers examined reach a stable output amplitude within the 10-millisecond observation period under all conditions of operation.

It is usually required in such an investigation that the time t_2 of Fig. 1 be of at least 1 to 3 seconds' duration, since the recovery time of most peak-limiting amplifiers is of this order of magnitude. Therefore, the cathode-ray tube used for viewing the transient phenomena should have a long-persistence type of screen phosphor, so that a visual impression of the transient trace will remain continuously on the screen between cycles of the recurrent transient phenomena.

The phenomena which occur for the first several cycles immediately after the establishment of amplitude b are usually of the greatest interest. By the use of the above-described measurement technique, the gain-reducing action of the amplifier can be observed cycle by cycle of the applied sine-wave signal, and the attack time is measured by counting the number of cycles of a given frequency to the point where no further change of amplitude takes place. Accompanying undesirable effects, such as thump and wave-form distortion, are also shown in as great detail as desired merely by changing the sweep speed of the oscillograph.

An important requirement of this method of transient analysis is that the change from amplitude a to amplitude b of Fig. 1 be made at a time when the applied sine-wave signal is crossing the axis of zero amplitude. If the amplitude change were to be made at any other part of the cycle an irregular wave front would be developed, rendering the transient analysis more difficult of interpretation.

IV. MEASURING EQUIPMENT

A block diagram of the required measuring equipment is shown in Fig. 2. A signal generator A, which may be a standard commercial type of audio oscillator, delivers a sinusoidal voltage of predetermined frequency to an electronic switch and synchronizer unit, B. The electronic switch and synchronizer unit consists of a combination of electronic circuits which provide the signal amplitude changes, phasing, and synchronizing functions required for the visual presentation of the transient phenomena on the cathode-ray oscillograph, C. The electronic switch and synchronizer unit supplies the input terminals of the peak-limiting amplifier under measurement (block D of Fig. 2) with voltage of the wave form shown in Fig. 1. It also supplies a synchronized triggering voltage to the linear-sweep-control circuits of the cathode-ray oscillograph, C. The cathode-ray oscillograph may be a standard commercial unit, providing it is designed for single-sweep, externally triggered operation.

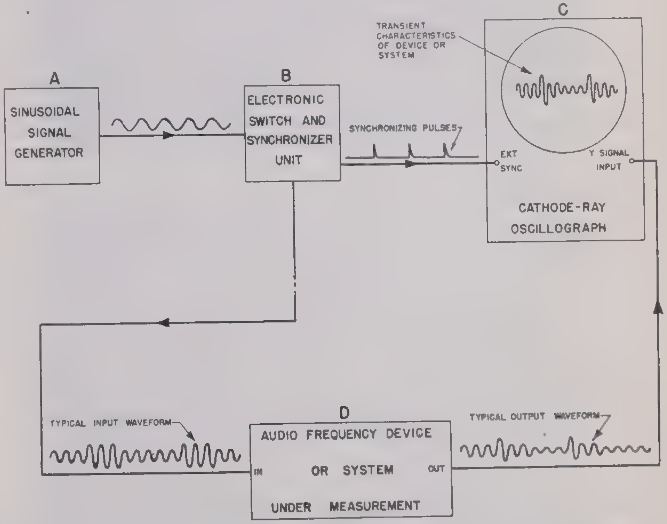
C
TRANSIENT CHARACTERISTICS OF DEVICE OR SYSTEM
A
SINUSOIDAL SIGNAL GENERATOR
B
ELECTRONIC SWITCH AND SYNCHRONIZER UNIT
SYNCHRONIZING PULSES
EXT SYNC
Y SIGNAL INPUT
CATHODE-RAY OSCILLOGRAPH
TYPICAL INPUT WAVEFORM
D
AUDIO FREQUENCY DEVICE OR SYSTEM UNDER MEASUREMENT
IN
OUT
TYPICAL OUTPUT WAVEFORM

Fig. 2—Block diagram of setup for analyzing dynamic performance of peak-limiting amplifiers.

The transient wave forms displayed on the cathode-ray-tube screen by this method lend themselves readily to photographing. The photographs, which form the basis of discussion for following sections of this paper, were selected from a considerable number taken of peak-limiting-amplifier performance under various operating conditions.

V. OBSERVED DYNAMIC PERFORMANCE OF TYPICAL COMMERCIAL PEAK-LIMITING AMPLIFIERS

The equipment described in the preceding section permits analysis of peak-limiting-amplifier performance at any frequency between 100 and 15,000 c.p.s., and at any desired ratio of peak signal level to threshold signal level (ratio of amplitude b of Fig. 1 to amplitude a). For the sake of brevity, however, results shown in this paper have been confined to two frequencies, 1000 and 10,000 c.p.s., and a single peak-to-threshold signal-amplitude ratio of approximately 18 db. The photographs shown in Fig. 3 are the transient signal wave forms applied successively to the input terminals of each of five different peak-limiting amplifiers. The application of these wave forms to the input terminals result in the output wave forms analyzed individually below for each of the amplifiers. Fig. 3(a) shows the 1000-cycle input wave form, while Fig. 3(b) shows the 10,000-cycle input wave form. These photographs are direct time exposures of the phenomena displayed on the cathode-ray-tube screen. For the purpose of analysis and discussion, reference axes and boundaries have been hand-drawn on many of the photographic prints shown in Figs. 3 through 7.

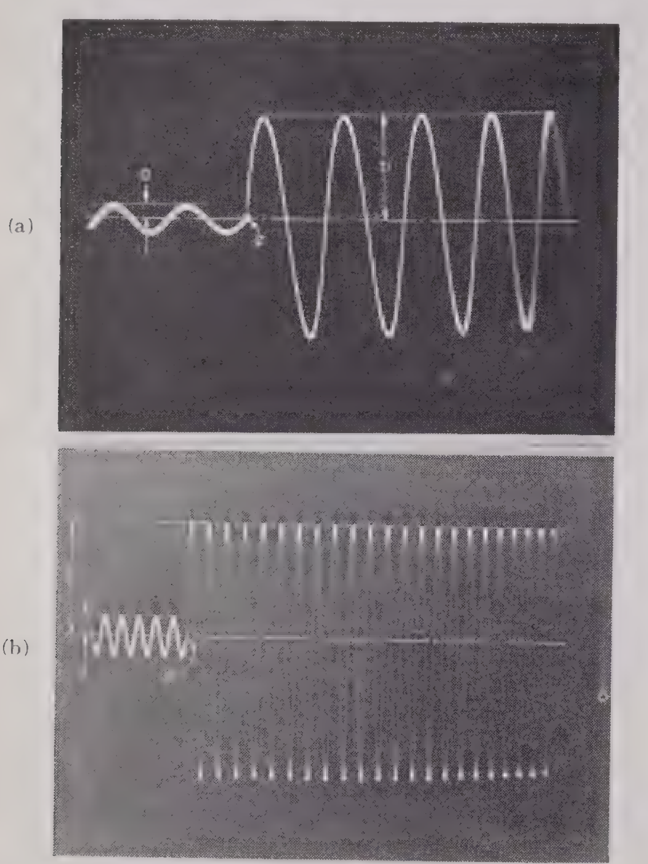

Fig. 3—Photographs of input wave forms applied to peak-limiting-amplifiers for analysis of dynamic performance. These are direct photographs of images appearing on the screen of the cathode-ray oscillograph. Amplitude *a* corresponds to the threshold of gain-reducing action. Amplitude *b* is approximately 18 db greater than *a*. Some second-harmonic distortion of the input wave form is evident, but this does not appreciably affect the results of the transient analyses to follow.
(a) 1000-c.p.s. sine-wave frequency.
(b) 10,000-c.p.s. sine-wave frequency.

The measuring equipment is so adjusted that some two to five cycles immediately preceding the arrival of the transient peak signal are shown for purposes of comparison with the phenomena occurring after the arrival of the transient. As mentioned above, the high-amplitude transient signal (amplitude *b* of Figs. 3(a) and 3(b)) persists for about 10 milliseconds, which is equivalent to 10 cycles of the 1000-c.p.s. signal, and 100 cycles of the 10,000-c.p.s. signal. The sweep speed of the oscillograph is adjusted for good resolution of each individual cycle, which usually results in only the first few cycles immediately after the onset of the peak being displayed on the screen. This is illustrated by Fig. 3(a), where two cycles before and four cycles after the onset of the peak appear on the screen of the cathode-ray tube. Obviously, merely by changing the sweep speed of the oscillograph each cycle can be studied in as great detail as desired, or, if the sweep speed is made sufficiently slow, the action of the peak-limiting amplifier may be observed throughout the entire 10-millisecond period. In general, a relatively fast sweep speed is used when it is desired to study wave-form distortion in detail, and a slower sweep speed is used when the peak envelope is of chief interest. The case of a relatively slow sweep speed is illustrated in Fig. 3(b) for the 10,000-c.p.s. signal, where the first twenty-odd cycles of high-amplitude transient appear on the cathode-ray tube. In this latter case, any cycle-to-cycle peak-amplitude variations would be clearly indicated.

Considerable care was taken in the generation of the applied wave forms of Fig. 3 to insure that no d.c. component of voltage was included in the high-amplitude signal after the points *p*. Close examination of these wave forms will reveal a slight dissymmetry of the positive and negative peak amplitudes due to second-harmonic distortion in the high-amplitude signal. This is not a desirable condition, but one imposed by signal-handling limitations in the electronic switch and synchronizer unit discussed in Section IV. Further development of the latter unit, since these photographs were taken, eliminated this distortion, but it was not considered of sufficient magnitude to affect substantially the results of the present analyses of peak-limiting-amplifier performance.

The response of several commercial peak-limiting amplifiers to the applied wave forms of Fig. 3 will now be analyzed. The sole purpose of these analyses is to describe dynamic phenomena which occur in typical commercial peak-limiting amplifiers; they are intended to be neither a recommendation nor a condemnation of the subject amplifiers.

Peak-Limiting Amplifier 1, Fig. 4

The first two cycles shown at the left of Fig. 4(a) represent an output level corresponding to the threshold of gain reduction, prior to the onset of the sinusoidal signal peak. Study of the wave form beyond the point *p* reveals that the first half-cycle rises to an amplitude *c* approximately 12 db above the threshold amplitude, showing that gain-reducing action has been insufficiently fast to reduce the amplitude of the first half-cycle of the 18-db, 1000-cycle peak by more than approximately 6 db. The amplitude *d* of the second half-cycle is seen to be reduced further, but it is still some 9 db above the peak threshold level *a*. It is evident from Fig. 4(a) that approximately two complete cycles of the 1000-cycle peak are required for effectively complete gain reduction. This can be interpreted to mean that the attack time of this amplifier is 2 milliseconds (the period of two cycles of a 1000-cycle frequency), as indicated by the time t_a on Fig. 4(a). It can be seen from Fig. 4(a) that there has taken place an axial shift of the output voltage during the process of gain reduction, as indicated by the distance g between the axes of the sine wave before and after gain reduction. This is the result of a d.c. component of control voltage which has not been completely balanced out, and represents the "thump" component of this amplifier for the particular peak signal applied. Note that, even though the sine-wave amplitude after gain reduction is apparently no greater than before the arrival of the peak, the axial shift due to thump results in all negative peaks shown on Fig. 4(a) exceeding the negative peak threshold amplitude a by a value of approximately 4 db. Therefore, were amplitude a equivalent to 100 per cent modulation of an associated transmitter, substantial overmodulation would persist for a much longer period than the apparent attack time of 2 milliseconds.

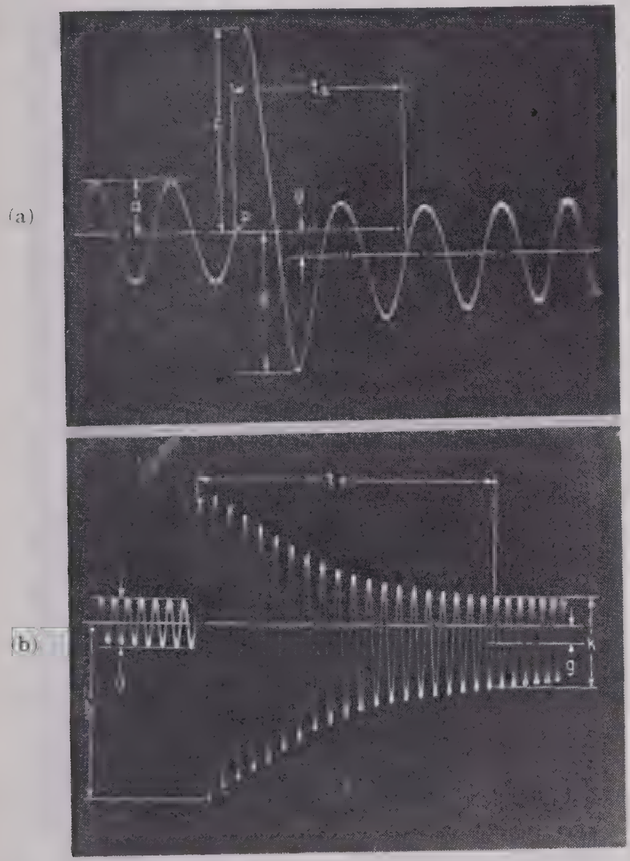

Fig. 4—Peak-limiting amplifier 1. Photographs of output wave forms when input wave forms are as shown in Fig. 3.

(a) 1000 c.p.s. The first cycle after arrival of the higher-amplitude peak at point p overshoots heavily due to slow attack time. Two complete cycles are required before a stable output amplitude is reached, indicating attack time t_a to be approximately 2 milliseconds. A strong thump component g is also shown.

(b) 10,000 c.p.s. The first twenty cycles after arrival of the peak show excessive amplitude, further confirming the attack time t_a to be 2 milliseconds. The steady-state amplitude k is approximately 6 db higher than the threshold amplitude a, indicating deficient high-frequency response in the control-voltage circuit. A thump component g is also indicated.

Since the signal path of no commercial peak-limiting amplifier can pass d.c., the time duration of the thump component indicated by g is a complicated function of the low-frequency response of the amplifier signal- and control-voltage circuits, as well as the feedback-loop gain of the control-voltage circuit. Frequently the amplitude of the thump component decreases in the form of a damped oscillation. This can be considered as an envelope modulation of the signal frequency, and an oscillation frequency on the order of 5 to 10 c.p.s. is common. Therefore, the 2- or 3-millisecond observation period of Fig. 4(a) is too short to indicate any appreciable decrease in the magnitude of the thump amplitude g.

A consideration of the above factors makes it evident that a constant output amplitude may not be reached for an appreciable fraction of a second after the application of a sustained peak signal. The actual time required for an essentially steady-state amplitude to be attained is thus a function of the original magnitude of the thump component and the decay period of the individual amplifier. This low-frequency thump component can very readily have a more disagreeable listening and operational effect on the signal than the short-duration, high-amplitude bursts which pass through the amplifier due to an insufficiently short attack time. For instance, it is not uncommon for the modulator of an amplitude-modulated transmitter using inverse feedback to have a sharply rising, subaudible, low-frequency response, the peak of which may coincide with the thump envelope frequency; in which case the thump is aggravated, and the modulator may be completely disabled for the duration of the thump. In an extreme case there might be developed an oscillation of sufficient amplitude to trip an overload circuit and remove the transmitter from the air.

The magnitude of the thump component in any amplifier varies with the amplitude of the peak which produces gain reduction. Some peak-limiting amplifiers have a so-called thump control which is effective in balancing the thump for any single amplitude of peak signal, but since the gain-reducing circuits seldom exhibit the same degree of balance at any other degree of gain reduction, these thump controls merely permit a compromise adjustment which has the lowest average thump content under normal program conditions.

The thump amplitude g of Fig. 4(a) is by no means of unusual magnitude, as peak-limiting amplifiers go. In fact, it is probably not great enough to be detected solely by a listening test of the audio output of the amplifier. Nor is it likely, either, that the high-amplitude bursts which are shown to occur for the first cycle or two can be detected by a simple listening test.

So far, no detailed tests have been made to correlate the transient effects observed on the oscillograph with the subjective listening effects of these transient phenomena. Preliminary observations, however, indicate that if the amplitude of the thump component, shown by the above sine-wave test, is as great as the threshold signal amplitude (i.e., if amplitude g of Fig. 4(a) is as great as amplitude a), then a listening test with ordinary program material is very likely to disclose a disagreeable "thump" each time heavy gain-reducing action occurs. Perhaps even more significant than the amount of audible thump observed at the output terminals of the amplifier, however, is the possible ill effect the thump component may have on subsequent audio equipment, such as the modulator described above.

Fig. 4(b) shows the effects on amplifier 1 of a peak signal having a frequency of 10,000 c.p.s. Here the 2-millisecond attack time t_a is perhaps more clearly illustrated than in the 1000-c.p.s. case. It is seen that approximately 20 cycles are required after the application of the peak for the output amplitude to approach the more or less constant value k of Fig. 4(b). The first few cycles of the 10,000-c.p.s. peak pass through the amplifier with little or no attenuation.

It is noted that the amplitude k of Fig. 4(b) is about 6 db greater than the amplitude a, a very undesirable condition probably indicating deficient high-frequency response in the control-voltage circuit. This is a deficiency which would also be indicated by steady-state measurements. A thump component g is also present in the 10,000-c.p.s. case.

Peak-Limiting Amplifier 2, Fig. 5

The photographs of Fig. 5 show that amplifier 2 has considerably less amplitude of overshoot than amplifier 1 during the period while gain reduction is taking place. This particular amplifier is designed to produce peak-chopping action at an output amplitude approximately 3 db above the threshold amplitude. The peak-chopping action is independent of automatic gain reduction and, hence, limits the maximum peak amplitude to about 3 db above the threshold value, regardless of how long it takes for complete gain reduction to be effected. Amplitude c of Fig. 5(a) and Fig. 5(b) corresponds to the peak-chopping level of this amplifier, and, were there no gain-reducing action, the output wave form after point p would be flat-topped and of amplitude c. Note, in the 1000-cycle case, Fig. 5(a), that a substantial part of the first half-cycle remains at or near the peak-chopping level, before sufficient gain reduction has occurred to reduce the output amplitude below this value. Fig. 5(b) shows that the output level remains near the peak-chopping value for about the first three cycles of a 10,000-cycle peak.

It may be noted from Fig. 5(a) that considerable wave-form distortion is evident near the peaks of at least the first four complete cycles after the arrival of the 1000-cycle peak. This indicates that gain-reducing action is still going on, even though the peak amplitude reaches a relatively stable value d after the first cycle. If the photograph of Fig. 5(b) were expanded on a faster sweep, considerable wave-form distortion would also be observable over the first 30 or 40 cycles after the arrival of the 10,000-cycle peak. From Fig. 5(b) it is seen that approximately six cycles are required for the output amplitude to reach its stable value d, which indicates that the attack time of amplifier 2 is approximately 0.6 millisecond. In view of the fact that considerable wave-form distortion persists for a much longer period, however, this factor should probably be taken into account. If the attack time of amplifier 2 is based upon the time required for the output wave form to become essentially sinusoidal, the value would be on the order of 4 milliseconds, instead of 0.6 millisecond.

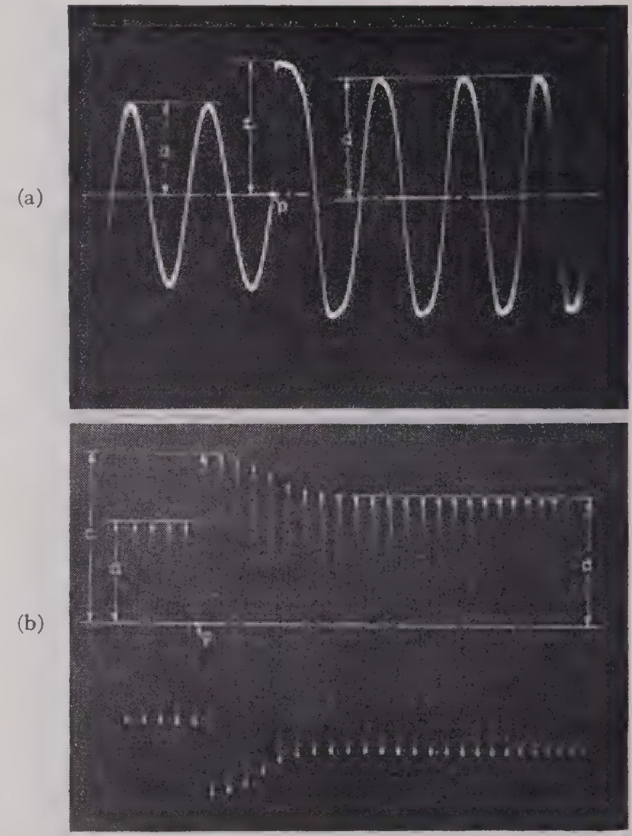

Fig. 5—Peak-limiting amplifier 2. Photographs of output wave forms when input wave forms are as shown in Fig. 3.

(a) 1000 c.p.s. This amplifier includes peak-chopping action for all input peaks more than approximately 3 db above limiting threshold level. The first half-cycle after arrival of the peak reaches the peak-chopping amplitude c. The next several half-cycles, while of reduced amplitude, show considerable distortion on peaks. The thump component is low.

(b) 10,000 c.p.s. The first two or three cycles remain at peak-chopping amplitude c. Approximately six cycles are required for full gain reduction, making the attack time approximately 0.6 millisecond.

Amplifier 2 appears to have a low thump component, as indicated by very little axial shift of the wave form before and after gain reduction. This particular amplifier is provided with a "thump" control, and optimum adjustment of this control was made before the photographs of Figs. 5(a) and 5(b) were taken. However, as noted in the discussion of amplifier 1, the thump control insures a low thump component for only one particular amplitude of peak signal; for some lower or higher amplitude of peak, amplifier 2 might exhibit appreciable thumps.

Peak-Limiting Amplifier 3, Fig. 6

As evidenced in Fig. 6, this amplifier exhibits a heavy thump component. The thump effect of amplifier 3 is great enough to be definitely audible on a listening test with ordinary program material. It is observable from Fig. 6(a) that the initial thump (amplitude *c*) is almost twice the peak threshold amplitude *a*. Note that the zero-signal axis of Fig. 6(a) after the application of the 1000-cycle peak has a definite upward slope to it. This indicates that amplifier 3 has a more rapid thump-decay period than was exhibited by amplifier 1.

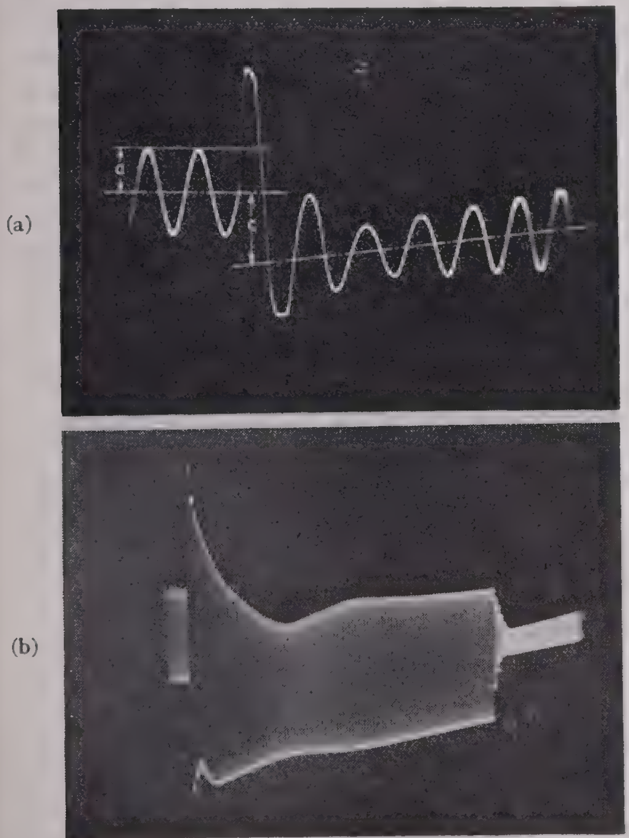

Fig. 6—Peak-limiting amplifier 3. Photographs of output wave forms when input wave forms are as shown in Fig. 3.

(a) 1000 c.p.s. Extremely heavy thump component *c* greater than peak threshold amplitude *a* is shown. The amplitude of the first cycle after arrival of the peak appears to be limited only by the overload characteristics of the amplifier. The fourth half-cycle and several successive half-cycles show severe over-control wherein the amplitude is *less* than the threshold value *a*.

(b) 10,000 c.p.s. Somewhat slower sweep speed was employed for this photograph, so that the entire 10-millisecond period of duration of the peak is visible. No stable output amplitude has been reached during the 10-millisecond interval, so it is not possible to specify with meaning the attack time of this amplifier.

Fig. 6(a) illustrates an effect discussed in Section II of this paper, namely, over-control, or excessive gain reduction. It can be observed that the fourth half-cycle has an amplitude (as also have the next several cycles thereafter) *less* than the threshold amplitude *a*. This is a direct result of too heavy a thump component, and the thump voltage is rectified along with the signal voltage, producing excessive control voltage in the gain-reducing circuit.

Fig. 6(b) shows the 10,000-cycle output when the wave form of Fig. 3(b) is applied to the input. This photograph differs slightly from the 10,000-cycle photographs of Figs. 3, 4, and 5 in that a slower sweep speed has been employed. In this photograph the entire 10-millisecond period of duration of the peak is visible. So close are the individual cycles under this condition that the resulting picture is essentially an envelope of the output peak amplitudes. It is difficult to offer a rational explanation for the shape of this 10,000-cycle envelope, since it is such a complicated function of the transient characteristic of the amplifier circuits.

At the end of the 10-millisecond peak, the output voltage of the amplifier is seen to be less than that immediately preceding the onset of the peak, the difference between the two amplitudes being a measure of the gain reduction that has taken place in the amplifier.

Due to the severe thump components of amplifier 3, it is difficult to specify definitely its attack time. For instance, although Fig. 6(a) indicates that maximum gain reduction occurs about 2 milliseconds after the application of the peak, the negative peak amplitude at that point is still more than 6 db greater than the threshold amplitude *a*, due to the magnitude of the thump. Nor has a stable output amplitude been reached within the 10-millisecond period of duration of the peak.

VI. CBS Experimental Amplifier

In one or several ways it has been observed that each of the peak-limiting amplifiers analyzed in Section V leaves considerable room for improvement. The Columbia Broadcasting System recently developed a unit which has outstanding dynamic-performance characteristics. The dynamic performance of this experimental amplifier is shown in Fig. 7.

The CBS amplifier has a maximum control range of 14 db; therefore, the analyses of Fig. 7 differ from those covered in Figs. 3, 4, 5, and 6 in that the transient peak amplitude is 14 db above the threshold value rather than 18 db. The 14-db transient was simulated at each of two frequencies, 1000 and 10,000 c.p.s. Except for the 4-db difference in amplitude, the input wave forms were similar to those shown in Fig. 3, and the resulting output wave forms of the CBS amplifier are shown in Figs. 7(a) and 7(b).

With reference to the 1000-cycle dynamic performance of Fig. 7(a), the first two cycles at the left of the photograph show the output voltage immediately before the arrival of the transient peak, while the next six cycles correspond to the output voltage immediately after the arrival of the peak. Note that not even the first half-cycle after the arrival of the peak shows any appreciable amplitude overshoot. Thus, the attack time of the CBS amplifier under the above conditions is effectively zero. What may seem more surprising is the fact that there is little wave-form distortion of even the first quarter-cycle after the arrival of the 1000-cycle transient.

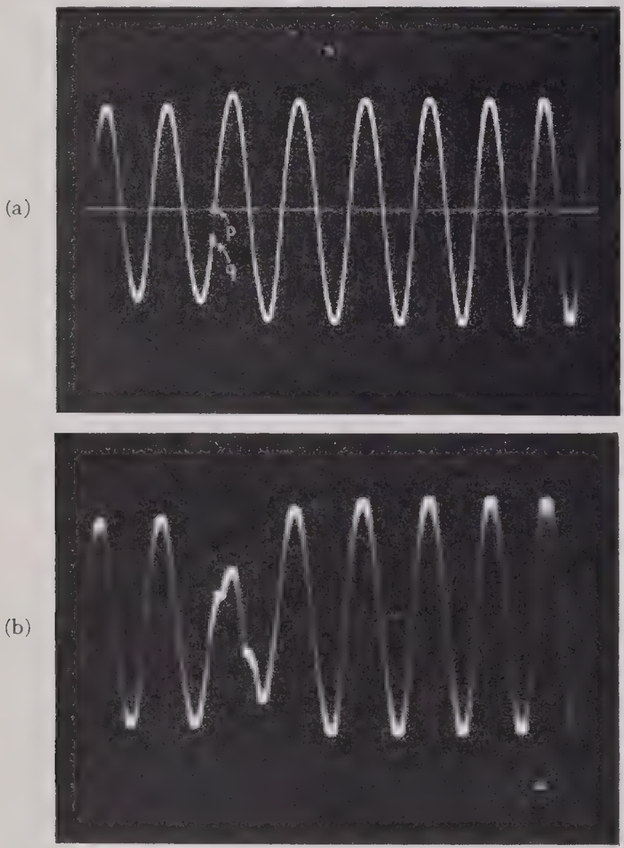

Fig. 7—CBS experimental peak-limiting amplifier, early model. Photographs of output wave forms. Input wave forms are the same as in Fig. 3, except that the amplitude of the transient peak is 14 instead of 18 db.

(a) 1000 c.p.s. No appreciable amplitude overshoot occurs; therefore the attack time is effectively zero. Note that even the first half-cycle is essentially undistorted. The thump component is negligible. The amplifier is seen to "anticipate" the arrival of the peak, since gain-reduction takes place at point *q* in time, whereas the peak does not start until point *p*.

(b) 10,000 c.p.s. No amplitude overshoot is present even on the first half-cycle after the arrival of the signal peak. The first cycle is over-controlled in amplitude.

This excellent performance is attributable to a unique circuit design wherein the automatic-gain-control voltage is a function of the input signal voltage, rather than of the output signal voltage. The control-voltage generating section of the amplifier incorporates large power-type amplifier and rectifier tubes in low-impedance circuit arrangements, resulting in extremely fast development of the automatic control voltage. Another major factor contributing to the exceptional performance shown in Fig. 7(a) is the use of a special time-delay network in the signal channel just ahead of the point where gain reduction takes place. This network acts to delay the signal by approximately 80 microseconds, and the gain is already reduced by the required amount upon the arrival of the peak at the point where gain control is effected. A close examination of Fig. 7(a) will reveal that automatic gain reduction occurs near the point *q* in time, whereas the 14-db peak does not arrive until a later time at point *p*.

The 10,000-cycle performance shown by Fig. 7(b) again illustrates the extremely short effective attack time of the amplifier. Even at 10,000 cycles, the 14-db peak which arrives at the point *p* in time is effectively prevented from exceeding the maximum steady-state value. Fig. 7(b) indicates excessive gain reduction (over-control) for the first cycle after the arrival of the peak. Over-control which persists for so short a time as shown in Fig. 7(b) (approximately 100 microseconds) cannot be perceived by a listening test, and is certainly preferable to under-control, since it renders overmodulation of subsequent equipment impossible.

It can be observed from Fig. 7 that the "thump" component of the amplifier is of very small amplitude, an additional design feature of this unit.

The amplifier described above was developed by E. E. Schroeder of the CBS-Chicago technical staff, under the direction of J. J. Beloungy, and has been used at station WBBM since 1945. Additional amplifiers, based upon this development, are in service in other Columbia Broadcasting System stations and are also available commercially from a well-known manufacturer.

VII. CONCLUSION

It is beyond the scope of this paper to attempt to set forth minimum standards for satisfactory transient performance of peak-limiting amplifiers. However, it seems evident that the more nearly the dynamic performance of a given peak-limiting amplifier conforms to the requirements set forth in this paper, the more satisfactory the operational results are likely to be.

The measuring technique and equipment used to obtain the results described in this paper are applicable to a wide variety of transient measurements of audio devices and systems, such as the transient performance of loudspeakers and recording and reproducing systems, and the build-up and decay characteristics of reverberant acoustical structures.

The technical developments and investigations which form the basis for this paper were carried out under the general direction of Howard A. Chinn, chief audio engineer of the Columbia Broadcasting System.

Radio Doppler Effect for Aircraft Speed Measurements[*]

LEONARD R. MALLING[†], ASSOCIATE, I.R.E.

Summary—**Measurement of the ground speed of aircraft by the use of the radio doppler effect is discussed, and the technical details of one complete system are presented. In this particular system, radio signals are transmitted from the ground, received in an airplane, and retransmitted to the ground for measurement of the doppler beat frequency. An accuracy of 0.1 per cent is obtained using simple techniques for frequency stabilization. Some experimental results of flight tests are given.**

INTRODUCTION

THE CONTINUAL trend of aircraft design toward higher and higher speed has created many problems for flight-test engineers who are responsible for performance tests of prototype airplanes. One of these is the problem of calibrating the conventional pitot-static air-speed system at high velocities. A customary method of performing this calibration has been to fly at very low altitude over a measured course while timing the flight with stop watches. By averaging the times required to fly the course in opposite directions, the effect of wind can be eliminated and a true measure of air speed obtained. This method has been extensively used but is subject to the following limitations:

1. Air conditions are uncertain at low altitude, so flights are frequently unsuccessful.
2. It is extremely hazardous to fly at low altitude with high-speed airplanes.
3. In the Seattle area it has been necessary to use an overwater course because of the rugged terrain and, if the crosswind exceeds 10 m.p.h., the airplane drifts so far off course that timing becomes difficult.

An alternative method of performing air-speed calibrations by means of a so-called "trailing bomb" has the advantage of measuring air speed directly without corrections for wind, but it has the disadvantage that with present techniques it cannot be used at speeds in excess of 350 m.p.h.

GENERAL PRINCIPLES OF DOPPLER SYSTEM

Various electronic means have been considered for the measurement of ground speed of airplanes, and the most satisfactory from the standpoint of simplicity and accuracy appear to be those based on the doppler effect of radio waves. According to the doppler principle, the frequency of a radio wave is increased if the source is moving toward the observer, or decreased if the source is moving away from the observer, according to the equation

$$f_0 = \frac{1 + \dfrac{V}{c}\cos\theta}{\left[1 - \left(\dfrac{V}{c}\right)^2\right]^{1/2}} f_s \qquad (1)$$

where f_s = source frequency, f_0 = observed frequency, V = speed of source, c = speed of propagation, and θ = angle between motion of the source and the line of sight. Since $V \ll c$, the denominator is very nearly equal to 1. If we assume that the observer is on an airplane headed at constant altitude in the direction of a source on the ground, the angle θ lies in a vertical plane, as shown in Fig. 1. Furthermore, with the airplane flying level at an altitude of 5000 feet and 25 miles from the source, the angularity correction is of the order of 0.1 per cent, so that comparatively large errors in altitude or distance measurements have little effect on the accuracy of speed measurements. Omitting the angularity correction, (1) becomes

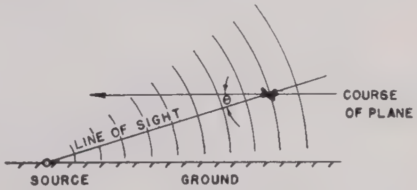

Fig. 1—Relation of course flown by a plane at constant altitude to line-of-sight.

$$f_0 - f_s = \frac{V}{c} f_s \qquad (2)$$

or

$$\frac{V}{c} f_s = \Delta f. \qquad (3)$$

Substituting typical values, $f_s = 200$ Mc., $V = 200$ miles per hour, $c = 186{,}000$ miles per second, we obtain $\Delta f \cong 60$ c.p.s. It will be seen at once from (2) that it would be impossible to measure V by separate independent measurements of f_0 and f_s because an error of 1 part in 200 million in either of them would cause an error of 2 per cent in determining V. If, however, the two frequencies are heterodyned to obtain the difference frequency Δf, V can be determined from (3) with whatever accuracy f_s and Δf are known. Both of these frequencies can be measured with very high precision by the use of quartz-crystal oscillators, although for ground-speed measurement quite mediocre oscillators will suffice, since it is only necessary to measure V within 0.1 per cent.

---

[*] Decimal classification: R520×621.375.614. Original manuscript received by the Institute, October 18, 1946; revised manuscript received, February 3, 1947.

[†] Formerly, Boeing Aircraft Company, Seattle, Wash.; now, Malling Laboratories, Seattle, Wash.

Requirements for Doppler System

A considerable variety of systems based on the doppler principle can be devised, and in order to choose among them it is necessary to specify the desired performance. The requirements for the Boeing radio-doppler ground-speed meter were as follows:

1. A 50-mile range in order to minimize angularity corrections for airplanes flying at high altitude, and to extend the area within which test flights can be made.
2. Elimination of altitude restrictions for test flights.
3. Use of a single ground installation to minimize setup time and simplify co-ordination.
4. Freedom for the pilot to fly in any direction, so that he can always fly with or against the wind.
5. Accuracy 0.1 per cent, with the time over which measurements must be averaged for a single observation reduced to the shortest possible interval.
6. The method used for recording the doppler beat frequency should be simple to use, and the data recorded should be in convenient form for analysis.

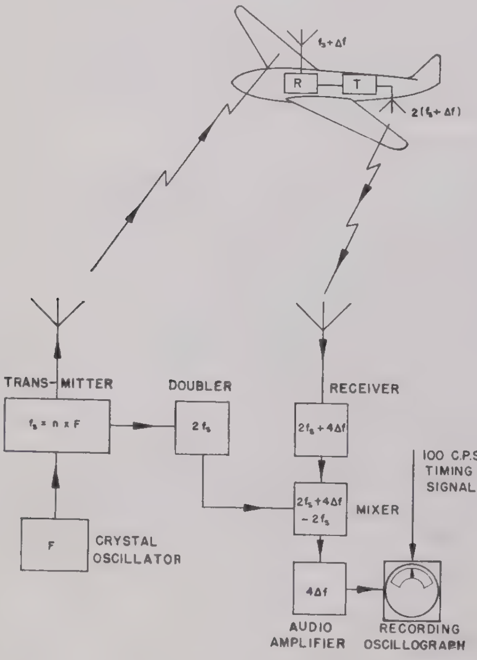

Fig. 2—Block diagram of the Boeing doppler ground-speed meter.

In order to eliminate the necessity of installing equipment in the airplane, a radar-echo type of system would be very desirable. However, radar equipment which meets all the requirements is not at present available, and would necessarily be fairly elaborate and expensive. Hastings has developed a system[1] using a radio transmitter in the airplane. However, this system requires the airplane to fly along a line between two fixed ground stations, and so fails to meet requirements 3 and 4. This restriction to a fixed line of flight could be eliminated by the use of three ground stations, but this further complicates the problems of ground installation and co-ordination.

The requirements have been met in the Boeing system by an arrangement somewhat analogous to a c.w. ground radar station, but with a small relay transmitter in the airplane to increase synthetically the intensity of reflected signals. In order to separate the output from the input of the relay station and prevent oscillation, the frequency of the received signal is doubled before retransmission. A block diagram of the system is shown in Fig. 2. In order to make speed measurements with this system, it is necessary for the airplane to fly radially toward or away from the ground station, but the pilot can choose any desired direction of flight provided the ground station has at least 180-degree vision.

Description of Equipment

A simplified schematic, Fig. 3, shows the circuit arrangements of the plane and ground equipment. The 200-Mc. signals, at a level as low as 1 millivolt, are received by the plane relay link, amplified, doubled in frequency, and retransmitted at 400 Mc. with a power of about 5 watts. To prevent instability because of mutual coupling between the transmitting and receiving antennas, the 200-Mc. antenna is mounted vertically below the fuselage, while the 400-Mc. antenna is mounted horizontally on the vertical stabilizer. Both antennas are quarter-wave stubs. A series-resonant transmission-line section reduces the 200-Mc. component in the 400-Mc. antenna, further improving stability of the plane relay system.

The ground-station equipment, including antennas and recording oscillograph, are contained in a test truck, shown in Fig. 4 with the antennas in the raised position. The horizontal corner reflector used for the 400-Mc. receiver and the 200-Mc. vertical antenna for the transmitter can be seen on the truck roof. The ground transmitter is of conventional v.h.f. design and has a temperature-controlled 12.5-Mc. crystal oscillator. The crystal frequency is multiplied by a series of doubler and power stages to a final frequency of 200-Mc. and an output power of 10 watts.

The 400-Mc. signal received from the airplane is amplified and combined in a mixer with the second harmonic of the signal being transmitted. The resultant audio beat is the doppler signal having a frequency proportional to plane speed. This frequency could be measured by means of a frequency meter or a counter. However, direct-reading frequency meters are not very accurate, and a counter might respond to occasional noise peaks or miss counts at points of low signal strength. Therefore, in order to be able to monitor the quality of the doppler signal, and also measure its frequency with high precision, it is recorded on one galvanometer of a recording oscillograph, while a 100-c.p.s. standard-fre-

---

[1] C. H. Hastings, "Radio ground speed system for aircraft," N.A.C.A. Report.

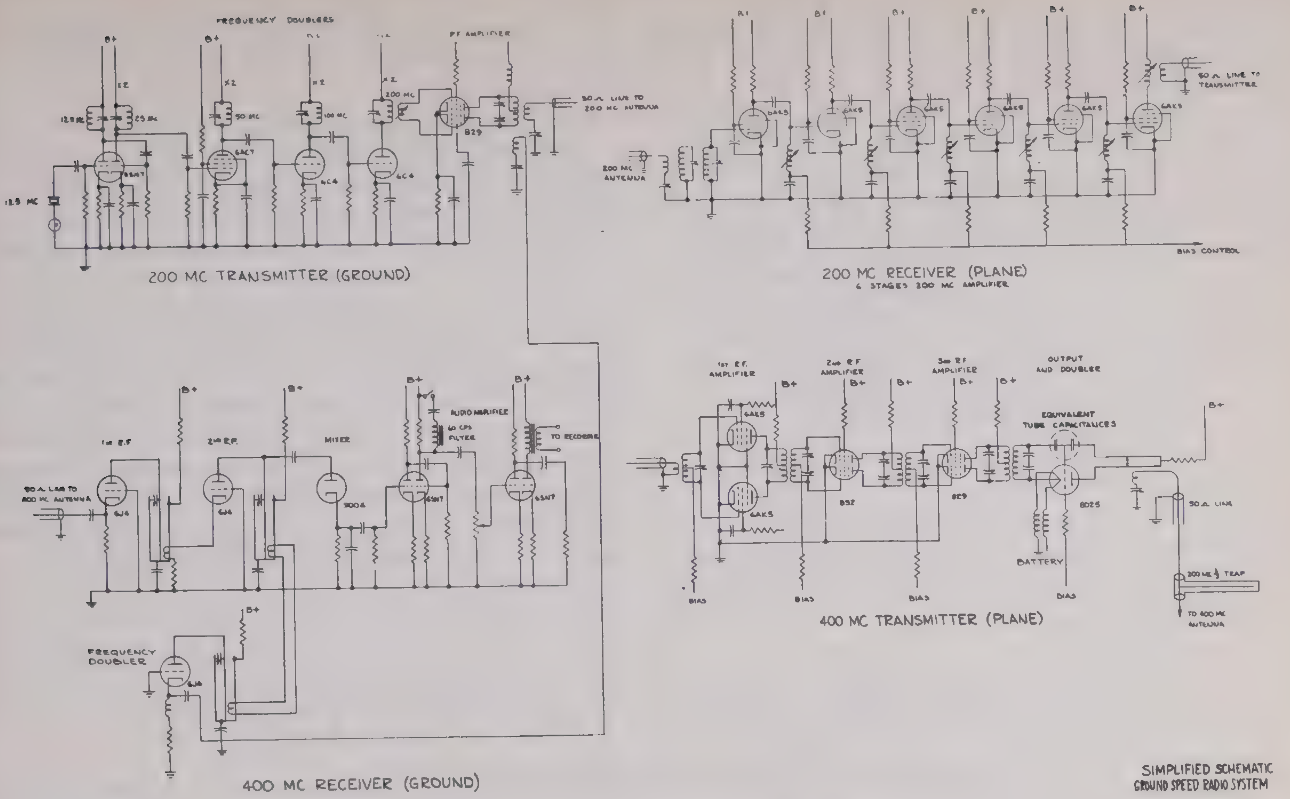
FREQUENCY DOUBLERS
RF AMPLIFIER
50 Ω LINE TO 200 MC ANTENNA
12.5 MC
829
200 MC TRANSMITTER (GROUND)
50 Ω LINE TO TRANSMITTER
200 MC ANTENNA
BIAS CONTROL
200 MC RECEIVER (PLANE)
6 STAGES 200 MC AMPLIFIER
1st R.F.
2nd R.F.
MIXER
AUDIO AMPLIFIER
60 CPS FILTER
TO RECORDER
50 Ω LINE TO 400 MC ANTENNA
FREQUENCY DOUBLER
400 MC RECEIVER (GROUND)
1st R.F. AMPLIFIER
2nd R.F. AMPLIFIER
3rd R.F. AMPLIFIER
OUTPUT AND DOUBLER
EQUIVALENT TUBE CAPACITANCES
BATTERY
BIAS
50 Ω LINE
200 MC ¼ TRAP
TO 400 MC ANTENNA
400 MC TRANSMITTER (PLANE)
SIMPLIFIED SCHEMATIC
GROUND SPEED RADIO SYSTEM

Fig. 3—Simplified schematic of the radio ground-speed meter.

quency timing wave is recorded on another galvanometer.

Experimental Results

Fig. 5 is a section of a typical oscillogram, from which the doppler frequency can be determined by counting the number of doppler cycles within any desired time interval.

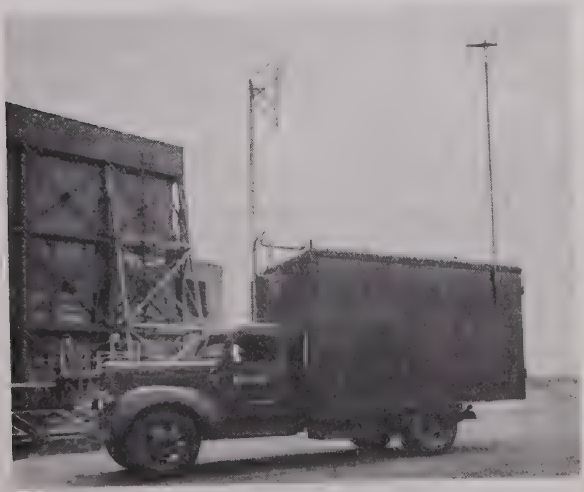

Fig. 4—Ground-speed-meter truck installation.

The 100-c.p.s. timing frequency and the frequency of the ground transmitter are both known within 0.01 per cent or less, so the error in measuring the radial component of velocity of the airplane is determined entirely by the error in counting cycles on the oscillogram. There are approximately 290 doppler cycles in one second, so that it is only necessary to estimate within $\frac{1}{3}$ of a cycle in order to obtain the average airplane ground speed during 1 second with an accuracy of 0.1 per cent. If it were of any value, still greater accuracy could be obtained by counting cycles over a longer period of time.

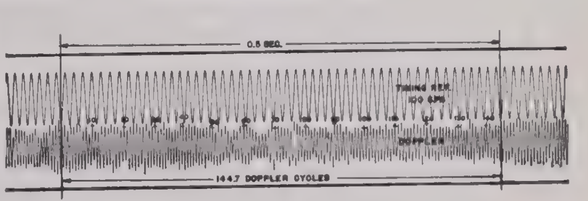

Fig. 5—Oscillogram of doppler signals.

Fig. 6 shows the results of a test in which doppler speed measurements were made during a timed flight over a measured speed course. It was necessary to fly at very low altitude in order to obtain accurate timing with stop watches, and the terrain was such that the doppler station had to be located slightly to the side at one end of the course. Consequently, angularity errors were large for the first few seconds of the run. The average of the doppler readings after the first 20 seconds, without making any corrections for angular error, was 229.4 m.p.h., while the average for the whole course as obtained by stop watches was 229.8 m.p.h.

The principal advantages claimed for the doppler ground-speed meter are:

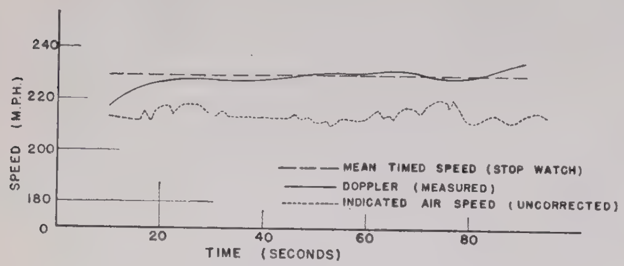

Fig. 6—Experimental results of a timed flight over a measured speed course.

1. Very high accuracy.
2. Speed is measured practically instantaneously, so that a flight condition does not have to be maintained for an extended period. This also facilitates corrections for wind, because the pilot can turn immediately and fly the reverse course with a minimum interval between the two tests.
3. The system can be used at high speeds without the hazard of low-altitude flying.
4. The pilot can always choose his course so as to fly exactly into or with the wind, because he can fly any radial course with respect to a single ground station.

ACKNOWLEDGMENTS

The advantages of a doppler system requiring only a single ground station, and means for achieving this using frequency doubling in the airplane, were first suggested in the latter part of 1943 by C. K. Stedman, physical research chief, Boeing Aircraft Company. Thanks are due to various members of the Physical Research Section who assisted with the development, and to personnel of the flight-test unit for their assistance with the test flights.

Force at the Stylus Tip While Cutting Lacquer Disk-Recording Blanks*

H. E. ROYS†, ASSOCIATE, I.R.E.

Summary—**Lacquer used for disk-recording purposes, being harder than wax, imposes a greater load on the cutting stylus and, consequently, upon the turntable drive system. In order to study the requirements, equipment has been developed to measure the force at the stylus tip while cutting unmodulated grooves. Reducing cutting bounce, a form of instability resulting in a groove of varying width, by using an advance ball or air dashpot was studied. The effect of height of the axis about which the recorder is pivoted above the record surface was also investigated.**

INTRODUCTION

WITHIN the past ten years a new disk-recording medium, of a cellulose nitrate base commonly called "lacquer," has been developed. This medium is harder than the wax compound used for commercial disk recording, and immediate playback of the recorded disk without appreciable impairment in quality is possible. The increased hardness of the lacquer medium over the wax imposes an additional load on the recording head and turntable driving system. Equipment has been developed for studying the cutting characteristics of the lacquer.

FORCE GAUGE

A simple device was constructed to permit measurement of the force at the tip of the stylus while cutting a blank groove. The pole piece and armature of a recording head was rotated 90 degrees from its normal position. This permits movement of the armature in a direction tangent to the groove, as shown in Fig. 1. The stylus, of course, is mounted so that the cutting surface remains in its normal plane. The deflection of the stylus is measured electrically. A 3000-c.p.s. field supply is used, and movement of the stylus induces a 3000-c.p.s. voltage in the armature coil which is proportional to displacement.

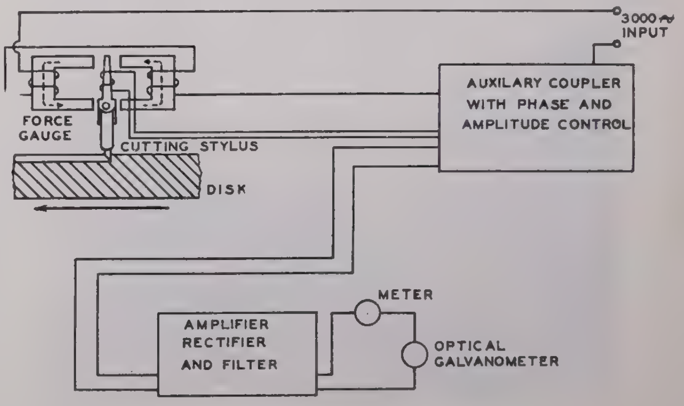
3000 ~ INPUT
AUXILARY COUPLER WITH PHASE AND AMPLITUDE CONTROL
FORCE GAUGE
CUTTING STYLUS
DISK
METER
AMPLIFIER RECTIFIER AND FILTER
OPTICAL GALVANOMETER

Fig. 1—Disk cutting-force equipment.

For steady forces or forces which vary at a very low rate, a direct-current meter is used to measure the rectified 3000-c.p.s. voltage. For variations at a higher rate, a galvanometer is used to indicate the modulation after the 3000-c.p.s. carrier has been filtered out.

---

* Decimal classification: R391.1. Original manuscript received by the Institute, June 7, 1946; revised manuscript received, February 2, 1947.

† Radio Corporation of America, RCA-Victor Division, Camden, N. J.

CUTTING FORCE INDEPENDENT OF SPEED

Measurements were made of the horizontal force at the stylus tip while cutting a groove of normal depth at different groove velocities. These measurements were started on the outside of a 16-inch-diameter "lacquer," and short bands were cut at 78 and 33⅓ revolutions per minute. The force-measuring gauge was freely suspended and was operated without the aid of a depth-regulating advance ball. The spring controlling the vertical force at the stylus was adjusted for a groove 5 mils in width and was not changed during the tests. The groove velocity, or cutting speed, was varied from 63 to 5 inches per second. The measured force at the cutting tip remained constant through the tests, and the groove showed no change in width. These results demonstrate that the cutting force is independent of the cutting speed. The observation can be checked quite easily by disconnecting the drive and allowing the turntable to coast to a stop while the stylus is cutting a blank groove. No change in width will be observed until the very end, when the stylus digs in slightly as the turntable stops.

CUTTING FORCE

Measurements of the cutting force required for different groove depths were made with both steel and sapphire styluses. The steel stylus had a sharp cutting edge and a pointed tip, and gave the results shown in Fig. 2. The ratio of the horizontal force to cutting area was calculated, and a "cutting stress" of 36,400 pounds per square inch resulted. A paper by Kornei[1] gives a figure of 8.5×10^9 dynes/cm.^{2} (123,000 pounds per square inch) for Young's modulus for the cellulose nitrate used in lacquer disks. The modulus of shear is approximately one-third of the modulus of elasticity for most metals (and presumably about the same for many other materials). Our calculated value of 36,400 pounds per square inch is believed to be a fair check with 41,000 pounds per square inch, or one-third of the value obtained by Kornei.

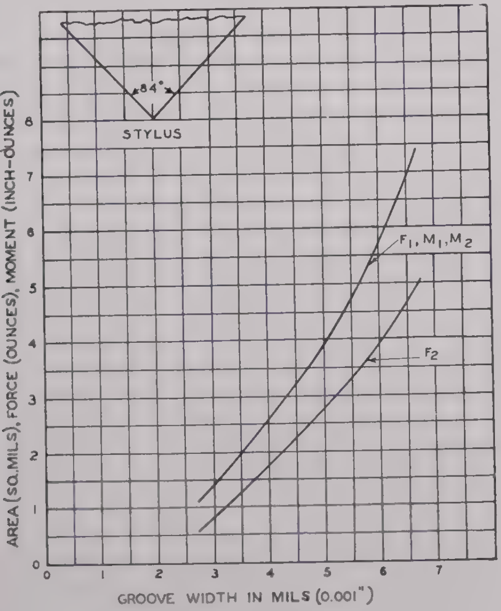

Fig. 2—Cutting force, steel stylus.

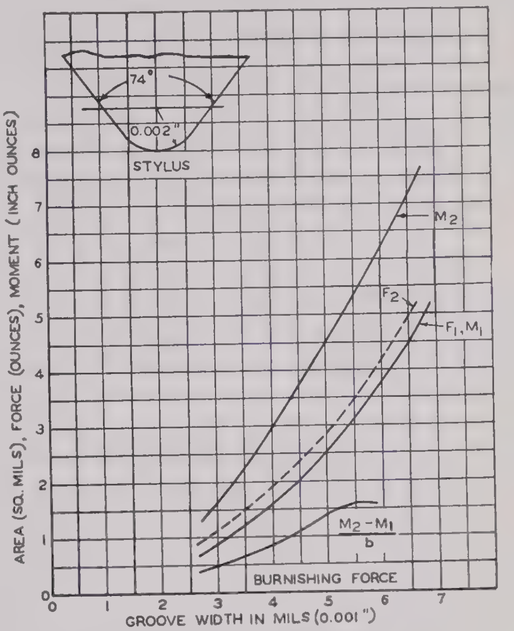

Fig. 3—Cutting force, sapphire stylus.

The cutting-force test was repeated with a sapphire stylus, and the results are shown in Fig. 3. In this case, the moment due to the downward force was found to be greater than that due to the horizontal force. A sapphire stylus for lacquer disk recording has a burnishing edge to smooth the side walls and produce a quiet groove, and it is only logical to assume that some additional force is needed to hold the sapphire down in place while performing this operation. Calculations of the cutting stress are meaningless, since part of the groove width is due to the widening action of the burnishing edge.

CUTTER BOUNCE

In some designs, the recording head oscillates or "bounces" vertically at some low frequency, depending upon the mass of the recording head and an effective stiffness, which depends on the rate at which the lifting moment due to the cutting force increases with downward displacement of the stylus into the recording medium. The vertical motion attained during oscillation cuts a groove of varying width and depth, and in extreme cases the tip may even clear the disk entirely, leaving an uncut portion. Naturally, a groove of varying depth does not promote good pickup tracking or low distortion.

---

[1] O. Kornei, "Playback loss of phonograph records," *Jour. Soc. Mot. Pict. Eng.*, vol. 37, pp. 569–590; December, 1941.

Since the bounce is an oscillating condition, it can be suppressed by introducing resistance into the mechanical system. Fig. 4(b) shows a recording of the vertical oscillation at 78 revolutions per minute, and Fig. 4(a) shows how it was reduced by means of an air dashpot. The dashpot is effective, but suffers a disadvantage when the disk is titled due to warpage or turntable wobble.

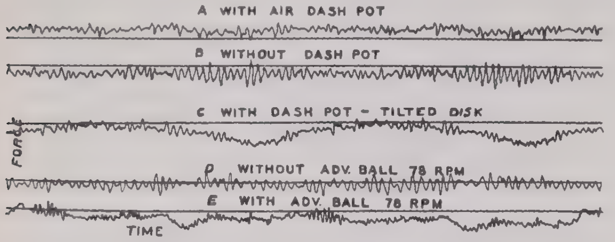

Fig. 4—Cutter bounce.

If enough resistance is used to reduce the oscillation effectively, it may cause the recording head to act sluggishly on warped disks and cut a groove of varying depth. Fig. 4(c) shows the force variation with the dashpot on a 16-inch-diameter lacquer disk which was tilted 0.025 inch to simulate the motion produced when the blank is warped. The once-around variation in force, due to the tilt, is plainly evident. It is interesting to note that the average force without the dashpot shows almost no variation, thus illustrating the self-regulating action of the recording head.

Since the dashpot had some disadvantages, an advance ball was tried. Figs. 4(d) and 4(e) show the cutting forces obtained without and with the use of the advance ball. The frequency of oscillation is raised and the amplitude of oscillation is decreased, but the force now varies considerably due to the fact that the self-regulating action of the head has been sacrificed by using the advance ball, which holds the stylus at some predetermined depth independent of hardness of the lacquer.

LACQUER HARDNESS VARIATION

Measurements were made of the variation in lacquer hardness by using an advance ball with the gauge. Fig. 5(b) shows the cutting-force variation on the outside of a 16-inch disk, and 5(a) shows the results obtained near the center of the same disk. Part of the once-around variation may be due to warped disks, although every effort was made to reduce such an error by using a long arm between the recording head and its pivot bearings. Any unevenness of the surface would also cause some variation, for the advance ball could not be located closer than about $\frac{1}{8}$ inch from the cutting tip. This unevenness probably accounts for some of the difference noted between the measurements made on the outside and on the inside of the disk, for the disk surfaces are noticeably more wavy near the edge. These variations are not too serious, however, as good recordings can be made with such disks. As an example of what extreme variations may be encountered in disks of the very inexpensive class, the results obtained with a cheap paper-base disk are shown in Fig. 5(c).

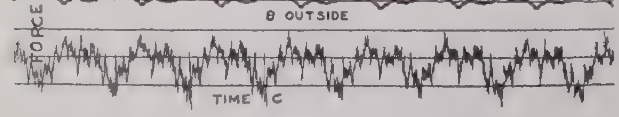

Fig. 5—Lacquer hardness.

TURNTABLE REQUIREMENTS

If the recording is being made without the aid of an advance ball, the self-regulating action of the cutter tends to maintain a constant average load regardless of the hard spots encountered throughout the disk. If there is bounce present, there will be a varying force of a frequency which is usually high enough not to cause serious changes in turntable speed, unless the inertia of the turntable is low and the bounce excessive. However, if an advance ball is used, there may be some low-frequency variations in load (due to hard spots and surface imperfections over which the advance ball rides) which may affect the speed even of a turntable of considerable inertia. Measurements of speed variation were made with laboratory equipment[2] while recording with and without the aid of an advance ball. Fig. 6(a) shows the speed variations obtained at no load; Fig. 6(b) shows the variation when cutting with an advance ball; and Fig. 6(c) shows the variation when cutting without the advance ball. There is some once-around speed variation (variation at turntable speed) which has to be discounted, but there is an evident increase in speed variation when the advance ball is used. The turntable in this case was 16 inches in diameter and 25 pounds in weight, with most of the mass located near the rim. The rate of variation is low, and therefore difficult to overcome.

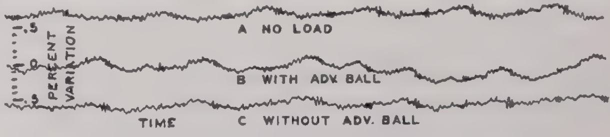

Fig. 6—Turntable speed variations while cutting with and without an advance ball.

Perhaps the best way to use the advance ball is to adjust it so that it barely touches the disk, and so that it clears entirely when the recording head is raised by hard spots but does not dig in too deeply when cutting softer portions. In this way the self-regulating action of the cutter is partially retained, the beneficial action in reducing bounce is partially retained, and the protection of the stylus tip from damage (due to dropping or recutting the same groove) is wholly retained.

---

[2] E. W. Kellogg and A. R. Morgan, "Measurement of speed fluctuation in sound recording and reproducing equipment," *Jour. Acous. Soc. Amer.*, vol. 7, pp. 271–280; April, 1936.

RECORDER ACTION

The oscillograms, with the recording head suspended freely, show the average force to be nearly constant; low-frequency variations due to hard spots or record warpage are not evident. The horizontal force F_1 of Fig. 7, at the stylus tip while cutting, creates a moment M_1 about the pivotal axis which tends to raise the recorder. Opposing this is the downward moment M_2 created by the vertical force F_2, also acting about the same axis. F_2 is measured with the stylus clear of the record but with the stylus at the same height relative to the pivot as when cutting the groove. During cutting equilibrium is attained when the two moments are equal, and the depth of cut is regulated by adjusting the vertical force by spring or counterweight adjustment. The data taken with a sharp-edged cutting stylus, illustrated in Fig. 2, show these two moments to be equal. The product of the horizontal and vertical forces, F_1 and F_2, by their effective distances from the pivotal axis, a and b, resulted in $M_1=M_2$, showing that the record material does not exert a vertical force on the stylus.

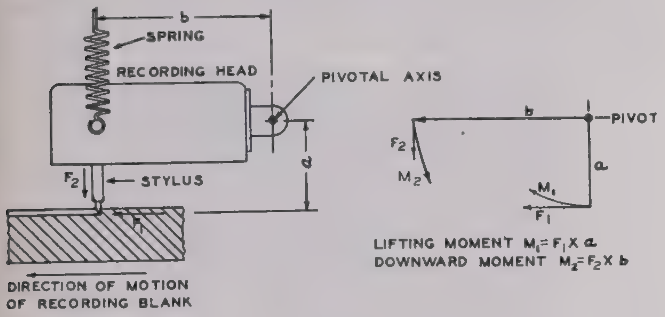

Fig. 7—Forces on recording head.

When a sapphire stylus is used, having a burnishing edge for polishing the groove side walls, some additional force to accomplish this action is required. With this stylus, the downward-acting moment M_2 was found to exceed the lifting moment M_1. The difference is due to the upward-force reaction on the cutting stylus exerted by the record material. In other words, the moment which provides the downward force must overcome the lifting moments due to the horizontal cutting force, plus a pressure to force the stylus into the record material. Taking the difference of M_2 and M_1 and dividing by b, the horizontal distance between the pivotal axis and the stylus tip, gives this force, which, as seen in Fig. 3, is an appreciable part of the total vertical force. In other words, the total or resultant force exerted on the stylus by the record is inclined to the horizontal at a considerable angle.

CUTTER BOUNCE AND DEPTH REGULATION

Theoretical considerations do not readily show cause for recorder instability, but cutter bounce does exist and is troublesome in many cases. Experiments indicate that the height of the pivotal axis above the surface of the disk is important, and if too low, oscillation occurs, which results in variations in depth of cut. Fig. 8 illustrates the variations in the width of the groove experienced with a tilted disk as the pivot height was changed. The decrease in the width variation with increased pivot height is believed to be due to several practical factors which perhaps may best be illustrated by the following example. If the pivot point is only 0.25 inch above the cutting plane, a cutting force of 2.4 ounces (for a groove about 5 mils wide) results in a lifting moment of 0.6 inch-ounce. If b, Fig. 7, is 2 inches, the vertical force for balanced moments is then only 0.3 ounce. With a recording head having an effective weight of 5 ounces about the pivotal axis, the frictional force at the pivots and between mechanical linkages used for raising and lowering the recorder may be of the same order of magnitude as this balancing force. Likewise, the additional vertical force required for burnishing when a sapphire is used may be greater, and so result in a depth regulation which is only partially due to the cutting force at the stylus tip. When a spring is used for groove-depth adjustment, the design should be such that small variations in extension of the spring, due to the rise and fall of the recorder because of record warpage or turntable wobble, will not alter the vertical force appreciably and change the depth of cut. In the design just discussed, when using a suitable spring, raising the pivot height to 1 inch increased the vertical force to 1.2 ounces and greatly improved the controlling action due to the cutting force. Satisfactory results were then obtained without the aid of an advance ball or dashpot.

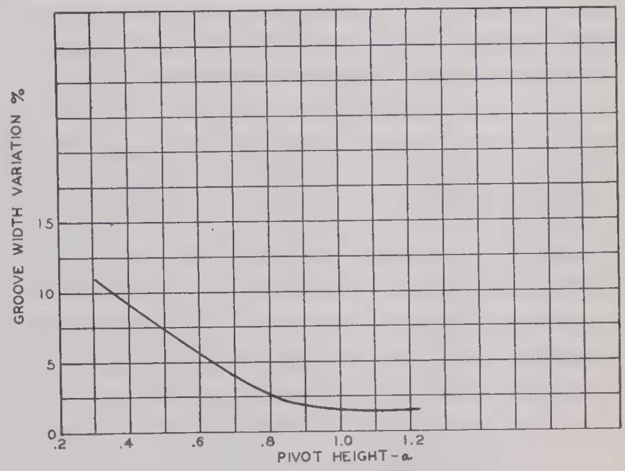

Fig. 8—Groove-width variation with pivot height.

Such practical design fulfillments probably account for the satisfactory operation observed in cases where a light-weight recorder is pivoted low, and when a heavy recorder is used but pivoted high.

Coaxial-Cable Networks*

FRANK A. COWAN†, SENIOR MEMBER, I.R.E.

Summary—**This paper discusses the general features of the coaxial system, its application for both telephone and television, and the future prospects for very-broad-band transmission facilities in the communication network.**

INTRODUCTION

THE UNPRECEDENTED growth in the volume of communications in recent years has spurred the development of means for handling long-distance communication channels in large bundles over transmission paths having broad frequency bands. Developments started in the early 1920's have extended the frequency band to about 150 kc. on open wire and about 60 kc. on 19-gauge cable pairs, thus providing for twelve or more telephone channels, or several high-grade program channels or many telegraph channels, per pair. The shielding against high-frequency external fields provided by the coaxial form of conductor makes its use attractive for transmission over long distances of still wider bands, and it is now being introduced extensively into the nationwide telephone network. Fortunately, this is occurring just when the telephone plant is beginning to be called upon to serve the new television industry by providing wide-band facilities for interconnecting television broadcasting stations in the same way as the telephone plant has been serving the sound broadcasting industry for many years.

GENERAL FEATURES OF THE COAXIAL-CABLE SYSTEM

Coaxial Conductors

The coaxial conductors used for long-distance transmission are of two types: an earlier type employed a 13-gauge (72-mil) copper wire for the central conductor held by polyethylene-disk insulators in the center of a longitudinal-seam copper tube 0.27 inch in diameter. In the present standard coaxial unit the central conductor is approximately 10 gauge (100 mil), and the outer conductor has an inner diameter of 0.375 inch. Fig. 1 shows the construction of this unit. The two steel tapes are provided to give added mechanical strength, and also added shielding at the lower frequencies.

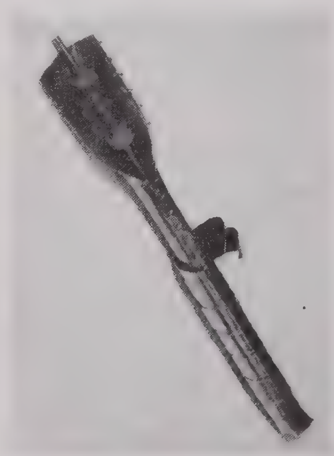

Fig. 1—Construction of coaxial unit.

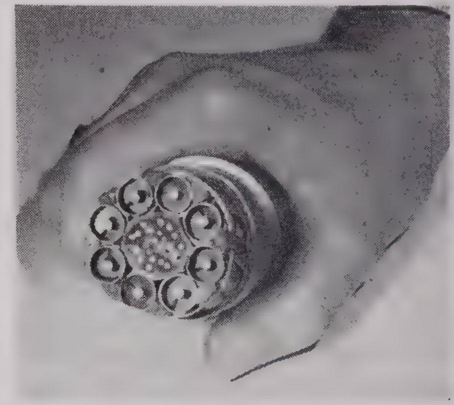

Fig. 2—View of section of eight-coaxial-unit cable.

As many as eight coaxial units, together with wire circuits for maintenance and testing and, in some cases, for short-haul telephone, program, or telegraph circuits, are included in a single cable. An end view of a typical cable is shown in Fig. 2. These cables are, in general, placed underground to reduce the chances of trouble and the difficulties of correcting transmission variations due to temperature changes.

Repeaters

The present coaxial system employs repeaters at intervals of about 5.5 miles for 0.27-inch coaxials and about 8 miles for 0.375-inch coaxials. Most of these repeater stations are called auxiliary stations and are unattended. The buildings are unheated but are so constructed that temperature changes inside are slow and of limited range. Fig. 3 shows the nature of the equipment within the housing, one such unit being required for two coaxials. The two shaded square boxes near the top of the equipment assembly are the amplifiers, each serving a particular coaxial. To avoid on-the-job amplifier maintenance, the amplifiers are of plug-in design, so that in case of trouble a new amplifier can be substituted and the defective unit sent to a maintenance center. The amplifier, with cover removed, is illustrated in Fig. 4. Each stage employs two tubes in parallel, so that failure of one tube will not interrupt the circuit. Negative feedback is used for stability and low modulation. Power for operation of the auxiliary repeaters is supplied over the central coaxial conductors from main

---

* Decimal classification: R117.2. Original manuscript received by the Institute, October 10, 1946; revised manuscript received, February 6, 1947.

† American Telephone and Telegraph Company, New York, N. Y.

stations located at intervals of 50 to 165 miles. These main stations also house supplementary equalizing and regulating equipment, and serve as the centers from which most of the testing and maintenance adjustments are made.

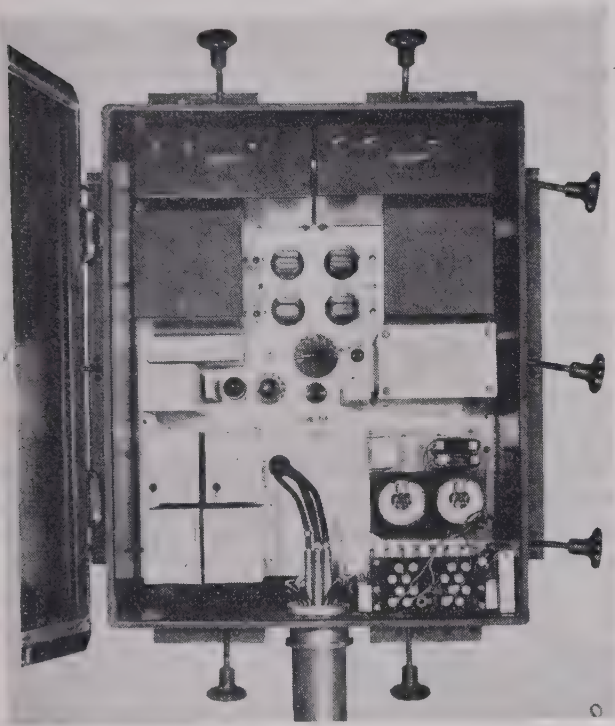

Fig. 3—Auxiliary-station equipment.

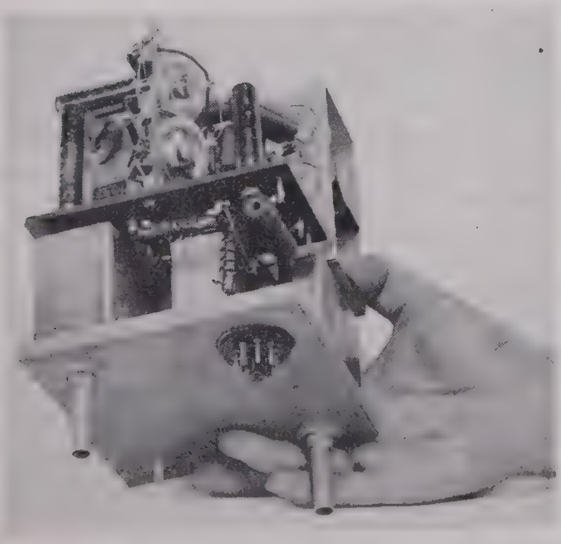

Fig. 4—Amplifier with cover removed.

Transmission Characteristics

The transmission loss of the bare coaxial unit varies, at normal temperature, from about 8 db at 60 kc. to about 52 db at 3000 kc. per repeater section. Equalizing and regulating equipment at each repeater station, controlled by a pilot frequency of about 2000 kc., and supplementary equipment at main stations, controlled by three additional pilot frequencies, compensate for these variations as well as for variations due to temperature. Typical over-all characteristics are shown in Fig. 5.

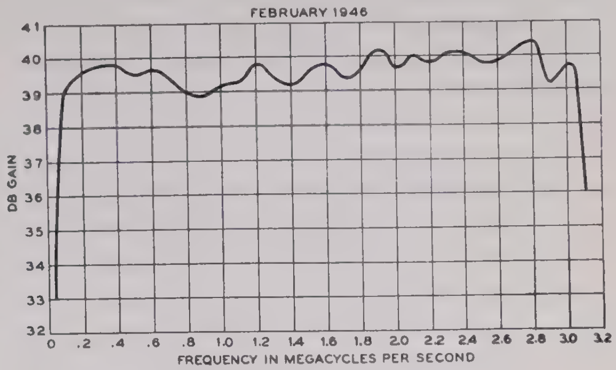

Fig. 5—Gain versus frequency characteristic of Washington-New York coaxial.

The shielding afforded by the coaxial units keeps noise due to atmospherics and inter-system cross talk low. The controlling noise is, therefore, generally thermal noise in the first circuits of the amplifiers.

When the coaxial line is used for television transmission, it must be carefully equalized from a delay standpoint. Such equalization is provided at intervals of 100 to 200 miles or at points where television programs are to be dropped or introduced.

Terminal Equipment

For flexibility, all broad-band carrier systems use a basic grouping of twelve telephone channels in the range 60 to 108 kc. This group is then moved by modulation to other appropriate frequencies.[1,2] In the coaxial system, five of the basic twelve-channel groups are assembled as a sixty-channel supergroup in the range

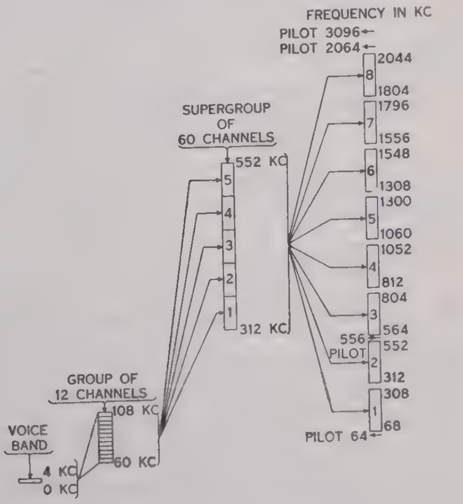

Fig. 6—Frequency translations in coaxial system (telephone).

---

[1] R. W. Chesnut, L. M. Ilgenfritz, and A. Kenner, "Cable carrier telephone terminals," *Bell Sys. Tech. Jour.*, vol. 17, pp. 106–124; January, 1938. Also, *Elec. Eng.*, vol. 57, pp. 237–245; May, 1938.

[2] C. E. Lane, "Crystal channel filters for the cable carrier system," *Bell Sys. Tech. Jour.*, vol. 17, pp. 125–136; January, 1938. Also, *Elec. Eng.*, vol. 57, pp. 245–250; May, 1938.

between 312 and 552 kc.[3,4] At present, eight such supergroups are positioned on the line between 64 and 2064 kc. These frequency translations are indicated in Fig. 6. There is under development equipment which will place two additional sixty-channel supergroups in the frequency space between about 2000 and 3000 kc.

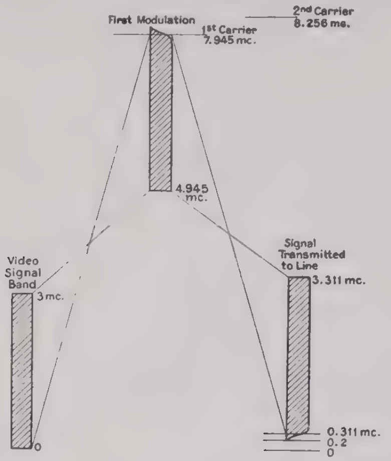
First Modulation
1st Carrier 7.945 mc.
2nd Carrier 8.256 mc.
4.945 mc.
Video Signal Band
3 mc.
0
Signal Transmitted to Line
3.311 mc.
0.311 mc.
0.2
0

Fig. 7—Frequency translations in coaxial system (television).

For television transmission the video band is positioned for transmission over the coaxial line as shown by Fig. 7. The sound channel associated with the television channel generally is transmitted over the same unit on a single-sideband basis between 80 and 88 kc.

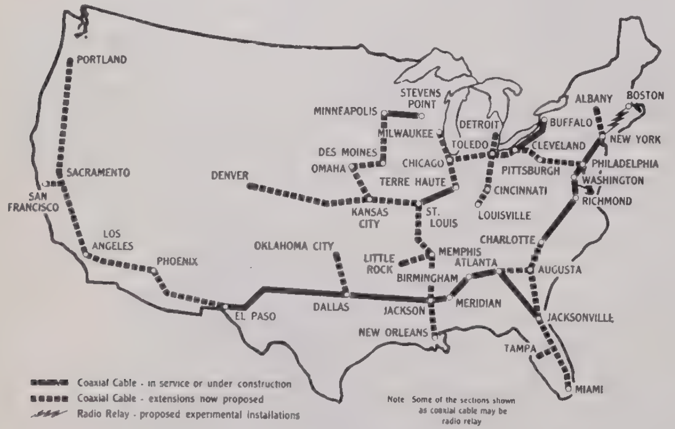
PORTLAND
SACRAMENTO
SAN FRANCISCO
LOS ANGELES
PHOENIX
EL PASO
DENVER
OKLAHOMA CITY
DALLAS
MINNEAPOLIS
STEVENS POINT
MILWAUKEE
DES MOINES
OMAHA
CHICAGO
TERRE HAUTE
KANSAS CITY
ST. LOUIS
LITTLE ROCK
MEMPHIS
BIRMINGHAM
JACKSON
NEW ORLEANS
MERIDIAN
ATLANTA
AUGUSTA
CHARLOTTE
JACKSONVILLE
TAMPA
MIAMI
DETROIT
TOLEDO
CLEVELAND
PITTSBURGH
CINCINNATI
LOUISVILLE
BUFFALO
ALBANY
BOSTON
NEW YORK
PHILADELPHIA
WASHINGTON
RICHMOND
Coaxial Cable - in service or under construction
Coaxial Cable - extensions now proposed
Radio Relay - proposed experimental installations
Note Some of the sections shown as coaxial cable may be radio relay

Fig. 8—Network facilities capable of television transmission.

Application of Coaxial-Cable Systems

In broad terms, the coaxial-type telephone system is and will be used principally for supplementing heavy cable routes, and for replacing open wire where the expected growth is heavy. Routes now in service, together with other cables under construction and cables expected to be added to the communication network within the next few years, are shown in Fig. 8.

Coaxial Cable for Television Transmission

In 1927, television transmission was demonstrated between Washington and New York (225 miles) using a 20-kc. band over an open-wire line.[5] In 1937, there was a similar demonstration between New York and Philadelphia using a 1-Mc. band over an experimental coaxial cable which was looped to provide a total circuit length of 180 miles. Many other tests and demonstrations have been carried out.[6–9]

In 1945 and 1946, techniques for handling television pickups and switching, paralleling in many respects the methods used in the sound-program transmission field, were sufficiently advanced to be demonstrated on many occasions. Experimental television transmission over the coaxial by several broadcasters is now continuing on a regular schedule. In 1946 color television was sent over the coaxial from New York to Washington and back.

Local Facilities

Pickup loops and other intracity television-system links are an important element in the nation-wide television network. During the past year over twenty-five such circuits have been in service in six cities, some having been in regular use for several years. To date, such facilities furnished by the telephone companies have been largely exchange-type paper-insulated cable pairs with special equalization and video amplifiers at intervals of about one mile.[10]

Experimental lengths of copper-shielded balanced 16-gauge pairs, string insulated with polyethylene, have been made for use within cities. This structure is expected to permit increasing repeater spacing to about three miles and to be sufficiently good, from the crosstalk standpoint, to permit opposite directions of television transmission in adjacent units.

In some cases, microwave radio may be the best method for supplying pickup loops or studio-transmitter facilities, and systems are under development at Bell Laboratories for this purpose. They seem well adapted for one-occasion pickups, or where the terrain favors radio but makes wire-line construction difficult. A trial microwave system was set up between the Yankee Stadium and the long-distance operating center in lower Manhattan for the Louis-Conn fight. It gave results comparable to that provided by the wire line which was actually used during the fight telecast. Also, this microwave system has been demonstrated between Hollywood and Mt. Wilson.

---

[3] L. Espenschied and M. E. Strieby, "System for wide-band transmission over coaxial lines," *Bell Sys. Tech. Jour.*, vol. 13, pp. 654–679; October, 1934.

[4] M. E. Strieby, "A million-cycle telephone system," *Bell Sys. Tech. Jour.*, vol. 26, pp. 1–10; January, 1937.

[5] D. K. Gannett and E. I. Green, "Wire transmission system for television," *Bell Sys. Tech. Jour.*, vol. 6, pp. 616–633; October, 1927.

[6] Herbert Ives, Frank Gray, and M. W. Baldwin, "Image transmission system for two-way television," *Bell Sys. Tech. Jour.*, vol. 9, pp. 448–470; July, 1930.

[7] M. E. Strieby, "Coaxial cable system for television transmission," *Bell Sys. Tech. Jour.*, vol. 27, pp. 438–458; July, 1938.

[8] M. E. Strieby and C. L. Weiss, "Television transmission," Proc. I.R.E., vol. 29, pp. 371–382; July, 1941.

[9] K. C. Black, "Stevens Point and Minneapolis linked by coaxial system," *Bell. Lab. Rec.*, vol. 20, p. 127; January, 1942.

[10] H. S. Osborne, "Transmission networks for frequency modulation and television," *Elec. Eng.*, vol. 64, pp. 392–398; November, 1945.

Radio Relay

Radio relay is a possible alternative to coaxial cable as a means of providing long-distance television, telephone, or other communication forms. Experiments are under way in this connection as a part of which a full-scale radio-relay system is being constructed between New York and Boston. This system will operate principally in the 4000-Mc. range and will use seven intermediate repeater points. If such a system should prove successful and be capable of being operated at a reasonable cost, there is a possibility that the future will see extensive use of radio relay in long-distance intercity communication. It would be expected that, as in the case of coaxial, the broad frequency bands provided might be utilized for television, telephone, or other types of communication.

LOOKING AHEAD

Past experience has shown a continued trend toward the use of wider and wider frequency bands for communication purposes. Equipment is now under development for use with coaxial cables which will provide wider bands; for example, a 7-Mc. band capable of being used in furnishing an effective 4-Mc. television circuit together with 480 telephone circuits.

For more than a decade the Bell System has conducted research work on a system of transmission in which super-high-frequency waves are guided through hollow pipes. The technique for generation, amplification, and control of the very-high frequencies used in the wave-guide system may also be employed when these frequencies are used for microwave radio. The relative extent to which guided waves or radio beams in space will be used in the future cannot accurately be predicted at this time. Wave guides have the advantage of avoiding some of the possible sources of interference in radio, but they do require the construction of the guiding structure over the route used.

Just how any of these future possibilities will develop, or what other arrangements might be introduced, can not be foretold with any certainty, but it seems clear that the frontiers of broad-band frequency transmission have ample room in which to move forward.

Mutual Impedance Between Vertical Antennas of Unequal Heights*

C. RUSSELL COX†, ASSOCIATE, I.R.E.

Summary—**An expression is derived for the resistive and reactive components of the mutual impedance between vertical antennas of unequal heights, located above a perfectly conducting ground. Mutual-impedance curves for typical combinations of antenna heights are plotted for spacings between 0.1 and 1.0 wavelength.**

I. INTRODUCTION

TO THE DESIGNER of power-distribution apparatus for directional antenna arrays, the evaluation of mutual impedance between elements of the array is the first step in a series of calculations leading eventually to the determination of all system parameters. Sufficient data exist in the literature to accommodate the usual problem in which all radiating elements are equal in height, but for the occasional instance involving radiators of unequal heights no mutual-impedance data are available. It is the purpose of this paper to derive an expression from which may be calculated the mutual impedance between radiators of unequal heights, mounted vertically above a perfectly conducting earth, and thus to fill in a gap which in some cases hinders the proper design of antenna-phasing networks.

II. FORMULATION OF INTEGRAL

In Fig. 1, two antennas of heights l_1 and l_2 are shown separated by a distance d. The current at the base of antenna *1* is I_{01}, while that at any distance z above ground is I_{z1}. Similarly, the current at the base of antenna *2* is I_{02}, while that at any distance z above ground is I_{z2}. The term E_{z21} represents the vertical com-

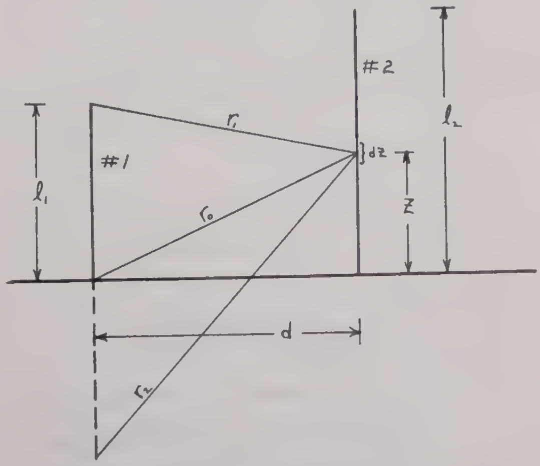

Fig. 1—Two antennas of unequal height above a perfectly conducting earth.

---

* Decimal classification: R125.1×R244. Original manuscript received by the Institute, July 22, 1946.

† Andrew Company, Chicago 19, Ill.

ponent of electric field at a point z on antenna *2* due to currents in antenna *1*, and V_{21} represents the voltage appearing at the base of antenna *2* due to antenna *1*.

By application of the reciprocity theorem to the currents and voltages in antenna *2*, one can write:

$$V_{21} = \int_0^{l_2} \frac{E_{z21} I_{z2}}{I_{02}} dz. \tag{1}$$

Since the antenna currents are assumed to be sinusoidally distributed, I_{z2} becomes:

$$I_{z2} = \frac{I_{02} \sin \beta(l_2 - z)}{\sin \beta l_2} \tag{2}$$

which, inserted in (1), gives

$$V_{21} = \int_0^{l_2} \frac{E_{z21} \sin \beta(l_2 - z)}{\sin \beta l_2} dz. \tag{3}$$

The mutual impedance, referred to the bases of both antennas, is

$$Z_{21} = -\frac{V_{21}}{I_{01}} = -\int_0^{l_2} \frac{E_{z21} \sin \beta(l_2 - z)}{I_{01} \sin \beta l_2} dz. \tag{4}$$

It is convenient to write (4) in terms of exponentials:

$$Z_{21} = -\int_0^{l_2} \frac{E_{z21}\left[e^{j\beta(l_2-z)} - e^{-j\beta(l_2-z)}\right]}{2jI_{01} \sin \beta l_2} dz. \tag{5}$$

Brown's[1] expression for the vertical component of electric field E_{z21} may now be introduced.

$$E_{z21} = \frac{-j30 I_{01} e^{j\omega t}}{\sin \beta l_1} \left\{ \frac{e^{-j\beta r_1}}{r_1} + \frac{e^{-j\beta r_2}}{r_2} - 2\frac{e^{-j\beta r_0}}{r_0} \cos \beta l_1 \right\}. \tag{6}$$

Inserting (6) into (5) and dropping the time-variant $c^{j\omega t}$, the mutual impedance is found to be the sum of six integrals.

$$\begin{aligned} z_{21} = \frac{15}{\sin \beta l_1 \sin \beta l_2} \Bigg\{ & \int_0^{l_2} \frac{e^{-j\beta(r_1 - l_2 + z)}}{r_1} dz \\ & - \int_0^{l_2} \frac{e^{-j\beta(r_1 + l_2 - z)}}{r_1} dz + \int_0^{l_2} \frac{e^{-j\beta(r_2 - l_2 + z)}}{r_2} dz \\ & - \int_0^{l_2} \frac{e^{-j\beta(r_2 + l_2 - z)}}{r_2} dz \\ & - 2\int_0^{l_2} \frac{e^{-j\beta(r_0 - l_2 + z)}}{r_0} dz \cos \beta l_1 \\ & + 2\int_0^{l_2} \frac{e^{-j\beta(r_0 + l_2 - z)}}{r_0} dz \cos \beta l_1 \Bigg\}. \end{aligned} \tag{7}$$

III. Evaluation of Integrals

From the geometry of Fig. 1, the following expressions are apparent:

$$r_1 = \sqrt{d^2 + (l_1 - z)^2} \tag{8}$$

$$r_2 = \sqrt{d^2 + (l_1 + z)^2} \tag{9}$$

$$r_0 = \sqrt{d^2 + z^2}. \tag{10}$$

On differentiating (8), (9), and (10), one obtains

$$\frac{dz}{r_1} = \frac{dr_1}{z - l_1} \tag{11}$$

$$\frac{dz}{r_2} = \frac{dr_2}{z + l_1} \tag{12}$$

$$\frac{dz}{r_0} = \frac{dr_0}{z}. \tag{13}$$

For convenience, let the sum and difference of the radiator lengths be given by

$$\Delta = l_2 - l_1 \tag{14}$$

$$L = l_2 + l_1. \tag{15}$$

By making suitable changes of variable, each integral will now be reduced to the form

$$\int_{u_0}^{u_1} \frac{e^{-ju}}{u} du = [Ci(u_1) - Ci(u_0)] + j[Si(u_0) - Si(u_1)] \tag{16}$$

in which $Ci(u)$ and $Si(u)$ are the cosine and sine integrals, respectively. Tables of these integral functions are available for values of the argument ranging from 0 to 100, the best available compilation having been published in 1940 under WPA sponsorship.[2]

In the first integral, let

$$u = \beta(r_1 - l_1 + z). \tag{17}$$

Then, from (11),

$$du = \beta(dr_1 + dz) = \beta\left(\frac{z - l_1 + r_1}{r_1}\right) lz = \frac{udz}{r_1}$$

and

$$\frac{du}{u} = \frac{dz}{r_1}. \tag{18}$$

New limits of integration u_0 and u_1 are obtained by letting $z=0$ and $z=l_2$, respectively, in (17).

$$\begin{aligned} u_0 &= \beta\left[\sqrt{d^2 + l_1^2} - l_1\right] \\ u_1 &= \beta\left[\sqrt{d^2 + \Delta^2} + \Delta\right]. \end{aligned} \tag{19}$$

The first integral in (7) then becomes

$$\begin{aligned} \int_0^{l_2} \frac{e^{-j\beta(r_1 - l_2 + z)}}{r_1} dz &= \int_{u_0}^{u_1} \frac{e^{-j(u + \beta l_1 - \beta l_2)}}{u} du \\ &= e^{j\beta\Delta} \int_{u_0}^{u_1} \frac{e^{-ju}}{u} du. \end{aligned} \tag{20}$$

In the second integral, let

$$v = \beta(r_1 + l_1 - z). \tag{21}$$

Differentiating and using (11), one obtains

$$\frac{dv}{v} = -\frac{dz}{r_1}. \tag{22}$$

---

[1] G. H. Brown, "Directional antennas," Proc. I.R.E., vol. 25, pp. 81–145; January, 1937.

[2] "Tables of Sine, Cosine, and Exponential integrals," Federal Works Agency, Work Projects Administration, 1940.

The new limits of integration are

$$\begin{aligned} v_0 &= \beta[\sqrt{d^2 + l_1^2} + l_1] \\ v_1 &= \beta[\sqrt{d^2 + \Delta^2} - \Delta]. \end{aligned} \tag{23}$$

The second integral in (7) then becomes

$$-\int_0^{l_2} \frac{e^{-j\beta(r_1+l_2-z)}}{r_1}\,dz = e^{-j\beta\Delta}\int_{v_0}^{v_1}\frac{e^{-jv}}{v}\,dv. \tag{24}$$

The remaining four integrals are transformed in similar fashion.

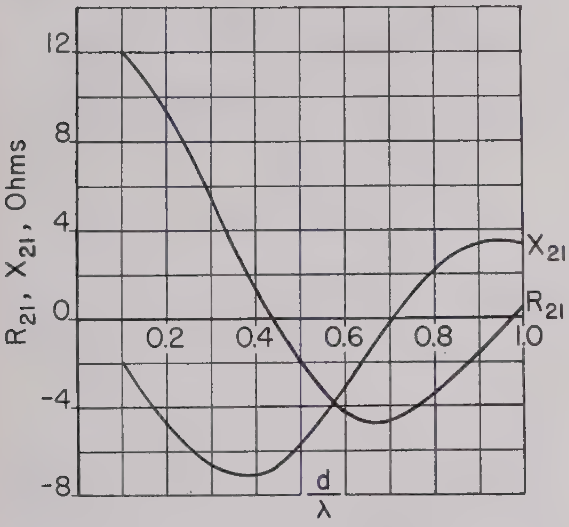

Fig. 2—Resistive and reactive components of mutual impedance between antennas of heights of 40 and 90 degrees.

Changes of variable are made as follows:

$$\begin{aligned} w &= \beta(r_2 + l_1 + z) \\ x &= \beta(r_2 - l_1 - z) \\ y &= \beta(r_0 + z) \\ s &= \beta(r_0 - z). \end{aligned} \tag{25}$$

The limits of integration are

$$\begin{aligned} w_0 &= \beta[\sqrt{d^2 + l_1^2} + l_1] = v_0 \\ w_1 &= \beta[\sqrt{d^2 + L^2} + L] \\ x_0 &= \beta[\sqrt{d^2 + l_1^2} - l_1] = u_0 \\ x_1 &= \beta[\sqrt{d^2 + L^2} - L] \\ y_0 &= \beta[d] \\ y_1 &= \beta[\sqrt{d^2 + l_2^2} + l_2] \\ s_0 &= \beta[d] = y_0 \\ s_1 &= \beta[\sqrt{d^2 + l_2^2} - l_2]. \end{aligned} \tag{26}$$

After undergoing the transformations indicated, (7) takes the form

$$\begin{aligned} z_{21} = \frac{15}{\sin\beta l_1 \sin\beta l_2}\Bigg\{ & e^{j\beta}\int_{u_0}^{u_1}\frac{e^{-ju}}{u}\,du \\ & + e^{-j\beta\Delta}\int_{v_0}^{v_1}\frac{e^{-jv}}{v}\,dv + e^{j\beta L}\int_{v_0}^{w_1}\frac{e^{-jw}}{w}\,dw \\ & + e^{-j\beta L}\int_{u_0}^{x_1}\frac{e^{-jx}}{x}\,dx - 2\cos\beta l_1 e^{j\beta l_2}\int_{y_0}^{y_1}\frac{e^{-jy}}{y}\,dy \\ & - 2\cos\beta l_1 e^{-j\beta l_2}\int_{y_0}^{s_1}\frac{e^{-js}}{s}\,ds\Bigg\}. \end{aligned} \tag{27}$$

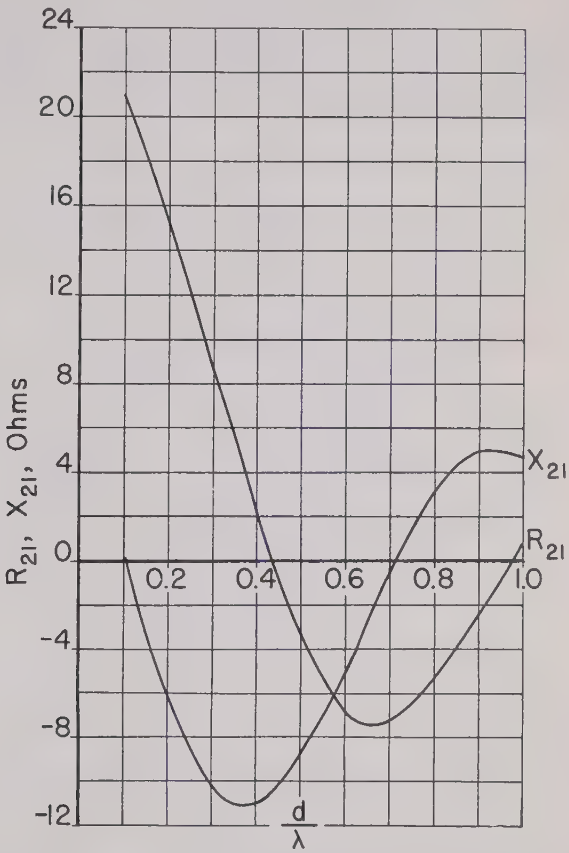

Fig. 3—Resistive and reactive components of mutual impedance between antennas of heights of 60 and 90 degrees.

The final answer is obtained by inserting the cosine and sine integrals of (16) into (27).

$$\begin{aligned} R_{21} = \frac{15}{\sin\beta l_1 \sin\beta l_2}\{ & \cos\beta\Delta[Ci(u_1) - Ci(u_0) \\ & + Ci(v_1) - Ci(v_0) + 2Ci(y_0) - Ci(y_1) - Ci(s_1)] \\ & + \sin\beta\Delta[Si(u_1) - Si(u_0) + Si(v_0) \\ & - Si(v_1) - Si(y_1) + Si(s_1)] \\ & + \cos\beta L[Ci(w_1) - Ci(v_0) + Ci(x_1) - Ci(u_0) \\ & + 2Ci(y_0) - Ci(y_1) - Ci(s_1)] \\ & + \sin\beta L[Si(w_1) - Si(v_0) + Si(u_0) \\ & - Si(x_1) - Si(y_1) + Si(s_1)]\} \end{aligned} \tag{28}$$

$$\begin{aligned} X_{21} = \frac{15}{\sin\beta l_1 \sin\beta l_2}\{ & \cos\beta\Delta[Si(u_0) - Si(u_1) \\ & + Si(v_0) - Si(v_1) + Si(y_1) - 2Si(y_0) + Si(s_1)] \end{aligned}$$

$$
\begin{aligned}
&+ \sin \beta\Delta[Ci(u_1) - Ci(u_0) + Ci(v_0) \\
&- Ci(v_1) - Ci(y_1) + Ci(s_1)] \\
&+ \cos \beta L[Si(v_0) - Si(w_1) + Si(u_0) - Si(x_1) \\
&+ Si(y_1) - 2Si(y_0) + Si(s_1)] \\
&+ \sin \beta L[Ci(w_1) - Ci(v_0) + Ci(u_0) \\
&- Ci(x_1) - Ci(y_1) + Ci(s_1)]\}. \qquad (29)
\end{aligned}
$$

Examination of (28) and (29) reveals that, to obtain X_{21} from R_{21}, it is necessary only to replace $Ci(p)$ by $-Si(p)$, and $Si(q)$ by $Ci(q)$.

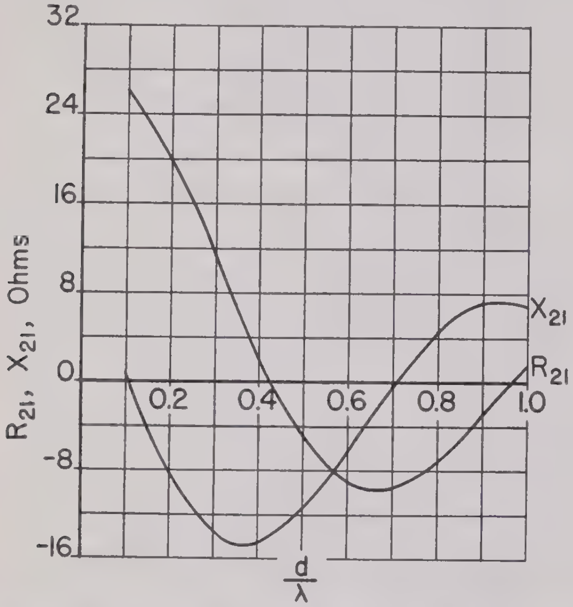

Fig. 4—Resistive and reactive components of mutual impedance between antennas of heights of 75 and 90 degrees.

IV. Special Cases

It is easily shown that when the radiators are equal in height, $l_1 = l_2$ and (28) and (29) become

$$
\begin{aligned}
R_{21} = \frac{15}{\sin^2 \beta l} &\{4Ci(u_1) - 2Ci(u_0) - 2Ci(v_0) \\
&+ \cos 2\beta l[Ci(w_1) - 2Ci(v_0) + Ci(x_1) \\
&- 2Ci(u_0) + 2Ci(u_1)] \\
&+ \sin 2\beta l[Si(w_1) - 2Si(v_0) \\
&- Si(x_1) + 2Si(u_0)]\} \qquad (30)
\end{aligned}
$$

$$
\begin{aligned}
X_{21} = \frac{15}{\sin^2 \beta l} &\{- 4Si(u_1) + 2Si(u_0) + 2Si(v_0) \\
&+ \cos 2\beta l[- Si(w_1) + 2Si(v_0) - Si(x_1) \\
&+ 2Si(u_0) - 2Si(u_1)] \\
&+ \sin 2\beta l[Ci(w_1) - 2Ci(v_0) \\
&- Ci(x_1) + 2Ci(u_0)]\}. \qquad (31)
\end{aligned}
$$

Considerable simplification of (28) and (29) results if one of the antennas (say l_2) is a quarter-wave in height. In this case, the resistive and reactive components of z_{21} become

$$
\begin{aligned}
R_{21} = 15\{&Ci(u_1) + Ci(v_1) - Ci(w_1) - Ci(x_1) \\
&+ \cot \beta l_1[Si(u_1) - Si(v_1) - 2Si(y_1) \\
&+ 2Si(s_1) + Si(w_1) - Si(x_1)]\} \qquad (32)
\end{aligned}
$$

$$
\begin{aligned}
X_{21} = 15\{&Si(w_1) + Si(x_1) - Si(u_1) - Si(v_1) \\
&+ \cot \beta l_1[Ci(u_1) - Ci(v_1) - 2Ci(y_1) \\
&+ 2Ci(s_1) + Ci(w_1) - Ci(x_1)]\}. \qquad (33)
\end{aligned}
$$

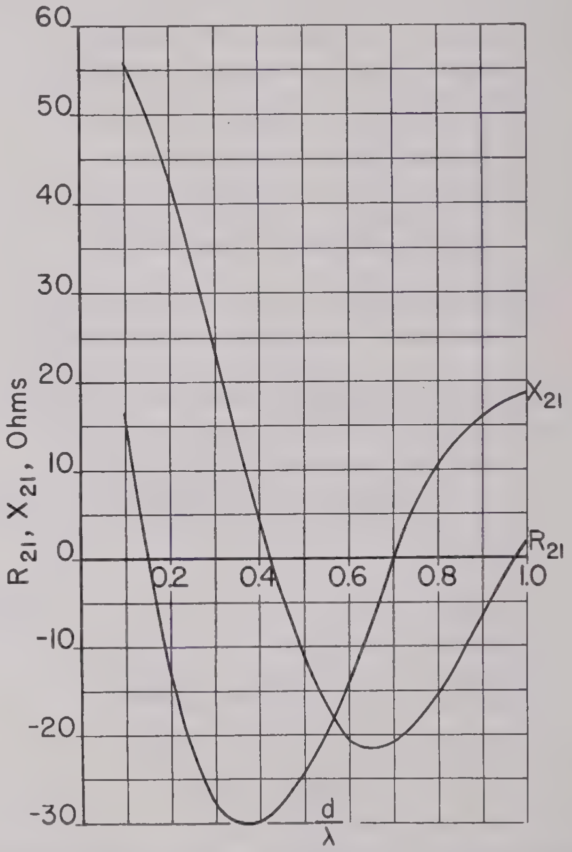

Fig. 5—Resistive and reactive components of mutual impedance between antennas of heights of 120 and 90 degrees.

Figs. 2, 3, 4, and 5 are plots of (32) and (33) for values of l_1 corresponding to angular heights of 40, 60, 75, and 120 degrees, respectively.

V. Conclusion

As is the case for previously available data on mutual impedance with equal heights, the expressions presented here are only approximate, because sinusoidal current distributions are assumed in both members. However, the present calculations are no less accurate, and should prove useful to the same extent as previously published information.

VI. Acknowledgments

The writer acknowledges the assistance of R. E. Beam, who carefully checked the mathematics, and of Peter Andris, who calculated and prepared Figs. 2, 3, 4, and 5.

A Wide-Band 550-Megacycle Amplifier*

RAYMOND O. PETRICH†, ASSOCIATE, I.R.E.

Summary—**This paper describes a five-stage 550-megacycle amplifier having an over-all bandwidth of 20 megacycles and a gain of 10 decibels per stage. It uses a 2C43 triode in a grounded-grid circuit with an impedance-transforming band-pass filter in the output to give the desired bandwidth. A visual method of alignment with a sweep-frequency oscillator is described, and important design considerations are given. The voltage gain per stage for a wide-band amplifier of this type is shown to be**

$$G=(\mu+1)\sqrt{R_L/(R_p+R_L[\mu+1+(R_p+R_L)/R_t]}$$

where R_t is the equivalent shunt resistance between grid and cathode due to transit-time loading and cathode-lead-inductance loading, and R_L is the optimum value of load resistance in the plate circuit consistent with the bandwidth of the amplifier and the grid-plate capacitance of the tube.

DESCRIPTION

A GAIN per stage of over 10 db for a bandwidth of 20 megacycles has been obtained at 550 megacycles using a 2C43 "lighthouse" triode in a grounded-grid amplifier circuit. The center frequency of the amplifier may be tuned from 500 to 600 megacycles and the bandwidth varied from 10 to 30 megacycles. Five stages have been connected in tandem, giving an over-all gain of 50 db for a 20-megacycle bandwidth. The first four stages are operated as voltage amplifiers drawing a cathode current of 25 milliamperes at a plate voltage of 250 volts, while the output stage is operated class AB at 20 milliamperes and 400 volts. A continuous-wave output of 5 watts may be obtained without external cooling. Impedance-transforming networks are used at both the input and output of the tube, so that standard 50-ohm concentric cables and connectors may be used for coupling into and out of each stage. This type of design provides for the most flexible use of the amplifier, since each stage is identical and may be used either separately or connected in tandem with several similar stages if more gain is desired.

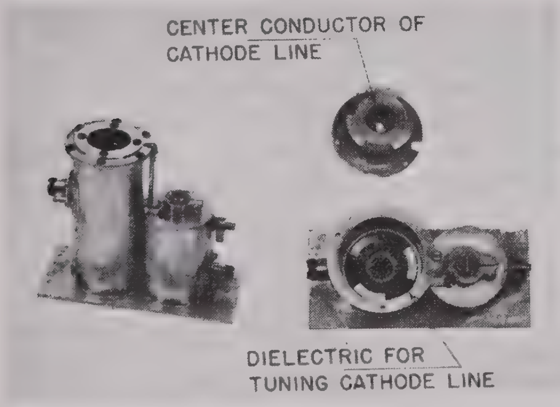
CENTER CONDUCTOR OF CATHODE LINE
DIELECTRIC FOR TUNING CATHODE LINE

Fig. 1—Views of a single stage.

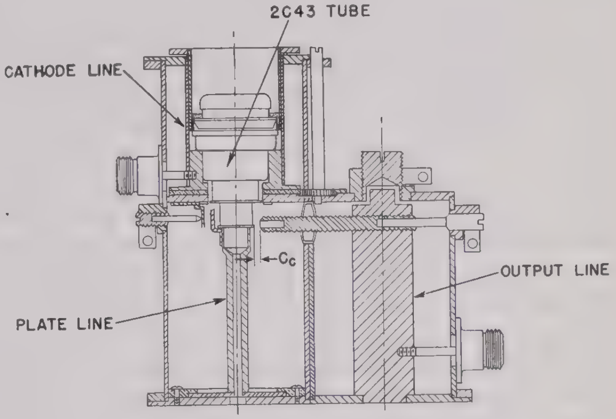

Fig. 2—Cross-sectional view.

Photographs of a single stage of the amplifier are shown in Fig. 1, and a cross-sectional view showing the the actual construction is given in Fig. 2. An equivalent circuit of the radio-frequency components may be represented as shown in Fig. 3.

Each stage of the amplifier is of the grounded-grid type with an impedance-transforming band-pass filter in the output circuit to give the required bandwidth. The output filter is a double-tuned circuit consisting of two resonant cavities capacitively coupled together. The plate cavity is a short concentric line tuned by the grid-plate capacitance of the tube plus a small trimming capacitor. The output cavity is of similar construction, using a short concentric-line inductance with capacitive tuning at the end. The coupling between the two circuits is through the capacitance C_c which is indicated in Figs. 2 and 3. Physically, this is the capacitance between the plate of the tube and the end of the coupling rod which is threaded through the center con-

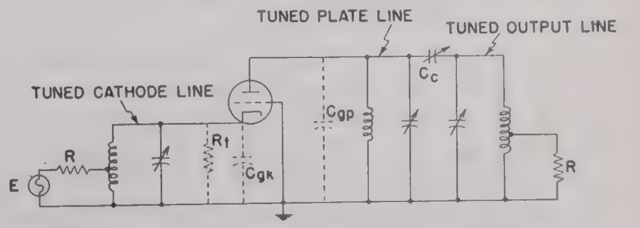

Fig. 3—Equivalent circuit of radio-frequency components.

---

* Decimal classification: R363.11. Original manuscript received by the Institute, September 19, 1946; revised manuscript received, November 15, 1946. This paper is based on work done for the Office of Scientific Research and Development under Contract OEMsr-411 with the President and Fellows of Harvard College.

† Airborne Instruments Laboratory, Inc., Mineola, Long Island, N. Y.

ductor of the output cavity. The inductance of the coupling rod was omitted in the equivalent circuit since its reactance is in the order of 50 ohms, whereas the reactance of the coupling capacitor, which is in series with this inductance, is nearly 4000 ohms. For maximum gain the output filter should be designed to match the output impedance of the tube. However, if this is not possible for the given bandwidth and grid-plate capacitance of the tube, the impedance should be made as high as these two factors will allow. The output tap is adjusted to work into a 50-ohm load.

A double-tuned circuit similar to that used in the output is not necessary at the input since the tube loading effect is sufficient to give a broad response with a single-tuned circuit. The input cavity consists of a short length of concentric line of low characteristic impedance. Since the impedance level is low due to the loading by the tube, a high-Q cavity is not necessary, thus making it possible to use a low-impedance line in which the base of the tube and socket are housed inside the center conductor. The tuning is accomplished by changing the amount of dielectric under three equally spaced conducting fins extending from the end of the center conductor. The shape of the dielectric piece is shown in Fig. 1, and the tuning adjustment is made by rotating it with respect to the fins on the end of the center conductor. The input tap is adjusted to work from a 50-ohm source.

ALIGNMENT

Because of the numerous tuning adjustments, the alignment of an amplifier of this type would be a very tedious process using the conventional point-by-point method of plotting response curves. However, the use of a sweep-frequency oscillator with visual presentation of the output on a cathode-ray oscilloscope provides an extremely simple and accurate method of checking the response.

A beat-frequency oscillator employing two frequency-modulated 3-centimeter reflex klystrons is used to obtain a sweep width of 100 megacycles over the desired range. The modulating source is capable of sweeping each of the tubes over a range of 50 megacycles by applying a low-frequency sawtooth voltage to each of the repellers. The modulating voltages are applied to the repellers 180 degrees out of phase, causing the tubes to change frequency in opposite direction, so that the difference-frequency output from the mixer sweeps over twice the range that would be obtainable if the modulating voltage were applied to a single tube only.

The radio-frequency output from the sweep oscillator is fed through an attenuator and matching section to the amplifier, which is terminated by a 50-ohm load. With proper matching the output of the sweep oscillator is nearly constant throughout the range, so that a true indication of the amplifier response is obtained. A single stage is aligned by tuning all three cavities to the desired center frequency and adjusting the coupling rod to give the desired bandwidth. To align a multistage amplifier, each stage may be aligned separately into a 50-ohm dummy load before connecting them in tandem. This may be done since the feedback between plate and cathode circuits is small, and the impedance level is 50 ohms at both the input and output of each stage. It should be noted that the over-all bandwidth decreases as each successive stage is added, so that in order to obtain a given over-all bandwidth each stage must have a bandwidth n times greater than the over-all bandwidth. If a 3-db dip may be tolerated in the over-all response and the bandwidth is measured down 3 db, Table I gives an approximate value for n for two to six stages in tandem.

TABLE I

Number of Stages	n for a 3-db dip
2	1.11
3	1.19
4	1.25
5	1.30
6	1.35

When the stages have been prealigned in this manner, they may be connected directly in tandem with only slight retuning to keep a symmetrical response as each successive stage is added. The output stage should be aligned for the load into which it will be working, and the additional stages added to the input.

GAIN CONSIDERATIONS

Neglecting the direct voltages applied to the tube, the radio-frequency circuit of the amplifier may be represented by Fig. 4.

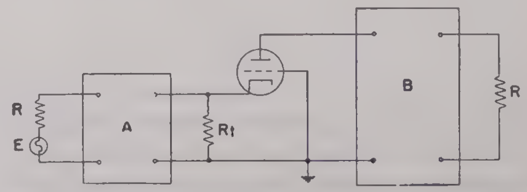

Fig. 4—General circuit of a grounded-grid amplifier.

E = open-circuit voltage of generator
R = load resistance and generator resistance
R_t = shunt resistance between grid and cathode due to transit-time loading and cathode-lead-inductance loading
A = impedance-transforming band-pass filter with an effective step-up ratio N_1
$N_1 = \sqrt{R_a/R}$ where R_a equals the shunt impedance at the output terminals of filter A
B = impedance-transforming band-pass filter with an effective step-up ratio N_2.

$N_2 = \sqrt{R/R_b}$ where R_b equals the shunt impedance at the input terminals of filter B.

In the circuit shown in Fig. 4, the input filter includes the dynamic input capacitance of the tube, and the output filter includes the dynamic output capacitance. Since the grid forms a screen between the input and output circuits in a grounded-grid amplifier, for all practical purposes the input capacitance may be considered equal to the grid-cathode capacitance of the tube, and the output capacitance equal to the grid-plate capacitance.

An analysis of a circuit similar to that shown in Fig. 4 has been made by Dishal, who has shown that the input impedance of the tube will be[1]

$$Z_{\text{in}} = R_t(R_p + R/N_2^2)/[R_p + R/N_2^2 + R_t(\mu + 1)] \qquad (1)$$

where

R_p = plate resistance of the tube

μ = amplification factor.

The output impedance of the tube was shown to be

$$Z_{\text{out}} = R_p + [N_1^2RR_t(\mu + 1)/(N_1^2R + R_t)]. \qquad (2)$$

The equivalent input circuit may be represented as shown in Fig. 5(a), and the equivalent output circuit as shown in Fig. 5(b).

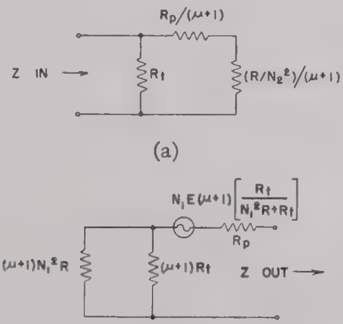

(a)

(b)

Fig. 5—(a) Equivalent input circuit. (b) Equivalent output circuit.

The condition for maximum gain was shown to be when N_1^2R was matched to the input impedance of the tube and R/N_2^2 was matched to the output impedance of the tube. Replacing N_1^2R for the input impedance in (1) and R/N_2^2 for the output impedance in (2) and solving the resulting simultaneous equations gives for the condition of maximum gain

$$(N_1^2R)' = R_t/\sqrt{1 + (\mu + 1)R_t/R_p} \qquad (3)$$

and

$$(R/N_2^2)' = R_p\sqrt{1 + (\mu + 1)R_t/R_p}. \qquad (4)$$

However, the maximum impedance which can be developed in the output circuit is limited by the bandwidth of the amplifier and the grid-plate capacitance of tube.[2]

$$R_L = 1/2\pi\Delta fC_{gp} \qquad (5)$$

where

R_L = maximum load resistance at the plate of the tube

Δf = bandwidth of the amplifier

C_{gp} = grid-plate capacitance of the tube.

If the value of R_L given by (5) is smaller than the optimum value of $(R/N_2^2)'$ given by (4), it will not be possible to match the output filter to the output impedance of the tube, and the maximum gain for this case will be obtained when R/N_2^2 is made equal to R_L and N_1^2R is made equal to the resulting input impedance of the tube. Therefore, when

$$R_L < R_p\sqrt{1 + (\mu + 1)R_t/R_p}, \qquad (R/N_2^2)'' = R_L \qquad (6)$$

and

$$(N_1^2R)'' = (R_p + R_L)/[\mu + 1 + (R_p + R_L)/R_t]. \qquad (7)$$

If the gain of the amplifier is expressed as the ratio of the voltage appearing across the load resistance R to that appearing across the output terminals of the generator under matched conditions, the expression for gain becomes[3]

$$G = \frac{(\mu+1)}{\sqrt{(R/N_2^2)/(R_p+R/N_2^2)[\mu+1+(R_p+R/N_2^2)/R_t]}}. \qquad (8)$$

Substituting (4) into (8) gives for the maximum value of gain

$$G' = (\mu + 1)/[\sqrt{R_p/R_t} + \sqrt{\mu + 1 + R_p/R_t}] \qquad (9)$$

when

$$R_L > R_p\sqrt{1 + (\mu + 1)R_t/R_p}.$$

Substituting (6) into (8) gives a gain of

$$G'' = (\mu+1)\sqrt{R_L/(R_p+R_L)[\mu+1+(R_p+R_L)/R_t]} \qquad (10)$$

when

$$R_L < R_p\sqrt{1 + (\mu + 1)R_t/R_p}.$$

The total input loading R_t may be considered equal to the combination of the transit-time loading R_g and the cathode-lead-inductance loading R_k, in parallel. Ferris[4] has shown that the loading due to the transit time of electrons between the cathode and grid is

---

[1] Milton Dishal, "Theoretical gain and signal-to-noise ratio of the grounded-grid amplifier at ultra-high frequencies," PROC. I.R.E., vol. 32, pp. 276–280; May, 1944.

[2] F. E. Terman, "Radio Engineers' Handbook," McGraw-Hill Book Co., New York, N. Y., 1943; Section 3, pp. 230–231. Actually, equation (5) is derived for a circuit containing lumped inductances and capacitances, but it may be used with reasonable accuracy for a short-circuited quarter-wave line heavily loaded with shunt capacitance.

[3] This definition is equivalent to the concept of gain advanced by Friis in a more general form in his paper, "Noise Figures of Radio Receivers," in which he defines gain in terms of available power. It should be noted that equation (8) gives twice the gain given by Dishal, since he defines gain as the ratio of the voltage across the final load resistance to the open-circuit voltage of the generator. Equation (8) may be used directly to compute the gain of amplifiers connected in tandem, whereas the definition given by Dishal would give a gain that would be incorrect by a factor of two for each successive stage that is added.

$$R_g = 1/kg_m f^2 T^2 \tag{11}$$

where

g_m = tube transconductance
f = frequency
T = time required for an electron to travel from cathode to grid
k = a constant determined by the tube voltages and geometry.

Strutt and van der Ziel[5] have shown that the cathode-lead-inductance loading is

$$R_k = 1/\omega^2 g_m L_k C_{gk} \tag{12}$$

where

L_k = cathode-lead inductance
C_{gp} = grid-cathode capacitance of the tube
$\omega = 2\pi f$.

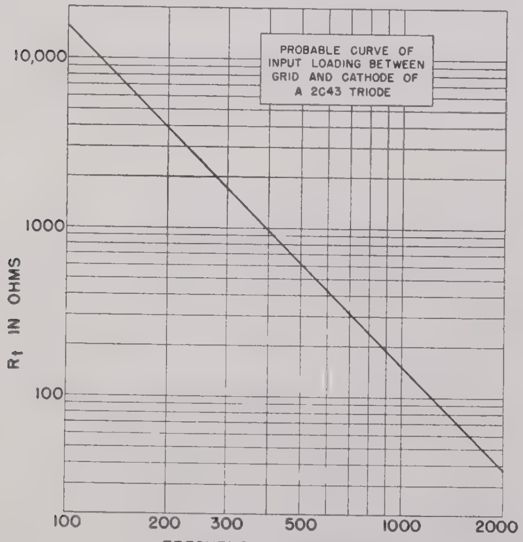

Fig. 6—Input loading for a 2C43.

It is important to note that the effects of both the transit-time loading and the cathode-lead-inductance loading increase as the square of the frequency, so that at higher frequencies they have a decided effect on the gain. Experimental results have shown that the total loading at the input to a 2C43 tube at 550 megacycles is in the order of 500 ohms. Using this as a basis, a probable curve of the loading versus frequency is given in Fig. 6. Using the value of R_t obtained from this curve, the gain versus frequency is computed for a 2C43 tube in an amplifier having a bandwidth of 20 megacycles, and the results are shown in Fig. 7.

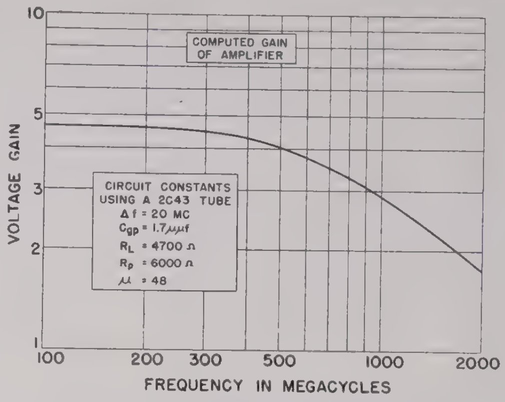

Fig. 7—Gain versus frequency for a 2C43.

DESIGN CONSIDERATIONS

Standard filter design may be used in determining the "lumped-constant" values of the components in the filter circuits. A pi-section filter similar to the one shown in Fig. 3, where C_{gp} is the grid-plate capacitance of the tube, has proved to be a suitable output circuit. The impedance developed across this section is determined by either (4) or (5), whichever is applicable for the given bandwidth, grid-plate capacitance, and input loading. The impedance transformation between the plate circuit and the output is accomplished by tapping down on the output line at the desired point.

Because of the small magnitude of the inductance and capacitance required for the circuit elements, short concentric lines capacitively loaded at the end are readily adaptable for the tuned circuits. Foreshortened one-quarter-wavelength lines should be used in preference to higher multiples, since the impedance will vary less rapidly with frequency and will provide a closer approximation to the "lumped-constant" values of the filter components.

The response of the input filter is not as critical as the output filter, since the output circuit is the main factor determining the bandwidth of the amplifier. It should have a bandwidth as wide as the output filter but the cutoff does not need to be as sharp, so that a heavily loaded single-tuned circuit is sufficient. This is simple to obtain at high frequencies since the response of the input circuit is determined by the input loading of the tube. Matching is accomplished by adjusting the position of the input tap.

ACKNOWLEDGMENT

Grateful acknowledgment is made to John P. Woods, under whose supervision the development of this amplifier was carried out.

---

[4] W. R. Ferris, "Input resistance of vacuum tubes as ultra-high-frequency amplifiers," PROC. I.R.E., vol. 24, pp. 82–107; January, 1936.

[5] M. J. O. Strutt and A. van der Zeil, "The causes for the increase of the admittance of modern high-frequency amplifier tubes on short waves," PROC. I.R.E., vol. 26, pp. 1011–1033; August, 1938.

Special Magnetic Amplifiers and Their Use in Computing Circuits*

H. S. SACK†, R. T. BEYER‡, G. H. MILLER†, MEMBER, I.R.E., AND J. W. TRISCHKA§

Summary—A special design of a magnetic amplifier is described which can be used as a summer, differentiator, or integrator in electronic computers. The incorporation of a negative feedback gives a high degree of precision and stability (0.1 per cent or better) to the system, with a minimum of precision parts.

IT IS CUSTOMARY to designate by the term "magnetic amplifier" certain circuits in which transformers operated in the nonlinear region form basic elements. In particular, it is possible to transform direct-current signals into alternating-current signals by means of such transformers in making use of certain hysteresis properties of the ferromagnetic core material.

Many radar and related devices, such as gun directors, navigational aids, etc., contain computers which transform the intelligence received from the radar beam into other signals appropriate for the further use of the device. These computers have to perform certain mathematical operations on the input signals, such as summing, differentiating, etc., or more complex operations such as co-ordinate transformations. In most cases, these computers are made up of a series of component circuits, each of which performs one specific mathematical operation (or a combination of a few, perhaps two or three). They may contain purely electrical elements, purely mechanical, or combinations of both electrical and mechanical elements.

The magnetic amplifier combined with a very high percentage of negative feedback can be used advantageously in such component circuits of computers, and can replace some of the more conventional designs; e.g., resistance networks in adders. In this paper the design, operation, and test results of magnetic-amplifier circuits for the use as summers, differentiators, and integrators will be discussed.[1]

I. Principle of the Magnetic Amplifier

The use of nonlinear transformers (NLT's) in the application here described depends in particular on a phenomenon observed by Epstein in 1902.[2] If a sinusoidal voltage is applied to the primary of a transformer containing a ferromagnetic core, of an amplitude sufficient to extend the hysteresis loop into the region of saturation, the potential appearing on the secondary winding will possess the same frequency and odd harmonics.[3–8] As long as the hysteresis loop is symmetrical (with respect to the origin), this will be the case, since the symmetry precludes the production of even harmonics. If a small direct-current flux is superimposed on the transformer, however, even harmonics will also appear in the output.

In the first approximation, the amplitude of the even harmonics will be proportional to the superimposed direct-current flux, and therefore to the magnitude of the direct-current bias which is used.

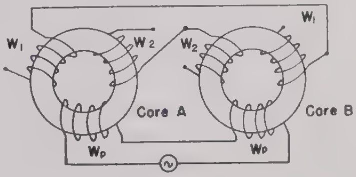

Fig. 1—Schematic diagram of the arrangements of windings on a pair of NLT's.

To remove the fundamental signal and the odd harmonics from the output, the transformers are wound as shown in Fig. 1. It is assumed here that the two transformers are identical, and that the windings are all wound in the same sense. W_p are the primary windings, and W_1 and W_2 are the pickup (output) and bias secondaries. These secondaries are so connected in series that the fundamental and odd harmonics will cancel out across them, while the even harmonics will add.

In some of the earlier work, the second-harmonic output, after amplification, was used as a measure of the

---

* Decimal classification: 621.375.2. Original manuscript received by the Institute, October 7, 1946; revised manuscript received, December 9, 1946. This paper is based in whole on work done for the Office of Scientific Research and Development under Contract OEMsr 768, with Cornell University.

† Cornell University, Ithaca, N. Y.
‡ Brown University, Providence, R. I.
§ Columbia University, New York, N. Y.

[1] This research was initiated by Bruno Rossi, now at the Massachusetts Institute of Technology, Cambridge, Mass., and continued by the present group. For more details, see National Defense Research Committee, Division 14, Reports 436 and 437, December, 1944, and May, 1945.

[2] T. Epstein, "German Pat. No. 149761, August, 1902.

[3] G. Vallauri, "Statischer frequentverdoppler," *Elek. Tech. Zeit.*, vol. 32, pp. 988–989; September, 1911.

[4] L. Kühn, "Über ein neues radiotelephonisches system," *Jahr für Draht Teleg.*, vol. 9, pp. 502–534; June, 1915.

[5] E. F. W. Alexanderson and S. P. Nixdorff, "A magnetic amplifier for radio telephony," Proc. I.R.E., vol. 4, pp. 101–121; April, 1916.

[6] T. Minohara, "Some characteristics of the frequency doubler as applied to radio transmission," Proc. I.R.E., vol. 8, pp. 493–509; December, 1920.

[7] A. Hund, "Phenomena in High-Frequency Systems," McGraw-Hill Book Co., New York, N. Y., 1936; p. 185.

[8] J. Zenneck, "A contribution to the theory of magnetic frequency changers, "Proc. I.R.E., vol. 8, pp. 468–493; December, 1920.

bias current. While high sensitivity can be obtained in this way, there are many disadvantages. The linearity between the amplitude of the second harmonic and the bias current is limited by the characteristics of the transformers, and is also dependent on external conditions such as temperature, constancy of primary voltage, etc. Also, the stability of such amplifiers is not always good. These disadvantages are overcome by introducing a negative feedback. A fourth pair of windings, similar to the bias windings, is added to the transformers. The second harmonic from the pickup windings is amplified and detected. The resultant direct current is fed into this added pair of windings (compensation or feedback windings) in such a way that its magnetic field opposes that of the direct-current bias. The magnitude of the compensating current can be shown to be

$$I_c = \frac{I_1}{\dfrac{1}{k} + \dfrac{N_c}{N_1}} \tag{1}$$

where I_c is the bias current, I_c the compensating current, k the amplification of the system, defined as the ratio of the output current of the amplifier system to the bias current if the compensating coils are not connected, and N_1 and N_c the numbers of turns on the bias and compensation windings, respectively.[9]

If k is sufficiently high, then $I_c = N_c I_1 / N_1$ and the linearity between input and output does not depend on a constant k, and therefore does not require good linearity in the transformers or very high stability of the amplifying system.

II. Detailed Description of the Circuit

A block diagram of a typical circuit is shown in Fig. 2. The two NLT's are designated by A and B, the bias (input) windings by S_1, the feedback windings by S_2, and the pickup windings by S_3. An audio-frequency oscillator is used to excite the NLT's. It must have a potential sufficiently large to drive the NLT's into the nonlinear region, and must not have a large content of even harmonics. The pickup windings are connected to an amplifier and detector stage, while the bias windings S_1 are connected to a separate input circuit. The output of the amplifier and detector stages is fed back through a feedback circuit into the windings S_2. The design of the feedback circuit depends on the particular application of the circuit, as does also the design of the input stage.

Although all the windings are drawn separately in the diagram, it is possible to use one winding for two purposes. In general, for example, the pickup winding and the input winding are the same windings. This reduces by one the number of windings required, and may be of importance where a larger number of windings are required; e.g., in a circuit for adding currents.

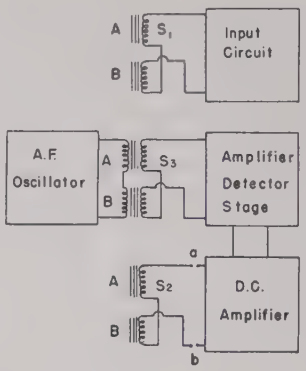

Fig. 2—Block diagram of a magnetic amplifier with feedback.

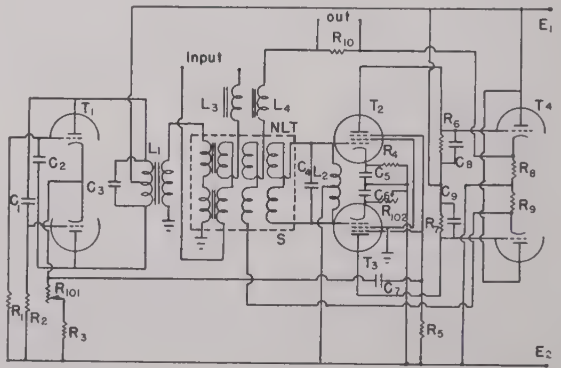

Fig. 3—Wiring diagram for a magnetic amplifier with voltage output.
Tubes (T): (1) 6N7; (2) 6SJ7; (3) 6SJ7; (4) 6SN7.
Chokes and transformers (L): (1) Western Electric type 645 (250 additional turns secondary); (2) Western Electric type 645 (2 sections in series); (3) 6 henries; (4) 6 henries.
Resistors (fixed) (R): (1) 100,000 ohms; (2) 100,000 ohms; (3) 3000 ohms; (4) 2000 ohms; (5) 1000 ohms; (6) 250,000 ohms; (7) 250,000 ohms; (8) 3000 ohms; (9) 3000 ohms; (10) 1000 ohms.
Resistors (variable) (R): (101) 2500 ohms; (102) 2500 ohms.
Capacitors (C): (1) 0.5 microfarad; (2) 0.5 microfarad; (3) 0.13 microfarad; (4) 0.03 microfarad; (5) 20 microfarads; (6) 20 microfarads; (7) 0.05 microfarad; (8) 0.5 microfarad; (9) 0.5 microfarad.
$E_1 = 250$, electron-tube-regulated.
$E_2 = 150$, VR-regulated.

The different stages of the circuit will now be discussed in more detail, referring to Fig. 3, which is a complete circuit diagram of one of the models developed.

---

[9] If k is the amplification as defined, the current in the output circuit, without feedback, is $I_c' = kI_1$. This current corresponds to a magnetic flux produced by $N_1 I_1$ ampere-turns. The output current for 1 ampere-turn is then k/N_1. If the output current is fed back, the the total flux in the NLT will be determined by the total ampere-turns $(N_1 I_1 - N_c I_c)$, and therefore the output current is

$$I_c = \frac{k}{N_1}(N_1 I_1 - N_c I_c)$$

from which equation (1) of the text follows immediately.

A. Nonlinear Transformers

The cores of the NLT's used in all the circuits described in this paper were made of molybdenum permalloy ribbon, 0.05 millimeter thick, wound as a spiral into a ring of rectangular cross section, 0.7 centimeter high, with inner and outer diameters of 2.9 and 3.8 centimeters, respectively. Each core weighed 25 grams and was placed in a phenol fiber box with a winding of 200 turns of No. 32 Formex wire for the primaries, and five separate windings of 800 turns each of No. 36 Formex wire for the secondaries.

Because the cancellation of the primary and odd harmonics requires identity in the two transformers, it is necessary that the pair be matched very carefully. The two transformers are connected together as in actual use; the primaries are excited, and the output is observed across that pair of secondaries which will form the pickup winding. Such transformers are chosen to form a pair in which the second-harmonic output is as nearly zero as possible. There may still be some fundamental signal left, but this can be easily eliminated later in the circuit, whereas the presence of a residual second harmonic would be more harmful.

Since bias produced by the earth's magnetic field or stray fields has serious effects on the zero level, it is necessary to shield the NLT's magnetically. A set of permalloy and copper shields is very effective for this purpose. The different windings must be well insulated from each other. Otherwise, leakage currents will greatly reduce the sensitivity of the NLT's. If the cores are to be subjected to mechanical vibration, they should be mounted in a shockproof case, since such vibrations may influence the magnetic properties of the cores.

B. Oscillator

The oscillator is a balanced negative-resistance oscillator. It not only satisfies the requirements of small even-harmonic content, but may also simultaneously serve as a source of a second-harmonic signal which is necessary for modulating purposes in another part of the circuit. This second harmonic is obtained from the common cathode of the twin triode.

The coil in the tuned plate circuit serves simultaneously as the primary of a matching transformer, the number of turns on the secondary being determined by the impedance of the NLT's. The frequency of the oscillator is 1000 cycles.

C. Detector and Amplifier

The output of the NLT's must be rectified by a phase-sensitive detector, i.e., a detector in which the direct-current output changes sign if the phase of the input signal changes by 180 degrees. Such a change of phase occurs when the bias (input) current changes its sign. But even if the input current were always of the same direction, a phase-sensitive detector is necessary because a system with a normal detector would not be stable.

Several types of phase-sensitive detectors were employed which could be classified as balanced modulators. They vary principally in the method of introducing the modulating signal. The design most frequently employed is shown in Fig. 3. The pickup coil on the NLT's is connected to a circuit tuned to the second harmonic whose inductance is center-tapped. This puts the signals at the ends of the coil 180 degrees out of phase. These signals are then applied to the control grids of two pentodes. The modulating signal, which is obtained from the oscillator, is applied to the suppressor grids of the tubes. This signal is in phase with one of the signals from the pickup coil, and is therefore 180 degrees out of phase with the other. The plate circuit of each pentode consists of a resistance-capacitance parallel combination with a time constant long in comparison with the period of the signal voltage. The magnitude of the modulating signal is such that the two tubes are effectively conducting only during half the period. The sign of the potential difference between the two plates then depends evidently on which of the two grids is more positive. The output thus changes its sign if the grid (input) signal changes its phase by 180 degrees.

Amplifications of between 70 and 120 direct-current volts per volt root-mean-square for pentodes such as 6SJ7, 6AC7, 6AS6, etc., can be obtained. The modulating signal must be of the order of 30 to 40 volts. The variable resistor R_{100} in the cathode of one of the pentodes permits a balancing of the two pentodes for zero input signal.

In other designs a twin triode is used, with the modulating signal applied across a common cathode resistance. This gives a much lower amplification (about 20 to 30), but requires one less tube envelope.

Another way of employing twin triodes is to apply the modulating signal to the grids over a resistance network. This method has the disadvantage that coupling between the two signals may occur.

D. Tuning of the Pickup Coil

In most of the circuits designed, the pickup coil was tuned to the second harmonic. This has two definite advantages. It increases the sensitivity by a factor of as much as 20 or more, depending on the sharpness of the tuning, and it reduces the relative content of the fundamental or other harmonics with respect to the second harmonic. It is desired to reduce this fundamental background in order that the detection stage will not be saturated with it, and also so that no phase detection can occur between it and any fundamental which may be present in the modulating signal.

The chief disadvantage of tuning is that slight changes in the frequency (resulting, say, from a change in the oscillator voltage) can produce a large variation in the input applied to the detector stage. Also, the time constant is increased due to this tuning, and, finally, if the tuning is too sharp, the output of the NLT's may jump into an unstable region. Therefore, this method requires careful tuning and a frequency-stable oscillator.

On the other hand, without tuning, the magnitude of the output of the NLT's might be too small for a direct application to the detector. An alternating-current preamplifier is then necessary. Also, the discrimination between the second harmonic and other harmonics is done only by the detector. The advantage of this method is the relative independence of frequency.

E. Feedback

The choice of the feedback system will depend on the output requirements—whether the device should give current amplification, voltage amplification, or yield another type of output as, for instance, an angular rotation, a mechanical speed, etc. The simplest method of feedback would be to connect the compensating winding in series with a large resistance or a large inductance, across the plates of the detector tubes. However, it may be that not enough current can be supplied by the detectors for this purpose. In that case a stage of direct-current or voltage amplification is necessary. In Fig. 3, this is accomplished by a differential cathode follower.

A second method of feedback was employed in an application which required the output of the circuit to cause a mechanical angular velocity. In this case it was more advantageous to use the output from the detector to drive a generator with linear characteristics, and then take the feedback current from the output of this generator. In this way the circuits connecting the detector output to the motor are also stabilized, and linearity between the input and the speed (output) is guaranteed.

In another application (differentiation) the output was desired in the form of an angular shaft rotation which was proportional to the input current of the NLT's. In this case, a linear potentiometer was connected to the output axle and a constant potential was applied across it. The feedback current was then taken from the variable contact of the potentiometer.

Of course, there are many other ways in which the feedback could have been accomplished. The final feedback is always a current, and if the output is desired in another form, such as a potential or a shaft rotation, it is important that the desired relation between the current and this other form of output be satisfied within the permitted error.

F. Input Circuit

The magnetic amplifier is a current-sensitive device and the input impedance is relatively low. Much care must be taken that this low impedance of the input coils does not influence those circuits which feed into the input circuit.

The impedance of the input circuit as seen from the input to the NLT's must not be too low, for instability again may be encountered. Since this impedance is reflected back into the primaries, a change in the value of the impedance can change the sensitivity. To avoid these difficulties, a large choke was put in series with the input windings, and all resistances which were subject to change during operation were shunted by capacitances of low impedance.

III. Circuit Operation and General Results

Before considering specific applications of the magnetic amplifier, the operation of the circuit in a general way will first be discussed, and those results described which are common to all applications.

A. Definition of Sensitivity and Precision

By sensitivity is meant the ratio of output to input. In regard to NLT's, the input is the current passing through an input winding, and the output is an alternating-current potential across the pickup winding. By this definition, the sensitivity depends on the number of turns in the different windings. For reasons of easier comparison it is preferable to refer all results to similar input and output windings, each having 800 turns. It may be noted that a current of 1 microampere in such a winding produces a magnetic field in the core of approximately 10^{-4} gauss.

By percentage precision is meant the mean per cent error of the result with respect to the maximum output for which the particular circuit was designed.

B. Number of Turns on the NLT's

The choice of the number of turns on the NLT's depends on the particular problem at hand. Since the absolute sensitivity of the NLT's increases with the number of pickup turns, and also with the number of input turns, a large number of such turns is certainly desirable. However, there is an upper limit to the number of turns apart from consideration of space, for, if it becomes too large, the potential of fundamental frequency appearing on each single NLT secondary will be very high and may cause insulation difficulties. This difficulty can be avoided by a particular arrangement of windings: several windings of fewer turns are wound on the NLT'S and then are connected in such a way that, for example, winding No. 1 of transformer 1 is connected to winding No. 1 of transformer 2; then to winding No. 2 of transformer 1; then to winding No. 2 of transformer 2, etc. In this way the net potential of fundamental frequency appearing across any winding can be kept within reasonable limits.

The number of windings on the primaries is not important, so long as there are means for matching the output impedance of the oscillator to the impedance of the primaries of the NLT's.

The choice of the number of turns for the compensation winding depends on the amount of current which is available in the output. If this current is sufficiently great, then very few turns will be sufficient.

C. Primary Frequency and Potential

As already mentioned, the fundamental frequency was 1000 cycles. While the sensitivity of the open-circuit NLT's increases with frequency, losses in the core material and the primary potential necessary to drive the NLT's to saturation also increase with frequency. On the other hand, the frequency should not be too low, for larger capacitors, chokes, etc., are then required in tuned circuits and filters.

The choice of the amplitude of the exciting potential on the primary of the NLT's is a critical one. The sensitivity of the open-circuit NLT's increases very rapidly with primary potential until a peak is reached. It then falls off with a further increase in the potential. For greatest stability, it is best to operate at the edge of this latter region, i.e., just beyond saturation. This particular potential can be determined by examining the hysteresis loop on an oscilloscope under operating conditions.

Under the operating conditions in this research, the open-circuit sensitivity was 43 millivolts root-mean-square secondary output per microampere input.

When tuned circuits are used on the pickup coil, the behavior of the NLT's is quite different. The investigation of such phenomena is complicated by the fact that the oscillator frequency and output voltage vary simultaneously in the type of oscillator here used. If the secondary is sharply tuned, the sensitivity of the NLT's increases very rapidly with the exciting voltage until an instability results. This has already been mentioned.

In a typical case of a sharply tuned secondary, the sensitivity increased from 168 to 612 millivolts per microampere and passed into instability as the oscillator voltage increased by 1 volt. If the tuning is less sharp, such instabilities do not occur.

These difficulties show that, if the circuit is used with a high sensitivity, the potential must not vary, and also the impedances in the secondaries must not change. In practice, a sensitivity of about 100 millivolts per microampere was found adequate and sufficiently stable.

D. Over-All Sensitivity and Linearity

Over-all current sensitivities, referred to 800-turn windings, of as high as 5000 have been obtained with these circuits. This high amplification indicates that the net magnetic field will be very small, and therefore the linearity should be very good. The results bear out this surmise. In the best tests, a mean error of 0.0025 per cent was obtained for a maximum current of 1.1 milliamperes (with an amplification of 5000).

In most cases, the amplification is not so high, and therefore the linearity is somewhat less good. However, it is always possible to remain within 0.1 per cent as long as the maximum output current is 100 microamperes or greater.

E. Limits of Sensitivity, Precision, and Range

No systematic deviations from linearity should occur with these circuits, provided the necessary zero adjustments can be kept constant. The error in microamperes of a particular reading seems to be independent of the magnitude of the input current. The precision of the apparatus is then limited by short-time fluctuations.

These fluctuations apparently depend on the over-all amplification, varying in the different models tested from 5 microamperes for a model in which the amplification was 70, down to 0.025 microampere for one in which the over-all amplification was 5000.

The larger fluctuations are possibly due to the amplifying stages following the NLT's. Another possible cause of fluctuations would be the discontinuities in magnetization (Barkhausen effect). However, for the large cores used in these experiments such fluctuations should be below 0.01 microampere. This is not very much smaller than the lowest value of fluctuations thus far obtained.

The maximum range of the circuit depends, for sufficiently large k, only on the amplifier stages, and is particularly determined by the saturation of the final stage. In the circuit just described, the maximum range is 5 milliamperes with a cathode follower in the last stage and about 0.2 milliampere with a differential amplifier (voltage amplification).

F. Long-Time Stability; Zero or Background Current

The long-time stability depends mainly on what is called the "background." A second-harmonic signal exists in the NLT's even if the input currents are zero. This gives rise to a finite compensation current which constitutes a zero error or zero current. The whole phenomenon of residual second harmonic is known as the background. It apparently varies with time, therefore producing a shift in the zero of the current. Such fluctuations seem to depend somewhat on the value of k. For the model just described, the observed fluctuations are of the order of 0.3 microampere over a period of eight days. For a similar circuit employing miniature tubes, the stability is somewhat less. In general, however, one can say that the long-time stability without any adjustments is 1 microampere or better over several weeks' time, provided that large temperature changes are avoided.

Some fluctuations may occur in the value of k, but since it is so large this has a negligible effect on the stability, provided that the region of instability of the NLT's is not reached. The long-time stability can be improved by using an automatic zero correction, as described in the next section.

G. Stability Under Change of External Conditions

Here, again, it is the background which causes variations under changes of external conditions. While no general rules can be stated, a few observations on particular models will give a general view of the problem. When broad tuning and a low k was used, the value of k changed very little when the NLT's were heated in the interval 5 to 65 degrees centigrade, while the background increased by about 0.2 microampere per degree centigrade. In the later model, with a certain tuning the zero current changed from 0.06 microampere to -1.8 microamperes, passing through a maximum of 0.4 microampere between 4 and 65 degrees centigrade, k varying from 120 to 230. Measurement of the sensitivity of the NLT's with the tuned circuit showed that it increased from 20 to 150. The largest influence of the temperature then appears to be on the tuning. Later measurements showed that, while the temperature variation could be very disturbing if only the NLT's were heated, the variations were kept within the limit of error when the whole circuit was kept at uniform temperature.

Vibration tests, without shock-proof mounting, showed that the change in the background stays within 1 microampere under a vibration of 10 g, provided that the vibration remains steady.

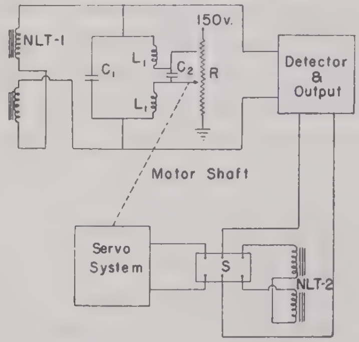

Fig. 4—Block diagram for automatic zero correction.

The general results of various stability tests show that, with the regulated power supplies normally available and with temperature variations of not more than 5 to 10 degrees centigrade, an over-all stability of about 0.1 microampere over a week can be expected, provided that k is 1000 or greater.

The long-time instabilities can be reduced even further by the use of a device to provide frequent zero corrections. One such arrangement is shown in Fig. 4. The zero is corrected by superimposing an additional bias current in one of the windings—say, the pickup winding—and by giving this current such a value that it compensates for the background and for any unbalancing in the later stages. This can be done automatically by adding a servo system in such a way that the output of the detector can be connected by a switch to the feedback winding or to a servomotor. This motor drives a potentiometer which regulates the zero correction current. If the switch is thrown to the servo position, then the feedback circuit is opened, and if simultaneously the input circuits are opened, then the servomotor will run until the zero current compensates the background. If care is taken that the opening of the input and feedback current is done in such a way that the alternating-current impedance is not changed, this method provides a very effective adjustment for the long-range fluctuations.

H. Use of Miniature Tubes

Although most measurements were made with circuits employing tubes of ordinary size, some tests were made with miniature tubes. Models of this type exhibited nearly the same behavior as the models thus far described, except that the long-time fluctuations are somewhat greater. This is apparently due to the twin triodes 6J6, the characteristics of which are not so constant as those of the 6SL7 or 6SN7.

IV. APPLICATIONS

A. Direct-Current Amplifier

The circuits which have been described can be used for the amplification, with high stability, of small direct currents from low-impedance sources. The current to be measured is entered on an input winding. If the compensating winding is connected in series with a large resistance (300,000 ohms) in a differential amplifier as a final stage, a relatively large potential output is obtained.

The amplification can be further increased by increasing the ratio of turns on the input winding to turns on the feedback winding.

B. Algebraic Addition of Currents

The magnetic amplifier can also be used for algebraic addition of currents. A number of input windings are placed on the NLT's, this number being the number of potentials or currents to be added. If the current in the jth winding is I_j and the number of turns in that winding is N_j, I_c is the compensating current and N_c is the number of turns on the compensating winding; and if k, the amplification factor, is sufficiently high, then

$$I_c = \frac{\sum_j N_j I_j}{N_c}. \tag{2}$$

Hence, the compensating current will give any desired linear combination of the input currents.

The simplest circuit performing such addition or subtraction is one in which the current is fed back from the detector stage directly over a resistance if the compensation current is small, or over a direct-current amplifier, e.g., a cathode follower, if the current is larger.

The operation of this circuit, except for the use of several input windings, follows the general description given above. Tests were made with two currents entered on windings with the same number of turns, and the precision was better than 0.1 per cent.

A somewhat different output system was designed for a special application. This circuit provided for an output in the form of an angular speed proportional to the sum of two currents. The motor employed was a permanent-field direct-current motor and the speed could only be varied by varying the armature current. This current (maximum 250 milliamperes) was too large for convenient direct control by vacuum tubes, so that a relay system was employed in which the potential necessary to drive the motor to maximum speed is periodically switched on and off, the average armature current therefore being determined by the relative length of time during which the motor is connected and disconnected, respectively. In order to have a good linearity between the speed and the sum of the inputs, a generator with linear characteristics was connected to the motor, and the output potential of this generator used to feed into the feedback winding of the NLT's.

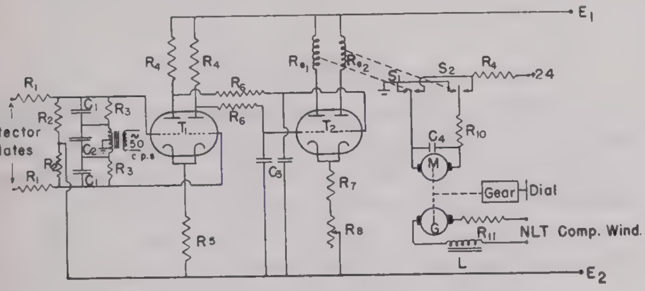

Fig. 5—Magnetic amplifier used as an adder followed by a mechanical integrator.

Tubes (T): (1) 6SL7; (2) 6SN7.

Resistors (R): (1) 0.5 megohm; (2) 0.5 megohm; (3) 0.1 megohm; (4) 100,000 ohms; (5) 20,000 ohms; (6) 300,000 ohms; (7) 10,000 ohms: (8) 10,000 ohms; (9) 10 ohms, 10 watts; (10) 10 ohms, 10 watts; (11) 875 ohms (precision).

Capacitors (C): (1) 4 microfarads; (2) 0.25 microfarad; (3) 0.01 microfarad; (4) 0.5 microfarad.

Inductance (L): 6 henries; R_e-S: relay (BTL 168479); M: motor (Delco, 24-volt); G generator (Delco, 24-volt).

Fig. 5 shows that part of the circuit which follows the detector stage, and which is characteristic for this particular application. The periodic switching is obtained by producing a square wave of variable width through superposition of an auxiliary alternating voltage (50 to 100 cycles) and the direct-current output voltage of the detector stage. The switching itself is done by Bell Telephone Laboratories mercury switches inserted in the plates of the last tube. Another switching system developed by Bell Telephone Laboratories, in which the switching is done by a self-oscillating circuit, was also tried with equally good success. With a maximum input of 1 milliampere direct current, a precision of 0.25 per cent was accomplished with no adjustments needed over a period of a week.

The advantages of the magnetic amplifier for current addition are the independence of input and output potential levels; good accuracy with no precision parts; virtually no dependence on tube drift; and high stability, particularly if used with zero correction. Its disadvantages are relatively high input currents and probably a need for more tubes than in a circuit with addition by a resistance network.

C. Application to Differentiation and Integration

The magnetic amplifier can be used for differentiation by applying a variable input potential through a capacitor C_0 to the input winding. The current in this winding is, in a first approximation, equal to $C_0(dV/dt)$. This is, then, the input, and hence the output will be proportional to dV/dt. This circuit has the advantage over direct electronic direct-current amplifiers in that the low input resistance of the coils eliminates the need for a compensation of the IR drop across the resistance of the winding. Some consideration must be given to the limitations in accuracy caused by the presence of resistance R and inductance L in the input circuit. The correct value of the current will, in general, contain higher derivatives of the potential than dV/dt, their importance being determined by the relative values of the circuit constants. It can be shown that the relative error in the current introduced by these higher terms is given by

$$\frac{\Delta i}{i} = \frac{\sum_{k=2}^{\infty} (RC_0)^{k-1} \left| \frac{d^kV}{dt^k} \right|}{\frac{dV}{dt}}. \tag{3}$$

For instance, if $R=2000$ ohms and $C_0=10$ microfarads, this formula shows that, in order to have a precision of 2 per cent, the second derivative may have a numerical value of the same order of magnitude as the first. Hence, the difficulties arising from higher terms are, in general, not very serious with low resistance values.

A second possibility of error lies in transients which will be set up whenever a sudden change occurs in the potential. However, with the proper choice of circuit constants (such as those above), the transients will become negligible after about 0.1 second, i.e., they will fall to within 1 per cent of the normal differentiation current CdV/dt. Hence, this is no serious difficulty in cases where dV/dt is changing slowly.

A more serious problem is that of the differentiating capacitor. It must be large in order that appreciable input currents be obtained. However, large capacitors generally exhibit absorption phenomena (after-effects) and leakage. This leads to additional currents not proportional to dV/dt. Even with some of the better makes of capacitors, errors as high as 3 per cent may occur. Furthermore, the leakage currents increase rapidly with temperature. Polystyrene capacitors were found to be the most successful, but have the disadvantage that they are rather bulky.

Because of the small size of the available input currents, it is advantageous to use a great number of turns on the input windings. In this case, care must be taken that sufficiently large chokes are inserted in the input circuit in order to make the reflected impedances large enough.

In the testing of the circuit for differentiating, several kinds of time functions of potentials were chosen as input signals. The first was obtained by the discharge of a large capacitor which results in a dV/dt proportional to an exponential. In such tests, the accuracy obtained was better than 1 per cent, with a maximum input current of 40 microamperes. In Fig. 6, results are reproduced which were obtained by giving the input potential a sawtooth shape. The circles represent the value of dV/dt calculated from the observation of the time variation of the input potential, while the curve shows the observed output values. As the measurements themselves are delicate, the coincidence of calculated and observed values must be considered quite satisfactory. The curve shows in particular that the transient occurring during the rapid rise in the sawtooth does not disturb the performance of the apparatus.

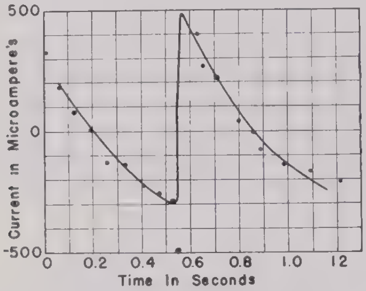

Fig. 6—Test results on a differentiator. (The input is a sawtooth potential.)

The general results of these experiments indicate that the magnetic amplifier lends itself very well to differentiation, having the advantage of a short time constant and of no need for a correction circuit for the IR drop. It does not require any precision parts, with the exception of the input capacitor. It has the only disadvantage that it needs a rather big differentiating capacitor.

Another possible use of the magnetic amplifier is in integration. The input potential to be integrated would be applied to one of the input windings, whereas the feedback current is obtained by connecting the output stage through a big capacitor to the feedback winding. Under such conditions, the feedback current is equal to CdV_0/dt where C is the capacitance of the capacitor just mentioned, and V_0 is the potential appearing at the output stage. As this feedback current is equal to the input current I, it is evident that

$$V_0 = \frac{1}{C}\int I dt. \tag{4}$$

As before, the advantages of the magnetic amplifier are the independence of the input and output levels, and the good precision and stability that can be obtained without any precision components. No comprehensive tests were made on a circuit of this design.

V. Conclusions

It may be seen from the above that magnetic-amplifier circuits can be applied to advantage in summer, differentiator, and integrator circuits, used in computing devices where high precision and high stability are desired. Particular advantages are the independence of input and output levels, and the achievement of good precision and stability with few precision parts. These circuits have a relatively low direct-current input impedance which, in certain applications, may be advantageous. A disadvantage to all these circuits is the relatively high input current, which is of the order of 10 microamperes or greater.

The lowest input current used in these experiments was 8 microamperes (through five input windings in series). The precision was $\frac{1}{2}$ per cent with good stability, which means that 0.04 microampere can still be detected. In other words, with an 8-microfarad capacitor as a differentiating capacitance, a dV/dt of 1 volt per second can be measured with $\frac{1}{2}$ per cent precision, or in other terms, since five windings in series have a resistance of 250 ohms, the sensitivity of the apparatus for direct voltages is 10 microvolts. With larger input currents, precisions of 0.1 per cent and better can be obtained.

The models described in this paper were designed with an aim towards ruggedness and good operation over long periods without adjustments. If it were a question of building a laboratory instrument, considerably higher sensitivity or precision could be obtained.

Dimensional Analysis of Electromagnetic Equations*

A. M. WINZEMER†, ASSOCIATE, I.R.E.

Summary—**The physical quantities of interest in electromagnetic theory are tabulated in terms of the basic physical quantities: mass, length, time, and charge; and a method for checking the dimensional validity of an equation is indicated.**

IT IS VERY often necessary to check equations dimensionally. The present paper describes a method of dimensional analysis by which equations can be checked with a minimum of effort.

In Table I, the various physical quantities of interest in electromagnetic theory are listed alphabetically. Dimensionally, each of these can be expressed in terms of four or less basic physical quantities. In the extended Giorgi system, the four basic quantities used are mass (kilogram), length (meter), time (second), and charge (coulomb). The symbols used to designate these are, respectively, M, L, T, and Q. For example, the units of acceleration are meters per second per second, expressed in shorter form as $[a]=LT^{-2}$.

TABLE I

Number	Quantity	Letter	M	L	T	Q	Equivalent Units
1	Acceleration	a	0	+1	−2	0	Meter/Second^2
2	Area	A	0	+2	0	0	Meter^2
3	Capacitance	C	−1	−2	+2	+2	Farad [Coulomb/volt]
4	Capacitance, distributed	c	−1	−3	+2	+2	Farad/Meter
5	Charge	Q	0	0	0	+1	Coulomb-[Ampere Second]
6	Charge density, line	q_l	0	−1	0	+1	Coulomb/Meter
7	Charge density, surface	q_s	0	−2	0	+1	Coulomb/Meter^2
8	Charge density, volume	q_v	0	−3	0	+1	Coulomb/Meter^3
9	Conductance	$\mathcal{G}$	−1	−2	+1	+2	Mho
10	Conductance, distributed	g	−1	−3	+1	+2	Mho/Meter
11	Conductivity	γ	−1	−3	+1	+2	Mho/Meter
12	Current	I	0	0	−1	+1	Ampere
13	Current density, line	J	0	−1	−1	+1	Ampere/Meter
14	Current density, surface	G	0	−2	−1	+1	Ampere/Meter^2
15	Dielectric constant	ϵ	−1	−3	+2	+2	Farad/Meter
16	Displacement, dielectric	D	0	−2	0	+1	Coulomb/Meter^2
17	Energy	W	+1	+2	−2	0	Joule [Watt-Second]
18	Energy density, volume	w	+1	−1	−2	0	Joule/Meter^3
19	Field intensity, electric	E	+1	+1	−2	−1	Volt/Meter
20	Field intensity, magnetic	H	0	−1	−1	+1	Ampere/Meter
21	Flux, dielectric	ψ	0	0	0	+1	Coulomb
22	Flux density, dielectric	D	0	−2	0	+1	Coulomb/Meter^2
23	Flux density, magnetic	B	+1	0	−1	−1	Weber/Meter^2
24	Flux, magnetic	ϕ	+1	+2	−1	−1	Weber [Volt-Second]
25	Force	F	+1	+1	−2	0	Newton [Joule/meter]
26	Force, electromotive	V	+1	+2	−2	−1	Volt
27	Force, magnetizing	H	0	−1	−1	+1	Ampere/Meter
28	Force, magnetomotive	$\mathcal{F}$	0	0	−1	+1	Ampere
29	Frequency	f	0	0	−1	0	Cycles/Second
30	Inductance	L	+1	+2	0	−2	Henry [Volt-Second/Ampere]
31	Inductance, distributed	l	+1	+1	0	−2	Henry/Meter
32	Length	s	0	+1	0	0	Meter
33	Magnetization	m_v	+1	0	−1	−1	Weber/Meter^2
34	Mass	M	+1	0	0	0	Kilogram
35	Moment, electric	M_e	0	+1	0	+1	Coulomb-Meter
36	Moment, magnetic	M_m	0	+2	−1	+1	Ampere-Meter^2
37	Permeability	μ	+1	+1	0	−2	Henry/Meter
38	Polarization, electric	p_e	0	−2	0	+1	Coulomb/Meter^2
39	Polarization, magnetic	p_m	0	−1	−1	+1	Ampere/Meter
40	Potential, electric	V	+1	+2	−2	−1	Volt
41	Power	P	+1	+2	−3	0	Watt [Joule/Second]
42	Power density, surface	N	+1	0	−3	0	Watt/Meter^2
43	Power density, volume	p	+1	−1	−3	0	Watt/Meter^3
44	Reluctance, magnetic	$\mathcal{R}$	−1	−2	0	+2	Ampere/Weber
45	Resistance	R	+1	+2	−1	−2	Ohm [Volt-Second/Coulomb]
46	Resistance, distributed	r	+1	+1	−1	−2	Ohm/Meter
47	Resistivity	ρ	+1	+3	−1	−2	Ohm-Meter
48	Time	T	0	0	+1	0	Second
49	Torque	$\mathfrak{T}$	+1	+2	−2	0	Joule
50	Velocity, angular	ω	0	0	−1	0	Radians/Second
51	Velocity, linear	v	0	+1	−1	0	Meter/Second
52	Voltage	V	+1	+2	−2	−1	Volt
53	Volume	τ	0	+3	0	0	Meter^3
54	Work	W	+1	+2	−2	0	Joule [Watt-Second]

---

* Decimal classification: 537.1×510. Original manuscript received by the Institute, July 25, 1946.

† Naval Research Laboratory, Washington, D. C.

We can use the notation $[a]=0+1-2\ \ 0$, where the numbers represent, in order, the powers of mass, length, time, and charge which characterize the physical quantity. All the other quantities in Table I are expressed in this manner.

In Table II, the physical quantities are listed in the descending numerical order of their powers. The symbol or letter which designates each of the physical quantities appears next to each set of powers. Also tabulated is a reference number which refers the user to the same physical quantity in Table I.

In each term of an equation, the various physical quantities are combined by means of the fundamental operations, multiplication, division, inverse, root, and power. It is easily seen that the following rules govern operations on combinations of physical quantities.

Rule number	Operation	
1	nth root	divide each power by n
2	nth power	multiply each power by n
3	inverse	reverse sign of each power
4	multiplication	add corresponding powers
5	division	subtract powers of denominator from corresponding ones of numerator.

As an illustration of the method of applying these rules, consider the following equation, which gives the power input to a smooth, lossless transmission line:

$$P=\frac{V^2}{\sqrt{l/c}}$$

From Table I, number 31, $[l]=+1+1\ \ 0-2.$
From Table I, number 4, $[c]=-1-3+2+2.$
Using rule 5, $[l/c]=+2+4-2-4.$
Using rule 1, $[\sqrt{l/c}]=+1+2-1-2.$
Using rule 3, $1/\sqrt{l/c}=-1-2+1+2.$
From Table I, number 26, $[V]=+1+2-2-1.$
Using rule 2, $[V^2]=+2+4-4-2.$
Using rule 4, $[V^2/\sqrt{l/c}]=+1+2-3\ \ 0.$

TABLE II

M	L	T	Q	Letter	Number
+1	+3	−1	−2	ρ	47
+1	+2	0	−2	L	30
+1	+2	−1	−1	ϕ	24
+1	+2	−1	−2	R	45
+1	+2	−2	0	$W, \mathfrak{J}, W$	17, 49, 54
+1	+2	−2	−1	V	26, 40, 52
+1	+2	−3	0	P	41
+1	+1	0	−2	l, μ	31, 37
+1	+1	−1	−2	r	46
+1	+1	−2	0	F	25
+1	+1	−2	−1	E	19
+1	0	0	0	M	34
+1	0	−1	−1	B, m_v	23, 33
+1	0	−3	0	N	42
+1	−1	−2	0	w	18
+1	−1	−3	0	p	43
0	+3	0	0	τ	53
0	+2	0	0	A	2
0	+2	−1	+1	M_m	36
0	+1	0	+1	M_e	35
0	+1	0	0	s	32
0	+1	−1	0	v	51
0	+1	−2	0	a	1
0	0	+1	0	T	48
0	0	0	+1	Q, ψ	5, 21
0	0	−1	+1	$I, \mathcal{J}$	12, 28
0	0	−1	0	f, ω	29, 50
0	−1	0	+1	q_l	6
0	−1	−1	+1	J, H, H, p_m	13, 20, 27, 39
0	−2	0	+1	q_s, D, D, p_e	7, 16, 22, 38
0	−2	−1	+1	G	14
0	−3	0	+1	q_v	8
−1	−2	+2	+2	C	3
−1	−2	+1	+2	$\mathcal{G}$	9
−1	−2	0	+2	$\mathcal{R}$	44
−1	−3	+2	+2	c, ϵ	4, 15
−1	−3	+1	+2	g, γ	10, 11

From Table II, $+1+2-3\ \ 0=[P]$, and the reference number is 41.

From Table I, number 41, P is the power in watts.[1]

---

[1] Note that more steps than necessary have been used in the above example, in order to illustrate the use of each of the rules.

Contributors to Waves and Electrons Section

Robert T. Beyer was born in Harrisburg, Penn., on January 27, 1920. He received the B.A. degree in mathematics from Hofstra College in 1942. His graduate work was done at Cornell University from 1942 to 1945, during which time he was a teaching assistant in physics. He received his Ph.D. in physics in 1945. While at Cornell, he engaged in war research under an Office of Scientific Research and Development contract.

Since 1945, Dr. Beyer has been an instructor in physics at Brown University, where he has conducted research in ultrasonics. He is a member of the American Physical Society and Sigma Xi.

❖

Frank A. Cowan (M'30–SM'43) was born on August 30, 1898, at Escatawpa, Ala. He received the B.S. degree in electrical engineering in 1919 from the Georgia School of Technology. From 1929 to the present date he has been associated with the Bell System and is currently the Transmission Engineer of the American Telephone and Telegraph Company, New York, N. Y. He holds a commission as lieutenant commander in the United States Naval Reserve. Mr. Cowan is a Fellow of the American Institute of Electrical Engineers.

Robert T. Beyer

❖

C. Russell Cox (A'39) was born in Chicago, Ill., in 1916, and attended the University of Chicago, receiving the B.S. degree in 1937, and the M.S. degree in physics in 1939. Since January 1, 1940, he has been associated with Andrew Company in Chicago, where he is now chief engineer and sales manager.

Mr. Cox is the author of numerous technical papers on coaxial transmission lines, and has presented several such papers at I.R.E. Section meetings. He is a member of Phi Beta Kappa, and has served on the Radio Manufacturers Association subcommittees to develop standards on coaxial transmission lines.

❖

Leonard R. Malling (A'31) was born in Acton, England, in 1909. He received the E.E. degree from the Northampton Technical Institute, England. From 1927 until 1931 he was engaged in the research laboratories of the Electrical and Musical Industries. In 1932 he joined the International Telephone and Telegraph Company to work on radio links, and the following year he became associated with Marconi-Ecko, doing instrument development. From 1934 until 1938 Mr. Malling was employed by the Baird Television Company in England, occupied with television research. He left Baird to join the Hazeltine Electronic Corporation, where he remained until 1943, engaged in both television research and electronic war developments.

Mr. Malling spent 1944 at the University of California, doing research on underwater sound. He joined the Boeing Aircraft Corporation in 1945, where he was associated with guided missile and antenna research. In 1947 he formed his own laboratory, where he is now engaged in special instrument manufacturing and consulting work.

❖

Frank A. Cowan

❖

C. Russell Cox

❖

Leonard R. Malling

❖

Donald E. Maxwell (A'46–SM'46) was born at Lynn, Mass., on April 18, 1913. In 1937 he received the B.S. degree in electrical engineering from Tufts College, and in 1939 the M.S. degree in communication engineering from Harvard University. From 1937 to 1938 he was employed by the General Electric Company as a student engineer at the Lynn and Pittsfield plants.

In 1939 Mr. Maxwell rejoined the General Electric Company as a student engineer in the radio transmitter department at Schenectady, and shortly thereafter became a development engineer in the broadcast engineering section of the transmitter division. From 1940 to 1945 he was project engineer of the audio facilities group, and was responsible for the development of a complete line of broadcasting audio facilities. During the war years he was engaged chiefly in the development of airborne radar equipment.

Since 1945 Mr. Maxwell has been with the Columbia Broadcasting System as a member of the audio division of the general engineering department, where he coordinates the activities of the audio development and measurement group. Mr. Maxwell is a member of Tau Beta Pi.

Donald E. Maxwell

❖

Glenn H. Miller (M'46) was born on June 15, 1920, in Washington, D. C. He received the B.S. degree in physics from Wake Forest College in 1942. From 1942 to 1944, he was a graduate assistant in physics at Cornell University. During that time he did research work on electronic computers under a contract with the Office of Scientific Research and Development.

In 1944 he accepted a position in the research laboratory at the Stromberg-Carlson Company, where he worked until October, 1946. At that time, he returned to Cornell, where he is now working toward the Ph.D. degree.

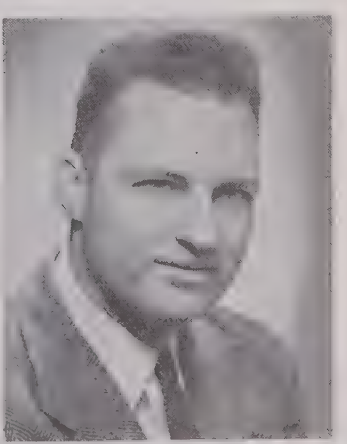

Glenn H. Miller

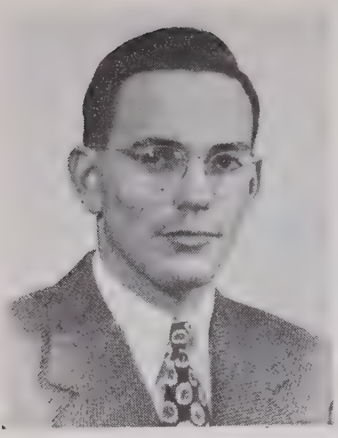

Raymond O. Petrich

Raymond O. Petrich (S'43–A'45) was born on September 14, 1922, at Cleveland, Ohio. He received the degree of B.S. in electrical engineering from the University of Washington in 1943. From 1943 through 1945 he was employed as a research associate at the Radio Research Laboratory, Harvard University. There he participated in the development of ultra-high-frequency and microwave receivers. In 1946, he became a staff member at the Airborne Instruments Laboratory, Inc., Mineola, N. Y., where he is continuing his work on the development of microwave receiver components.

Mr. Petrich is a member of Tau Beta Pi, and an associate member of Sigma Xi and the American Institute of Electrical Engineers.

◆

For a photograph and biography of H. E. Roys, see page 1162 of the September, 1947, issue of the Proceedings of the I.R.E.

◆

Henri S. Sack was born in Davos, Switzerland, on November 25, 1903. He received his diploma for physics and mathematics in 1925, and the Dr. of Sc. degree in 1927 at the Eidgen Techn. Hochschule in Zürich, Switzerland. He was an assistant and later "Chef de Travaux" in Zürich, then in Leipzig, Germany, and in Bruxelles, Belgium. In 1940 he became a research associate at the college of engineering of Cornell University. He is now associate professor of engineering physics in the new department of engineering physics of Cornell University.

Mr. Sack is a member of the American Physical Society, the American Chemical Society, the Swiss Physical Society, and the New York Academy of Science, and of Sigma Xi.

Henri S. Sack

◆

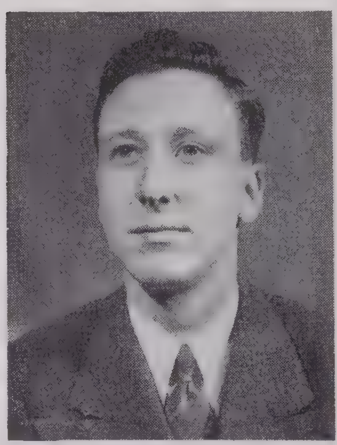

Otto J. M. Smith

Otto J. M. Smith (M'44) was born on August 6, 1917, in Urbana, Ill. He received the B.S. degree in chemistry from Oklahoma Agricultural and Mechanical College in 1938; the B.S. degree in electrical engineering from the University of Oklahoma in 1938; and the Ph.D. in electrical engineering from Stanford University in 1941. He was a research assistant at the H. J. Ryan High Voltage Laboratory at Stanford from 1938 to 1941.

Dr. Smith was an instructor in power and high voltage at Tufts College from 1941 to 1943; assistant professor of communications at Denver University 1943 to 1944; research engineer in the electronics department of the Westinghouse Research Laboratories, May, 1944, to October, 1945; and chief electrical engineer of the Summit Research and Development Laboratory, October, 1945, to date.

Dr. Smith is a member of the A.I.E.E., American Chemical Society, American Physical Society, American Institute of Physics, American Association for the Advancement of Science, and American Society for Engineering Education. He also is associated with Sigma Xi, Phi Kappa Phi, Tau Beta Pi, Eta Kappa Nu, Phi Lambda Upsilon, Kappa Tau Pi, and Phi Eta Sigma.

◆

J. W. Trischka was born on December 30, 1916, in Bisbee, Ariz. He received the B.S. degree in electrical engineering from the University of Arizona in 1937. He then worked for a year for the General Electric Company at Schenectady, N. Y., where he was a test engineer and where he took the advanced course in engineering. From 1938 to 1942 he was a graduate student and assistant in physics at Cornell University, receiving his Ph.D. degree in 1943 after completing a thesis on X-ray absorption fine structure. From 1942 to 1945 he was an instructor in physics at Cornell University, doing research first under a Naval Ordnance Laboratory contract and subsequently on a project sponsored by the National Defense Research Committee.

J. W. Trischka

From the middle to the end of 1945 Dr. Trischka worked on the Manhattan Project at Los Alamos. In 1946 he became an associate in physics at Columbia University, where he is now teaching and doing research on molecular beams. Dr. Trischka is a member of Tau Beta Pi, Sigma Xi, and the American Physical Society.

◆

A. M. Winzemer (A'42) was born on November 15, 1917, at Cleveland, Ohio. He received the B.E.E. degree from the City College of New York in 1940 and has taken graduate courses at the Polytechnic Institute of Brooklyn. From 1941 to 1944, Mr. Winzemer was an inspector of electrical instruments for the Navy Department. Since 1945 he has been employed as a radio engineer in the Antenna Subsection, Radio Division III, Naval Research Laboratory, Washington, D. C.

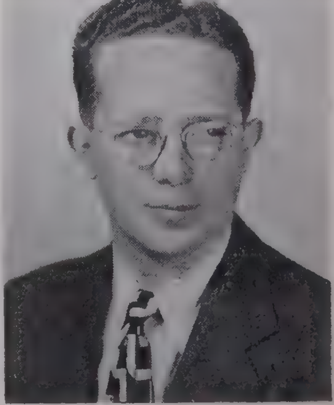

A. M. Winzemer

Abstracts and References

Prepared by the National Physical Laboratory, Teddington, England, Published by Arrangement with the Department of Scientific and Industrial Research, England, and *Wireless Engineer*, London, England

NOTE: The Institute of Radio Engineers does not have available copies of the publications mentioned in these pages, nor does it have reprints of the articles abstracted. Correspondence regarding these articles and requests for their procurement should be addressed to the individual publications and not to the I.R.E.

The Annual Index to these Abstracts and References, covering those published from January, 1946, through December, 1946, may be obtained for 2s. 8d., postage included from the *Wireless Engineer,* Dorset House, Stamford St., London S. E., England

Acoustics and Audio Frequencies...... 1387
Aerials and Transmission Lines....... 1387
Circuits and Circuit Elements........ 1388
General Physics...................... 1390
Geophysical and Extraterrestrial Phenomena.......................... 1391
Location and Aids to Navigation........ 1391
Materials and Subsidiary Techniques.. 1392
Mathematics.......................... 1393
Measurements and Test Gear......... 1393
Other Applications of Radio and Electronics........................ 1394
Propagation of Waves................ 1395
Reception........................... 1396
Stations and Communication Systems.. 1396
Subsidiary Apparatus................. 1397
Television and Phototelegraphy 1397
Transmission........................ 1398
Vacuum Tubes and Thermionics....... 1399
Miscellaneous........................ 1400

The number in heavy type at the upper left of each Abstract is its Universal Decimal Classification number and is not to be confused with the Decimal Classification used by the United States National Bureau of Standards. The number in heavy type at the top right is the serial number of the Abstract.

ACOUSTICS AND AUDIO FREQUENCIES

534.42:621.38 **3001**

A Method for Changing the Frequency of a Complex Wave—Kent. (*See* 3048.)

534.62:621.396.001.42 **3002**

The Silent Room of the National Centre for the Study of Telecommunications—P. Chavasse. (*Compt. Rend. Acad. Sci.* (Paris), vol. 224, pp. 1341–1343; May 12, 1947.) A special arrangement of absorbing screens enables waves to be obtained which, in a test-space of 1.5 m^3, are uniform to within ±1 db for all frequencies from 200 to 10,000 c.p.s.

534.756 **3003**

Acoustical Quanta and the Theory of Hearing—D. Gabor. (*Nature* (London), vol. 159, pp. 591–594; May 3, 1947.) A summary of the first two parts of 1057 of May with emphasis on the physical and physiological aspects of the problem.

534.78:621.396.619.11/.13 **3004**

Narrow-Band F.M. for Voice Communication—Bishop. (*See* 3275.)

534.845 **3005**

Functional Sound Absorbers—H. F. Olson. (*RCA Rev.*, vol. 7, pp. 503–521; December, 1946.) Sound absorbers are described whose high efficiency depends upon the shape and the fact that the absorbers are not required also to act as building material.

534.851 **3006**

The Reduction of Background Noise in the Reproduction of Music from Records—H. H. Scott. (*Proc. Nat. Electronics Conference* (Chicago), vol. 2, pp. 586–596.)

534.86:534.322.1 **3007**

Experiments in Listening—N. D. Webster and F. C. McPeak. (*Electronics*, vol. 20, pp. 90–95; April, 1947.) Audience reaction to reproduced music, from both live and transcribed sources, is tested with a high-quality audio system.

534.861.1 **3008**

Acoustical Design of Studios for A.M. and F.M.—C. R. Jacobs. (*Tele-Tech*, vol. 6, pp. 46–50; June, 1947.) Details of the lay-out and construction of the New York WNEW studios, with particulars of the insulation of floors, walls, ceilings, windows, and doors. To minimize background noise, the air-conditioning system is lined throughout with rigid rockwool material 1 inch thick. A feature of the inner lining of the studios is that no large area of any one type of absorbing material is used. Five different types are used in combination with serrated and curved plywood and plaster areas.

534.861.1 **3009**

Audio Problems in A.M. Broadcasting—H. L. Blatterman. (*Communications*, vol. 27, pp. 18–21, 51; April, 1947.) The subjective effect of a given broadcast depends not only on the characteristics of the electrical circuits between studio and home, but also on the reverberation introduced. An equipment interposed between studio microphone and the transmitter is described, which gives a controllable amount of reverberation. The variation in high frequency transmission with the diameter of the playing groove in a disk recording may be compensated electrically. An arrangement for achieving this is described.

534.862.1 **3010**

Recording Studio 3A—G. M. Nixon. (*RCA Rev.*, vol. 7, pp. 634–640; December, 1946.) The acoustical design problems encountered in remodeling a studio for recording both broadcast transcriptions and records for home use are discussed and some methods of solution given.

621.395.625 **3011**

Lateral Recording: Part 2—W. H. Robinson. (*Communications*, vol. 27, pp. 38–40, 58; April, 1947.) Discussion of cutter measurement technique, frequency run recordings, stylus, cutting angles, disks, scratch filters, and pre-emphasis. To be continued. For part 1 see 1993 of August.

621.395.625.2 **3012**

Embossing Type Sound Recorder—(*Tele-Tech*, vol. 6, p. 55; June, 1947.) Uses Vinylite disks of diameter 3 and three-quarter inches. These have a moulded guide groove, with 350 lines to the inch, on the underside and a sound groove is embossed on the smooth upper surface by a recording stylus which also serves for reproduction.

621.395.625.2:016"1921/1947" **3013**

Bibliography of Disc Recording—A. Jlrysz. (*Tele-Tech*, vol. 6, pp. 73–77, 104; June, 1947.) From 1921 to 1947, with brief summaries.

621.395.625.3 **3014**

Recent Developments in Magnetic Recording of Sound—R. B. Vaile, Jr. (*Proc. Nat. Electronics Conference* (Chicago), vol. 2, pp. 597–602.)

AERIALS AND TRANSMISSION LINES

621.315.211.9:621.315.616.1 **3015**

Making Rubber Cables—(*Elec. Rev.* (London), vol. 141, pp. 278–283; August 22, 1947.) A description of the essential processes.

621.315.212:621.317.73.029.63 **3016**

Comparator for Coaxial Line Adjustments—O. M. Woodward, Jr. (*Electronics*, vol. 20, pp. 116–120; April, 1947.) The instrument, consisting of a T-junction and rotating loop coupling to the lines, can be used in place of a slotted line and probe to measure standing-wave ratios and load impedances at u.h.f.

621.315.212:621.317.79 **3017**

A Standing-Wave Meter for Coaxial Lines—Pattison, Morris, and Smith. (*See* 3196.)

621.315.212.029.6:[621.317.333+621.317.37 **3018**

The Voltage Characteristics of Polythene Cables—Davis, Austen, and Jackson. (*See* 3179.)

621.392:621.317.79 **3019**

The Theory and Design of Several Types of Wave Selectors—N. I. Korman. (*Proc. Nat. Electronics Conference* (Chicago), vol. 2, pp. 404–423.) Wave selectors are devices which, when attached to a transmission line or waveguide, set up in another system a response proportional to either the forward or the backward traveling wave in the line or guide. Lumped-constant and distributed-constant wave selectors for frequencies lower and higher than 1000 Mc. respectively are described, with methods of adjustment.

621.392.029.64 **3020**

Wave Guides for Slow Waves—L. Brillouin. (*Phys. Rev.*, vol. 71, p. 483; April 1, 1947.) Summary of American Physical Society paper. Pipes fitted with equidistant diaphragms which behave as band-pass filters, show a very marked variation of phase velocity with respect to frequency.

621.392.029.64:549.623.5 **3021**

Mica Windows as Elements in Microwave Systems—L. Malter, R. L. Jepsen, and L. R. Bloom. (*RCA Rev.*, vol. 7, pp. 622–633; December, 1946.) "The design of a virtually reflectionless, vacuum-tight window made of mica for use in a wave-guide system is described. The technique of manufacture and the experimental results with a number of models are given. Such mica windows have many applications but are particularly useful for the transmission of microwave power or electromagnetic radiation in particular portions of the spectrum."

621.392.21:621.315.1+621.396.664]:621.396.712 3022

The Design and Use of Radio-Frequency Open-Wire Transmission-Lines and Switchgear for Broadcasting Systems—F. C. McLean and F. D. Bolt. (*Jour. I.E.E.* (London), Part III, vol. 94, pp. 216–217; May, 1947.) Discussion on 2139 of 1946.

621.392.43 3023

An Exponential Transmission Line Employing Straight Conductors—W. N. Christiansen. (PROC. I.R.E., vol. 35, pp. 576–581; June, 1947.) The design is described of a 4-wire wide-band matching line, of constant wire diameter, in which the horizontal and vertical wire spacings vary linearly with distance to produce a characteristic impedance which rises nearly exponentially from 300 to 600 Ω.

621.392.43 3024

Matching the Line to the Ground-Plane Antenna—J. T. McWatters. (*QST*, vol. 31, pp. 56–58; May, 1947.) Simple calculations give the dimensions of the antenna and shunt corrective stub.

621.392.43:[621.317.72.029.56/.58 3025

Additional Notes on the "Micromatch"—Jones and Sontheimer. (*See* 3188.)

621.396.67 3026

Problems in Wide-Band Antenna Design—A. G. Kandoian. (*Proc. Nat. Electronics Conference* (Chicago), vol. 2, p. 142.) Summary only. The most general requirement is that both the impedance and radiation patterns be essentially independent of frequency over the operating range, but in some specialized applications a predetermined variation of the radiation pattern with frequency is required. Examples and measured results of various types of wide-band aerial are discussed.

621.396.67:621.396.97 3027

Theoretical and Practical Aspects of F.M. Broadcast Antenna Design—P. H. Smith. (*Communications*, vol. 27, pp. 14–15; March, 1947.) Summary of 1947 I.R.E. Convention paper.

621.396.67:621.397.5 3028

Load Characteristics of Television Antenna Systems: Part 3—Hamilton and Olsen. (*See* 3303.)

621.396.67:621.397.5 3029

Television Antenna Installations Giving Multiple Receiver Outlets—R. J. Ehret. (*Tele-Tech*, vol. 6, pp. 26–29, 100; June, 1947.) A distribution system, for hotel use, with a single aerial. Three or six receivers are fed through 300-Ω lines without interference.

621.396.674:621.396.712:621.396.619.13 3030

Loop Antennas for F.M. Broadcasting: Part 1—N. Marchand. (*Communications*, vol. 27, pp. 34–35, 63; April, 1947.) Discussion of aerial requirements for f.m., with particular reference to loop type aerials. To be continued.

621.396.676 3031

Aircraft Antenna Pattern Measuring System—O. Schmitt. (*Proc. Nat. Electronics Conference* (Chicago), vol. 2, p. 132.) Summary only. A system for drawing automatically the radiation patterns of aircraft aerials by use of scale models. See also 2684 of October (Schmitt and Peyser).

621.396.677 3032

Directional Patterns with a 54A Array—H. R. Whaley. (*Radio News*, vol. 37, pp. 53, 143; April, 1947.) Directional aerial arrays are described, using as elements standard single aerials whose horizontal radiation pattern is circular.

621.396.677 3033

Helical Beam Antenna—J. D. Kraus. (*Electronics*, vol. 20, pp. 109–111; April, 1947.) Axial mode of operation gives circular polarization, with readily controlled directivity and gain. Aerial dimensions are given for λ 10 cm.

621.396.677 3034

Long Slot Antennas—A. Alford. (*Proc. Nat. Electronics Conference* (Chicago), vol. 2, pp. 143–155.) Brief account of aerials with slot as long as possible and to which metal wings are added to control the radiation pattern in the plane perpendicular to the axis, and of the use of arrays of such aerials to obtain directivity.

621.396.96:621.396.82 3035

Theory of Radar Reflection from Wires or Thin Metallic Strips—J. H. Van Vleck, F. Bloch, and M. Hamermesh. (*Jour. Appl. Phys.*, vol. 18, pp. 274–294; March, 1947.) The radar reflecting properties of wires and thin metallic strips are analyzed mathematically by two independent methods. The efficiency of a reflector is expressed by the concept of "radar cross section," defined as 4π times the power per unit solid angle returned in the direction of the source divided by the incident power density. This quantity, when expressed in units of area equal to the square of the wavelength, depends only on the ratios of the length of the wire to its diameter and to the wavelength. For several wires in random orientation an averaged "radar crosssection" is calculated which is small when the wavelength is longer than the wire and passes through maxima when the wire is slighty less than an integral number of half wavelengths long. The ratio of maxima to minima decreases and their magnitude increases as the number of wavelengths of the wire increases. The values of the minima increase with the thickness of the wire. See also 1687 of July (Block, Hamermesh and Phillips).

CIRCUITS AND CIRCUIT ELEMENTS

538.3:621.396.694:[621.385.029.63/.64 3036

On the Helix Circuit Used in Progressive-Wave Valves—É. Roubine. (*Onde Élec.*, vol. 27, pp. 203–208; May, 1947.) A complete account of the work referred to in 2339 and 2340 of September.

621.314.2.029.5:621.396.69 3037

Very-Wide Band Radio-Frequency Transformers—D. Maurice and R. H. Minns. (*Wireless Eng.*, vol. 24, pp. 168–177 and 209–216; June and July, 1947.) Toroidal transformers may be used for impedance matching, balanced-unbalanced coupling, d.c. isolation, and the provision of accurate voltage or current ratios. The equivalent circuit of the 2-winding transformer is used to deduce the lf. loss of the winding data for 2-db loss are shown graphically for various commercial cores (dust and alloy-strip). The leakage inductance and shunt capacitance for various forms of winding are evaluated; their effect on the h.f. performance is minimized by a low-pass filter design technique. Multiwinding and auto-transformers are briefly discussed; balance and its measurement are described. The design procedure is illustrated by a numerical example.

621.314.23:621.396.69 3038

Practical Transformer Design and Construction: Part 1—C. Roeschke. (*Radio News*, vol. 37, pp. 60–61, 165; June, 1947.) Simple method of calculating winding data from graphs and tables.

621.314.26:629.135 3039

Electronic Frequency Changers for Aircraft—O. E. Bowlus and P. T. Nims. (*Elec. Eng.*, (New York), vol. 66, pp. 463–466; May, 1947.) The frequency changer incorporates two distinct cirucits: (a) power circuit for frequency conversion, and (b) control circuit to establish output frequency. Design and performance details of an experimental test unit are given. By using a similar unit with each alternator, several main aircraft engine-driven alternators can be operated in parallel.

621.314.671 3040

Circuit Cushioning of Gas-Filled Grid-Controlled Rectifiers—D. V. Edwards and E. K. Smith. (*Trans. A.I.E.E.* (*Elec. Eng.*, December Supplement, 1946), vol. 65, p. 1131.) Discussion on 361 of March.

621.315.2.011.3 3041

The Inductance of Wires and Tubes—A. H. M. Arnold. (*Jour. I. E. E.* (London), Part I, vol. 94, pp. 116–118; February, 1947.) Summary of 1017 of May.

621.316.313.025 3042

A New Design for the A.C. Network Analyzer—J. D. Ryder and W. B. Boast. (*Trans. A.I.E.E.* (*Elec. Eng.*, December Supplement, 1946), vol. 65, pp. 1162–1165.) Discussion on 362 of March.

621.316.726.029.64.078.3 3043

Microwave Frequency Stability—Harrison. (*See* 3321.).

621.316.86 3044

Thermistors—W. Rosenberg. (*Electronic Eng.*, vol. 19, pp. 185–187; June, 1947.) Discussion of characteristics and applications, including methods of use with ohmic resistors in amplifiers and oscillators.

621.318.323.2.042.15 3045

Permeability of Dust Cores—Friedlaender. (*See* 3163.)

621.318.371.011.2/.4 3046

Q of Solenoid Coils—M. V. Callendar. (*Wireless Eng.*, vol. 24, p. 185; June, 1947.) Within the limits of Medhurst's data (1694 of July) $Q=0.15\sqrt{f}/(1/R+1/l)$ is accurate within a few per cent provided $l>R$.

621.318.572:621.396.615.015.33 3047

Electronic Switch for the Production of Pulses—C. R. Smitley and R. E. Graber. (*Electronics*, vol. 20, pp. 128–130; April, 1947.) A circuit providing variable pulse length and rate, variable delay of synchronizing pip and means for introducing a steady-state signal upon which pulses may be superimposed, in a laboratory generator.

621.38:534.42 3048

A Method for Changing the Frequency of a Complex Wave—E. L. Kent. (*Proc. Nat. Electronics Conference* (Chicago), vol. 2, pp. 329–338.) A method retaining essentially the original wave form. Variants are obtained by different sampling procedures.

621.392.1 3049

On Methods for the Construction of Networks Dual to Non-Planar Networks—A. Bloch. (*Proc. Phys. Soc.*, vol. 58, pp. 677–694; November, 1946.) A network having a non-planar circuit diagram (i.e., one with crossings between some of its branches) cannot be converted into its dual counterpart directly, but must first be converted to an equivalent planar network. The paper describes a number of methods for determining the equivalent planar network.

621.395.661 3050

Mica Capacitors for Carrier Telephone Systems—A. J. Christopher and J. A. Kater. (*Trans. A.I.E.E.*, (*Elec. Eng.*, December Supplement, 1946), vol. 65, pp. 1116–1117.) Discussion on 374 of March.

621.396.611.4+621.385.1 3051

F.M./TV P-A Tube and Grounded-Grid Cavity Cicruit—Wells and Reed. (*See* 3337.)

621.396.615 3052

Non-Linear Regenerative Circuits—D. G. Tucker. (*Wireless Eng.*, vol. 24, pp. 178–184; June, 1947.) Analysis and curves for the frequency and amplitude discrimination of the synchronized oscillator with an unwanted signal mixed with the injected locking tone. Some discrimination occurs over the whole frequency range, and within limits a relatively pure tone can be obtained from a signal having other frequencies mixed with it that cannot be separated by ordinary frequency-selective circuits.

The experimental results of Byard and Eccles (750 of 1941) are shown to be consistent with the theory given.

621.396.615:371.66 3053

A Demonstration Valve Oscillator—E. Bradshaw. (*Electronic Eng.*, vol. 19, pp. 162–163; May, 1947.) Meters in all parts of the circuit facilitate study of operating conditions of tuned-anode oscillator.

621.396.615.015.33+621.396.619.16 3054

Some Notes on Pulse Technique—M. M. Levy. (*Jour. Brit. I.R.E.*, vol. 7, pp. 99–116; May and June, 1947.) The transmission of pulses through ideal filters and delay lines is discussed in detail and practical formulas are given for the design of delay networks. The use of pulsed tubes is considered together with methods of obtaining high efficiency in practical circuits for power pulse generators. Pulse modulation and demodulation processes are studied, with particular reference to the choice of conveniently shaped pulses, in order to simplify the circuit design and eliminate harmonic distortion.

621.396.615.12:621.396.619.13 3055

Frequency Modulation of High-Frequency Power Oscillators—W. R. Rambo. (*Proc. Nat. Electronics Conference* (Chicago), vol. 2, pp. 577–585.) An account with particular reference to common-grid reactance-tube circuits and to class-C operation of reactance tubes.

621.396.615.14 3056

Study of a V.H.F. Oscillator—L. Liot. (*Télév. Franç.*, no. 24, Supplement *Électronique*, pp. 11–14; April, 1947.) A detailed description of a symmetrical arrangement using two 955 tubes with λ/4 feeding lines the anodes and between the cathodes and earth. Short-circuiting bars across these lines give wavelength adjustment from 0.7 m. to 2 m.

621.396.615.142:621.396.621.54:621.396.96 3057

Reflex Oscillators for Radar Systems—J. O. McNally and W. G. Shepherd. (*Proc. Nat. Electronics Conference* (Chicago), vol. 2, p. 157.) Summary only. Design problems for oscillators for military radar receivers.

621.396.615.142.2 3058

Design of Wide-Range Coaxial-Cavity Oscillators Using Reflex Klystron Tubes in the 1000 to 11,000 Megacycle Frequency Region—J. W. Kearney. (*Proc. Nat. Electronics Conference* (Chicago), vol. 2, pp. 624–636.) The design of an external-resonator type of reflex klystron oscillator, for use in standard signal generators and superheterodyne receivers. The tuning range is about 2:1 in frequency. Details of operation, and methods of adaptation of present day tubes for use as coaxial resonators are given. Design characteristics are outlined for (a) optimum cavity dimensions, (b) suitable contacts to the tubes, (c) noncontact, short circuiting tuning plungers, (d) output coupling devices. The factors involved in the choice of cavity and repeller modes, and precautions for the suppression of interference from undesirable modes, are discussed in some detail.

621.396.619 3059

Selective Demodulation—D. B. Harris. (Proc. I.R.E., vol. 35, pp. 565–572; June, 1947. When an amplitude-modulated carrier f, together with other modulated carriers on frequencies harmonically related to f, is multiplied by the instantaneous value of a plain carrier whose frequency and phase are identical with f, only the modulation component of f appears in the output. The modulation components of two carriers in phase quadrature on the same frequency may be separated similarly. A suitable linear multiplicative pentagrid demodulator is described. The advantages and disadvantages of a system using these principles for multichannel carrier working are discussed, and a design for a hypothetical 8-channel system is outlined.

621.396.622 3060

F. M. Detector Systems—B. D. Loughlin. (*Communications*, vol. 27, p. 18; March, 1947.) Summary of 1947 I.R.E. Convention paper.

621.396.622 3061

A New Detector for Frequency Modulation—Bradley. (*See* 3264.)

621.396/.397].645 3062

Bandwidth and Speed of Build-Up as Performance Criteria for Pulse and Television Amplifiers—D. G. Tucker. (*Jour. I.E.E.* (London), Part III, vol. 94, pp. 218–226; May, 1947.) "A comparison is made of the two main methods of describing the performance of pulse and television amplifiers, namely bandwidth, and speed of build-up of a suddenly applied signal. It is shown for a variety of circuit arrangements (including asymmetrical circuits) that equal speeds of build-up based on the slope of the build-up curve at half the steady-state amplitude correspond fairly closely to equal bandwidths measured between the points at which the response is 3 db below that at the applied frequency. It is therefore concluded that either of these criteria would be satisfactory in practice, since they are mutually consistent. Other methods of defining the speed of build-up are discussed, and the main inconsistency is shown to be that, for only one or two stages, but not for larger numbers, the use of the maximum slope of the build-up curve gives misleading results."

621.396.645 3063

Stabilised Amplifiers—J. J. Zaalberg van Zelst. (*Philips Tech. Rev.*, vol. 9, pp. 25–32; January, 1947.) Two groups of circuits are discussed. The first adds a compensating quantity to the input or output signal of the main amplifier and uses either a negative feedback circuit or an auxiliary amplifier. The second group uses an auxiliary alternating voltage, generated either outside or inside the amplifier and passed through the same circuit as the main signal to keep the slope of the amplifying tube constant.

621.396.645 3064

Input Admittance of Cathode-Follower Amplifiers—H. J. Reich. (Proc. I.R.E., vol. 35, pp. 573–576; June, 1947.) General expressions are derived, taking the tube interelectrode capacitances into account, and curves of conductance and susceptance for typical tube constants are given. It is shown that capacitance across the cathode load resistance can produce a negative input conductance, and oscillations may result. Means of preventing such oscillations are discussed.

621.396.645:518.3 3065

Exact Design and Analysis of Double- and Triple-Tuned Band-Pass Amplifiers—M. Dishal. (Proc. I.R.E., vol. 35, pp. 606–626; June, 1947.) Nomograms for designing double and triple-tuned coupled circuits to achieve desired band-pass, gain, skirt-rejection, and phase-change characteristics are developed from conventional theory. Both inductive and capacitance coupling are considered. The work is extended to cover multistage band-pass amplifiers.

621.396.645:518.4 3066

A Graphical Analysis of the Cathode-Coupled Amplifier—M. S. Rifkin. (*Communications*, vol. 26, pp. 16, 43; December, 1946.)

621.396.645.029.6+621.396.621.54.029.6 3067

Gain and Sensitivity of Amplifier and Frequency-Changer Stages for Metre and Decimetre Waves—M. J. O. Strutt. (*Onde Élec.*, vol. 27, pp. 184–193; May, 1947.) Methods are given for estimating the optimum gain for both narrow and wide-frequency bands. For narrow bandwidths the optimum gain is equal to the square of the effective slope divided by the product of the effective input and output admittances. For wide bands the admittance product must be replaced by that of the input and output capacitances. The power gain of amplifiers with grid coupling is treated in detail. Three important properties of the noise factor are stated; these form a basis for applications which enable the noise factor to be reduced considerably, especially in the case of grid-coupling stages and multigrid frequency changers.

621.396/.397].645.029.62 3068

Wide-Band I.F. Amplifier Above 100 Mc/s—M. T. Lebenbaum. (*Communications*, vol. 26, pp. 25, 50; December, 1946.) Summary of Rochester Fall Meeting paper. A brief outline of the general features and design considerations. The advantages of staggered tuning and the effect of grid-anode capacitance are discussed. For the full paper see *Electronics*, vol. 20, pp. 138–149; April, 1947.

621.396.645.029.62 3069

A Compact Lightweight Amplifier for Radar—P. L. Hammann. (*Bell Lab. Rec.*, vol. 25, pp. 146–149; April, 1947.) Design and construction details of the 6AK5 amplifier used in AN/APS-4 radar equipment and in the Bat radar-directed bomb.

621.396.645.029.62.076.2 3070

A Permeability-Tuned 100-Mc/s Amplifier of Specialized Coil Design—Z. Benin. (*Proc. Nat. Electronics Conference* (Chicago), vol. 2, pp. 548–556.) Suitable spacing of coil turns and choice of core and coil lengths reduces frequency drift and makes trimmer capacitors unnecessary.

621.396.645.371.029.4 3071

The Parallel-T Bridge Amplifier—A. B. Hillan. (*Jour. I.E.E.* (London), Part I, vol. 94, pp. 188–189; April, 1947.) Summary of 2051 of August.

621.396.662 3072

The Design of Band-Spread Tuned Circuits for Broadcast Receivers—D. H. Hughes. (*Jour. I.E.E.* (London), Part III, vol. 94, p. 227; May, 1947.) Discussion on 1803 of 1946.

621.396.662.2:621.397.62 3073

Variable Inductance Tuning for TV Receivers—M. F. Melvin. (*Communications*, vol. 27, pp. 48–49, 63; April, 1947.) Description of a 3-gang tuning unit and its application in a television receiver covering the frequency range 44 to 216 Mc. Methods of adjusting the design to provide tracking and suitable bandwidths are described.

621.396.662.3 3074

The Design of Resonant Filters—S. Y. White. (*Tele-Tech*, vol. 6, pp. 56–57; June, 1947.) Discussion of pendulum analogy results in tuned filter with rapid rise, immunity from shock excitation and complete cutoff at 7 per cent off resonance.

621.396.662.3:534.12 3075

Compact Electromechanical Filter—R. Adler. (*Electronics*, vol. 20, pp. 100–105; April, 1947.) The design and performance of a transmission-line type of filter consisting of a number of steel plates interconnected by steel wires. A model for a 455-kc. i.f. channel is described.

621.396.662.34:621.396.645.37 3076
RC Bandpass Filter Design—J. L. Bowers. (*Electronics*, vol. 20, pp. 131–133; April, 1947.) Design curves and applications to l.f. filters of a parallel-T RC network, used as the feed-back loop in an amplifier to give narrow band-pass characteristics similar to those of an LC circuit.

621.396.69+621.317.7+621.38 3077
The Physical Society's Exhibition—(*Electronics Eng.*, vol. 19, pp. 195–198; June, 1947.) See also 2494 of September.

621.396.69+621.317.7 3078
The R.C.M.F. [Radio Component Manufacturers' Federation] Exhibition—(*Electronics Eng.*, vol. 19, pp. 164–165; May, 1947.) A further selection of exhibits. See also 2376 of September.

621.396.69 3079
Electronic Wiring Techniques—C. Brunetti. (*Communications*, vol. 27, p. 16; March, 1947.) Summary of 1947 I.R.E. Convention paper.

621.396.69 3080
Evolution of Printed Circuits for Miniature Tubes—A. F. Murray. (*Tele-Tech*, vol. 6, pp. 58–61, 112; June, 1947.)

621.396.69 3081
Materials and Techniques for Printed Electrical Circuits—Rose. (*See* 3164.)

621.396.69:669.228 3082
New Types of Silver Coatings—Hopf. (*See* 3166.)

621.396.96:531.76 3083
Timer for Radar Echoes—L. A. Meacham. (*Bell Lab. Rec.*, vol. 25, pp. 231–236; June 1947.) A range measuring unit for radar systems which use irregularly spaced pulses. Each transmitted pulse initiates a sine wave reaching steady state immediately. This is passed through a continuously variable phase shifter and is formed into pulses, one of which is selected as a marker. By means of the phase shifter control, which is calibrated in distance, the marker can be continuously moved over the radar display.

GENERAL PHYSICS

531.18:531.15 3084
Absolute Rotation and a Rotating Magnet—Chang-Pen Hsü. (*Wireless Eng.*, vol. 24, pp. 185–187; June, 1947.) Comment on 3564 of 1946 (G.W.O.H.); see also 2727 of September (Stedman) and back reference. Einstein's principle of equivalence, properly applied for any particular instant, gives a simple explanation of so-called "absolute rotation." The electromagnetic reaction upon a rotating magnet and the resultant electric field distribution in it can then be obtained from Maxwell's equations modified for the relativity effect.

537.291:621.385.833 3085
Oil-Drop Method for Electron Trajectories—L. Jacob. (*Nature* (London), vol. 159, pp. 475–476; April 5, 1947.) Visual study of trajectories in air at atmospheric pressure of charged oil drops falling undergravity through enlarged model of electrostatic electron lens.

537.311.33 3086
Surface States and Rectification at a Metal Semi-Conductor Contact—J. Bardeen. (*Phys. Rev.*, vol. 71, pp. 717–727; May 15, 1947.)

537.312.62 3087
Super-Conductivity—E. Schroter. (*Metal Ind.* (London), vol. 70, pp. 444–445; June 13, 1947.) A review of recent researches, abstracted from "Zentralblatt für die Österr Industrie und Technik," discussing (a) the critical temperatures of pure metals, alloys, and certain metallic compounds such as nitrides, carbides, etc., (b) the transition from normal conductivity to superconductivity and (c) the effects produced in superconducting materials by the application of a magnetic field. A result of practical importance has been the discovery of materials with critical temperatures in the region of the temperature of boiling hydrogen. Further research may reveal substances with critical temperatures easily attained.

537.312.62 3088
The Magnetic Quenching of Superconductivity—J. W. Stout. (*Phys. Rev.*, vol. 71, p. 741; May 15, 1947.)

537.523.3 3089
The Mechanism of the Negative Point Corona at Atmospheric Pressure in Relation to the First Townsend Coefficient—L. B. Loeb. (*Phys. Rev.*, vol. 71, pp. 712–714; May 15, 1947.)

537.525:621.3.015.5.027.7 3090
The Insulation of High Voltages in Vacuum—J. G. Trump and R. J. Van de Graaff. (*Jour. Appl. Phys.*, vol. 18, pp. 327–332; March, 1947.) A description of research into the mechanism of electrical breakdown in vacuum for voltages from 50 kv to 700 kv. Results are given graphically supporting a theory of breakdown at these voltages due to secondary emission. See also 3545 of 1946.

538.3 3091
The Experimental Basis of Electro-Magnetism: The Direct-Current Circuit—N. R. Campbell and L. Hartshorn. (*Proc. Phys. Soc.*, vol. 58, pp. 634–653; November 1, 1946.) The first part of an investigation of the extent to which the working principles of electromagnetism can be soundly based on real experimental facts as distinct from imaginary experiments such as those involving point charges and unit magnetic poles.

The general principles of measurement are outlined. Current, resistance, conductance, and voltage are then established independently of a knowledge of any other magnitudes. Ohm's Law and the conception of e.m.f. follow. An examination of the relations between these magnitudes and geometrical and mechanical magnitudes leads to the consideration of Ampère's two laws. See also 3092 below.

538.3 3092
The Experimental Basis of Electromagnetism—G.W.O.H. (*Wireless Eng.*, vol. 24, pp. 161–162; June, 1947.)
Editorial discussion of 3091 above.

538.52:537.123 3093
On a New Electromagnetic Induction Effect Due to Negative Ions—T. V. Ionescu and V. P. Mihu [Mihul]. (*Compt. Rend. Acad. Sci.* (Paris), vol. 224, pp. 1349–1351; May 12, 1947.) If a Geissler tube is placed within a coil forming part of an oscillatory circuit, the intensity of the current through the coil varies with the intensity of the tube current. A detailed study of this effect is described. In general an absorption of energy occurs in the discharge tube, but for certain frequencies the resonator current is much greater with the discharge than without it.

538.56:[621.396.615.142+621.392.029.64 3094
Generalized Boundary Conditions in Electromagnetic Theory—S. A. Schelkunoff. (*Proc. Nat. Electronics Conference* (Chicago), vol. 2, pp. 317–322.) Generalization of the conception of an idealized perfectly conducting boundary, and its application to wave guides, magnetrons, and velocity-modulation tubes. The generalized condition is that E_t/H_t is constant, E_t and H_t being the tangential components of the electric and magnetic vectors at a given surface. The condition may be extended to distinguish between isotropic and anisotropic boundaries, and the ratio E_t/H_t may be a given function of position on the boundary.

538.566.2:517.94 3095
Two Notes on Phase-Integral Methods—W. H. Furry. (*Phys. Rev.*, vol. 71, pp. 360–371; March 15, 1947.) In the first note, entitled "A New Derivation of the Connection Formulas," proof is based only on the fact that actual solutions of the differential equation must be single-valued. The results serve to establish the validity of Eckersley's phase-integral method for the treatment of problems of wave propagation. The second note, entitled "Normalization of Approximate Wave Functions of the Anharmonic Oscillator," discusses the accuracy of the usual asymptotic formula for the normalization factor for the lowest quantum states of the oscillator.

538.569.4.029.64:546.171.1 3096
Inversion Spectrum of Ammonia—M. W. P. Strandberg, T. Kyhl, T. Wentink, Jr., and R. E. Hillger. (*Phys. Rev.*, vol. 71, p. 326; March 1, 1947.) Measurements of the frequencies of some of the lines have been made to an accuracy of ±50 kc. A formula for these frequencies in terms of rotational angular momenta is discussed. See also 1399 of June (Townes) and back references, and 3097 below.

538.569.4.029.64:546.171.1 3097
Microwave Absorption Frequencies of $N_{14}H_3$ and $N_{15}H_3$—W. E. Good and D. K. Coles. (*Phys. Rev.*, vol. 71, pp. 383–384; March 15, 1947.) Measurements of the frequencies of some of the lines to an accuracy of ±20 kc. See also 3096 above.

538.569.4.029.64:546.21 3098
The Absorption of Microwaves by Oxygen—J. H. Van Vleck. (*Phys. Rev.*, vol. 71, pp. 413-424; April 1, 1947.) A theoretical paper in which the features of the oxygen absorption spectrum at millimeter and centimeter wavelengths are derived and compared with existing experimental data. The absorption is caused by the interaction of the magnetic moment of O_2 with electromagnetic fields, and is most pronounced at a wavelength of about 5 mm. where it exceeds 10 db per kilometer. The theoretical dependence of absorption on pressure is considered.

538.569.4.029.64:[546.212+546.212.02 3099
Expected Microwave Absorption Coefficients of Water and Related Molecules—G. W. King, R. M. Hainer, and P. C. Cross. (*Phys. Rev.*, vol. 71, pp. 433–443; April 1, 1947.) A theoretical paper. The predicted positions and strengths of the absorption lines at centimeter and millimeter wavelengths are tabulated for H_2O, D_2O, HDO, H_2S, and H_2Se, and, where possible, compared with experimental data. It is pointed out that HDS and HDSe will also have many absorption lines in this wavelength region. See also 3100 below.

538.569.4.029.64:546.212 3100
The Absorption of Microwaves by Uncondensed Water Vapor—J. H. Van Vleck. (*Phys. Rev.*, vol. 71, pp. 425–433; April 1, 1947.) A theoretical paper in which the characteristics of the absorption spectrum at centimeter and millimeter wavelengths are computed and compared with existing experimental data. Agreement is generally satisfactory and the comparison yields precise information concerning the wavelength and breadth of the absorption line at about 1.35 centimeters (attenuation 0.2 db/km. per gm./$m.^3$). The predicted attenuation "due to the combined effect of all the other lines whose wavelengths are too short for resonance" is about a quarter of the observed value; possible explanations of this discrepancy are discussed. See also 3099 above.

GEOPHYSICAL AND EXTRATERRESTRIAL PHENOMENA

523.53:621.396.11 3101

Meteor Detection by Amateur Radio—O. G. Villard, Jr. (*QST*, vol. 31, pp. 13–18; July, 1947.) A general explanation of the effect of meteors on radio propagation, and an account of experimental equipment used for their detection.

523.7+550.385]"1946.10.12" 3102

Solar and Magnetic Data, October to December, 1946, Mount Wilson Observatory—S. B. Nicholson and E. S. Mulders. (*Terr. Mag. Atmo. Elec.*, vol. 52, pp. 65–66; March, 1947.)

523.72+523.32]:621.396.822.029.64 3103

Microwave Radiation from the Sun and Moon—R. H. Dicke and R. Beringer (*Astrophys. Jour.*, vol. 103, pp. 375–376; May, 1946.) Measurement of thermal radiation at 1.25 centimeters; half-power beam width of 18-inch parabolic reflector was 2 degrees and measured gain 6000 times that of isotropic radiator. Size of sun's disk at 1.25 centimeters found to be nearly similar to that at optical wavelengths; effective black-body temperature of sun and moon found to be about 1.1×10^4 and 292 degrees K respectively.

523.72:621.396.822 3104

Origin of Solar 'Static'—C. E. R. Bruce. (*Nature* (London), vol. 159, p. 580; April 26, 1947.) Comment on 2088 of August (Martyn). Suggestion that "discharges occur in the radial electric field set up by the emission of highly charged atoms from nuclear reactions in the sun's interior."

523.74:551.593.9 3105

Relations Between Solar Activity and the Luminescence of the Earth's Upper Atmosphere—J. Cabannes, J. Dufay, and Tcheng Mao-Lin. (*Compt. Rend. Acad. Sci.* (Paris), vol. 224, pp. 1393–1395; May 19, 1937.)

523.746 "1946.10/.12" 3106

Provisional Sunspot-Numbers for October to December, 1946—M. Waldmeier. (*Terr. Mag. Atmo. Elec.*, vol. 52, p. 14; March, 1947.)

523.746 "1947.03/.04" 3107

Solar Notes—H.W.N. (*Observatory*, vol. 67, p. 74; April, 1947.) Two sunspots occurred in March and April, 1947, without associated magnetic storms. The April spot was the largest ever recorded.

523.78"1945.07.02":621.396.822.029.64 3108

Radio Noise from the Sun at 3.2 cm—K. F. Sander. (*Nature* (London), vol. 159, pp. 506–507; April 12, 1947. Comment on 716 of April (Martyn). Observations during the partial eclipse of July 2, 1945, indicate that the noise mainly emanates from the solar circumference and has a value of 4×10^{-18} watts per square centimeter per Mc.

523.78"1947.05.20":551.510.535 3109

To the Question of the Coefficient of the Ionosphere's Recombination and the Determination of Its Quantity at the Time of the Eclipse on the 20th of May 1947 in Brazil—J. L. Alpert and A. A. Einberg. (*Bull. Acad. Sci.* (U.R.S.S.), *sér. géogr. géophys.*, vol. 11, no. 2, pp. 137–140; 1947. In Russian with English summary.) Measurements at Tromse during the eclipse of June 9, 1945, gave for the effective recombination coefficient of the E layer: $\alpha E = 4.65 \times 10^{-9}$ and for the F_1 layer: $\alpha F_1 = 6.9 \times 10^{-9}$. The changes of ionization to be expected during the 1947 eclipse are calculated.

537.591 3110

Cosmic-Ray Research in B-29 Laboratory Determines Nature of Secondary Particles—G. Grosvenor. (*Terr. Mag. Atmos. Elec.*, vol. 52, pp. 84–87; March, 1947.) Proof that a large proportion of mesotrons are produced by electrically-charged particles.

537.591 3111

The Mass of the Mesotron as Determined by Cosmic-Ray Measurements—D. J. Hughes. (*Phys. Rev.*, vol. 71, pp. 387–392; April 1, 1947.) "The great majority of the results are statistically reconcilable with a single mass."

538.12:521.15 3112

The Magnetic Field of Massive Rotating Bodies—P. M. S. Blackett. (*Nature* (London), vol. 159, pp. 658–666; May 17, 1947.) It is known that the magnetic moment and the angular momentum of the earth and sun are nearly proportional and that the constant of proportionality is nearly the square root of the gravitational constant divided by the velocity of light. The author points out that recent measurements of the magnetic moment of a star are in agreement with this relationship and that since its validity has been demonstrated over such a wide range of values of the parameters it should be given further consideration as a possible general law of nature. A review of previous theories of the magnetic field of the earth and sun is followed by a discussion of the application of the above relationship and of the possibilities of further measurements both for stars and in the laboratory.

550.38"1884/1889" 3113

Daily International Magnetic Character-Figures, C, for the Years 1884 to 1889—J. Bartels. (*Terr. Mag. Atmo. Elec.*, vol. 52, pp. 33–38; March, 1947.)

550.38"1945" 3114

Mean K-Indices from Thirty Magnetic Observatories and Preliminary International Character-Figures, *C*, for 1945—W. E. Scott. (*Terr. Mag. Atmo. Elec.*, vol. 52, pp. 25–31; March, 1947.)

550.38"1946.04/.06" 3115

Five International Quiet and Disturbed Days for April to June, 1946—W. E. Scott. (*Terr. Mag. Atmo. Elec.*, vol. 52, p. 87; March, 1947.)

550.38"1946.10/.12" 3116

American Magnetic Character-Figure, C_A, Three-Hour-Range Indices, K, and Mean K-Indices, K_A, for October to December, 1946, and Summary for Year 1946—W. E. Scott. (*Terr. Mag. Atmo. Elec.*, vol. 52, pp. 15–24; March, 1947.) See also 1770 of July.

550.385:523.755"1942.08/1944.07" 3117

The Correlation of Magnetic Disturbances with Intense Emission Regions of the Solar Corona—A. H. Shapley and W. O. Roberts. (*Astrophys. Jour.*, vol. 103, pp. 257–274; May, 1946.) Observations during 1942–1944 show that magnetic disturbance occurred when intense emission regions of the corona were situated in the eastern hemisphere of the solar disk.

550.385:621.396.11 3118

Effect of Magnetic Perturbations on the Velocity of Short Radio Waves—Stoyko. (*See* 3251.)

551.5:621.396.9 3119

Recent Developments in Meteorological Equipment—A. F. Spilhaus. (*Bull. Amer. Met. Soc.*, vol. 27, pp. 399–409; September, 1946.) A review of wartime developments in electronics and other equipment for use both in aircraft and on the ground.

551.510.535 3120

The Ionosphere—(*Observatory*, vol. 67, pp. 51–53; April, 1947.) Sir Edward Appleton, introducing a geophysical discussion, pointed out that though the general structure of the ionosphere is well known, anomalies occur, especially in the F_2 layer with its winter ionization maximum and dependence on magnetic dip (see 2898 of 1946). A. H. Mumford described transatlantic experiments on the reciprocity of long-distance transmission, and H. L. Kirke experiments on lateral deviation between London and New Delhi. J. W. Cox described work by the Interservice Ionosphere Bureau on possible ways of using existing knowledge. J. S. Hey considered radiations associated with solar disturbances at wavelengths between 1.5 and 15 meters. "Scatter bursts" were discussed; they occur at a height of about 95 km. and are believed to originate from meteors. Finally, H. S. W. Massey considered the processes by which the ionospheric layers are formed.

551.510.535 3121

Ionospheric Studies in South Africa: Telecommunications Research Laboratory Ionospheric Sounder—T. L. Wadley. (*Terr. Mag. Atmo. Elec.*, vol. 52, pp. 67–69; March, 1947.) A description of the ionospheric recorder in use at Johannesburg. The instrument covers the frequency range of 2 to 14 Mc. in 8 seconds. The height frequency graph is formed on a long-afterglow c.r. tube and photographed on a single frame of 16 mm. film. The transmitter and receiver are kept in tune by means of a common oscillator, and the r.f. tracking is obtained by cams which operate the tuning capacitors.

551.510.535 3122

Echoes at D-Heights with Special Reference to the Pacific Islands—C. D. Ellyett. (*Terr. Mag. Atmo. Elec.*, vol. 52, pp. 1–13; March, 1947.) Radio echoes obtained from an equivalent height of 50 km. above Pitcairn Island during 1944 and 1945 by the usual vertical-incidence pulse technique are attributed to D-layer reflections. Earlier data are collected and compared with these observations, which are analyzed with respect to frequency range, diurnal and seasonal variations, and echo strength.

551.510.535 3123

Temperature of the Upper Atmosphere—S. L. Seaton. (*Phys. Rev.*, vol. 71, p. 557; April 15, 1947.) Calculations are made of the temperature at various heights for three widely different latitudes. At E-layer heights of about 100 km., high temperatures are to be expected, while the F_1 and F_2 layers at about 200 km. and 350 km. respectively may be at considerably lower temperatures, with a wide variation from night to day.

551.510.535:621.396.11 3124

Equivalent Path and Absorption in an Ionospheric Region—Jaeger. (*See* 3252.)

551.510.535:621.396.11.029.58 3125

Doppler Effect in Propagation—Griffiths. (*See* 3254.)

551.593.5 3126

The Equilibrium of Atmospheric Sodium [Na-Na⁺ and Na-NaO]—D. R. Bates. (*Terr. Mag. Atmo. Elec.*, vol. 52, pp. 71–75; March, 1947.)

551.593.9+[551.510.535:523.7 3127

[Minutes of the] Meeting of the Royal Astronomical Society [14th March] 1947—(*Observatory*, vol. 67, pp. 46–51; April, 1947.) Short papers read and discussed included: The origin of the Night Sky Light, by D. R. Bates, and The Relations between the Ionosphere, Sunspots, and Solar Corona, by K. O. Kiepenheuer (an account by R. d'E. Atkinson).

LOCATION AND AIDS TO NAVIGATION

621.396.663 3128

4-Band Automatic Radio Direction Finder for Transport Planes—R. H. Bailey. (*Radio News*, vol. 37, pp. 68–69, 130; June, 1947.) An account of a new light-weight radio compass covering all normal broadcast transmissions and marine beacons. Improved bearings are obtained because the compass loop is automatically turned to face the incoming signal. High altitude and atmosphere effects are reduced by hermetic sealing of components and eliminating the receiver power pack.

621.396.9:551.5 3129

Applications of Electronics to Meteorology—C. M. Reber (*Bull. Amer. Met. Soc.*, vol. 27, pp. 365–372; September, 1946.) A brief account of the application of radar to the detection of thunderstorms, fronts, and other precipitation areas, and also to the following of free balloons for wind determination. The use of the cathode-ray direction finder to obtain the position of sources of atmospherics is also described.

621.396.9:551.5 3130

Recent Developments in Meteorological Equipment—Spilhaus. (*See* 3119.)

621.396.93 3131

Raydist—A Radio Navigation and Tracking System—C. E. Hastings. (*Tele-Tech*, vol. 6, pp. 30–33, 103; June, 1947.) A portable system depending on the relative phase relationship between c.w. transmitters operating on frequencies of the order of 2 to 15 Mc. Block diagrams show the arrangement of equipment at the master and relay stations for (a) determining the position of a ship or an aeroplane, (b) measuring the distance between two stations, and (c) charting the flight path of a guided missile.

621.396.93:551.594.6 3132

Location of Thunderstorm Centres from Directional Observations of Atmospherics During Sunrise and Sunset—S. R. Khastgir, M. K. Das Gupta, and D. K. Ganguli. (*Nature* (London), vol. 159, pp. 572–573; April 26, 1947.) The time variation of the intensity of atmospherics is in agreement with the theory of Khastgir (1379 of 1943) and enables the difference of the longitudes of the source and receiver to be estimated.

621.396.93:621.396.663 3133

The Design of Electromagnetic Radiogoniometers for Use in Medium-Frequency Direction-Finding—J. H. Moon. (*Jour. I.E.E.* (London), Part I, vol. 94, pp. 185–186; April, 1947.) Summary of 2127 of August.

621.396.932 3134

Radio Aids to Marine Navigation—(*Nature* (London), vol. 159, p. 647; May 10, 1947.) Brief description of the International Meeting, London, May, 1946, during which ship and shore d.f., hyperbolic systems (Loran, Gee, Decca) and radar were discussed. For the complete account see 3135 below.

621.396.932 3135

Radio Aids to Marine Navigation. Vol. 1. Record of the [International] Meeting Held in London [in May 1946] and of Demonstrations and Visits. Vol. 2. Radio Navigation Radar and Position Fixing Systems for Use in Marine Navigation [Book Notice]—H.M. Stationery Office., vol. 1, 2s. 6d. vol. 2, 5s. (*Govt. Publ.* (London), p. 16 and p. 16; November and December, 1946.

621.396.932 3136

Postwar Marine Radar in Great Britain—M. G. Scroggie. (*Communications*, vol. 26, pp. 9–11, 41; December, 1946.) The design of the prototype set developed by the British Admiralty and demonstrated at the International meeting on Radio Aids (3135 above). Choice of frequency, pulse duration, horizontal and vertical beam widths, transmitter power, and performance monitoring are discussed in some detail. New design features include facilities for superimposing the p.p.i. picture upon charts and a monitoring device which indicates voltages at 20 points as vertical lines on the display tube. A safety device automatically cuts out the p.p.i. should the performance of either transmitter or receiver fall below a certain level.

621.396.933 3137

Trends in Air Navigation—H. Davis and L. Lader. (*Communications*, vol. 27, pp. 15–16; March, 1947.) Summary of 1947 I.R.E. Convention paper.

621.396.933 3138

Teleran—D. H. Ewing and R. W. K. Smith. (*RCA Rev.*, vol. 7, pp. 601–621; December, 1946.) A system for air navigation and traffic control using television and radar. See also 3139 below.

621.396.933 3139

Teleran Air Navigation and Traffic Control by Means of Television and Radar—D. H. Ewing and R. W. K. Smith. (*Proc. Nat. Electronics Conference* (Chicago), vol. 2, pp. 299–316.) See also 1546 of 1946 (Herbst *et al.*) and 3138 above.

621.396.933 3140

Navaglobe Long-Range Radio Navigation System—P. R. Adams and R. I. Colin. (*Proc. Nat. Electronics Conference* (Chicago), vol. 2, pp. 288–298.)

621.396.933:629.135 3141

Automatic Radio Flight Control—F. L. Moseley and C. B. Watts. (*Proc. Nat. Electronics Conference* (Chicago), vol. 2, pp. 268–287.) An outline of various radio navigational facilities for automatic aircraft guidance.

621.396.933.029.5/.6 3142

Ground-Air Communications Unit—Meacham. (*See* 3325.)

621.396.933.2 3143

Improvements in 75-Megacycle Aircraft Marker Systems—B. Montgomery. (*Proc. Nat. Electronics Conference* (Chicago), vol. 2, pp. 133–141.)

621.396.96+621.396.93 3144

A Survey of the Development of Radar—R. A. Smith. (*Jour. I.E.E.* (London), Part I, vol. 94, pp. 172–178; April, 1947.)

621.396.96:531.76 3145

Timer for Radar Echoes—Meacham. (*See* 3083.)

621.396.96:621.396.82 3146

Theory of Radar Reflection from Wires or Thin Metallic Strips—Van Vleck, Block, and Hamermesh. (*See* 3035.)

621.396.96:629.135 3147

Radar Eyes for the Black Widow—J. B. Maggio. (*Bell Lab. Rec.*, vol. 25, pp. 221–226; June, 1947.) Describes a night fighter radar system. A dipole rotating in a parabolic mirror scans a 15 degree cone. The mirror searches automatically or can be directed by the radar operator on to a chosen aircraft which it then follows, ignoring aircraft at different ranges. Indication is given to the pilot of range, azimuth, and rate of overtaking.

MATERIALS AND SUBSIDIARY TECHNIQUES

535.37:535.215.9 3148

The Influence of Irradiation with Light on the Dielectric Properties of ZnS Phosphors—W. de Groot. (*Phillips Tech. Rev.*, vol. 8, p. 370; December, 1946.) Brief summary of *Physica* paper. The change in dielectric behavior is probably due to free electrons.

537.312.62:546.883 3149

Magnetic Transition Curves in Superconducting Tantalum.—R. T. Webber. (*Phys. Rev.* vol. 71, p. 471; April 1, 1947.) Summary of American Physical Society paper on the results of measurements made at the temperature of liquid helium with thin wires of pure tantalum in uniform longitudinal magnetic fields. Unannealed wires were used and the effects of annealing and outgassing were also determined. Experiments with pulse magnetic fields are mentioned.

538.221 3150

On the Isothermal Remanent Magnetization of Iron Sesquioxide—J. Roquet. (*Compt. Rend. Acad. Sci.* (Paris), vol. 224, pp. 1418–1420; May 19, 1947.) Measurements on stabilized Fe_2O_3 α to field strengths of 32300 gauss.

538.221 3151

Properties of a Fine-Grain Cubic Ferromagnetic Material—L. Néel. (*Compt. Rend. Acad. Sci.* (Paris), vol. 224, pp. 1488–1490; May 28, 1947.) See also 3152 below. Calculation for spherical grains shows that below a critical diameter of about 300 Å the magnetization is uniform. Powders have been obtained with a grain size of 200 to 300 Å and coercive field as high as 1000 gauss; this field is too large to be satisfactorily explained by magnetocrystalline anisotropy and must probably be attributed to anistropy of grain shape. Discussion of powders consisting of ellipsoids of different eccentricities confirms this view.

538.221 3152

The Coercive Field of a Cubic Ferromagnetic Powder with Anisotropic Grains—L. Néel. (*Compt. Rend. Aacd. Sci.* (Paris), vol. 224, pp. 1550–1551; June 2, 1947.) Abstracted with 3151 above.

538.221:621.317.41.029.62 3153

Ferromagnetism at Very High Frequencies: Part 1—Magnetic Iron at 200 Mc/s—Johnson, Rado, and Maloof. (*See* 3182.)

538.221:621.317.41.029.62 3154

Complex Permeability of Magnetic Iron at 200 Mc/s as a Function of Polarizing Field—Rado, Johnson, and Maloof. (*See* 3183.)

538.245:621.318.323.2 3155

Non-Metallic Magnetic Material for High Frequencies—J. L. Snoek. (*Philips Tech. Rev.*, vol. 8, pp. 353–360; December, 1946.) "Ferrites of the type MFe_2O_4, in which *M* is a bivalent metal, have specific resistance 10^7–10^{12} times that of iron, so that eddy currents are negligible; hysteresis can be made small, while initial permeability is of the order of 1000.

538.3:539.215.2 3156

The Electrical Constants of a Material Loaded with Spherical Particles—L. Lewin. (*Jour. I.E.E.* (London), Part I, vol. 94, p. 186; April, 1947.) Summary of 2139 of July.

538.63:549.289 3157

Hall Effect and Magneto-Resistance in Germanium—W. C. Dunlap, Jr. (*Phys. Rev.*, vol. 71, p. 471; April 1, 1947.) Summary of American Physical Society paper on the results of measurements made with polycrystalline and single-crystal specimens. "The magneto-resistance effect in germanium appears to be at least an order of magnitude larger than is expected from the free electron theory for semiconductors."

546.431.284:621.385.1.032.216 3158

A Study of the Barium Silicate Interface of Oxide Coated Cathodes—A. Eisenstein. (*Phys. Rev.*, vol. 71, p. 473; April 1, 1947.) Summary of American Physical Society paper. "The interface compound which is formed in the case of a BaO or (BaSr)O coating on a Si-Ni base is believed to be Ba_2SiO_4 rather than $BaSiO_3$. . . . " The relation of the compound to an anomalous voltage at the interface region (thickness from 5×10^{-4} to 10^{-3} cm.) has been examined.

620.19"19/20" 3159

Corrosion Processes—U. R. Evans. (*Metal Ind.* (London), vol. 70, pp. 335–337 and 355–357; May 9 and 16, 1947.) A survey, covering the last hundred years, of the British contribution to the understanding of metallic corrosion. A bibliography of 78 items is included.

621.315.615.2 3160

The Influence of the Concentration and Mobility of Ions on Dielectric Loss of Insulating Oils—B. P. Kang. (*Trans. A.I.E.E.* (*Elec. Eng.*, December Supplement, 1946.) vol. 65, p. 1132.) Discussion on 443 of March.

621.315.616.018.14 3161

A Note on the Effect of Combined Carbon Monoxide on the Power Factor of Polythene—W. Jackson and T. S. A. Forsyth. (*Jour. I.E.E.* (London), Part I, vol. 94, p. 187; April, 1947.) Summary of 2145 of August.

621.318.322:[621.314.2.029.4/.5 3162

Use of Thin Permalloy Tape in H.F. Transformers—(*Tech. Mod.*, vol. 39, pp. 68–69; February 1 and 15, 1947. In French.) Summary of 2225 of 1946 (Ganz).

621.318.323.2.042.15 3163

Permeability of Dust Cores—E. R. Friedlaender. (*Wireless Eng.*, vol. 24, pp. 187–188; June, 1947.) The observed increase of permeability may be explained by the assumption of irregular shaped particles and uneven distribution of air pockets. See also 1692 and 1693 of July.

621.396.69 3164

Materials and Techniques for Printed Electrical Circuits—K. Rose. (*Materials and Methods*, vol. 25, pp. 73–76; March, 1947.) A war time development having many post-war applications whereby electrical components and circuit connections are produced as metallic and carbonaceous deposits on a ceramic plate thus enabling overall size of an instrument to be reduced while its mechanical stability is increased. See also 1913 of July.

669.14–41:538.221:621.314.1/.2 3165

Magnetic Sheet Steel—D. Edmundson. (*Jour. I.E.E.* (London), Part I, vol. 94, pp. 180–182; April, 1947.) An account of recent American improvements in both quality and production technique, special attention being given to heat treatment, cold rolling, and subsequent reannealing.

669.228:621.396.69 3166

New Types of Silver Coatings—P. P. Hopf. (*Electronic Eng.*, vol. 19, p. 193–194, 198; June, 1947.) A colloid containing up to 70 per cent of metallic silver and containing no organic matter may be used in an offset printing press for depositing circuits such as spiral aerials and can facilitate the manufacture of silvered polythene capacitors by h.f. eddy current heating methods.

678.1:537.226 3167

Dielectric Properties of Rubber—Particularly of Loaded Stock—L. V. Holroyd, B. A. Mrowca, and E. Guth. (*Phys. Rev.*, vol. 71, p. 488; April 1, 1947.) Summary of American Physical Society paper.

678.1:621.3.011.2 3168

The Electrical Resistivity of Conducting Rubber—P. E. Wack. (*Phys. Rev.*, vol. 71, p. 489; April 1, 1947.) Summary of American Physical Society paper.

679.5 3169

Fugitive Fluorine Works for Industry—H. C. E. Johnson. (*Sci. Amer.*, vol. 176, pp. 60–62; February, 1947.) Short descriptions of commercial methods for the production of fluorine and some of its compounds. These include a new plastic called "Teflon" which is a polymer of tetrafluorethylene, is stable and tough from −75 degrees to 250 degrees centigrade, is not attacked by any chemical except molten alkali metals and has excellent electrical properties. See also 1121 of May.

679.5:537.226 3170

Some Dielectric Properties of Butadiene-Containing Polymers and Copolymers—R. F. Boyer, E. B. Baker, and P. C. Woodland. (*Phys. Rev.*, vol. 71, p. 488; April 1, 1947.) Summary of American Physical Society paper.

MATHEMATICS

517.54:621.385.1 3171

Conformal Transformations in Orthogonal Reference Systems—C. S. Roys. (*Proc. Nat. Electronics Conference* (Chicago), vol. 2, pp. 323–328.) General equations are derived for transformations which correspond to the Cauchy-Riemann equations for Cartesian coordinates; these are applied to shielding and tube problems involving recurrent structures.

518.5 3172

The Mechanical-Transients Analyzer—G. D. McCann. (*Proc. Nat. Electronics Conference* (Chicago), vol. 2, pp. 372–392.) An electric analogue computer for the solution of complex algebraic and differential equations. It is designed primarily for the analysis of mechanical vibration problems and servomechanisms.

519.28:621.3 3173

A New Approach to Probability Problems in Electrical Engineering—H. A. Adler and K. W. Miller. (*Trans. A.I.E.E.* (*Elec. Eng.*, December Supplement, 1946.) vol. 65, pp. 1118–1119.) Discussion on 465 of March.

517.512.4(083.5) 3174

Tables of Spherical Bessel Functions, Vol. 1 [Book Review]—Mathematical Tables Project, National Bureau of Standards. Columbia University Press, New York, 1947, 378 pp., $7.50. (*Gen. Elec. Rev.*, vol. 50, p. 60; May, 1947.) The Introduction summarizes their properties, expresses the Fresnel integrals in terms of them, and describes methods of computation. The present tables, with their great scope and accuracy, now make possible the solution of a large number of important problems in a wide variety of fields.

MEASUREMENTS AND TEST GEAR

620.16:621.319.4.011.5 3175

Metallized Capacitor Tests—P. Godley and J. C. Balsbaugh. (*Electronics*, vol. 20, pp. 112–115; April, 1947.)

620.163:621.385 3176

Electrical Production Tests for High-Power Tubes—Sheren. (*See* 3334.)

620.163:621.385 3177

Production Test Facilities for High-Power Tubes—Lyndon. (*See* 3335.)

621.317.32:621.317.755 3178

Measurement of H.T. by Cathode-Ray Tube E.M.I. Laboratories—(*Electronic Eng.*, vol. 19, p. 177; June, 1947.) A special tube is used with two anode systems. The unknown voltage is applied to the second of these and a calibrated lower voltage to the first. The value of this lower voltage for accurate focusing of the beam is a measure of the unknown voltage.

621.317.333+621.317.37]:621.315.212.029.6 3179

The Voltage Characteristics of Polythene Cables—R. Davis, A. E. W. Austen, and W. Jackson. (*Jour. I.E.E.* (London), Part III, vol. 94, pp. 154–165; May, 1947. Discussion, pp. 165–170.) An experimental investigation of breakdown voltage, power factor, life with pulse voltages and discharge characteristics at power frequencies and performance with 600-Mc. r.f. pulse operation. Tentative voltage ratings based on this work are proposed.

621.317.333.027.3 3180

High Voltage D.C. Testing of Rubber-Insulated Wire—W. N. Eddy and W. D. Fenn. (*Trans. A.I.E.E.* (*Elec. Eng.*, December Supplement, 1946.) vol. 65, p. 1126.) Discussion on 3668 of 1946.

621.317.34 3181

Highly-Selective Transmission-Measuring Equipment for Communication Circuits—D. G. Tucker. (*Jour. I.E.E.* (London), Part III, vol. 94, pp. 211–216; May, 1947.) The equipment can be designed to be within a specified degree of accuracy; ±0.25 db is readily obtainable. Basic principles are: (a) direct demodulation of the test signal by means of an identical frequency obtained from an oscillator synchronized to the test tone, (b) discrimination against unwanted line signals obtained by means of low-pass filters, (c) the elimination of the effect of the phase difference between the test and demodulating tones by Barber's two-path method (2697 of October), and (d) the use of an envelope-modulated test signal.

621.317.41.029.62:538.221 3182

Ferrogmagnetism at Very High Frequencies: Part 1—Magnetic Iron at 200 Mc/s—M. H. Johnson, G. T. Rado, and M. Maloof. (*Phys. Rev.*, vol. 71, pp. 322–323; March 1, 1947.) A method of determining the complex permeability by measuring the phase velocity and attenuation in a coaxial line whose center conductor is the metal under investigation. The results at 200 Mc. suggest that magnetization by displacement of domain boundary walls is greatly reduced and magnetization by rotation is the dominant effect.

621.317.41.029.62:538.221 3183

Complex Permeability of Magnetic Iron at 200 Mc/s as a Function of Polarizing Field—G. T. Rado, M. H. Johnson, and M. Maloof. (*Phys. Rev.*, vol. 71, p. 472; April 1, 1947.) Summary of American Physical Society paper. Results obtained by extension of method of 2852 of October.

621.317.44.025 3184

Alternating Current Probe for the Measurement of Magnetic Fields—E. C. Gregg. (*Phys. Rev.*, vol. 71, p. 482; April 1, 1947.) Summary of American Physical Society paper. The probe consisted of a 150-turn primary winding and a 100-turn secondary wound on a 0.1-inch length of Permalloy wire 0.01 inch in diameter. The probe had the dimensions of a cylinder 0.1 inch long and 0.08 inch in diameter. An a.c. null detector method was used, an adjustable d.c. current in the primary serving as a measure of the unknown magnetic field. The accuracy of the probe measurements was about 0.2 per cent.

621.317.7+621.38+621.396.69 3185

The Physical Society's Exhibition—(*Electronic Eng.*, vol. 19, pp. 195–198; June, 1947.) See also 2494 of September.

621.317.7+621.396.69 3186

The R.C.M.F. [Radio Component Manufacturers' Federation] Exhibition—(*See* 3078.)

621.317.7.029.64:621.396.611.4 3187

Cavity Resonators for Measurements with Centimeter Electromagnetic Waves—B. Bleaney, J. H. N. Loubser, and R. P. Penrose. (*Proc. Phys. Soc.*, vol. 59, pp. 185–199; March 1, 1947.) "A wave-meter for wavelengths of about a centimeter, with an accuracy of 1 to 2 parts in 10,000, is described." Measurements at wavelengths of 3.2 and 1.35 centimeters of the dielectric constant and power factor of six nonpolar liquids are described and tabulated.

621.317.72.029.56/.58]:621.392.43 3188
Additional Notes on the "Micromatch"—M. C. Jones and C. Sontheimer. (*QST*, vol. 31, p. 45; July, 1947.) A complete account of the modifications to the original design (2853 of October) to improve the performance at 30 Mc.; details of the revised circuit and components and the best method of assembly are given.

621.317.73.029.63:621.315.212 3189
Comparator for Coaxial Line Adjustments—Woodward. (*See* 3016.)

621.317.733 3190
Measuring Megohms to a Few Parts in a Million—H. T. Wilhelm. (*Bell Lab. Rec.*, vol. 25, pp. 155–158; April, 1947.) Bridge method of measurement used in production to obtain resistance-ratios constant to <100 parts in 10^6 for a range of temperature from -40 degrees to 60 degrees Centigrade.

621.317.755 3191
Trends in Cathode-Ray Oscillograph Design—W. L. Gaines. (*Proc. Nat. Electronics Conference* (Chicago), vol. 2, p. 454.) Summary only.

621.317.755:621.394.813 3192
A Cathode-Ray Telegraph Distortion Measuring Set—W. T. Rea. (*Bell Lab. Rec.*, vol. 25, pp. 150–154; April, 1947.) A portable set with a built-in supply unit. A simplified circuit of diagram is given.

621.317.761:621.165 3193
An Electronic Frequency Meter and Speed Regulator—E. Levin. (*Trans. A.I.E.E.* (*Elec. Eng.*, December Supplement, 1946) vol. 65, pp. 1181–1182.) Discussion on 1148 of May.

621.317.761.029.64 3194
S.H.F. Heterodyne Frequency Meter—C. D. Jeffries. (*Electronics*, vol. 20, pp. 134–137; April, 1947.) Portable instrument for the range 450 to 10,000 Mc. with a maximum error less than 0.05 per cent.

621.317.784:621.3.015.33 3195
The Notch Wattmeter for Low-Level Power Measurement of Microwave Pulses—D. F. Bowman. (*Proc. Nat. Electronics Conference* (Chicago), vol. 2, pp. 361–371.) The r.f. pulse of unknown amplitude is matched in amplitude with an interrupted c.w. signal. The interrupted portion or notch of the c.w. signal is adjusted to equal in length and to coincide in time with the unknown pulse. The amplitude is then measured by a self-balancing thermistor bridge, an instrument which indicates average power, and measures accurately the peak pulse power of the unknown signal. Powers from 20 to 200 μW can be measured within 5 per cent; accuracy is independent of pulse shape, pulse length, repetition rate, and frequency modulation during the pulse.

621.317.79:621.315.212 3196
A Standing-Wave Meter for Coaxial Lines—H. O. Pattison, Jr., R. M. Morris, and J. W. Smith. (*QST*, vol. 31, pp. 41–43; July, 1947.) A full account of the construction and performance, with diagrams and details of circuit and components. The meter is essentially a resistance bridge with R_1 equal to the impedance of the line under test, in this case 52Ω, so that substitution of R_1 is necessary for other cables. A calibration curve is given for the instrument shown, and the method of calibration is described fully.

621.317.79:621.392 3197
The Theory and Design of Several Types of Wave Selectors—Korman. (*See* 3019.)

621.317.79:621.396.611 3198
The Design of a Universal Automatic Circuit Tester and Its Application to Mass-Production Testing—R. C. G. Williams, J. E. Marshall, H. G. T. Bissmire, and J. W. Crawley. (*Jour. I.E.E.* (London), Part I, vol. 94, pp. 194–196; April, 1947.) Summary of 2181 of August.

621.317.79:621.396.615 3199
The Sweep-Frequency Signal Generator—R. Endall. (*Radio News*, vol. 37, pp. 47–50, 114; June, 1947.) A full general description of instruments used for testing i.f. and r.f. circuits and video amplifiers. The frequency response curve is observed visually on an oscilloscope screen.

621.317.79:621.396.615.14 3200
A New Frequency-Modulated Signal Generator—D. M. Hill. (*Communications*, vol. 26, pp. 50–51; December, 1946.) Summary of a Rochester Fall Meeting paper. Covers the range 54 to 216 Mc. and can be used for amplitude or frequency modulation either separately or simultaneously. A circuit diagram is given.

621.317.79.029.62 3201
Standing-Wave Ratio Meter for V.H.F.—G. Glinski. (*Tele-Tech*, vol. 6, pp. 34–35; June, 1947.) A simple directional coupler, consisting essentially of a section of auxiliary transmission line with matched terminations, coupled to the main transmission line. It can also be used as a power meter.

621.317.79.089.6:[621.396.615.12/.14 3202
A Method of Calibrating Standard-Signal Generators and Radio-Frequency Attenuators—G. F. Gainsborough. (*Jour. I.E.E.* (London), Part III, vol. 94, pp. 203–210; May, 1947.) The relative magnitudes of r.f. signals are measured by passing the signals through a linear heterodyne frequency-converter and comparing the magnitudes of the resultant i.f. signals with those of signals from a standard i.f. generator of known performance. Signal ratios up to 10 db can be measured to 0.02 db; greater ratios up to 90 db can be measured to within 0.2 per cent of their decibel values. Signals 16 db below noise can be measured to 0.5 db. The method has been used for frequencies betseen 3 and 3000 Mc. and this range can be extended.

621.396.11+538.566 3203
Velocity of Electromagnetic Waves—Essen. (*See* 3249.)

OTHER APPLICATIONS OF RADIO AND ELECTRONICS

533.5:539.163.2.08:620.191.33 3204
The Mass Spectrometer as an Industrial Tool—A. O. Nier. (*Proc. Nat. Electronics Conference* (Chicago), vol. 2, pp. 190–197). Applications to continuous process gas analysis and to leak detection in high-vacuum systems.

535.33.072.029.63 3205
A Microwave Spectrograph—R. H. Hughes and E. B. Wilson, Jr. (*Phys. Rev.*, vol. 71, pp. 562–563; April 15, 1947.) The basic principle is the use of a r.f. Stark effect field which modulates the absorption by the gas so that a radio receiver can be used for detection purposes.

538.74:621.385.832 3206
Cathode-Ray Compass—R. T. Squier. (*Electronics*, vol. 20, pp. 121–123; April, 1947.) Uses a vertical electron beam in a gimbal-mounted tube with four horizontal quadrantal targets. The action depends on the varying target currents due to the deflection of the beam by the earth's magnetic field.

539.16.08 3207
Velocity of Propagation of the Discharge in Geiger-Müller Counters—E. Wantuch. (*Phys. Rev.*, vol. 71, p. 646; May 1, 1947.) Experimental results support the theory that the positive-ion sheath spreads by photon emission and ionization. Values of the propagation velocity are lower than those found by Huber, Alder, and Baldinger (2867 of October).

539.17:620.93 3208
Some Fundamental Problems of Nuclear Power-Plant Engineering—E. T. P. Neubauer. (*Proc. Nat. Electronics Conference* (Chicago), vol. 2, pp. 673–679.)

621.313.2-9:621.314.653 3209
Large Electronic Direct-Current Motor Drives—M. M. Morack. (*Proc. Nat. Electronics Conference* (Chicago), vol. 2, pp. 212–225.) The use of sealed ignitrons extends electronics drives up to about 600 h.p. where reversing is not required.

621.313.2-9:621.316.721.076.7 3210
Constant-Current Systems for Electronic Control of D.C. Motors—O. W. Livingston. (*Gen. Elec. Rev.*, vol. 50, pp. 38–44; May, 1947.) Adjustment of speed for a wide variety of applications is effectively accomplished through suitable modification of the basic constant-torque system.

621.313.2-9:621.316.721.076.7 3211
Electronic Constant-Current Motor Systems—O. W. Livingston. (*Elec. Eng.* (New York), vol. 66, pp. 432–437; May, 1947.) Constant torque characteristics simplify use for certain applications. As adjustable speed drive, similar characteristics to variable voltage system, with minimum number of power tubes.

621.316.7:621.313.2-9 3212
Basic Procedures in Motor Control: Part 1—D.C. Series Motors—G. W. Heumann. (*Gen. Elec. Rev.*, vol. 50, pp. 23–34; May, 1947. Methods of calculating performance and of selecting types of control for matching motor characteristics to the operating requirements. To be continued.

621.316.718.5.076.7:621.313.3-9 3213
Electric Speed Control of A.C. Motors—W. H. Elliot. (*Proc. Nat. Electronics Conference* (Chicago), vol. 2, pp. 226–238.) A review of basic circuits, with practical applications.

621.317.39:[531.71+531.787 3214
The Pressuregraph—A. Crossley. (*Proc. Nat. Electronics Conference* (Chicago), vol. 2, pp. 352–360.) A compact pickup is used to modulate an h.f. source and transform pressure variation or mechanical motion into a pressure-time or displacement-time graph on a c.r.o.

621.317.39:531.717.1 3215
The Z-Callipers—A. G. Long. (*Electronic Eng.*, vol. 19, p. 187; June, 1947.) Details of a simple instrument for measuring bulb wall thickness in terms of readings of an a.c. milliammeter.

621.317.39:6 3216
Electric Gauges in Quality Control—J. Manuele. (*Elec. Eng.* (New York), vol. 66, pp. 441–444; May, 1947.)

621.317.39:620.178.3 3217
A Modern Vibration Measurement Laboratory: Part 3—Types of Apparatus—A. J. Cogman. (*Electronic Eng.*, vol. 19, pp. 152–156; May, 1947.) D.c. bridge methods of stress measurement using temperature compensation. An a.c. bridge circuit for measuring steady stress by means of a c.r.o. is illustrated. A mobile recording unit includes an amplifier of almost uniform response from 2 cycles to 10 kc. Some preliminary notes are also given on the measurement of h.f. vibrations. For part 4 see 3218 below.

621.317.39:620.178.3 3218
A Modern Vibration Measurement Laboratory: Part 4—Fatigue Testing—D. M. Corke. (*Electronic Eng.*, vol. 19, pp. 189–192; June, 1947.) The test apparatus is arranged as part of a regenerative electromechanical system; instability is reduced by limiting the amplitude and adjusting the phase of the electrical feedback. For part 3 see 3217 above.

621.317.755:535.33 3219

The Cathode-Ray Spectrograph—R. Feldt and C. Berkley. (*Proc. Nat. Electronics Conference* (Chicago), vol. 2, pp. 198–211.) Produces complete spectral distribution curves on a c.r. screen. Applications to color matching, etc., are suggested.

621.317.755:771.36 3220

Cathode-Ray Tube Shutter-Testing Instrument—D. T. R. Dighton and H. McG. Ross. (*Jour. Sci. Instr.*, vol. 24, pp. 128–133; May, 1947.) The apparatus gives, on an after-glow c.r. tube, the characteristic curve of a camera shutter, i.e., the variation with time of the light passing through the shutter. Full details are provided of the various circuits used in the instrument.

621.365.5+621.365.92]:621.316.726.078.3 3221

The Problem of Constant Frequency in Industrial High-Frequency Heating Generators—E. Mittelmann. (*Proc. Nat. Electronics Conference* (Chicago), vol. 2, pp. 503–510.)

621.365.5:621.314.653 3222

Ignitron Converters for Induction Heating—R. J. Ballard and J. L. Boyer. (*Proc. Nat. Electronics Conference* (Chicago), vol. 2, pp. 455–469.) A "cyclo-inverter" circuit converting directly 3-phase 60-cycle power to single-phase power at a higher frequency.

621.365.52 3223

Coreless Induction Furnaces—M. J. Marchbanks. (*Jour. I.E.E.* (London), Part I, vol. 94, pp. 119–120; February, 1947.) Summary of I.E.E. paper. Another account noted in 1987 of 1946.

621.365.92 3224

Heating by Dielectric Losses—G. Gourod. (*Tech. Mod.*, vol. 39, pp. 45–49 and 113–119; February 1, 15 and April 1, 15, 1947. In French.) Formulas and graphical methods are given for finding the h.f. power required to raise a given quantity of a dielectric to a given temperature. Applications to many branches of industry are reviewed.

621.365.92:679.5 3225

Dielectric Preheating in the Plastics Industry—G. F. Leland, D. E. Watts, and T. N. Willcox. (*Proc. Nat. Electronics Conference* (Chicago), vol. 2, pp. 488–502.)

621.365.92.029.64 3226

Microwaves and Their Possible Use in High-Frequency Heating—T. P. Kinn and J. Marcum. (*Proc. Nat. Electronics Conference* (Chicago), vol. 2, pp. 470–487.) Sources of c.w. power for r.f. heating at frequencies from 1500 to 30,000 Mc. are discussed and microwave coaxial transmission line and wave guide technique, including matching methods, described. Possible methods of using waveguides, aerials, and resonators to apply r.f. power to dielectric materials of various shapes are suggested.

621.38:621.9 3227

The Electronic Method of Contouring Control—J. Morgan. (*Proc. Nat. Electronics Conference* (Chicago), vol. 2, pp. 239–249.) See also 207 of February.

621.38:655.324.5 3228

Electronic Register Control for Multicolor Printing—W. D. Cockrell. (*Trans. A.I.E.E.* (*Elec. Eng.*), December Supplement, 1946), vol. 65, pp. 1117–1118.) Discussion on 3697 of 1946.

621.383.001.8 3229

An Electronic Reading Aid for the Blind—V. K. Zworykin and L. E. Flory. (*Proc. Amer. Phil. Soc.*, vol. 91, pp. 139–142; April 5, 1947.) A description of the equipment and a critical account of its application. It is not considered that the apparatus is ready for general use, although after about 60 hours training two blind readers were able to identify letters at random with about 80 per cent accuracy. See also 3700 of 1946.

621.383.5.001.8+[621.383.5:621.318.57 3230

The A.C. Behavior of the Barrier Layer Photo Cell—Sargrove. (*See* 3332.)

621.384.3 3231

Military Application of Infrared Viewers—G. E. Brown. (*Proc. Nat. Electronics Conference* (Chicago), vol. 2, pp. 181–188.)

621.384.6 3232

Optimum Disturbing Field for Synchrotron Beam Ejection—F. K. Goward and J. Dain. (*Nature* (London), vol. 159, pp. 636–637; May, 1947.) Theoretical analysis of the reactive power required to build up the disturbing field and of the conditions that minimize this power.

621.384.6 3233

Nuclear Research With the 100-MeV Betatron—E. E. Charlton and G. C. Baldwin. (*Proc. Nat. Electronics Conference* (Chicago), vol. 2, pp. 650–672.) A description of the General Electric betatron, with experimental results.

621.384.6 3234

Initial Performance of the 184-Inch Cyclotron of the University of California—W. M. Brobeck, E. O. Lawrence, K. R. MacKenzie, E. M. McMillan, R. Serber, D. C. Sewell, K. M. Simpson, and R. L. Thornton. (*Phys. Rev.*, vol. 71, pp. 449–450; April 1, 1947.) A brief description of equipment and experiments by which deuteron and alpha-particle beams, of approximately 200 and 400 Mev respectively, have been produced. The characteristics of the high-power (18 kw input) frequency-modulated h.f. generator are mentioned.

621.384.6 3235

An Accelerator Column for Two to Six Million Volts—R. R. Machlett. (*Proc. Nat. Electronics Conference* (Chicago), vol. 2, pp. 680–687.) Manufacturing techniques for multi-section tubes.

621.385.833 3236

Summarized Proceedings of Conference on the Electron Microscope. Oxford 1946—(*Jour. Sci. Instr.*, vol. 24, pp. 113–119; May, 1947.) Sessions were devoted to: (a) construction, including descriptions of various recent developments and discussion of design principles, (b) the technique of specimen preparation, and (c) special applications.

621.385.833 3237

Proceedings of the Electron Microscope Society of America—(*Jour. Appl. Phys.*, vol. 18, pp. 269–273; March, 1947.) Titles and abstracts of 36 papers presented at the 1946 annual meeting.

621.385.833 3238

On the Limit of Resolution of the Electron Microscope: Round Lens.—H. Bruck. (*Compt. Rend. Acad. Sci.* (Paris), vol. 224, pp. 1553–1555; June 2, 1947.) A discussion of the different values obtained for the limit of resolution in the Gauss plane by use of the superposition formula, that of Born and Glaser and Rayleigh's $\lambda/4$ rule, with graphs and a numerical table.

621.385.833 3239

A Methyl Methacrylate-Silica Replica Technique for Electron Microscopy—A. F. Brown and W. M. Jones. (*Nature* (London), vol. 159, pp. 635–636; May 10, 1947.) A method requiring neither pressure nor high temperature and applicable to many types of material.

621.386.001.8 3240

One-Millionth-Second Radiography and Its Applications—C. M. Slack and D. C. Dickson, Jr. (Proc. I.R.E., vol. 35, pp. 600–606; June, 1947.) Outline of development of the modern cold-cathode X-ray tube, in which 1000-Ampere microsecond pulses are obtained, and of the associated 300-kv. surge-generator. The equipment has had particular application to studying the effect of bullets passing through material opaque to light. Summary noted in 1613 of 1946.

621.391.64 3241

Modulation of Infrared Sources for Signaling Purposes—W. S. Huxford. (*Proc. Nat. Electronics Conference* (Chicago), vol. 2, pp. 158–170.) An account of various modulation methods, including mechanical modulation used by the Japanese, and German mechanical and optical methods. Details are given of two new types of electrically modulated arc lamps, (a) the concentrated arc, and (b) the calcium vapor arc.

621.396.9.083.7:551.5 3242

Telemetering from V-2 Rockets: Part 2—V. L. Heeren, C. H. Hoeppner, J. R. Kauke, S. W. Lichtman, and P. R. Shifflett. (*Electronics*, vol. 20, pp. 124–127; April, 1947.) A time-modulated pulse system is used. The output of the ground station 1000-Mc. receiver contains trains of pulses spaced according to instrument readings in the rocket. Circuits for decoding these pulses into individual voltages for recording are given. For part 1 see 2536 of September.

621.398:621.397.6 3243

Television Equipment for Guided Missiles—C. J. Marshall and L. Katz. (*Proc. Nat. Electronics Conference* (Chicago), vol. 2, pp. 115–129.)

623.26:621.396.9 3244

Detectors for Buried Metallic Bodies—L. F. Curtis. (*Proc. Nat. Electronics Conference* (Chicago), vol. 2, pp. 339–351.) Various development problems are discussed and a description is given of the SCR-625 detector, which uses a 1-kc. transmitter and receiver and a balanced coil system.

623.978+550.838]:538.71 3245

Magnetic Prospecting—W. J. Shackelton. (*Bell Lab. Rec.*, vol. 25, pp. 142–145; April, 1947.) Short account of an airborne magnetic detector, and its application to submarine detection and geophysical prospecting.

778.332 3246

Electronic Timing Provides Uniform X-Ray Exposures—H. D. Moreland. (*Radiography*, vol. 13, pp. 51–54; May, 1947.) X-ray radiation, after passing through an object, is converted to visible radiation measured by a photoelectric cell which opens a relay switch in the X-ray circuit.

PROPAGATION OF WAVES

538.566.2:517.94 3247

Two Notes on Phase-Integral Methods—Furry. (*See* 3095.)

538.569.4.029.64 3248

Various Papers on Absorption of Microwaves—(*See* 3096 to 3100.)

621.396.11+538.566 3249

Velocity of Electromagnetic Waves—L. Essen. (*Nature* (London), vol. 159, pp. 611–612; May 3, 1947.) An account of the results obtained from velocity determination by resonance of a short length of a wave guide closed at both ends, using centimeter waves. The accuracy is comparable with that of light velocity measurements, and the average result obtained is 17 kilometers higher than that generally accepted for light waves, although this discrepancy is within the combined limits of error for the two measurements.

621.396.11 3250

The Elements of Wave Propagation Using the Impedance Concept—H. G. Booker. (*Jour. I.E.E.* (London), Part III, vol. 94, pp. 171–198; May, 1947. Discussion, pp. 199–202.) The theory of transmission lines is normally approached from the point of view of circuits and developed in terms of the impedance concept, whereas the theory of more general forms of wave propagation tends to be developed from Maxwell's equations. By using the concept of field impedance, propagation and transmission line phenomena can be integrated into a single picture. Phenomena such as the Brewster angle, the critical angle, propagation in hollow metal pipes, reflection, and transmission by wire netting, etc., all have their counterparts in transmission line theory. For example, it is easier to explain the part played by the less dense medium in total internal reflection by regarding total internal reflection as analogous to a reactive load on the end of a simple transmission system. The impedance concept can, in fact, be regarded as complementary to the optical approach to electromagnetic phenomena.

The impedance concept is here applied to: (a) a simple infinite plane wave; (b) reflection at a discontinuity between two dielectrics, (c) extension of (b) to conducting media and to oblique incidence, (d) extension of the use of circle diagrams, (e) the effect of obstacles such as an infinite plane sheet of wire netting on an incident plane wave, (f) propagation along a wave guide. Energy, metal losses, the use of matrices and radiation from aerials are also discussed. The correspondence between transmission-line and propagation phenomena is made clear by placing corresponding equations in parallel columns; for example, the obstacles mentioned in (e), above, correspond to lumped shunt impedances.

621.396.11:550.385 3251

Effect of Magnetic Perturbations on the Velocity of Short Radio Waves—N. Stoyko. (*Compt. Rend. Acad. Sci.* (Paris), vol. 224, p. 1281; May 5, 1947.) From reception results for 17–35 m. at Buenos Aires, Paris, Tokyo, and Washington, and magnetic data provided by the University of Paris, it is found that for direct propagation the apparent velocity diminishes from 275 660 kilometers per second for magnetically calm conditions to 272 090 kilometers per second for very disturbed conditions, while for "super-propagation" (along the longer arc of the great circle) the apparent velocity increases from 284, 502 kilometers per second for calm days to 288, 283 kilometers per second for very disturbed conditions. For earlier work see 3780 of 1945, 945 of 1942, and back references.

611.396.11:551.510.535 3252

Equivalent Path and Absorption in an Ionospheric Region—J. C. Jaeger. (*Proc. Phys. Soc.*, vol. 59, pp. 87–96; January 1, 1947.) Formulas for the calculation of absorption and equivalent path for rays vertically incident on an ionized region, the ionization of which varies exponentially (a Chapman region), are deduced for the cases of transmision and of reflection from above and below. Tables of numerical values are appended. The results are compared with those obtained on the basis of a parabolic variation of ionization.

621.396.11:551.510.535 3253

Predicting World Area Coverage by Reflected Waves—N. A. Atwood. (*Tele-Tech*, vol. 6, pp. 38–42, 104; June, 1947.) Technical details of a new method for predicting the maximum usable frequency and the optimum working frequency for any radio link. Use is made of a slide-rule type of device consisting of a transparent world map, a transparent time-frequency chart, and a series of great-circle charts. These are similar to the maps and charts contained in the C.R.P.L. Basic Radio Propagation Predictions.

621.396.11.029.58:551.510.535 3254

Doppler Effect in Propagation—H. V. Griffiths. (*Wireless Eng.*, vol. 24, pp. 162–166; June, 1947.) Changes of 2 to 7 parts in 10^8 have been observed in the received frequency of WWV standard transmissions on 15 Mc., which are accurate to ± 2 parts in 10^8. Further measurements under different conditions have shown that the divergence is not wholly or largely due to the difference in frequency standards.

Trigonometrical formulas for the path length and the Doppler effect resulting from the changes in path length are deduced. A rate of change of the virtual height of the reflecting layer of the order of 3 to 6 meters could account for the observed frequency difference between the received and transmitted signals.

621.396.11.029.6 3255

Radio Propagation at Frequencies Above 30 Megacycles—K. Bullington. *Proc. Nat. Electronics Conference* (Chicago), vol. 2, p. 130.) Summary only. Discusses the effect on propagation of frequency, range, aerial height, curvature of the earth, atmospheric conditions, etc. Charts are given from which an estimate of received power and field intensity for a given transmission path can be obtained quickly.

621.396.11.029.6:621.397.81 3256

Analyzing TV Propagation at U.H.F.—R. P. Wakeman. (*Tele-Tech*, vol. 6, pp. 62–65, 115; June, 1947.) From investigations by the F.C.C. of diffraction effects, u.h.f. at present carrier power levels appears to be useful only for line-of-sight service.

621.396.11.029.64:535.434 3257

Radar Echoes from the Sea Surface at Centimeter WaveLengths—H. Davies and G. G. Macfarlane. (*Proc. Phys. Soc.*, vol. 58, pp. 717–729; November 1, 1946.) An account is given of quantitative measurements of the echoes obtained from the sea surface under various weather conditions with radars operating on wavelengths of 1.25, 3, and 10 centimeters. The necessary theoretical treatment is given; a "scattering coefficient" of the surface is defined and its variation with sea conditions and angle of elevation is shown. See also 423 of March and 2218 of August, for which the above U.D.C. would have been preferable.

621.396.81.029.63:621.397.81 3258

Results of Field Tests on U.H.F. (490 Mc/s) Color Television Transmissions in the New York Metropolitan Area—E. B. Lodge. (*Proc. Nat. Electronics Conference* (Chicago), vol. 2, p. 156.) Summary only.

RECEPTION

621.396.621+621.396.662.2.029.62 3259

Front-End Design of F.M. Receivers—C. R. Miner. (*Proc. Nat. Electronics Conference* (Chicago), vol. 2, pp. 564–569.) Details of a new type of guillotine tuner for receivers for the 100-Mc. band. See also 2052 of August.

621.396.621 3260

High-Fidelity Miniature Tube Receiver—J. C. Hoadley. (*Radio News*, vol. 37, pp. 47–49, 171; April, 1947.)

621.396.621:621.396.681 3261

28 Volts H.T. and L.T.—R. Terlecki and J. W. Whitehead. (*Electronic Eng.*, vol. 19, pp. 157–159; May, 1947.) Discusses the design of receivers for operation direct from a 28-volt supply, without either rotary converters or vibrators. Tests with a modified American communications receiver gave very satisfactory results. Suitable tubes are listed.

621.396.621.54:621.396.615.142:621.396.96 3262

Reflex Oscillators for Radar Systems—McNally and Shepherd. (*See* 3057.)

621.396.621.54.029.6:621.396.5 3263

An Experimental Receiver for Ultra-Short-Wave Radio-Telephony with Frequency Modulation—A. van Weel. (*Philips Tech. Rev.*, vol. 8, pp. 193–198; July, 1946.) Description of a superheterodyne receiver for a mean carrier frequency of about 300 Mc. The push-pull mixing stage is made self-oscillating by introducing an "asymmetric" input circuit tuned to the local oscillator frequency. As no separate oscillator is required there is a reduction in fluctuation noise, so that an h.f. amplifier can be omitted with only a small reduction in the signal-to-noise ratio. For a description of the transmitter used for the same Tilburg-Eindhoven link, see 2606 of September.

621.396.622 3264

A New Detector for Frequency Modulation—W. E. Bradley. (*Proc. Nat. Electronics Conference* (Chicago), vol. 2, pp. 570–576.) A description of the circuit, design procedure, and alignment of a single stage f.m. detector. Tests show it to be comparatively unresponsive to a.m. and free from practical defects.

621.396.662:621.396.621.54.029.62 3265

V.H.F. Tuner Design—G. Wallin and C. W. Dymond. (*Proc. Nat. Electronics Conference* (Chicago), vol. 2, pp. 557–563.) The design of a single-oscillator double-superheterodyne circuit for use on the 88 to 108 Mc. f.m. band is described. Receiver performance characteristics are given.

621.396.82:621.396.619.13 3266

Frequency Modulation Distortion Caused by Common- and Adjacent-Channel Interference—M. S. Corrington. (*RCA Rev.*, vol. 7, pp. 522–560; December, 1946.) Formulas are developed for computing the amplitudes of harmonics and cross-modulation formed by the interference of two f.m. waves. From these the effects on f.m. reception of a de-emphasis network following the discriminator, of a low-pass audio filter and of nonlinear phase shift in the amplifiers are calculated.

621.396.82.029.5 3267

Interference Between V.H.F. Radio Communication Circuits—W. R. Young, Jr. (*Proc. Nat. Electronics Conference* (Chicago), vol. 2, p. 131.) Summary only. A discussion of common causes of such interference, with measurement results and computation formulas.

621.396.822:621.396.615.141.2 3268

Excess Noise in Cavity Magnetrons—R. L. Sproull. (*Jour. Appl. Phys.*, vol. 18, pp. 314–320; March, 1947.) A fluctuating noise modulation in excess of shot noise in 4000-Mc. magnetron oscillations is described. The effects of gas pressure and cathode material on the ratio of noise to r.f. output were investigated and the gas near the cathode examined by spectrograph. The excess noise is attributed to the liberation of metal atoms from the oxide coated cathode by bombarding electrons. Details are given of a cathode in which the oblique path of bombardment is used to separate the emitting and bombarded surfaces.

621.396.828:621.396.619.16 3269

Pulse Modulation Noise Suppression Characteristics—S. Moskowitz and D. D. Grieg. (*Communications*, vol. 27, pp. 42–43; March, 1947.) Summary of 1947 I.R.E. Convention paper.

STATIONS AND COMMUNICATION SYSTEMS

621.394.44 3270

Carrier Telegraphy—J. te Winkel. (*Philips Tech. Rev.*, vol. 8, pp. 206–213; July, 1946.) A method in which 18 telegraphic channels are contained in the frequency band of a single telephone connection.

621.395.44:621.315.052.63 3271

Rural Carrier Telephony—(*Elec. Eng.*, vol. 66, pp. 425–431; May, 1947.) A carrier system for application on power lines. Summary of "A Carrier Telephone System for Rural Service," by T. M. Barstow and "Application of Rural Carrier Telephone System," by E. H. B. Bartelink, L. E. Cook, F. A. Cowan, and G. R. Messmer.

621.395.44:621.315.052.63 3272

Field Tests on Power-Line Carrier-Current Equipment—R. H. Miller and E. S. Prud'homme. (*Trans. A.I.E.E.* (*Elec. Eng.*, December Supplement, 1946), vol. 65, pp. 1177–1178.) Discussion 1207 of May.

621.395.5:621.317.34 3273

Transmission Rating of Telephone Systems—W. A. Codd. (*Trans. A.I.E.E.* (*Elec. Eng.*, December Supplement, 1946), vol. 65, p. 1123.) Discussion on 1208 of May.

621.396.1 3274

The Job Ahead—C. R. Denny. (PROC. I.R.E., vol. 35, pp. 598–599; June, 1947.) The chairman of the F.C.C. asks radio engineers for ways and means of winning the battle for ether-space.

621.396.619.11/.13:534.78 3275

Narrow-Band F.M. for Voice Communication—N. Bishop. (*QST*, vol. 31, pp. 20–23; May, 1947.) Comparison of a.m. and narrow-band f.m. shows that the latter gives greater intelligibility with weak signals.

621.396.619.11/.13].029.62:621.396.931 3276

Amplitude-Modulated Communication in the V.H.F. Band—D. H. Hughes. (*Electronic Eng.*, vol. 19, pp. 143–146, 151; May, 1947.) The relative merits of f.m. and a.m. are discussed and miniature mobile radiotelephone equipment using a.m. is described. It occupies 1 ft.^{3} for a weight of 40 pounds and radiates 12 watts at frequency between 80 and 100 Mc. The results of some field tests are given.

621.396.619.16:621.396.13:621.396.97 3277

Pulse-Time Multiplex Broadcasting on the Ultra-High Frequencies—D. D. Grieg and S. Moskowitz. (*Proc. Nat. Electronics Conference* (Chicago), vol. 2, pp. 531–547.) The advantages of a multiplex broadcast system over a simplex system are discussed. Details are given of time-division and frequency-division multiplex systems, apparatus employed, and results obtained. See also 3049 of 1946 (Grieg).

621.396.619.16:621.396.41 3278

Multiplex Employing Pulse Time and Pulsed F.M. Modulation—H. Goldberg and C. C. Bath. (*Communications*, vol. 27, pp. 41–42; March, 1947.) Summary of 1947 I.R.E. Convention paper.

621.396.65+621.397.26]:629.135 3279

Stratovision System of Communication—C. E. Nobles. (*Proc. Nat. Electronics Conference* (Chicago), vol. 2, pp. 54–72.) The proposed system uses high-altitude aircraft transmission. The same aircraft may carry television and f.m. transmitters, as well as radio-relaying transmitters. Experimental curves are given of field-strengths at various distances from an aircraft transmitting on 107.5 Mc. and 514 Mc. at about 20,000 ft. For previous accounts see 3970 of 1945, 3090 and 3801 of 1946, and 2588 of September.

621.396.65+621.397.26]:629.135 3280

The Stratovision System of Communication—Aircraft Requirements—W. K. Ebel. (*Proc. Nat. Electronics Conference* (Chicago), vol. 2, pp. 73–81.) Design considerations for reliability and economy of operation.

621.396.65.029.63:621.396.619.16 3281

Pulse Time Division Radio Relay—B. Trevor, O. E. Dow, and W. D. Houghton. (*RCA Rev.*, vol. 7, pp. 561–575; December, 1946.) Description of a radio relay set developed for the U. S. Army. Two sets provide eight two-way telephone circuits, over a line-of-sight path of between 50 and 100 miles. The frequency range is 1350 to 1500 Mc.; a time division multiplex system and pulse position modulation are used. See also 3283 below.

621.396.65.029.64 3282

A Microwave Relay Communication System—G. G. Gerlach. (*Proc. Nat. Electronics Conference* (Chicago), vol. 2, pp. 511–530.) A description of a multichannel f.m. 4000-Mc. relay system using a 1-Mc. f.m. sub-carrier. The intermediate relay stations are unattended. See also 1578 of June (Thompson).

621.396.65.029.64 3283

A Microwave Relay Communication System—G. G. Gerlach. (*RCA Rev.*, vol. 7, pp. 576–600; December, 1946.) A review of experimental results obtained with a 4000 Mc. multichannel relay system using a f.m. sub-carrier for frequency-modulation of the final carrier. Demodulation to sub-carrier frequency is effected at the relay stations. The equipment developed from these experiments and to be used commercially for linking New York, Washington, and Pittsburgh, is described in detail. See also 3048 and 3748 of 1946 and 2935 of October.

621.396.712.2 3284

WNEW Program Dispatching System—J. Peterson. (*Tele-Tech*, vol. 6, pp. 50–51, 111; June, 1947.) A master control console is designed for flexibility in handling multiple programs and can deal with seven studios and three remote channels simultaneously.

621.396.931 3285

Vehicle Radiotelephony Becomes a Bell System Practice—A. C. Peterson, Jr. (*Bell Lab. Rec.*, vol. 25, pp. 137–141; April, 1947.) A brief description of a mobile radio-telephone system, operating on frequencies in the range 100 to 200 Mc. and providing two-way communication between any subscriber's vehicle and the normal telephone system.

621.396.931 3286

Selective-Calling Systems in Mobile Radio Communication—L. Morris. (*Proc. Nat. Electronics Conference* (Chicago), vol. 2, pp. 644–649.)

SUBSIDIARY APPARATUS

621-526 3287

Dimensionless Analysis of Servomechanisms by Electrical Analogy—S. W. Herwald and G. D. McCann. (*Trans. A.I.E.E.* (*Elec. Eng.*, December Supplement, 1946), vol. 65, p. 1132.) Discussion on 543 of March.

621-526 3288

Parallel Circuits in Servomechanisms—H. T. Marcy. (*Trans. A.I.E.E.* (*Elec. Eng.*, December Supplement, 1946), vol. 65, p. 1128.) Discussion on 3763 of 1946.

621-526 3289

The Frequency Response of Automatic Control Systems—H. Harris, Jr. (*Trans. A.I.E.E.* (*Elec. Eng.*, December Supplement, 1946), vol 65, pp. 1131–1132.) Discussion on 3764 of 1946.

621-526 3290

High-Performance Demodulators for Servomechanisms—K. E. Schreiner. (*Proc. Nat. Electronics Conference* (Chicago), vol. 2, pp. 393–403.)

621.313.2 3291

The "Electrotor"—J. V. Eurich. (*Electronic Eng.*, vol. 19, pp. 160–161; May, 1947.) For another account of this equipment see 2943 of October.

621.317.755 3292

Trends in Cathode-Ray Oscillograph Design—Gaines. (*See* 3191.)

621.318.3 3293

A.C. Magnets and Solenoids—L. T. Rader. (*Elec. Eng.*, vol. 66, pp. 487–492; May, 1947.) The design and construction of single phase a.c. magnets. Their advantages over d.c. magnets are briefly discussed.

621.318.5 3294

Telephone Relays—and Their Use in Electronic Circuits: Part 1—A. A. Chubb. (*Electronic Eng.*, vol. 19, pp. 172–177; June, 1947.) The operating conditions of common types of relay are described and the load-line method of matching a relay to a tube is discussed. To be continued.

621.352.8 3295

Characteristics of the Silver Chloride-Magnesium Water Activated Battery—J. B. Mullen and P. L. Howard. (*Electrochemical Society*, Preprint 90-33, pp. 411–422.) The full account of a new type of cell referred to in 2948 of October.

TELEVISION AND PHOTO-TELEGRAPHY

537.291+538.691]:621.385.832 3296

Electron Optics of Deflection Fields—R. G. E. Hutter. (*Proc. Nat. Electronics Conference* (Chicago), vol. 2, pp. 424–453; October 3 and 5, 1946.)

621.397.3 3297

Simultaneous All-Electronic Color Television—RCA Laboratories Division. (*RCA Rev.*, vol. 7, pp. 459–468; December, 1946.) The first progress report on the new system which enables the three color images to be transmitted simultaneously. Each color channel employs the same standards as are in use for black and white transmission, so that the green channel can transmit monochrome pictures. Undesirable obsolescence is thus avoided, as the system can be interchanged with ordinary black-and-white television. Apparatus for scanning, color slides and color motion-picture film is described in detail, and the construction of the receivers used in the experimental work is explained.

621.397.44 3298

Television Relaying—P. H. Reedy. (*Communications*, vol. 26, pp. 18–21; December, 1946.) Summary of a Rochester Fall Meeting Paper. Color television relaying by means of cable and radio. Tests on short-range transmissions are outlined and a description of a 530-Mc relay transmitter is given. Long-distance cable tests indicate the superiority of color over black and white, despite bandwidth limitations.

621.397.5 3299

A Report on the 1946 Rochester Fall Meeting—L. Winner. (*Communications*, vol. 26, pp. 18–25, 51; December, 1946.

621.397.5 3300

Television as a Public Service—R. F. Guy. (*Communications*, vol. 26, pp. 21–22.) Summary of a Rochester Fall Meeting paper.

621.397.5 3301

Television—(*RCA Rev.*, vol. 7, pp. 641–655; December, 1946.) A list of some 275 papers published by R.C.A. authors from 1929 to 1946 on television and related subjects.

621.397.5:621.318.572 3302

Counter-Timer for Television—C. E. Hallmark. (*Communications*, vol. 27, p. 14; March, 1947.) Summary of 1947 I.R.E. Convention paper.

621.397.5:621.396.67 3303

Load Characteristics of Television Antenna Systems: Part 3—G. E. Hamilton and R. K. Olsen. (*Communications*, vol. 27, pp. 20–25; March, 1947.) Aerial impedance characteristics are discussed and phrasing and matching methods for transmitting aerials are given, with particular reference to (a) the doughnut type of folded dipole with elements of the same or unequal diameter, (b) a double-folded system in turnstile and (c) three-element folded dipoles. Where many measurements are found necessary and the complex nature of the load must be plotted, transmission line charts may be used to simplify the calculation. Suitable charts are "Chart for Transmission Line Measurements and Computations," by P. S. Carter, (*RCA Review*, January 1939); "Practical Analysis of Ultra-High-Frequency," by J. R. Meagher and H. J. Markley, (RCA Service Co.) and "Transmission Line Calculator," by P. H. Smith (*Electronics*, January, 1939.) For parts 1 and 2 see 2262 of August.

621.397.5:621.396.67 3304

Television Antenna Installations Giving Multiple Receiver Outlets—Ehret. (*See* 3029.)

621.397.6 3305

Television Deflection Circuits: Part 1—Molded Iron Dust Cores for Use in Horizontal [line] Deflection Circuits. Part 2—Theory and Design of Combined Low-Loss Horizontal Deflecting and High-Voltage Power-Supply Systems—A. W. Friend. (*RCA Rev.*, vol. 8, pp. 98–138; March, 1947.) Part 1: A low-loss, inexpensive system using compressed sponge-iron cores for transformers and yokes enables line deflection to be obtained for a 27-kb kinescope from two type 807 tubes. Curves of the properties of the core material, photographs of typical yokes and transformers and circuit details are given. Part 2: A complete analysis with design equations and charts.

621.397.6 3306

The Use of Powdered Iron in Television Deflecting Circuits—A. W. Friend. (*Proc. Nat. Electronics Conference* (Chicago), vol. 2, pp. 89–114.) A shortened version of 3305 above.

621.397.6 3307

Westinghouse Color Television Studio Equipment—D. L. Balthis. (*Proc. Nat. Electronics Conference* (Chicago), vol. 2, pp. 27–39.) A descriptive account of the electrical and optical equipment required to convert a 35-mm. color slide, or a 16-mm. color film and its associated sound into signals suitable for an u.h.f. color television transmitter (480 to 920 Mc.). The color operation is based on the use of three primary colors with sequential scanning by means of color filters. Sound and picture signals are transmitted on the same frequency.

621.397.6:621.398 3308

Television Equipment for Guided Missiles—C. J. Marshall and L. Katz. (*Proc. Nat. Electronics Conference* (Chicago), vol. 2, pp. 115–129.)

621.397.6:629.135 3309

Television Equipment for Aircraft—M. A. Trainer and W. J. Poch. (*RCA Rev.*, vol. 7, pp. 459–502; December, 1946.) A light-weight airborne television equipment operating on a frequency of about 100 Mc. is described, and the design considerations involved are listed and discussed. The transmitter and camera are enclosed in a single unit which, together with a monitor and power supply, comprises the transmitting station. Flight tests of the equipment showed difficulties peculiar to the transmission of television signals from aircraft; methods used for minimizing these difficulties are discussed. In particular instability of synchronization was overcome by use of a keyed automatic volume control and difficulties due to multi-path transmission from one plane to another by keeping the frequency modulation of the transmitter to a minimum.

621.397.61 3310

High-Power Television Transmitters—Some Aspects of Their Design: Parts 1 and 2—P. A. T. Bevan. (*Electronic Eng.*, vol. 19, pp. 138–142 and 181–184, 204; May and June, 1947.) Considers the problems associated with peak power outputs up to 50 kW, involving bandwidths up to ±5 Mc., with special reference to the B.B.C. 405-line system. Wide bandwidth requires "maximally flat" coupled circuits of low Q and this implies a low anode load resistance for the amplifier tube, thus limiting the power output and anode conversion efficiency. Recent short single-ended water cooled tubes such as the CAT21 give the small grid-lead inductance required for neutralized push-pull grid-modulated amplifiers at 50 Mc. The estimated peak power of a CAT21 is shown graphically in terms of the bandwidth response. The requirements for capacitors, insulators, and resistors are briefly described. After expressing the need for more accurate measurement of large currents in v.h.f. tank circuits, the idealized linear operating conditions of a grid-modulated push-pull r.f. amplifier are illustrated and the requirements for neutralization are given. Methods described for overcoming the effects of nonlinearity include loading the grid circuit of the modulated amplifier with resistance and the use of a cathode-follower driver stage. The advantages and disadvantages of the grounded-grid r.f. amplifier, and the requirements for output transmission lines, and cables are described.

621.397.61 3311

Television Transmitter for Black-and-White and Color Television—N. H. Young. (*Proc. Nat. Electronics Conference* (Chicago), vol. 2, pp. 40–53). A general description of a 490-Mc. transmitter giving a peak power output of 1 kW. It is designed for operation from 3-phase 60-c.p.s. mains at either 208 or 220 volts. The total power consumption is 25 k.v.a.

621.397.611 3312

The Electrostatic [image] Dissector—H. Salinger. (*Proc. Nat. Electronics Conference* (Chicago), vol. 2, pp. 82–88.) Magnetic focusing is used, but scanning is done by electrostatic deflection. The deflection is achieved by means of a number of wires (twelve in this case) disposed axially inside the tube. The two scanning saw-tooth voltages are applied in different proportions to each wire. Special networks to effect proper voltage distribution have been developed.

621.397.62 3313

A Simple and Practical Television Receiver—M. Mars. (*Télévis. Franç.*, no. 24, pp. 15–17; April, 1947.) Circuit diagrams and constructional details of a receiver using only 18 tubes, including the three rectifiers in the supply unit. Sensitivity can be improved by the addition of another h.f. stage.

621.397.62 3314

Color Television for Theatres—H. G. Shea. (*Tele-Tech*, vol. 6, pp. 44–45; June, 1947.) General principles of a R.C.A. system giving pictures 7 and one-half feet by 10 feet. The colors are obtained by special phosphors in the three c.r. tubes. See also 1246 of May.

621.397.62 3315

Television Sound Channels—R. B. Dome. (*Communications*, vol. 26, pp. 22–25; December, 1946.) Summary of a Rochester Fall Meeting paper. A television receiver using a single wide-band i.f. amplifier for both sound and vision signals. Final separation depends on the frequency difference between sound and vision channels.

621.397.62:621.396.662.2 3316

Variable Inductance Tuning for TV Receivers—Melvin. (*See* 3073.)

621.397.743 3317

Television Network Facilities—L. G. Abraham and H. I. Romnes. (*Elec. Eng.*, vol. 66, pp. 477–482; May, 1947.) A discussion on the use of (a) balanced wire pairs, (b) coaxial cables, and (c) radio relays for the interconnection of television studios.

621.397.81:621.396.11.029.6 3318

Analyzing TV Propagation at U.H.F.—Wakeman. (*See* 3256.)

621.397:621.396.81.81.029.63 3319

Results of Field Tests on U.H.F. (490 Mc/s) Color Television Transmissions in the New York Metropolitan Area—Lodge. (*See* 3257.)

621.397.5 3320

Television: Vols. 3 and 4. [Book Notice]—A. N. Goldsmith, A. F. Van Dyck, R. S. Burnap, E. T. Dickey, and G. M. K. Baker (Eds.). Radio Corporation of America, Princeton, N. J. A collection of papers dealing with all aspects of television. Volumes 1 and 2 are now out of print, but summaries of the papers in them are included in Volume 3, which covers the period 1938 to 1941. Volume 4 covers the period 1942 to 1946.

TRANSMISSION

621.316.726.029.64.078.3 3321

Microwave Frequency Stability—A. E. Harrison. (*Proc. Nat. Electronics Conference* (Chicago), vol. 2, pp. 615–622.) A discussion of the principles of operation of klystron frequency multipliers and power amplifiers for direct crystal control of the microwave power.

621.396.61:621.396.662.1 3322

Mono-Sequence Tuning—J. N. Whitaker. (*Radio News*, vol. 37, pp. 44–45, 92; June, 1947.) A full description of a single-dial tuning system for the oscillator and frequency multiplier stages of a multiband transmitter, using identical variable capacitors. Circuit details are given.

621.396.61:621.396.97 3323

2-Control 250-W A.M. Braodcast Transmitter—H. Kees. (*Communications*, vol. 27, pp. 11–13, 37; March, 1947.) A design with only one tunable r.f. circuit, simplified metering and controls, and accessible components.

621.396.61.029.5 3324

Transmitter with Efficient Band Switching—R. P. Turner. (*Radio News*, vol. 37, pp. 53–55, 150; June, 1947.) The coils for the range 10 to 80 meters are mounted on a sliding carriage, with rack and pinion operation from the front panel, which carries all controls.

621.396.61.029.5/.62]:621.396.933 3325

Ground-Air Communications Unit—S. A. Meacham. (*Communications*, vol. 27, pp. 22–23, 54; April, 1947.) A medium-power transmitter covering the bands 125 to 525 kc., 2 to 20 Mc., and 100 to 160 Mc.

621.396.61.21.029.56/.58 3326

A Table-Top Kilowatt—G. Grammer, D. Mix, and B. Goodman. (*QST*, vol. 31, pp. 13–19, 154; May, 1947.) Triode-tetrode crystal oscillator and frequency multiplier drive an 813 push-pull amplifier. With input of 1 kW, output of 600 watts is obtained at all amateur frequencies from 3.5 to 30 Mc.

621.396.619.13/.14 3327

Low-Frequency N.F.M. [narrow-band frequency modulation]—B. Goodman. (*QST*, vol. 31, pp. 21–27; July, 1947.) Comparison with narrow-band phase modulation and description of a simple phase modulator.

VACUUM TUBES AND THERMIONICS

537.533.7+621.385.1 3328

Electron Optics and Space Charge in Strip-Cathode Emission Systems—O. Klemperer. (*Proc. Phys. Soc.*, vol. 59, pp. 302–323; March, 1947.) For small emission, electron-optical laws can be applied. Simple space charge theory does not hold for special systems of the type proposed by Pierce (4275 of 1940 and back references). In these systems, the potential distribution in the beam causes a lack of homocentricity, revealed by ray-tracing results.

621.383 3329

Spontaneous Fluctuations of Current in a Photo-Electric Cell—D. K. C. MacDonald. (*Nature* (London), vol. 159, pp. 608–609; May 3, 1947.) Graphical presentation of the results of shot-effect measurements, with brief discussion.

621.383 3330

Photodetectors for Ultraviolet, Visible and Infrared Radiation—R. J. Cashman. (*Proc. Nat. Electronics Conference* (Chicago), vol. 2, pp. 171–180.) Review of recent developments, including (a) protoemissive cells with activated and pure metal cathodes, (b) photovoltaic cells as used in exposure meters, and (c) photoconductive cells and their uses.

621.383:522.615 3331

Application of the Multiplier Phototube to Astronomical Photoelectric Photometry—G. E. Kron. (*Astrophys. Jour.*, vol. 103, pp. 326–331; May, 1946.) Characteristics of 1P21 multiplier phototube, which is many times superior to light-sensitive units previously used in the blue region of the spectrum.

621.383.5:621.318.57]+621.383.5.001.8 3332

The A.C. Behaviour of the Barrier Layer Photo Cell—J. A. Sargrove. (*Jour. Brit. I.R.E.*, vol. 7, pp. 86–97; May and June, 1947.) When the cell is illuminated, it acts as a nonlinear conductor to current in both directions, whereas in darkness it behaves as a rectifier. This property enables the cell to be used directly for operating relays, with a sensitivity some 300 times greater than when used as a detector. A high degree of electrical stability is obtained by operating the cell from the same a.c. supply as the lamp which illuminates it. A number of industrial applications of the method are described.

621.385 3333

Similitude of Valves—F. H. Raymond. (*Onde Élec.*, vol. 27, pp. 209–212; May, 1947.) A demonstration of the agreement between the general theory of similitude and the technical aspect of its application to tubes described by Lehmann (3821 of 1946). The similitude of tubes with a common cathode is considered in particular, the possibility of other types of similitude is discussed and the law of similitude for the magnetron derived simply.

621.385:620.163 3334

Electrical Production Tests for High-Power Tubes—B. Sheren. (*Proc. Nat. Electronics Conference* (Chicago), vol. 2, pp. 250–255.)

621.385:620.163 3335

Production Test Facilities for High-Power Tubes—W. L. Lyndon. (*Proc. Nat. Electronics Conference* (Chicago), vol. 2, pp. 256–267.) R.C.A. equipment for testing modern high-power tubes. It consists of a 25-Mc. oscillator unit, a 1.5-Mc. oscillator unit, and associated dummy loads, power supplies, sub-station, control and water-cooling equipment.

621.385.029.63/.64]:538.3:621.396.694 3336

On the Helix Circuit Used in Progressive-Wave Valves—Roubine. (*See* 3036.)

621.385.1+621.396.611.4 3337

F.M.+TV P-A Tube and Grounded-Grid Cavity Circuit—H. D. Wells and R. I. Reed. (*Communications*, vol. 27, p. 16; March, 1947.) Summary of 1947 I.R.E. Convention paper.

621.385.1:517.54 3338

Conformal Transformations in Orthogonal Reference Systems—Roys. (*See* 3171.)

621.385.1:621.396.813 3339

Microphony of Radio Valves—Chamagne and Guyot. (*Télévis. Franç.*, no. 24, Supplement *Électronique*, pp. 7–10; April ,1947.) Discusses definition and gives methods of measurement.

621.385.1:621.396.813 3340

Microphonism in a Subminiature Triode—V. W. Cohen and A. Bloom. (*Communications*, vol. 27, pp. 18, 41; March, 1947.) Summary of 1947 I.R.E. Convention paper.

621.385.1.032.216:546.431.284 3341

A Study of the Barium Silicate Interface of Oxide Coated Cathodes—Eisenstein. (*See* 3158.)

621.385.16+621.396.615.141.2 3342

The Donutron. An All-Metal Tunable Squirrel-Cage Magnetron—F. H. Crawford and M. D. Hare. (*Proc. Nat. Electronics Conference* (Chicago), vol. 2, p. 623.) Summary only. For another account see 947 of April.

621.385.2 3343

Total Emission Noise in Diodes—A. van der Ziel and A. Versnel. (*Nature* (London), vol. 159, pp. 640–641; May 10, 1947.) Measurements at λ 7.25 meters on a diode with negative anode voltage show that the equivalent noise temperature of the conductance is approximately equal to the cathode temperature; this relationship is expected to hold over a wide frequency range.

621.385.2 3344

Total Emission Damping in Diodes—A. van der Ziel. (*Nature* (London), vol. 159, pp. 675–676; May 17, 1947.) Results of measurements at λ 5.8 meters of the additional admittance in a diode due to the space charge are given in curves which show the dependence of the admittance on the anode voltage and the saturation current. See also 3109 of 1946 (Smyth).

621.385.3:621.396.694.012.8 3345

The Equivalent Diode—J. Eastabrook. (*Wireless Eng.*, vol. 24, pp. 188–189; June, 1947.) It is concluded that experimental discrimination between the formulas of Walker (949 of April) and Tellegen (*Physica*, vol. 5, p. 301; 1925.) is not possible; between these two and Fremlin's (3166 of 1939) it is possible but unimportant. Walker's approach is preferred on account of its simplicity and because it is theoretically sounder and does not involve the three-halves law. See also 2622 and 2623 of September.

621.385.832:[537.291+538.691 3346

Electron Optics of Deflection Fields—R. G. E. Hutter. (*Proc. Nat. Electronics Conference* (Chicago), vol. 2, pp. 424–453.)

621.396.615.14 3347

The Generator of Centimeter Waves—H. D. Hagstrum. Proc. I.R.E., vol. 35, pp. 548–564; June, 1947.) The physical principles and performance of three types of cavity-resonator magnetron oscillator are described and discussed in some detail. Disk-seal triodes (with built-in cavity-resonators) and velocity-variation oscillators are described briefly. References to basic papers are given.

621.396.615.14+621.385.1].029.63/.64 3348

The Generation of Ultra-High-Frequency Power at the Fifty-Kilowatt Level—W. G. Dow and H. W. Welch, Jr. (*Proc. Nat. Electronics Conference* (Chicago), vol. 2, pp. 603–614.) A comprehensive description of the cavity and electrode structures of the resnatron. The effects of transit time are considered with special reference to frequency stability. See also 1732 of 1946 (Salisbury).

621.396.615.141.2 3349

A Magnetron Oscillator with a Series Field Winding—L. H. Ford. (*Jour. I.E.E.* (London), Part I, vol. 94, pp. 187–188; April, 1947.) Summary of 2631 of September.

621.396.615.141.2:621.396.645.35 3350

A Magnetron for D.C. Voltage Amplification—H. B. G. Casimir. (*Philips Tech. Rev.*, vol. 8, pp. 361–367; December, 1946.) Use of diode in which magnetic field is excited by input circuit; input and output circuits thus separated; introduction of grid at cathode potential near anode increases magnetic sensitivity, which is comparable with the amplification factor of a triode.

621.396.615.141.2:621.396.822 3351

Excess Noise in Cavity Magnetrons—Sproull. (*See* 3268.)

621.396.615.142 3352

Velocity Modulation: Parts 1 and 2—J. H. Fremlin. (*Electronic Eng.*, vol. 19, pp. 147–151 and 199–201; May and June, 1947.) A general discussion of the various types of tubes. The conditions for oscillation in the Heil tube are derived and it is shown how the power from the electron beam in a rhumbatron varies with the oscillation amplitude. The methods for increasing bunching efficiency using the reflex klystron oscillator are compared and the mechanism of bunching for different field distributions using a reflector at high negative potential is explained with the aid of mechanical analogies. By considering the voltage and current conditions in the working gap it is shown how instantaneous frequency changes are effected in a klystron by variation of the high voltage or in a reflexoscillator by variation of the reflector potential.

621.396.615.142 3353

Velocity-Modulation Valves—F. M. Penning. (*Philips Tech. Rev.*, vol. 8, pp, 214–224; July, 1946.) A theoretical discussion of the principles involved in their use as amplifiers and as oscillators.

[621.396.615.142+621.392.029.64]:538.56 3354

Generalized Boundary Conditions in Electromagnetic Theory—Schelkunoff. (*See* 3094.)

621.396.615.142.2.029.64 3355

The Klystron as Amplifier at Centimetric Wavelengths—R. Kompfner. (*Jour. Brit. I.R.E.*, vol. 7, pp. 117–123; May and June, 1947. Discussion, pp. 123–124.) It is shown that in theory a klystron is capable of giving r.f. amplification; a detailed examination shows that noise is the limiting factor. The reduction of shot noise by suitable design is discussed briefly but it is concluded that the practical difficulties in the case of the klystron are much greater than for other devices.

621.396.694 3356

Empirical Formula for [Valve] Amplification Factor—E. W. Herold. (*Proc. I.R.E.*, vol. 35, p. 493; May, 1947.) A simple formula based on Herne's table (2210 of 1944). See also 2406 of 1946.

621.396.694 3357

Triode Characteristics—S. Rodda. (*Wireless Eng.*, vol. 24, p. 157; May, 1947.) Method of calculating the equivalent grid voltage of a triode. A first approximation gives a result in agreement with that of Tellegen, a second approximation includes the effect of space charge in the grid-anode region.

621.383 3358

Photoelectric Cells [Book Review]—A. Sommer. Methuen and Co., 104 pp., 5s. (*P. O.*

Elec. Eng. Jour., vol. 39, part 4, p. 180; January, 1947.) Describes the theory of photoemission, the properties of commercial photo electric cathodes, the matching of light sources and photocathodes, the mechanism of gas amplification and multiplier cells, and applications.

MISCELLANEOUS

061.3:621.39 3359
A Report on the 1947 I.R.E. National Convention—(*Communications*, vol. 27, pp. 14–16, 43; March, 1947.) For titles of some of the papers read see individual sections.

061.6(54):666 3360
Central Glass and Ceramic Research Institute, India—Y. P. Varshney. (*Nature* (London), vol. 159, pp. 290–292; March 1, 1947.) A description covering the functions of, and facilities to be provided by, the Institute which is in process of erection at Calcutta.

5+6]:016 3361
Bibliography of Scientific and Industrial Reports—A weekly publication by the U. S. Department of Commerce, giving abstracts of reports and patents dealing with electronics, plastics, electrical machinery, equipment and supplies, instruments, metals and metal products, physics, and other subjects.

5:3 3362
Science, Politics, and the National Welfare—F. L. Hovde. (*Proc. Nat. Electronics Conference* (Chicago), vol. 2, pp. 15–19.)

5:6 3363
Physics of To-day Becomes the Engineering of To-morrow—C. G. Suits. (*Proc. Nat. Electronics Conference* (Chicago), vol. 2, pp. 20–26.) A discussion of developments resulting from physical research, illustrated by special reference to the magnetron. See also *Elec. Eng.*, vol. 66, pp. 241–243; March, 1947.

538.3:001.5 3364
The Electric-Magnetic Analogy—G.W.O.H: G. H. Livens. (*Wireless Eng.*, vol. 24, pp. 131–132 and 156; May, 1947.) Comment on 970 of April. Various manipulations of the Lagrangian and Hamiltonian functions L and A for both electric and magnetic fields tend to show that in some cases E is analogous to B rather than to H, while D ($MP = E/4\pi$, where P is the material polarization) is analogous to H rather than to B.

The advantages and disadvantages of exchanging the roles of the vectors B and H are discussed.

539 Rutherford 3365
Rutherford: Life and Work After the Year 1919, with Personal Reminiscences of the Cambridge Period—J. D. Cockcroft. (*Proc. Phys. Soc.*, vol. 58, pp. 625–633; November, 1946.) The second Rutherford Memorial Lecture.

539 Rutherford 3366
Rutherford and the Modern World—M. L. Oliphant. (*Proc. Phys. Soc.* (London), vol. 59, pp. 144–155; January 1, 1947.) The third Rutherford Memorial Lecture.

539.1:62 3367
Atoms, Electrons and Engineers—T. E. Allibone. (*Jour. I.E.E.* (London), Part I, vol. 94, pp. 165–171; April, 1947.) The Faraday Lecture. Salient features of modern atomic theory. Common substances and processes used in engineering are examined in the light of this theory. Uranium fission and its applications are described.

614.825 3368
Dangerous Electric Currents—C. F. Dalziel. (*Trans. A.I.E.E.* (*Elec. Eng.*, December Supplement, 1946.) vol. 65, pp. 1123–1124.) Discussion on 310 of February.

621.3.016.25 3369
The Sign of Reactive Power—(*Elec. Eng.*, vol. 66, pp. 514–517; May, 1947.) Sixteen further comments on 971 of April. See also 1972 of July.

621.3"1920/1946" 3370
A Synoptic Review of Electrical Engineering Progress, Particularly During the Last Quarter Century—J. D. Ferguson. (*Jour. I.E.E.* (London), Part I, vol. 94, pp. 73–81; February, 1947.) Abstract of Chairman's address to Irish branch of I.E.E.

621.38/.39 3371
Electronics and the Future—E. U. Condon. (*Proc. Nat. Electronics Conference* (Chicago), vol. 2, pp. 1–14.) The opening address at the Conference.

621.38/.39 3372
Some Aspects of Electronic Engineering—T. P. Allen. (*Jour. I.E.E.* (London), Part I, vol. 94, pp. 113–115; February, 1947.) Abstract of Chairman's address to Northern Ireland Centre of I.E.E.

621.395:061.24 C.C.I.F. 3373
The 14th Plenary Session of the Comité Consultatif International Téléphonique (C.C.I.F.) in Montreux, 21st–31st October 1946—W. Schiess. (*Tech. Mitt. Schweiz. Telegr.-Teleph. Verw.*, vol. 25, pp. 73–82; April 1, 1947. In German.) A general account of the proceedings.

621.396 3374
Scientific Problems of Contemporary Radio—N. D. Papalexi. (*Viestnik Akad. Nauk.* (U.S.S.R.), no. 7, pp. 9–15; 1946. In Russian.)

621.396 3375
[Radio Society of Great Britain] Presidential Address—S. K. Lewer. (*Proc. R.S.G.B.*, no. 1, pp. 1–6; Spring, 1947.) Discusses the revival of obsolete radio techniques to solve new problems.

621.396:06.053 URSI 3376
Summary Report of the Seventh General Assembly of the International Scientific Radio Union (URSI) in Paris, September 27–October 25, 1946—Newbern Smith. (*Terr. Mag. Atmo. Elec.*, vol. 52, pp. 80–83; March, 1947.) Statement of resolutions adopted. For a summary of selected papers read at the Conference, see 2758 of October.

621.396"1939/1946" 3377
Radio-Communication Developments—(*Wireless World*, vol. 53, pp. 158–160, 181; May, 1947.) Report of the I.E.E. Radio-Communication Convention of March 1947 which covered advances made since 1939.

621.396.1.029 3378
Proposed Frequency Band Designations—*Elec. Eng.*, vol. 66, p. 471; May, 1947.) Explanation, by the technical committee on standard frequency bands, of a "decade frequency system" in which the designation of each band is the characteristic of the logarithm to base 10 of all the frequencies within the band. Band 5, for example, includes frequencies from 10^5 to 10^6 c.p.s. See also 3742 of 1945.

621.396.97:621.396.82 3379
The War of Broadcasting—E. Wolf. (*Tech. Mitt. Schweiz. Telegr.-Teleph. Verw.*, vol. 25, pp. 64–72; April 1, 1947.) In German and French. Discusses the part played by broadcasting during the war and describes the development of methods of attack and defense, from simple jamming of enemy transmissions to intrusion on the single sideband of the enemy carrier wave.

491.7-3=2 3380
Russian-English Technical and Chemical Dictionary [Book Review]—L. I. Callahan. John Wiley and Sons, New York, N. Y., 1947, 794 pp., $10.00. (*Amer. Jour. Sci.*, vol. 245, p. 463; July, 1947.) The book leans towards chemistry, but nearly every natural science, medicine, mathematics, engineering, etc., receives some attention.

621.38/.39 3381
Proceedings of the National Electronics Conference, Vol. 2 [Book Notice]—R. E. Beam (Ed.), Electrical Engineering Department, Northwestern University, Evanston, Illinois, 1947, 741 pp., $3.50. A collection of papers presented at the Second National Electronics Conference held at Chicago, October 3 and 5, 1946. For abstracts of selected individual papers, see other sections.

621.396 3382
Radio's Conquest of Space [Book Review]—D. McNicol. Murray Hill Books, Inc., 364 pp., $4.00. (*Electronic Eng.*, vol. 19, p. 202; June, 1947.) The author traces "the evolution of radio as a disinterested observer. . . . This is a good book and an authoritative book."

621.396 3383
Reference Data for Radio Engineers [Book Review]—W. L. McPherson. Standard Telephones and Cables, London, 175 pp., 5s. (*Overseas Eng.*, vol. 20, p. 278; March, 1947.) "It consists of a series of tables which list mathematical theorems and short reminders of essential definitions. It is profusely illustrated with curves and diagrams relating to every important aspect of radio engineering."

621.396 3384
Second Year Radio Technology. [Book Review]—W. H. Date. Longmans, Green and Co., London, 222 pp., 7s. 6d. (*Elec. Rev.*, vol. 141, p. 304; August 22, 1947.)

621.396 3385
The Radio Amateurs' Handbook [Book Review]—Headquarters Staff of the American Radio Relay League. American Radio Relay League, West Hartford, Conn., 24th edition, 1947, 470 pp., $1.25 in U.S., $2.00 elsewhere. (PROC. I.R.E., vol. 35, p. 707; July, 1947.) For review of 1946 edition see 1303 of May. The section on equipment construction is revised, and information on the mechanical construction of aerials has been added.